

TYOLOGY OF RECENT GROUNDWATERS FROM DIFFERENT AQUIFER ENVIRONMENTS BASED ON GEOGENIC TRACER ELEMENTS

THÈSE N° 2411 (2001)

PRÉSENTÉE AU DÉPARTEMENT DE GÉNIE CIVIL

ÉCOLE POLYTECHNIQUE FÉDÉRALE DE LAUSANNE

POUR L'OBTENTION DU GRADE DE DOCTEUR ÈS SCIENCES

PAR

Sybille KILCHMANN

Diplom-Phil.-nat, Université de Berne
de nationalité suisse et originaire de Kriens (LU)

acceptée sur proposition du jury:

Prof. A. Parriaux, directeur de thèse
Dr M. Bensimon, rapporteur
Dr V. Labiouse, rapporteur
Prof. J.-L. Michelot, rapporteur
Dr N. Waber, rapporteur
Dr J. Zobrist, rapporteur

Lausanne, EPFL
2001

Abstract	XXIII
Résumé	XXVII
Zusammenfassung	XXXI
Acknowledgements	XXXV

I. INTRODUCTION **1**

1. 1. Framework	2
1. 1. 1. The AQUITYP project: previous studies	3
Spatial observation network	3
Long-term monitoring network	4
1. 2. Objectives	5
1. 3. Basic principles	6
1. 3. 1. Concept of aquifer classification	6
1. 3. 2. Groundwater as a part of the global water cycle	8
1. 3. 3. Factors controlling groundwater composition	9
Mineral dissolution and precipitation	10
Oxidation and reduction	11
Sorption	12
1. 4. Geochemical modelling	16
1. 4. 1. Aqueous speciation and saturation state modelling	16
1. 4. 2. Inverse modelling	17
1. 4. 3. Forward modelling	17

II. WATER DATA **19**

2. 1. Analytical methods applied in the AQUITYP project	20
2. 1. 1. Introduction	20
2. 1. 2. Field measurements	23
2. 1. 3. Sampling techniques, water sample treatment and conservation	23
Suspended particles and colloids	24
Filtration test	26
2. 1. 4. Laboratory analytical methods	28

Current major and minor elements analytical methods	28
Current trace elements analytical methods	29
Quality control of the chemical data	29
2. 2. Selection of data	32
2. 2. 1. Field measurements	32
2. 2. 2. Major elements	33
2. 2. 3. Trace elements	35
2. 3. AQUITYP DataBase	39
2. 3. 1. Database structure	39

III. TYPOLOGY OF RECENT GROUNDWATERS 41

3. 1. Introduction	42
3. 2. Sampling sites and groundwater data	43
3. 3. Geologic and hydrogeologic setting	45
3. 3. 1. Crystalline rocks	45
3. 3. 2. Carbonate rocks	47
3. 3. 3. Evaporite rocks	51
3. 3. 4. Molasse	54
3. 3. 5. Flysch	57
3. 4. Hydrochemistry	59
3. 4. 1. Recent groundwaters derived from crystalline rocks	60
Physical-chemical parameters.....	60
Major element concentrations.....	60
Trace element concentrations	61
Geochemical evolution	63
3. 4. 2. Recent groundwaters derived from carbonate rocks	69
Physical-chemical parameters.....	69
Major element concentrations.....	69
Trace element concentrations	70
Geochemical evolution	73
3. 4. 3. Recent groundwaters derived from evaporite rocks	81
Physical-chemical parameters.....	81
Major element concentrations.....	81
Trace element concentrations	82
Geochemical evolution	84
3. 4. 4. Recent groundwaters derived from molasse	91
Physical-chemical parameters.....	91
Major element concentrations.....	91
Trace element concentrations	92
Geochemical evolution	95

3. 4. 5. Recent groundwaters derived from Flysch	98
Physical-chemical parameters	98
Major element concentrations	98
Trace element concentrations	100
Geochemical evolution.....	102
3. 5. Comparison of aquifer types	106
3. 5. 1. Physical-chemical parameters of the groundwaters	106
Water temperature and total mineralisation	107
pH and redox conditions	108
3. 5. 2. Major elements	109
3. 5. 3. Trace elements	114
Natural tracers of groundwaters in the crystalline Mont-Blanc and	
Aiguilles-Rouges Massifs	118
Natural tracers of groundwaters from carbonate rocks	118
Natural tracers of groundwaters from evaporite rocks.....	119
Natural tracers of molasse groundwaters	119
Natural tracers of groundwaters in the flysch	119
3. 6. Groundwater quality	122
3. 6. 1. Groundwaters from granite and gneiss aquifers	
in the Mont-Blanc region	125
3. 6. 2. Groundwaters from carbonate karst aquifers	125
3. 6. 3. Groundwaters from evaporite rocks in the Swiss Rhone valley	125
3. 6. 4. Groundwaters from molasse aquifers	126
3. 6. 5. Groundwaters from flysch aquifers	126
3. 6. 6. Conclusions	127

IV. CHEMICAL WEATHERING OF BURDIGALIAN SANDSTONE:

SOURCES AND BEHAVIOUR OF CHROMIUM 129

4. 1. Introduction	130
4. 1. 1. Selection of the study site	130
4. 1. 2. Previous studies and data	131
4. 2. Hydrogeologic setting	133
4. 2. 1. Localisation of the study site	133
4. 2. 2. Geological background	136
Soil	136
Bedrock sandstone	137
Origin of the detrital material.....	138
4. 2. 3. Hydrogeology	140
4. 3. Weathering of the Burdigalian sandstone	142

4. 3. 1. Mineralogy	142
4. 3. 2. Geochemistry	146
4. 4. Chromium in the Burdigalian sandstone	149
4. 4. 1. Primary Cr-minerals	149
4. 4. 2. Secondary Cr-minerals	150
4. 4. 3. Summary	152
4. 5. Hydrochemistry	153
4. 5. 1. Water compositions	153
Rainwater and throughfall solution.....	153
Soil solutions.....	154
Groundwater	155
4. 5. 2. Chromium as geogenic tracer	162
4. 5. 3. Chemical evolution of the Lutry springwater	163
Major elements.....	166
Trace elements	168
Mass balance calculations.....	168
4. 6. Geochemistry of chromium	172
4. 6. 1. Natural and anthropogenic sources of chromium	172
4. 6. 2. Toxicology	173
4. 6. 3. Aqueous geochemistry of chromium	173
Oxidation-reduction reactions.....	173
Speciation.....	174
Solubility of chromium compounds.....	175
Adsorption and complexation	176
Summary	176
4. 6. 4. Chromium in groundwater from the Burdigalian sandstone	177
4. 7. Leaching experiments	181
4. 7. 1. Substratum	181
4. 7. 2. Experimental method	183
Column characteristics.....	186
Experimental artefacts	187
4. 7. 3. Results	190
4. 7. 4. Conclusions	195

V. SUMMARY AND CONCLUSIONS 197

5. 1. Creation of a groundwater database	198
5. 2. Definition of an aquifer typology	199
5. 2. 1. Hydrochemical characteristics of recent groundwaters from the different aquifer types	200
Physical-chemical parameters.....	200

Major and trace elements	200
5. 2. 2. Groundwater quality	202
5. 3. Identification of the leaching processes of Cr from a molasse sandstone	202
5. 3. 1. Field study	202
5. 3. 2. Leaching experiments	203
5. 4. Applicability of the groundwater typology	203
5. 5. Further research	207

List of Figures

Figure 1-1:	The flow path of groundwater is important for the evaluation of the impact of underground construction on groundwater resources. If the water discharged in the tunnel spring in the example comes from formation 1, then the consequences of a lowering of the water table are limited to the tunnel itself and the water can be drained. On the other hand, if the water comes from formation 2, the spring used for drinking water supply will run dry and measures are needed to prevent this (e.g. sealing of the tunnel).....	2
Figure 1-2:	Porosity types (after Hölting, 1992). Dark = porosity, light = rock.....	6
Figure 1-3:	Groundwater is part of the global hydrologic cycle. Along its flow path through soil and aquifer the chemical composition of groundwater evolves by interacting with soil and aquifer materials.....	8
Figure 2-1:	Size spectrum of water-borne particles (after Stumm, 1977).	25
Figure 2-2:	Results of the filtration test. Filtered and non-filtered samples from the Lutry (LRY) and the Pierre-Ozaire (POZ) springs in the molasse sediments, as well as samples from the Brocard spring (BRO) in the crystalline at low (4.2.1999) and high water period (26.5.1999) are compared. A HAWP filter membrane with 0.45 μ mesh diameter was used.	27
Figure 2-3:	Correlation plot of Sc analysed with a standard ICP-MS system and Si, revealing spectral interference.	30
Figure 2-4:	Comparison of duplicate iodine analyses made on the same samples suggesting a systematic but not uniform overestimation due analytical artefacts in analyses performed before 1994.	31
Figure 2-5:	Structure of the AQUITYP DataBase.....	39
Figure 2-6:	Data sheet of the AQUITYP DataBase (print model).	40
Figure 3-1:	AQUITYP spatial observation network with locations of sampling sites in and around Switzerland.	44
Figure 3-2:	Lithologic diagram of the molasse (after Matter and others, 1980).	55
Figure 3-3:	Piper-diagram showing the average chemistry of recent groundwaters from the granite and gneiss of the Mont-Blanc and Aiguilles-Rouges massifs (milliequivalents normalised to 100%). Granite: open rhombs, gneiss: crosses.	61
Figure 3-4:	Fluorite saturation state of the different water types occurring in the granite and gneiss of the Mont-Blanc and Aiguilles-Rouges massifs compared to the average F^- activity (GW = groundwaters).....	65

Figure 3-5:	Average molar $\text{Na}^+/\text{Ca}^{2+}$ ratios in the groundwaters from the Mont-Blanc and Aiguilles-Rouges massifs, in granitoid rocks and plagioclase, as well as average molar alkalinity/ Ca^{2+} ratios in these groundwaters. Plag An 20% = plagioclase with 20% anorthite component, i.e. with a Na/Ca ratio of 4; Plag An 80% = plagioclase with 80% anorthite component, i.e. with a Na/Ca ratio of 0.25.	65
Figure 3-6:	Piper-diagram depicting the distribution of the average groundwater chemistry in the investigated carbonate aquifers (milliequivalents normalised to 100%).	70
Figure 3-7:	Calcite and dolomite saturation state of the investigated carbonate karst groundwaters compared to average Ca^{2+} and Mg^{2+} activities and water temperature (for marked springs see table 3-15).	73
Figure 3-8:	Average molar alkalinity/ Ca^{2+} ratios in groundwaters of the different water types occurring in carbonate aquifers (after Dematteis, 1995; for marked springs see table 3-15).	75
Figure 3-9:	Average Ca^{2+} activities in carbonate karst groundwaters and calculated solubilities of calcite and dolomite in pure water (constant $P_{\text{CO}_2} = 10^{-2}$) as a function of water temperature (for marked springs see table 3-15).....	76
Figure 3-10:	A plot of average HCO_3^- concentrations versus pH in the investigated carbonate karst springwaters. Dashed lines indicate the evolution of groundwater composition towards equilibrium with calcite or dolomite in the case of a system open to CO_2 ($P_{\text{CO}_2} = \text{constant}$) or closed with respect to CO_2 (no CO_2 added). Solid lines indicate equilibrium with calcite and dolomite (after Langmuir, 1971).	77
Figure 3-11:	Saturation state of barite compared to average SO_4^{2-} and Ba^{2+} activities in the carbonate karst groundwaters (for marked springs see table 3-15).	80
Figure 3-12:	Comparison of average Sr^{2+} and SO_4^{2-} contents in evaporite groundwaters. .	81
Figure 3-13:	Piper-diagram showing the average chemistry of the investigated evaporite groundwaters (milliequivalents normalised to 100%).	82
Figure 3-14:	Saturation state of the investigated evaporite groundwaters with respect to gypsum, calcite, dolomite, celestite and barite compared to average SO_4^{2-} activities (see table 3-17 for marked groundwaters).....	88
Figure 3-15:	Comparison of average dissolved concentrations of Ca^{2+} , Mg^{2+} and SO_4^{2-} for the investigated evaporite groundwaters (see table 3-17 for marked groundwaters). Full lines indicate expected trends when groundwater is in exact equilibrium with calcite and dolomite, and dashed lines when $\text{SI}_{\text{calcite}} = 0.5$ (relation 3.12). Modified after Appelo and Postma, 1996.	89
Figure 3-16:	Piper-diagram showing the distribution of the average groundwater chemistry in the investigated molasse aquifers in Switzerland and neighbouring France,	

	Germany and Austria (milliequivalents normalised to 100%). Molasse groundwaters: open circles. Special cases: groundwaters from the "Glimmersand" molasse: grey squares; groundwaters from the "Gypsum-bearing Molasse": black triangles.	91
Figure 3-17:	Example of the relation between aquifer lithology and trace element contents in the corresponding groundwaters (after Hesske, 1995). AM = Autochthonous molasse; SM = Subalpine molasse.	93
Figure 3-18:	Calcite and dolomite saturation state of recent molasse groundwaters compared to average Ca^{2+} and Mg^{2+} activities (for marked groundwaters see table 3-21).	95
Figure 3-19:	Average molar alkalinity/ Ca^{2+} ratios in the investigated molasse groundwaters.	97
Figure 3-20:	The comparison of average Mg, Na, and silica concentrations in flysch groundwaters from natural springs and from springs in the Arnon tunnel shows that the tunnel springwaters are more evolved than the subsurface groundwaters discharged in natural springs.	99
Figure 3-21:	Piper-diagram showing the distribution of the average groundwater chemistry in the investigated flysch aquifers in the Niesen and Gurnigel nappes (milliequivalents normalised to 100%).	99
Figure 3-22:	Calcite and dolomite saturation state of recent flysch groundwaters compared to average Ca^{2+} and Mg^{2+} activities.	102
Figure 3-23:	Average molar alkalinity/ Ca^{2+} ratios in the flysch groundwaters.	104
Figure 3-24:	Average molar Na^+/Cl^- ratios in the investigated flysch groundwaters compared to precipitation. The arrow indicates the evolution of the Na^+/Cl^- ratios in the groundwaters resulting from ion exchange.	104
Figure 3-25:	Saturation state of recent flysch groundwaters with respect to barite and Fe-hydroxide compared to average Ba^{2+} activities and total Fe content, respectively.	105
Figure 3-26:	Relations between water temperature, altitude of the sampling site, and groundwater mineralisation.	108
Figure 3-27:	Ranges of pH and E_H conditions in the investigated groundwaters and precipitation waters in the stability field of water.	108
Figure 3-28:	Schoeller plot showing the median major element compositions of the groundwaters from the different aquifer types.	110
Figure 3-29:	Box plots comparing major element concentrations and their ranges in the groundwaters from the different aquifer types (see table 3-26). The boxes show the inter quartile range (25 th percentile to 75 th percentile) and median	

	values (the line through the middle of the box). The whiskers extend from the 10 th percentile to the 90 th percentile. The black point displays the arithmetic mean. Outliers (lower than 10 th percentile or higher than the 90 th percentile) are not plotted.	111
Figure 3-30:	Piper-diagram illustrating the distribution of the major element compositions in each of the five investigated aquifer types (milliequivalents normalised to 100%)......	112
Figure 3-31:	Ca ²⁺ concentrations in the groundwaters from different aquifer types compared to total amounts of dissolved solids (A) and alkalinity (B).	113
Figure 3-32:	Comparison of the fluorite solubility in Ca ²⁺ -poor groundwaters (e.g. from crystalline rocks) and in Ca ²⁺ -rich groundwaters (e.g. from evaporite rocks). Plotted values are activities.	114
Figure 3-33:	Box plots showing natural concentration ranges of alkali and earth-alkali trace elements, as well as halides and non-metal trace elements in groundwaters from the different aquifer types (see table 3-27). The boxes show the inter quartile range (25 th percentile to 75 th percentile) and median values (the line through the middle of the box). The whiskers extend from the 10 th percentile to the 90 th percentile and the black point displays the arithmetic mean. Outliers (lower than 10 th percentile or higher than the 90 th percentile) are not plotted. D.L. = detection limit, values below are qualitative; if no D.L. is indicated on the plot, it is below the measured concentrations. Q = quality target values and L = intervention values for drinking water in Switzerland.	116
Figure 3-34:	Box plots illustrating natural concentration ranges of metal trace elements in groundwaters from the different investigated aquifer types (see also table 3-27)......	117
Figure 3-35:	Comparison of dissolved Mo and U in the groundwaters from the different aquifer types.	120
Figure 3-36:	Comparison of the calculated barite solubility in SO ₄ ²⁻ -poor groundwaters and in SO ₄ ²⁻ - rich groundwaters such as those found in evaporite rocks. Plotted values are activities.....	121
Figure 4-1:	Geographic and tectonic situation (after Weidmann, 1988)......	133
Figure 4-2:	Close-up map showing the locations of the Lutry spring (LRY, coordinates 544'620 / 157'350) and the Pierre-Ozaire spring (POZ, coordinates 544'860 / 156'690), and the approximate extension of the catchments.	135
Figure 4-3:	Lutry catchment:schematic profile through soil and bedrock sandstone....	136
Figure 4-4:	Colour variations of the OMM sandstone according to its alteration state. The springs emerge in the yellow parts of the sandstone, usually on top of impermeable marl beds. The sandstone which is not in direct contact with	

	oxygenated groundwater remains in the reduced state displayed by its bluish colour.	138
Figure 4-5:	Origin of diagnostic heavy minerals such as hornblende, serpentine and pumpellyite occurring in the Burdigalian sandstone in western Switzerland (after Allen, 1985).....	139
Figure 4-6:	Discharge hydrographs of the Lutry (LRY) and Pierre-Ozaire (POZ) springs (example 1997), compared to daily precipitation at Villars-Tiercelin (SMA meteorologic station, altitude 850 m), as well as water temperature and electric conductivity (E.C.).	140
Figure 4-7:	Relative amounts of main and clay minerals in a depth profile through the soil and in different varieties of the bedrock sandstone. Mineralogic data of soil (abbreviations see table 4-2) and the bedrock samples RM90 to RM92 are from Dalla Piazza, 1996.....	142
Figure 4-8:	Corroded chromite grain (picture width 87 μm).	144
Figure 4-9:	Strongly corroded Cr-bearing pyroxene grain (picture width 43 μm).	144
Figure 4-10:	Exfoliated and chloritised biotite flake (picture width 87 μm).	144
Figure 4-11:	Typical aggregate of weathered glauconite (picture width 87 μm).	144
Figure 4-12:	Corroded quartz grain (picture width 87 μm).	145
Figure 4-13:	Relatively fresh muscovite grain (picture width 580 μm).	145
Figure 4-14:	Corroded plagioclase grain (picture width 87 μm).	145
Figure 4-15:	Slightly corroded K-feldspar grain (picture width 87 μm).	145
Figure 4-16:	Major element composition along a compiled depth profile through the soil and bedrock sandstone. Chemical data from the soil and partly from the bedrock are from Dalla Piazza (1996) and Hesske (1995).	146
Figure 4-17:	Major and trace element composition along a compiled depth profile through the soil and bedrock sandstone. Chemical data from the soil and partly from the bedrock are from Dalla Piazza (1996) and Hesske (1995).	147
Figure 4-18:	Comparison of the Na^+/Cl^- ratios in the precipitation at the Lutry site with the ratio of sea water.	154
Figure 4-19:	Lutry springwater: Time series of discharge, total mineralisation (TDS), total hardness, water temperature, pH and E_{H}	158
Figure 4-20:	Lutry springwater: Time series of major elements.	159

Figure 4-21: Pierre-Ozaire spring: Time series of discharge, total mineralisation (TDS), total hardness, water temperature, pH and E_H	160
Figure 4-22: Pierre-Ozaire springwater: Time series of major elements.	161
Figure 4-23: Time variation of the Cr concentration in the Lutry and Pierre-Ozaire springwaters.....	162
Figure 4-24: Distribution of dissolved major and trace elements and saturation state from rainwater to groundwater (data see table 4-6).	165
Figure 4-25: Evolution of the major element composition from rainwater to groundwater. Chemical data of rainwater, throughfall and soil solutions are from Atteia (1992).....	166
Figure 4-26: Areas of dominance of aqueous inorganic Cr hydrolysis species at equilibrium in the system $Cr + H_2O + O_2$ at standard state conditions (Ball and Nordstrom, 1998). The hatched area indicates the predominance region of $Cr(OH)_{3(cr)}$ at $[Cr_{tot}] = 10^{-6}$ M (i.e. 52 $\mu g/L$).....	175
Figure 4-27: Qualitative influence of the solution pH on different processes influencing the mobility of Cr.	177
Figure 4-28: Evolution of the dissolved Cr concentration and the saturation state with amorphous Cr-hydroxide from rainwater to groundwater.....	177
Figure 4-29: Evolution from rainwater to groundwater of the dissolved Fe and Mn concentrations and saturation states with amorphous Fe-hydroxide and manganite.....	178
Figure 4-30: pH and redox conditions of the average soil solutions and groundwater of the Lutry site plotted in the pH-EH diagram for Cr (after Ball and Nordstrom, 1998; see figure 4-26).....	180
Figure 4-31: Results of speciation calculations of dissolved Cr in soil solution and groundwater.	180
Figure 4-32: Grain-size distribution of the reduced and oxidised sandstone used in the leaching experiments determined by dry sieving.	182
Figure 4-33: Experimental setup.	185
Figure 4-34: Results of a bank-test using the same experimental setup and measuring electrodes as in the leaching experiments but without substratum indicating K and Cl input from the pH-electrode.	188
Figure 4-35: Contamination with KCl from the pH electrode occurring in the leaching experiments with reduced and oxidised sandstone.....	188

Figure 4-36: Decrease of the redox potential resulting from the presence of oxygen consuming micro-organisms..... 189

Figure 4-37: Evolution of the flow rate with time, showing that a fairly constant flow rate has been attained by using a HPLC pump. 189

Figure 4-38: Estimated volume of solution and electric conductivity measured during the experiments. The evolution of these two parameters suggests that the step-wise increase of the electric conductivity is due to the losses of solution which occurred in the pump..... 190

Figure 4-39: Evolution of the P_{CO_2} and pH, and of the alkalinity, Ca^{2+} , and Mg^{2+} concentrations in the solutions from the leaching experiments, as well as their saturation states with respect to calcite and dolomite..... 193

Figure 4-40: Evolution of pH and Cr and Fe concentrations in the solutions from the leaching experiments, as well as their saturation states with respect to amorphous Cr- and Fe-hydroxide. 194

List of Tables

Table 1-1:	Principal aquifer types in the alpine region and their typical hydrogeologic characteristics.	7
Table 1-2:	Mean chemical weathering rates of some common minerals determined in the laboratory at standard state conditions (25°C, 1 bar) and a pH of 5.	11
Table 1-3:	Cation exchange capacities (CEC) of common soil and aquifer minerals (from Appelo & Postma, 1996).	13
Table 1-4:	pH _{PZNPC} values of common soil and aquifer minerals (from Appelo & Postma, 1996).	14
Table 1-5:	Approximate selectivity coefficients for different ions I with a charge i, with respect to Na ⁺ based on the Gaines-Thomas convention (from Appelo & Postma, 1996). β is the equivalent fraction of adsorbed ions. A range is given when many measurements in different soils or for different clay minerals are available.	15
Table 2-1:	Overview of analytical equipment and water sample treatment applied in the AQUITYP project. Analyses were made in the laboratory if not specified otherwise. Authors: 1: Dubois, 1993; 2: Mandia, 1993; 3: Basabe, 1993; 4: Dematteis, 1995; 5: Hesske, 1995; 6: GEOLEP. Abbreviations: a: Wissenschaftlich Technische Werkstätten GmbH, Weilheim, Germany; b: liquid ion chromatography; c: atomic absorption spectro-photometry / flame emission spectro-photometry; d: high pressure liquid ion chromatography; e: inductively coupled plasma source mass spectrometry; f: high resolution inductively coupled plasma source mass spectrometry. .	21
Table 2-2:	Overview of the evolution of chemical analytical methods applied by the different authors. Analyses were made in the laboratory if not specified otherwise. Authors: 1: Dubois, 1993; 2: Mandia, 1993; 3: Basabe, 1993; 4: Dematteis, 1995; 5: Hesske, 1995; 6: GEOLEP. a: long-term monitoring network, samples analysed before 1997; b: samples analysed after 1997. .	22
Table 2-3:	Trace elements analysed by the previous researchers.	28
Table 2-4:	Current major and minor elements analytical methods.	28
Table 2-5:	Field measurements: overview of analytical methods used in the AQUITYP project, their application range and accuracy, potential sampling- and analytical problems, as well as a general evaluation of the data produced by the respective methods.	33
Table 2-6:	Major and minor elements: analytical methods used in the AQUITYP project, their equipment-related detection limits and accuracy, potential sampling and	

	analytical problems, as well as a general evaluation of the data produced by the respective methods.	34
Table 2-7:	Trace elements 1: Analytical methods used in the AQUITYP project, their equipment-related detection limits and accuracy, potential sampling and analytical problems, as well as a general evaluation of the data produced by the respective methods.	36
Table 2-8:	Trace elements 2: Analytical methods used in the AQUITYP project, their equipment-related detection limits and accuracy, potential sampling and analytical problems, as well as a general evaluation of the data produced by the respective methods.	37
Table 3-1:	Data base used for the typology of recent groundwaters.	43
Table 3-2:	Common hydrothermal minerals occurring in the Mont-Blanc and Aiguilles-Rouges massifs (based on the review by Dubois, 1993).	46
Table 3-3:	Time variations of discharge (Q), water temperature (T), and total mineralisation (TDS) of seven selected springs in granite and gneiss units of the Mont-Blanc and Aiguilles-Rouges massifs, observed over a time span of 2 to 14 years (Dubois, 1993).	47
Table 3-4:	Locations of studied carbonate karst regions (after Dematteis, 1995).	48
Table 3-5:	Carbonate rocks in the investigated regions (geographic region numbers refer to table 3-4; after Dematteis, 1995): Lithostratigraphic units, age, predominant sedimentary environment (P = carbonate platform, L = lagoon, R = reef, S = continental slope, B = deep-sea basin) and predominant rock types (LS = limestone, LS-M = marly limestone, LS-D = dolomitic limestone, D = dolostone, E = evaporite minerals, mainly gypsum).	49
Table 3-6:	Time variations of discharge (Q), water temperature (T), and total mineralisation (TDS) of three selected karst springs in Switzerland (data from 1982 to 1996).	50
Table 3-7:	Common minerals occurring in the Triassic rocks of the Swiss Rhone basin (Mandia, 1993 and references therein).	52
Table 3-8:	Time variations of discharge (Q), water temperature (T), and total mineralisation (TDS) of twelve selected evaporite springs observed over 2 to 14 years (Mandia, 1993).	53
Table 3-9:	Time variations of discharge (Q), water temperature (T), and total mineralisation (TDS) of three selected molasse springs in Switzerland (data from 1982 to 1996).	56
Table 3-10:	Time variations of discharge (Q), water temperature (T), and total mineralisation (TDS) of nine selected Flysch springs (data from 1982 to 1996; Basabe, 1993).	58

Table 3-11:	Chemical composition of recent groundwaters in granite and gneiss aquifers in the Mont-Blanc and Aiguilles Rouges Massifs (- = not analysed; data from Dubois, 1993).	62
Table 3-12:	Average chemical compositions and saturation states with respect to selected minerals of precipitation water and eight springwaters from granite and gneiss of the Mont-Blanc and Aiguilles-Rouges Massifs. n.d. = not detected; - = not analysed. The “EMOW/71” and “EMOE/84” springs discharge the least mineralised gneiss- and granite-derived groundwater, respectively. The other springs discharge the most mineralised groundwaters of the corresponding water types.	64
Table 3-13:	NETPATH results: Amounts of minerals weathered from infiltration to discharge in mmol per kg H ₂ O. Positive values indicate dissolution, negative values indicate precipitation of the corresponding mineral phase.	68
Table 3-14:	Chemical composition of the investigated carbonate karst groundwaters (data from Dematteis, 1995. - = not analysed).	72
Table 3-15:	Average chemical composition and saturation states with respect to selected minerals of four carbonate karst waters (region numbers refer to table 3-4) and precipitation water from two sites in Switzerland. n.d. = not detected; - = not analysed. The “SA2” spring discharges the least mineralised groundwater, while the other springs discharge the most mineralised groundwaters of the corresponding water types.	74
Table 3-16:	Chemical composition of recent groundwaters from evaporite aquifers in the Swiss Rhone basin (data from Mandia, 1993).	83
Table 3-17:	Average chemical composition and saturation states with respect to selected minerals of precipitation and two evaporite springwaters. n.d. = not detected. The “FEY” and “QUE” springs discharge the least mineralised groundwater and one of the most mineralised groundwaters, respectively.	85
Table 3-18:	NETPATH results: Amounts of minerals weathered from infiltration to discharge in mmol per kg H ₂ O. Positive values indicate dissolution, negative values indicate precipitation of the corresponding mineral phase (for composition of selected groundwaters see table 3-17).	87
Table 3-19:	Average concentrations of Mn, Cu, and Ni, percentages of the most abundant corresponding species, and saturation state with possible secondary minerals in the least mineralised (FEY, pH = 7.4) and most mineralised evaporite groundwater (QUE, pH= 7.0). A pe of 7.00 has been assumed for the calculations. (See table 3-17 for compositions of the selected groundwaters, n.d. = not detected).	90
Table 3-20:	Chemical composition of recent groundwaters from molasse aquifers in Switzerland and neighbouring France, Germany and Austria (data from Hesske, 1995).	94

Table 3-21:	Chemical composition and saturation states with respect to selected minerals of four molasse springwaters and precipitation. n.d. = not detected; - = not analysed. The “69b” spring discharges the least mineralised, and the “124b” spring the most mineralised molasse groundwater, respectively. The “109b” and “148c” springs discharge the most mineralised groundwaters from the “Glimmersand” and “Gypsum-bearing Molasse”.96
Table 3-22:	Chemical composition of recent groundwaters from the investigated flysch aquifers in the Niesen and Gurnigel nappes (data from Basabe, 1993).101
Table 3-23:	Chemical composition and saturation states with respect to selected minerals of two flysch springwaters and precipitation. n.d. = not detected; - = not analysed. The “RN” spring discharges the least mineralised, and the “TF” spring the most mineralised groundwater, respectively.103
Table 3-24:	Mineralogy of the different aquifer types.106
Table 3-25:	Physical-chemical parameters of recent groundwaters from different aquifer types (median values and the number of samples). CRY = crystalline, CARB = carbonates, EVAP = evaporites, MOL = molasse, FLY = flysch. ...107
Table 3-26:	Comparison of major element concentrations in recent groundwaters from the different aquifer types (median values and number of samples). CRY = crystalline, CARB = carbonates, EVAP = evaporites, MOL = molasse, FLY = flysch.110
Table 3-27:	Median concentrations of trace elements in recent groundwaters from the different aquifer types (median values and number of samples). CRY = crystalline, CARB = carbonates, EVAP = evaporites, MOL = molasse, FLY = flysch. - = not analysed. Note that Li and B analyses for crystalline and evaporite groundwaters have higher detection limits (see page 35).115
Table 3-28:	Swiss drinking water standards and WHO recommendations.123
Table 3-29:	Comparison of groundwaters from different aquifer types to Swiss drinking-water standards. Given are the percentages of groundwaters with concentrations of specific elements above the limit and above or below the quality target value.124
Table 4-1:	Chromium concentrations in groundwaters from different aquifer types (median, minimum and maximum values, and number of springs). Mol = molasse groundwaters in general and OMM W-CH = groundwaters from OMM sandstone in western Switzerland (Hesske, 1995); Mafic = groundwaters from mafic rocks and Ultram = groundwaters from ultramafic rocks (Derron, 1999); Fly = flysch groundwaters (Basabe, 1993); Evap = evaporite groundwaters (Mandia, 1993); Carb = carbonate karst groundwaters (Dematteis, 1995).131
Table 4-2:	Description of the soil layers in a typical profile in the Lutry catchment (after Dalla Piazza, 1996).137

Table 4-3:	Primary (detrital and diagenetic) and secondary minerals (authigenic weathering products formed due to the alteration of the sandstone by the infiltrating rain water) constituting the OMM sandstone and soil at the study site and their properties as potential Cr-sources or Cr-sinks.	151
Table 4-4:	Compositions of rain water, throughfall solution, and soil solutions at the Lutry site (Atteia, 1992; n.d. = not detected).	155
Table 4-5:	Chemical compositions of the Lutry and Pierre-Ozaire springwaters (n.d. = not detected).	157
Table 4-6:	Median chemical compositions and saturation states with respect to selected minerals of rainwater, throughfall, soil solutions (data from 1990-1991; Atteia, 1992) and springwater (sampling period 1981 to 2001, median values, high water and low water periods). Concentrations are in $\mu\text{mol/L}$. n.d. = not detected; n.a. = not analysed.	164
Table 4-7:	Compositions of the initial and final solutions used in the mass balance calculations.	169
Table 4-8:	Six different models obtained by NETPATH mass balance calculations using different mineral assemblages. Amounts of mass transfer of dissolving (positive) and precipitating (negative) mineral phases are given in $\mu\text{mol/kg H}_2\text{O}$; n.c. = not considered.	170
Table 4-9:	Average Cr-concentrations in different rock types and in water.	172
Table 4-10:	Main aqueous Cr-species in natural groundwaters.	175
Table 4-11:	Bulk mineralogy (weight%) and clay mineralogy (relative amounts in percent) of the sandstones used in the leaching experiments determined by X-ray diffraction analysis. The values in brackets are qualitative.	183
Table 4-12:	Column characteristics: results of four tracer experiments.	187
Table 4-13:	Chemical composition of the solution sampled during the leaching experiment with the reduced sandstone (n.d. = not detected; n.a = not analysed).	191
Table 4-14:	Chemical composition of the solution sampled during the leaching experiment with the oxidised sandstone (n.d. = not detected; n.a = not analysed).	192
Table 5-1:	Potential sources and solubility limiting processes for geogenic tracer elements at the given conditions reigning in the investigated recent groundwaters, i.e. at temperatures below 20°C , oxidising conditions, near-neutral pH, and typical element concentrations.	206

List of Appendices

<i>Appendix A:</i>	<i>Median Chemical Composition of Precipitation Water</i>	<i>229</i>
<i>Appendix B:</i>	<i>Groundwater Composition in Different Aquifer Types</i>	<i>231</i>
<i>Appendix C:</i>	<i>Chemical Groundwater Classification</i>	<i>245</i>
<i>Appendix D:</i>	<i>Lutry Site: Porosity and Specific Permeability of Bedrock Sandstone Samples</i>	<i>249</i>
<i>Appendix E:</i>	<i>Lutry Site: Mineralogical Composition of Bedrock and Soil</i>	<i>251</i>
<i>Appendix F:</i>	<i>Lutry Site: Chemical Composition of Bedrock and Soil</i>	<i>253</i>

A key problem in environmental science and in engineering geology is the often incomplete understanding of the origin of dissolved components in groundwater. The dissolved contents of trace elements in groundwater are of special importance for groundwater quality control. The AQUITYP project aims to establish a detailed typology of recent groundwaters based on their geogenic trace element compositions, and to derive a so-called "geo-reference" for groundwaters from five principal aquifer lithologies in the Alpine belt. This geo-reference provides a database for investigations related to groundwater contamination, groundwater resources management and engineering geology. Groundwaters from crystalline, carbonate, and evaporite rocks, as well as molasse and flysch sediments in Switzerland and in neighbouring countries were sampled and documented by previous researchers (Dubois, 1993; Dematteis, 1995; Mandia, 1993; Hesske, 1995; Basabe, 1993). Based on a statistical analysis of the data and examination of the relationship between aquifer lithology and chemical groundwater composition these researchers identified a number of characteristic tracer elements (geogenic tracers).

The present study includes (1) a synthesis of the hydrogeology and the hydrochemistry of recent groundwaters in these five aquifer types based on groundwater data acquired within the AQUITYP project, and (2) a hydro-geochemical investigation of the origin and chemical behaviour of the geogenic tracer chromium, based on a comprehensive field and laboratory study.

To enable a comparison of the chemical groundwater data gathered and analysed over a time span of 20 years, a rigorous quality control of the entire database was made. An assessment was made of the sampling techniques, the sample treatment and the analytical methods applied in the AQUITYP project since 1981. Different tests were carried out to evaluate the quality and comparability of the data, including geochemical model calculations, comparison of different analytical techniques, and tests to estimate the influence of the filtration procedure. In order to make this large number of quality controlled data accessible also for future investigations, a groundwater data storage system was developed (*AQUITYP-DataBase*).

1.) Typology of recent groundwaters

In the synthesis of groundwater hydrochemistry, the emphasis was laid on the hydro-geochemical evolution leading to the characteristic groundwater composition in each of the five aquifer types. Chemical characteristics and differences between the groundwaters from the different aquifer types were identified and natural concentration ranges for each aquifer type derived. The proposed geogenic tracers were evaluated and the potential sources of these tracers identified. The dominant processes leading to the typical mineralisation of recent groundwaters were investigated using geochemical modelling strategies. Finally, the concentrations of chemical elements in the groundwaters from the different aquifer types were compared to the Swiss drinking water standards in order to assess the quality of the investigated groundwaters. It has been found that each rock type contributes in a characteristic way to the major and trace element composition of the corresponding groundwater:

The groundwaters derived from the **crystalline** Mont-Blanc and Aiguilles-Rouges massifs are characterised by a low total mineralisation (TDS 22 to 158 mg/L) dominated by

Ca²⁺, Na⁺, Mg²⁺, alkalinity, SO₄²⁻, and F⁻ (Ca-Na-HCO₃-SO₄ waters). Elevated amounts of Mo, U, W, and As occur. These groundwaters derive their mineralisation mainly from the interaction with hydrothermal minerals present along fractures. Fractures act as major groundwater flow paths. Minerals relevant for groundwater mineralisation include carbonates (Ca²⁺, Mg²⁺, HCO₃⁻), clay minerals (Ca-Na ion exchange), fluorite (F⁻, Ca²⁺), Fe-, As-, and Mo-sulphides (SO₄²⁻, As, Mo), and U- and W-minerals (U, W). In these crystalline groundwaters the natural concentrations of F⁻ (23% of the investigated springs) and As (7%) exceed the Swiss limits for drinking water. In addition, the WHO guideline values for U are exceeded in 65% of the cases and for Mo in 15% of the cases.

The **carbonate karst** groundwaters obtain their low to intermediate mineralisation (TDS 161 to 547 mg/L) from the dissolution of calcite (Ca-HCO₃ waters), as well as in certain regions dolomite (Ca-Mg-HCO₃ waters) and gypsum (Ca-Mg-HCO₃-SO₄ waters). Together with their very short residence times, the carbonate karst groundwaters generally contain very low trace element contents. Nevertheless, geogenic trace elements occur in specific regions in relation with fossil organic matter (I, V) and accessory minerals such as barite in deep sea limestones (Ba), evaporite minerals (gypsum, celestite: Sr, Li), clay- and Fe-minerals (V), and Mo-sulphides and U-minerals in dolomitic limestones (Mo, U). In 18% of the carbonate karst springs atmospheric derived Pb exceeds the Swiss drinking water quality target value.

The groundwaters from Triassic **evaporites** in the Swiss Rhone basin are characterised by a high total mineralisation (TDS 760 to 2788 mg/L) expressed by elevated amounts of Ca²⁺, Mg²⁺, Sr²⁺, SO₄²⁻, and alkalinity (Ca-Mg-SO₄-HCO₃ waters). Elevated amounts of the trace elements Mn, Ni, Cu, Li, Rb, Y, and Cd occur. The hydrochemical evolution of these groundwaters is governed by incipient dedolomitisation, involving dissolution of gypsum, celestite and dolomite and simultaneous precipitation of calcite. The Na⁺ and K⁺ contents probably controlled by ion-exchange reactions on clay minerals. Characteristic trace elements originate mainly from the dissolution of dolomite (Mn, Ni) and small amounts of apatite (Y, Cd), and from the oxidation of sulphide minerals (Cu, Ni, Cd). The elevated concentrations of the highly soluble Li and Rb may be related to brine inclusions in evaporite minerals and eventually to clay minerals. These evaporite groundwaters contain SO₄²⁻ concentrations exceeding the Swiss quality target for drinking water in all springs, and the concentrations of U and Ni exceed the WHO guideline values in respectively 58% and 2% of the cases. In addition, Mn, Cd, and As concentrations exceed the Swiss quality targets in respectively 11%, 10%, and 7% of the investigated springs.

Recent groundwaters circulating in the porous and fissured **molasse** sandstones and conglomerates acquire their intermediate mineralisation (TDS 48 to 714 mg/L) primarily by dissolution of calcite and minor dolomite (Ca-Mg-HCO₃ waters). The particular mineralogy of certain Molasse formations is reflected in specific trace element compositions of corresponding groundwaters: ophiolite detritus in OMM sandstones in western Switzerland (Cr), barite fracture mineralisations in subalpine and folded Molasse units (Ba), granitic detritus containing sulphides (Mo), U-minerals (U) and abundant mica (Li) in the “Glimmersand” (OSM, Ca-Mg-HCO₃-SO₄ waters), and evaporite minerals (Li, Sr), sulphides (Mo), and U-minerals (U) in the “Gypsum-bearing Molasse” (USM, highly mineralised Ca-Mg-SO₄-HCO₃ waters, TDS 984 to 1346 mg/L). In these molasse groundwaters the Swiss quality target values for drinking water of Cr and Pb are exceeded in 36% and 6% of the springs, respectively. The U concentrations of 14% of the molasse groundwaters (“Gypsum-bearing Molasse” and “Glimmersand”), exceed the WHO guideline value. The groundwaters from the “Gypsum-bearing Molasse” display similar quality problems as the evaporite groundwaters.

Groundwaters derived from the shallow **flysch** aquifers in the Niesen and Gurnigel nappes are poorly evolved Ca-(Mg)-HCO₃ waters. Their low to intermediate total mineralisation (TDS 160 to 459 mg/L) is acquired primarily by dissolution of calcite and to a lesser degree dolomite. The low trace element content is dominated by Ba originating from barite fracture mineralisations. The poor chemical evolution of recent flysch groundwaters results from (1) their short residence time in the fractured flysch rocks, and (2) the absence of readily dissolving minerals except carbonates and barite. In 32% of the flysch springs Pb derived from atmospheric sources exceeds the Swiss quality target value.

2.) Case study on the chemical weathering of molasse sandstone: Sources and chemical behaviour of Cr

For the characterisation of the potentially toxic tracer element Cr a comprehensive field study was carried out on a selected catchment (Lutry spring catchment near Lausanne) situated in a molasse sandstone (OMM, Burdigalian). The investigation of the processes controlling the dissolved Cr content in these groundwaters was based on the groundwater chemical data, as well as on mineralogical, geochemical, and hydrological data. Relic Cr-bearing spinel and pyroxene in the sandstone were identified to be the primary sources of Cr. An electron microscope study showed that in the Burdigalian sandstone and overlying soil these minerals are strongly weathered. The slow weathering of these minerals is the major Cr releasing process. Under the oxidising conditions reigning in the investigated groundwaters, Cr prevails in solution in its highly soluble and toxic hexavalent state (CrO₄²⁻). In this case, retention by secondary Cr-hydroxide phases does not occur, as can be shown by geochemical model calculations.

Laboratory leaching experiments were carried out with Burdigalian molasse sandstone from the field site, in order to support the field study findings and to quantify the processes responsible for the Cr mineralisation observed in the Lutry groundwater. Two experiments with mountain-wet oxidised and reduced sandstone were carried out over a time span of 2 months each, to obtain information about the influence of the oxidation state of the substratum on the mobilisation of Cr. The experiments clearly showed that the Cr-releasing processes are fast enough to explain the Cr contents found in the groundwater, and that the release of Cr into the groundwater depends on the weathering state of the sandstone. In the oxidised, Fe-hydroxide-coated sandstone, Cr is faster released into solution than in the less altered reduced sandstone. This indicates that the Cr contained in the reduced sandstone is in a more stable state, i.e. mainly incorporated in detrital minerals, while in the oxidised sandstone, the Cr is partly in a unstable state, i.e. adsorbed on the surface of secondary Fe-hydroxides, from where it is more easily leached.

Key words: natural groundwater composition, geogenic tracer elements, rock-water interaction, geochemical modelling, groundwater observation networks

Un problème clé des sciences de l'environnement ainsi que de la géologie de l'ingénieur réside dans le manque de connaissances sur l'origine des composants dissous dans les eaux souterraines. La qualité de ces eaux est fortement dépendante de leur composition en éléments traces dissous. Le projet AQUITYP a pour ambition d'établir une typologie des eaux souterraines récentes sur la base de leur composition géogène en éléments traces et d'en dégager une "géo-référence" pour les cinq principaux types d'aquifères de l'arc alpin. Une telle "géo-référence" servira comme base de données pour l'étude de sites contaminés et pour la gestion des ressources en eau. Des eaux souterraines provenant des roches cristallines, carbonatées et évaporites, ainsi que des sédiments de la molasse et du flysch, principalement en Suisse mais également dans les pays limitrophes, ont été échantillonnées et documentées par des recherches antérieures (Dubois, 1993; Dematteis, 1995; Mandia, 1993; Hesske, 1995; Basabe, 1993). Grâce à ces travaux de recherche des traceurs géogènes ont été proposés.

Dans cette étude, sont présentées (1) une synthèse de l'hydrogéologie et de l'hydrochimie des eaux souterraines récentes issues des cinq types d'aquifères basée sur les données acquises précédemment dans le cadre du projet AQUITYP et (2) une étude hydro-géochimique sur les origines et le comportement chimique du chrome en tant que traceur géogène, appuyée par des travaux de terrain et de laboratoire.

La comparaison des données concernant les eaux récoltées sur une période de vingt ans et pour lesquelles les méthodes d'analyse chimique ont évolué, a nécessité un contrôle préalable et rigoureux de la qualité de toute la banque de données. Les techniques d'échantillonnage, de traitement des échantillons et d'analyse utilisées tout au long du projet AQUITYP depuis 1981 ont été évaluées. Pour permettre de juger la qualité et la comparabilité des techniques d'analyses, différents tests ont été effectués. Afin de faciliter l'accès à ce grand nombre de données hydrochimiques vérifiées lors de future investigations, une base de données a été développée (*AQUITYP-DataBase*).

1.) Typologie des eaux souterraines récentes

L'analyse de l'évolution hydro-géochimique a été réalisée pour les eaux souterraines caractéristiques de chacun des 5 aquifères types. Les caractéristiques chimiques ont été analysées pour chaque type d'aquifère, puis comparées entre elles. Ce travail a conduit à la détermination des ordres de grandeur des concentrations naturelles en éléments minéraux dans les eaux souterraines de chaque aquifère type. La validité des traceurs géogènes proposés dans les travaux antérieurs a été vérifiée. On a également identifié les sources potentielles de ces traceurs pour chacune des formations aquifères. Une modélisation géochimique a permis de mettre en évidence les principaux processus contrôlant la composition chimique des eaux issues de chaque type d'aquifère. Enfin, pour chaque élément, les concentrations typiques de chaque aquifère ont été comparées aux normes suisses pour les eaux destinées à la consommation humaine, afin d'en estimer la qualité.

Les eaux souterraines provenant des massifs **cristallins** silicatés du Mont-Blanc et des Aiguilles-Rouges se caractérisent par un faible taux de minéralisation (TDS 22 à 158 mg/L), dominée par Ca^{2+} , Na^+ , Mg^{2+} , alcalinité, SO_4^{2-} , et F^- (eaux $\text{Ca-Na-HCO}_3\text{-SO}_4$). On note des concentrations élevées en Mo, U, W, et As. Ces signatures géochimiques proviennent essentiellement des interactions de l'eau avec les minéraux hydrothermaux

lorsqu'elle circule dans les fractures. Ces minéraux correspondent à des carbonates (Ca^{2+} , Mg^{2+} , HCO_3^-), des argiles (échange ionique Ca-Na), de la fluorite (F^- , Ca^{2+}), sulfures de Fe, As, et Mo (SO_4^{2-} , As, Mo), et des minéraux d'U et de W (U, W). Dans ces eaux souterraines d'origine cristalline, les concentrations naturelles en F^- (23% des sources analysées) et As (7%) sont supérieures aux normes suisses. De plus, les valeurs recommandées par l'OMS sont dépassées pour U (65%) et pour Mo (15%).

La minéralisation des eaux issues des **karsts carbonatés** est faible à moyenne (TDS 161 à 547 mg/L) et provient essentiellement de la calcite (eaux Ca- HCO_3) ou, dans certaines régions, de la dolomite (eaux Ca-Mg- HCO_3) et du gypse (eaux Ca-Mg- HCO_3 - SO_4). Les éléments traces sont présents en très faibles quantités, en raison du faible temps de résidence de l'eau dans le karst. Localement, on peut trouver des concentrations en traces géogènes de iode provenant de matières organiques fossiles; de Ba provenant de la barytine contenue dans les calcaires de mer profonde; de Sr et Li provenant de minéraux évaporitiques comme le gypse et la célestine; de V provenant des argiles et des minéraux du fer et, enfin, de Mo et U provenant des sulfures et minéraux uranifères contenus dans les calcaires dolomitiques. Dans 18% des sources karstiques analysées, les concentrations en Pb dépassent la norme suisse.

Les eaux souterraines échantillonnées dans les **roches évaporitiques** du Trias se caractérisent par un fort taux de minéralisation (TDS 760 à 2788 mg/L) provenant de concentrations élevées en Ca^{2+} , Mg^{2+} , Sr^{2+} , SO_4^{2-} , et de l'alcalinité (eaux Ca-Mg- SO_4 - HCO_3). On y trouve les éléments traces suivants en concentrations élevées: Mn, Ni, Cu, Li, Rb, Y, et Cd. La signature géochimique de ces eaux provient de la dédolomitisation des roches, qui correspond à la dissolution du gypse, de la célestite et de la dolomite, ainsi qu'à la précipitation simultanée de calcite. Les concentrations en Na^+ et K^+ y sont probablement contrôlées par des réactions d'échanges ioniques avec les argiles. On y trouve des éléments traces typiques de la dissolution de la dolomite (Mn, Ni) et de l'apatite (Y, Cd), ainsi que de l'oxydation de certains sulfures (Cu, Ni, Cd). Les concentrations élevées en Li et Rb proviennent probablement de la dissolution d'inclusions de saumure dans les minéraux évaporitiques ou d'argiles. Ces eaux sulfatées contiennent des SO_4^{2-} en concentrations qui excèdent l'objectif de qualité suisses dans toutes les sources testées. Les concentrations en U et Ni dépassent les valeurs recommandées par l'OMS dans 58%, respectivement 2% des cas. De plus, les concentrations en Mn, Cd et As dépassent l'objectif suisse de qualité dans respectivement 11%, 10% et 7% des sources.

Les eaux provenant des grès et des conglomérats de la **molasse** se caractérisent par un taux de minéralisation intermédiaire (TDS 48 à 714 mg/L) provenant essentiellement de la dissolution de la calcite et, de façon moins importante, de la dolomite (eaux Ca-Mg- HCO_3). La composition minéralogique caractéristique de certaines formations molassiques confère aux eaux une signature particulière en éléments traces. C'est le cas des ophiolites détritiques contenus dans les grès de l'OMM en Suisse occidentale (Cr); des minéralisations de barytine dans les fractures dans les unités de la Molasse subalpine (Ba); des granites détritiques contenant des sulfures (Mo), des minéraux uranifères (U) et d'abondants micas (Li) dans la molasse du "Glimmersand" (OSM, eaux Ca-Mg- HCO_3 - SO_4); des minéraux évaporitiques (Li, Sr), des sulfures (Mo) et des minéraux uranifères (U) de la "Molasse à gypse" (USM, eaux fortement minéralisées de type Ca-Mg- SO_4 - HCO_3 , TDS 984 à 1346 mg/L). Dans ces eaux souterraines typiques de la molasse, les valeurs correspondant aux objectifs de qualité suisses sont dépassées pour le Cr et le Pb dans 36%, respectivement 6% des sources testées. Les concentrations en U sont supérieures à la valeur recommandée par l'OMS pour 14% ("Molasse à gypse" et "Glimmersand"). Les eaux souterraines issues de la "Molasse à gypse" présentent les mêmes problèmes de qualité que les eaux provenant des roches évaporitiques.

Les eaux provenant du **flysch** des nappes du Niesen et du Gurnigel sont de type Ca-(Mg)-HCO₃ et sont peu minéralisées (TDS 160 à 459 mg/L). La minéralisation provient essentiellement de la dissolution de calcite et, de façon moins importante, de dolomite. Les concentrations en éléments traces sont faibles et correspondent surtout à du Ba provenant des minéralisations de barytine dans les fractures. Le caractère peu évolué des eaux du flysch est dû (1) à leur bref temps de résidence dans les fractures (ou fissures) et (2) à l'absence de minéraux très solubles, à l'exception des carbonates et de la barytine. Les concentrations en Pb dépassent les normes suisses (ou l'objectif de qualité) dans 32% des sources testées.

2.) Etude de l'altération chimique du grès molassique Burdigalien: origine et comportement chimique du chrome

Afin de caractériser le traceur géogène de l'élément Cr, une étude sur un site prédéterminé dans le grès molassique (source de Lutry, près de Lausanne) a été entreprise. La description quantitative du processus régissant la concentration en Cr dissous de l'eau souterraine découle d'une investigation minéralogique, géochimique et hydrologique en complément aux résultats des analyses chimiques des eaux. Le chrome dissous provient principalement des spinels et pyroxènes détritiques contenus dans le grès Burdigalien. Une analyse au microscope électronique a montré que ces minéraux sont fortement corrodés. Le processus de libération du Cr provient, pour la plus grande part, de la lente altération de ces minéraux. Dans les conditions oxydantes régnant dans les eaux souterraines étudiées, le Cr dissous prédomine sous forme de chromate (CrO₄²⁻), qui est la forme la plus soluble, mais aussi la plus toxique. Dans de telles conditions, il n'y a pas de rétention par la précipitation d'hydroxides de Cr secondaires, ainsi que démontré par modélisation géochimique.

Des expériences de lixiviation en laboratoire avec du grès molassique provenant du site étudié ont été entreprises pour valider les résultats de l'étude de terrain et pour quantifier les processus responsables de la minéralisation en Cr observée dans les eaux de la source de Lutry. Deux tests, s'étendant sur une période de deux mois chacun, effectués avec du grès oxydé et réduit ont permis d'obtenir des données montrant l'influence de l'état d'oxydation du substrat sur la mobilité du Cr. Ces tests ont montré que les processus responsables de la dissolution du Cr sont assez rapides, ce que permet d'expliquer la concentration en Cr mesurée dans les eaux souterraines. Il a été découvert que ces processus dépendent de l'état d'altération du grès. Dans le grès oxydé, où les grains sont recouverts d'hydroxides de fer, le Cr passe plus vite en solution que dans le grès réduit moins altéré. Ceci implique que dans le grès réduit, le Cr est présent principalement sous une forme relativement stable (incorporé dans les minéraux détritiques), tandis que dans le grès oxydé, le Cr se trouve sous une forme plus rapidement mobilisable (adsorbé sur les hydroxides de fer).

Mots clé: composition naturelle de l'eau souterraine, traceurs géogènes, interactions eaux-roche, modélisation géochimique, réseaux d'observation de l'eau souterraine

Die oft ungenügende Kenntnis der Herkunft von Grundwasserinhaltsstoffen stellt ein grundlegendes Problem dar, sowohl in den Umweltwissenschaften, als auch in der Ingenieurgeologie. Insbesondere die Gehalte an gelösten Spurenelementen sind von Bedeutung für die Grundwasserqualität. Ein Hauptziel des AQUITYP-Projektes ist es, basierend auf geogenen Spurenelementgehalten eine detaillierte Typologie natürlicher Grundwässer aus fünf Haupt-Aquifertypen auszuarbeiten, und eine sogenannte "Geo-Referenz" daraus abzuleiten. Diese "Geo-Referenz" stellt eine wertvolle Datenbasis dar für Untersuchungen im Zusammenhang mit Grundwasserverschmutzungen, mit der Verwaltung von Grundwasserreserven, sowie mit ingenieurgeologischen Problemen. Während früherer Arbeiten im Rahmen des AQUITYP-Projektes wurden Grundwässer aus dem Kristallin, aus Karbonat-, und Evaporitgesteinen, sowie aus Molasse- und Flyschsedimenten in der Schweiz und in Nachbarländern beprobt und dokumentiert (Dubois, 1993; Dematteis, 1995; Mandia, 1993; Hesske, 1995; Basabe, 1993). Mittels statistischer Auswertungen dieser Grundwasserdaten und der Untersuchung des Zusammenhangs zwischen Aquiferlithologie und chemischer Grundwasserzusammensetzung konnten eine Anzahl charakteristische Tracer-Elemente identifiziert werden (geogene Tracer).

Die vorliegende Studie beinhaltet (1) eine Synthese der Hydrogeologie und Hydrochemie junger Grundwässer in den oben erwähnten fünf Aquifertypen, basierend auf den vorhandenen Grundwasserdaten, und (2) eine hydro-geochemische Studie über die Herkunft und das chemische Verhalten von Chrom in Molasse-Grundwässern, welche sich auf umfassende Feld- und Laboruntersuchungen stützt.

Eine strenge Qualitätskontrolle der gesamten Datenbank wurde vorgenommen, um einen Vergleich der über eine Zeitspanne von 20 Jahren gesammelten Grundwasserdaten zu ermöglichen. Dafür wurde eine Bestandsaufnahme der seit 1981 angewandten Probennahmetechniken, Probenbehandlungen, und Analysemethoden gemacht. Diverse Tests wie Filtrationstests, geochemische Modellrechnungen und Vergleiche verschiedener Analyse-Methoden erlaubten eine Abschätzung der Qualität und Vergleichbarkeit der Daten. Um diese grosse Anzahl von kontrollierten Grundwasserdaten auch für zukünftige Untersuchungen verfügbar zu machen, wurde eine Grundwasser-Datenbank entwickelt (AQUITYP-DataBase).

1.) Typologie junger Grundwässer

Der Schwerpunkt dieser Synthesearbeit wurde auf die Erforschung der hydro-geochemischen Prozesse gelegt, welche zu den typischen Grundwasserzusammensetzungen in den fünf Aquifertypen führen. Chemische Besonderheiten und Unterschiede zwischen den Grundwässern aus den verschiedenen Aquifertypen wurden identifiziert und die natürlichen Konzentrationsbereiche für jeden der fünf Aquifertypen bestimmt. Die in den früheren Arbeiten vorgeschlagenen geogenen Tracer wurden überprüft und ihre potentiellen Quellen ermittelt. Die massgebenden hydro-geochemischen Prozesse wurden mittels Modellrechnungen untersucht. Schliesslich wurden die Zusammensetzungen der verschiedenen Grundwassertypen mit den schweizerischen Trinkwassernormen verglichen, um einen Überblick über die Qualität der untersuchten natürlichen Grundwässer zu gewinnen. Es stellte sich heraus, dass jeder der untersuchten Gesteinstypen in einer charakteristischen Weise zur Haupt- und Spurenelement-Mineralisation der entsprechenden Grundwässer beiträgt.

Die Grundwässer aus dem **Kristallin** der Mont-Blanc und Aiguilles-Rouges Massive sind durch eine tiefe Gesamtmineralisation charakterisiert (TDS 22 bis 158 mg/L), welche durch Ca^{2+} , Na^+ , Mg^{2+} , HCO_3^- , SO_4^{2-} , und F^- dominiert ist (Ca-Na- HCO_3 - SO_4 Wässer). Erhöhte Mo-, U-, W-, und As-Gehalte sind typisch. Da diese Kristallin-Grundwässer entlang von Klüften zirkulieren, erlangen sie ihre Mineralisation hauptsächlich aus Wechselwirkungen mit hydrothermalen Kluftmineralien. Folgende Mineralien sind für die Grundwassermineralisation relevant: Karbonate (Ca^{2+} , Mg^{2+} , HCO_3^-), Tonmineralien (Ca-Na Ionen-Austausch), Fluorit (F^- , Ca^{2+}), Fe-, As-, und Mo-Sulfide (SO_4^{2-} , As, Mo), sowie U- und W-Mineralien (U, W). Die natürlichen F^- und As-Konzentrationen liegen in 23%, respektive 7% der untersuchten Quellen über den Schweizerischen Grenzwerten für Trinkwasser. Ausserdem übertreffen die U-Gehalte in 65% der Fälle und die Mo-Gehalte in 15% der Fälle die empfohlenen Maximalwerte der WHO.

Die Grundwässer aus dem **Karbonatkarst** erlangen ihre tiefe bis mittlere Mineralisation (TDS 161 bis 547 mg/L) aus der Auflösung von Kalzit (Ca- HCO_3 Wässer), sowie in gewissen Regionen von Dolomit (Ca-Mg- HCO_3 Wässer) und Gips (Ca-Mg- HCO_3 - SO_4 Wässer). Karbonatkarst-Grundwässer weisen gewöhnlich eine sehr kurze Aufenthaltszeit im Kalkgestein auf und enthalten meist nur sehr geringe Mengen an Spurenelementen. Erhöhte Spurenelementgehalte kommen indessen in gewissen Regionen vor, hauptsächlich im Zusammenhang mit fossilen organischen Stoffen (I, V) und Mineralien wie Baryt in pelagischen Kalken (Ba), Evaporitmineralien (Sr, Li), Ton- und Fe-Mineralien (V), sowie Mo-Sulfiden und U-Mineralien in dolomitischen Kalken (Mo, U). In 18% der untersuchten Karbonatkarst-Quellen überschreiten die aus der Atmosphäre stammenden Pb-Gehalte das Schweizerische Qualitätsziel für Trinkwasser.

Die Grundwässer aus den Triassischen **Evaporiten** im Schweizer Rhonetal weisen eine hohe Gesamtmineralisation auf (TDS 760 bis 2788 mg/L), welche sich aus Ca^{2+} , Mg^{2+} , Sr^{2+} , SO_4^{2-} , und HCO_3^- zusammensetzt (Ca-Mg- SO_4 - HCO_3 Wässer). Erhöhte Gehalte an Mn, Ni, Cu, Li, Rb, Y, und Cd sind typisch. Die Mineralisation dieser Grundwässer wird durch eine beginnende Dedolomitisation dominiert (Auflösung von Gips, Cölestin und Dolomit unter gleichzeitiger Ausfällung von Kalzit). Die Na^+ - und K^+ -Gehalte sind vermutlich auf Kationenaustausch-Reaktionen an Tonmineralien zurück zu führen. Die charakteristischen Spurenelemente stammen hauptsächlich aus der Auflösung von Dolomit (Mn, Ni) und wenig Apatit (Y, Cd), sowie aus der Oxydation von Sulfidmineralien (Cu, Ni, Cd). Die hohen Gehalte an leicht löslichem Li und Rb stammen vermutlich aus Salzwassereinschlüssen in Evaporitmineralien und aus Tonmineralien. Alle Evaporit-Grundwässer weisen SO_4^{2-} Konzentrationen über dem Schweizerischen Qualitätsziel für Trinkwasser auf. Ferner überschreiten die Mn-, Cd-, und As-Konzentrationen die Qualitätsziele in 11%, 10%, respektive 7% der untersuchten Quellen. Die U- und Ni-Konzentrationen überschreiten die empfohlenen Maximalwerte der WHO in 58% respektive 2% der Fälle.

Junge Grundwässer aus porösen und geklüfteten **Molassegesteinen** erlangen ihre mittlere Gesamtmineralisation (TDS 48 bis 714 mg/L) hauptsächlich aus der Auflösung von Kalzit und wenig Dolomit (Ca-Mg- HCO_3 Wässer). Die besondere mineralogische Zusammensetzung einzelner Molasseformationen widerspiegelt sich in einer spezifischen Spurenelement-Zusammensetzung der entsprechenden Grundwässer: Ophiolitdetritus im OMM-Sandstein der Westschweiz (Cr), Baryt in Kluftmineralisationen der subalpinen und gefalteten Molasse (Ba), granitischer Detritus mit Sulfiden (Mo), U-Mineralien (U) und grossen Mengen an Glimmer (Li) in den "Glimmersanden" (OSM, Ca-Mg- HCO_3 - SO_4 Wässer), sowie Evaporitmineralien (Li, Sr), Mo-Sulfide und U-Mineralien (Mo, U) in der "Gips-Molasse" (USM, stark mineralisierte Ca-Mg- SO_4 - HCO_3 Wässer, TDS 984 bis 1346 mg/L). Die Cr- und Pb-Gehalte überschreiten in 36%, respektive 4% der untersuchten Molasse-Quellen die Schweizerischen Qualitätsziele für Trinkwasser. Die

U-Konzentrationen liegen in 14% der Quellen ("Gips-Molasse" und "Glimmersande") über dem empfohlenen Maximalwert der WHO. Ferner zeigen die Grundwässer aus der "Gips-Molasse" ähnliche Qualitätsprobleme wie die Evaporit-Grundwässer.

Junge Grundwässer aus den **Flysch**-Aquiferen der Niesen- und Gurnigel-Decke sind schwach mineralisierte Ca-(Mg)-HCO₃ Wässer. Ihre tiefe bis mittlere Gesamtmineralisation (TDS 160 bis 459 mg/L) stammt hauptsächlich aus der Auflösung von Kalzit und zu einem kleinen Teil Dolomit. Der tiefe Spurenelement-Gehalt ist dominiert durch Ba aus Barythaltigen Kluftmineralisationen. Die tiefe Gesamtmineralisation junger Flysch-Grundwässer kann erklärt werden durch (1) ihre kurze Aufenthaltszeit in den geklüfteten Flysch-Gesteinen, und (2) durch die Abwesenheit von leichtlöslichen Mineralien ausser Karbonaten und Baryt. In 32% der Flysch-Quellen überschreiten die aus der Atmosphäre stammenden Pb-Gehalte das Schweizerische Qualitätsziel für Trinkwasser.

2.) Fallstudie über die chemische Verwitterung von Molasse Sandstein: Herkunft und chemisches Verhalten von Cr im Grundwasser

Um das toxische Tracer-Element Cr besser zu charakterisieren wurde eine umfassende Felduntersuchung in einem ausgewählten Einzugsgebiet im Molasse-Sandstein (Burdigalien) durchgeführt (Einzugsgebiet der Lutry-Quelle in der Nähe von Lausanne). Die Untersuchung der Prozesse, welche den Gehalt an gelöstem Cr in diesen Grundwässern kontrollieren, stützte sich auf chemische Grundwasserdaten, sowie auf mineralogische, geochemische, und hydrologische Daten. Reliktische Cr-Spinelle und Cr-haltige Pyroxene im Sandstein stellen die wichtigsten Cr-Quellen dar. Eine Elektronenmikroskop-Studie zeigte, dass diese Mineralien im Sandstein und im darüber liegenden Boden stark korrodiert sind. Durch die langsame Verwitterung dieser Mineralien gelangt das Cr in Lösung. Unter den oxydierenden Bedingungen, welche in den untersuchten Grundwässern herrschen, liegt das Cr in seiner leichtlöslichen und toxischen Form vor (CrO₄²⁻). Geochemische Modellrechnungen zeigten, dass das Cr in diesem Fall kaum zurückgehalten wird (keine Ausfällung von sekundären Cr-Hydroxyd-Phasen).

Im Labor wurden Auslaugversuche mit Molassesandstein aus dem Untersuchungsgebiet durchgeführt, um die Ergebnisse der Felduntersuchung zu bestätigen, und um die für die Cr-Mineralisation des Lutry-Grundwassers massgeblichen Prozesse zu quantifizieren. Zwei Experimente mit bergfeuchtem oxydiertem und reduziertem Sandstein wurden durchgeführt, um Informationen über den Einfluss des Oxydationszustandes des Substrats auf die Mobilisation von Cr zu erhalten. Die Dauer der Experimente betrug 2 Monate pro Experiment. Diese Auslaugversuche zeigten klar, dass die Cr-abgebenden Prozesse schnell genug sind, um die im Grundwasser beobachteten Cr-Gehalte zu erklären. Es stellte sich auch heraus, dass die Abgabe von Cr ins Grundwasser vom Verwitterungszustand des Sandsteins abhängt: Aus dem oxydierten, Fe-Hydroxyd-haltigen Sandstein gelangte das Cr schneller in Lösung als aus dem weniger verwitterten, reduzierten Sandstein. Dies zeigt, dass das Cr im reduzierten Sandstein in einem relativ stabilen Zustand vorliegt (in den detritischen Mineralien), währenddem das Cr im oxydierten Sandstein teilweise in einem instabilen Zustand vorliegt (adsorbiert auf den sekundären Fe-Hydroxyden), von wo es leichter in Lösung gelangt.

Schlüsselbegriffe: natürliche Grundwasserzusammensetzung, geogene Tracer-Elemente, Gestein-Wasser Wechselwirkungen, geochemische Modellierung, Grundwasser-Beobachtungsmessnetze

Acknowledgements

This study was carried out under the supervision and with the support of Prof. A. Parriaux from the Laboratory of Geology (GEOLEP) of the Swiss Federal Institute of Technology, whom I would like to thank for his support and advice. Considerable thanks are due to Dr M. Bensimon for his assistance in the laboratory and fruitful discussions during the accomplishment of this study. Further, I am particularly indebted to Dr N. Waber from the Rock-Water Interaction Group (GGWW) at the Mineralogical and Geological Institutes of the University of Berne, whose careful reviews and constructive criticism added greatly to the quality of the manuscript.

Prof. I. Mercolli and G. Rizzoli from the Mineralogical Institute of the University of Berne are thanked for their analytical support and advise with geochemical and mineralogical rock analyses. Thanks are also due to Dr M. Herweg and A. Jenni from the Geological Institute of the University of Berne for their assistance in the scanning electron microscope lab. I also express my thanks to H. Haas for providing porosity and permeability measurements.

Dr V. Maître, J.-Ph. Rey, and G. Franciosi are thanked for their help and generosity. Furthermore, I would like to thank the technical staff at the GEOLEP, P. Gallay, B. Sperandio, M. Tiercy, A. Tomaniak, R. Menendes, and J. Bourquin for their help.

I also extend sincere appreciation to N. Ruder and R. Borloz for providing linguistic reviews of the manuscript and to M. Bovey for his help with the AQUITYP database.

All my colleagues at the GEOLEP and at the Mineralogical and Geological Institutes of the University of Berne are thanked for their support and for sharing the period of this study with me.

My personal thanks go to my parents and friends for supporting me during this part of my life.

This study was financially supported by the Swiss National Science Foundation (grant N° 20-45730.95).

I. INTRODUCTION

1.1. Framework

In recent times groundwater quality issues have become a major concern world-wide. While drinking water management strategies in the past used to concentrate mainly on the major element composition of groundwaters, the increase in potential groundwater pollution sources requires a deeper insight into the chemical behaviour of trace elements. Previous studies on trace elements in shallow groundwater were mainly local studies at watershed scale and at point-source polluted sites such as industrial sites. More recently, attention was drawn to the geochemistry of trace elements by non-point source pollution such as for example the use of certain fertilisers in agriculture (e.g. Nriagu, 1991; Adriano, 1986; Salomons & Förstner, 1984; Moore & Ramamoorthy, 1984). In deep circulating groundwater systems the geochemistry of trace element has been explored mainly within the scope of radioactive waste disposal investigations (e.g. Middlesworth & Wood, 1998; Schmassmann and others, 1984, 1992; Schmassmann, 1990; Ménager and others, 1989; Pearson and others, 1986; Swedish nuclear fuel and waste management, 1985). However, until now there has been little systematic research on trace element geochemistry of recent groundwaters, i.e. tritium containing groundwaters with a residence time of a few years to a few decades. Only in the past years the increased awareness of groundwater quality led to a more systematic approach and the development of national groundwater-monitoring networks in several countries (e.g. NL: Frapporti and others, 1996; CH: BUWAL, 1998). The geogenic background concentrations of many trace elements in recent groundwaters are thus still insufficiently recognised. The study of trace elements in active groundwater systems in different geologic environments, their long-term evolution, and the processes leading to this mineralisation is therefore of great importance.

One of the key problems in environmental science and in engineering geology is the often incomplete understanding of the origin of groundwater compositions. Additionally, studies on groundwater pollution often suffer from the lack of reliable data for the natural background levels of dissolved trace elements. The concentrations of trace and ultra-trace elements in recent groundwaters, which are of importance to water quality and thus human health and to aspects of engineering geology, depend on the aquifer lithology. It is important to recognize the origin of the observed water composition particularly for the identification of adequate measures for the protection of groundwater resources. Further, in engineering geology the flow path of groundwater encountered in underground work is central to the evaluation of the impact of such construction on groundwater resources (Maréchal, 1998) (see figure 1-1).

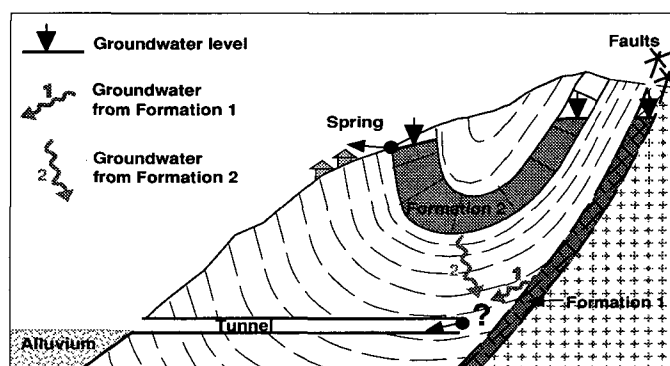


Figure 1-1: The flow path of groundwater is important for the evaluation of the impact of underground construction on groundwater resources. If the water discharged in the tunnel spring in the example comes from formation 1, then the consequences of a lowering of the water table are limited to the tunnel itself and the water can be drained. On the other

hand, if the water comes from formation 2, the spring used for drinking water supply will run dry and measures are needed to prevent this (e.g. sealing of the tunnel).

Several groundwater typologies based on geologic, hydrodynamic and major element chemical parameters have been proposed (e.g. Piper and others, 1953; Schoeller, 1960; Jäckli, 1970; Hem, 1985; Jahnke, 1999). However, these typologies do not include trace elements. To establish a detailed typology of recent groundwaters as a reference for the geogenic groundwater trace element composition in different lithologic environments – called “geo-reference” - is crucial in dealing with groundwater contamination. Such a geo-reference may help to differentiate between anthropogenic contamination and natural background concentrations of dissolved trace elements in a particular aquifer type. We hope that this geo-reference will provide a tool for groundwater quality management by state and local authorities. Furthermore, in engineering geology a detailed groundwater typology also contributes to a better understanding of groundwater flow paths, which will make a better evaluation of the impact of underground work on groundwater resources possible.

1. 1. 1. The AQUITYP project: previous studies

The AQUITYP and AQUISOL projects have been conducted at the Swiss Federal Institute of Technology at Lausanne (Geology laboratory GEOLEP of the Civil Engineering Department and soil science group of the Rural Engineering Department) with the support of the Swiss National Science Foundation. The principal goal of these projects was the investigation of trace elements in recent groundwaters and in soils from different lithologic environments in the alpine belt.

The AQUITYP project (Parriaux and others, 1990) was focused on the chemistry of recent groundwaters from different rock types, i.e. crystalline (granite and gneiss, Dubois, 1993), carbonate (Dematteis, 1995), and evaporite rocks (Mandia, 1993), as well as molasse (Hesske, 1995) and flysch sediments (Basabe, 1993). These rock types represent the major aquifer types in the alpine belt. On the other hand, the AQUISOL project aimed at the investigation of trace element cycling in soil ecosystems developed on these rock types (Atteia, 1992; Dalla Piazza, 1996).

In the AQUITYP project groundwater hydrochemistry was investigated in these different aquifer types in areas with low anthropogenic input. To achieve this objective, a vast network for *spatial* and *long-term groundwater monitoring* was set up by the GEOLEP.

Spatial observation network

The spatial observation network allowed the characterisation of the geochemical imprint and its spatial variability of a given geologic unit on the groundwater. This observation network covers a large part of the alpine belt (Switzerland, France, Italy, Austria and Germany) as well as several karst regions in southern Europe. It comprises 564 sampling sites (springs and wells) and provides the basis for the above mentioned geo-reference, which has been established in the present work.

The water samples were analysed in the field for physical-chemical parameters and in the laboratory for major and trace elements. The results of these studies are documented in five PhD thesis (Dubois, 1993; Mandia, 1993; Basabe, 1993; Dematteis, 1995; Hesske, 1995). Statistical analysis of the data and the examination of the relationship between aquifer geology and the chemical composition of the corresponding groundwater led to the identification of a number of specific geogenic tracer elements. Batch leaching experiments with representative rock samples allowed to test the geogenic origins of these elements.

Long-term monitoring network

In addition to the large number of sampling sites of the spatial observation network, 14 reference sites were selected for long-term monitoring. This network allows the documentation of seasonal variations and long-term changing of the chemical composition over the last 20 years (1981 to 2001). The 14 reference sites represent the major aquifer types and are situated on a transect in western Switzerland, from the Jura mountains southwards to the Alps.

Water samples for chemical analyses have been collected twice a year at each site, once in spring during high water period and once in autumn during low water period. At each site water temperature and electric conductivity have been measured monthly and discharge or water level have been recorded continuously. At present, a chemical data set of 535 complete groundwater analyses of these 14 reference sites is available, including major and trace element analyses, physical-chemical field measurements, and discharge recordings.

A co-operation with the Swiss Groundwater Quality Monitoring Network NAQUA (BUWAL, 1998) has recently been established for three of these observation sites.

1. 2. Objectives

The present research is part of the AQUITYP project and focuses on the following objectives:

- 1.) **Synthesis of the typology of recent groundwaters from crystalline, carbonate, evaporite, molasse and flysch rocks based on the groundwater data acquired during the previous studies**
 - a) Homogenisation and thorough quality control of the data gathered by different authors over a time span of 20 years
 - b) Identification of the chemical characteristics and differences of groundwaters from the different aquifer types: natural major and trace element concentration ranges
 - c) Investigation of the sources of the geogenic tracers and of the rock-water interaction processes controlling groundwater chemistry under natural conditions by using geochemical modelling strategies
 - d) Comparison of the concentrations of chemical elements in the groundwaters from the different aquifer types to the Swiss drinking water standards, in order to assess the quality of the investigated groundwaters as drinking waters.
- 2.) **Case study: Chromium in groundwaters from Burdigalian molasse sandstone**
 - a) Conduction of a comprehensive field study of a selected catchment in the Burdigalian molasse sandstone (geology, hydrogeology and geochemistry) in order to get a *quantitative* description of the processes controlling this geogenic marker element
 - b) Geochemical comparison of long-term hydrochemical data from two reference springs (Lutry and Pierre-Ozaire)
 - c) Conduction of laboratory leaching experiments to support the study at catchment-scale

1. 3. Basic principles

1. 3. 1. Concept of aquifer classification

For an aquifers classification both geologic and hydrogeologic criteria can be applied. Water passing through a rock tries to chemically equilibrate with it. The chemical composition of groundwater depends on the mineralogic composition of the rock and the residence time of the groundwater in the rock. Therefore, both the lithologic and hydrogeologic characteristics of aquifers have been considered in the design of the groundwater observation networks of the AQUITYP project (Parriaux and others, 1990).

An aquifer is defined as a *permeable sequence of rocks* that can contain and transmit significant quantities of groundwater under ordinary hydraulic gradients (Freeze & Cherry, 1979). It can be unconfined or confined. An *unconfined aquifer* or *watertable aquifer* is an aquifer in which the water table forms the upper boundary. A *confined aquifer* is an aquifer that is confined by aquitards, i.e. semi-confining strata permitting some groundwater flow at a very low transmission rate. Usually, unconfined aquifers occur near the surface and confined aquifers at depth.

The nature and distribution of aquifers and aquitards in a geologic system are controlled by the lithology and the structure of the geologic system. The *lithology* is the physical make-up of a rock type, including its mineralogic composition and texture. *Structural features*, such as cleavages, fractures, folds, and faults are the geometric properties of the geologic system produced by deformation after deposition or crystallisation.

Water infiltrates into an aquifer in the *recharge area* or *catchment* and is discharged naturally from an aquifer in the *discharge area*. Groundwater discharge can be either diffuse or restricted to a spring, depending on the structure of the geologic system. Alternatively, groundwater can be produced from an aquifer by pumping in a well. The sampling sites of the AQUITYP observation networks are either natural or artificial springs, e.g. springs in tunnels, or wells.

Void spaces within a rock sequence, so-called pores, are the space in which groundwater can circulate. The shape of the pores, the size of their apertures, their arrangement, and interconnectedness determine the permeability of a geologic unit. In general, three porosity types are distinguished (e.g. Hölting, 1992; see figure 1-2): inter-granular porosity, fracture

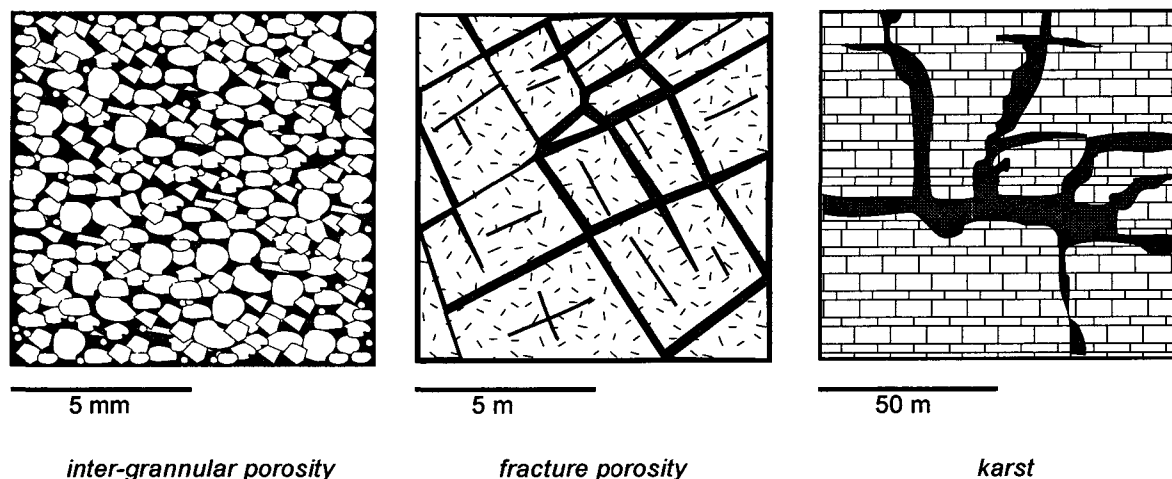


Figure 1-2: Porosity types (after Hölting, 1992). Dark = porosity, light = rock.

porosity, and conduit porosity (karst). Inter-granular porosity is characteristic of clastic sedimentary rocks, fracture porosity is typical of crystalline rocks and diagenetic or metamorphic sedimentary rocks, and conduit porosity (karst) occurs in rocks composed of soluble minerals, such as carbonate rocks and certain types of evaporite rocks.

The permeability and hydraulic gradient of the aquifer are the basic factors that determine the flow rate and residence time of a groundwater. High flow rates occur in highly permeable karstic and fractured rocks which are situated in steep mountain areas (high hydraulic gradient). Hence, the groundwater residence time in such geologic units is short.

In the alpine belt the major rock types acting as aquifers, are clastic sedimentary rocks, carbonate, evaporite, and crystalline rocks. In addition to their specific lithology, these rock types occur in distinctive topographic settings, e.g. crystalline and flysch rocks form steep mountains and molasse rocks form smooth hills. Aquifers composed of these different rock types therefore have particular hydrogeologic properties. In the following, the term “aquifer type” is used in the sense of combined lithologic and hydrogeologic characteristics: crystalline aquifers, carbonate aquifers, evaporite aquifers, molasse aquifers, and flysch aquifers.

During previous studies the lithologic and structural properties of these five aquifer types were investigated by means of literature studies and completed with mineralogic and chemical rock analyses (Dubois, 1993; Mandia, 1993; Basabe, 1993; Dematteis, 1995; Hesske, 1995). An assessment of the hydrogeologic characteristics was achieved by analysing time-series of discharge recordings, water temperatures and electric conductivities of selected springs, as well as by conducting tracer tests. The typical lithologic and hydrogeologic characteristics of these major aquifer types investigated in the AQUITYP project are summarised in table 1-1 and in chapter 3. 3. on page 45.

Rock type	Lithology	Aquifer type	Predominant porosity type	Predominant groundwater flow
Crystalline rocks	Gneiss and granite	Crystalline	fractures	fracture flow
Rocks composed of soluble minerals	Carbonate rocks	Carbonate karst	Karst conduits and fractures	conduit and fracture flow
	Evaporite rocks	Evaporite karst		
Clastic sediments	Molasse	Molasse	fractures and inter-granular porosity	inter-granular and fracture flow
	Flysch	Flysch		fracture flow

Table 1-1: Principal aquifer types in the alpine region and their typical hydrogeologic characteristics.

1.3.2. Groundwater as a part of the global water cycle

Groundwater is part of the global hydrologic cycle (see figure 1-3). In Switzerland groundwater recharge occurs almost exclusively through infiltration of meteoric water, i.e. rainwater and snowmelt. Generally, the composition of rainwater and snow is determined by the source of the water vapour and by the ions acquired during transport through the atmosphere (Appelo & Postma, 1996). The sea is the source of approximately 30% of all water in continental precipitation worldwide (Garrels and others, 1975). Rainwater with a purely marine origin resembles very diluted seawater. The concentration of marine aerosols transported in the atmosphere decreases with increasing distance from the sea. In addition to this “marine” part of the meteoric water composition, continental dust and gases of natural or anthropogenic origin dissolve in the water particles during atmospheric transport.

In groundwaters, which have a short residence time in the underground environment (within a few years), many chemical elements are present in very low concentrations, not much higher than those found in rainwater or snow. It is therefore particularly important to recognise the atmospheric input when studying trace elements in groundwaters with a fast transit time (Atteia, 1992). In recent years, the atmosphere has become increasingly loaded with anthropogenic pollutants, and it is important to understand the consequences for groundwater quality. Particularly the effect of acid deposition - so-called “acid rain¹” - on groundwater quality has become a major concern in recent years. The strong acids HNO_3 , H_2SO_4 and HCl produced by industry and traffic are the main cause for acid rain, and can disturb the delicate proton balance in water and soil systems (Stumm & Morgan, 1996). The production of natural bases originating from the dissolution of carbonate containing dust is often too weak to neutralise this anthropogenic acidity. Additional base is produced by

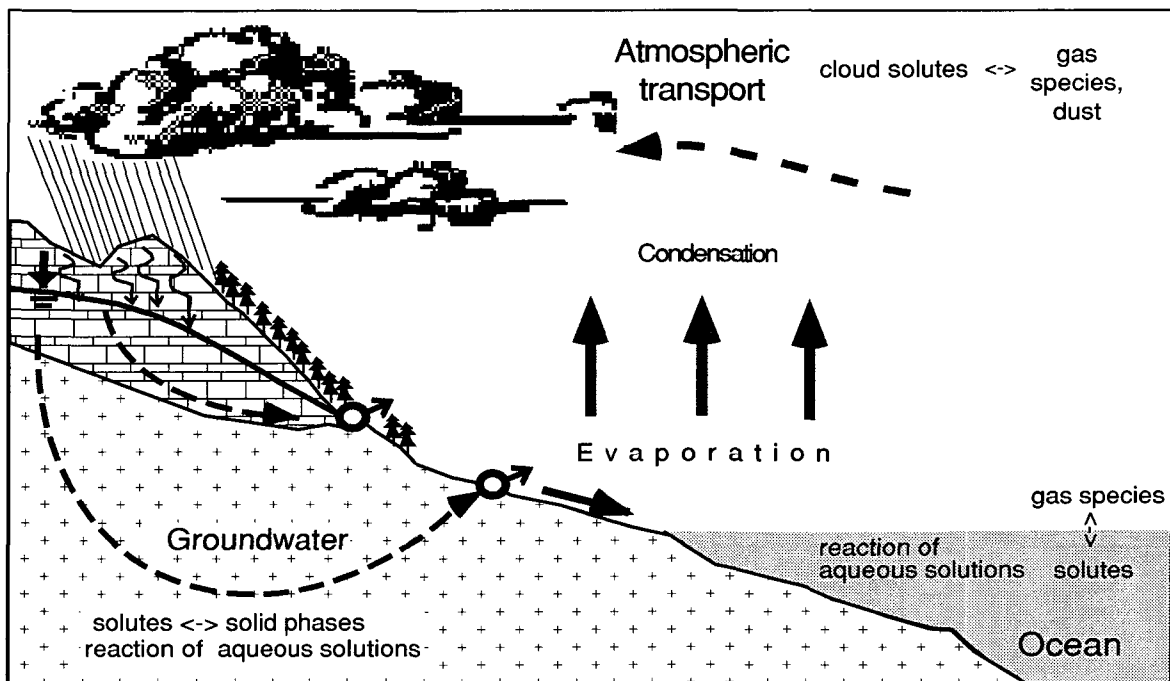


Figure 1-3: Groundwater is part of the global hydrologic cycle. Along its flow path through soil and aquifer the chemical composition of groundwater evolves by interacting with soil and aquifer materials.

1. Rain water with a pH <5.6 is referred to as acid rain

intensive agriculture in the form of NH_4OH , which evaporates from manure and is found in rainwater as NH_4^+ . However, in the soil the oxidation of NH_4^+ leads to further acidification (see below).

Throughfall solutions under forest canopies are more mineralised than rainwater without influence of a vegetation canopy. Evaporation on the plant surface leads to an increase of concentrations, which is proportional to the water that evaporates for non-reactive components. Further, throughfall solutions take up chemical compounds from dry deposition on the plant surface, i.e. atmospheric fallout of dust and aerosols, as well as gases that are adsorbed on the plant surface during dry periods.

The infiltration of meteoric water into the soil represents the next stage in the water cycle. The soil is the interface between atmosphere, geosphere, biosphere, and hydrosphere, and soil processes play an important role in the mineralisation of the infiltrating meteoric water. Weathering of soil minerals and ion exchange processes buffer the acidity of the infiltrating water. In fact, soils consist from bottom to top of the progressively weathered equivalents of the underlying material. In addition, the vegetation itself also influences the chemical composition of the infiltrating water by selectively uptaking or releasing ions. The acidity of the soil solution, which is the driving force of weathering processes, can have both natural and anthropogenic origins: Natural acidification of the soil solution occurs by dissolution of soil CO_2 from the oxidation of organic matter and root respiration. Anthropogenic acidification of the soil solution results from acid input and the oxidation of NH_4^+ . If plants consumed all the nitrate produced by NH_4^+ -oxidation in the soil, the proton production would be balanced by the HCO_3^- production from the denitrification process. Yet, the frequent presence of NO_3^- in the groundwater is proof of incomplete denitrification.

Finally, the water reaches the aquifer. By interacting with the rocks in the aquifer it attains its characteristic chemical composition, which leads us to the next section.

1. 3. 3. Factors controlling groundwater composition

Groundwater acquires its chemical characteristics during residence in the subsurface environment and by interacting with the aquifer rocks. More precisely, the difference in composition between meteoric water that infiltrates into the subsoil and the groundwater that emerges at the spring is the result of the interaction of the groundwater with the rock along its flow path. The groundwater composition in different lithologic units is controlled by *mineralogic*, *chemical* and *hydrogeologic* factors. The potential sources of solutes are determined by the exposure of reactive mineral surfaces to the groundwater. The basic rock-water interaction processes occurring in the subsurface environment are:

- mineral dissolution and precipitation
- oxidation and reduction of aqueous species
- sorption (surface complexation and ion exchange)

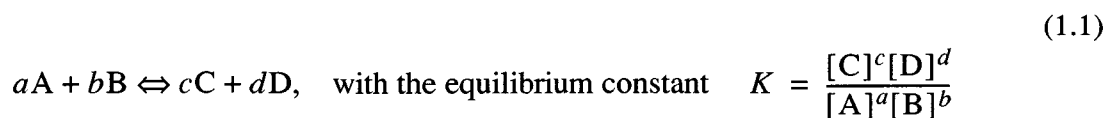
All of these basic processes are subject to specific *reaction kinetics*. The concentration of a specific element is either controlled by equilibrium (usually in case of fast reactions), or it is determined by reaction kinetics (in case of slow reactions). When studying rock-water interaction processes the residence time of the groundwater in the subsurface environment is therefore a crucial factor.

Hydrogeologic characteristics, such as the porosity and related hydraulic conductivity of the rocks in the aquifer establish the boundary conditions for potential chemical reactions. Tracer tests conducted in selected catchments of the AQUITYP observation network showed that the investigated recent groundwaters have residence times ranging from a few hours to a few years (Dubois, 1993; Mandia, 1993; Basabe, 1993; Hesske, 1995; Dematteis, 1995 and references therein; see chapter 3. 3. on page 45). The shortest residence times occur in karst aquifers composed of carbonate or evaporite rocks and in aquifers composed of fractured crystalline and flysch rocks. The processes leading to the mineralisation of such groundwaters must therefore be fast. Among the fastest rock-water interaction processes are the dissolution of soluble carbonate and sulphate minerals, i.e. calcite, dolomite, and gypsum, the oxidation of sulphides, such as pyrite, and ion exchange and surface complexation reactions. In contrast, Al-silicate alteration is very slow at near-neutral pH and therefore influences such recent groundwaters only marginally.

Trace elements in groundwater tend to be more characteristic of different lithologic and hydrogeologic properties of aquifers than major elements. Like major elements, dissolved trace elements are controlled by mineral dissolution or precipitation, redox processes and sorption. Relatively few minerals exist that are composed of trace elements alone. Some of them may act as solubility controls for certain dissolved trace elements, e.g. Sr- and Ba-carbonates and -sulphates (strontianite, witherite, celestite and barite, respectively) or U-oxides and -carbonates. The majority of dissolved trace elements, however, is also incorporated as trace elements in different major element mineral phases. The dissolution of such trace elements therefore depends on the dissolution kinetics of their host mineral.

Mineral dissolution and precipitation

The relation between minerals and dissolved species can be quantified by the *law of mass action* (Garrels & Christ, 1965). This equilibrium approach has proved to be very useful to describe the limits set to concentrations of dissolved substances in natural systems.



The bracketed quantities denote activities. Since the activity of pure solids is equal to 1 by definition, a simple relation results between the equilibrium constant of the mineral of interest and the activities of its dissociation products. Activities of dissolved species are always smaller than their molal concentrations, because of the effect of electrostatic shielding and the presence of aqueous complexes. A correction term, the *activity coefficient*, relates activities to molal concentrations. In the present study activity coefficients are calculated with PHREEQC (Parkhurst, 1995; see chapter 1. 4. 1. on page 16) using the extended Debye-Hückel theory (Appelo & Postma, 1996: 49, and references therein).

The saturation index (SI) of a solution for a mineral X is calculated from the equilibrium constant of this mineral (K_x) and the ion activity product (IAP) of its dissociation products in solution:

$$SI_x = \log IAP / K_x \quad (1.2)$$

The saturation state indicates the tendency of a solution to dissolve or precipitate minerals. For $SI = 0$ there is equilibrium between the solution and the mineral, $SI < 0$ reflects subsaturation (dissolution is expected) and $SI > 0$ supersaturation (precipitation is expected).

The reaction kinetics of weathering processes, and thus the dissolution rate of a given mineral phase depends on its reactive surface area (accessible surface per weight unit of substratum), and on the saturation condition, pH, redox potential, ionic strength, and temperature of the solution. Chemical weathering rates from literature of some important minerals are reported in table 2-2. Note that different solvents were used for determining these rates, and that rather large differences exist between laboratory weathering rates and field weathering rates (e.g. White and others, 1998; Lasaga and others, 1994; Velbel, 1993; Sverdrup, 1990).

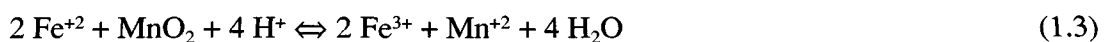
Mineral	Chemical weathering rate moles/m ² *s	Reference
Calcite	10 ^{-5.64}	Schott et al., 1989
Dolomite	10 ^{-5.92}	Gautelier et al., 1999
Anorthite	10 ^{-8.55}	Lasaga et al., 1994
Diopside	10 ^{-10.02}	Sverdrup, 1990
Serpentine	10 ^{-10.61}	Sverdrup, 1990
Enstatite	10 ^{-11.10}	Sverdrup, 1990
Montmorillonite	10 ^{-11.61}	Sverdrup, 1990
Biotite	10 ⁻¹¹ to 10 ⁻¹⁵	Murphy et al., 1998
Albite	10 ^{-12.26}	Chou & Wollast, 1984
Hornblende	10 ^{-12.40}	Frogner & Schweda, 1998
Mg-Chlorite	10 ^{-12.42}	Sverdrup, 1990
K-feldspar	10 ^{-12.50}	Lasaga et al., 1994
Epidote	10 ^{-12.61}	Rose, 1991
Muscovite	10 ^{-13.07}	Lasaga et al., 1994
Quartz	10 ^{-13.39}	Rimstidt & Barnes, 1980

Table 1-2: Mean chemical weathering rates of some common minerals determined in the laboratory at standard state conditions (25°C, 1 bar) and a pH of 5.

Oxidation and reduction

Oxidation and reduction processes, so-called redox processes, control the aqueous species distribution of redox-sensitive elements in groundwater including H₂S/SO₄⁻², CH₄/HCO₃⁻, or NH₄⁺/NO₃⁻ (Appelo & Postma, 1996: 239 ff.). Many trace elements, particularly metals are also redox-sensitive. Therefore redox processes play an important role in the mobility of many trace elements.

Redox reactions involve electron transfer from one atom to another, e.g. in the reaction between Fe and Mn:



In this reaction one electron per Fe^{II} is transferred to reduce Mn^{IV} from MnO₂ to Mn^{II}. Fe⁺² acts as *reductant* or *electron donor*, while MnO₂ is the *oxidant* or *electron acceptor*. In redox reactions the relation between ion activities and voltage is expressed by the Nernst equation (Anderson, 1996).

$$E_H = E^0 + \frac{RT}{nF} \ln \frac{[D_{ox}]^d}{[B_{red}]^b} \quad (1.4)$$

E_H = redox potential (standard hydrogen electrode) [Volt]

E^0 = standard potential [Volt]

F = Faraday's constant [96.42 kJ/Volt gram equivalent]

T = absolute temperature

n = number of electrons transferred in the reaction

$[D_{ox}]$, $[B_{red}]$ = activities of oxidised/reduced species

Electron transfer reactions are often very slow when occurring inorganically, but they may be accelerated by bacterial catalysis. Reaction 1.3 also shows that redox reactions may have a significant effect on the solution pH.

The so-called *pe* concept is used as an alternative definition of the redox state instead of E_H . "Free" electrons are treated as a concentration ($pe = -\log [e^-]$), even though a "free" electron never exists. The *pe* concept simplifies calculations considerably, as the electron activity appears explicitly in the activity product. This allows to treat redox reactions algebraically in a similar way as other mass action expressions. The relationship between *pe* and E_H is:

$$E_H = \frac{2.303RT}{F} pe \quad (1.5)$$

at 25°C the relationship is: $E_H = 0.0592 pe$ (1.6)

Sorption

This chapter is based on the text books by Appelo & Postma (1996) and Stumm & Morgan (1996), as well as on Hochella (1990).

Soils and aquifers contain materials that are able to adsorb solutes from the water. Sorption is the change in concentration of a chemical in the solid matter as a result of mass transfer between solution and solid. Sorption processes can be subdivided into

- **adsorption:** a chemical adheres to the surface of a solid phase
- **desorption:** a chemical is detached from a solid phase
- **absorption:** a chemical is taken up into a solid phase
- **exchange:** a replacement of one ion for another at the solid surface or in interlayers

Adsorption of ions by soil or aquifer material may retard a solute component with respect to groundwater flow velocity. Ion exchange acts as a temporary buffer in non-steady state situations, which are the result of acidification, pollution, or moving salt/fresh water boundaries. The adsorbed amount of a chemical in the substratum is usually large compared to the amount of that chemical in solution. Ion exchange therefore tends to smooth changes in water composition. On the other hand, ion exchange can completely alter the dissolved cation concentrations through a process known as ion chromatography. In general, sorption reactions proceed fast compared to mineral dissolution/precipitation reactions and equilibrium is almost always established.

Sorption is limited by the exchange or sorption capacity of the substratum. Each mineral has a specific exchange capacity for cations and anions, the so-called *cation exchange capacity* (CEC, see table 1-3). The CEC depends on the surface and interlayer charge and the specific surface area of a mineral. It is therefore considerably influenced by the type of mineral and grain size. Among the materials commonly occurring in soils and aquifers, the most efficient sorbing materials are clay minerals, Fe- and Mn-oxides and -hydroxides, and organic matter. The latter are often found as coatings on coarser grains, and therefore play an important role for the chemical evolution of groundwater.

Mineral	CEC [meq/100 g]
kaolinite	3-15
montmorillonite	80-120
vermiculite	100-200
glauconite	5-40
illite	20-50
chlorite	10-40

Table 1-3: Cation exchange capacities (CEC) of common soil and aquifer minerals (from Appelo & Postma, 1996).

Adsorption occurs, because dissolved ions are attracted to mineral surfaces that have a net electrical charge. Clay minerals usually have a negative *structural charge* due to substitutions of cations in the crystal lattice (e.g. substitution of Al^{3+} for Si^{4+}), or due to the exchange of interlayer cations (e.g. substitution of Na^{+} for Ca^{2+}). *Surface charge* arises from the protonation of surface oxygen or the deprotonation of surface hydroxyl, which is due to ongoing dissolution. The surface charge of Fe- and Mn-oxides and -hydroxides, kaolinite and silicates are attributed to such surface reactions.

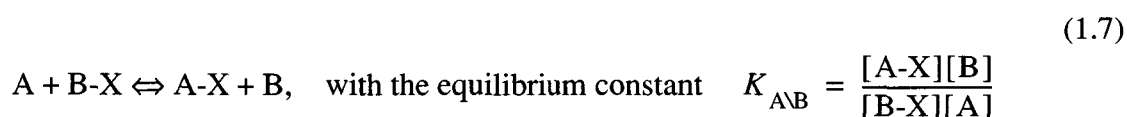
The surface charge of a mineral depends on the pH of the solution. It is zero at the pH value, where the surface oxygens are protonated just enough to compensate for broken bonds and small internal charge, i.e. at the *point of zero net proton charge* or pH_{PZNPC} . The *magnitude* of the adsorption capacity depends on the difference between the solution pH and the pH_{PZNPC} , as well as on solute concentrations and ionic strength of the solution.

Minerals have a capacity for cation adsorption when the pH of the solution is above the pH_{PZNPC} (negative surface charge), and for anion adsorption when the pH of the solution is below the pH_{PZNPC} (positive surface charge). In table 1-4 the pH_{PZNPC} values of common soil and aquifer minerals are listed. Clay minerals, quartz, and feldspars have a low pH_{PZNPC} . In the pH-range found in natural groundwaters (pH 6 to 8) these minerals therefore behave as *cation adsorbents* only. Anion exchange capacity may be present on minerals that have a high pH_{PZNPC} , such as carbonates and Fe-hydroxides.

Mineral	pH _{PZNPC}	Source
birnessite	2.2	Davis & Kent, 1990
montmorillonite	<2.5	Parks, 1967
quartz, feldspar	2.9	Davis & Kent, 1990
kaolinite	4.6	Parks, 1967
α-Al(OH) ₃	5.0	Stumm & Morgan, 1996
goethite	7.3	Davis & Kent, 1990
ferrihydrite	8.5	Stumm & Morgan, 1996
haematite	8.5	Davis & Kent, 1990
calcite	9.5	Parks, 1967

Table 1-4: pH_{PZNPC} values of common soil and aquifer minerals (from Appelo & Postma, 1996).

Sorption processes are modelled with equations that are derived from the law of mass action. While the model equations for adsorption/desorption use the concentration of only one chemical and neglect the effect of other solutes, ion exchange equations explicitly account for all ions that compete for the exchange site. Ion exchange processes are treated as a system of chemical reactions (mass actions) between the exchangeable species (*A* and *B*) on the exchanger (*X*) and the aqueous species available for exchange:



Activity coefficients for ions on the exchanger are commonly unknown, and there is no universally accepted model for activities of ions on the exchanger, as it is the case for solute activities. Activities of adsorbed ions are sometimes calculated as *molar fractions* (Vanselow convention; Vanselow, 1932), but more often as *equivalent fractions* (Gaines & Thomas convention; Gaines & Thomas 1953). In a third approach, the Gapon convention (Gapon, 1933), the activities of the adsorbed ions are assumed proportional to the number of exchange sites that are occupied by the ions. The molar and the equivalent fraction are therefore identical in the Gapon convention, both are based on a single exchanger site with charge -1. For homovalent exchanges it makes no difference which convention is used, but for heterovalent exchange the difference is notable. The standard state, i.e. the state where the activity of the exchangeable ion is equal to 1, is in all cases an exchanger that is fully covered with one cation only.

The *exchange or selectivity coefficient* indicates the relative tendency of two elements to become adsorbed (approximate values are given in table 1-5). The selectivity coefficients vary with the exchanger and the solution composition. If anion exchange is important, the sequence of high to low sorption is $PO_4^{-3} > F^- > SO_4^{-2} > HCO_3^- > Cl^-$. However, this sequence may be affected by the presence of cations and complexes.

Equation: $\text{Na} + 1/i\text{I-X}_i \rightleftharpoons \text{Na-X} + 1/i \text{I}^{+i}$ with $K_{\text{NaI}} = \frac{[\text{Na-X}][\text{I}^{+i}]^{1/i}}{[\text{I-X}_i]^{1/i}[\text{Na}^+]} = \frac{\beta_{\text{Na}}[\text{I}^{+i}]^{1/i}}{\beta_{\text{I}}^{1/i}[\text{Na}^+]}$

Ion I ⁺	K _{NaI}	Ion I ⁺²	K _{NaI}	Ion I ⁺³	K _{NaI}
Li ⁺	1.2 (0.95-1.2)	Fe ⁺²	0.6	Al ⁺³	0.6 (0.5-0.9)
K ⁺	0.20 (0.15-0.25)	Co ⁺²	0.6		
NH ₄ ⁺	0.25 (0.2-0.3)	Mn ⁺²	0.55		
Rb ⁺	0.10	Ni ⁺²	0.5		
Cs ⁺	0.08	Cu ⁺²	0.5		
		Mg ⁺²	0.50 (0.4-0.6)		
		Ca ⁺²	0.40 (0.3-0.6)		
		Zn ⁺²	0.4 (0.3-0.6)		
		Cd ⁺²	0.4 (0.3-0.6)		
		Sr ⁺²	0.35 (0.3-0.6)		
		Ba ⁺²	0.35 (0.2-0.5)		
		Pb ⁺²	0.3		

Table 1-5: Approximate selectivity coefficients for different ions I with a charge i, with respect to Na⁺ based on the Gaines-Thomas convention (from Appelo & Postma, 1996). β is the equivalent fraction of adsorbed ions. A range is given when many measurements in different soils or for different clay minerals are available.

1. 4. Geochemical modelling

The following chapter is based on the notes of the short course “Geochemical Modelling of Natural and Contaminated Groundwaters” (Mäder & Waber, 1997) and on the paper by Plummer (1992).

Geochemical modelling attempts to quantitatively interpret and/or predict chemical reactions of minerals, gases and organic matter with aqueous solutions in rock-water systems. Geochemical models are based on chemical and thermodynamic principles that are independent of the geologic environment. In many cases they are the only recourse to analyse environmental processes in inaccessible systems (e.g. in aquifers) or when predictions must be carried out over geologic time spans. However, numerical models cannot reproduce nature in full detail, and they are only as good as their input data, the available thermodynamic, kinetic and hydraulic data, and their interpretation.

Geochemical modelling began 40 years ago as an attempt to apply more quantitative techniques to the interpretation of water-rock interactions. Plummer (1992) offers a detailed review of the older studies. Principally two approaches of geochemical modelling have evolved: “inverse modelling”, which uses observed water and rock compositions to identify and quantify geochemical reactions, and “forward modelling”, which uses hypothesised geochemical reactions to predict water and rock compositions.

1. 4. 1. Aqueous speciation and saturation state modelling

Aqueous geochemical models are used in the inverse and forward geochemical modelling approaches (see sections 1. 4. 2 and 1. 4. 3), but in somewhat different ways. In inverse modelling the selected reactants and the calculated mass transfer have to be consistent with the calculated saturation states for these phases. In forward simulations, the combined aqueous and solid data set can be used to predict mineral solubilities, reactions paths and mass transfer.

Aqueous speciation and saturation state calculations have been performed for the spring waters of the spatial observation network (see chapter 3. 4. on page 59), for rain water, soil solutions and groundwater of the Lutry site (chapter 4. 5. 3. on page 163), and for the solutions from the leaching experiments (chapter 4. 7. on page 181). The computer code PHREEQC (Parkhurst, 1995; Parkhurst & Appelo, 1999) has been used for these calculations, together with the internally consistent WATEQ4F thermodynamic database based on Nordstrom and others (1990).

PHREEQC is based on ion association models, which account for the non-ideality of aqueous solutions by individual ion activity coefficients (derived from extensions of the Debye-Hückel theory) and for the formation of aqueous complexes from the individual ions (mass-action relations). Ion association models consist of sets of mass balance equations for each element, mass action equations and their equilibrium constants for complex-ion formation, and of equations that define individual ion-activity coefficients.

PHREEQC uses as input field measurements of temperature, pH, and E_H , together with chemical data of water samples. The distribution of aqueous species, ion activities, and mineral saturation indices are then calculated as a function of solution composition, pH, E_H , and temperature. This code uses the equilibrium approach for the calculation of the aqueous species distribution and for the reactions between the aqueous and the solid phases. The equilibrium approach gives a good first approximation and is adequate for fast reacting

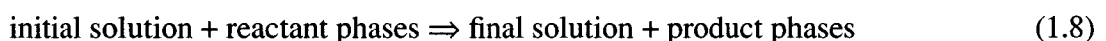
mineral assemblages in recent groundwater systems. Unfortunately, the calculation of saturation states for clay minerals such as illite, chlorite, smectites, and primary silicates such as feldspars, amphiboles, pyroxenes and mica, is hampered by the lack of reliable stability constants (Drever, 1988). In addition, these minerals react very sluggishly (see table 1-2). For the investigated recent groundwaters the P_{CO_2} and the saturation states have been calculated with respect to calcite, dolomite, gypsum, barite, celestite, strontianite, fluorite, and chalcedony, as well as Fe-, Al-, Mn-, and Cr-oxides and -hydroxides. These are potential sources or sinks of dissolved elements.

1.4.2. Inverse modelling

Inverse geochemical modelling combines information on mineral saturation states with mass balance modelling, to identify and quantify mineral reactions in the system. In a mass balance calculation the changes in total concentrations of the elements in *evolutionary* waters are used to calculate the masses of minerals and gases that enter or leave the aqueous phase, to account for the observed changes in composition (Plummer & Back, 1980). The equations of mass-balance models include element mass balance equations, electron conservation equations, and, where appropriate, isotope mass balance equations.

Inverse modelling has been performed to investigate water mineralisation processes occurring between rainwater and groundwater of selected springs of the spatial observation network, between rain water, soil solutions and groundwater at the Lutry site, and between the solutions from the beginning and the end of the leaching experiments.

The computer code NETPATH (Plummer and others, 1994) has been used to calculate the net geochemical mass-balance between the different initial and final waters along hypothesised hydrologic flow paths. NETPATH allows to include several processes, such as dissolution/precipitation, ion exchange, oxidation/reduction, gas exchange, mixing, evaporation, and isotope fractionation and exchange. For a set of mineral and gas phases assumed to be the reactive phases in the system, NETPATH calculates the mass transfer in mol/kg H₂O for every possible combination of these phases that account for the observed changes in water composition along a flow path. The model is of the form



In inverse modelling there are usually several solutions to one geochemical problem, which have to be judged based on the consistency with mineral saturation calculations. For example, a mass balance model that requires the precipitation of a particular mineral is invalid, if saturation calculations indicate that the water is subsaturated with this particular mineral along the flow path. Similarly, mass-balance models are invalid that require dissolution of minerals known to be supersaturated in the system.

1.4.3. Forward modelling

Forward geochemical modelling uses an aqueous speciation model to predict the results of hypothetical reactions. Forward geochemical modelling has been performed with PHREEQC to investigate the geochemical evolution of the spring waters of the spatial observation network and at the Lutry site, as well as the solution evolution in the leaching experiments. Forward modelling includes calculations of non-available or unreliable

dissolved element concentrations at a given gas or mineral saturation state. PHREEQC calculates pH and pe as a function of reaction progress, and mineral solubilities and mass transfer resulting from reversible reactions (aqueous, gas, mineral, solid-solution, surface complexation, and ion exchange equilibria) or irreversible reactions (specified mole-transfer of reactants, kinetically controlled reactions, mixing of solutions, and temperature changes).

II. WATER DATA

2. 1. Analytical methods applied in the AQUITYP project

2. 1. 1. Introduction

As the analytical methods applied in the AQUITYP project have evolved and improved with technological progress and experience, the number of analysed parameters has increased in the more recent studies. This is particularly true for the number of field measurements and the number of analysed trace elements.

A comparison of different groundwater data requires a sound knowledge of sampling methods and analytical processing of the samples. In order to compare the data gathered over the whole time period of the AQUITYP project, a complete overview of the different analytical methods was established. The different types of analytical methods and equipment used since 1981 is shown in the synoptic table 2-1 and table 2-2. During the investigations of each aquifer type (each study) the same analytical equipment and methods were used for comparability reasons. This chapter describes the analytical methods present and past used in the AQUITYP project.

A quality control of the chemical analyses was necessary, because different types of errors might have occurred during sampling, sample treatment and storage, as well as during analytical procedures. Data quality can be judged by the precision and accuracy of the data, and by the detection limit of the method applied (Rollinson, 1993). While *precision* refers to the repeatability of a measurement and reflects random fluctuations in the analytical procedure, *accuracy* displays systematic errors due to faulty procedures or interferences during analysis. The *detection limit* (d.l.) is the lowest concentration which can be “seen” by a particular method. It depends on the blank level (background noise) relative to the element concentration in the sample and on the sensitivity of the analytical method (e.g. Schwedt, 1995).

In order to compare groundwater data from the different authors contributing to the AQUITYP project, a thorough quality control of the chemical water data was performed including several tests to assess data quality and comparability:

- Filtration tests were performed allowing an estimation of the influence on the water chemistry of the filtration procedure.
- Charge balance was recalculated for all water analyses in order to estimate the accuracy of the major ion analyses from the electro-neutrality condition.
- Trace element analyses were checked for specific analytical problems and internal inconsistencies. In particular, element-element scatter plots were made to reveal known spectral interferences and duplicate analyses of a number of samples (same site and sampling date, but different analysis date and methods) were compared.

The result is a compilation of all analytical methods used in the AQUITYP project, a list of potential sampling- and analytical problems, as well as their equipment-related detection limits and accuracy (table 2-5 to table 2-7). A general evaluation of the data produced by the respective methods was made in order to select chemical water data for interpretation during this study.

Parameter	Author	Year, referring to sampling date																			
		81	82	83	84	85	86	87	88	89	90	91	92	93	94	95	96	97	98	99	00
Sampling period																					
	1																				
	2																				
	3																				
	4																				
	5																				
	6																				
Equipment																					
Discharge	1-6	measuring container/chromometer, water stage recorder																			
Temperature	1-6	Horiba, on site										WTW ^a , on site									
E. C.	1-6	Horiba, on site																			
pH	1, 2, 3	pH-paper, on site																			
	4, 5, 6	WTW pH-meter (Ag/AgCl pH-electrode), on site																			
E _H	1-6	WTW pH-meter (Ag/AgCl reference electrode), on site																			
	3, 4, 5, 6	WTW Oxi, on site																			
Dissolved O ₂	1-6	IC ^b (Perkin-Elmer LC10), AAS/FES ^c (Pye-Unicam SP 1900), EDTA- titration (Ca), ion-selective electrode (F)																			
Major elements	1-6	AAS/FES (Pye-Unicam SP 1900), colorimetry (B)										ICP-MS ^e (VG PQ+)					HR-ICP-MS ^f (Fisons instruments Winsford, Cheshire, GB				
Trace elements	1-6	HPLC-IC ^d (Dionex DX 120)																			
Sample treatment																					
Filtration	2, 3, 4, 5, 6	generally not filtered																			
	1	Tunnel springs: 0.45 µm, on site																			
Acidification	2, 3, 4, 5, 6	HCl										HNO ₃ supra pure									
	1	not acidified																			

Table 2-1: Overview of analytical equipment and water sample treatment applied in the AQUITYP project. Analyses were made in the laboratory if not specified otherwise. Authors: 1: Dubois, 1993; 2: Mandia, 1993; 3: Basabe, 1993; 4: Dematteis, 1995; 5: Hesske, 1995; 6: GEOLEP. Abbreviations: a: Wissenschaftlich Technische Werkstätten GmbH, Weilheim, Germany; b: liquid ion chromatography; c: atomic absorption spectro-photometry / flame emission spectro-photometry; d: high pressure liquid ion chromatography; e: inductively coupled plasma source mass spectrometry; f: high resolution inductively coupled plasma source mass spectrometry.

Parameter	Author	Year, referring to sampling date																			
		81	82	83	84	85	86	87	88	89	90	91	92	93	94	95	96	97	98	99	00
Alkalinity (HCO ₃)	1, 2, 3, 5, 6																				
	4																				
Cl, NO ₃ , SO ₄	1-6																				
F	1-6																				
Na, K, Mg	1, 2																				
	3, 4, 5, 6 ^a																				
Sr	6 ^b																				
	2, (3)																				
Ca	1 (3)																				
	4, 5, 6																				
Total Hardness	1, 2																				
	3																				
Si	4, 5																				
	6 ^a																				
Trace elements	6 ^b																				
	1, 2, 3, 5, 6																				
Li	4																				
	1-6																				
B	1, 2, 3																				
	4, 5, 6																				

Table 2-2: Overview of the evolution of chemical analytical methods applied by the different authors. Analyses were made in the laboratory if not specified otherwise. Authors: 1: Dubois, 1993; 2: Mandia, 1993; 3: Basabe, 1993; 4: Dematteis, 1995; 5: Hesske, 1995; 6: GEOLEP. a: long-term monitoring network, samples analysed before 1997; b: samples analysed after 1997.

2. 1. 2. Field measurements

For each groundwater sample a number of physical-chemical parameters were measured on site: discharge (Q), electric conductivity (E.C.), water temperature (T), pH, and redox potential (E_H). Current field measurement procedures are as follows:

- **Discharge (Q)** is measured with a measuring container and a chronometer. Water gauges are installed at the springs of the long-term monitoring network and at other selected sites in order to obtain continuous measurements. To enable the conversion of such water level measurements into discharge values, the water level is measured in a channel of known dimensions. Discharge is proportional to the water level, provided a laminar streaming behaviour in the channel is given (Hölting, 1996:39). Based on individual calibration curves the discharge in L/min is calculated for each spring.
- **Electric conductivity (E.C. corrected to the value at 20°C)** and water **temperature (T)** are measured using a digital apparatus (WTW). Using this method, the temperature measurement has a precision of $\pm 0.2^\circ\text{C}$ and the E.C. measurement of $\pm 1.5\%$.
- The **pH** is measured by means of a digital WTW pH-meter with an Ag/AgCl reference electrode (SenTix combination electrode, analytical precision ± 0.01 pH-units). The apparatus is controlled regularly before sampling campaigns and calibrated when necessary.
- The **redox potential** is measured by a digital apparatus (WTW pH), with an Ag/AgCl reference electrode (reference potential $E_{\text{ref}} = 217$ mV at 10°C , analytical precision ± 2 mV). In order to obtain the redox potential relative to the standard hydrogen electrode (E_H), the measured potential (E_m) is corrected using the reference potential at 10°C according to relation 2.1. In the investigated cold groundwaters, the error introduced by the temperature dependency of the reference potential is smaller than the accuracy of the data.

$$E_H = E_m + E_{\text{ref}} \quad (2.1)$$

- **Dissolved oxygen** is measured by a WTW Oxi apparatus with a membrane covered galvanic sensor.

2. 1. 3. Sampling techniques, water sample treatment and conservation

Groundwater emerging at a spring may be subject to changes in its chemical composition due to the different environmental conditions at the surface. Changes in temperature, redox conditions, and dissolved gases may provoke precipitation of mineral phases and sorption of dissolved compounds and thus alter the in-situ groundwater composition. In addition, the contact with certain materials used in technical installations of the spring surrounding (metal conduits, concrete, etc.) may lead to important modifications of the trace element content of the groundwater (Parriaux & Bensimon, 1990). Finally, changes in the chemical water composition may occur due to inadequate sample storage or contamination during the

period between sampling and analysis. Therefore, sampling techniques and water sample treatment have a major influence on the comparability of chemical groundwater analyses. This is particularly true for trace element analyses.

Several measures have been taken to avoid problems related to changes of natural physical-chemical conditions of the groundwater or to sample contamination. This leads to the following standardisation in sampling, sample treatment and sample conservation techniques in the AQUITYP project:

- To avoid contamination by materials used in technical installations of spring surroundings, springwaters emerging directly from the rock have been preferred (see chapter 3. 2. "Sampling sites and groundwater data" on page 43).
- Bottles of an unbreakable and inert material (PE) are used for sampling and storing the groundwater samples. The bottles are previously rinsed with dilute HNO_3 and distilled water. They are filled completely, in order to avoid gas exchange of the water sample with the atmosphere.
- Water samples are kept at a cool and dark place (refrigerator).
- Groundwater samples are generally *not filtered*. Most samples are from springs used for public water supply, and normally show no visible turbidity. Only when a visibly turbid sample could cause analytical problems, it is filtered with a membrane filtering-device (0.45 μm).
- The samples for cation and trace element analysis are acidified for conservation immediately after sampling to a $\text{pH} < 2$ (addition of 2 ml HNO_3 65% supra-pure per litre of sample). The low pH prevents adsorption on bottle walls and mineral precipitation, as well as microbial activity. This is important, because numerous samples of the long-term monitoring network were stored for several years before analysed.

Suspended particles and colloids

Natural groundwaters contain not only dissolved ions, but also variable amounts of fine suspended matter (e.g. McCarthy & Zachara, 1989). Suspended particles with a diameter of 0.003 to 10 μm (Puls & Barcelona, 1989) or 0.001 to 0.1 μm (Matthess, 1994) are called colloids. Clay minerals, mineral precipitates (e.g. calcite) and weathering products such as Fe- and Al-hydroxides, as well as organic compounds such as humic substances may be present in the water as suspended particles of colloidal size (see figure 2-1). Clay minerals usually constitute the main colloid fraction.

The inorganic colloid load of groundwaters originates from the aquifer material. The mobilisation of colloidal matter may have various causes. Colloids can be mobilised due to increased water flow during high water periods, or they form as a consequence of changes in chemical parameters of the water. For example, when the groundwater gets in contact with the atmosphere at the spring, carbonate or Fe-hydroxide colloids may form due to gas exchanges with the atmosphere and redox state changes, respectively.

Trace elements can move through fractured or porous media not only as dissolved species, but also as solid phases or polymeric species. If a water sample is acidified without previous filtration, colloids and small suspended particles dissolve and cannot be

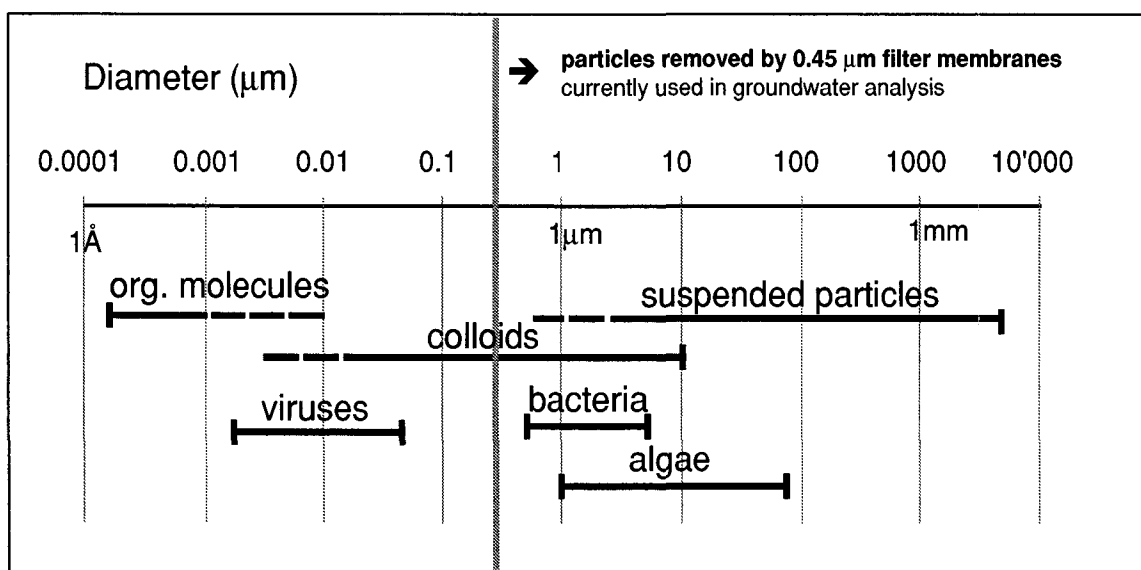


Figure 2-1: Size spectrum of water-borne particles (after Stumm, 1977).

distinguished any more from originally dissolved components. Hence, the values for certain elements do not always correspond to the amounts of truly dissolved ions. Especially for elements including Al, Fe, Mn, and Si, the presence of colloids can bias measured concentrations. Filtration with 0.45 μm mesh diameter membranes removes most of the suspended matter (figure 2-1). Aluminium is typically part of colloid particles with a very small size and passes through such filter membranes (Kennedy and others, 1974). To obtain the true concentration of dissolved Al (which is an extremely insoluble element in dilute waters at near-neutral pH and usually present in concentrations of 2-4 μg dissolved Al /L), filtration through a 0.1 μm filter is necessary. In addition, obtaining correct values of dissolved Al is even more problematic, because Al is ubiquitous and contamination is difficult to prevent.

The capacity of colloidal matter to *adsorb* trace elements has to be considered in the study of ultra-trace elements. Depending on their behaviour and mobility in the water, colloids can retard or accelerate the transport of adsorbed trace metals (McCarthy & Zachara, 1989). Filtration of the water samples removes the adsorbed fraction from solution and thus results in an underestimation of the concentrations of certain trace elements of importance to groundwater quality. As it has been pointed out earlier (e.g. Puls & Barcelona, 1989), the decision whether to filter or not to filter the water samples should depend on the aim of the investigation. When looking at trace element analyses, it is important to know if a water sample has been filtered or not, at what time filtration took place (before or after acidification), and which was the size of the filter mesh.

The study of geogenic trace elements requires filtration; for engineering-type groundwater quality studies though filtration might not be required. In the AQUITYP project the majority of groundwater samples are taken from springs used for public water supply and normally show no visible turbidity. Furthermore, drinking water standards are based on total amounts of chemical elements in the water, and it is important, not to underestimate element concentrations by removing the colloidal fraction.

Filtration test

As shown above, for the interpretation of trace elements in groundwaters investigated in the AQUITYP project, it is necessary to understand possible effects of the filtration procedure applied on the trace element composition. To better estimate the effects of the filtration procedure, a comparative test has been performed. For this purpose water samples of three typical springs were analysed in filtered and non-filtered state, two in the Molasse and one in the crystalline. The two Molasse springs (Lutry spring and Pierre-Ozaire spring) were chosen, because they were going to be investigated in more detail (chapter IV. "Chemical Weathering of Burdigalian Sandstone: Sources and Behaviour of Chromium" on page 129). The crystalline Brocard spring was selected, because the crystalline groundwaters mostly come from artificial springs in tunnels and galleries and therefore had to be filtered (syringe filtering system, 0.45 µm, on site). Because the colloid load is higher during high water periods, samples from low water conditions (4.2.1999) and high water conditions (26.5.1999) have been compared. None of the samples was visibly turbid.

Filtration was performed before sample acidification with a Pyrex filtering device equipped with a filter membrane with 0.45 µm mesh diameter (HAWP type hydrophilic cellulose-ester mixture, Millipore). Tests at the GEOLEP laboratory have shown that this filter type generates a very low contamination of trace elements (Dauchy, 1994). The filter device and the bottles were rinsed first with a nitric acid solution (2 ml/L HNO₃ supra-pure, MERCK), then three times with distilled water, and finally with part of the sample solution. Subsequently, filtered samples and non-filtered samples were analysed for trace elements.

The results of the filtration test are displayed in figure 2-2. The test shows that the Al concentrations are 25-30% lower in the filtered samples from the Brocard spring. As clay minerals typically constitute the main colloid fraction, silica is also influenced by the colloid load. However, this effect is negligible compared to the total amount of silica (several mg total silica/L vs. some µg/L of colloidal silica). The Fe concentrations were also slightly lower in all filtered samples, but as the concentrations are very near the detection limit the absolute differences are very small. This indicates that Al, Si and probably also Fe are partly present as colloids and not only as dissolved ions. It confirms the hypothesis that Al, Si, and Fe are the elements most influenced by the presence of colloids.

The concentrations of Li, Mn, Co, Cu, Cd, Rb, and Pb in all three springs, as well as in addition Mo, As and U in the Lutry and Pierre-Ozaire springs are below or near detection limit. The small absolute differences in the concentrations of these elements lie within the range of analytical accuracy and are therefore insignificant. The differences in composition between the filtered samples from low and high water conditions from the Brocard spring are also within analytical accuracy.

The test shows further, that there is a potential risk of sample contamination during the filtration procedure. The samples from the Lutry and Pierre-Ozaire springs and the low water sample from the Brocard spring were contaminated with Zn (up to 90% more Zn in the filtered samples). As the filtering device itself induces negligible trace element contamination (Dauchy, 1994), and because the GEOLEP laboratory is a routine chemistry lab equipped with an adequate air filtering system, but not a high-purity "clean-lab", the Zn could originate from the contact with dust particles in the laboratory air during the filtration procedure. Alternatively, as tap water often contains high Zn concentrations from conduits, the solution used for rinsing is another possible source of contamination (malfunction of the ion exchanger or confusion of water bottles).

Concluding it can be said that in the three analysed spring waters the influence of colloids on the trace element content appears to be very small, except for Al and probably Fe, which can also be part of colloidal matter. The trace element analyses of the tunnel

springs in the crystalline, which were filtered on site can therefore be compared to the non-filtered spring waters. On the other hand, it appears that the error induced by potential sample contamination during the filtration procedure may be larger than the error induced by the effect of colloids. Not filtering the samples routinely seems therefore to be the most coherent choice to attain the objectives of the AQUITYP project.

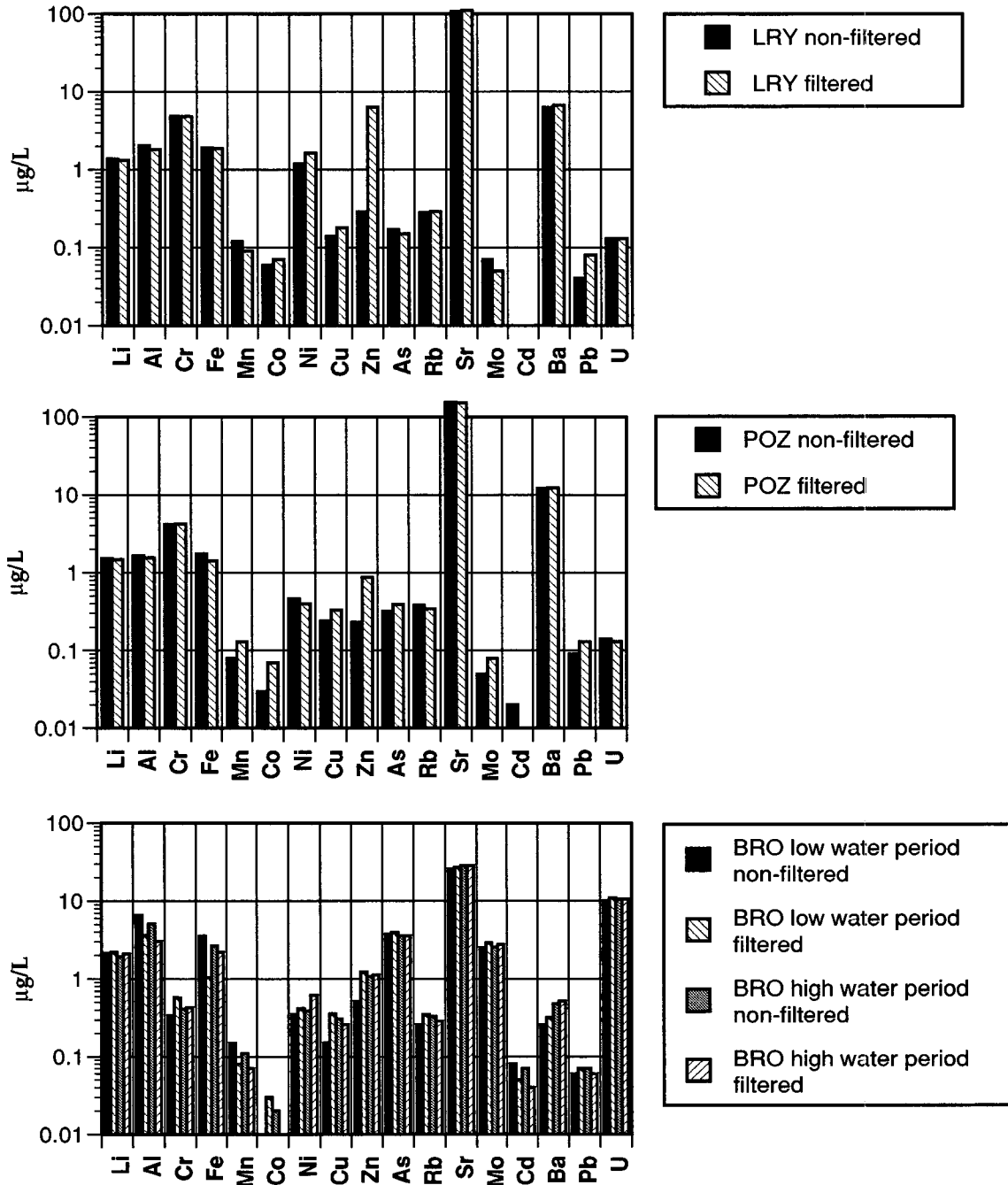


Figure 2-2: Results of the filtration test. Filtered and non-filtered samples from the Lutry (LRY) and the Pierre-Ozaire (POZ) springs in the molasse sediments, as well as samples from the Brocard spring (BRO) in the crystalline at low (4.2.1999) and high water period (26.5.1999) are compared. A HAWP filter membrane with 0.45 µ mesh diameter was used.

2.1.4. Laboratory analytical methods

Chemical groundwater analyses were performed in the chemistry laboratory of the GEOLEP, under the direction of Th. Lutz (until 1989) and Dr. M. Bensimon (since 1989). In each sample 10 major and minor anions (Cl^- , SO_4^{2-} , NO_3^- , F^- , and alkalinity) and cations (Na^+ , K^+ , Mg^{2+} , Ca^{2+} , and Sr^{2+}), dissolved silica, and total hardness were analysed. Based on the availability of analytical methods at the time of the different studies up to 28 trace elements were analysed (table 2-3). Since 1989, when the HR-ICP-MS system got into service, most of the remaining elements of the periodic table have been checked, but they were generally not detected.

	Aquifer type	Author	Analysed trace elements
Spatial observation network	Crystalline	Dubois, 1993	Li, B, Ba, As, Rb, Mo, W, U
	Evaporites	Mandia, 1993	Al, As, B, Ba, Br, Cd, Cr, Cu, Ge, Li, Mn, Ni, Rb, Sc, U, V, Y, Zn
	Flysch	Basabe, 1993	Al, B, Ba, Br, Co, Cr, Cu, Fe, La, Li, Mn, Mo, Ni, Pb, Rb, Ti, U, V, Zn
	Carbonates	Dematteis, 1995	Al, As, B, Ba, Br, Cd, Co, Cr, Cu, Fe, I, Li, Mn, Mo, Ni, Pb, Rb, Sc, Ti, U, V, Zn
	Molasse	Hesske, 1995	Al, As, B, Ba, Be, Bi, Br, Cd, Co, Cr, Cu, Fe, Ga, Ge, I, Li, Mn, Mo, Ni, Pb, Rb, Sc, Se, Sn, Ti, U, V, Zn
Long-term monitoring network	All above mentioned plus quaternary	GEOLEP	Al, As, B, Ba, Br, Cd, Co, Cr, Cs, Cu, Fe, I, Li, Mn, Mo, Ni, Pb, Rb, Sc, Se, Ti, U, V, W, Zn

Table 2-3: Trace elements analysed by the previous researchers.

Current major and minor elements analytical methods

Major anion analyses were carried out as soon as possible after sampling in order to avoid sample conservation problems. Alkalinity was analysed in the laboratory, if possible within a day after sampling, and the other major anions and total hardness were analysed within one week after sampling. Current major elements analytical methods are listed in table 2-4.

Compound	Unit	Analytical method
alkalinity	mg/L	titration (0.1 N HCl titration to pH 4.3)
Cl^- , SO_4^{2-} , NO_3^- , F^- , Na^+ , K^+ , Mg^{2+} , Ca^{2+}	mg/L	high-pressure liquid ion chromatography (HPLC-IC, Dionex DX 120, equipped with an auto-suppressor)
Sr^{2+}	mg/L	HR-ICP-MS
Si	mg/L	colorimetry (ammonium molybdate)
total hardness	°F ^a	titration (EDTA)

Table 2-4: Current major and minor elements analytical methods.

a. French hardness degrees; 1°F \equiv 10 mg/L CaCO_3

Current trace elements analytical methods

All trace elements are currently analysed by HR-ICP-MS in the GEOLEP laboratory. HR-ICP-MS is a very sensitive and fast method with low detection limits in routine analyses of most elements of the periodic table (about 0.2 µg/L). This method is characterised by a large dynamic range of six orders of magnitude, which allows analysing element concentrations ranging from 0.1 µg/L to 100 mg/L in the same sample without additional treatment. Furthermore, the interpretation of the mass spectrum is relatively simple. All these properties make HR-ICP-MS a convenient method for the analysis of trace elements in groundwaters. Trace element analyses are performed in routine mass resolution mode (resolution $\approx 3000^1$) at 10% transmission (diaphragm aperture).

Quality control of the chemical data

Major elements

The accuracy of major ion analyses is checked with the electro-neutrality condition (E.N.), which says that the sums of negatively and positively charged ions in meq/L must be balanced:

$$\text{E.N. [\%]} = 100 \cdot \frac{(\sum \text{cations} + \sum \text{anions})}{(\sum \text{cations} - \sum \text{anions})} \quad (2.2)$$

An error of up to $\pm 5\%$ on the charge balance is generally acceptable for routine analysis (e.g. Schmassmann 1984, Appelo & Postma, 1996:17) and was allowed for the data used in this study.

Trace elements

The accuracy of trace element analyses is much more difficult to estimate than the accuracy of major element analyses. Per definition, trace elements represent less than 1% of the total dissolved compounds in a water sample. Therefore, results of trace element analyses cannot be checked by charge balance calculations. For the same reason, trace elements are also much more liable to sample contamination than major elements. However, the data can be checked for *specific analytical problems* and *inconsistencies*. Furthermore, the *long-term monitoring* allows a certain control over the natural fluctuations. A single outstanding value must then be interpreted with caution, because the probability that sample contamination or a faulty measurement have occurred is higher than the probability of a natural anomaly.

Trace element analyses made with a standard ICP-MS *mass unit resolution* system, i.e. the trace element analyses of crystalline, flysch and evaporite groundwaters made before 1993, can be problematic for certain trace elements. This is mainly due to spectral interferences and so-called memory effects, which are related to insufficient instrumental resolution of the mass spectra of analysed trace elements and other elements in the sample

1. The resolution (dimensionless number) is the isotope mass divided through the mass difference (peak width) at 10% intensity.

(Bensimon and others 1994, 1996; Dauchy, 1994). With the currently used high resolution ICP-MS system a mass resolution as high as 8000 can be reached, and such problems can today be avoided.

Spectral interference

Different types of spectral interferences occur with a standard ICP-MS *mass unit resolution* system (Dauchy, 1994). The most important spectral interferences occur, when elements such as O, H, C, Na, Si, K, Cl and S from the sample, and Ar from the plasma-gas react within the plasma. The resulting molecules may have masses similar to those of the analysed trace elements and interfere with their peaks in the mass spectrum (matrix-effect). Spectral interferences therefore depend on the sample composition. The higher the concentrations of interfering elements in a sample are, the greater is the chance that problematic molecules of even rare isotopes interfere with the analysed trace elements. Matrix effects are therefore particularly annoying in highly mineralised waters, such as in the evaporite groundwaters, or in samples that were acidified with HCl instead of HNO₃ (springs of the long term monitoring network sampled before 1985).

In practice, spectral interference result in higher detection limits and a lower accuracy for the involved trace elements. Precautions can be taken for known spectral interferences to minimise their effect on the quantification of the trace element of interest; however, the problem persists for unknown spectral interference pairs. Trace elements affected by spectral interference such as V, Cr, Fe, Ni, Cu, and Zn can be quantified using a different isotope. This may though lead to a loss in sensitivity, due to the lower natural abundance of this isotope. Elements that consist of only one naturally occurring stable isotope such as Be, Al, Sc, Mn, Co, As, Y, I, Cs, Bi, and Th are consequently the most problematic ones.

The older trace element data analysed before 1993 with a standard ICP-MS system (crystalline, evaporite, and flysch groundwaters) were checked for potential spectral interferences. Scatter plots were made of those elements with known spectral interferences to reveal potential problems.

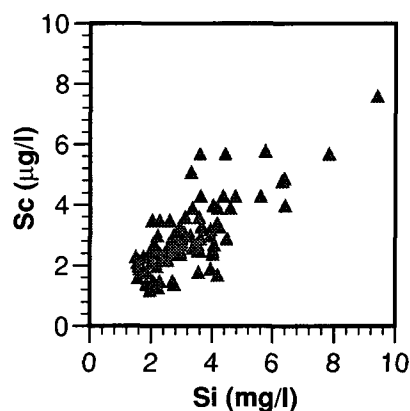


Figure 2-3: Correlation plot of Sc analysed with a standard ICP-MS system and Si, revealing spectral interference.

A spectral interference of Si and Sc has been identified in the evaporite groundwaters, which may be important even in dilute groundwaters (figure 2-3). At Si concentrations ranging from 1 to 20 mg/L, Si complexes formed in the plasma generate a signal, which cannot be distinguished from the signal of the ⁴⁵Sc isotope in measurements performed standard ICP-MS systems (Bensimon and others, 1994). Tests with Si standard solutions showed, that 1 mg Si/L generates a signal at mass 45 that corresponds to approximately 1 µg Sc/L. Indeed, the scatter plot of Sc and Si analysed by this method in the evaporite groundwaters, shows a trend between these two elements, which strongly indicates spectral interference. ⁴⁵Sc is the only stable Sc isotope, the problem can therefore not be avoided by measuring a different isotope. Therefore Sc must be disregarded in the interpretation of evaporite groundwaters.

Memory effects

Hg, halogens, as well as B and Li may be affected by a so-called “memory effect”. This is due to partial adsorption of these elements onto the walls of the glassware within the spectrometer, leading to falsified measurements and a higher detection limit to 5-10 µg/L for these elements. This effect is largest for Hg and I and less pronounced for B, Br and Li. Therefore, the detection limit is higher for these elements.

Systematic errors

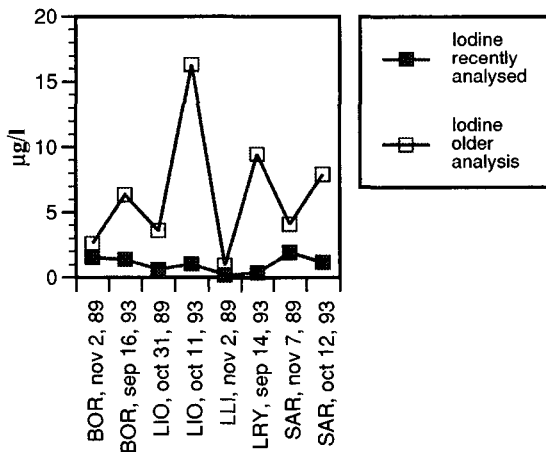


Figure 2-4: Comparison of duplicate iodine analyses made on the same samples suggesting a systematic but not uniform overestimation due analytical artefacts in analyses performed before 1994.

An internal inconsistency has been discovered by comparing samples analysed in duplicate. Some samples from springs of the long-term monitoring network were analysed twice (same spring/same sampling date), once in 1989 by previous researchers (Dematteis, 1995; Hesske, 1995; Basabe, 1993) and once recently together with the whole stored sample series of these springs. All of the recently repeated iodine analyses have shown *lower* concentrations than the earlier analyses made on the same samples (figure 2-4). Because of an analytical artefact, the iodine concentrations have been overestimated in the analyses performed before 1994 (Bensimon, personal comm.). Evaporation of the acidified iodine standard is suspected to be the reason of this artefact.

2. 2. Selection of data

The following tables (table 2-5 to table 2-7) give an overview of the analytical methods applied in the AQUITYP project, their equipment-related detection limits and accuracy, and potential sampling and analytical problems. The last column gives a general evaluation of the data produced by the respective methods.

2. 2. 1. Field measurements

In the long term monitoring network, a HORIBA apparatus was used until 1985 for the measurement of E.C., pH, and temperature. In the spatial observation network, mainly in crystalline, evaporite and flysch groundwaters, pH measurements were earlier made by pH indicator paper (MERCK). Later, all physical-chemical parameters were determined on-site by electrode measurements with digital WTW measuring devices. Sometimes, pH indicator paper (MERCK) was also used as a semi-quantitative backup in case of malfunction of the apparatus, or the pH was measured in the laboratory. pH is a crucial parameter, which has major importance in quantitative calculations of water saturation states with respect to minerals. The problems involved in pH measurements are mainly related to CO₂ out-gassing which increases the pH, and to the temperature dependency of the electrode calibration. pH-measurements made with indicator paper and those measured in the laboratory have to be regarded as semi-quantitative and they limit the interpretation of trace elements in these groundwaters. The data obtained with the HORIBA apparatus are used with care because the quality of the data is doubtful.

E_H has been measured regularly since 1987, and dissolved oxygen since 1989. Because both measurements are problematic, the obtained field values are considered to be semi-quantitative.

Parameter	Unit	Method	Sampling and analytical problems	Application range	Accuracy	General evaluation
Field measurements						
Q	L/min	measuring container / chronometer	poor accuracy at high discharge		±10%	quantitative
E.C.	µS/cm	WTW	instrumental drift	1-2·10 ⁶	±5%	quantitative
		Horiba			ca. ±5%	used with care
T	°C	WTW		-5 to +100	±0.2°C	quantitative
		Horiba			ca. ±0.2°C	used with care
pH	pH-units	WTW pH-meter, (Ag/AgCl pH-electrode)	CO ₂ out-gassing; T-dependency	0-14	±0.1 pH-units	quantitative
		Horiba			ca. ±0.2 pH-units	used with care
		MERCK indicator paper	CO ₂ out-gassing, subjective perception of small colour differences, alteration of colour indicators		±0.2-0.5 pH-units	semi-quantitative
E _H	mV	WTW pH-meter, (Ag/AgCl ref. electrode)	no unique E _H due to disequilibrium of redox pairs	-1250 to +1250	±20 mV	semi-quantitative
O ₂ (aq)	mg/L	WTW Oxi (galvanic sensor)	O ₂ in-gassing from the atmosphere, T-dependency	0-50	±10%	semi-quantitative

Table 2-5: Field measurements: overview of analytical methods used in the AQUITYP project, their application range and accuracy, potential sampling- and analytical problems, as well as a general evaluation of the data produced by the respective methods.

2.2.2. Major elements

In the AQUITYP project, analytical methods for major elements were most subject to changes. Particularly Ca²⁺ was analysed by many different methods, according to concentration ranges in the different groundwater types and available equipment. Together with alkalinity, Ca²⁺ is the most concentrated ion in virtually all investigated groundwaters, and obtaining reliable values for these two constituents is particularly important. Calcite precipitation due to CO₂ out-gassing is the main disturbing factor for both elements. In the case of the carbonate karst groundwaters, which were gathered over southern Europe, a field titration set was used to analyse alkalinity and Ca²⁺, in order to avoid carbonate precipitation during the long transport which would have resulted in an underestimation of these constituents (Dematteis, 1995). Analytical inaccuracies in major element analysis can be revealed by using the charge balance equation. Of a total of 1824 groundwater analyses 150 had incomplete major element analyses or more than 5% error on the charge balance. These data were not used.

Parameter	Unit	Method	Sampling and analytical problems	Detection limit	Accuracy	General evaluation
Major and minor anions						
F	mg/L	HPLC-IC		0.2	±10%	quantitative
		ion selective electrode		0.2	±10%	
Cl	mg/L	HPLC-IC		0.2	±5%	quantitative
		IC		1	±5%	
NO₃	mg/L	HPLC-IC		0.2	±5%	quantitative
		IC		1-2	±5%	
SO₄	mg/L	HPLC-IC		0.2	±5%	quantitative
		IC		1-2	±5%	
Alkalinity	mg/L	titration (HCl)	calcite-precipitation due to CO ₂ out-gassing	0.5	±5-10%	quantitative
Major and minor cations						
Mg	mg/L	HPLC-IC		0.2	±5-10%	quantitative
		HR-ICP-MS		0.2	±5-10%	
		AAS/FES		0.2	±5-10%	
Ca	mg/L	HPLC-IC	calcite-precipitation due to CO ₂ out-gassing	0.2	±5-10%	quantitative
		HR-ICP-MS		2-4	±5-10%	
		ICP-MS		2-4	±5-10%	
		titration (EDTA)		2-4	±5-10%	
		AAS/FES		2-4	±5-10%	
Sr	mg/L	HR-ICP-MS		0.001	±10%	quantitative
		ICP-MS		0.010	±10%	
	mg/L	AAS/FES		0.01-0.02	±10%	
Na	mg/L	HPLC-IC		0.2	±5-10%	quantitative
		HR-ICP-MS		0.2	±5-10%	
		AAS/FES		0.2	±5-10%	
K	mg/L	HPLC-IC		0.2	±5-10%	quantitative
		HR-ICP-MS		0.2	±5-10%	
		AAS/FES		0.2	±5-10%	
Silica and total hardness						
Si	mg/L	colorimetry (ammonium molybdate)		0.5	±5-10%	quantitative
Total hardness	°F ^a	titration (EDTA)		0.2-0.5	±1-5%	quantitative

Table 2-6: Major and minor elements: analytical methods used in the AQUITYP project, their equipment-related detection limits and accuracy, potential sampling and analytical problems, as well as a general evaluation of the data produced by the respective methods.

a. French hardness degrees; 1°F ≡ 10 mg/L CaCO₃

2.2.3. Trace elements

The filtration test (see chapter "Suspended particles and colloids" on page 24) showed that the influence of colloidal matter is generally very small, except for Al, Fe, and Si, which may partly be present in colloidal matter. Filtered and non-filtered samples can therefore be compared. The Al and Fe concentrations in the unfiltered samples represent total concentrations (i.e. dissolved + colloidal) and are therefore not used in saturation state calculations. The potential contamination problems arising from the filtration procedure have no limiting consequences on the data quality of the filtered crystalline groundwater samples, because (1) only a restricted number of trace elements were analysed, and (2) the analysed elements are present at relatively high concentrations and therefore less prone to contamination by air-contact.

In the AQUITYP project, trace elements were mostly analysed by ICP-MS. Only the Li and B analyses in crystalline and evaporite groundwaters have been performed by FES and azomethine-H colorimetry and thus have higher detection limits.

The detection limit of trace elements depends on the element concentration in the sample relative to the blank level (background noise) and on the sensitivity of the analytical method. Blank values include all sorts of potential contamination, which can occur during sample storage and preparation, as well as during the analytical procedure itself. In a routine chemistry laboratory the air has to be considered as an important source of contamination. Generally, Al, Zn, and to a minor extent Cu and Pb are most sensitive to this type of contamination. Furthermore, the acid used for sample acidification (HNO_3 , 65% supra-pure, MERCK) contains traces of nearly all elements. Guaranteed concentrations of most concentrated elements in this acid are $<10 \mu\text{g Fe/L}$, $<10 \mu\text{g Ni/L}$, $<5 \mu\text{g Al/L}$, and $<5 \mu\text{g Zn/L}$. However, considering the very low concentrations and the small quantity of acid added to a sample (2-4 ml/L), this source of contamination can be neglected. There is also a small contamination of B possible from the glassware. A blank correction was routinely made for all trace element analyses.

Considering all of this, an accuracy of $\pm 10\%$ is accepted for all the data used in this study. Because of the matrix effects, no exact detection limit but a range for each element is given (table 2-7). For most trace elements in the investigated dilute groundwaters the detection limit is about $0.2 \mu\text{g/L}$. The trace elements As, B, Li, Sr, I, Br, Fe, and Al have higher detection limits due to the analytical problems described earlier. When no spectral interference of the sample matrix is present) there can be a significant signal even below this given detection limit. Elements that gave no signal at all are referred to as „not detected“. The trace elements Be, Sc, Ti, Co, Ga, Ge, Sn, La, Bi, and Se are generally below $0.2 \mu\text{g/L}$ and will therefore not be discussed further. The Sc values of the evaporite groundwaters, are not used for further discussion, because spectral interference problems were discovered only after the analyses were made. Other elements liable to spectral interference such as Al, V, Cr, Mn, Fe, Ni, Cu, and Zn analysed with the standard ICP-MS system have higher detection limits and are thus interpreted with caution. Spectral interference of a Cl-complex with As results in a higher detection limit of up to $1 \mu\text{g/L}$ for As in samples with Cl concentrations higher than a few mg/L. The As data analysed with the standard ICP-MS system were therefore also interpreted with caution. In samples acidified with HCl (i.e. samples of the long-term monitoring network gathered before 1985) the As values were corrected for the effect of Cl interference (Bensimon, personal communication). The trace elements B, Br, Li, and particularly iodine are affected by a so-called memory effect resulting in an increase of their detection limits to 5-10 $\mu\text{g/L}$. As these elements are usually present in concentrations as low as a few $\mu\text{g/L}$ in the investigated recent groundwaters, their concentrations are considered to be semi-quantitative. The iodine concentrations have been

overestimated in the analyses performed before 1994 because of an analytical artefact. These data are therefore not used.

All samples of the long-term monitoring network were analysed for trace elements by HR-ICP-MS between 1994 and 1996, under the same analytical conditions. In contrast to major elements, which have been analysed immediately after each sampling campaign, the about thirty acidified trace element samples from each site were analysed together as series. This circumstance is very important, as it allows to exclude influences of variable analytical conditions. The trace element data quality and comparability in these time series is therefore better than for the older trace element data of the spatial observation network.

Parameter	Unit	Method	Sampling and analytical problems	Detection limit	Accuracy	General evaluation
Alkali and earth-alkali trace elements						
Li	µg/L	HR-ICP-MS	memory effect, transmission efficiency	≈1-10	±10%	semi-quantitative
		ICP-MS		≈1-10	±10%	
		FES		5 ^a	±10%	
Rb	µg/L	HR-ICP-MS		≈0.2	±5-10%	quantitative
		ICP-MS		≈0.2	±5-10%	
Be	µg/L	HR-ICP-MS		≈0.2	±10%	generally b.d.l. ^b
Ba	µg/L	HR-ICP-MS		≈0.2	±5-10%	quantitative
		ICP-MS		≈0.2	±5-10%	
Halides and non-metal trace elements						
Br	µg/L	HR-ICP-MS	memory effect	≈1-10	±10%	semi-quantitative
		ICP-MS		≈1-10	±10%	
I	µg/L	HR-ICP-MS	memory effect	≈1-10	±10%	semi-quantitative; analyses older than 1994 are not used
		ICP-MS		≈1-10	±10%	
B	µg/L	HR-ICP-MS	memory effect	≈1-10	±10%	semi-quantitative
		ICP-MS	memory effect, spectral interference	≈1-10	±10%	
		colorimetry (azomethine H)		25 ^a	±10%	
As	µg/L	HR-ICP-MS	spectral interference	≈0.5 (1 ^c)	±5-10%	quantitative
		ICP-MS		≈0.5 (1 ^c)	±10%	
Se	µg/L	HR-ICP-MS		≈0.2	±10%	generally b.d.l.

Table 2-7: Trace elements 1: Analytical methods used in the AQUITYP project, their equipment-related detection limits and accuracy, potential sampling and analytical problems, as well as a general evaluation of the data produced by the respective methods.

a. Rodier, 1996

b. b.d.l.: below detection limit

c. higher detection limit in samples with Cl concentrations higher than a few mg/L

Parameter	Unit	Method	Sampling and analytical problems	Detection limit	Accuracy	General evaluation
Metal trace elements						
Al	µg/L	HR-ICP-MS	colloids	≈0.2	±10%	semi-quantitative
		ICP-MS	colloids, spectral interference	≈0.2-0.5	±10%	
Sc	µg/L	HR-ICP-MS		≈0.2	±5-10%	generally b.d.l. ^a
		ICP-MS	spectral interference	≈0.2-0.5	±10%	not used
Ti	µg/L	HR-ICP-MS		≈0.4	±10%	generally b.d.l.
V	µg/L	HR-ICP-MS		≈0.2	±5-10%	quantitative
		ICP-MS	spectral interference	≈0.2-0.5	±10%	used with caution
Cr	µg/L	HR-ICP-MS		≈0.2	±5-10%	quantitative
		ICP-MS	spectral interference	≈0.2-0.5	±10%	used with caution
Mn	µg/L	HR-ICP-MS	colloids	≈0.2	±5-10%	quantitative
		ICP-MS	colloids, spectral interference	≈0.2-0.5	±10%	used with caution
Fe	µg/L	HR-ICP-MS	colloids, spectral interference	≈2	±10%	semi-quantitative
		ICP-MS		≈2	±10%	
Co	µg/L	HR-ICP-MS		≈0.2	±5-10%	generally b.d.l.
		ICP-MS	spectral interference	≈0.2-0.5	±10%	
Ni	µg/L	HR-ICP-MS		≈0.2	±5-10%	quantitative
		ICP-MS	spectral interference	≈0.2-0.5	±10%	used with caution
Cu	µg/L	HR-ICP-MS		≈0.2	±5-10%	quantitative
		ICP-MS	spectral interference	≈0.2-0.5	±10%	used with caution
Zn	µg/L	HR-ICP-MS	potential pollution	≈0.2	±5-10%	used with caution
		ICP-MS	spectral interference	≈0.2-0.5	±10%	
Ga	µg/L	HR-ICP-MS		≈0.2	±5-10%	generally b.d.l.
Ge	µg/L	HR-ICP-MS		≈0.2	±5-10%	generally b.d.l.
Y	µg/L	ICP-MS		≈0.2	±5-10%	used with caution
Mo	µg/L	HR-ICP-MS		≈0.2	±5-10%	quantitative
		ICP-MS		≈0.2	±5-10%	
Cd	µg/L	HR-ICP-MS		≈0.2	±5-10%	quantitative
		ICP-MS	spectral interference	≈0.2	±5-10%	used with caution
Sn	µg/L	HR-ICP-MS		≈0.2	±10%	generally b.d.l.
La	µg/L	ICP-MS		≈0.2	±10%	generally b.d.l.

Table 2-8: Trace elements 2: Analytical methods used in the AQUITYP project, their equipment-related detection limits and accuracy, potential sampling and analytical problems, as well as a general evaluation of the data produced by the respective methods.

Parameter	Unit	Method	Sampling and analytical problems	Detection limit	Accuracy	General evaluation
W	µg/L	HR-ICP-MS		≈0.2	±5-10%	quantitative
		ICP-MS		≈0.2	±5-10%	
Pb	µg/L	HR-ICP-MS		≈0.2	±5-10%	quantitative
		ICP-MS		≈0.2	±5-10%	
Bi	µg/L	HR-ICP-MS		≈0.2	±5-10%	generally b.d.l.
U	µg/L	HR-ICP-MS		≈0.2	±5-10%	quantitative
		ICP-MS		≈0.2	±5-10%	

Table 2-8: Trace elements 2: Analytical methods used in the AQUITYP project, their equipment-related detection limits and accuracy, potential sampling and analytical problems, as well as a general evaluation of the data produced by the respective methods.

a. b.d.l.: below detection limit

2.3. AQUITYP DataBase

The *AQUITYP-DataBase* was designed in order to allow fast sorting and data retrieval, and to make this large number of quality controlled water data accessible to different users in the GEOLEP in the future. All water data from the different previous studies in the AQUITYP project were standardised and fed into this database.

2.3.1. Database structure

The *AQUITYP DataBase* is a FileMaker Pro 4 database (Claris Corporation, 1997). It contains the two files “Sites” and “Analyses”, which are related by an internal ID-number (see figure 2-5). Each site is identified by a unique code, while the different water analyses from a particular site are identified by their sample number.

The different data categories, such as site location data, aquifer geology and site characteristics, field measurements, major and minor elements, trace elements, isotopes, and analytical details, are organised in separate data sheets with distinctive colours, to allow a straightforward navigation. The chemical data can be viewed as individual data sheets of selected samples or as a list of all water analyses from a particular site. Chemical concentrations in moles and equivalents, total dissolved solids and charge balance are calculated automatically. In addition, the average values of all analyses from a particular site are calculated automatically.

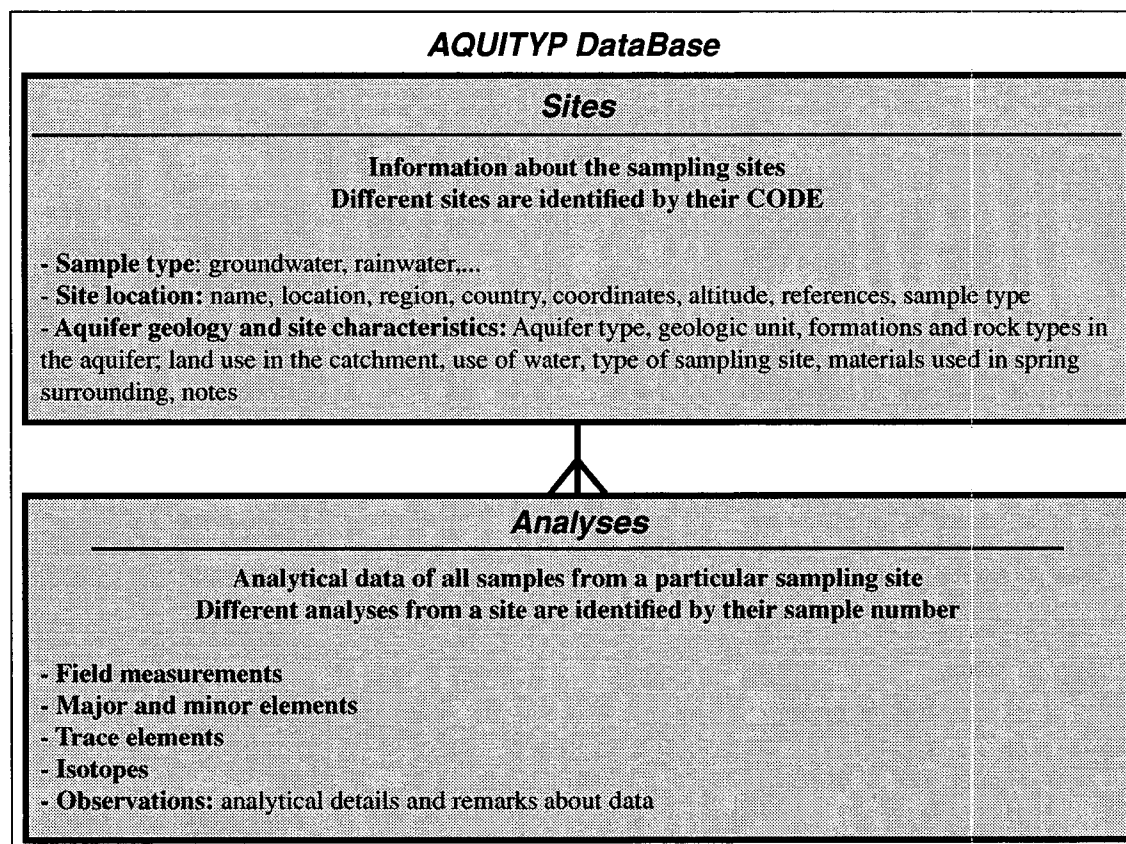


Figure 2-5: Structure of the AQUITYP DataBase.

AQUITYP DataBase

ID 13

CODEBOR		Geological Unit: Préalpes médianes rigides	
Sample Type: Recent GW		Formations: Trias. - Malm	
Aquifer Type: Carbonates		Rocktypes: Limestone, dolostone, marl, evaporite rocks	
Name: Bornels		Catchment land use:	
Location: L'Etivaz		Use of water: drinking water	
Region/Canton: VD	Country: Switzerland	Type of sampling site: surrounded spring	
Coordinates: 576.780 / 142.260 / 1140 m		Materials used in spring surrounding:	
MapN°: 1265		Notes:	
Information, Refs.:			

Sample N°	24	Sampling Date	15.10.1992	Author	GEOLEP	Author's Ref N°	
-----------	----	---------------	------------	--------	--------	-----------------	--

Field measurements							
Discharge [l/min]	3200	Water Temp [°C]	5.7	E _i [mV]	441	O ₂ diss. [mg/L]	11.8
E.C. at 20°C [mS/cm]	289	pH [pH-units]	7.90	pe	7.449	O ₂ sat [%]	107

Major and Minor Elements			
		[mg/L]	[mmol/L]
Anions	HCO ₃ ⁻	123.5	2.024
	F ⁻	0.06	0.003
	Cl ⁻	0.4	0.011
	NO ₃ ⁻	3.0	0.048
	SO ₄ ²⁻	50.2	0.523
Cations	Ca ²⁺	50.2	1.252
	Mg ²⁺	6.25	0.257
	Sr ²⁺	0.32	0.004
	Na ⁺	0.28	0.012
	K ⁺	0.13	0.003
	NH ₄ ⁺		
Other dissolved substances			
	Si	0.56	0.020
	P		
Total Hardness [°F]		14.70	
Temporary hardness [°F]			
TDS [mg]		235.67	
Σ Anions [meq]		3.13	
Σ Cations [meq]		3.04	
Ionic balance [%error]		-1.45	

Filtration no					
Analytical Notes Trace elements analysed (sample from 9.10.1996), but not detected: Be, Sc, Co, Ga, Ge, Se, Y, Zr, Nb, Ru, Rh, Pd, Ag, In, Sn, Sb, Te, Cs, La, Ce, Pr, Nd, Sm, Eu, Gd, Tb, Dy, Ho, Er, Tm, Yb, Lu, Hf, Ta, W, Re, Os, Ir, Pt, Au, Hg, Tl, Pb, Bi, Bk, Th.					
Observations					

Trace Elements					
Alkali and earth-alkali trace elements			Metal trace elements		
	[mg/L]	[mmol/L]	[mg/L]	[mmol/L]	[mg/L] [mmol/L]
Li	0.83	0.1196	Al	82.49	3.0573 Ga
Rb	0.30	0.0035	Sc		Ge
Cs			Ti	0.00	0.0000 Y
Be			V	0.15	0.0029 Mo 0.22 0.0023
Ba	17.86	0.1301	Cr	0.64	0.0123 Cd 0.02 0.0002
			Mn		Sn
Halids & non-metals			Fe	5.47	0.0979 La
	[mg/L]	[mmol/L]	Co		W
Br	5.14	0.0643	Ni	0.92	0.0157 Pb
I	1.40	0.0110	Cu	0.59	0.0093 Bi
B	3.10	0.2867	Zn	2.86	0.0437 U 0.46 0.0019
As	0.61	0.0081			
Se					

Bacteria (qualitative)	
aerobic germs	+ E. Coli -

Isotopes	
Tritium [UT]	Carbon-13 [δ‰]
Deuterium [δ‰]	Oxygen-18 [δ‰]

Figure 2-6: Data sheet of the AQUITYP DataBase (print model).

III. TYPOLOGY OF RECENT GROUNDWATERS

3. 1. Introduction

The present chapter gives a synthesis of the geology and hydrogeology of five aquifer types and the hydrochemistry of recent groundwaters from these aquifer types. This synthesis is based on groundwater data acquired during the previous studies in the AQUITYP project, on hydrogeological investigations such as tracer tests and reviews of the geology and hydrogeology of the aquifers made during these previous studies, as well as on additional mineralogical and geochemical data from the literature. The investigated aquifer types include crystalline rocks (Dubois, 1993), carbonate rocks (Dematteis, 1995), evaporite rocks (Mandia, 1993), molasse (Hesske, 1995), and flysch rocks (Basabe, 1993). To compare the recent groundwater compositions to the atmospheric input, chemical data of rainwater and snow from the study of Atteia (1992) have been used (appendix A).

The present study focuses on recent groundwaters from active, relatively local flow systems. In the first part, the criteria applied for the selection of sampling sites and water data are presented (section 3. 2).

Then, an overview of geologic and hydrogeologic characteristics of each aquifer type is given, including structural aspects and the mineralogic compositions of the geologic units (section 3. 3).

Section 3. 4 summarises the chemical composition of the recent groundwaters in each aquifer type. The hydrochemical characteristics of the groundwaters in the different aquifer types were summarised and compared, and concentration ranges of major and trace elements for groundwaters in each aquifer type were deduced. Within the different aquifer types especially trace elements show a strongly asymmetric distribution, with outliers (observations that are distant from the bulk of the data set) towards high concentrations. In order to avoid a distortion of the arithmetic mean value by these outliers median values have been used instead to describe the typical compositions of the groundwaters from the different aquifer types.

In this study the emphasis has been laid on the geochemical evolution leading to the characteristic groundwater composition in each aquifer type. Groundwater mineralisation was set into relation with aquifer lithology and hydrogeology and the dominant processes leading to the typical mineralisation of recent groundwaters were investigated using geochemical modelling strategies. The geogenic tracers proposed in the previous studies were evaluated and potential element sources identified.

Finally, the concentrations of chemical elements in the groundwaters from the different aquifer types were compared to the Swiss drinking water standards, in order to assess the quality of the investigated groundwaters as drinking waters.

3. 2. Sampling sites and groundwater data

The spatial groundwater observation network of the AQUITYP project provides a representative selection of groundwater samples from active and mostly small-scaled flow systems in different geologic environments. The geologic, hydrogeologic and environmental criteria applied for the selection of the sampling sites are as follows:

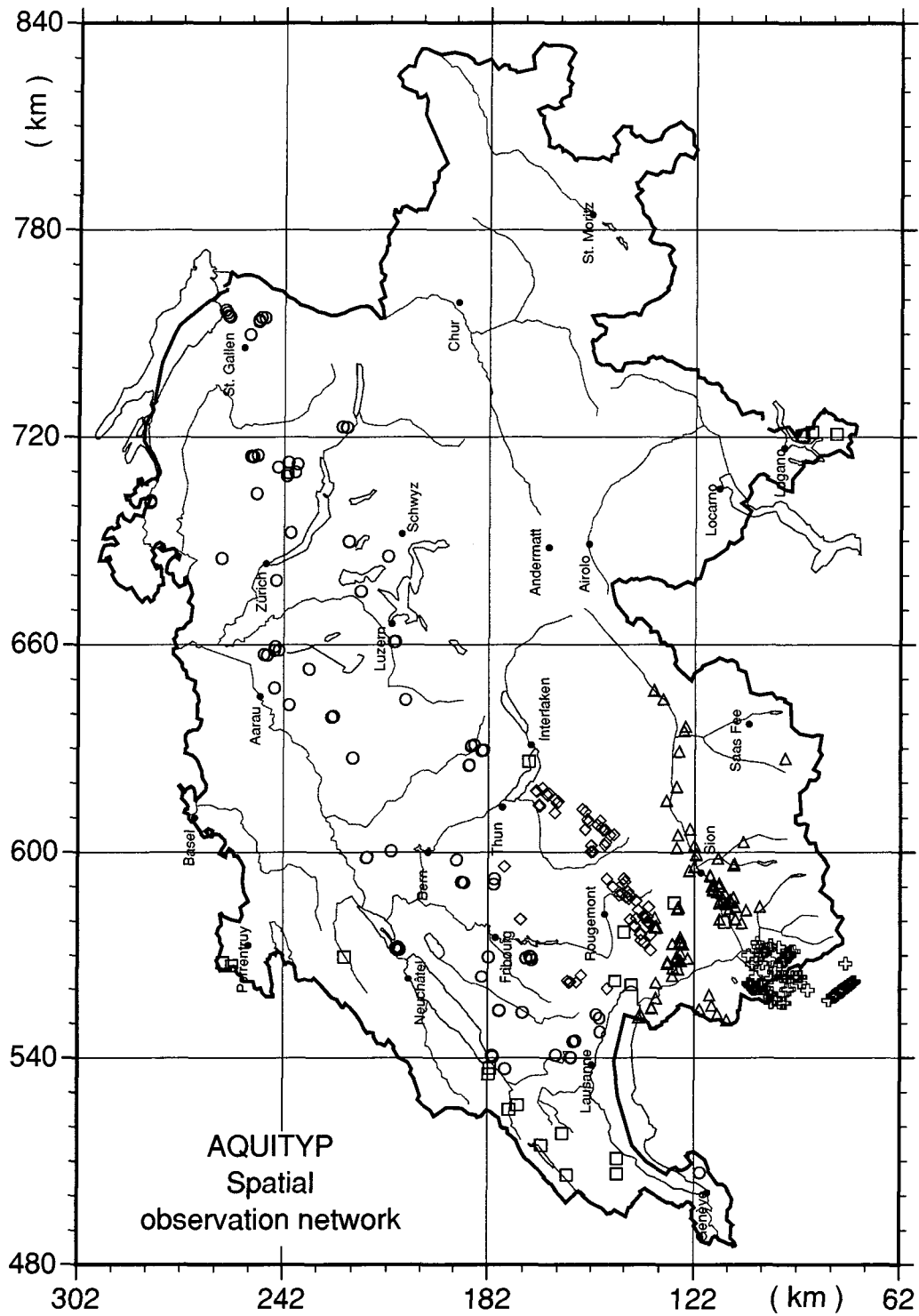
- 1.) Only catchments in relatively remote regions were considered, where point source pollution (runoff from urban sites, waste deposits, traffic ways) was thought to be minimal. Areas with intensive agricultural activity were avoided as far as possible, to exclude such influences onto the groundwater composition.
- 2.) The aquifer had to consist, as far as possible, of a single lithologic unit within a simple tectonic context, thus excluding the influences of other lithologic units. Only catchments covered with little quaternary deposits differing in their mineralogic composition from the aquifer lithology were taken into consideration.
- 3.) The springs had to be perennial in order to exclude waters from very superficial flow systems.
- 4.) Springs emerging directly from the aquifer rock were preferred, in order to minimise contamination by technical installations.

From a total of 1824 groundwater analyses 1674 analyses passed the quality check described in chapter II. on page 19. From these, 1475 are analyses of *recent* groundwaters and have been selected for further investigation (see also table 2-1). The geographical distribution of the sampling sites in and around Switzerland is shown in figure 3-1. Additional molasse springs are located in Austria and France, and additional carbonate karst springs were sampled in Austria, France, Italy, Slovenia and Greece (see table 2-4).

Aquifer type	Sites	Analyses	Reference
Crystalline	119	338	Dubois, 1993
Carbonates	87	207	Dematteis, 1995
Evaporites	91	473	Mandia, 1993
Molasse	108	193	Hesske, 1995
Flysch	53	264	Basabe, 1993
Total	458	1475	

Table 3-1: Data base used for the typology of recent groundwaters.

The groundwater from most sampling sites was analysed once or twice in the period of 1981 to 2000, in order to study the spacial variation of natural groundwater chemistry in a given aquifer type. In addition, a number of sites were sampled several times or observed continuously over a certain period, in order to obtain insight into long-term variations of the chemical groundwater composition. These time series comprise physical-chemical field measurements and a selection of chemical components. For the following hydrochemical synthesis average values of all analyses have been used.



- Aquifer types :**
- | | |
|--------------|---------------|
| ○ Molasse | △ Evaporites |
| ◇ Flysch | ⊕ Crystalline |
| □ Carbonates | |

Figure 3-1: AQUITYP spatial observation network with locations of sampling sites in and around Switzerland.

3. 3. Geologic and hydrogeologic setting

3. 3. 1. Crystalline rocks

The investigated catchments in crystalline rocks are situated in the Mont-Blanc and Aiguilles-Rouges massifs, in southwestern Switzerland and neighbouring France and Italy. This area is characterised by a very steep topography, culminating in the summit of the Mont-Blanc (altitude 4807 m). A large part of the catchments surface is situated at high altitudes and covered by glaciers and perennial snow or bare rock. The lower regions are covered by an alpine-type vegetation; the timber line is situated at about 2000 m. In approximately half of the crystalline catchments area there is practically no soil cover.

Mean annual precipitation at the meteorologic station of Grand St. Bernard (altitude 2472 m) is 2336 mm (30 years mean value 1961-1990, MeteoSwiss). This value is representative of the precipitation conditions in a large part of the investigated area.

Major rock types present in the Mont-Blanc and Aiguilles-Rouges massifs include granites, mainly the porphyritic Mont-Blanc granite, and poly-metamorphic and partly migmatitic ortho- and para-gneisses and mica-schists of pre-Mesozoic age¹. The granites are composed of quartz (25 to 35%), altered plagioclase (30 to 38%, mainly sericitic and saussuritic oligoclase), relatively fresh K-feldspar (22 to 35%), chloritised biotite (ca. 6%) and minor amounts of amphibole and epidote (<1%) (Marro, 1986). The predominantly felsic ortho- and para-gneisses show a characteristic decimetre- to metre-thick banding. They are composed of largely the same minerals as the granites, including 25 to 40% quartz, 20 to 56% altered plagioclase, and 3 to 32% relatively fresh K-feldspar. In addition, the gneisses contain garnet (up to 2%), as well as biotite and white mica (10 to 20%) (Niggli and others, 1930). In the para-gneiss units minor amounts of calcareous sediments and basalt dykes occur intercalated as thin layers or lenses of calcite and dolomite marble, calc-silicate rocks and amphibolites (Collet and others, 1952).

The crystalline rocks of the Mont-Blanc and Aiguilles-Rouges massifs underwent several episodes of ductile and brittle tectonic deformation (Corbin & Oulianoff, 1959; von Raumer, 1987; Jamier, 1975). Mylonite zones were often reactivated during later brittle deformation. The result are extensive fissure and fracture systems in N-S and NE-SW direction. These open fracture and fissures act as preferential pathways of groundwater flow (fracture flow). The abundance of open fractures and fissures leads to a relatively high permeability, despite of the very low permeability of undisturbed crystalline rocks.

Dubois (1993) gives a detailed review of the various hydrothermal vein mineralisations, which have been described at several locations within the Mont-Blanc and Aiguilles-Rouges massifs and near the contacts with adjacent sediments². Even a number of small ancient mines exist. Hydrothermal mineralisations can be widely found associated with mylonites and in fractured zones. However, not every fracture contains hydrothermal mineralisations; some fractures were formed during brittle deformation without extensive water-rock interaction. Generally, hydrothermal mineralisations form when fluids separate from a rising magma body as a consequence of decreasing pressure and intrude into the overlying

1. Niggli et al. 1930; Rybach et al. 1966; Burri & Jemelin, 1983; von Raumer, 1984, 1987; von Raumer et al., 1990; Marro, 1986; Ayrton et al. 1987; Bussy, 1990

2. Baggio, 1958; Canet, 1960; Rigault & Ferraris, 1962; Labhart & Rybach, 1972, 1974; Ravagnani, 1974; Burri & Jemelin, 1983; Gilliéron, 1986; Woodtli et al., 1987; Dumont, 1988

rocks. Hydrothermal fluids are often rich in volatile constituents, such as H₂O, CO₂, S, F, Cl, B and P (Philpotts, 1990). In addition, they may be enriched in various incompatible elements that do not readily enter common rock forming minerals, such as Li, Be, Sc, Ga, Ge, As, Rb, Y, Zr, Nb, Mo, Ag, In, Sn, Sb, Cs, Ba, rare earth elements (REE), Hf, Ta, W, Re, Au, Pb, Bi, Th, and U. The hydrothermal minerals found in the Mont-Blanc and Aiguilles-Rouges massifs, which are significant for groundwater mineralisation are listed in table 3-2. Fluorite, molybdenite, U- and W-minerals are principally associated with the Mont-Blanc granite, while arseno-pyrite and barite appear to be more abundant in the gneiss units. In addition, clay minerals such as chlorite, illite, and smectite occur in fracture zones.

	Mineral	Formula
Carbonates	calcite	CaCO ₃
	dolomite	CaMg(CO ₃) ₂
Fluorides	fluorite	CaF ₂
Sulphates	barite	BaSO ₄
Sulphides	pyrite	FeS ₂
	arsenopyrite	FeAsS
	molybdenite	MoS ₂
	chalcopyrite	FeCuS ₂
	galena	PbS
	sphalerite	ZnS
Oxides & hydroxides	haematite	Fe ₂ O ₃
	goethite	FeOOH
	uraninite or pitchblende	UO ₂ -U ₃ O ₈
W-minerals	scheelite	CaWO ₄
	wolframite	(Fe,Mn)WO ₄

Table 3-2: Common hydrothermal minerals occurring in the Mont-Blanc and Aiguilles-Rouges massifs (based on the review by Dubois, 1993).

Long-term observations of discharge, water temperature and total mineralisation of seven selected springs allowed to study the hydrogeology of the granite and gneiss units of the Mont-Blanc and Aiguilles-Rouges massifs (Dubois, 1993). These observations revealed that there is generally a much higher variation of discharge than of water temperature and mineralisation (see table 3-3). Strong seasonal fluctuations of discharge are common. High water periods typically occur during snow melt from May to July. The variation of discharge in gneiss springs tends to be smaller than in granite springs. Dubois (1993) suggested that this is related to the higher permeability of the granites due to the influence of both regional fracture systems and small fissures, compared to the gneisses, where groundwater flow occurs primarily in surface-near fissured zones.

Site (data base code)		Altitude (m)	Av. Q (L/min)	coeff. of variation	Av. T (°C)	coeff. of variation	Av. TDS (mg/L)	coeff. of variation
Gneiss	CHAT EAU	1930	521±280	53.7%	5.0±0.4	8.0%	91.0±3.7	4.1%
	NANT PROV	1200	771±267	34.6%	6.3±0.4	6.3%	157.7±4.2	2.7%
	BRO	570	1725±304	17.6%	7.2±0.2	2.8%	74.5±7.8	10.5%
Granite	FINFON/19	1360	1905±190	10.0%	5.1±0.2	3.9%	45.8±2.7	5.9%
	CHAP SUP	1720	2450±1506	61.5%	3.3±0.1	3.0%	44.6±2.3	5.2%
	CHAMOIS	1100	242±262	108.3%	6.9±0.2	2.9%	56.2±5.7	10.1%
	COL MONT	1530	255±63	24.7%	5.8±0.8	13.8%	40.9±0.8	2.0%

Table 3-3: Time variations of discharge (Q), water temperature (T), and total mineralisation (TDS) of seven selected springs in granite and gneiss units of the Mont-Blanc and Aiguilles-Rouges massifs, observed over a time span of 2 to 14 years (Dubois, 1993).

Tracer tests and calculations based on tritium data have revealed very short residence times of groundwater in the Mont-Blanc and Aiguilles-Rouges massifs (Dubois, 1993; Maréchal, 1998). In two tracer tests carried out in the region of the Glacier du Toule (altitude ca. 3300 m) the tracer reappeared after less than 4 months in the springs located in zones of intense fracturing in the Mont-Blanc road tunnel, 2000 m below the surface. This indicates that (1) there is a direct hydraulic connection between the surface and the springs in fractured zones in the Mont-Blanc tunnel, and (2) the flow in these fracture zones is very fast (up to 17 m/day). Calculations based on tritium data indicate a mean residence time of 1 to 2 years for the waters emerging at the springs in the Mont-Blanc tunnel (Maréchal, 1998). This result is consistent with the findings of the tracer tests.

3.3.2. Carbonate rocks

To study karst catchments in carbonate rocks from different sedimentary environments and tectonic contexts, the study area was extended. Catchments in karst regions in the Swiss and French Jura Mountains, in the Swiss, French, Italian, and Austrian Alps, as well as in parts of the Apennine in Italy, in the Dinarids in Slovenia, and in the Hellenids in Greece were included (table 3-4). This involves that not only geologic factors but also external factors such as topography, climate, and type of soil and vegetation, are characterised by a greater variation. In addition, the composition of precipitation (atmospheric input) varies more strongly in this extended area than in Switzerland alone. This is particularly true for the concentrations of atmospheric pollutants and marine aerosols. For instance, the catchments in Italy, Slovenia and Greece receive higher amounts of marine aerosols than the catchments in the Jura mountains and in the Alps, due to their shorter distance to the sea.

In the Swiss Jura mean annual precipitation is 1886 mm at La Dôle (altitude 1670 m) and 1155 mm at the Chasseral (altitude 1599 m; 30 years mean values 1961-1990, MeteoSwiss). In the Alps, at the meteorological station of Gryon (altitude 1085 m), mean annual precipitation is 1206 mm (30 years mean values 1930-1960, MeteoSwiss).

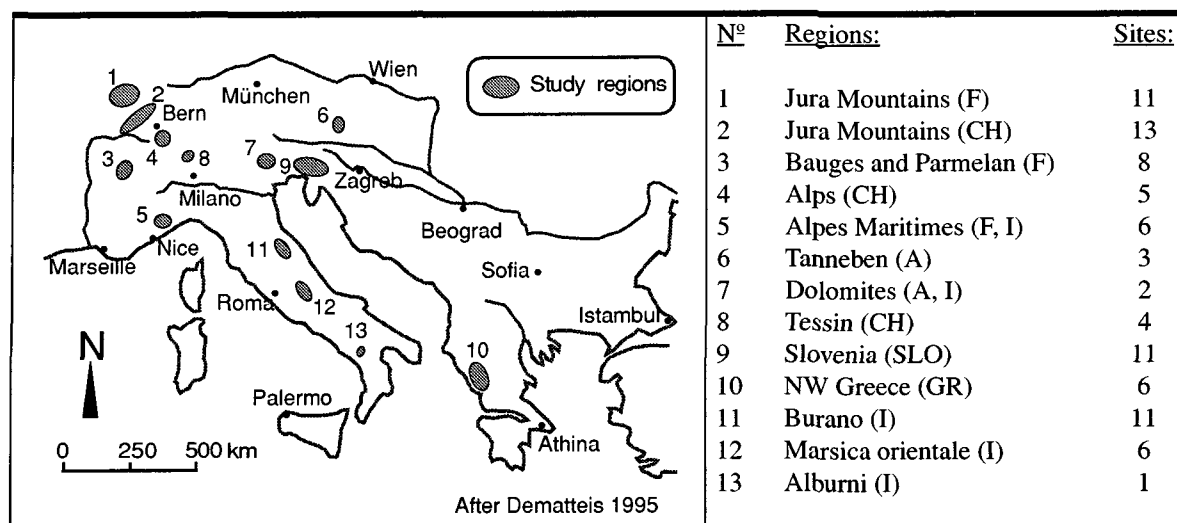


Table 3-4: Locations of studied carbonate karst regions (after Dematteis, 1995).

The lithology of carbonate rocks (mineralogic composition and texture) depends on the conditions reigning at their formation, i.e. temperature and depth of the sea, oxygen content, marine biology, input of detrital material, and rate of sedimentation. The carbonate rocks in the investigated catchments represent different sedimentary environments (see table 3-5). Rock types include pure limestone, marly limestone, dolomitic limestone, and dolostone of Devonian to Eocene age. They are essentially composed of calcite (CaCO_3) or dolomite ($\text{CaMg}(\text{CO}_3)_2$), with variable amounts of detrital minerals including clay minerals, quartz and minor amounts of feldspars and mica. Further, accessory fossil organic matter (bitumen, kerogens, graphite), sulphides (usually pyrite), as well as secondary Fe-hydroxides may be present. Dispersed micro-crystalline barite (BaSO_4) occurs in carbonate rocks from deep sea environments in amounts of up to 10% (Church, 1979). Gypsum ($\text{CaSO}_4 \cdot 2\text{H}_2\text{O}$) and celestite (SrSO_4) are common in evaporitic carbonate series (Holser, 1979a, 1979b).

In particular, dolostones and dolomitic limestones dominate in the Dolomiti Bellunesi (region N° 7) and in the Slovenian Dinarids (region N° 9). Marly deep sea limestones dominate in NW Greece (region N° 7) and in the Mte Catria - Mte Acuto region in Italy (region N° 11). Evaporitic beds with sulphate minerals occur in the Triassic rock series at the bottom of the Mesozoic, mainly in the Swiss Alps (region N° 4) and in Mte Catria and Mte Acuto region (Apennine, region N° 11).

Geographic regions		Lithostratigraphic units	Age	Sed. enviro	rock types
1	Haute Saône Lons-le-Saunier	“Dogger”	Dogger	P/S	LS
2	Swiss Jura ^a	“Malm” “Cretaceous”	Malm Cret.	P/R L	LS, LS-M LS, LS-M
3	Haute Vallée du Chéran Massif du Parmelan	Senonien Urgonien Tithonique	u. Cret. l. Cret. Malm	B L-R B	LS, LS-M LS LS, LS-M
4	Chablais ^b Saillon ^c Derborence ^d Beatenberg ^e	“Trias”, “Lias”, “Malm” “Trias”, “Malm”, “Cret.,” Eocene” Drusberg, Val. calc., calc. bleutés Schrattenkalk, Hogantsandstein	Trias. - Malm Trias. - Eoc. Cret. - Eoc. Malm - l. Cret.	R/L	D, LS, LS-M, E D, LS, LS-M, E LS, LS-M LS
5	Alpes Maritimes ^f	Calc. dolomitici, Calc. a Cellette	Trias. - Malm	P	LS, LS-D
6	Tanneben ^g	Schöckelkalk	Devonian	P	LS, LS-D
7	Dolomiti Bellunesi ^h	“Jurassic”, “Cretaceous” Dolomia Principale Dolomia d. Sciliar	Jura. -Cret. u. Trias. m. Trias	L L	LS D, LS-D D, LS-D
8	Monte Generoso ⁱ	Calcare selcifero lombardo	Lias	B	LS
9	Suhadolnitce region Julian alpes Banjsitce region Tcitcarija region Carso triestino	Dachstein	m. Trias u. Trias. Jura. - l. Cret. Cret. Cret. - Eoc.	L L L L	D LS, D LS LS LS
10	Pinde Massif Ionian Zone ^j	Vigla, Sinais	u. Trias - u. Cret. Lias. - Eoc.	B B	LS, LS-M
11	Mte Catria, Mte Acuto ^k	Scaglia Maiolica Corniola, Calcare Massiccio	Cret. - Paleoc. Malm - l. Cret. u. Trias. - Malm	B B R	LS-M LS, LS-M LS, E
12	Marsica orientale ^l	Formazione della Terratta	l. Lias - u. Cret.	P	LS, LS-D
13	Mti. Alburni ^m		Trias. - Cret.	P	LS, LS-D

Table 3-5: Carbonate rocks in the investigated regions (geographic region numbers refer to table 3-4; after Dematteis, 1995): Lithostratigraphic units, age, predominant sedimentary environment (P = carbonate platform, L = lagoon, R = reef, S = continental slope, B = deep-sea basin) and predominant rock types (LS = limestone, LS-M = marly limestone, LS-D = dolomitic limestone, D = dolostone, E = evaporite minerals, mainly gypsum).

- a. Falconier, 1931; Aubert et al. 1979
b. Badoux, 1965; Mosar, 1988; Mosar & Borel, 1992; Masson, 1992; Weidmann, 1993
c. Perrin, 1996
d. Badoux & Gabus, 1991
e. Bitterli, 1988
f. Malaroda, 1970
g. Behrens et al., 1992
h. Castiglioni, 1931; Rossi, 1967; Leonardi, 1968a, 1968b; Lombardi, 1968; Bosellini, 1989; Appelo et al. 1984
i. Bernoulli, 1964; Cavalli & Bianchi-Demicheli, 1982; Cantone Ticino, 1990
j. Institut Français du Pétrole, 1967
k. Centamore & Valletta, 1976; Servizio Geologico d'Italia, 1972, 1976; Calamita et al. 1990; Arrà et al., 1994
l. Colacicchi, 1967; Celico, 1983; Boni et al., 1986; Governa et al., 1989
m. Bellucci et al., 1991

Karst aquifers are characterised by their conduit porosity (e.g. Ford & Williams, 1989; Ford, 1998). They can be understood as very permeable conduits systems, which drain a large volume of carbonate rocks with a low permeability (e.g. Kiraly, 1975; Mangin, 1975). Therefore, the permeability of carbonate aquifers strongly depends on the extent of the development of karst systems. Atkinson (1975) showed from hydrograph analysis and other parameters in the Mendip Hills, England, that the major part (60 to 80%) of groundwater in carbonate karst aquifers flows through fissures and larger openings, whereas only a small part of the groundwater is transmitted through the pores of the carbonate rock. The recharge areas of karst aquifers often extend over several tens of km², and their exact limits are difficult to determine. Further, karst aquifers typically possess different types of recharge, each yielding a specific water mineralisation: fast infiltration in sink-holes yields a very low mineralisation, while slow infiltration through the soil and epikarst zone results in more mineralised groundwaters. In addition, surface water courses disappearing in sinkholes often originate in neighbouring regions and can have evolved in different rock types.

In consequence of these particular recharge and hydraulic conditions, the mineralisation of karst waters typically varies strongly in response to seasonal changes in recharge (table 3-6). The complex relationship between recharge conditions, heterogeneous permeability of carbonate aquifers and variability of karst springwater chemistry is the subject of continuously ongoing studies (e.g. Bakalowicz, 1974, 1979; Kiraly & Muller, 1979; Schoeller, 1980; Lastennet, 1994; Eisenlohr, 1995; Grasso & Jeannin, 1998). Variations in the discharge of a karst spring are usually accompanied by opposite variations of the springwater mineralisation, i.e. the highest mineralisation occurs during low water periods and vice-versa. Mayer (1999) showed that strong variations in karst water mineralisation can be related to mixing of distinct “end-member” karst waters of different origins within the aquifer (conduit flow versus fissure flow). These “end-member” karst waters consist of rapidly infiltrating, dilute waters that dominate during high water conditions, and slowly infiltrating, more mineralised waters that dominate during low water conditions.

In conduits and fractures, the flow velocity of karst water is very fast, in the order of several 100 m to several km per day, as long as natural discharge is provided. The residence time of such waters is consequently very short, ranging from a few hours to some weeks. However, within a karst aquifer the water residence time and therefore its mineralisation can vary considerably over very short distances, depending on whether the sample is drawn from a highly permeable conduit or from a small fissure in the rock (e.g. Mayer, 1999). The sampling sites considered in the present study are karst springs, i.e. karst waters from major conduits were sampled at the natural outlet of the aquifer. The investigated karst springs generally have a high discharge owing to their large recharge areas (table 3-6).

Site data base code		Altitude (m)	Av. Q (L/min)	coeff. of variation	Av. T (°C)	coeff. of variation	Av. TDS (mg/L)	coeff. of variation
Jura	LIO	1040			6.1±0.2	3.3%	287.8±34.3	11.9%
Alps	BOR	1140	3595±413	11.5%	5.6±0.1	1.8%	211.4±11.8	5.6%
	SAR	470	19416±12699	65.4%	7.1±0.4	5.6%	240.8±31.1	12.9%

Table 3-6: Time variations of discharge (Q), water temperature (T), and total mineralisation (TDS) of three selected karst springs in Switzerland (data from 1982 to 1996).

3.3.3. Evaporite rocks

The investigated catchments in evaporite rocks are situated in the Alps, in the region of the Swiss Rhone valley (canton Wallis and Vaud). This region is characterised by a pronounced alpine topography. The altitudes of the studied springs range from 375 m near Lac Léman and 2220 m in the south.

In the investigated region precipitation varies strongly as a function of altitude and exposition: Mean annual precipitation is 2336 mm at the meteorologic station of Grand St. Bernard, located on the main ridge of the Alps near the Italian border (altitude of 2472 m), and 982 mm at Montana (altitude 1508 m), situated on the northern slope of the Rhone valley and thus protected from the main rain-bringing westerly winds (30 years mean values 1961-1990, MeteoSwiss).

In the investigated region Triassic evaporite rocks occur in the following tectonic units: Préalpes Médiannes Plastiques, Helvetic, Ultrahelvetic (Meilleret, Bex, and Sex-Mort nappes), and Pennine (Grand St-Bernard nappe, Sion-Courmayeur zone)¹. The Triassic rocks of the Helvetic and Ultrahelvetic tectonic units include a restricted sequence of mid to upper Triassic clastic, carbonate and evaporite rocks (upper Muschelkalk and Keuper), which are thought to belong to the so-called germanic domain (Gwinner, 1978). The Triassic rocks of the Préalpes and the Pennine include Lower Triassic clastic sediments (Werfenian or Scythian), and Middle to Upper Triassic carbonate and evaporite rocks, which are thought to belong to the so-called "Alpine Triassic". The Triassic units in the Pennine show a metamorphic overprint reaching green-schist facies in the south.

The *evaporite rock series* of the Aigle region is typically composed of laminated gypsum or anhydrite rocks with detrital and calcareous interlayers (NAGRA, 1993). Rock forming minerals include gypsum or anhydrite, some dolomite and calcite, and variable amounts of detrital and partly authigenic silicate minerals such as quartz, chalcedony, feldspars, talc, and clay minerals (illite, chlorite, smectite, and corrensite, which is a chlorite-vermiculite mixed-layered clay mineral) (see table 3-7). Accessory fluorite, celestite, barite, apatite and sulphide minerals (pyrite, sphalerite, galena and chalcopyrite) can be present.

The *carbonate series* consist of a succession of limestones with variable dolomite content and intercalated shale layers. The carbonate rocks themselves are composed of calcite and dolomite, and variable amounts of detrital and partly authigenic silicates (mainly quartz, chalcedony, feldspars, and the clay minerals illite, chlorite, and smectite). Accessory minerals include celestite, variable amounts of fluorite, apatite and sulphides.

The *detrital rock series* include feldspar- and mica-bearing calcareous sandstones or quartzites with intercalated marls or shales. Ore beds with barite and sulphides occur locally.

The soft evaporites and shales often acted as gliding material between the pre-Triassic crystalline basement and the overthrust nappes. Therefore, the Triassic rocks are usually strongly deformed and occur in discontinuous shreds and lenses of varying thickness. Large masses of evaporite rocks occur in the Ultrahelvetic tectonic unit, particularly in the region of the Col de la Croix. Here, usually both the recharge and the discharge areas lie within the Triassic evaporite rocks ("modèle jointif", Mandia, 1993). The tectonic structure of the Préalpes Médiannes, the Helvetic, and the Pennine nappes, however, is such that infiltrating water usually passes through various other rock types (e.g. carbonate rocks, gneiss, schist) before reaching the evaporites ("modèle non-jointif", Mandia, 1993). Particularly the

1. Bearth, 1953; Badoux, 1963; Badoux et al., 1971; Baud, 1972, 1987; Masson et al., 1980; Escher et al., 1987; Escher, 1988; Marthaler, 1984; Jeanbourquin & Burri, 1989,

Pennine Grand St-Bernard nappe presents a very complex structure. It consists of a pile of several imbricated gneiss and schist slabs with intercalated evaporite rocks.

The majority of the investigated aquifers are composed of Triassic evaporite and carbonate rocks. The Lower Triassic sandstones and fractured quartzites occur in certain aquifers in the Pennine, where this rock type reaches the greatest thickness.

	Mineral	Formula
Sulphates	gypsum	CaSO ₄ ·2H ₂ O
	anhydrite	CaSO ₄
	celestite	SrSO ₄
	barite	BaSO ₄
Carbonates	calcite	CaCO ₃
	dolomite	CaMg(CO ₃) ₂
Fluorides	fluorite	CaF ₂
Phosphates	apatite	Ca ₅ (F,Cl,OH)(PO ₄) ₃
Silicates ^a	chalcedony / quartz	SiO ₂
	illite	K _{1-1.5} Al ₄ [(OH) ₄ /(Si,Al) ₈ O ₂₀]
	chlorite	(Mg,Fe ^{II} ,Fe ^{III} ,Mn,Al) ₁₂ [(Si,Al) ₈ O ₂₀](OH) ₁₆
	smectite	Al _{1.67} Mg _{0.33} [(OH) ₂ /Si ₄ O ₁₀]·Na _{0.33} ·(H ₂ O) ₄
	talc	Mg ₃ [(OH) ₂ /Si ₄ O ₁₀]
	plagioclase	(Na,Ca)[Al(Si,Al)Si ₂ O ₈]
	K-feldspar	K[AlSi ₃ O ₈]
	muscovite	KAl ₂ [(OH) ₂ /AlSi ₃ O ₁₀]
Sulphides ^b	pyrite	FeS ₂
	sphalerite	ZnS
	chalcopyrite	FeCuS ₂
	galena	PbS

Table 3-7: Common minerals occurring in the Triassic rocks of the Swiss Rhone basin (Mandia, 1993 and references therein).

- a. Note that in the investigated area no pure evaporite rocks occur.
- b. Sulphide minerals are particularly widespread in the metamorphic evaporite units of the Pennine.

Calcium sulphate rocks are almost always composed of gypsum in surface-near zones and in zones along fractures and lithologic contacts (so-called "Gips-Hut"). Anhydrite occurs only at a depth of several tens of meters. Calcium-sulphate rocks form either in large standing bodies of water, or in the vadose zone of tidal flats (so-called sabkhas) or desert playas, where brine has become concentrated by evaporation to the point of gypsum precipitation (Blatt and others, 1980; Krauskopf, 1995). Only at a very final stage of evaporation, anhydrite might precipitate. Gypsum dehydration and formation of anhydrite occurs during diagenesis and eventually metamorphism of the evaporite sediments at temperatures above 42°C. Hence, the sulphate rocks in the Alps consisted entirely of anhydrite, until they were uplifted, exposed to erosion, and the present groundwater flow system became active, turning them into gypsum again.

Calcium sulphate rocks therefore exhibit a characteristic hydrogeology: On the one hand, the high solubility of gypsum (2.5 g gypsum per litre can be dissolved in pure water) leads to the development of dissolution conduits in the surface-near zones and to the related high

permeability which is typical of karst aquifers¹. On the other hand, observations in underground construction and bore holes have shown that the anhydrite rocks found at depth have an extremely low permeability (e.g. Paul, 1993). Near the surface and along lithologic contacts and fractures with groundwater circulation anhydrite re-hydrates and is replaced by gypsum. This re-crystallisation involves a volume increase of up to 61% (Holser, 1979), which leads to a partial, if not complete sealing of the groundwater pathways. The hydration of anhydrite can then only continue if the pathway remains open. The permeability of calcium sulphate rocks therefore depends strongly on the geologic context, particularly on the thickness of the formation and on extent of fracturing (e.g. Parriaux and others, 1990c).

The study of variations of discharge, water mineralisation and temperature of twelve selected springs revealed strong seasonal fluctuations of discharge, linked to snow melt in the recharge area (Mandia, 1993; table 3-8). High water periods occur from April to July, depending on the altitude of the recharge area. During these high water periods the springwater is generally less mineralised.

Site (data base code)	Altitude (m)	Average Q (L/min)	coeff. of variation	Av. T (°C)	coeff. of variation	Average TDS (mg/L)	coeff. of variation	
Préalpes Médianes	LED	400	138±50	36.2%	8.7±0.4	4.6%	2045.5±164.8	8.1%
	LEI	385	157±10	6.4%	9.4±1.3	13.8%	1508.5±118.2	7.8%
	SEM	375	373±34	9.1%	9.9±0.2	2.0%	1620.3±81.8	5.0%
Helvetic	DAP	880	3±2	66.7%	7.1±2.5	35.2%	2398.2±263.4	11.0%
	OBE	840			8.3±0.1	0.9%	2058.6±49.4	2.4%
	DAG	880			7.5±0.2	3.2%	2327.9±26.0	1.1%
Ultra- helvetic	EAR	1360	600±0	0.0%	6.4±0.1	1.6%	2179.8±25.0	1.1%
	MAU	1810	841±519	61.7%	4.2±0.2	4.8%	1312.3±252.9	19.3%
	NOC	395	2106±953	45.3%	11.0±0.1	0.9%	1409.1±38.3	2.7%
Pennine	MUL	630	861±533	61.9%	9.0±0.1	1.1%	2097.1±23.6	1.1%
	PER	1400	123±21	17.1%	5.5±0.1	1.8%	2325.5±38.3	1.6%
	QUE	620	34±2	5.9%	9.3±1.6	17.2%	2407.8±25.5	1.1%

Table 3-8: Time variations of discharge (Q), water temperature (T), and total mineralisation (TDS) of twelve selected evaporite springs observed over 2 to 14 years (Mandia, 1993).

Mandia (1993) also performed several tracer tests, which allowed to determine maximum flow velocities ranging from 10 to >1000 m per day, based on transit times of the tracer between 22 h and 4 months. In catchments where both the recharge and discharge area lie within evaporite rocks, as it is the case in the Ultrahelvetic, the flow velocities tend to be faster than in catchments where water first passes through other rock types. The observed short residence times show that the investigated evaporite groundwaters are recent, as it is typical of permeable aquifers with fracture and conduit porosity. This is also consistent with the fact that all of the observed springwaters contain tritium (Mandia, 1993).

1. Eleven small caves in gypsum rocks are known in the Valais and Vaud region (Bitterli, 1998). The most important cave is the *Crête de Vaas* near Sierre with a length of 1343 m. The largest known caves in gypsum rocks in the world are the *Optimisticheskaja* (203 km length) and the *Ozernaja* (117 km length) caves in Ukraine (Klimchouk, 2000).

3.3.4. Molasse

The investigated catchments are distributed over the molasse basin between Chambéry (France) and Linz (Austria), with most of the sampling sites being situated in Switzerland. This area is characterised by a hilly topography and relatively low altitudes. The altitudes of the investigated springs range from 340 to 1430 m. Typically, rich vegetation and deep soils cover the catchments.

In the Swiss plateau region mean annual precipitation ranges from 954 mm at Changins (altitude 430 m) to 1736 mm at the Napf at an altitude of 1406 m (30 years mean values 1961-1990, MeteoSwiss).

The molasse basin originated during the early Oligocene (Tertiary) as a part of the peri-Alpine foredeep (Trümpy, 1980a). Molasse consists of clastic sediments that formed in shallow marine or fluvial environments and are derived mainly from the rising Alps. Four groups are generally distinguished: *Lower Marine Molasse* (UMM; Middle Oligocene), *Lower Freshwater Molasse* (USM; Upper Oligocene to early Lower Miocene), *Upper Marine Molasse* (OMM; late Lower Miocene), and *Upper Freshwater Molasse* (OSM; Middle and early Upper Miocene) (see figure 3-2). Structurally, one can distinguish between the autochthonous molasse, generally flat-lying but with a folded belt to the south, and the Subalpine molasse, which forms a zone up to 25 km wide at the margin of the Alps and which is strongly overthrust.

The different molasse formations in the investigated area have been extensively investigated; a comprehensive literature review including regional and many local studies is given by Hesske (1995)¹. Molasse sandstones and conglomerates typically consist of quartz and feldspar grains and lithic fragments of metamorphic, igneous, and sedimentary rocks, contained in a carbonate or clay matrix. Clay minerals include illite, smectite, chlorite and small amounts of kaolinite. The proportions of these major constituents in a particular formation depend on the type of the source rocks from which they are derived, and on the sedimentary environment. Predominant rock types and the environments in which they were deposited are briefly summarised in the following (after Trümpy, 1980a):

- UMM: Marine and brackish black shales with thin intercalated sandstone bands were deposited in a shallow, brackish and poorly aerated narrow sea.
- USM: Large conglomerate alluvial fans at the northern margin of the Alps, grading outwards into flood plains and lakes, where sandstones and shales with thin limestone bands were deposited. Drainage occurred essentially eastwards. Source rocks include Mesozoic carbonates, flysch, igneous, metamorphic, and rare ophiolite rocks from Prealpine and Austroalpine nappes.
- OMM: Thick-bedded feldspar-rich and often glauconitic marine sandstones were deposited in a shallow sea. The seas were generally shallow and pebbles and sand were transported by strong long-shore currents from southwest to

1. Aberer, 1957; Allen et al., 1985; Berger, 1985, 1992; Büchi, 1950, 1958; Büchi & Welti, 1951; Büchi & Schlanke, 1977; Bürgisser, 1980; Fasel, 1986; Füchtbauer, 1954, 1955, 1964; Gasser, 1966, 1968, 1966; Grimm, 1965; Habicht, 1945, 1987; Hofmann, 1957, 1959; Homewood & Allen, 1981; Homewood et al., 1982; Homewood & Lateltin, 1988; Homewood et al., 1989a, 1989b; Jordi, 1955; Keller, 1987, 1989; Kissling, 1974; Lemcke et al., 1953; Lemcke, 1972; Matter et al., 1980; Maurer et al., 1978; Maurer, 1983; Monnier, 1979, 1982; Mornod, 1949; Pavoni, 1957; Renz, 1937; Schlanke, 1974; Schlunegger et al., 1993; Schmid, 1970; Schoepfer, 1989; Schwerd & Unger, 1981; Speck, 1953; Unger, 1989; Vernet, 1964; von Moos, 1935; Ziegler, 1992.

northeast. At the boundary of the “Burdigalian” to “Helvetian” time a second cycle of alluvial fans was built up. Pebbles from Helvetic nappes first appear towards the top of the OMM.

OSM: Alluvial fans extending further north. Source rocks are the same as before, but with predominance of flysch. The intensity of gravel and sand transport varied repeatedly, leading to the formation of thin coal seams and freshwater limestones in areas where the detrital input was reduced. The drainage pattern is reversed; a great river coming from the Austrian Alps and from the Bohemian massif flowed in ENE-WSW direction along the foot of the future Jura. It brought pure mica rich sands (“Glimmersande”). In the Hegau area volcanic tuff debris occur in the uppermost OSM.

Two molasse formations stand out due to their uncommon lithology, which is also transmitted in a characteristic groundwater chemistry (Hesske, 1995). The “Gypsum-bearing Molasse” (USM, upper Chattian) consists of gypsum-bearing sandstones and marls and thin intercalated dolomitic limestone layers (Angelillo, 1987). It occurs in western Switzerland, at the foot of the Jura Mountains. The “Glimmersand” formation (OSM) consists of well sorted mica-rich calcareous sands (Hofmann, 1960). The “Glimmersand” formation is poorly cemented and therefore comparable in its hydraulic behaviour to unconsolidated sediments. It occurs in a narrow band along the foot of the Jura Mountains and of the Schwäbische and Fränkische Alb.

Even more than the main constituents, the heavy mineral assemblage is characteristic of the type of the source rocks and therefore shows characteristic regional variations. Most heavy minerals such as zircon, rutile, ilmenite, and epidote are very insoluble and resistant to weathering. However, certain molasse formations, such as the OMM sandstones in western Switzerland, contain more easily weatherable heavy minerals including biotite, amphiboles, pyroxenes, and spinels (Allen and others, 1985). Such heavy minerals are very important to understand groundwater compositions in the molasse.

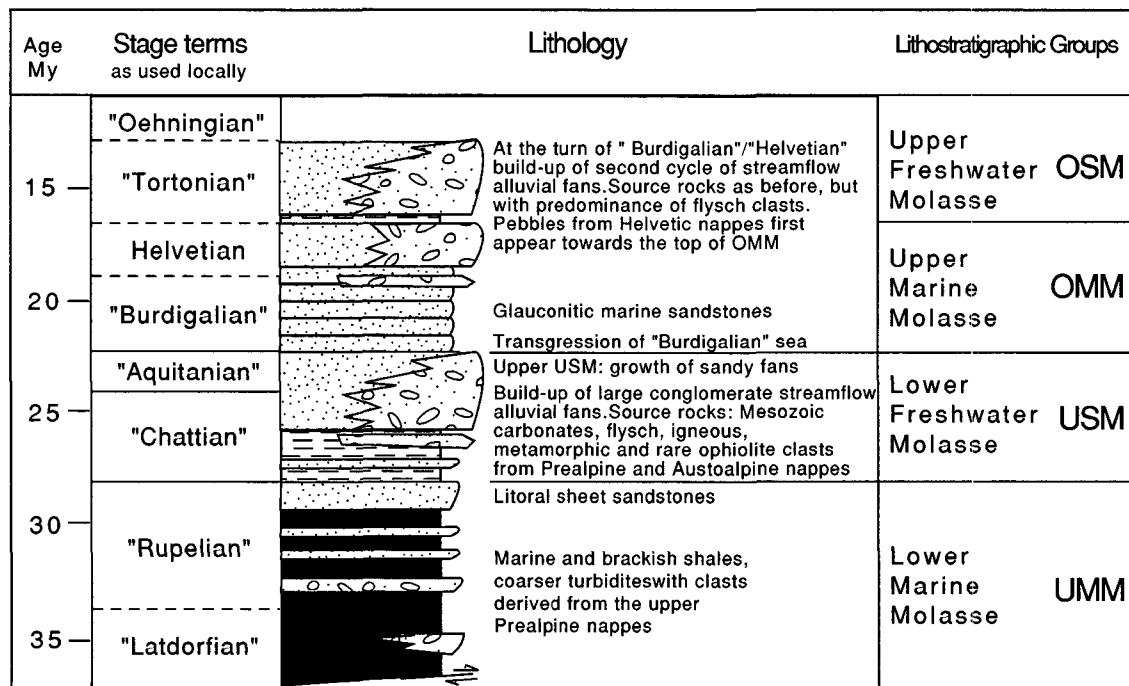


Figure 3-2: Lithologic diagram of the molasse (after Matter and others, 1980).

The sandstones and conglomerates of the USM, OMM and OSM are important aquifers in Switzerland and in neighbouring regions (Keller, 1992; Pearson and others, 1991). Particularly the thick-bedded sandstones of the OMM represent important aquifers in a large part of the Swiss plateau. The fluvial sediments of the USM and OSM include abundant conglomerates and sandstones grading into silty shales. Therefore, the USM and OSM sediments normally contain small aquifers of local extension. Outcrops of the UMM are only found in the Subalpine molasse. The marine and brackish UMM shales act as aquitards.

The investigated catchments are situated in the USM, OMM and OSM lithostratigraphic groups and are relatively small. At catchment-scale the composition of molasse rocks can be considered as homogeneous. The springs are commonly the natural outlets of local flow systems in the altered surface-near parts of the molasse. Usually, shaly layers act as hydraulic barriers (e.g. Balderer, 1979b) and the small springs emerge on top of them.

Molasse aquifers are generally characterised by a double porosity. Groundwater can circulate relatively fast along fractures and joints (“fracture flow”), and slowly within inter-granular pores (“matrix flow”). Fracture flow dominates in tectonically deformed areas, such as in the Subalpine molasse at the margin of the Alps (Parriaux, 1981; Schoepfer, 1989). Matrix flow can be dominant in weakly deformed or undeformed areas, such as in the autochthonous molasse. Long-term monitoring of three molasse springs revealed that the discharge shows large seasonal variations, which suggests that fracture flow is important in these three springs (table 3-9).

Site (data base code)		Altitude (m)	Average Q (L/min)	coeff. of variation	Av. T (°C)	coeff. of variation	Average TDS (mg/L)	coeff. of variation
Autochth. molasse	LRY	878	26±21	83.0%	7.4±1.4	19.5%	213.1±54.1	25.4%
	POZ	848	61±30	49.8%	8.3±1.4	16.5%	253.2±27.0	10.7%
Subalpine molasse	COR	597	26±23	89.5%	10.9±0.2	2.0%	535.7±23.7	4.4%

Table 3-9: Time variations of discharge (Q), water temperature (T), and total mineralisation (TDS) of three selected molasse springs in Switzerland (data from 1982 to 1996).

A review of hydrogeological data (Hesske, 1995) showed that the investigated molasse derived groundwaters contain tritium (20 to 99 TU in samples from 1985 to 1990). The residence times of these groundwaters ranging from a few days or weeks to several years (Balderer, 1990a) vary depending on aquifer permeability. The results of a number of local studies illustrate this fact (Baumann, 1987; Geologisches Landesamt Baden-Württemberg, 1990, 1992; Thierrin, 1990). The groundwaters in the “Glimmersand” appear to have relatively longer residence times, ranging from 4 to 20 years, than the groundwaters in other molasse formations (Geologisches Landesamt Baden- Württemberg, 1990, 1992). As expected, long term observation of molasse springs show a negative correlation between seasonal variations in groundwater flow and water mineralisation, which confirms the influence of the residence time on groundwater mineralisation (Petch, 1970).

In order to allow a comparison of the different molasse groundwaters taking into account the variable mineralogic composition, grain-size and hydraulic conductivity of the molasse formations, Hesske (1995) defined aquifer sub-types, according to the following hierarchy: 15 feeder systems of detritus (“Schüttungen”) are divided into 32 aquifer sub-types. The feeder systems are defined by the origin and composition of the detrital material, while the aquifer sub-types are defined by the sedimentary environment (see figure 3-17, page 93).

3.3.5. Flysch

Catchments in flysch rocks have been studied in the Niesen nappe (the majority of the sampling sites) and in the Gurnigel nappe, which both belong to the Prealps (Basabe, 1993). These flysch units build up two mountain chains extending over a distance of 60 km in SW-NE direction between Lac Léman and Thunersee in western Switzerland. The topography of this area is relatively steep, with the highest point at the Albristhorn (2762 m). The altitudes of the investigated springs range from 650 to 1950 m. While the lower slopes are covered with meadows and forest, bare rock crops out the higher regions, often as a result of landslides and rock fall. The soil cover is thickest at the valley bottoms.

In the investigated region mean annual precipitation totals 1496 mm at Les Diablerets (altitude 1162 m; 30 years mean value 1930-1960, MeteoSwiss) and 1346 mm at Adelboden at an altitude of 1320 m (30 years mean value 1961-1990, MeteoSwiss).

The Flysch of the Niesen and Gurnigel nappes consists of elastic turbidite sediments with some intercalated carbonate beds. These sediments were deposited in deep marine environments at Mid Cretaceous and Early Tertiary time (Homewood & Lateltin, 1988). The turbidite sediments, which formed from the detritus of the uplifting Alps, are composed of graded coarse-grained to fine-grained detrital material of both intra- and extra-basin origin (Caron and others, 1989). Rock types comprise polygenic conglomerates and breccias, sandstones, and intercalated shales and limestones.

The flysch sediments of the Niesen nappe are divided into the following lithostratigraphic units; from bottom to top there are the "Frutigen-Flysch", "Niesenkulm-Flysch", "Seron-Flysch" and "Chesselbach-Flysch". These units are distinguished by their slightly different lithology: The "Frutigen-Flysch" is composed of graded turbidite sediments with important conglomerate layers. It occurs in large parts of the Niesen nappe, essentially in the SE. The "Niesenkulm-Flysch" is characterised by the occurrence of decimetre-thick limestone banks intercalated in the turbidite sediments. It occurs in the central part of the Niesen nappe and forms the top of the Niesen mountain chain. The "Seron-Flysch" is again composed of graded turbidite sediments and occurs in the NW part of the Niesen nappe. It contains important polygenic and poorly cemented conglomerates with abundant carbonate components (Lombard and others, 1975). The "Chesselbach-Flysch" consists of more fine-grained turbidite sediments including sandstones and shales. Therefore, and because it crops out only in a small area, the "Chesselbach Flysch" is insignificant as an aquifer.

The detrital components found in the conglomerates include debris of various alpine rock types, such as carbonates, shales, sandstones, schists, gneisses, quartzite, amphibolite, and various igneous rocks (Ackermann, 1986; Bornhauser, 1929). The sandstones are composed in average of 60% quartz, 20% feldspars and 20% lithic fragments, mainly of sedimentary rocks. Ackermann (1986) reports a heavy mineral assemblage in the sandstones of the Niesen nappe dominated by tourmaline and zircon, with minor amounts of apatite and TiO₂ minerals. Conglomerates and sandstones are partly cemented by carbonates, partly they contain a clay matrix. In contrast to the molasse, the flysch units underwent an anchi-metamorphic overprint. As a consequence, only the clay minerals illite and Fe-chlorite occur.

A very strong tectonic deformation gave rise to sub-vertical SSE-NNW directed faults and a complicated internal folding and over-thrusting of the flysch rocks. The flysch units are mainly preserved as "décollement" nappes and thrust sheets. The Niesen nappe overlays Ultrahelvetic units in the south and is limited by the overthrust Zone Submédiane to the north.

The conglomerates and sandstones of the Niesen nappe (“Frutigen Flysch”, “Niesenkulm Flysch”, and “Seron-Flysch”) represent the majority of the investigated aquifers. The abundant intercalated shale and fine-grained siltstone beds limit regional ground water circulation. Therefore, small mountain catchments with a size of some hectares are common. The abundant limestone bands in the “Niesenkulm Flysch” give rise to local micro-karst features.

The investigated flysch groundwaters are characterised by fast flow velocities. Several tracer tests revealed groundwater flow velocities ranging from 0.5 m/h to 90 m/h (Basabe, 1993; CSD, 1985; Geotest, 1982; Kunz, 1986; Norbert, 1988). Basabe, 1993 systems of open fractures in the strongly deformed rocks favour such fast groundwater flow. In addition, in regions with abundant limestones, local micro-karst features play a significant role in flysch groundwater hydrodynamics.

Seasonal discharge variations of recent flysch groundwaters are usually high (see table 3-10), while the variations of temperature and mineralisation are small. There is a weak correlation between the altitude of the spring, its temperature and its mineralisation, with the warmer and more mineralised springs occurring at low altitudes.

Site (data base code)		Altitude (m)	Av. Q (L/min.)	coeff. of variation	Av. T (°C)	coeff. of variation	Av. TDS (mg/L)	coeff. of variation
Gurnigel nappe	GJ	1204	53±11	20.8%	5.9±0.2	3.6%	279.8±8.0	2.9%
	GT	1204	9±4	41.4%	6.0±0.7	11.3%	270.2±11.9	4.4%
Niesen nappe	AS	1560	10±4	41.1%	6.1±0.5	7.9%	428.4±16.4	3.8%
	TL	1120	2247±741	33.0%	6.3±0.3	4.8%	419.2±32.8	7.8%
	WM	660	513±253	49.4%	8.0±0.1	1.8%	359.4±27.6	7.7%
	SE	1435	729±901	123.7%	4.3±0.1	1.7%	234.0±20.0	8.5%
	SL	1430	665±256	38.5%	5.6±0.5	9.2%	271.9±13.8	5.1%
	VB	1450	593±246	41.6%	4.3±0.1	3.2%	271.7±36.7	13.5%
	LLI	1845	2311±1149	49.7%	3.3±0.2	6.4%	159.3±7.2	4.5%

Table 3-10: Time variations of discharge (Q), water temperature (T), and total mineralisation (TDS) of nine selected Flysch springs (data from 1982 to 1996; Basabe, 1993).

3.4. Hydrochemistry

For the groundwaters from each aquifer type the physical-chemical parameters, and major and trace element compositions are given in appendix B (minimum, 25th percentile, median, 75th percentile and maximum values).

Several ways exist to compare and classify large numbers of groundwater data based on major elements. The *water type* or *hydrochemical facies* refers to a water classification based on the proportions of major cations and anions (Jäckli, 1970). The water types are named using a multiple-ion designation in decreasing order of dominance. The distribution of water types in each of the aquifer types is given in appendix C.

So-called *Piper-diagrams* (Piper and others, 1953) are used to plot the distribution of major ions in the groundwaters of each aquifer type. Dominant major cations (Ca^{2+} , Mg^{2+} , and $\text{Na}^+ + \text{K}^+$) and anions (SO_4^{2-} , Cl^- , and $\text{HCO}_3^- + \text{CO}_3^{2-}$) are represented in two triangular diagrams as percentage of milliequivalents in solution. Subsequently, the data points from the cation and anion triangles are transferred to the diamond diagram by drawing lines parallel to the outer boundary until they meet in the diamond. Piper-diagrams have the advantage that dominant major element compositions can be easily compared and geochemical evolutionary trends become visible.

The distribution of aqueous species, ion activities, and mineral saturation indices of the investigated groundwaters have been calculated as a function of measured solution compositions, pH, E_{H} , and temperature. Only groundwater data with known pH values have been considered for these calculations. Unfortunately, pH data are available only for 37% of the springs in the crystalline, and for 22% of the springs in the evaporites.

Mineral saturation indices are used to evaluate if a groundwater is in equilibrium with the minerals in the aquifer. Saturation state calculations were performed using an equilibrium approach. For the young groundwaters considered here such calculations yield only saturation state indications about kinetically fast reacting minerals with which potential equilibrium could have been reached within the underground residence time of the groundwaters. Relatively fast reacting minerals that occur in the various aquifer rocks include calcite, dolomite, gypsum, barite, celestite, strontianite, fluorite, and chalcedony. In addition, the saturation states of certain groundwaters with metalliferous oxide and hydroxide phases of Ni, Mn, Cu and Cr were calculated. Chalcedony is the more soluble silica phase than quartz. However, the rate of crystallisation of quartz is so slow at low temperatures that the solubility of such soluble silica phases like amorphous silica or chalcedony represent the upper limit of dissolved silica (Stumm & Morgan, 1996). The sluggish reaction kinetics of primary Al-silicates such as feldspars, the lack of reliable stability constants (Drever, 1988), and the difficulties attached to good quality Al-analyses impede the calculation of saturation states with respect to primary Al-silicates.

Mass balance calculations have been performed with selected springwaters to test the likelihood of geologically reasonable mineral phases to get involved in the hydrochemical evolution of the groundwater from infiltrating rainwater to the spring. The difference in composition between these two solutions is due to reactions of the groundwater with minerals in the aquifer. The mineralogy of the aquifer rock is used to calculate the mass transfer for every combination of these plausible phases to fit the observed changes in solute composition. A model is realistic when the results are consistent with thermodynamic considerations (saturation states).

3. 4. 1. Recent groundwaters derived from crystalline rocks

Physical-chemical parameters

Granite and gneiss groundwaters from the Mont-Blanc and Aiguilles-Rouges massifs typically have temperatures below 10°C (table 3-11; Dubois, 1993), with the exception of granite groundwaters sampled from a number of tunnel springs situated in the Mont-Blanc road tunnel and in the galleries of the hydro-electric complex of Emosson, up to 2000 m below surface. These springs may have temperatures of up to 35°C, depending on the depth below surface. These thermal springs with temperatures >20°C were not considered in this study. However, some of the tunnel springs occur in very permeable zones with sub-vertical fractures. In these fracture zones large quantities (up to 1600 L/min) of cold groundwater circulate so fast that the water temperature remains lower than would be expected from the regional geothermal gradient (Maréchal, 1998). This is also consistent with the results of the tracer tests made in such zones (see page 47).

The pH values measured in the investigated groundwaters range from 5.9 to 8.5. Granite ground waters usually have a significantly lower pH (median pH = 6.5) than gneiss groundwaters (median pH = 7.6). The lowest pH values were measured in the most dilute granite groundwaters, which also have the lowest temperatures.

Major element concentrations

The investigated crystalline-derived groundwaters are very dilute with total amounts of dissolved solids (TDS) ranging from 22.3 to 157.7 mg/L. The most mineralised groundwaters are generally those with the highest temperatures. The hydrochemistry is dominated by Ca²⁺, alkalinity, and SO₄²⁻, and minor amounts of Na⁺, Mg²⁺, and F⁻ (figure 3-3 and table 3-11). The main water types present are: Ca-HCO₃-SO₄, Ca-Mg-HCO₃-SO₄, Ca-Na-HCO₃-SO₄, and Ca-Na-HCO₃-SO₄-F. In the majority of the samples Cl⁻ and NO₃⁻ were not detected. Although in the investigated groundwaters the Na⁺ and Cl⁻ concentrations are very low, the Na⁺/Cl⁻ ratios are always higher than in the precipitation of the investigated area.

Groundwaters evolving in granite and gneiss aquifers differ in their chemical composition. In general, gneiss groundwaters have a slightly higher total mineralisation (median TDS 75 mg/l) than granite groundwaters (median TDS 69 mg/l). This is mainly due to the higher concentrations of Mg²⁺, Ca²⁺, Sr²⁺, and alkalinity. Gneiss groundwaters are mainly of the Ca-Mg-HCO₃-SO₄ or Ca-HCO₃-SO₄ water types, and more rarely of the Ca-Na-HCO₃-SO₄ water type. The most mineralised gneiss groundwaters are Ca-Mg-HCO₃-SO₄ type waters (mean pH 7.8). On the other hand, granite groundwaters are mainly of the Ca-Na-HCO₃-SO₄-F or Ca-Na-HCO₃-SO₄ water types and rarely of the Ca-HCO₃-SO₄ water type. They typically contain higher concentrations of Na⁺, K⁺, and F⁻ than gneiss groundwaters. The Ca-Na-HCO₃-SO₄-F type groundwaters are characterised by a low pH (average pH 6.4). There is a rough correlation between water temperature and dissolved silica concentration.

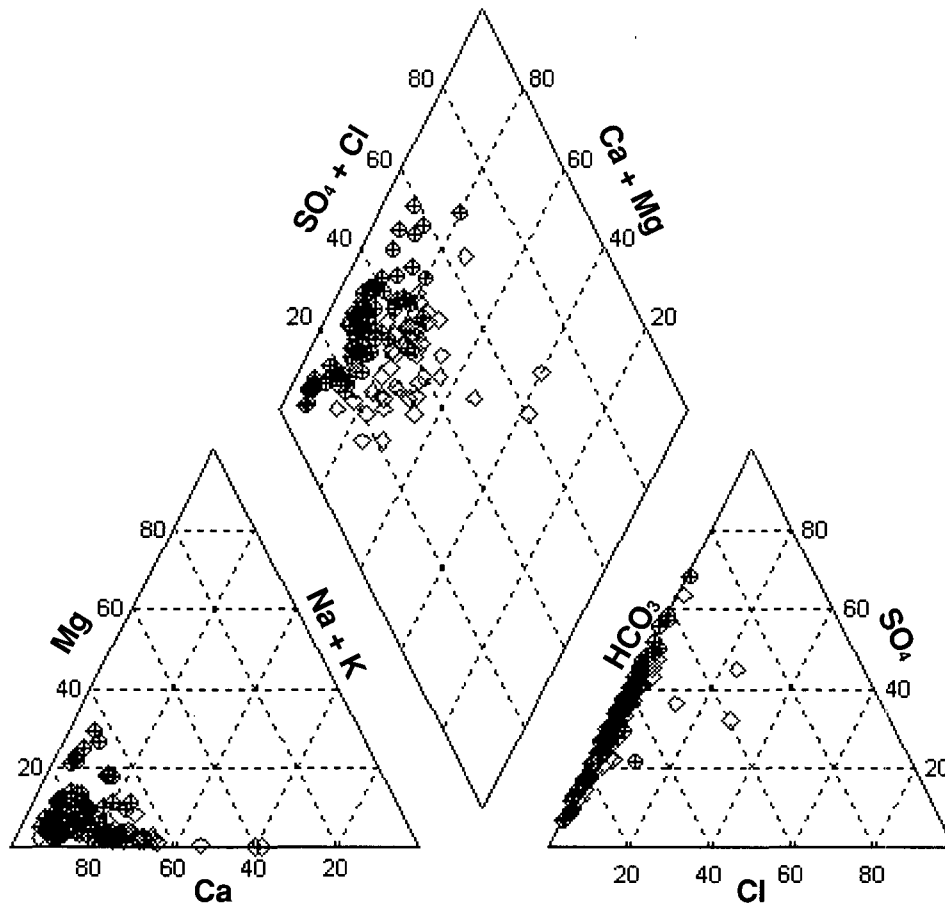


Figure 3-3: Piper-diagram showing the average chemistry of recent groundwaters from the granite and gneiss of the Mont-Blanc and Aiguilles-Rouges massifs (milliequivalents normalised to 100%). Granite: open rhombs, gneiss: crosses.

Trace element concentrations

Despite of their low total mineralisation, the investigated granite- and gneiss-derived groundwaters are characterised by high concentrations of certain trace elements. The trace element concentrations are different in granite and gneiss groundwaters (table 3-11). The granite groundwaters are characterised by elevated concentrations of Mo (median 66.9 µg/l), U (median 135.2 µg/l), W (median 3.1 µg/l), As (median 5.81 µg/l), and Rb (median 1.4 µg/l) (Dubois, 1993). The highest concentrations of U, Mo, and W occur in groundwaters with a pH between 6.2 and 7.2. There is a rough correlation between water temperature and Mo, W, and Rb concentrations. Groundwaters in gneiss often contain higher Ba (median 2.9 µg/l) and As concentrations (median 13.8 µg/l) than in granite (Dubois, 1993). The highest As concentration of 225 µg/L has been measured in a gneiss spring in “Emosson gallery South”. The high As concentrations in groundwaters in the Mont-Blanc region in relation to the rock composition and mining activities were also investigated by Pfeifer and others (1995, 2000).

Parameter	Unit	Gneiss-derived groundwaters				Granite-derived groundwaters			
		min	median	max	n	min	median	max	n
T	°C	1.4	4.7	8.6	63	0.2	8.9	18.3	46
pH	pH-units	6.6	7.6	8.5	17	5.9	6.5	8.0	35
Eh	mV	284	439	511	6	254	402	428	6
O2 diss.	mg/L	-	13	-	1	-	-	-	0
E.C. at 20°C	µS/cm	21	83	190	63	22	79	159	55
Total Hardness	°F	0.98	4.1	8.8	64	2.0	3.1	6.8	47
TDS	mg/L	22.25	75.2	157.7	64	28.7	69.1	145.8	54
Alk. as HCO ₃ ⁻	mg/L	9.15	39.1	77.5	64	15.0	29.9	54.1	55
F ⁻	mg/L	<0.2	<0.2	1.4	64	<0.2	1.1	4.0	55
Cl ⁻	mg/L	<1	<1	<1	64	<1	<1	17.1	55
NO ₃ ⁻	mg/L	<1	<1	2.5	64	<1	<1	5.0	55
SO ₄ ²⁻	mg/L	4.60	12.1	46.0	64	3.0	12.5	38.7	55
Mg ²⁺	mg/L	<0.2	0.7	6.1	64	<0.2	0.3	1.4	55
Ca ²⁺	mg/L	3.45	14.2	33.1	64	7.0	11.8	25.6	55
Sr ²⁺	mg/L	<0.010	0.041	0.852	63	<0.010	0.036	0.452	55
Na ⁺	mg/L	0.60	1.5	5.4	64	0.5	3.4	23.7	55
K ⁺	mg/L	<0.2	0.7	3.3	64	<0.2	1.3	3.2	55
Si total	mg/L	1.24	2.5	4.6	63	1.6	3.2	9.8	46
Li total	µg/L	<5	<5	43	64	<5	<5	210	55
Rb total	µg/L	<0.2	0.7	7.6	58	<0.2	1.4	7.2	42
Ba total	µg/L	0.20	2.9	40.1	57	<0.2	0.6	10.4	41
Al total	µg/L	-	21.8	-	1	-	-	-	0
V total	µg/L	-	0.2	-	1	-	-	-	0
Cr total	µg/L	-	0.6	-	1	-	-	-	0
Mn total	µg/L	-	0.4	-	1	-	-	-	0
Fe total	µg/L	-	11.4	-	1	-	-	-	0
Co total	µg/L	-	<0.2	-	1	-	-	-	0
Ni total	µg/L	-	0.6	-	1	-	-	-	0
Cu total	µg/L	-	0.5	-	1	-	-	-	0
Zn total	µg/L	-	2.4	-	1	-	-	-	0
Mo total	µg/L	<0.2	3.1	21.6	58	0.2	66.9	140.4	42
Cd total	µg/L	-	0.2	-	1	-	-	-	0
W total	µg/L	<0.2	0.2	32.4	40	<0.2	3.1	14.0	38
Pb total	µg/L	-	<0.2	-	1	-	-	-	0
U total	µg/L	<0.2	5.1	50.5	58	<0.2	135.2	2092.7	42
Br total	µg/L	-	4	-	1	-	-	-	0
I total	µg/L	-	1	-	1	-	-	-	0
B total	µg/L	<25	<25	47	45	<25	25.5	56	38
As total	µg/L	<0.5	13.8	225.2	58	<0.5	5.8	76.4	42
Tritium	TU	17	47	79	43	8	45	90	37
Deuterium	δ‰	-	-99.6	-	1	-	-	-	0
Oxygen-18	δ‰	-20.0	-13.4	-13.0	6	-14.0	-14.0	-13.0	5
Carbon-13	δ‰	-	-	-	0	-	-	-	0

Table 3-11: Chemical composition of recent groundwaters in granite and gneiss aquifers in the Mont-Blanc and Aiguilles Rouges Massifs (- = not analysed; data from Dubois, 1993).

Geochemical evolution

Crystalline rocks have low to very low matrix permeabilities and active groundwater circulation in such rocks occurs essentially along tectonic discontinuities (fracture flow). Therefore the hydrochemistry of recent groundwaters in crystalline rocks will be controlled by the minerals present along fracture and fissure planes. If a hydrothermal event had occurred at some time in the geological evolution, the minerals present in fractures are often substantially different from the bulk rock composition (see page 45). Hydrothermal minerals make up only a very small part of the total rock, nevertheless they are exposed along the preferential pathways and therefore determine the mineralisation of fast-circulating groundwater in the fracture networks. Along the same line of evidence goes the fact that secondary fracture mineral assemblages often include more easily dissolvable minerals, such as certain sulphides, carbonate minerals, and fluorite, than the Al-silicates of the rock matrix. In addition, clay minerals give rise to cation exchange reactions and the abundant Fe-hydroxides may act as sorbing material.

Major elements

The sources of major cations are not only important when investigating the base cation fluxes (e.g. in the context of acid rain buffering capacity and plant nutrient availability; e.g. Sverdrup, 1990), and field weathering rates (White and others, 1999) but also when investigating the sources and the chemical behaviour of dissolved trace elements. Based on the analyses of dissolved major cation concentrations, weathering reactions involving trace elements can be deduced. For example, Ba is not likely to be leached from feldspars, if the major element mineralisation of a corresponding groundwater does not show clear evidence of Al-silicate weathering.

Of the minerals considered for the saturation state calculations, especially calcite, barite, fluorite, and dolomite occur in hydrothermal mineralisations present along fractures or in calc-silicate lenses intercalated in the investigated crystalline rocks and are potential sources of groundwater mineralisation. Gypsum, barite, celestite, strontianite, fluorite, and chalcedony are potential sinks of dissolved elements.

The saturation state calculations show that within the analytical uncertainties most groundwaters from the granite and gneiss aquifers of the Mont-Blanc and Aiguilles-Rouges massifs are subsaturated with respect to all considered minerals, except chalcedony (see table 3-12). Calculated P_{CO_2} values range from $10^{-1.5}$ to $10^{-3.9}$. Granite groundwaters tend to have higher P_{CO_2} values together with their lower pH than the gneiss groundwaters. All groundwaters are slightly subsaturated to saturated with chalcedony, indicating that the solubility of chalcedony represents the upper limit of dissolved silica.

Site code	ARG ^a	Gneiss				Granite			
		EMOW/71	EMOW/72	EMOW/66	NANTPR	EMOE/84	EMOE/107	EMOE/103	EMOE/94
		Ca-Na- HCO3-SO4	Ca-Na- SO4-HCO3	Ca-Mg- HCO3-SO4	Ca-HCO3 -SO4	Ca-Na- HCO3-SO4-F	Ca-HCO3 -SO4	Ca-Na- HCO3-SO4	Ca-Na- HCO3-SO4-F
Alt. (m)	2000	1948	1947	1956	1200	1543	1553	1552	1549
TDS (mg/L)	3.8	71.1	134.0	151.0	157.7	41.4	111.7	83.6	103.6
T (°C)		4.7	4.8	7.3	6.3	4.2	5.5	9.9	11.8
pH (pH-units)	5.3	7.6	7.8	8	7.4	6.2	6.2	7.0	6.4
Alk. as HCO ₃ ⁻ (µmol/L)	0.36 ^b	560	751	1270	1165	356	887	624	645
F ⁻ (µmol/L)	-	5	5	11	11	76	21	47	150
Cl ⁻ (µmol/L)	8	8	n.d.	n.d.	24	4	11	6	13
SO ₄ ²⁻ (µmol/L)	9	119	470	325	412	41	249	187	290
NO ₃ ⁻ (µmol/L)	15	31	n.d.	n.d.	8	6	n.d.	n.d.	n.d.
Ca ²⁺ (µmol/L)	6	339	671	616	826	215	637	443	494
Mg ²⁺ (µmol/L)	n.d.	24	83	252	51	8	35	19	32
Sr ²⁺ (µmol/L)	0.02	0.89	6.72	9.72	0.15	0.12	3.83	1.31	0.61
Na ⁺ (µmol/L)	4	85	184	154	86	78	101	142	223
K ⁺ (µmol/L)	2	6	10	13	84	14	6	28	53
NH ₄ ⁺ (µmol/L)	5	-	-	-	-	-	-	-	-
Si total (µmol/L)	7	108	146	105	96	83	112	109	167
Li total (µmol/L)	-	0.14	0.29	0.29	0.80	0.07	0.07	0.14	0.14
Rb total (µmol/L)	n.d.	0.006	0.008	0.008	0.002	0.003	0.037	0.084	0.062
Ba total (µmol/L)	0.014	0.066	0.207	0.189	0.050	0.005	0.069	0.005	0.004
Mo total (µmol/L)	-	0.032	0.218	0.164	0.038	0.274	1.196	1.463	1.155
U total (µmol/L)	-	0.028	0.004	0.079	0.005	0.158	1.140	3.250	1.120
B total (µmol/L)	0.19	3.42	3.51	2.77	n.d.	0.74	2.96	2.13	2.22
As total (µmol/L)	-	2.120	0.824	0.088	0.053	0.044	0.212	0.116	0.065
log P _{CO2}	-3.50	-3.17	-3.25	-3.21	-2.65	-1.96	-1.57	-2.50	-1.87
SI calcite	-9.16	-1.38	-0.81	-0.38	-0.91	-3.16	-2.33	-1.75	-2.27
SI dolomite	-	-4.12	-2.72	-1.29	-3.19	-7.96	-6.10	-4.98	-5.80
SI fluorite	-	-3.30	-3.07	-2.47	-2.32	-1.10	-1.84	-1.34	-0.33
SI gypsum	-5.65	-2.95	-2.14	-2.36	-2.13	-3.57	-2.42	-2.68	-2.47
SI barite	-2.46	-0.92	0.07	-0.19	-0.65	-2.47	-0.66	-1.98	-2.01
SI celestite	-6.13	-3.48	-2.09	-2.11	-3.82	-4.77	-2.58	-3.17	-3.34
SI strontianite	-10.77	-3.04	-1.89	-1.28	-3.74	-5.49	-3.63	-3.41	-4.32
SI chalcedony	-1.30	-0.16	-0.04	-0.21	-0.24	-0.27	-0.16	-0.23	-0.06

Table 3-12: Average chemical compositions and saturation states with respect to selected minerals of precipitation water and eight springwaters from granite and gneiss of the Mont-Blanc and Aiguilles-Rouges Massifs. n.d. = not detected; - = not analysed. The "EMOW/71" and "EMOE/84" springs discharge the least mineralised gneiss- and granite-derived groundwater, respectively. The other springs discharge the most mineralised groundwaters of the corresponding water types.

a. Sampling site near Argentières, France; median of 13 samples (Atteia, 1992)

b. Calculated value, assuming equilibrium with CO₂(g) at atmospheric P_{CO2}=10^{-3.5}

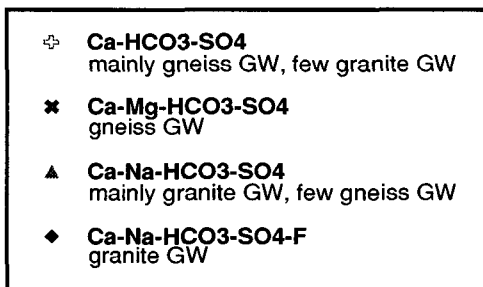
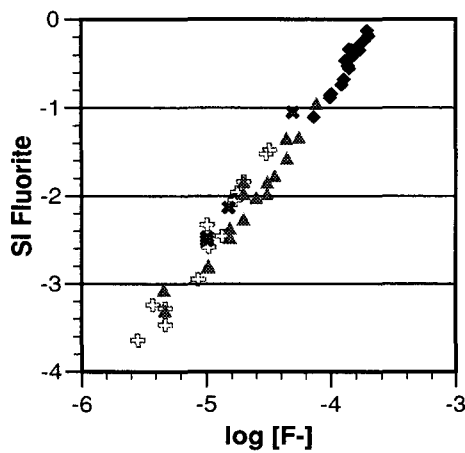


Figure 3-4: Fluorite saturation state of the different water types occurring in the granite and gneiss of the Mont-Blanc and Aiguilles-Rouges massifs compared to the average F^- activity (GW = groundwaters).

The gneiss groundwaters, particularly the more mineralised Ca-Mg-HCO₃-SO₄ type groundwaters, tend to be less subsaturated with respect to calcite, dolomite, gypsum, celestite, strontianite and barite than the granite groundwaters, due to their slightly higher CO₃²⁻, Ca²⁺, Mg²⁺, Sr²⁺, and Ba²⁺ activities and their higher pH (see table 3-11 and table 3-12). On the other hand, the granite-derived groundwaters with high F⁻ activities corresponding to concentrations of up to 4 mg/L (Ca-Na-HCO₃-SO₄-F type groundwaters) are less subsaturated with respect to fluorite than the gneiss groundwaters. There is a clear evolutionary trend towards solubility control by fluorite (figure 3-4).

In the investigated granite and gneiss groundwaters from the Mont-Blanc and Aiguilles-Rouges massifs, Ca²⁺ and alkalinity are the dominant dissolved components. Most groundwaters have a molar alkalinity/Ca²⁺ ratio between 1.0 and 2.3 (figure 3-5). The molar Na⁺/Ca²⁺ ratios range from 0.1 to 0.5 in gneiss groundwaters and from 0.2 to 1.0 in granite groundwaters. The molar Na⁺/Ca²⁺ ratios in the groundwaters are significantly different from the ratio in granitoid rocks. Therefore, the bulk rock does not contribute significantly to the groundwater chemistry.

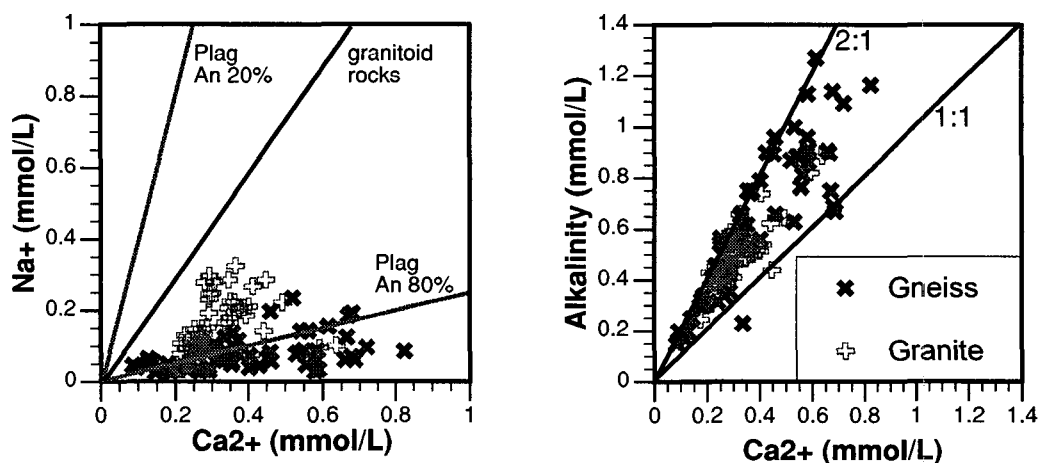


Figure 3-5: Average molar Na⁺/Ca²⁺ ratios in the groundwaters from the Mont-Blanc and Aiguilles-Rouges massifs, in granitoid rocks and plagioclase, as well as average molar alkalinity/Ca²⁺ ratios in these groundwaters. Plag An 20% = plagioclase with 20% anorthite component, i.e. with a Na/Ca ratio of 4; Plag An 80% = plagioclase with 80% anorthite component, i.e. with a Na/Ca ratio of 0.25.

In granitoid rocks, most of the Ca resides in plagioclase. Garrels (1967) suggested that the proportions of dissolved Ca^{2+} and Na^+ should reflect the stoichiometry of plagioclase, if this mineral is the principal source of Ca^{2+} . In the granite and gneiss of the Mont-Blanc and Aiguilles-Rouges Massifs the plagioclase occurring is mostly oligoclase, i.e. a plagioclase with a molar Na/Ca ratio of about 3.0. Therefore, the observed enrichment of Ca^{2+} in the investigated groundwaters has to be explained by a different Ca source than plagioclase. Two hypotheses can be proposed to explain the “excess” dissolved Ca^{2+} in recent groundwaters from crystalline rocks:

- 1.) The “excess” Ca^{2+} may be the result of dissolution of hydrothermal carbonate minerals.
- 2.) The source of the “excess” Ca^{2+} may be the weathering of other Ca-silicates such as hornblende (Clow and others, 1993) or the selective leaching of the anorthite-rich cores of plagioclase (Clayton, 1986; Williams and others, 1993).

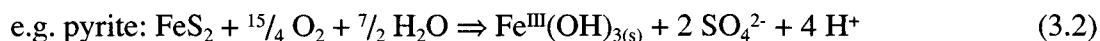
The second hypothesis is quite unlikely, because Ca-silicates such as hornblende occur only in very small amounts (<1% hornblende) in the Mont-Blanc granite and only little more in the gneisses of the Mont-Blanc and Aiguilles-Rouges massifs. Primary Al-silicate minerals are very insoluble and have sluggish reaction kinetics. At a pH of 5 the dissolution rate of hornblende ($\approx 10^{-12}$ moles m^{-2} s^{-1} ; Frogner & Schweda, 1998) is about seven orders of magnitude slower than the dissolution of calcite ($\approx 10^{-5}$ moles m^{-2} s^{-1} ; Schott and others, 1989; see table 1-2 on page 11) and also plagioclase dissolves 3 to 7 orders of magnitude slower than calcite. Such Ca-Al-silicates are therefore not likely to contribute large amounts of dissolved Ca^{2+} .

The first hypothesis has been shown to be relevant in several recent studies, which suggested that the dissolution of small amounts of carbonate minerals may have a dominant effect in the chemical weathering of granitoid rocks (White and others, 1999; Blum and others, 1998; Harris and others, 1998). Besides the marble and calc-silicate bands the para-gneisses of the Mont-Blanc and Aiguilles-Rouges massifs themselves contain small amounts of inherited carbonate minerals from their sedimentary origin. The granitic rocks contain trace amounts of calcite of late-magmatic or hydrothermal origin. This hydrothermal calcite is mainly present as crack fillings (see page 45). It also occurs as disseminated grains in the granite in amounts of a few hundred to some thousand ppm (White and others, 1999). As pointed out earlier, fractures and fissures are the preferential flow paths of groundwater in crystalline rocks. The contained carbonate minerals are therefore readily accessible to groundwater interaction. The availability of carbonate minerals and the fact that silicate minerals dissolve much more slowly than carbonates provide evidence that dissolved Ca^{2+} in the groundwater is mainly derived from dissolution of small amounts of carbonate minerals and not from weathering of silicate minerals.

If the dissolution of calcite enhanced by the uptake of atmospheric CO_2 and possibly small amounts of soil CO_2 in the catchments at lower altitudes were the primary process, then a molar alkalinity/ Ca^{2+} ratio of 2 would be the result (see reaction 3.5, page 75). However, the groundwaters from the crystalline often show lower molar alkalinity/ Ca^{2+} ratios (see figure 3-5). Additional Ca^{2+} is provided by the dissolution of fluorite (reaction 3.1), which shifts the molar alkalinity/ Ca^{2+} ratio towards lower values.



Further, in the investigated crystalline groundwaters the dissolution of carbonates is likely to be promoted not only by the acidity resulting from the dissolution of CO₂, but also by the acidity produced by the oxidation of sulphides. This process has also been proposed by Lebdioui and others (1990) from the results of a stable isotope study (³⁴S, ¹⁸O and ¹³C) on groundwaters from the Mont-Blanc road tunnel. The oxidation of the abundant hydrothermal sulphide minerals releases SO₄²⁻ and metals into solution, which subsequently precipitate as hydroxide phases:



The oxidation of sulphides explains the observed SO₄²⁻ and metal concentrations and also results in lower molar alkalinity/Ca²⁺ ratios, due to the reaction 3.3.



Most groundwaters from the crystalline aquifers show higher molar Na⁺/Cl⁻ ratios than precipitation water, indicating that besides marine aerosols an additional Na-source is required. However, the Na⁺ concentrations are mostly below 5 mg/L, which is very low, and Cl⁻ is generally below the detection limit, indicating that the Na⁺/Cl⁻ ratios cannot be determined exactly. A likely source of Na⁺ in the investigated crystalline aquifers is Ca-Na ion exchange, which liberates 2 moles of Na⁺ per mole of adsorbed Ca²⁺ (reaction 3.4). Ion exchange reactions proceed fast compared to mineral dissolution or precipitation reactions, and equilibrium is almost always established.



In this reaction, X indicates the exchanger. The abundant clay minerals present along fractures are likely exchangers in the crystalline rocks. During hydrothermal alteration of a Na-rich rock mainly Na-rich clay minerals such as smectite are formed. Clay minerals generally have a high cation exchange capacity (see table 1-3 on page 13). The approximate selectivity coefficient of 0.4 for Ca²⁺ with respect to Na⁺ indicates that Ca²⁺ is more strongly adsorbed than Na⁺ (Appelo & Postma, 1996; see table 1-5 on page 15). Due to the low Na⁺ concentrations, however, the amount of ion exchange is very small.

Mass balance calculations were conducted with selected granite and gneiss groundwaters to test these potential sources of dissolved elements (see table 3-12 and table 3-13). The likeliness of this weathering scenario was evaluated based on relative abundance and reactivity of the minerals present in the crystalline aquifers. Calcite dissolution was allowed as Ca²⁺ source, because of the reasons discussed above. Fluoride is derived from dissolution of fluorite, Na⁺ from Ca-Na ion exchange, and silica from a pure silica phase.

The mass balance calculation shows that it is possible to explain the mineralisation of the investigated granite and gneiss groundwaters by dissolution of calcite as source of Ca²⁺ and CO₃²⁻, fluorite (Ca²⁺ and F⁻), a pure silica phase (Si), by oxidation of sulphides (SO₄²⁻ and various trace metals), and by Na-Ca ion exchange as Na⁺ source. The positive correlation of the dissolved silica concentrations in the groundwaters and water temperature can be explained by the fact that silica phases are more soluble at higher temperature. The model shows that the more Na⁺ the groundwater contains, the more calcite has to dissolve to provide Ca²⁺ for the Ca-Na exchange.

Phases	Formula	Gneiss				Granite			
		EMOW/71	EMOW/72	EMOW/66	NANTPR	EMOE/84	EMOE/107	EMOE/103	EMOE/94
		Ca-Na- HCO ₃ -SO ₄	Ca-Na- SO ₄ -HCO ₃	Ca-Mg- HCO ₃ -SO ₄	Ca-HCO ₃ - -SO ₄	Ca-Na- HCO ₃ -SO ₄ -F	Ca-HCO ₃ - SO ₄	Ca-Na- HCO ₃ -SO ₄	Ca-Na- HCO ₃ -SO ₄ -F
CO ₂ gas	CO ₂	0.212	0.012	0.598	0.425	0.859	1.916	0.294	0.783
Calcite	CaCO ₃	0.371	0.752	0.679	0.855	0.208	0.669	0.482	0.522
Pyrite	FeS ₂	0.055	0.230	0.158	0.201	0.016	0.120	0.089	0.140
Fluorite	CaF ₂	0.003	0.003	0.006	0.006	0.038	0.011	0.024	0.075
Ion-exchange	Ca ²⁺ ↔ Na ⁺	0.040	0.090	0.075	0.041	0.037	0.048	0.069	0.109
SiO ₂	SiO ₂	0.101	0.139	0.098	0.089	0.076	0.105	0.102	0.160

Table 3-13: NETPATH results: Amounts of minerals weathered from infiltration to discharge in mmol per kg H₂O. Positive values indicate dissolution, negative values indicate precipitation of the corresponding mineral phase.

To conclude, the results of the mass balance models confirm that the hydrochemistry of the granite and gneiss groundwaters in the Mont-Blanc and Aiguilles-Rouges Massifs is dominated by interaction processes with the hydrothermal fracture mineralogy. Dominant processes are the rapidly occurring dissolution of carbonate minerals and fluorite, the oxidation of sulphides, and Na-Ca cation exchange on clays. Additional silicate weathering may only become important in the mineralisation of deeper thermal groundwaters with a longer residence time.

The subsaturation with respect to carbonate minerals is consistent with the short residence time of the groundwater in an aquifer system, which contains only small amounts of carbonate minerals. Besides the hydrothermal carbonates, the rare marble bands found in the para-gneiss units represent an additional source of Ca²⁺, Mg²⁺, Sr²⁺, and alkalinity. This is consistent with the higher pH, Ca²⁺ mineralisation, lower P_{CO₂} and mineral saturation values of the gneiss-derived groundwaters (see table 3-12).

Fluorite is a typical hydrothermal mineral in the Mont-Blanc granite. This mineral is likely to be the major source of F⁻ because fluorite is the most soluble F-bearing mineral. Because fluorite occurs predominantly in the granite, dissolved F⁻ is an excellent tracer of recent groundwaters from the Mont-Blanc granite. The F⁻ concentration is only limited by the solubility of fluorite. The saturation state calculations show that fluorite saturation is rarely attained. Following from the law of mass action, in groundwaters in equilibrium with fluorite, the F⁻ activities are higher at low Ca²⁺ activities and vice versa. With the given Ca²⁺ concentrations (median 11.8 mg/L) and pH values (median pH 6.5) in the granite groundwaters and at a temperature of 10°C, the equilibrium with fluorite is attained at dissolved F⁻ concentrations as high as 4.8 mg/L. This suggests that the F⁻ concentration is limited by the abundance and dissolution kinetics of fluorite.

Trace elements

The groundwater circulation in fractures explains the strong marking of groundwaters in the crystalline with trace elements such as U, Mo, As, W, and Ba, despite of the low total mineralisation. All of these trace elements are leached from the abundant hydrothermal mineralisations in the Mont-Blanc and Aiguilles-Rouges Massifs. Such mineralisations include molybdenite (MoS₂), diverse U-minerals, scheelite (CaWO₄), arsenopyrite (FeAsS),

barite, and clay minerals. Such hydrothermal veins represent zones of weakness and have been continuously reactivated from the alpine deformation to present earthquakes. It is in this network of open fractures and fissures that the bulk groundwater flow takes place.

Dissolved Ba is likely to be derived from hydrothermal barite, which is typically found associated with sulphide minerals. The trace elements Mo and As are mobilised by the oxidation of sulphides such as molybdenite and arsenopyrite or As-bearing pyrite. The dissolution of U- and W-minerals such as pitchblende, scheelite and wolframite liberates U and W. Speciation calculations show that at oxidising conditions and the given pH values U and As are present in solution in a soluble anion form, including U^{VI} -carbonate complexes and As^V -complexes. Under such conditions, dissolved Mo- and W-species occur as $Mo^{V,VI}$ - and W^{VI} -oxy-anions, respectively (Brookins, 1988). At the given element concentrations, pH, and redox conditions no solubility control exists for these elements, and they are transported in the groundwater as dissolved components. Differences in concentrations among different springwaters can be related to the variable natural abundance of the corresponding minerals and/or to sorption reactions on secondary Fe-hydroxides along the flow path. Rubidium has a similar chemical behaviour as K^+ and Na^+ and is roughly correlated with these major elements. Ion exchange reactions on clay minerals are therefore a likely source of this trace element.

3. 4. 2. Recent groundwaters derived from carbonate rocks

Physical-chemical parameters

The investigated groundwaters from carbonate aquifers have a water temperature of around 10°C (see table 3-14; Dematteis, 1995). There is a negative correlation between water temperature and altitude of the spring. Measured pH values range from 6.5 to 7.9 and most carbonate groundwaters have a near neutral pH (median pH = 7.2). Measured E_H values (median 440 mV) indicate oxidising conditions, which are consistent with the dissolved oxygen contents ranging from 6 to 14 mg/L.

Major element concentrations

The investigated carbonate karst groundwaters are characterised by an intermediate total mineralisation (median 345 mg TDS/L). The groundwaters discharged at low altitude springs tend to be more mineralised than at high altitude springs. The major element chemistry is dominated by Ca^{2+} and alkalinity and minor amounts of Mg^{2+} and SO_4^{2-} (figure 3-6 and table 3-14). The groundwaters are mostly of the Ca- HCO_3 water type (54%), as well as of the Ca-Mg- HCO_3 water type (30%), or the Ca-Mg- HCO_3 - SO_4 water type (16%). These three hydrochemical facies can be related to aquifer lithology (Dematteis, 1995): The Ca- HCO_3 water type is found in pure limestone aquifers. The Ca-Mg- HCO_3 water type occurs in dolomitic limestone or dolostone aquifers, while the Ca-Mg- HCO_3 - SO_4 water type is found in aquifers composed of carbonate series containing evaporite beds with gypsum and other sulphate minerals (see page 48).

In the investigated carbonate karst groundwaters Na^+ and Cl^- concentrations are generally very low, with the exception of the springs close to the coast in Slovenia and Greece, where sea spray has a considerable influence. The Na^+/Cl^- ratios are similar to the ratios found in

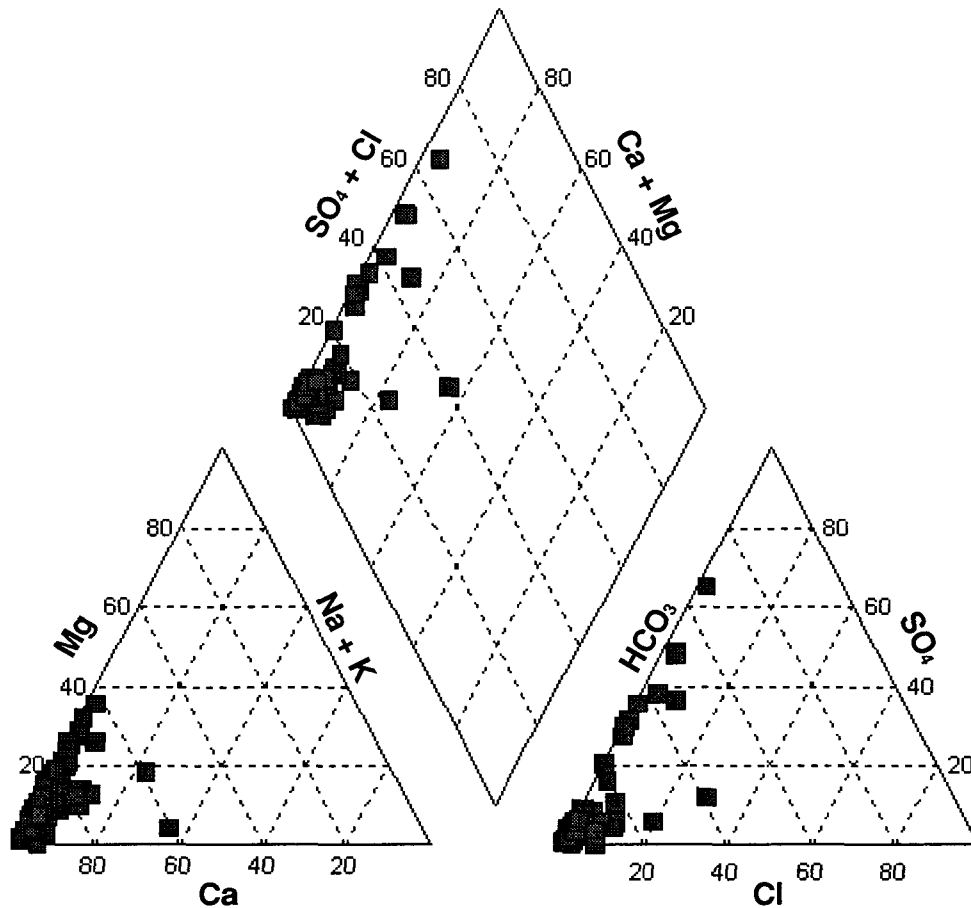


Figure 3-6: Piper-diagram depicting the distribution of the average groundwater chemistry in the investigated carbonate aquifers (milliequivalents normalised to 100%).

precipitation. Further, dissolved K^+ , F^- , and NO_3^- concentrations are usually very low, too. The dissolved silica concentration (median 3.0 mg Si/L), is positively correlated with water temperature.

Trace element concentrations

In the investigated carbonate karst groundwaters trace elements including Al, B, Ba, Br, Cr, Cu, Mn, Fe, I, Mo, Ni, Pb, Rb, U, V and Zn are present in small amounts, while the As, Cd, and Li concentrations are below or hardly above the detection limit (Dematteis, 1993).

Iodine (up to 37.7 $\mu\text{g/L}$) is generally elevated in carbonate karst groundwaters. However, only few reliable data are available.

In addition, specific trace elements occur in the groundwaters from certain carbonate units (Dematteis, 1995):

- Barium is most elevated (up to 220.0 $\mu\text{g/L}$) in the groundwaters from deep sea limestones, such as the Maiolica and Scaglia formations in the Apennine (Italy), the Vigla and Sinais formations in NW Greece, and the “Malm” of the Préalpes Médiannes.

- Vanadium is found in elevated concentrations (up to 1.4 µg/L) in the groundwaters from the “Malm” in the Jura mountains in western Switzerland, and in the groundwaters from the Cretaceous units of the Trieste region.
- Molybdenum (up to 10.7 µg/L) and uranium (up to 3.1 µg/L) are often elevated in the groundwaters from dolomite-bearing aquifers.

Parameter	Unit	minimum	median	maximum	n
T	°C	3.3	9.8	14.1	86
pH	pH-units	6.5	7.2	7.9	85
Eh	mV	207	440	519	72
O2 diss.	mg/L	6	12	16	66
E.C. at 20°C	µS/cm	147	347	609	79
Total Hardness	°F	9.5	20.0	47.8	86
TDS	mg/L	160.5	345.4	547.2	87
Alkalinity as HCO ₃ ⁻	mg/L	78.0	213.5	372.1	87
F ⁻	mg/L	<0.2	<0.2	0.4	87
Cl ⁻	mg/L	<1	2.7	52.9	87
NO ₃ ⁻	mg/L	<1	3.0	30.1	87
SO ₄ ²⁻	mg/L	<1	8.6	148.9	87
Mg ²⁺	mg/L	<0.2	4.1	19.8	87
Ca ²⁺	mg/L	28.7	72.3	126.6	87
Sr ²⁺	mg/L	0.010	0.150	1.750	87
Na ⁺	mg/L	<0.2	1.6	45.2	87
K ⁺	mg/L	<0.2	0.8	6.5	87
NH ₄ ⁺	mg/L				
Si total	mg/L	<0.5	3.0	8.2	87
Li total	µg/L	<1	<1	6	87
Rb total	µg/L	<0.2	0.6	7.5	87
Ba total	µg/L	<0.2	11.1	220.0	87
Al total	µg/L	<0.2	3.0	137.0	87
V total	µg/L	<0.2	0.4	1.4	87
Cr total	µg/L	<0.2	0.4	2.8	87
Mn total	µg/L	<0.2	1.1	36.9	87
Fe total	µg/L	<2	<2	1352.9	87
Co total	µg/L	<0.2	<0.2	0.5	87
Ni total	µg/L	<0.2	0.5	4.0	78
Cu total	µg/L	<0.2	0.3	50.8	87
Zn total	µg/L	<0.2	0.9	86.6	87
Mo total	µg/L	<0.2	0.3	10.7	87
Cd total	µg/L	<0.2	<0.2	0.2	18
W total	µg/L	-	-	-	0
Pb total	µg/L	<0.2	0.4	6.0	87
U total	µg/L	<0.2	0.3	3.1	87
Br total	µg/L	<1	3	96	87
I total	µg/L	<1	18	38	19
B total	µg/L	<1	8	49	87
As total	µg/L	<0.5	<0.5	1.4	87
Tritium	TU	-	-	-	0
Deuterium	‰	-	-	-	0
Oxygen-18	‰	-	-	-	0
Carbon-13	‰	-14.8	-11.3	-7.0	34

Table 3-14: Chemical composition of the investigated carbonate karst groundwaters (data from Dematteis, 1995. - = not analysed).

Geochemical evolution

In carbonate rocks water circulation occurs essentially along fractures and joints (fracture flow), which may be enlarged into conduits by dissolution processes (conduit flow). Due to the particular hydraulic and recharge conditions in karst aquifers (see page 50), the residence time of karst groundwaters varies strongly. In dolines and ponors, water infiltrates locally and passes directly into karst conduits. On the other hand, diffuse water infiltration passes through the soil and epikarst zone before it eventually gathers in karst conduits. Groundwater flow in conduits is rapid, sometimes even turbulent, leading to the very short residence times of karst groundwaters. In contrast, diffuse groundwater flow in small fissures and pores is much slower. Because a large part of the groundwater flow in karst aquifers takes place in conduits and fractures, the hydrochemistry of carbonate karst groundwaters is dominated by fast rock-water interaction reactions. The main minerals are calcite and dolomite, which react easily with groundwater. It is clear that high TDS values in these groundwaters are mainly related to increases in Ca^{2+} and alkalinity due to carbonate dissolution. Eventually, dissolution of rare gypsum in evaporite layers and oxidation of scarce sulphide minerals such as pyrite dispersed in the carbonate rocks can occur. Finally, clay minerals, which are of common occurrence in karst conduits, give rise to cation exchange reactions and Fe-hydroxides present along joints may act as sorbing materials.

Major elements

Although carbonate rocks are primarily composed of very reactive calcite, saturation state calculations indicate that the investigated carbonate karst groundwaters are not necessarily saturated with calcite (table 3-15 and figure 3-7). Particularly the cold and dilute groundwaters discharged by high altitude springs tend to be subsaturated with calcite. Only the warmer and more mineralised karst groundwaters discharged by low altitude springs attain equilibrium with calcite. Calculated P_{CO_2} values range from $10^{-1.14}$ to $10^{-2.75}$, which is higher than the atmospheric P_{CO_2} of $10^{-3.5}$. The investigated carbonate karst groundwaters are mostly subsaturated with dolomite, and all of them are subsaturated with respect to gypsum, fluorite, strontianite, and celestite. The Ca-Mg- HCO_3 - SO_4 type groundwaters are less subsaturated with respect to gypsum and celestite than the groundwaters of the other water types, due to their higher SO_4^{2-} activity. Saturation with chalcedony is only reached in part of the warmer and more mineralised groundwaters.

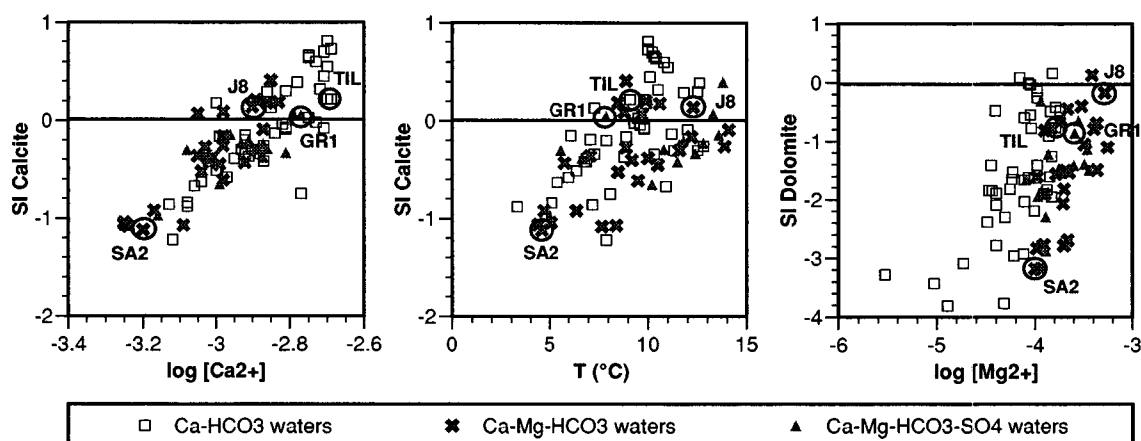


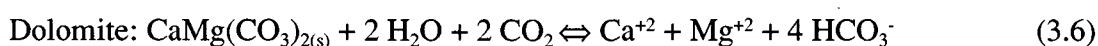
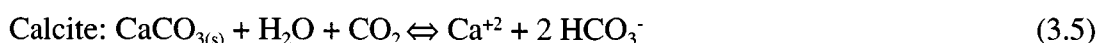
Figure 3-7: Calcite and dolomite saturation state of the investigated carbonate karst groundwaters compared to average Ca^{2+} and Mg^{2+} activities and water temperature (for marked springs see table 3-15).

Site code (Region)	Units	P-JUP ^a	P-SAR ^b	SA2 (9)	TIL (2)	J8 (2)	GR1 (4)
Water type		Precipitation		Ca-Mg-HCO ₃	Ca-HCO ₃	Ca-Mg-HCO ₃	Ca-Mg-HCO ₃ -SO ₄
Altitude	m	1350	2100	990	650	580	540
TDS	mg/L	6.92	11.12	160.55	547.17	443.69	497.73
T	°C	-	-	4.6	9.1	12.3	7.9
pH	pH-units	5.6	6.8	7.0	7.3	7.4	7.5
Alkalinity as HCO ₃ ⁻	µmol/L	2.49 ^c	39.54 ^c	1899	5687	5298	3426
F ⁻	µmol/L	-	-	2	1	19	4
Cl ⁻	µmol/L	11	12	28	408	113	47
SO ₄ ²⁻	µmol/L	13	10	45	119	98	1550
NO ₃ ⁻	µmol/L	21	21	52	485	50	39
Ca ²⁺	µmol/L	10	29	801	3159	1894	2814
Mg ²⁺	µmol/L	-	-	144	253	782	416
Sr ²⁺	µmol/L	n.d.	n.d.	0.11	1.46	6.73	19.97
Na ⁺	µmol/L	4	7	n.d.	174	61	122
K ⁺	µmol/L	1	5	5	43	18	19
NH ₄ ⁺	µmol/L	12	3	-	-	-	-
Si total	µmol/L	14	10	4	92	98	121
Li total	µmol/L	n.d.	n.d.	n.d.	0.2	0.3	0.9
Rb total	µmol/L	n.d.	n.d.	n.d.	0.008	0.007	0.008
Ba total	µmol/L	0.007	0.045	n.d.	0.102	0.103	0.577
Cr total	µmol/L	0.003	n.d.	0.012	0.005	n.d.	n.d.
Mn total	µmol/L	0.056	0.050	0.002	0.016	0.003	0.013
Fe total	µmol/L	0.036	0.036	n.d.	0.209	0.035	0.011
Ni total	µmol/L	n.d.	n.d.	0.038	0.009	0.008	0.009
Cu total	µmol/L	0.054	0.039	n.d.	0.042	0.002	0.015
Zn total	µmol/L	0.346	0.291	n.d.	0.002	0.027	0.017
Mo total	µmol/L	n.d.	n.d.	0.001	0.008	0.007	0.008
Pb total	µmol/L	0.019	n.d.	0.0005	n.d.	0.0003	0.002
U total	µmol/L	n.d.	n.d.	0.0004	0.002	0.005	0.002
I total	µmol/L	n.d.	n.d.	-	-	0.140	0.089
B total	µmol/L	0.4	0.2	0.1	0.6	0.4	4.0
log P _{CO2}		-3.50	-3.50	-2.04	-1.87	-1.98	-2.25
SI calcite		-7.19	-4.32	-1.12	0.22	0.14	0.05
SI dolomite		-	-	-3.18	-0.77	-0.17	-0.86
SI fluorite		-	-	-3.97	-4.18	-1.69	-2.8
SI gypsum		-5.34	-4.96	-3.08	-2.29	-2.56	-1.24
SI barite		-2.72	-2.03	-	-1.11	-1.22	0.7
SI celestite		-6.22	-5.89	-4.93	-3.57	-2.97	-1.34
SI strontianite		-9.21	-6.39	-4.1	-2.22	-1.45	-1.2
SI chalcidony		-1.05	-1.22	-1.57	-0.29	-0.3	-0.15

Table 3-15: Average chemical composition and saturation states with respect to selected minerals of four carbonate karst waters (region numbers refer to table 3-4) and precipitation water from two sites in Switzerland. n.d. = not detected; - = not analysed. The "SA2" spring discharges the least mineralised groundwater, while the other springs discharge the most mineralised groundwaters of the corresponding water types.

- a. P-JUP: Precipitation sampling site in the Jura mountains, median of 27 samples (Atteia, 1992);
- b. P-SAR: Precipitation sampling site in the Alps near Martigny (Valais), median of 14 samples.
- c. Calculated value, assuming equilibrium with CO₂(g) at atmospheric P_{CO2}=10^{-3.5}

Groundwaters in carbonate karst aquifers obtain their chemical characteristics from interactions with the carbonate minerals in the aquifer, mainly with calcite. Calculations show that only 0.06 mmol of calcite can be dissolved in pure water without dissolved CO_2 . However, the investigated groundwaters from carbonate karst aquifers contain Ca^{2+} concentrations ranging from 0.7 to 3.2 mmol, which is up to 50 times higher than this calculated value. The higher Ca^{2+} concentrations observed in the field result from the reaction with carbonic acid (H_2CO_3) derived from dissolved CO_2 gas. H_2CO_3 is the most important acid in natural aquifer systems. CO_2 gas is produced in the soil by decay of organic matter and root respiration. The acid provides protons (H^+) that associate with the carbonate ion (CO_3^{2-}) and form bicarbonate (HCO_3^-). Thus, further calcite can be dissolved until equilibrium is reached. Dissolution and precipitation of calcite and dolomite under field conditions can be summarised by the following equations:



If a source of CO_2 is available, dissolution of calcite will take place, while out-gassing of CO_2 will cause precipitation of calcite. According to the stoichiometry of reaction 3.5, waters in equilibrium with calcite have a molar alkalinity/ Ca^{2+} ratio of 2. The groundwaters of the Ca- HCO_3 water type, although not necessarily saturated with calcite, plot along this trend (figure 3-8). The groundwaters of the Ca-Mg- HCO_3 water type sometimes have higher alkalinity/ Ca^{2+} ratios due to their higher alkalinity from the dissolution of dolomite (reaction 3.6). The groundwaters of the Ca-Mg- HCO_3 - SO_4 water type show lower alkalinity/ Ca^{2+} ratios resulting from the higher Ca^{2+} content due to gypsum dissolution (reaction 3.7). The dissolution of associated celestite and Sr-bearing dolomite gives rise to the high Sr^{2+} contents observed in these groundwaters (see also chapter 3. 4. 3. on page 81).

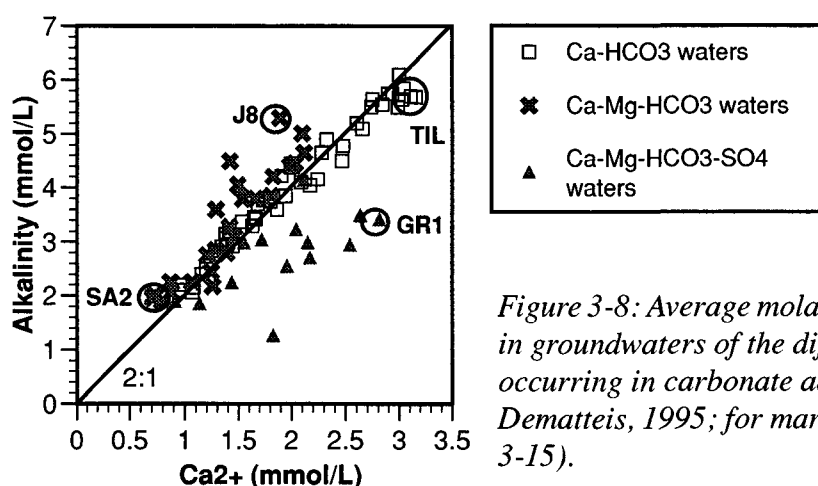
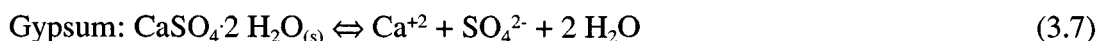


Figure 3-8: Average molar alkalinity/ Ca^{2+} ratios in groundwaters of the different water types occurring in carbonate aquifers (after Dematteis, 1995; for marked springs see table 3-15).

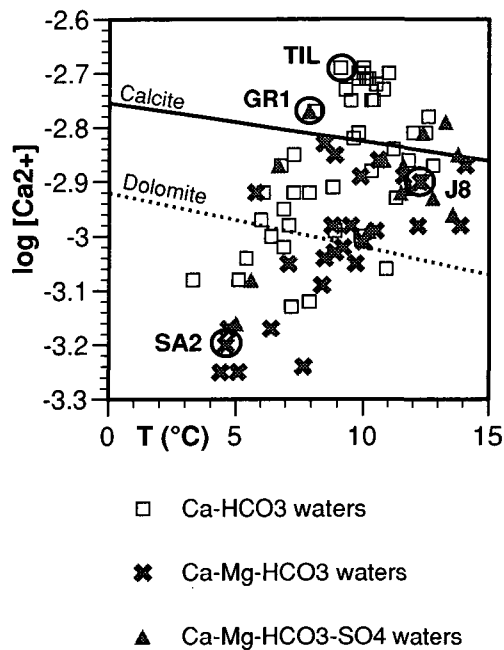


Figure 3-9: Average Ca^{2+} activities in carbonate karst groundwaters and calculated solubilities of calcite and dolomite in pure water (constant $P_{\text{CO}_2} = 10^{-2}$) as a function of water temperature (for marked springs see table 3-15).

CO_2 production occur (Buyanovsky & Wagner, 1983). The CO_2 pressure is highest when respiration is at maximum in summer and decreases during autumn and winter. CO_2 gas transfer reactions between the gaseous and the aqueous phase are often slower than reactions that produce or consume CO_2 in the aqueous phase, such as respiration, dissolution and precipitation reactions (Stumm & Morgan, 1996). Therefore, the amount of CO_2 uptake by infiltrating water also depends on the residence time of the water in the soil, and thus on the thickness and permeability of the soil.

Low altitude catchments in carbonate terrains are characterised by a mild climate, and they are usually covered by thick soils and rich vegetation. This favours CO_2 production (soil $P_{\text{CO}_2} = 10^{-1.5}$ to $10^{-2.5}$) and a certain storage of water in the soil, which leads to important uptake of soil CO_2 and thus enhanced carbonate dissolution. On the other hand, cold temperatures and poor soil development dominate in mountain catchments. Carbonate terrains at high altitudes are usually present as barren karst fields. In this case dissolved CO_2 in the infiltrating water is predominantly of atmospheric origin and the resulting low P_{CO_2} of the infiltrating water (atmospheric $P_{\text{CO}_2} = 10^{-3.5}$) leads to decreased carbonate dissolution.

The importance of soil CO_2 in the mineralisation of the carbonate groundwaters is confirmed by the distribution of the ^{13}C isotope in the investigated groundwaters (Dematteis, 1995). Due to isotope fractionation processes, carbon shows a specific ^{13}C signature in marine carbonate rocks ($\delta^{13}\text{C} = 0\text{‰}$, Morse & Mackenzie, 1990), in atmospheric CO_2 ($\delta^{13}\text{C} = -7.3\text{‰}$, Salomons & Mook, 1986), and in organically produced CO_2 ($\delta^{13}\text{C} = -27\text{‰}$, Cerling & Quade, 1993). The investigated groundwaters have ^{13}C signatures ranging from $\delta^{13}\text{C} = -14.8\text{‰}$ to -7‰ , indicating that the dissolved carbon is influenced by organically derived carbon. The lowest $\delta^{13}\text{C}$ values occur in groundwaters

In contrary to other minerals, calcite and dolomite are less soluble at higher water temperatures, because the solubility of CO_2 gas in water decreases with increasing temperature. Calculations show that at a P_{CO_2} of 10^{-2} and at a temperature of 1°C , 2.47 mmol of calcite can be dissolved, whereas at 15°C only 1.95 mmol of calcite can be dissolved. Comparison with field data shows, however, that this effect is negligible. In contrary, there is a positive correlation between Ca^{2+} activities and water temperature (see figure 3-9).

The amount of calcite to be dissolved is determined by the production of soil CO_2 . Thus, as Adams & Swinnerton pointed out first in 1937 and numerous other authors confirmed later (e.g. Drake & Wigley, 1975; Atkinson, 1977, Schoeller, 1980), the effect of increased carbonate dissolution resulting from CO_2 uptake in the soil is very important in the mineralisation of carbonate karst groundwaters. The amount of CO_2 produced in the soil by decay of organic matter and root respiration increases with temperature (e.g. Harmon and others, 1975). It also depends on the type of soil and vegetation, which again are a function of climate, and important seasonal fluctuations of

from low altitude catchments (e.g. in the French Jura mountains), while karst waters from high altitude catchments (e.g. in the dolomites) have a largely atmospheric ^{13}C signature.

One can distinguish between *open system* (constant P_{CO_2}) and *closed system* carbonate dissolution, where an initial content of CO_2 is consumed by reaction 3.5 and not replenished. Open system carbonate dissolution takes place primarily in the soil, where CO_2 is continuously produced. The open system extends through the whole unsaturated zone due to rapid gas exchange through the gas phase (Laursen, 1991). During open system carbonate dissolution the P_{CO_2} remains constant and the HCO_3^- concentration increases log-linearly with the pH. Farther down in the saturated zone, the water becomes isolated from the CO_2 source and carbonate dissolution occurs in a closed system. Here, the P_{CO_2} will decrease rapidly. Waters with low HCO_3^- and Ca^{2+} concentrations, a low P_{CO_2} , and a high pH are the result. For a given initial P_{CO_2} a much smaller amount of carbonates can be dissolved in a closed system than in an open system until equilibrium is reached.

Whether the composition of springwater evolves under open or closed system conditions can be evaluated by plotting pH against the HCO_3^- content (Langmuir, 1971, see figure 3-10). The data scatter in figure 3-10 can be explained by the variability of CO_2 production in the different soils and considering the error attached to pH and alkalinity measurements. With the available data it cannot be decided definitively whether the karst groundwaters evolve under open or closed system conditions. Nevertheless, the data mostly plot around the lines for an initial P_{CO_2} between $10^{-1.5}$ and $10^{-2.0}$, which is consistent with calculated P_{CO_2} values ranging from $10^{-1.14}$ to $10^{-2.75}$. This again illustrates clearly the influence of relatively high initial CO_2 pressures on groundwater mineralisation.

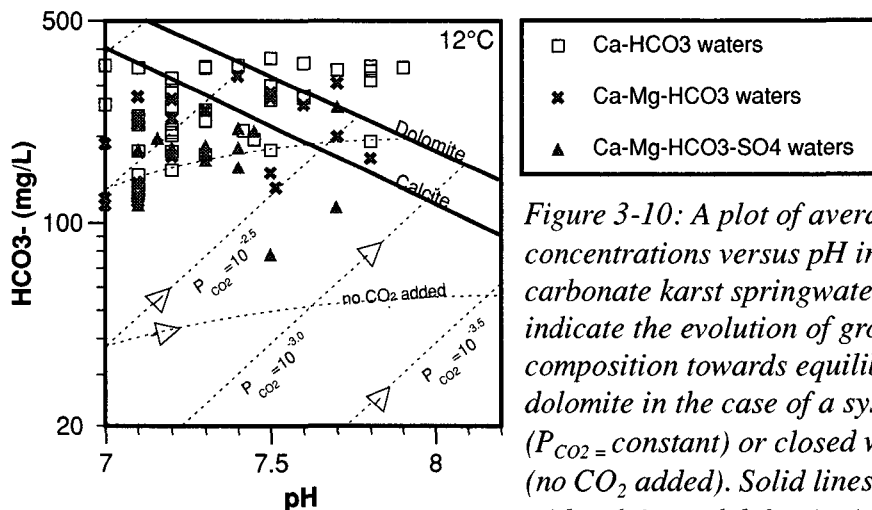


Figure 3-10: A plot of average HCO_3^- concentrations versus pH in the investigated carbonate karst springwaters. Dashed lines indicate the evolution of groundwater composition towards equilibrium with calcite or dolomite in the case of a system open to CO_2 ($P_{\text{CO}_2} = \text{constant}$) or closed with respect to CO_2 (no CO_2 added). Solid lines indicate equilibrium with calcite and dolomite (after Langmuir, 1971).

The majority of the springwaters are roughly in equilibrium with calcite. In addition to the process through which the water has attained equilibrium with calcite, other processes within the aquifer can also change the water composition up and down the equilibrium line in figure 3-10. For instance, out-gassing of CO_2 in caves will cause precipitation of calcite and the water composition will change along the equilibrium line towards higher pH and lower HCO_3^- concentrations. The result of this reaction is visible in caves where formation of speleothems is a widespread feature. The opposite case, i.e. the production of CO_2 in the aquifer, e.g. by oxidation of organic matter, will cause additional carbonate dissolution and the water composition will change towards lower pH and higher HCO_3^- concentrations. Carbonate rocks may contain small amounts of organic matter, but it is unlikely that this

plays a dominant role in the investigated aquifers. However, if an extended conduit system is developed, organic matter from the surface can be washed down into the deeper parts of the aquifer, particularly during high water periods. Decomposition of this organic matter is a source of CO₂ within the aquifer. Another explanation for increased carbonate dissolution is based on the fact that the mixing of waters with different CO₂ pressures in the aquifer will always result in *subsaturat*ion (Plummer, 1975). This effect was also described as “Mischungskorrosion” by Bögli (1978).

The subsaturation with respect to calcite of some of the investigated groundwaters (see table 3-15 and figure 3-7) can be related to the *kinetics* of carbonate dissolution reactions. Depending on the hydrogeologic conditions of the aquifer, the dissolution of carbonate rocks is controlled by several complex mechanisms, including the amount of CO₂ production in the soil, the amount of infiltrating water compared to the rock surface, the transport of solutes to and from the calcite surface either in laminar flow in small fissures or in turbulent flow in larger fissures and conduits, and the inhibition of surface reaction rates by the presence of impurities in natural carbonate minerals (Dreybrodt, 1998). Plummer and others (1978) showed that the calcite dissolution rate depends on pH and becomes increasingly dependant on P_{CO2} at a pH above 3.5. A sharp drop of the dissolution rate is observed near the equilibrium with calcite. Rickard and Sjöberg (1983) suggested that the calcite dissolution rate is controlled by both transport and surface reaction and proposed the following empirical rate expression:

$$\text{Rate [mmol} \cdot \text{cm}^{-2} \cdot \text{s}^{-1}] = k A/V (1-\Omega)^n \quad (3.8)$$

A = surface area

V = volume of solution

Ω = saturation state IAP/K

k, n = coefficients which depend on solution composition and temperature

Applying this empirical rate expression to a vertical shaft in limestone, along which water flows in thin films (e.g. 0.5 mm), Appelo and Postma (1996:123) have calculated that at a constant P_{CO2} of 10^{-1.5} and a temperature of 10°C 32 minutes are needed to reach a solution concentration of 95% of the concentration at calcite saturation. The average flow velocity of a 0.5 mm water film with a hydraulic gradient of 1 (vertical shaft) is 0.6 m/s or about 2 km/h. Accordingly, the distance covered in 32 min is about 1 km. The flow velocity increases with the square of the water film thickness. The calculations by Appelo & Postma (1996) clearly indicate that in a karst environment infiltrating groundwater can reach considerable depths and travel lengths, without reaching equilibrium with calcite. This subsaturation is necessary to explain cave formation.

Dolomite dissolves about a 100 times slower than calcite, although it is more soluble (Appelo and Postma, 1996). However, dolostones often show a higher porosity than limestones, and they are more friable, leading to large scree slopes. The contact time of water with such material is therefore often longer than with barren carbonate rock. Furthermore, the higher ratio of surface area over water volume increases the dissolution rate. This explains the large scatter of saturation states with respect to dolomite of the groundwater from dolomite bearing aquifers (see figure 3-7).

Based on these considerations, the following conclusions can be drawn: Carbonate aquifers in mountain areas are characterised by high hydraulic gradients (mainly shafts) and recharge areas show little soil development. This leads to poor rock-water contact, low CO₂ pressures of the infiltrating water, and relatively low calcite dissolution rates. The result are carbonate groundwaters with a low mineralisation that often attain the spring before

saturation with calcite is reached. In low-land carbonate aquifers hydraulic gradients are generally lower, and recharge areas usually show important soil development, leading to high CO₂ pressures of the infiltrating water. Consequently, calcite dissolution rates and the amount of calcite dissolution are higher, leading to more mineralised groundwaters which are usually saturated with calcite.

Trace elements

The trace element content of carbonate rocks depends on the sedimentary environment and on the later diagenetic and/or metamorphic overprint of the rock sequences (see Dematteis, 1995:7ff). Limestones and dolostones consist almost exclusively of calcite and dolomite. Most calcite is fairly close in composition to pure CaCO₃ and it can only contain small amounts of a few specific trace elements substituting for Ca, including Mg, Fe, Mn, Sr, and Ba, and traces of Co and Zn (Deer and others, 1992; Siegel, 1967). On the other hand, dolomite can incorporate more important amounts of trace elements substituting for Mg and Ca, including Fe, Mn, Zn, Pb, and Ni, which often results in a yellow tinge of hand specimens. In general, however, pure carbonate rocks have a low potential for specific trace elements. Most carbonate rocks are not pure. They contain a detrital component (marly or sandy layers), iron minerals such as pyrite or secondary Fe-hydroxide, fossil organic matter (bitumen, kerogen, and graphite), and - in metamorphic environments - possible hydrothermal mineralisations. In addition, dispersed micro-crystalline barite is common in the marly limestones from deep sea environments (Church, 1979), and evaporite minerals such as gypsum and celestite occur in evaporitic carbonate series (Holder, 1979a). Such accessory minerals and organic matter lead to higher amounts of dissolved trace elements in the corresponding groundwaters.

As pointed out above, the evolution of most investigated groundwaters from carbonate karst aquifers is dominated by calcite dissolution. Therefore, and because of the generally very short residence time of the groundwater in the rock, most of the investigated carbonate karst waters contain very low trace element contents. Nevertheless, groundwaters from certain carbonate units with a particular rock composition contain specific geogenic trace elements (Dematteis, 1995):

Iodine is elevated in many carbonate groundwaters. It is most concentrated in fossil organic matter such as bitumen and kerogen commonly contained in carbonate rocks (Wedepohl, 1978). The content of such organic matter in carbonate rocks is connected with their origin as biogenic detritus (debris of calcareous shells of marine organisms). Iodine is present as highly soluble anion (I⁻) in solution, which explains the high mobility of this element.

Karst waters from deep sea limestones, such as the Maiolica and Scaglia formations in the Apennine (Italy), the Vigla and Sinais formations in NW Greece, and the "Malm" of the Préalpes Médiannes in the Alps, are enriched in Ba. The Ba²⁺ activities in these low SO₄²⁻ groundwaters are so high that saturation with respect to barite is reached (figure 3-11). The fact, that barite solubility places an upper limit on the dissolved Ba concentrations at SO₄²⁻ contents surpassing 0.1 mmol (Dematteis, 1995) has been confirmed.

Uranium and molybdenum can reach high concentrations in Mg²⁺ and SO₄²⁻-rich groundwaters from dolomite-bearing aquifers. The observed U and Mo concentrations can be explained by the oxidation of Mo-bearing sulphides and the dissolution of associated U-mineralisations. Such mineralisations appear to occur particularly in aquifers containing dolomite and sulphate minerals. In addition, U and Mo mineralisations are widespread in the pre-Triassic metamorphic basement rocks below the carbonate series. It is therefore

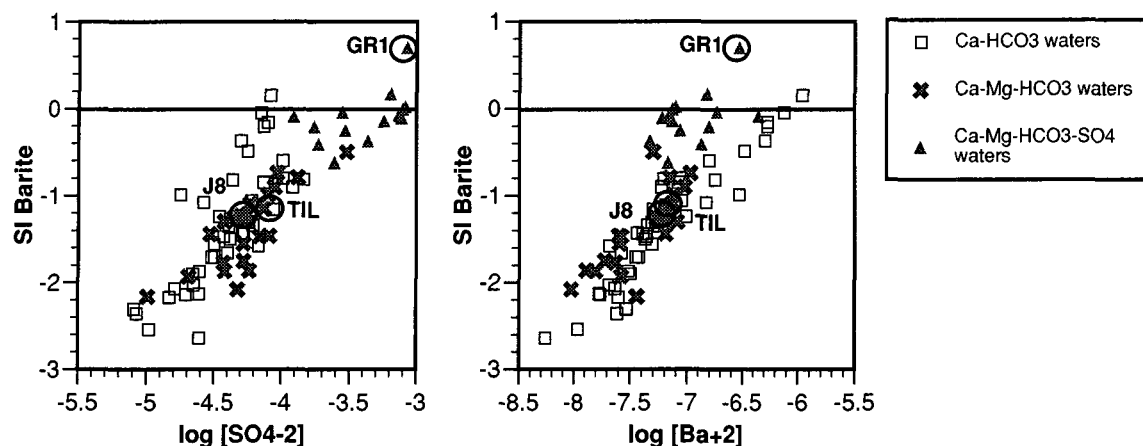


Figure 3-11: Saturation state of barite compared to average SO_4^{2-} and Ba^{2+} activities in the carbonate karst groundwaters (for marked springs see table 3-15).

possible that in certain cases the observed U and Mo anomalies originate from the underlying pre-Triassic rocks (chapter 3. 4. 3. on page 81). Another possibility is that U and Mo are contained in dolomite and associated evaporite minerals themselves (Wedepohl, 1978). This might be the case for the U - Mo anomalies observed in Jurassic dolomitic limestone formations, which are not likely to be influenced by hydrothermal mineralisations from the pre-Triassic basement.

The influence of evaporitic layers containing sulphate minerals on the water chemistry is obvious from the elevated SO_4^{2-} , Sr^{2+} , and Li concentrations. Groundwaters from carbonate series containing evaporitic rocks are less subsaturated with respect to gypsum, strontianite, celestite and barite than the other carbonate karst waters. The high Sr^{2+} and Li concentrations are associated with the dissolution of evaporite minerals (see also chapter 3. 4. 3. on page 81). Calcite can contain small amounts of Sr substituting for Ca, and micro-crystalline celestite (SrSO_4) commonly occurs in evaporite rocks as inclusions in gypsum (Holser, 1979b). The same author shows that Li is enriched in evaporite rocks, although this element does practically not occur in evaporite minerals. Lithium is very soluble and shows a low tendency to become adsorbed, which points to a presence in brine inclusions in evaporite minerals as source of dissolved Li.

Finally, V marks the groundwaters in contact with the "Malm" limestones of the western Swiss Jura mountains (particularly the "Portlandian" (upper Malm) is known for its V-anomaly) and the bituminous Cretaceous limestones of the region of Trieste. The geogenic origin of this element has been confirmed by rock leaching experiments (Dematteis, 1995). This element is usually associated with clay minerals, Fe-hydroxides and organic matter (Wedepohl, 1978). Under oxidising conditions, V appears to be present as rather soluble anion-complexes such as H_2VO_4^- and HVO_4^{2-} (Brookins, 1988), which explains its high mobility in oxygenated groundwaters.

In addition, Pb concentrations of up to 6 $\mu\text{g/L}$ have been observed. These maximum concentrations lie in the same range as in precipitation water (Atteia, 1992). Generally, Pb is strongly fixed to organic matter in the uppermost soil layers (Atteia, 1992). Atteia (1992) suggested that regarding the particular infiltration conditions in karst aquifers, it is likely that atmospheric derived Pb adsorbed to organic matter is transported into the subsoil with the groundwater. On the other hand, small concentrations of Pb have also been detected in the leachates of carbonate rocks (Dematteis, 1995), suggesting at least a partly geogenic

origin. Lead is contained in carbonate, sulphate and sulphide phases such as dolomite, cerrussite (PbCO_3), anglesite (PbSO_4), and (galena, PbS). However, the latter minerals are primarily associated with hydrothermal ore deposits and not likely to occur in the investigated carbonate units.

Certain carbonate karst groundwaters contain Cr concentrations of up to 2.8 $\mu\text{g/L}$. They are all from catchments with either a moraine cover containing ophiolite detritus, or with infiltration of water originating from non-carbonate terrains, which suggests a non-carbonate related origin of the Cr (Dematteis, 1995).

3. 4. 3. Recent groundwaters derived from evaporite rocks

Physical-chemical parameters

The investigated groundwaters from evaporite aquifers have temperatures ranging from 4.2 to 13.8°C, depending on the altitude of the spring (375 to 2220 m) (see table 3-16; Mandia, 1993). The greatest range of altitudes occurs in the Pennine and Ultrahelvetic units. The investigated evaporite groundwaters generally exhibit a near neutral pH ranging from 7 to 7.6. However, these pH data have to be regarded as semi-quantitative (see table 2-1 on page 21 and chapter “Field measurements” on page 32).

Major element concentrations

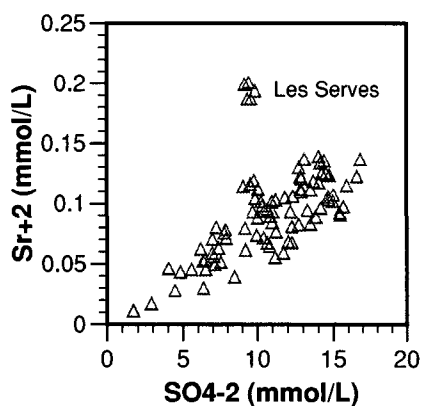


Figure 3-12: Comparison of average Sr^{2+} and SO_4^{2-} contents in evaporite groundwaters.

The investigated evaporite groundwaters are strongly mineralised (median 1782 mg TDS/L). The largest variation of groundwater mineralisation is found in the Pennine. The major element composition is dominated by Ca^{2+} , Mg^{2+} , and SO_4^{2-} (figure 3-13), which make up 80 to 90% of the groundwater mineralisation. The investigated groundwaters from evaporite rocks are typically of the $\text{Ca-Mg-SO}_4\text{-HCO}_3$ water type and show small compositional variation. SO_4^{2-} is by far the dominating anion, with average concentrations ranging from 165 to 1620 mg/L. Alkalinity generally makes up less than 20% of the total mineralisation. Groundwaters with elevated alkalinity contents only occur in aquifers predominantly composed of carbonate and detrital rocks and with a small part of calcium sulphate minerals. These groundwaters also show a lower total mineralisation than the

groundwaters circulating in rocks dominated by Ca-sulphate minerals. Average Ca^{2+} and Mg^{2+} concentrations range from 114.0 to 590.0 mg/L and 14.1 to 251.0 mg/L, respectively. The highest Mg^{2+} concentrations are found in the evaporite groundwaters of the Pennine and Helvetic units, where dolostone layers represent an important constituent of the Triassic rock sequence. Strontium is usually present at higher concentrations than Na^+ , K^+ , F^- and Cl^- , and shows a fairly good correlation with SO_4^{2-} (figure 3-12). NO_3^- is below the detection

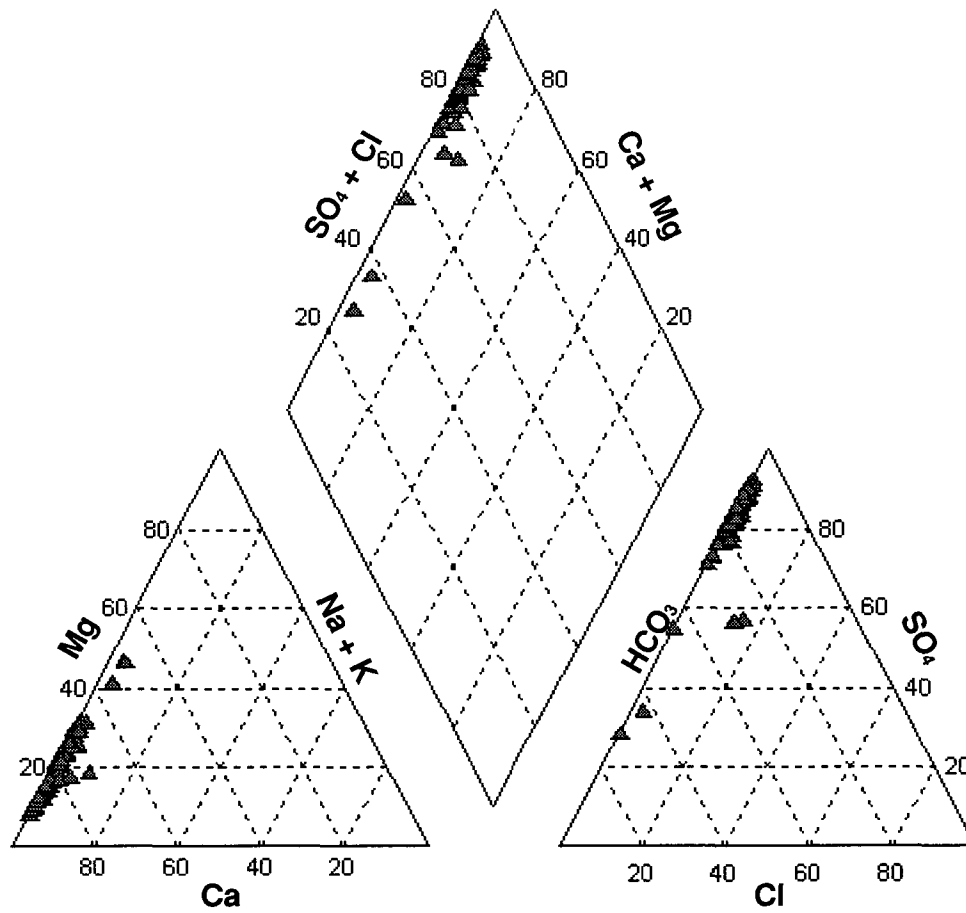


Figure 3-13: Piper-diagram showing the average chemistry of the investigated evaporite groundwaters (milliequivalents normalised to 100%).

limit in half of the samples. The highest silica concentrations (up to 9.4 mg/L) have been observed in aquifers of the Pennine.

Trace element concentrations

The trace elements Al, Ba, Br, Cu, Li, Mn, Ni, Rb, U, V, Y, Cd, and Zn occur in measurable amounts in the investigated evaporite groundwaters, while the concentrations of As, B, and Cr are usually below or hardly above the detection limit (Mandia, 1993; table 3-16).

Characteristic trace elements in evaporite-derived groundwaters are Li, Rb, Ni, Cu, Cd, Y, and Mn. These elements have all been detected in the leachates of Ca-sulphate rocks (gypsum and anhydrite), which is indicative for their geogenic origin (Mandia, 1993). In the evaporite groundwaters of the Helvetic and Pennine units, elevated U concentrations have been observed.

Parameter	Unit	minimum	median	maximum	n
T	°C	4.2	8.7	13.8	91
pH	pH-units	7.0	7.0	7.6	20
Eh	mV	-	406	-	1
O2 diss.	mg/L	-	7	-	1
E.C. at 20°C	µS/cm	750	1693	2347	91
Total Hardness	°F	49.5	130.3	196.3	91
TDS	mg/L	760.3	1782.2	2787.5	91
Alkalinity as HCO ₃ ⁻	mg/L	85.0	237.9	593.7	91
F ⁻	mg/L	<0.2	<0.2	0.9	83
Cl ⁻	mg/L	<1	2.9	78.1	91
NO ₃ ⁻	mg/L	<1	<1	41.7	91
SO ₄ ²⁻	mg/L	165.0	1043.3	1620.0	91
Mg ²⁺	mg/L	16.6	57.7	227.7	91
Ca ²⁺	mg/L	114.3	426.0	573.6	91
Sr ²⁺	mg/L	1.00	8.22	17.60	91
Na ⁺	mg/L	1.0	4.8	30.6	91
K ⁺	mg/L	0.4	1.6	17.7	91
NH ₄ ⁺	mg/L	-	-	-	0
Si total	mg/L	1.6	3.0	9.4	85
Li total	µg/L	<5	28	114	91
Rb total	µg/L	1.5	17.4	53.3	78
Ba total	µg/L	1.3	9.6	38.3	78
Al total	µg/L	<0.2	14.1	93.8	73
V total	µg/L	<0.2	0.4	1.1	70
Cr total	µg/L	<0.2	<0.2	1.1	73
Mn total	µg/L	<0.2	12.7	31.2	73
Fe total	µg/L	-	4.5	-	1
Co total	µg/L	-	<0.2	-	1
Ni total	µg/L	<0.2	3.1	35.7	78
Cu total	µg/L	<0.2	2.9	14.4	78
Zn total	µg/L	<0.2	2.1	156.2	78
Y total	µg/L	<0.2	0.6	2.4	72
Mo total	µg/L	-	2.8	-	1
Cd total	µg/L	<0.2	0.2	0.9	73
W total	µg/L	-	-	-	0
Pb total	µg/L	-	1.3	-	1
U total	µg/L	<0.2	5.2	67.0	78
Br total	µg/L	<1	8	58	73
I total	µg/L	-	2	-	1
B total	µg/L	<25	<25	95	80
As total	µg/L	<0.5	<0.5	4.3	72
Tritium	TU	-	-	-	0
Deuterium	‰	-	-	-	0
Oxygen-18	‰	-	-	-	0
Carbon-13	‰	-	-	-	0

Table 3-16: Chemical composition of recent groundwaters from evaporite aquifers in the Swiss Rhone basin (data from Mandia, 1993).

Geochemical evolution

The Triassic evaporite series in the investigated units in the Alps show a variable permeability related to their lithology and their degree of fracturing. In surface near zones composed of *gypsum*, and in the *carbonate series*, tectonic discontinuities can develop into dissolution conduits (see page 52), leading to the high permeability which is typical of karst aquifers. *Anhydrite rocks* found at depth, however, typically have an extremely low permeability. The presence of predominantly *detrital rock series* composed of sandstones, quartzites and shales, or an important detrital component in the calcium sulphate and carbonate series also reduces the permeability of Triassic rocks. Further, the very complicated tectonic structure which is present mainly in the Pennine unit has the same effect. There, the evaporite series usually occur as discontinuous shreds and lenses of varying thickness intercalated in other rocks such as schists and gneisses. Groundwater then flows mostly along fractures and extended karst systems are rare. Nevertheless, it has been shown that the investigated evaporite groundwaters generally have a short residence time (Mandia, 1993) ranging from days to months. The hydrochemistry of these groundwaters is therefore dominated by fast rock-water interaction reactions.

Major elements

Saturation state calculations show that within the analytical uncertainties most of the investigated recent groundwaters from evaporite rocks are saturated or slightly supersaturated with calcite and nearly saturated with respect to gypsum (see table 3-17 and figure 3-14). Further, the investigated evaporite groundwaters reach saturation with celestite, but are notably subsaturated with strontianite due to high Sr^{2+} and SO_4^{2-} and relatively low CO_3^{2-} activities. They also reach saturation with respect to chalcedony and dolomite. It appears that the mineral solubilities of calcite, gypsum, dolomite, chalcedony and celestite limit the concentrations of Ca^{2+} , Mg^{2+} , SO_4^{2-} , Sr^{2+} , alkalinity, and dissolved silica. Finally, the investigated evaporite groundwaters are slightly subsaturated with respect to fluorite.

Gypsum is the most soluble mineral present in the investigated evaporite aquifers and interacts readily with the groundwater. It is obvious that the high TDS values and the Ca^{2+} and SO_4^{2-} dominated hydrochemistry result from gypsum dissolution. In addition, oxidation of the sulphide minerals occurring in the Triassic units may contribute minor amounts of SO_4^{2-} as well. Further, dissolution of dolomite and calcite, which are common minerals in all Triassic rock types, contributes Ca^{2+} , Mg^{2+} , and alkalinity.

Site code	Units	P-SAR ^a	FEY	QUE
Water type		Precipitation	Ca-Mg-HCO ₃ -SO ₄	Ca-Mg-SO ₄ -(HCO ₃)
Altitude	m	2100	880	620
TDS	mg/L	11.1	760.3	2407.8
T	°C	-	8.4	9.3
pH	pH-units	6.8	7.0	7.5
Alkalinity as HCO ₃ ⁻	µmol/L	39.54 ^b	6464	4221
F ⁻	µmol/L	n.d.	3	3
Cl ⁻	µmol/L	12	342	129
SO ₄ ²⁻	µmol/L	10	1735	15459
NO ₃ ⁻	µmol/L	21	n.d.	n.d.
Ca ²⁺	µmol/L	29	2853	13344
Mg ²⁺	µmol/L	n.d.	2089	4001
Sr ²⁺	µmol/L	n.d.	11.57	91.17
Na ⁺	µmol/L	7	285	370
K ⁺	µmol/L	5	82	52
NH ₄ ⁺	µmol/L	3	-	-
Si total	µmol/L	10	185	164
Li total	µmol/L	n.d.	2.5	4.8
Rb total	µmol/L	-	0.103	0.263
Ba total	µmol/L	0.045	0.146	0.076
V total	µmol/L	-	0.021	0.017
Mn total	µmol/L	0.050	0.138	0.391
Ni total	µmol/L	-	n.d.	0.066
Cu total	µmol/L	0.039	n.d.	0.076
Zn total	µmol/L	0.291	0.028	0.009
U total	µmol/L	-	0.145	0.190
Br total	µmol/L	-	0.4	0.1
B total	µmol/L	0.2	0.5	2.8
log P _{CO2}		-3.50	-1.53	-2.25
SI calcite		-4.32	-0.15	0.58
SI dolomite		-	-0.57	0.55
SI fluorite		-	-3.19	-2.82
SI gypsum		-4.96	-1.27	-0.05
SI barite		-2.03	0.06	0.17
SI celestite		-5.89	-1.6	-0.17
SI strontianite		-6.39	-1.64	-0.69
SI chalcedony		-1.22	0.02	-0.04

Table 3-17: Average chemical composition and saturation states with respect to selected minerals of precipitation and two evaporite springwaters. *n.d.* = not detected. The “FEY” and “QUE” springs discharge the least mineralised groundwater and one of the most mineralised groundwaters, respectively.

a. P-SAR: precipitation sampling site near Martigny, Valais; median of 14 samples (Atteia, 1992)

b. Calculated value, assuming equilibrium with CO₂(g) at atmospheric P_{CO2}=10^{-3.5}

The elevated concentrations of Sr^{2+} in the investigated groundwaters can be related to the general enrichment of this element in evaporite rocks (e.g. Holser, 1979b). Sr occurs in the crystal structure of carbonate minerals, mainly in dolomite, or in celestite (SrSO_4), which is the most important Sr mineral. In calcium sulphate rocks, celestite commonly occurs as micro-crystalline inclusions in gypsum (Holser, 1979b). Secondary celestite is also a common vein mineral in the triassic dolomite series in the Alps (Baud, 1987; NAGRA, 1993). The presence of secondary celestite in veins has been related to the re-crystallisation of an aragonite sediment with a high Sr content to low-Mg calcite and dolomite. Aragonite may hold up to 8000 ppm Sr, whereas dolomite and calcite can contain only 200 to 600 ppm (Deer and others, 1992). As gypsum dissolves, the celestite inclusions dissolve as well. The dissolution of celestite in veins and Sr-bearing dolomite provide further Sr^{2+} . This explains the fairly good positive correlation of Sr^{2+} and SO_4^{2-} , both in the leachates of gypsum rocks and in most of the investigated evaporite groundwaters (Mandia, 1993; figure 3-12). The fact that some of the investigated evaporite groundwaters are saturated with respect to celestite might also indicate that some of the secondary celestite observed in veins has precipitated in recent times from the circulating groundwater.

The normally very low Cl^- concentrations indicate that dissolution of salt minerals such as halite is only significant in less than 5% of the investigated springs. The Na^+/Cl^- ratios are slightly higher than in precipitation, suggesting that a source of Na^+ must exist in the aquifer. As suggested in chapter 3. 4. 1. on page 60, in recent groundwaters a probable source of dissolved Na^+ is Ca-Na cation exchange (reaction 3.4). This would be fully consistent with the abundant occurrence of clay minerals in the Triassic evaporite series.

Fluorite occurs in variable amounts in the alpine Triassic formations (Baud, 1987; NAGRA, 1993). Dissolution of fluorite is the most probable source of the small F^- contents in the investigated evaporite groundwaters. Based on the solubility product of fluorite, much smaller quantities of fluorite can be dissolved before saturation is reached in these Ca-rich groundwaters compared to groundwaters with low Ca^{2+} concentrations, such as for example groundwaters in crystalline rocks (see page 68). This calculation shows that with the given Ca^{2+} concentrations (median 426.0 mg/L) and pH values (median pH 7.0) and at a temperature of 10°C, the equilibrium with fluorite is already attained at dissolved F^- concentrations of 1.1 mg/L. The F^- concentration in these evaporite groundwaters thus always remains very low. The subsaturation of the investigated evaporite groundwaters with respect to fluorite indicates that either fluorite occurs only locally in larger quantities in the Triassic evaporite series, or that dissolution kinetics of fluorite at neutral pH and in the highly mineralised groundwaters is too slow to attain equilibrium.

The highest silica concentrations (up to 9.4 mg/L) can be observed in groundwaters from Pennine evaporite aquifers. In contrast to the groundwaters from the Préalpes Médiannes, the Helvetic, and the Ultrahelvetic tectonic units where the aquifers are predominantly composed of sulphate and carbonate rock series, the groundwaters in the Pennine evaporite aquifers flow also through fractured calcareous quartzites and shales, and, due to the complicated tectonic structure, through other siliceous rock types such as schists and gneisses. The extent of karst development therefore tends to be lower and the residence time of groundwater in these detrital and metamorphic rocks longer (Mandia, 1993).

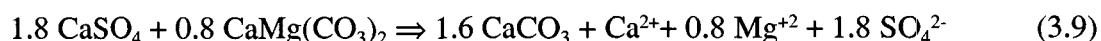
Mass balance calculations were carried out to test these potential sources of dissolved elements (see table 3-18). Two evaporite springwaters were selected for these calculations, the least mineralised (FEY) and one of the most mineralised springwater (QUE).

Phases	Formula	FEY	QUE
Gypsum	CaSO ₄ ·2H ₂ O	1.714	15.395
Celestite	SrSO ₄	0.012	0.091
Dolomite	CaMg(CO ₃) ₂	2.090	4.011
Calcite	CaCO ₃	-0.842	-5.878
CO ₂ gas	CO ₂	4.762	2.319
Ion exchange	Ca ²⁺ ↔ Na ⁺	0.139	0.182
Fluorite	CaF ₂	0.0016	0.0015
Barite	BaSO ₄	0.00011	0.00004
SiO ₂	SiO ₂	0.175	0.155

Table 3-18: NETPATH results: Amounts of minerals weathered from infiltration to discharge in mmol per kg H₂O. Positive values indicate dissolution, negative values indicate precipitation of the corresponding mineral phase (for composition of selected groundwaters see table 3-17).

The results of these mass balance calculations confirm that gypsum, and dolomite dissolution are the dominant processes in the evolution of the investigated evaporite groundwaters. In addition, small amounts of celestite, fluorite, silica phases, and barite dissolve. The Na content in the groundwater can indeed be related to Ca-Na ion exchange. The mass balance calculations further show that with the given water composition calcite must precipitate: The more gypsum and dolomite is dissolved, the more calcite must precipitate from the solution. The relatively large CO₂ gas mass transfer can be explained by CO₂ production in the soil by the decay of organic matter in an open system. Because of the low solubility of anhydrite rocks occurring in deeper zones, it is likely that most evaporite groundwaters evolve in shallow parts of the subsoil, where soil CO₂ may still have an influence on the water chemistry. If extended conduit systems have developed, organic matter from the surface may be washed down into deeper parts of the aquifer, providing a deeper source of CO₂ gas. Finally, small amounts of organic matter may also be present in the sediments in the aquifer, and its decay may produce further CO₂.

The elevated Ca²⁺, Mg²⁺, and SO₄²⁻ concentrations and the relatively low alkalinity of the investigated evaporite groundwaters can be related to a process known as *dedolomitisation*. Dedolomitisation has been described for dolomite bearing aquifers in combination with gypsum dissolution (Back & Hanshaw, 1970; Wigley, 1973; Atkinson, 1983; Back and others, 1984; Plummer and others 1990). As a result of gypsum dissolution, dolomite dissolves and calcite precipitates:



The increasing Ca²⁺ concentration due to gypsum dissolution causes calcite to precipitate. The CO₃²⁻ concentration decreases as calcite precipitates, and this provokes further dissolution of dolomite and an increase of the Mg²⁺ concentration. According to equation 3.9 two moles of calcite must precipitate for each mole of dolomite that dissolves.

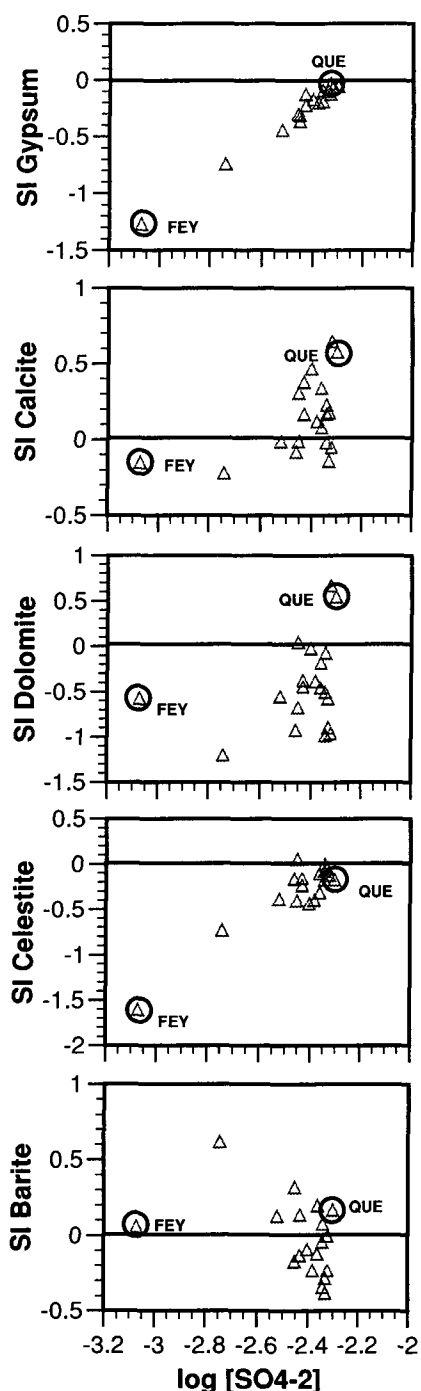


Figure 3-14: Saturation state of the investigated evaporite groundwaters with respect to gypsum, calcite, dolomite, celestite and barite compared to average SO_4^{2-} activities (see table 3-17 for marked groundwaters).

concentrations in the water (Berner, 1975). The latter is consistent with a similar supersaturation with calcite for groundwaters of the Madison aquifer observed by Plummer

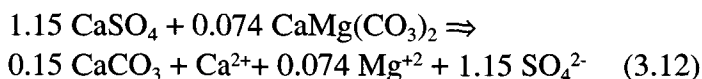
This situation has been described by Plummer and others (1990) for the Madison aquifer (USA), and is illustrated for the investigated evaporite groundwaters in figure 3-14. The SO_4^{2-} concentration can be used to deduce the extent of gypsum dissolution. The saturation state for gypsum ranges from subsaturated to saturated. All of the investigated evaporite springwaters are saturated or slightly supersaturated with calcite, regardless of the SO_4^{2-} concentration. The scatter for saturation with respect to dolomite is larger than for calcite, and some groundwaters are still subsaturated with dolomite. As long as equilibrium with calcite and dolomite is maintained, the ratio of the Mg^{2+}/Ca^{2+} activities must remain about 0.8 according to equation 3.9. Since the two ions behave similarly regarding complexation and activity coefficient corrections, the ratio of total concentrations should also remain about 0.8. The plots in figure 3-15 show that the investigated evaporite groundwaters do not exactly follow the expected trends, particularly the Mg concentrations are lower than expected. However, the apparent supersaturation with calcite influences the Mg^{2+}/Ca^{2+} ratio dramatically (Appelo & Postma, 1996:115). At a SI_{calcite} of +0.5 this ratio becomes:



$$\text{at } 25^\circ C \quad (3.11)$$

$$\frac{K_{Dol}}{K_{Cc}^2} = K_{4.22} = \frac{[Mg^{2+}]}{[Ca^{2+}]} = \frac{10^{-17.09}}{(10^{-8.48 + 0.5})^2} = 0.074$$

The overall mass transfer now changes to:



The graph illustrating this stoichiometry is shown in figure 3-15. This relation represents a lower boundary for the increase of Mg^{2+} and SO_4^{2-} , whereas the plot for Ca^{2+} and SO_4^{2-} follows the calculated trend quite well. It appears that the mass transfer coefficients depend on the degree of calcite supersaturation. This supersaturation is either due to analytical uncertainties, particularly the semi-quantitative pH measurements, or it may partly be caused by precipitation inhibitors such as the high Mg^{2+}

and others (1990). These authors found low average rates: $0.59 \mu\text{mol}\cdot\text{L}^{-1}\cdot\text{y}^{-1}$ for calcite precipitation, $0.25 \mu\text{mol}\cdot\text{L}^{-1}\cdot\text{y}^{-1}$ for dolomite dissolution, and $0.95 \mu\text{mol}\cdot\text{L}^{-1}\cdot\text{y}^{-1}$ for gypsum dissolution. The investigated evaporite groundwaters generally show shorter residence times than the groundwaters in the Madison aquifer, which infiltrated between 23'000 b. p. and recently (Plummer and others, 1990). If equilibrium is not attained in the older groundwaters in the Madison aquifer, it is well possible that equilibrium is not attained in the investigated groundwaters with short residence times.

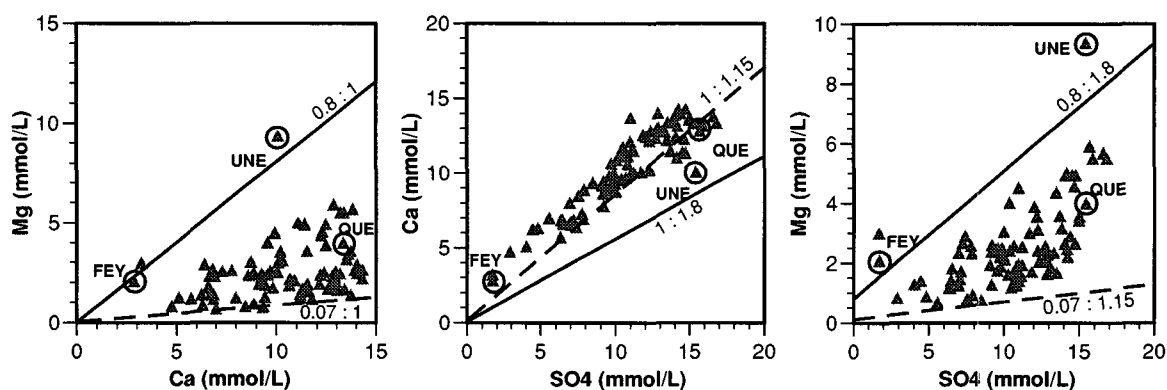


Figure 3-15: Comparison of average dissolved concentrations of Ca^{2+} , Mg^{2+} and SO_4^{2-} for the investigated evaporite groundwaters (see table 3-17 for marked groundwaters). Full lines indicate expected trends when groundwater is in exact equilibrium with calcite and dolomite, and dashed lines when $SI_{\text{calcite}} = 0.5$ (relation 3.12). Modified after Appelo and Postma, 1996.

Trace elements

The investigated evaporite groundwaters contain elevated concentrations of Li, Rb, Ni, Cu, Cd, Y, and Mn. Leaching experiments showed that these elements have a geogenic origin, related to the dissolution of gypsum-bearing evaporite rocks (Mandia, 1993). As gypsum is fairly close in composition to pure CaSO_4 (Deer and others, 1992), these trace elements are probably contained in associated carbonate, phosphate and clay minerals, and/or in brine inclusions.

Lithium and rubidium are both highly soluble, but not very reactive elements, and there seems to be no mechanism that removes significant amounts of Li or Rb from the solution. Therefore, with ongoing evaporation these trace elements are enriched in the brine and finally in evaporite rocks (Holser, 1979b). Lithium and rubidium are incompatible in the structure of the minerals commonly occurring in the investigated evaporite rocks. Therefore, they may be contained in brine inclusions in evaporite minerals. Rubidium is possibly also adsorbed on clay minerals. During dissolution of evaporite rocks, the highly soluble Li and Rb are enriched in the groundwater.

Yttrium occurs in rocks primarily in phosphate minerals such as apatite, and in fluorite (Wedepohl, 1978). This element has a chemical behaviour and solubility similar to heavy REE (Liu & Byrne, 1997). Bau and others (1997) have observed in the eastern Mediterranean sea that Y is relatively enriched in oxic seawater, compared to anoxic seawater. They explained this anomaly by the fact that Y is less easily adsorbed on Fe- and Mn-oxy-hydroxides than other heavy REE. It is therefore likely that this Y enrichment is also found in evaporite rocks. Apatite has been observed in the Triassic dolomite series near Aigle (Baud, 1987). In addition to Y, apatite often contains also appreciable amounts of Cd.

Dissolution of apatite may therefore explain the enrichment of Y and Cd in evaporite groundwaters. The dissolved Y concentrations are limited by sorption on secondary Fe-hydroxides (Bau, 1999).

Accessory barite has been reported from the Triassic evaporite series. Barite is the most likely source of dissolved Ba. The investigated evaporite groundwaters are about in equilibrium with barite (BaSO_4). The diagram with the barite saturation index plotted against the SO_4^{2-} activity (see figure 3-14) indicates that the Ba concentration is limited by the solubility of barite. Following from the solubility product of barite, these SO_4^{2-} -rich groundwaters can contain only small quantities of dissolved Ba before saturation with barite is reached. The apparent supersaturation of barite can be explained by the rather sluggish precipitation kinetics of barite, as the solution gets enriched with SO_4^{2-} due to the ongoing dissolution of gypsum.

Dolomite may hold significant amounts of Fe, Mn, and Sr, and smaller amounts of Zn, Pb, Co, and Ni substituting for Mg (Deer and others, 1992). Dissolution of large amounts of Mn- and Ni-bearing dolomite can explain the elevated Mn and Ni contents found in the evaporite groundwaters. In addition, sulphides such as pyrite, and Cu-, Pb-, and Zn-sulphides have widely been observed in the Triassic rock series of the Alps. Their oxidation releases SO_4^{2-} and the corresponding metals such as Cu, Ni, Zn, and possibly Cd into solution. Sulphide oxidation produces acidity, which is buffered by further carbonate dissolution (reaction 3.2). In oxygenated groundwaters with near neutral pH, the concentrations of dissolved Fe, Mn, Ni, and Cu is limited by the solubility of hydroxide and oxide phases including ferrihydrite ($\text{Fe}^{\text{III}}(\text{OH})_3$), manganite ($\text{Mn}^{\text{III}}\text{OOH}$), birnessite ($\text{Mn}^{\text{IV}}\text{O}_2$), $\text{Ni}(\text{OH})_2$, and malachite ($\text{Cu}^{\text{II}}_2\text{CO}_3(\text{OH})_2$) (Adriano, 1986). Saturation state calculations show, however, that the investigated groundwaters are subsaturated with manganite, $\text{Ni}(\text{OH})_2$ and malachite (see table 3-19). Inorganic complexation with SO_4^{2-} or CO_3^{2-} decreases the activity of M^{2+} ions such as Mn^{2+} , Ni^{2+} and Cu^{2+} , and thus leads to a greater subsaturation with the corresponding oxide or hydroxide phase. The solubility of these elements is thus enhanced. This is particularly important in strongly mineralised groundwaters, such as the investigated evaporite groundwaters. Speciation calculations show that these elements are not only present in solution as free ions, but to an important part as uncharged sulphate and carbonate complexes (table 3-19).

Site code	FEY	QUE		FEY	QUE		FEY	QUE
Mn ($\mu\text{mol/L}$)	0.138	0.391	Cu ($\mu\text{mol/L}$)	n.d.	0.076	Ni ($\mu\text{mol/L}$)	n.d.	0.066
Mn^{+2}	66.7%	63.1%	$\text{Cu}(\text{OH})_2^0$	-	47.3%	NiCO_3^0	-	86.6%
MnSO_4^0	4.4%	19.0%	CuCO_3^0	-	40.2%	Ni^{+2}	-	7.6%
MnHCO_3^+	23.2%	10.5%	Cu^{+2}	-	4.9%	NiSO_4^0	-	3.0%
MnCO_3^0	5.7%	7.7%	CuHCO_3^+	-	4.6%	NiHCO_3^+	-	2.0%
			CuSO_4^0	-	2.1%			
si_Manganite	-4.58	-2.78	SI Malachite	-	-3.46	SI $\text{Ni}(\text{OH})_{2(s)}$	-	-3.18

Table 3-19: Average concentrations of Mn, Cu, and Ni, percentages of the most abundant corresponding species, and saturation state with possible secondary minerals in the least mineralised (FEY, pH = 7.4) and most mineralised evaporite groundwater (QUE, pH= 7.0). A pe of 7.00 has been assumed for the calculations. (See table 3-17 for compositions of the selected groundwaters, n.d. = not detected).

3.4.4. Recent groundwaters derived from molasse

Physical-chemical parameters

The investigated recent molasse groundwaters have temperatures ranging from 6.5 to 12.9°C (median $T = 8.7$) (see table 3-20; Hesske, 1995). They show a mildly acid to mildly alkaline pH ranging from 6.5 to 8.1. Measured E_H values of 288 to 557 mV and dissolved oxygen contents of 5 to 15 mg/L reflect oxidising conditions.

Major element concentrations

The recent groundwaters derived from the investigated molasse aquifers generally have an intermediate mineralisation (median TDS = 418 mg/L). The hydrochemistry of these groundwaters is dominated by Ca^{2+} , Mg^{2+} and alkalinity (see figure 3-16 and table 3-20). Approximately 50% of the investigated molasse groundwaters are of the Ca-Mg-HCO₃ water type and another 16% are of the Ca-(Mg)-HCO₃ water type. The investigated

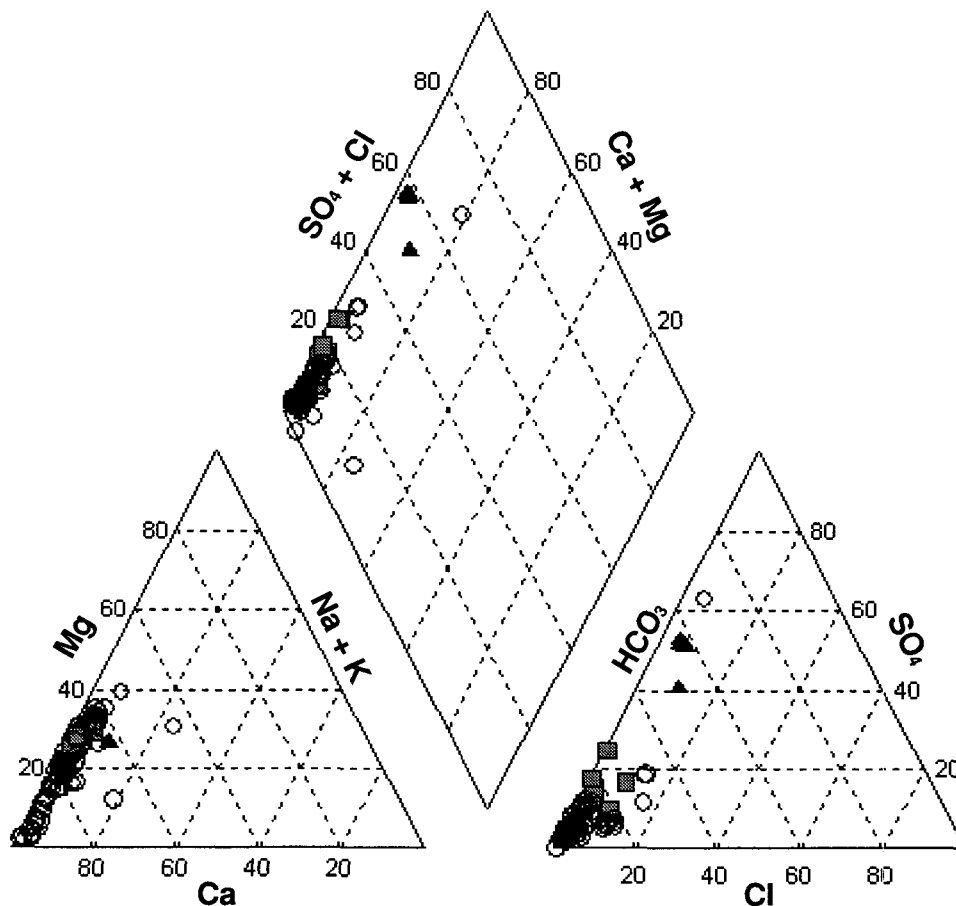


Figure 3-16: Piper-diagram showing the distribution of the average groundwater chemistry in the investigated molasse aquifers in Switzerland and neighbouring France, Germany and Austria (milliequivalents normalised to 100%). Molasse groundwaters: open circles. Special cases: groundwaters from the “Glimmersand” molasse: grey squares; groundwaters from the “Gypsum-bearing Molasse”: black triangles.

groundwaters contain elevated concentrations of dissolved silica (median 5.9 mg Si/L). High NO_3^- (up to 158 mg/L) and K^+ (up to 8.1 mg/L) concentrations reflect the influence of agriculture in certain catchments. As mentioned earlier, the “Gypsum-bearing Molasse” (USM) and the “Glimmersand” molasse (OSM) occurring at the foot of the Jura Mountains have an atypical lithology (see page 55), which is reflected in the chemical composition of the corresponding groundwaters. Typical compositions of groundwaters from these two formations are therefore listed separately (table 3-20). Groundwaters from both formations show a higher total mineralisation than the groundwaters from the other molasse formations. Groundwaters from the “Gypsum-bearing Molasse” have total mineralisations >1000 mg/L, which is expressed mainly in high SO_4^{2-} , Ca^{2+} , Mg^{2+} , and Sr^{2+} concentrations. These groundwaters have similar geochemical characteristics as the evaporite groundwaters discussed earlier (see chapter 3. 4. 3. on page 81). The groundwaters from the “Glimmersand” formation, too, show higher SO_4^{2-} contents than the groundwaters from the other molasse formations. However, in this case the high SO_4^{2-} contents are related to the oxidation of sulphides contained in the sediment.

Trace element concentrations

The trace elements Al, Ba, Cr, Cu, Fe, Mn, Mo, Ni, Rb, U, V and Zn have usually been detected in the investigated recent molasse groundwaters. On the other hand, As, B, Br, Cd, I, Li, and Pb are usually below or hardly above the detection limit (Hesske, 1995). This author has shown the link between the mineralogic composition of the different molasse formations and the trace element composition of corresponding groundwaters (see figure 2-17). A number of trace elements including Cr, Mo, U, Li, and Ba have been proposed as specific natural tracers for particular molasse formations:

- Groundwaters derived from the OMM in western Switzerland are characterised by elevated Cr concentrations (1.9 to 6.9 $\mu\text{g/L}$).
- Elevated concentrations of Ba (50.5 to 333.7 $\mu\text{g/L}$) occur in the groundwaters from the conglomerates of the Gubloux fan (OMM) and the “Rigi-Rossberg” fan (USM) and in groundwater from the “Grès de la Cornalle” (sandstone).
- The groundwaters from the “Gypsum-bearing Molasse” contain elevated amounts of Li (17.2 to 28.6 $\mu\text{g/L}$), Mo (1.3 to 16.0 $\mu\text{g/L}$), U (2.4 to 3.6 $\mu\text{g/L}$), Br (27.6 to 44.6 $\mu\text{g/L}$), and B (12.0 to 52.4 $\mu\text{g/L}$).
- The groundwaters from the “Glimmersand” formation contain elevated Mo (2.6 to 140.3 $\mu\text{g/L}$) and U (2.0 to 9.0 $\mu\text{g/L}$) contents and slightly elevated Li (5.0 to 13.4 $\mu\text{g/L}$) concentrations.

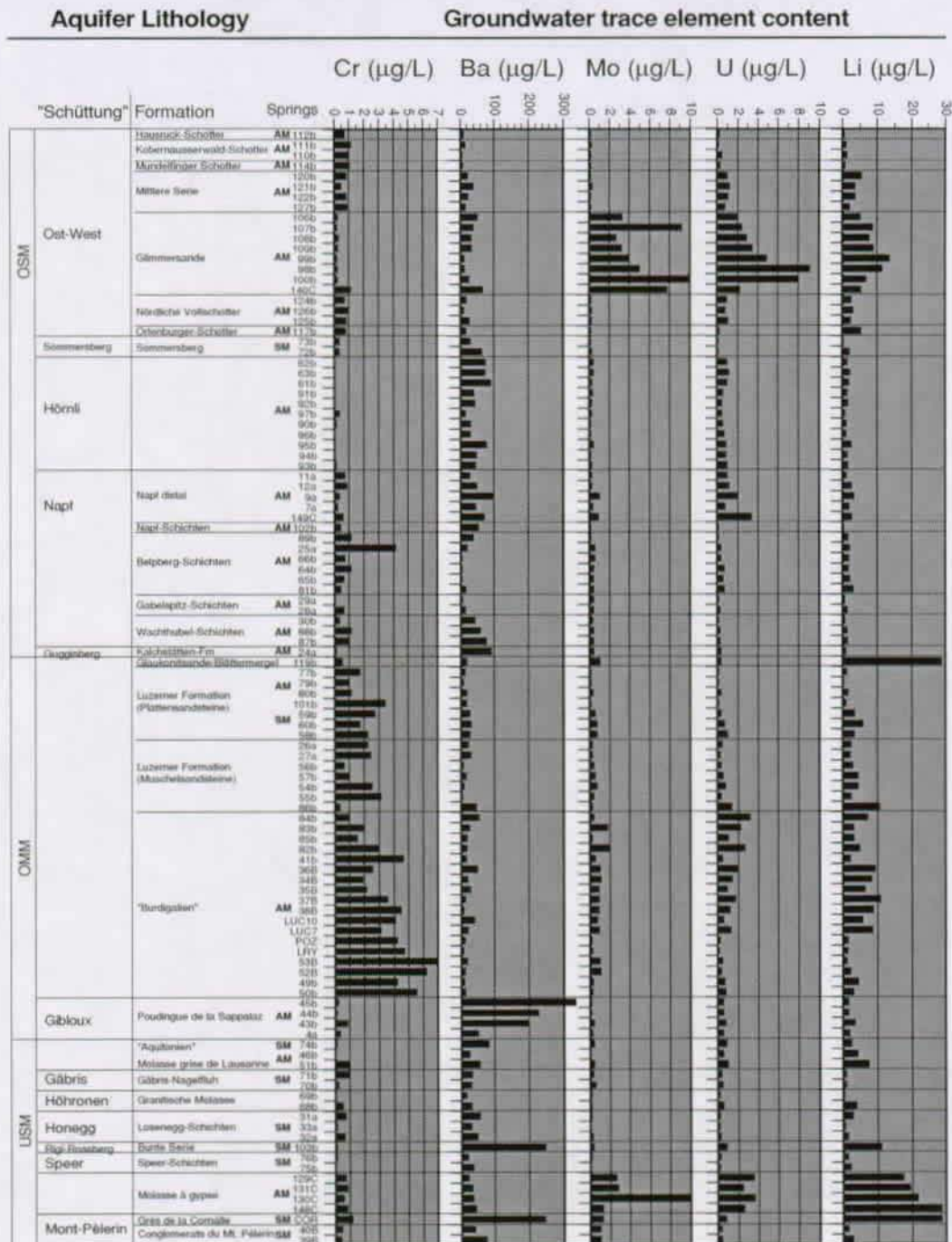


Figure 3-17: Example of the relation between aquifer lithology and trace element contents in the corresponding groundwaters (after Hesske, 1995). AM = Autochthonous molasse; SM = Subalpine molasse.

Typology of Recent Groundwaters

Parameter	Unit	Molasse groundwaters				"Gypsum-bearing Molasse"				"Glimmersande"			
		min	med.	max	n	min	med.	max	n	min	med.	max	n
T	°C	6.5	8.7	12.9	96	9.8	11.4	16.3	4	9.1	9.8	11.9	8
pH	pH-units	6.5	7.2	8.1	94	7.4	7.5	7.8	4	7.5	7.7	8.1	8
Eh	mV	288	391	484	94	333	417	434	4	337	401	440	8
O2 diss.	mg/L	5	11	15	32	-	-	-	0	-	9	-	1
E.C. at 20°C	µS/cm	22	420	806	96	1008	1141	1326	4	561	642	698	8
Total Hardness	°F	1.2	25.0	43.3	96	55.2	73.3	86.0	4	16.7	37.9	39.4	8
TDS	mg/L	48.4	418.3	714.4	96	984.4	1146.9	1346.0	4	556.9	638.0	674.4	8
Alk. as HCO ₃ ⁻	mg/L	7.3	281.5	432.9	96	375.8	403.9	463.5	4	357.7	394.3	430.1	8
F ⁻	mg/L	<0.2	<0.2	0.2	96	0.2	0.2	0.2	4	<0.2	<0.2	<0.2	8
Cl ⁻	mg/L	<1	3.0	32.0	96	28.0	34.5	50.0	4	2.0	8.3	27.7	8
NO ₃ ⁻	mg/L	<1	8.1	157.9	96	28.0	33.5	40.0	4	<1	3.5	32.3	8
SO ₄ ²⁻	mg/L	<1	12.1	60.6	96	255.0	386.5	445.0	4	32.9	56.3	92.6	8
Mg ²⁺	mg/L	0.7	13.5	36.1	96	35.4	39.5	43.2	4	25.3	26.1	30.8	8
Ca ²⁺	mg/L	6.5	82.2	117.4	96	168.5	234.3	289.2	4	94.7	117.3	123.7	8
Sr ²⁺	mg/L	0.010	0.215	0.996	96	4.030	4.693	4.797	4	0.160	0.265	0.681	8
Na ⁺	mg/L	0.3	2.4	36.4	96	7.6	9.6	29.5	4	2.4	2.6	8.5	8
K ⁺	mg/L	0.2	0.8	4.2	96	2.0	3.9	8.1	4	0.6	0.8	0.9	8
NH ₄ ⁺	mg/L	-	-	-	0	-	-	-	0	-	-	-	0
Si total	mg/L	2.0	5.9	19.0	96	3.7	4.9	7.4	4	2.8	7.0	8.6	8
Li total	µg/L	<1	2	29	96	17	20	29	4	5	8	13	8
Rb total	µg/L	<0.2	0.5	3.0	96	0.9	1.1	1.8	4	0.6	0.8	1.9	8
Ba total	µg/L	2.4	26.8	333.7	96	20.7	32.9	43.0	4	10.1	31.1	65.3	8
Al total	µg/L	<0.2	8.2	80.5	96	<0.2	3.6	6.3	4	1.1	1.4	212.0	8
V total	µg/L	<0.2	0.5	1.1	96	0.4	0.6	0.7	4	0.2	0.3	1.0	8
Cr total	µg/L	<0.2	0.8	6.9	96	0.6	0.7	0.8	4	0.2	0.2	1.1	8
Mn total	µg/L	<0.2	0.8	374.1	96	<0.2	0.5	0.6	4	<0.2	5.5	45.7	8
Fe total	µg/L	<2	<2	155.0	96	<2	<2	11.4	4	<2	<2	161.8	8
Co total	µg/L	<0.2	<0.2	0.8	96	0.4	0.4	0.6	4	<0.2	<0.2	0.2	8
Ni total	µg/L	<0.2	0.5	3.2	96	0.7	1.3	1.7	4	0.3	1.0	3.9	8
Cu total	µg/L	<0.2	<0.2	15.2	96	2.3	2.9	49.5	4	<0.2	0.3	2.8	8
Zn total	µg/L	<0.2	0.9	155.0	96	5.6	9.1	11.0	4	<0.2	0.4	4.9	8
Mo total	µg/L	<0.2	0.3	1.9	96	1.3	2.6	2.7	3	2.6	3.8	9.2	7
Cd total	µg/L	<0.2	<0.2	0.3	96	<0.2	<0.2	<0.2	4	<0.2	<0.2	<0.2	8
W total	µg/L	-	-	-	0	-	-	-	0	-	-	-	0
Pb total	µg/L	<0.2	<0.2	8.7	96	0.4	0.5	2.1	4	<0.2	<0.2	0.5	8
U total	µg/L	<0.2	0.5	3.3	96	2.4	3.0	3.6	4	2.0	3.1	9.0	8
Br total	µg/L	<1	9	126	96	28	37	45	4	2	22	37	8
I total	µg/L	<1	2	8	4	2	3	15	4	-	4	-	1
B total	µg/L	<1	3	99	96	12	26	52	4	2	3	7	8
As total	µg/L	<0.5	<0.5	1.2	96	<0.5	<0.5	0.5	4	<0.5	<0.5	2.5	8
Tritium	TU	20.0	30.0	86.8	4	-	-	-	0	20.0	25.0	52.0	3
Deuterium	δ‰	-80.1	-77.1	-71.6	3	-	-	-	0	-	-	-	0
Oxygen-18	δ‰	-11.3	-11.0	-10.2	3	-	-	-	0	-10.4	-10.4	-10.4	2
Carbon-13	δ‰	-	-	-	0	-	-	-	0	-	-	-	0

Table 3-20: Chemical composition of recent groundwaters from molasse aquifers in Switzerland and neighbouring France, Germany and Austria (data from Hesske, 1995).

Geochemical evolution

The investigated molasse catchments are situated at low altitudes and show a more extensive soil development than the previously described alpine catchments. Generally, the permeability of molasse rocks depends strongly on their grain-size distribution and on the extent of fracturing. Groundwater flow occurs primarily in the altered surface-near parts of the subsoil, which is characterised by abundant decompression cracks. Partly, groundwater follows preferential pathways along fractures and lithologic discontinuities ("fracture flow"), partly groundwater flow occurs within inter-granular pores of sandstones and conglomerates ("matrix flow"). Molasse groundwaters circulating primarily in porous sandstones and conglomerates therefore have a longer residence time compared to groundwaters circulating in fractures. This is particularly the case of the groundwaters from "Glimmersand" aquifers, which are composed of poorly cemented sands (see page 56). Nevertheless, the short observed residence times of the investigated molasse groundwaters, ranging from a few days or weeks to several years, indicate that the hydrochemistry will be dominated by the dissolution of fast-reacting minerals. In the molasse sandstones and conglomerates these are calcite and dolomite occurring as detrital components and as cement around the more inert grains. In addition, clay minerals, and scarce barite and detrital sulphide minerals are present. Gypsum and celestite occur in the "Gypsum-bearing Molasse". The alteration of silicate minerals plays a minor role because of the slow kinetics.

Major elements

Saturation state calculations show that the majority of the investigated molasse groundwaters are saturated with calcite (table 3-21 and figure 3-18). P_{CO_2} values range from $10^{-1.3}$ to $10^{-3.0}$, indicating that the uptake of soil CO_2 plays an important part in groundwater mineralisation. Dolomite saturation states range from subsaturated to saturated. Further, the molasse groundwaters are saturated or slightly subsaturated with chalcedony. The elevated dissolved silica contents are compatible with the relatively longer residence times compared to fractured or karst aquifers and the resulting intensive weathering processes in the sandy soils. Then, the molasse groundwaters are generally subsaturated with respect to gypsum, celestite, strontianite and fluorite due to low SO_4^{2-} , F⁻ and Sr^{2+} activities.

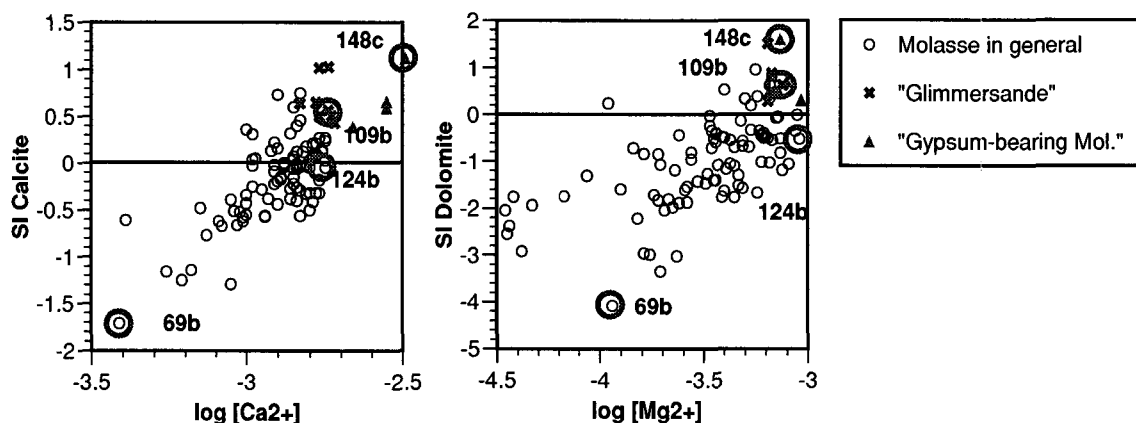


Figure 3-18: Calcite and dolomite saturation state of recent molasse groundwaters compared to average Ca^{2+} and Mg^{2+} activities (for marked groundwaters see table 3-21).

Site code	Units	P-LRY ^a	69b	124b	109b	148c
Geological Unit Formation			USM	OSM	OSM	USM
Water type			Granitische Molasse	Nördliche Vollsotter	Glimmersande	Gypsum-bearing Mol.
Altitude	m	Precip.	Ca-Mg-HCO ₃ -(SO ₄)	Ca-Mg-HCO ₃ -(SO ₄)	Ca-Mg-HCO ₃ -(SO ₄)	Ca-(Mg)-SO ₄ -HCO ₃
		885	1140	440	598	435
TDS	mg/L	8.3	114.9	714.4	674.4	1346.0
T	°C	-	7.9	8.6	9.3	16.3
pH	pH-units	4.9	6.8	7.2	7.6	7.8
Alk. as HCO ₃ ⁻	µmol/L	0.30 ^b	1080	4579	7049	7596
F ⁻	µmol/L	n.d.	5	n.d.	5	11
Cl ⁻	µmol/L	7	31	903	195	959
SO ₄ ²⁻	µmol/L	22	72	631	643	4633
NO ₃ ⁻	µmol/L	36	113	2547	n.d.	645
Ca ²⁺	µmol/L	18	477	2929	3061	7216
Mg ²⁺	µmol/L	n.d.	140	1485	1267	1605
Sr ²⁺	µmol/L	n.d.	0.46	1.14	3.42	54.75
Na ⁺	µmol/L	1	57	457	104	400
K ⁺	µmol/L	3	8	33	18	207
NH ₄ ⁺	µmol/L	59	-	-	-	-
Si total	µmol/L	15	162	314	308	213
Li total	µmol/L	-	n.d.	0.3	1.3	4.1
Rb total	µmol/L	-	0.014	0.010	0.009	0.011
Ba total	µmol/L	0.015	0.106	0.119	0.232	0.313
Cr total	µmol/L	-	n.d.	0.013	0.004	0.015
Mn total	µmol/L	0.164	0.005	0.052	0.003	0.010
Fe total	µmol/L	0.165	0.027	0.002	n.d.	0.205
Ni total	µmol/L	0.002	n.d.	0.011	0.012	0.027
Cu total	µmol/L	0.027	0.002	0.013	0.001	0.779
Zn total	µmol/L	0.297	0.413	0.023	n.d.	0.143
Mo total	µmol/L	-	0.001	0.001	0.033	0.013
Pb total	µmol/L	0.009	n.d.	n.d.	n.d.	0.010
U total	µmol/L	-	n.d.	0.004	0.014	0.011
log P _{CO2}		-3.50	-2.07	-1.87	-2.08	-2.25
SI calcite		-8.69	-1.71	-0.05	0.56	1.12
SI dolomite		-	-4.09	-0.52	0.63	1.61
SI fluorite		-	-3.18	-	-2.62	-1.92
SI gypsum		-4.88	-3.07	-1.66	-1.63	-0.64
SI barite		-2.31	-1.03	-0.40	-0.11	0.43
SI celestite		-5.73	-4.00	-3.04	-2.54	-0.72
SI strontianite		-10.70	-3.80	-2.59	-1.51	-0.15
SI chalcedony		-1.10	-0.03	0.25	0.23	-0.02
SI Cr(OH) ₃		-	-	-2.26	-5.23	-3.66

Table 3-21: Chemical composition and saturation states with respect to selected minerals of four molasse springwaters and precipitation. n.d. = not detected; - = not analysed. The “69b” spring discharges the least mineralised, and the “124b” spring the most mineralised molasse groundwater, respectively. The “109b” and “148c” springs discharge the most mineralised groundwaters from the “Glimmersand” and “Gypsum-bearing Molasse”.

a. P-LRY: precipitation sampling site near Lausanne; median of 11 samples (Atteia, 1992)

b. Calculated value, assuming equilibrium with CO₂(g) at atmospheric P_{CO2}=10^{-3.5}

Compared to the other molasse groundwaters, the groundwaters from the "Gypsum-bearing Molasse" are least subsaturated with gypsum ($SI_{\text{gypsum}} = -0.64$ to -0.99) and celestite (-0.72 to -0.84), and they are in equilibrium with respect to calcite and dolomite, due to the elevated activities of SO_4^{2-} and Ca^{2+} .

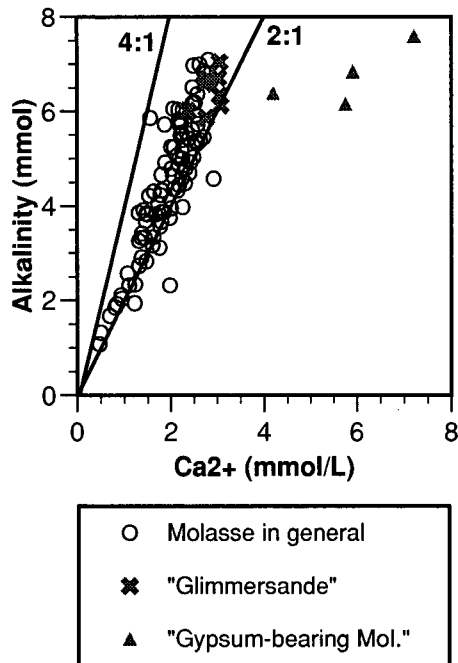


Figure 3-19: Average molar alkalinity/ Ca^{2+} ratios in the investigated molasse groundwaters.

The elevated concentrations of dissolved Ca^{2+} , Mg^{2+} , and alkalinity indicate that dissolution of calcite and dolomite enhanced by uptake of soil CO_2 governs the hydrochemistry of molasse groundwaters (reactions 3.5 and 3.6 page 75). Due to their high reactivity, carbonate minerals have a dominant effect on the groundwater chemistry, whereas the much slower processes such as silicate alteration play only a minor role. According to the stoichiometry of reaction 3.5, groundwaters in equilibrium with calcite have a molar alkalinity/ Ca^{2+} ratio of 2, if calcite dissolution is the dominating process. In analogy, groundwaters in equilibrium with dolomite have alkalinity/ Ca^{2+} ratio of 4, if dolomite dissolution is the dominating process. Although not necessarily saturated with calcite and dolomite, the molasse groundwaters including those from the "Glimmersande" generally plot nearer to the line for calcite dissolution than to the line for dolomite dissolution (figure 3-19). This indicates that dissolution of calcite dominates over dissolution of dolomite, which is consistent with the

generally greater abundance of calcite and the faster reaction kinetics of this mineral compared to dolomite (see page 78).

Contrasting this, the groundwaters from the "Gypsum-bearing Molasse" plot on the right side of the line for calcite dissolution. They have lower alkalinity/ Ca^{2+} ratios, due to their higher Ca^{2+} content from gypsum dissolution (reaction 3.7).

Trace elements

The mineralogic compositions of the different molasse formations are reflected in the trace element content of the corresponding groundwaters (Hesske, 1995). Groundwater flow in interstitial pores of the detrital sediments leads to relatively long residence times and allows an intensive rock water contact and weathering of the substratum.

Groundwaters from the calcareous and glauconitic OMM sandstones in western Switzerland contain significantly higher Cr concentrations than the groundwaters from the other molasse formations. The geogenic origin of the dissolved Cr in the groundwater has been confirmed by rock leaching experiments (Hesske, 1995, and this study, see chapter 4.7. on page 181). It is related to the alteration of ophiolite detritus in the OMM sandstone (Hesske, 1995; Dalla Piazza, 1996). The groundwaters from OMM sandstones at the southwestern border of the molasse basin contain the highest Cr values. Here, the proportion of detrital Cr-spinels and Cr-bearing pyroxenes derived from ophiolite rocks in the flysch nappes of the Préalpes is greatest (Allen and others, 1985). At oxidising

conditions and at a neutral to alkaline pH such as found in the investigated groundwaters, dissolved Cr is present as the highly soluble and mobile chromate anion ($\text{Cr}^{\text{VI}}\text{O}_4^{2-}$), and saturation with secondary Cr^{III} -hydroxide is not reached (table 3-21). The weathering of the OMM sandstone and the sources and chemical behaviour of Cr are discussed in more detail in part IV (see page 129).

Elevated Ba concentrations occur in the groundwaters from the conglomerate and sandstone formations of the Gibloux and Mont-Pelerin fan deposits north of Lake Geneva and of the Rigi fan deposits north of Lake Lucerne. These molasse units belong to the Subalpine molasse or to the folded autochthonous molasse and are more strongly fractured than the autochthonous molasse. The source is barite, which typically occurs as fracture mineralisation and is thus present in along the preferential flow paths of the groundwater (Hesske, 1995).

Groundwaters from the “Gypsum-bearing Molasse” contain elevated amounts of Li, B, Br, Cl, Cu, U, and Mo concentrations. The elevated Li, Cl, and Br contents can be explained by dissolution of evaporite minerals containing brine inclusions. The origin of Mo, Cu and U is related to the oxidation of Mo- and Cu-bearing sulphides and associated U-minerals (Hesske, 1995).

Likewise, the elevated Mo and U contents occurring in the groundwaters from the “Glimmersand” formation are related to the oxidation of sulphides and the dissolution of U-minerals contained in the fine-grained granitic detritus of the “Glimmersand” formation. However, the elevated Li concentrations are in this case explained by the weathering of the abundant mica by the slowly flowing groundwater in this unit (Hesske, 1995, compare page 55 and page 56).

3. 4. 5. Recent groundwaters derived from Flysch

Physical-chemical parameters

The investigated recent flysch groundwaters are cold; temperatures ranging from 1.2 to 9.2°C have been measured (see table 3-22, Basabe, 1993). They show a rough negative correlation between the altitude of the spring and the water temperature. The investigated groundwaters show a mildly acid to mildly alkaline pH ranging from 5.9 to 8.3. Measured E_{H} values of 449 to 477 mV reflect oxidising conditions.

Major element concentrations

The investigated recent flysch groundwaters have a low to intermediate total mineralisation (median 270 mg TDS/L). The major element chemistry is dominated by Ca^{2+} , alkalinity, and to a minor degree Mg^{2+} . 51% of the investigated flysch groundwaters are of the Ca-HCO₃ water type and 35% are of the Ca-(Mg)-HCO₃ water type. Flysch springwaters are poor in dissolved Sr^{2+} , Na^+ , K^+ , Cl^- , NO_3^- , SO_4^{2-} , and silica, and F^- has not been detected. Dissolved Mg^{2+} , Sr^{2+} , Na^+ , K^+ , and silica concentrations increase with increasing mineralisation.

A number of tunnel springs were sampled in the Arnon gallery near Les Diablerets. Four of these tunnel springwaters show exceptionally high Mg^{2+} , Sr^{2+} , silica, Na^+ , and K^+ values, but not particularly elevated Ca^{2+} and alkalinity.

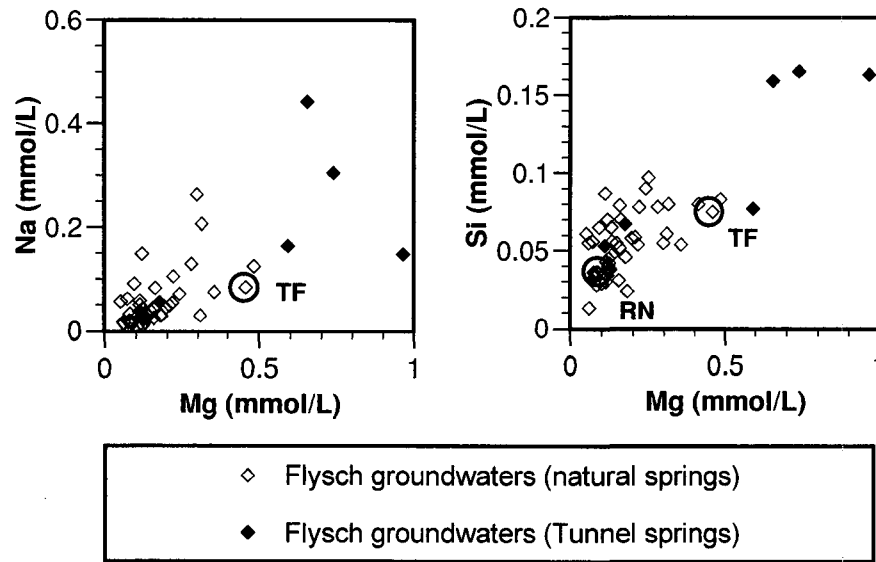


Figure 3-20: The comparison of average Mg, Na, and silica concentrations in flysch groundwaters from natural springs and from springs in the Arnon tunnel shows that the tunnel springwaters are more evolved than the subsurface groundwaters discharged in natural springs.

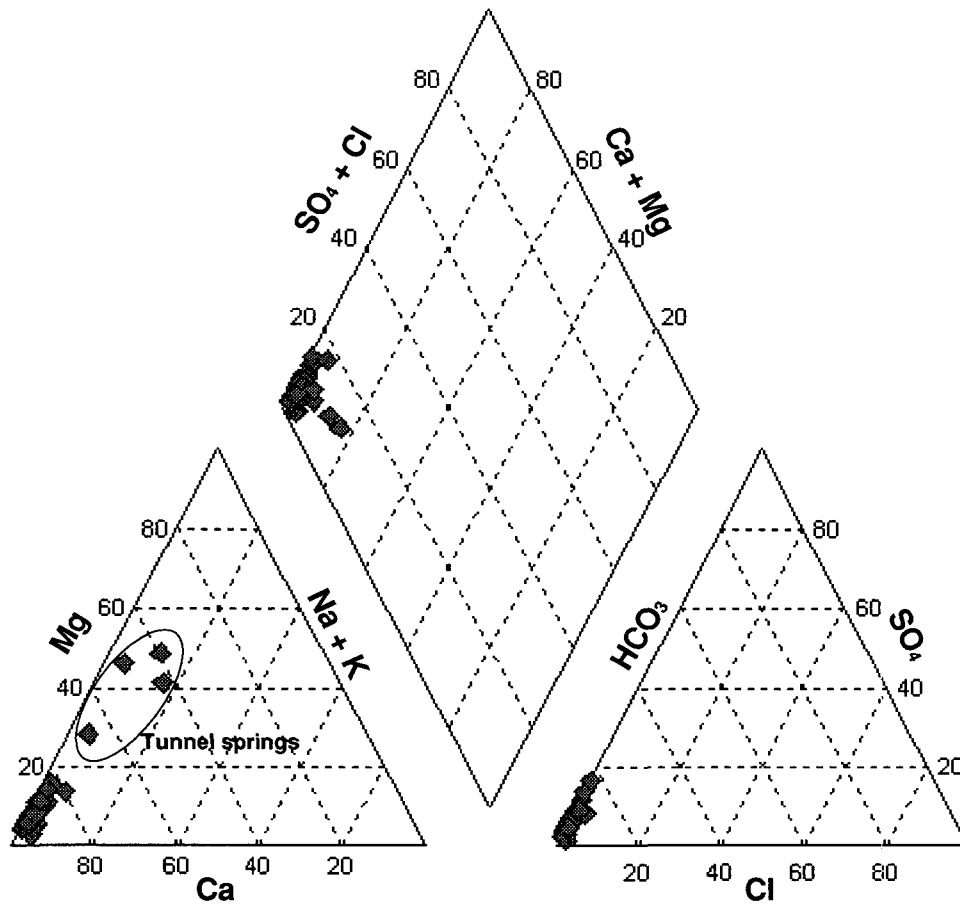


Figure 3-21: Piper-diagram showing the distribution of the average groundwater chemistry in the investigated flysch aquifers in the Niesen and Gurnigel nappes (milliequivalents normalised to 100%).

Trace element concentrations

The most concentrated trace elements found in the investigated recent flysch groundwaters are Ba (median 27.2 µg/L), Fe (median 10.9 µg/L), and B (median 7.4 µg/L). The trace elements Al, Cr, Cu, Zn, Mn, Ni, Pb, Rb, U, and V occur at low median concentrations ranging from 0.2 to 1.2 µg/L. The measured concentrations of Mo, Li, and Br are below or just above their respective detection limits (Basabe, 1993).

Parameter	Unit	minimum	median	maximum	n
T	°C	1.2	5.7	9.2	50
pH	pH-units	5.9	7.0	7.7	46
Eh	mV	449	454	477	5
O2 diss.	mg/L	-	12	-	1
E.C. at 20°C	µS/cm	159	270	474	53
Total Hardness	°F	9.7	16.3	27.9	53
TDS	mg/L	159.7	267.1	458.8	53
Alkalinity as HCO ₃ ⁻	mg/L	113.7	186.9	314.2	53
F ⁻	mg/L	<0.2	<0.2	<0.2	53
Cl ⁻	mg/L	<1	<1	3.5	51
NO ₃ ⁻	mg/L	<1	2.4	8.1	53
SO ₄ ²⁻	mg/L	2.5	8.2	36.2	53
Mg ²⁺	mg/L	1.3	3.2	23.5	53
Ca ²⁺	mg/L	24.0	56.2	97.3	53
Sr ²⁺	mg/L	0.111	0.368	3.114	53
Na ⁺	mg/L	0.3	0.8	10.2	51
K ⁺	mg/L	<0.2	0.4	3.0	53
NH ₄ ⁺	mg/L	-	-	-	0
Si total	mg/L	<0.5	1.5	4.6	53
Li total	µg/L	<1	3	29	53
Rb total	µg/L	0.3	0.6	5.8	53
Ba total	µg/L	5.1	26.5	128.0	53
Al total	µg/L	<0.2	0.9	23.2	53
V total	µg/L	<0.2	0.2	0.5	53
Cr total	µg/L	<0.2	0.2	1.1	53
Mn total	µg/L	<0.2	0.5	4.9	53
Fe total	µg/L	<2	10.7	57.9	44
Co total	µg/L	<0.2	<0.2	0.6	53
Ni total	µg/L	<0.2	0.5	4.0	49
Cu total	µg/L	<0.2	0.5	3.7	48
Zn total	µg/L	<0.2	1.1	75.0	46
Mo total	µg/L	-	<0.2	-	1
Cd total	µg/L	-	0.4	-	1
Pb total	µg/L	<0.2	0.3	6.3	53
U total	µg/L	<0.2	0.2	0.9	53
Br total	µg/L	<1	3	8	53
I total	µg/L	-	<1	-	1
B total	µg/L	2	7	73	53
As total	µg/L	-	-	-	0
Tritium	TU	-	-	-	0
Deuterium	‰	-	-	-	0
Oxygen-18	‰	-	-	-	0
Carbon-13	‰	-	-	-	0

Table 3-22: Chemical composition of recent groundwaters from the investigated flysch aquifers in the Niesen and Gurnigel nappes (data from Basabe, 1993).

Geochemical evolution

The particular sedimentary and structural characteristics of flysch make flysch aquifers a highly discontinuous environment. The abundant intercalated shale beds associated with conglomerates or sandstones results in a low primary permeability of flysch units on a catchment scale, which restricts active groundwater circulation systems to the shallow subsurface. In addition, the strong tectonic deformation favours fast groundwater flow along fractures and joints (fracture flow) which is expressed by fast flow velocities of the groundwater ranging from 0.5 m/h to 90 m/h observed in tracer tests. In the “Niesenkulm-Flysch” the occurrence of decimetre-thick limestone banks intercalated in the turbidite sediments gives rise to the development of micro-karst features, which can influence groundwater flow on a local scale. The short residence times of the flysch groundwaters imply that fast rock-water interaction processes such as the dissolution of carbonates and ion exchange reactions will dominate the groundwater hydrochemistry.

Major elements

Only a minority of the investigated flysch groundwaters reach saturation with calcite and even less with dolomite (table 3-23). The P_{CO_2} values of the investigated groundwaters between $10^{-9.85}$ and $10^{-2.76}$ are in the range as the P_{CO_2} values commonly occurring in soils. In addition, the flysch groundwaters are subsaturated with chalcedony and strontianite, as well as with respect to sulphate phases such as gypsum, celestite, and barite.

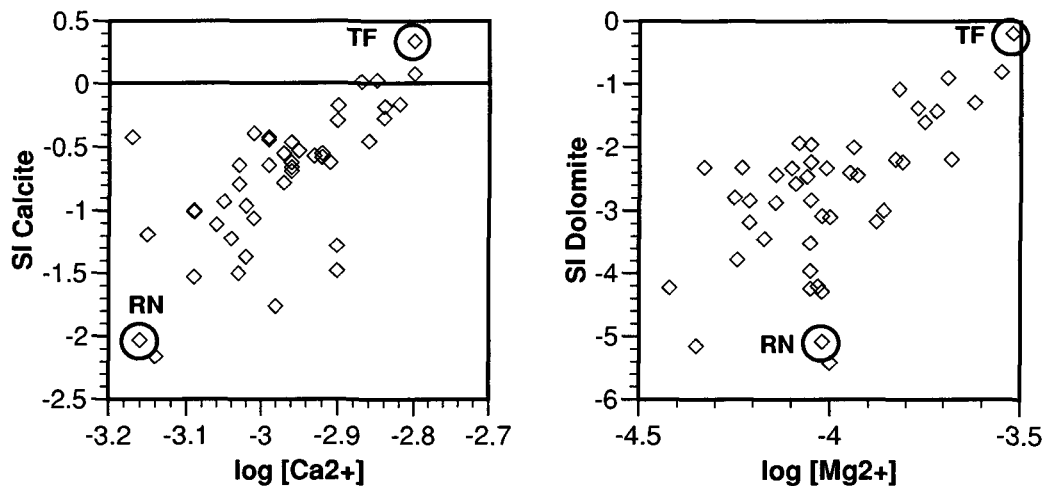


Figure 3-22: Calcite and dolomite saturation state of recent flysch groundwaters compared to average Ca^{2+} and Mg^{2+} activities.

Site (Region) Water type Altitude	Units m	P-BOR ^a Precipitation 2100	RN Ca-(Mg)-HCO ₃ 1760	TF Ca-(Mg)-HCO ₃ 1210
TDS	mg/L	6.51	169.76	458.75
T	°C	-	7.0	6.9
pH	pH-units	6.3	6.0	7.6
Alkalinity as HCO ₃ ⁻	µmol/L	12.90 ^b	1921	5149
F ⁻	µmol/L	n.d.	n.d.	n.d.
Cl ⁻	µmol/L	20	11	25
SO ₄ ²⁻	µmol/L	8	90	276
NO ₃ ⁻	µmol/L	25	24	n.d.
Ca ²⁺	µmol/L	19	894	2427
Mg ²⁺	µmol/L	2	122	459
Sr ²⁺	µmol/L	n.d.	2	14
Na ⁺	µmol/L	2	12	84
K ⁺	µmol/L	12	7	26
NH ₄ ⁺	µmol/L	16	-	-
Si total	µmol/L	11	41	75
Li total	µmol/L	n.d.	0.2	2.0
Rb total	µmol/L	0.008	0.003	0.027
Ba total	µmol/L	0.122	0.136	0.304
V total	µmol/L	0.006	0.001	0.004
Cr total	µmol/L	-	0.004	0.002
Mn total	µmol/L	0.018	0.029	0.003
Fe total	µmol/L	-	-	0.193
Co total	µmol/L	-	0.004	0.002
Ni total	µmol/L	-	0.016	0.008
Cu total	µmol/L	0.014	-	0.012
Zn total	µmol/L	0.104	-	0.016
Pb total	µmol/L	-	0.002	n.d.
U total	µmol/L	-	n.d.	0.001
log P _{CO2}		-3.50	-1.03	-2.22
SI calcite		-5.49	-2.03	0.34
SI dolomite		-12.22	-5.08	-0.20
SI gypsum		-5.29	-2.75	-2.00
SI barite		-1.73	-0.87	-0.20
SI celestite		-6.28	-3.28	-2.21
SI strontianite		-7.61	-3.70	-1.01
SI chalcedony		-1.14	-0.62	-0.35
SI Fe(OH) ₃		-	-	1.95

Table 3-23: Chemical composition and saturation states with respect to selected minerals of two flysch springwaters and precipitation. n.d. = not detected; - = not analysed. The "RN" spring discharges the least mineralised, and the "TF" spring the most mineralised groundwater, respectively.

a. P-BOR: precipitation sampling site in the Préalpes Vaudoises; median of 8 samples (Atteia, 1992)

b. Calculated value, assuming equilibrium with CO₂(g) at atmospheric P_{CO2}=10^{-3.5}

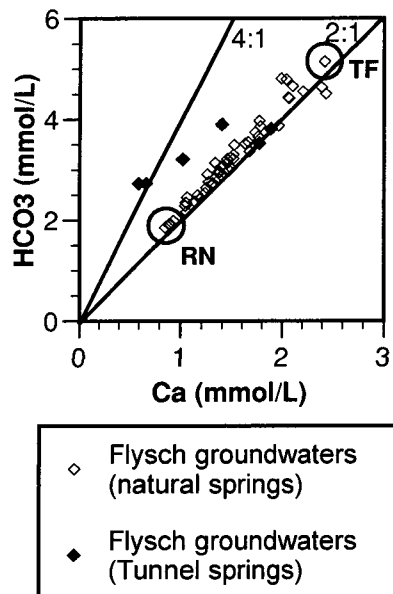


Figure 3-23: Average molar alkalinity/ Ca^{2+} ratios in the flysch groundwaters.

There is an excellent correlation between average Ca^{2+} and alkalinity concentrations in flysch groundwaters. The alkalinity/ Ca^{2+} ratios are close to 2, which is consistent with the overall reaction for calcite dissolution (reaction 3.5, page 75). This indicates that dissolution of calcite enhanced by CO_2 uptake in the soil is the dominant rock-water interaction process in recent flysch groundwaters. The groundwaters sampled in the Arnon tunnel show higher alkalinity/ Ca^{2+} ratios due to higher alkalinity values from dolomite dissolution (reaction 3.6, page 75). Unfortunately, no pH values are available for these tunnel springwaters, so that their saturation state cannot be calculated. Nevertheless, as dolomite has slower dissolution kinetics than calcite (see page 78), the higher Mg^{2+} values suggest that these tunnel springs are more evolved than the subsurface groundwaters discharged in natural springs. This is also consistent with the elevated Sr^{2+} , silica, Na^+ , and K^+ concentrations in these groundwaters. The fact that these tunnel springs are not the most mineralised springs in terms of Ca^{2+} and alkalinity may be explained by a limited availability of calcite.

In the most dilute flysch groundwaters the Na^+ and Cl^- concentrations are near the detection limit. However, in the more mineralised flysch groundwaters it appears clearly that the $\text{Na}^+ / \text{Cl}^-$ ratios evolve towards higher values (figure 3-24). The most likely Na^+ source in such groundwaters is Ca-Na ion exchange on the abundant clay minerals.

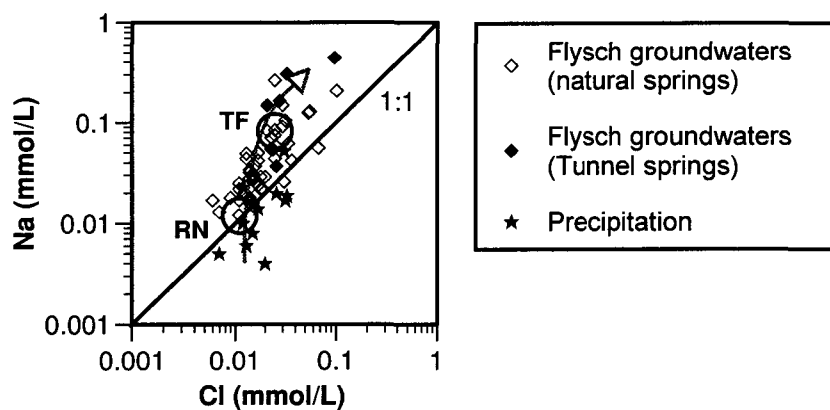


Figure 3-24: Average molar $\text{Na}^+ / \text{Cl}^-$ ratios in the investigated flysch groundwaters compared to precipitation. The arrow indicates the evolution of the $\text{Na}^+ / \text{Cl}^-$ ratios in the groundwaters resulting from ion exchange.

Trace elements

The poor chemical evolution of recent flysch groundwaters is one reason of the low trace element contents. Further, except for barite there are no other particular fracture mineralisations, which could mark the groundwaters circulating in these fractures.

The elevated Ba concentrations can be related to barite, which typically occurs in veins and fractures in sandstones and shales. There is an evolutionary trend towards solubility control by barite (see figure 3-25).

Lead concentrations of up to 6.3 $\mu\text{g/L}$ have been observed. The measured concentrations lie in the same range as in precipitation water (Atteia, 1992). The fact, that Pb has not been detected in the leachates of flysch rocks (Basabe, 1993), indicates that Pb must have an atmospheric origin.

The supersaturation of the large majority of flysch groundwaters with amorphous $\text{Fe}(\text{OH})_3$ with SI values ranging from -0.02 to +2.66 indicates that the measured Fe concentrations might not exactly represent dissolved Fe only. This corroborates the suggestion that the relatively elevated Fe contents are related to colloidal matter in the unfiltered groundwater samples. Fe-hydroxides are abundant secondary minerals in Flysch rocks. Cobalt and lead show a strong affinity for Fe- and Mn-oxides and -hydroxides (Manceau et al, 2000), which suggests that the elevated Co and Pb concentrations in these groundwaters are connected with suspended colloids.

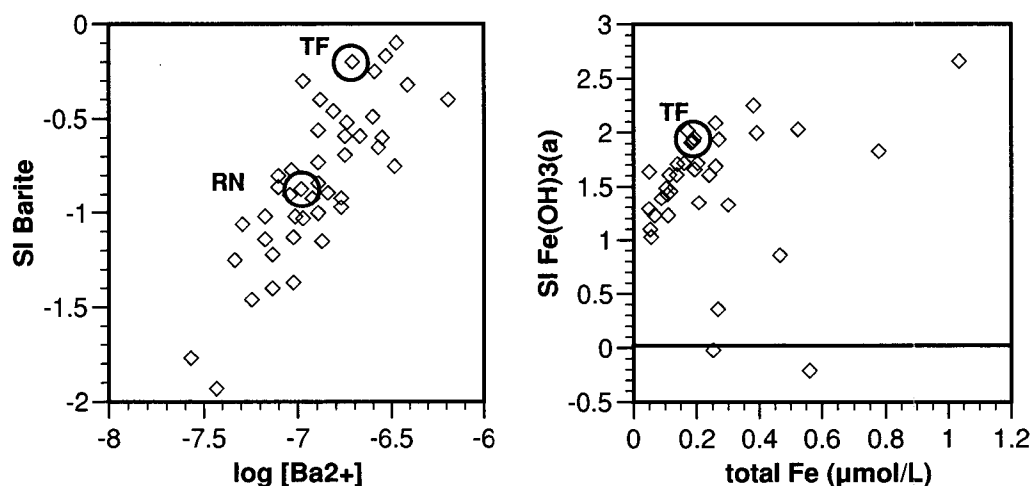


Figure 3-25: Saturation state of recent flysch groundwaters with respect to barite and Fe-hydroxide compared to average Ba^{2+} activities and total Fe content, respectively.

3. 5. Comparison of aquifer types

To start the comparison of recent groundwaters, an overview of the minerals occurring in the different aquifer types is given (table 2-24):

Aquifer types	Mineralogy
Crystalline rocks of the Mont-Blanc and Aiguilles-Rouges Massifs	<p>Main mineralogy of granite: quartz, K-feldspar, saussuritic plagioclase (mainly oligoclase) Accessory chloritised biotite, hornblende, epidote, and sericite</p> <p>Main mineralogy of ortho- and para-gneisses: quartz, plagioclase (partly saussuritic), K-feldspar, partly chloritised biotite and hornblende, garnet and white mica in variable proportions Accessory epidote, and diopside; carbonate minerals in marble bands and skarns</p> <p>Hydrothermal mineralisations: calcite, dolomite, fluorite, quartz, barite, pyrite and As-, Mo-, Pb-, Zn- and Cu-sulphides, scheelite, wolframite, and U-minerals Secondary minerals: calcite, Fe-hydroxides and clay minerals</p>
Carbonate rocks	<p>Main mineralogy: Calcite, dolomite; gypsum in evaporitic layers; detrital quartz, feldspars, and clay minerals in more sandy and marly units, Accessory pyrite, celestite, fossil organic matter (bitumen, kerogen, graphite); barite in deep-sea limestones; molybdenite and U-minerals in dolomitic limestones Secondary minerals: Fe-hydroxides and calcite</p>
Triassic evaporite series in the Swiss Rhone valley	<p>Main mineralogy: Gypsum or anhydrite, dolomite, calcite, and clay minerals (illite, chlorite and smectite, and corrensite); Accessory celestite, fluorite, apatite, barite, talc, chalcedony, feldspars, and sulphides (pyrite, chalcopyrite, sphalerite, galena) Secondary minerals: Fe-hydroxides and calcite</p>
Molasse	<p>Main mineralogy: Quartz, calcite, dolomite, feldspars, glauconite, clay minerals (illite, chlorite, smectite, and minor kaolinite), and micas; gypsum and celestite in the "Gypsum-bearing Molasse". Accessory minerals include various heavy minerals including epidote, spinels, pyroxenes, apatite, etc., barite in veins, and molybdenite and U-minerals ("Glimmersand" and "Gypsum-bearing Molasse") Secondary Fe-hydroxides and clay minerals (smectite, vermiculite)</p>
Flysch	<p>Main mineralogy: Quartz, feldspars, calcite, dolomite, clay minerals (illite and Fe-chlorite), micas, various heavy minerals Accessory barite in veins Secondary Fe-hydroxides and clay minerals (smectite, vermiculite)</p>

Table 3-24: Mineralogy of the different aquifer types.

3. 5. 1. Physical-chemical parameters of the groundwaters

In table 2-25 the median values of the measured physical-chemical parameters, altitude of the springs and total mineralisation of the different groundwater types are compared. The values show that the investigated recent groundwaters are generally cold and oxygenated and have a mildly acid to mildly alkaline pH. These characteristics are typical for recent groundwaters.

Parameter	Unit	CRY		CARB	EVAP	MOL	FLY
		Gneiss	Granite				
Altitude	m	1953 n=64	1491 n=50	510 n=83	1020 n=91	650 n=96	1502 n=53
T	°C	4.7 n=63	8.9 n=46	9.8 n=86	8.7 n=91	8.7 n=96	5.7 n=50
pH	pH-units	7.6 n=17	6.5 n=35	7.2 n=85	7.0 n=20	7.2 n=94	7.0 n=46
EH	mV	439 n=6	402 n=6	440 n=72	406 n=1	391 n=94	454 n=5
O ₂ (aq)	mg/L	13 n=1	- -	12 n=66	7 n=1	11 n=32	12 n=1
E.C. at 20°C	µS/cm	83 n=63	79 n=55	347 n=79	1693 n=91	420 n=96	270 n=53
TDS	mg/L	75.2 n=64	69.1 n=54	345.4 n=87	1782.2 n=91	418.3 n=96	267.1 n=53

Table 3-25: Physical-chemical parameters of recent groundwaters from different aquifer types (median values and the number of samples). CRY = crystalline, CARB = carbonates, EVAP = evaporites, MOL = molasse, FLY = flysch.

Water temperature and total mineralisation

A negative correlation can be observed between water temperatures and the altitude of the springs (figure 3-26 A), with the coldest springs occurring at the highest altitudes. The temperature of groundwaters in shallow aquifers is related to the altitude of the catchment, while in deeper groundwaters it is related to the geothermal gradient. The observed scatter can be explained by the differences in local climate and by seasonal temperature variation. Further, the groundwater temperature measured in very surface-near spring surroundings is often influenced by surface temperature variations and does not exactly correspond to the true groundwater temperature. The plot shows that the water temperatures of a number of groundwaters from crystalline and evaporite rocks (individual symbols) are significantly higher than expected from the altitude of the corresponding springs: These springs are located either in tunnels up to 2000 m below the surface such as the Mont-Blanc road tunnel and the galleries of the hydro-electric complex of Emosson, or in boreholes of several 10 m depth.

When comparing the water temperature to the total mineralisation (figure 3-26 B) one can see that the lithologic and hydrogeologic characteristics of the aquifers are more important for the groundwater mineralisation than the water temperature. Within a given aquifer type, however, the warmer springs are usually more mineralised. The water temperature is an important factor that influences the solubility of minerals (e.g. Stumm & Morgan, 1996). At higher temperatures, the solubility of most minerals increases, while at a given P_{CO_2} , the solubility of carbonate minerals decreases with increasing temperature. The dissolution of carbonate minerals is one of the major processes in the mineralisation of the investigated recent groundwaters. This suggests that the increasing groundwater mineralisation with increasing water temperature is inconsistent with the decreasing solubility of carbonate minerals. However, it has been shown that due to increased biological activity in the soils of the warmer low altitude catchments, the effect of the resulting increased soil CO_2 production dominates over the decreased carbonate solubility.

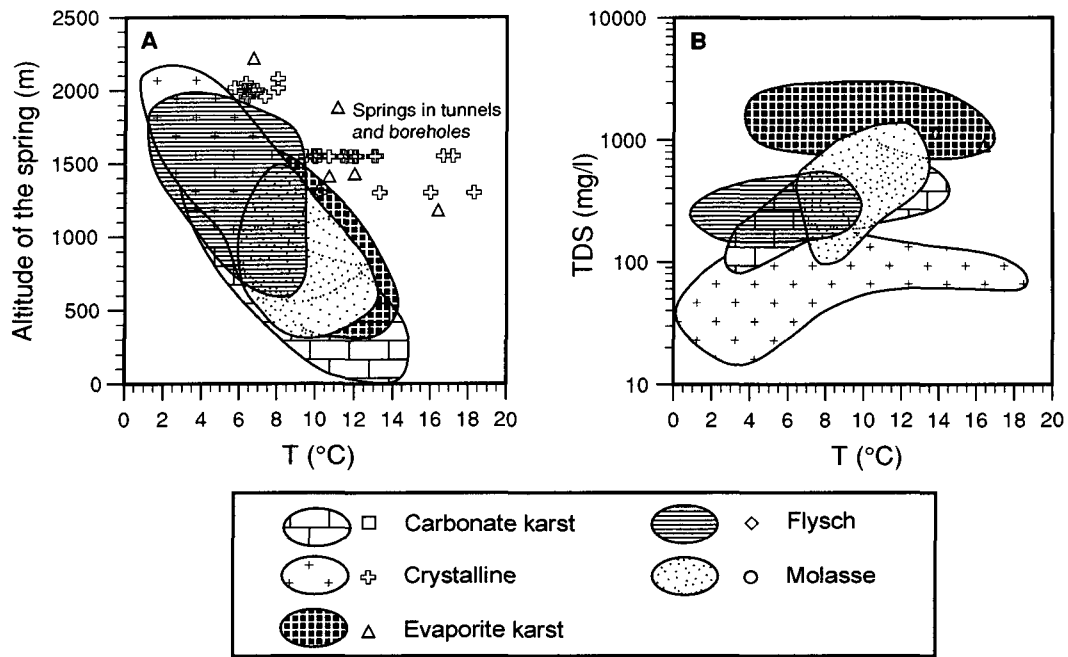


Figure 3-26: Relations between water temperature, altitude of the sampling site, and groundwater mineralisation.

pH and redox conditions

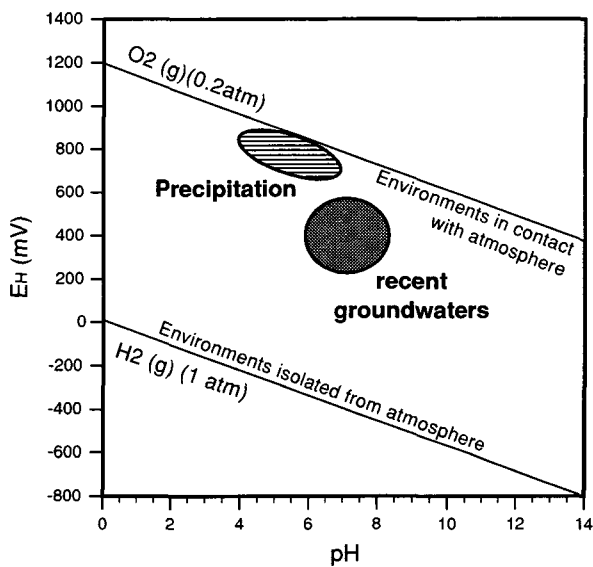


Figure 3-27: Ranges of pH and E_H conditions in the investigated groundwaters and precipitation waters in the stability field of water.

The pH- E_H -plot in figure 3-27 shows the distribution of precipitation water and the investigated recent groundwaters in the stability field of water. All of the pH and E_H values measured in the recent groundwaters plot in a restricted area, indicating oxidising and mildly acid to mildly alkaline conditions.

Unfortunately, pH and E_H have not been measured systematically at the beginning of the AQUITYP project, particularly in the groundwaters from crystalline, evaporite and flysch aquifers. Due to technical difficulties only few pH measurements and even less E_H measurements were made.

The pH evolves from acid conditions in precipitation water to the still mildly acid to mildly alkaline conditions observed in the groundwaters.

The pH of rain and snow melt in Switzerland ranges from 3.7 to 7.1 with a median value of 5.4 (Atteia, 1992). In

pristine environments the pH of precipitation water is governed by the atmospheric P_{CO_2} . Pure water, in equilibrium with atmospheric CO_2 ($P_{\text{CO}_2} = 10^{-3.5}$ at 20°C), has a pH of 5.6. This is slightly higher than the pH generally observed in the precipitation in Switzerland. Gases from anthropogenic origins (industry, traffic fumes, etc.) are oxidised and produce sulphuric, nitric, and hydrochloric acids, which are the cause of “acid rain”.

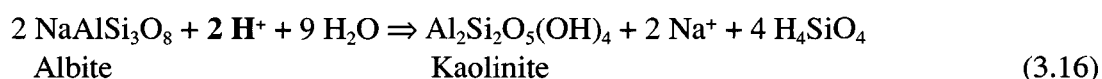
As the precipitation water percolates through the soil it is further acidified by natural and anthropogenic induced processes: Natural acidification of the soil solution occurs by dissolution of CO_2 produced by oxidation of organic matter and root respiration. Soil air typically has a P_{CO_2} ranging from $10^{-1.5}$ to $10^{-2.5}$ (e.g. Buyanovsky & Wagner, 1983; Scheffer & Schachtschabel, 1979), which is about 10 to 100 times higher than the atmospheric P_{CO_2} .



In addition, anthropogenic induced acidification of the soil solution results from acid input and the oxidation of NH_4^+ in the rainwater, which is produced by the dissolution of NH_4OH evaporating from manure. Compared to the acidification by the dissolution of soil CO_2 , this second process is less important in the investigated alpine catchments.



The acidity of the soil solution is the driving force behind mineral dissolution and weathering processes, which result in an increase of the pH. Both, the dissolution of carbonate minerals and the weathering of Al-silicates consume protons, as illustrated by the reactions 3.15 and 3.16:



The chemical weathering of Al-silicate minerals takes much more time than the dissolution of carbonate minerals (see table 1-2, page 11). Therefore, a pH increase caused by weathering of Al-silicate minerals takes several orders of magnitude longer than by the dissolution of carbonate minerals, and consequently has very little influence in the investigated recent groundwaters. In catchments where little carbonate minerals are available for dissolution, such as in the crystalline, or in karst and fractured aquifers, where flow is too fast for the groundwater to attain equilibrium with carbonate minerals, groundwaters with still mildly acid pH values occur.

3. 5. 2. Major elements

In order to compare concentrations of major ions, dissolved silica, total dissolved solids, and total hardness of the investigated recent groundwaters from the different aquifer types median concentrations are given in table 3-26. A Schoeller plot (Schoeller, 1960; figure 3-28) gives an overview of the median major element compositions in a graphical form. In addition, box plots of major element concentrations, total dissolved solids, and total hardness provide an overview of the concentration ranges (figure 3-29). The dominant

major element compositions of the groundwaters from the different aquifer types can be compared in a Piper-diagram (Piper and others, 1953; figure 3-30).

Parameter	Unit	CRY		CARB	EVAP	MOL	FLY
		Gneiss	Granite				
F ⁻	mg/L	<0.2 n=64	1.1 n=55	<0.2 n=87	<0.2 n=83	<0.2 n=96	<0.2 n=53
Cl ⁻	mg/L	<1 n=64	<1 n=55	2.7 n=87	2.9 n=91	3.0 n=96	<1 n=51
Alkalinity as HCO ₃ ⁻	mg/L	39.1 n=64	29.9 n=55	213.5 n=87	237.9 n=91	281.5 n=96	186.9 n=53
SO ₄ ²⁻	mg/L	12.1 n=64	12.5 n=55	8.6 n=87	1043.3 n=91	12.1 n=96	8.2 n=53
NO ₃ ⁻	mg/L	<1 n=64	<1 n=55	3.0 n=87	<1 n=91	8.1 n=96	2.4 n=53
Mg ²⁺	mg/L	0.7 n=64	0.3 n=55	4.1 n=87	57.7 n=91	13.5 n=96	3.2 n=53
Ca ²⁺	mg/L	14.2 n=64	11.8 n=55	72.3 n=87	426.0 n=91	82.2 n=96	56.2 n=53
Sr ²⁺	mg/L	0.04 n=63	0.04 n=55	0.15 n=87	8.22 n=91	0.22 n=96	0.37 n=53
Na ⁺	mg/L	1.5 n=64	3.4 n=55	1.6 n=87	4.8 n=91	2.4 n=96	0.8 n=51
K ⁺	mg/L	0.7 n=64	1.3 n=55	0.8 n=87	1.6 n=91	0.8 n=96	0.4 n=53
Si total	mg/L	2.5 n=64	3.2 n=46	3.0 n=87	3.1 n=85	5.9 n=96	1.5 n=53
TDS	mg/L	75.2 n=64	69.1 n=54	345.4 n=87	1782.2 n=91	418.3 n=96	267.1 n=53
Total Hardness	°F	4.1 n=64	3.1 n=47	20.0 n=86	130.3 n=91	25.0 n=96	16.3 n=53

Table 3-26: Comparison of major element concentrations in recent groundwaters from the different aquifer types (median values and number of samples). CRY = crystalline, CARB = carbonates, EVAP = evaporites, MOL = molasse, FLY = flysch.

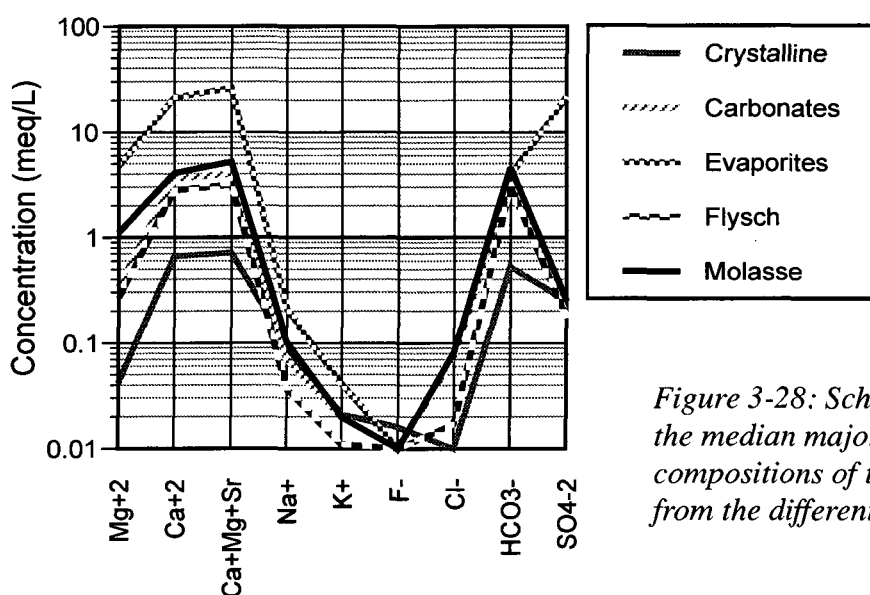


Figure 3-28: Schoeller plot showing the median major element compositions of the groundwaters from the different aquifer types.

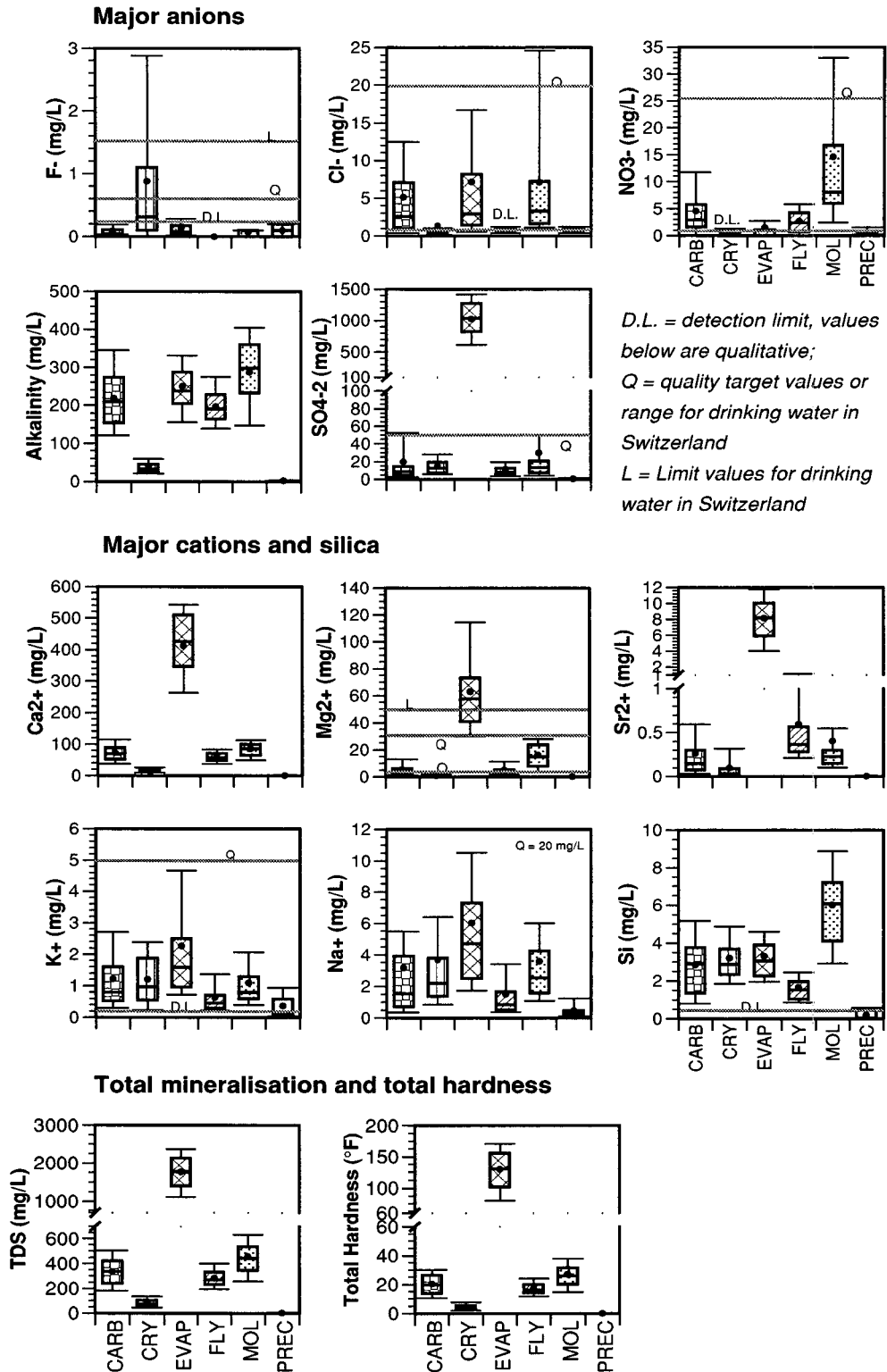


Figure 3-29: Box plots comparing major element concentrations and their ranges in the groundwaters from the different aquifer types (see table 3-26). The boxes show the inter quartile range (25th percentile to 75th percentile) and median values (the line through the middle of the box). The whiskers extend from the 10th percentile to the 90th percentile. The black point displays the arithmetic mean. Outliers (lower than 10th percentile or higher than the 90th percentile) are not plotted.

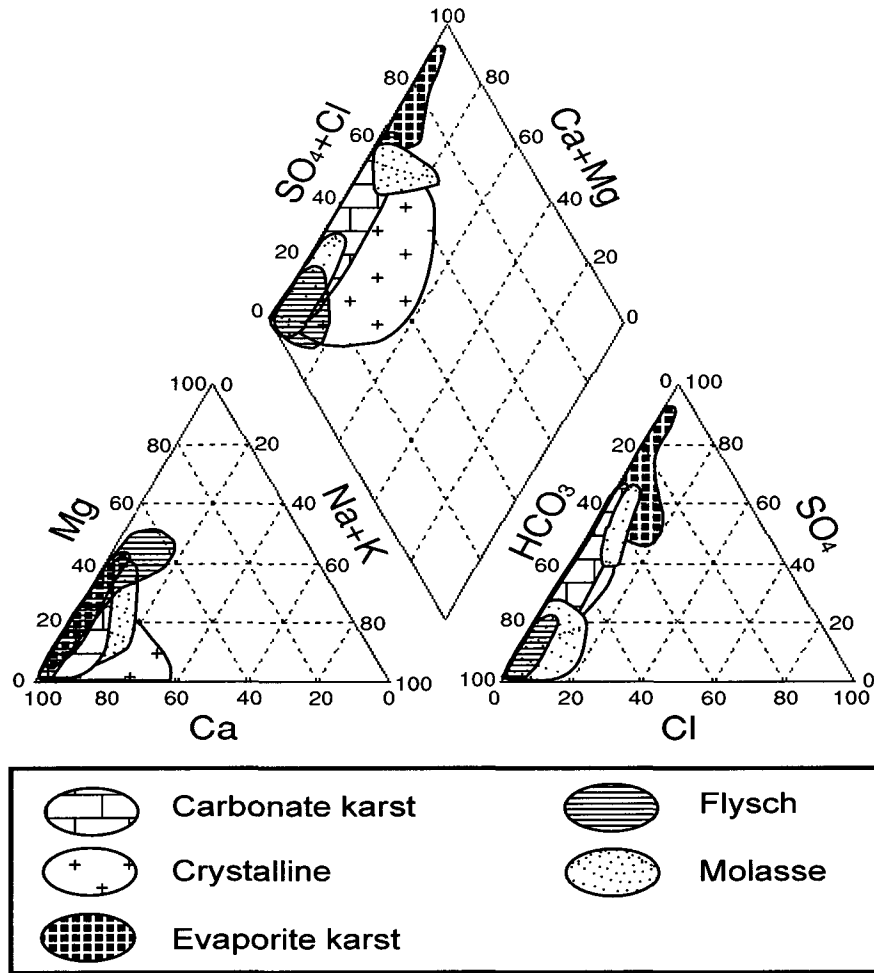


Figure 3-30: Piper-diagram illustrating the distribution of the major element compositions in each of the five investigated aquifer types (milliequivalents normalised to 100%).

Considering the major element chemistry and the total mineralisation of the investigated recent groundwaters, three hydrochemical facies can be distinguished:

- 1.) The **groundwaters from the crystalline rocks** of the Mont-Blanc and Aiguilles-Rouges Massifs, generally of the Ca-(Na)-HCO₃-(SO₄) type, are the most dilute groundwaters. They usually have a total mineralisation below 100 mg TDS/L, low Ca²⁺ and alkalinity concentrations and a very low total hardness. On the other hand, the F⁻ concentrations can reach values as high as 4.0 mg/L, particularly in the groundwaters from the granite.
- 2.) The **groundwaters from carbonate rocks and from calcareous clastic sediments (molasse and flysch)** are generally of the Ca-(Mg)-HCO₃-(SO₄) water type. These groundwaters generally have an intermediate mineralisation of around 300 mg TDS/L and a similar major element chemistry. The total mineralisation of recent flysch groundwaters and carbonate karst groundwaters is generally slightly lower than in the recent molasse groundwaters. Molasse groundwaters generally have longer residence times and contain somewhat higher Mg²⁺, alkalinity, silica, and NO₃⁻ concentrations than the groundwaters from carbonate and flysch rocks.

- 3.) The **groundwaters from evaporite rocks** are by far the most mineralised groundwaters, usually of the $\text{Ca-Mg-SO}_4\text{-HCO}_3$ type. These groundwaters owe their high total mineralisation of around 1800 mg TDS /L and their very high total hardness to the high concentrations of SO_4^{2-} , Ca^{2+} , Mg^{2+} , and Sr^{2+} .

It arises that Ca^{2+} is the dominant cation in all investigated recent groundwaters (figure 3-31). Mg^{2+} generally dominates over Na^+ , except in the groundwaters from crystalline rocks, where Na^+ is often slightly more concentrated than Mg^{2+} . The dominant anion of the recent groundwaters from crystalline, carbonate, molasse and flysch rocks is typically HCO_3^- , while the major anion in groundwaters from evaporite rocks is SO_4^{2-} . Chloride concentrations are typically low in the investigated recent groundwaters. In more evolved groundwaters, higher Na^+/Cl^- ratios than in precipitation occur, due to additional Na^+ from Ca-Na cation exchange reactions.

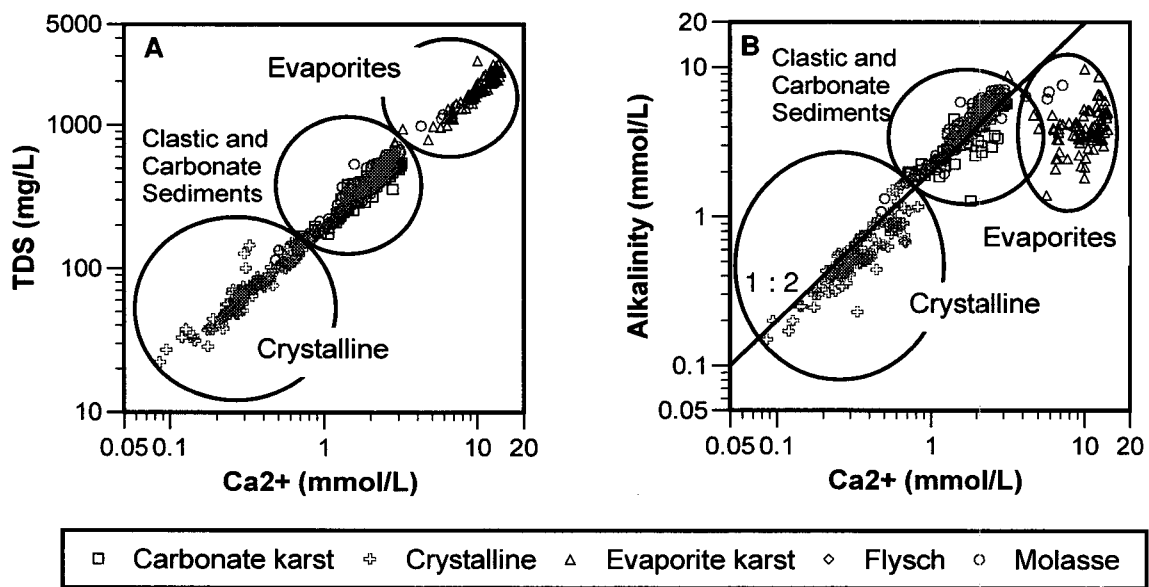


Figure 3-31: Ca^{2+} concentrations in the groundwaters from different aquifer types compared to total amounts of dissolved solids (A) and alkalinity (B).

The hydrochemical evolution of the recent groundwaters in crystalline rocks appears to be dominated by the dissolution of small amounts of hydrothermal calcite. Compared to the molar alkalinity/ Ca^{2+} ratio of 2, which results from calcite dissolution enhanced by the uptake of atmospheric and possibly soil CO_2 (reaction 3.5, page 75), these groundwaters often show lower molar alkalinity/ Ca^{2+} ratios. This can be explained by the dissolution of fluorite, which provides additional dissolved Ca^{2+} . Further, in the investigated crystalline groundwaters the dissolution of carbonates is promoted not only by acidity resulting from CO_2 uptake, but also by the acidity produced by the oxidation of sulphides (reaction 3.2 page 67 combined with reaction 3.15), which also results in lower molar alkalinity/ Ca^{2+} ratios. As granite and gneiss groundwaters contain very low Ca^{2+} activities, the solubility control by fluorite only sets in at high F^- activities (corresponding to F^- concentrations as high as 4.8 mg/L), while in the groundwaters with high Ca^{2+} activities such as the evaporite groundwaters, saturation with fluorite is attained already at relatively lower F^- activities (corresponding to F^- concentrations of about 1.1 mg/L; see figure 3-32). The low total

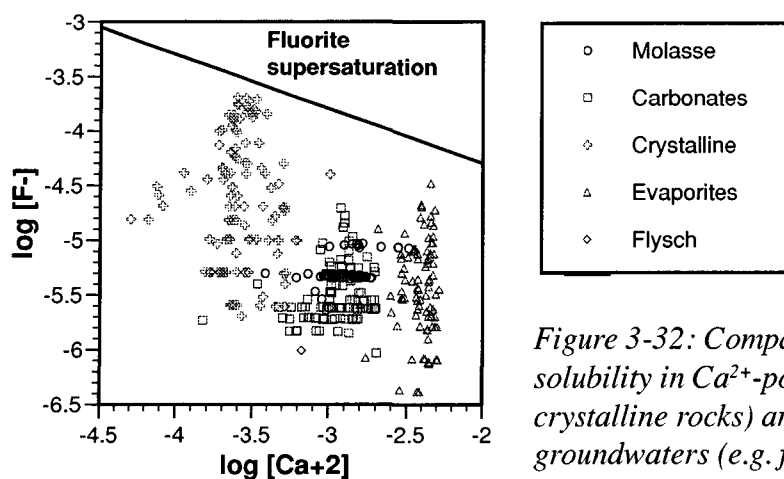


Figure 3-32: Comparison of the fluorite solubility in Ca^{2+} -poor groundwaters (e.g. from crystalline rocks) and in Ca^{2+} -rich groundwaters (e.g. from evaporite rocks). Plotted values are activities.

mineralisation of the groundwaters in the crystalline is a consequence of the small amount of readily dissolving minerals including carbonates, fluorite and sulphides available in granite and gneiss.

The hydrochemical evolution of the groundwaters from carbonate sediments as well as calcareous molasse and flysch rocks is dominated by the dissolution of calcite, which is enhanced by the uptake of soil CO_2 (reaction 3.5, page 75). The molar alkalinity/ Ca^{2+} ratio of around 2 illustrates this relationship. If additional dolomite dissolution becomes important, as it is the case in the more evolved groundwaters in dolomite-bearing aquifers, the alkalinity/ Ca^{2+} ratio shifts towards higher values (reaction 3.6, page 75). This explains the higher alkalinity and Mg^{2+} concentrations usually occurring in the molasse groundwaters and in some more evolved carbonate karst and flysch groundwaters. The more evolved groundwaters generally also contain higher Si concentrations. On the other hand, dissolution of gypsum or anhydrite induces a shift in the opposite direction, towards higher Ca^{2+} concentrations (reaction 3.7, page 75). Dissolution of gypsum is important in the mineralisation of groundwaters from the “Gypsum-bearing Molasse” and from certain carbonate karst aquifers containing evaporite beds.

The hydrochemical evolution of the groundwaters from evaporite rocks is governed by incipient dedolomitisation, which involves the dissolution of gypsum and dolomite and the simultaneous precipitation of calcite. The dissolution of gypsum leads to the observed low alkalinity/ Ca^{2+} ratios and the high SO_4^{2-} contents. The alkalinity remains low due to the precipitation of calcite. In pure water, gypsum is about 225 times more soluble than calcite, and still about 167 times more soluble than dolomite. This explains the much higher total mineralisation of these evaporite groundwaters compared to the groundwaters from the other aquifer types. The high Sr^{2+} concentrations result from the dissolution of important amounts of celestite and Sr^{2+} bearing dolomite.

3.5.3. Trace elements

The median trace element concentrations in the groundwaters from the different aquifer types are compared in table 3-27, and the figures 3-33 and 3-34 give a graphical overview of the concentration ranges.

Parameter	Unit	CRY		CARB	EVAP	MOL	FLY
		Gneiss	Granite				
Alkali and earth-alkali trace elements							
Li total	µg/L	<5 n=64	<5 n=54	<1 n=87	28 n=91	2 n=96	3 n=53
Rb total	µg/L	0.7 n=58	1.4 n=42	0.6 n=87	17.4 n=78	0.5 n=96	0.6 n=53
Ba total	µg/L	2.9 n=57	0.6 n=41	11.1 n=87	9.6 n=78	26.8 n=96	26.5 n=53
Metal trace elements							
Al total	µg/L	21.8 n=1	- -	3.0 n=87	14.1 n=73	8.2 n=96	0.9 n=53
V total	µg/L	0.2 n=1	- -	0.4 n=87	0.4 n=70	0.5 n=96	0.2 n=53
Cr total	µg/L	0.6 n=1	- -	0.4 n=87	<0.2 n=73	0.8 n=96	0.2 n=53
Mn total	µg/L	0.4 n=1	- -	1.1 n=87	12.7 n=73	0.8 n=96	0.5 n=53
Fe total	µg/L	11.4 n=1	- -	<2 n=87	4.6 n=1	<2 n=96	10.7 n=44
Co total	µg/L	<0.2 n=1	- -	<0.2 n=87	<0.2 n=1	<0.2 n=96	<0.2 n=53
Ni total	µg/L	0.6 n=1	- -	0.5 n=78	3.1 n=78	0.5 n=96	0.5 n=49
Cu total	µg/L	0.5 n=1	- -	0.3 n=87	2.9 n=78	<0.2 n=96	0.5 n=48
Zn total	µg/L	2.4 n=1	- -	0.9 n=87	2.1 n=78	0.9 n=96	1.1 n=46
Y total	µg/L	- -	- -	- -	0.6 n=72	- -	- -
Mo total	µg/L	3.1 n=58	66.9 n=42	0.3 n=87	2.8 n=1	0.3 n=96	0.1 n=1
Cd total	µg/L	0.2 n=1	- -	<0.2 n=18	0.2 n=73	<0.2 n=96	0.5 n=1
W total	µg/L	0.2 n=40	3.1 n=38	- -	- -	- -	- -
Pb total	µg/L	<0.2 n=1	- -	0.4 n=87	1.3 n=1	<0.2 n=96	0.3 n=53
U total	µg/L	5.1 n=58	135.2 n=42	0.3 n=87	5.2 n=78	0.5 n=96	0.2 n=53
Halides and non-metal trace elements							
Br total	µg/L	4 n=1	- -	3 n=87	8 n=73	8 n=96	3 n=53
I total	µg/L	1 n=1	- -	18 n=19	2 n=1	2 n=4	<1 n=1
B total	µg/L	<25 n=46	26 n=38	8 n=87	<25 n=80	3 n=96	7 n=53
As total	µg/L	13.8 n=58	5.8 n=42	<0.5 n=87	<0.5 n=72	<0.5 n=96	- -

Table 3-27: Median concentrations of trace elements in recent groundwaters from the different aquifer types (median values and number of samples). CRY = crystalline, CARB = carbonates, EVAP = evaporites, MOL = molasse, FLY = flysch. - = not analysed. Note that Li and B analyses for crystalline and evaporite groundwaters have higher detection limits (see page 35).

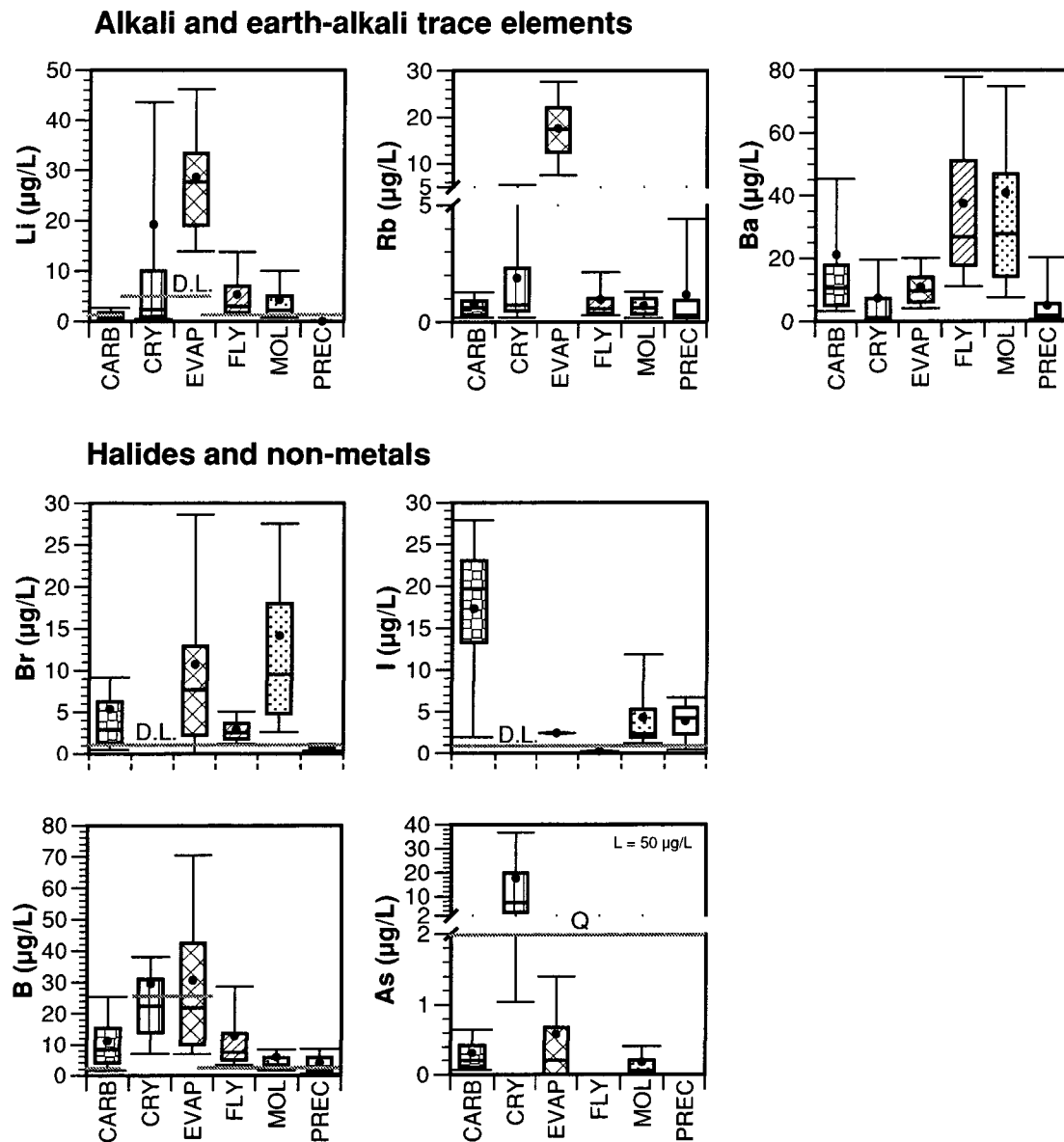


Figure 3-33: Box plots showing natural concentration ranges of alkali and earth-alkali trace elements, as well as halides and non-metal trace elements in groundwaters from the different aquifer types (see table 3-27). The boxes show the inter quartile range (25th percentile to 75th percentile) and median values (the line through the middle of the box). The whiskers extend from the 10th percentile to the 90th percentile and the black point displays the arithmetic mean. Outliers (lower than 10th percentile or higher than the 90th percentile) are not plotted. D.L. = detection limit, values below are qualitative; if no D.L. is indicated on the plot, it is below the measured concentrations. Q = quality target values and L = intervention values for drinking water in Switzerland.

Metal trace elements

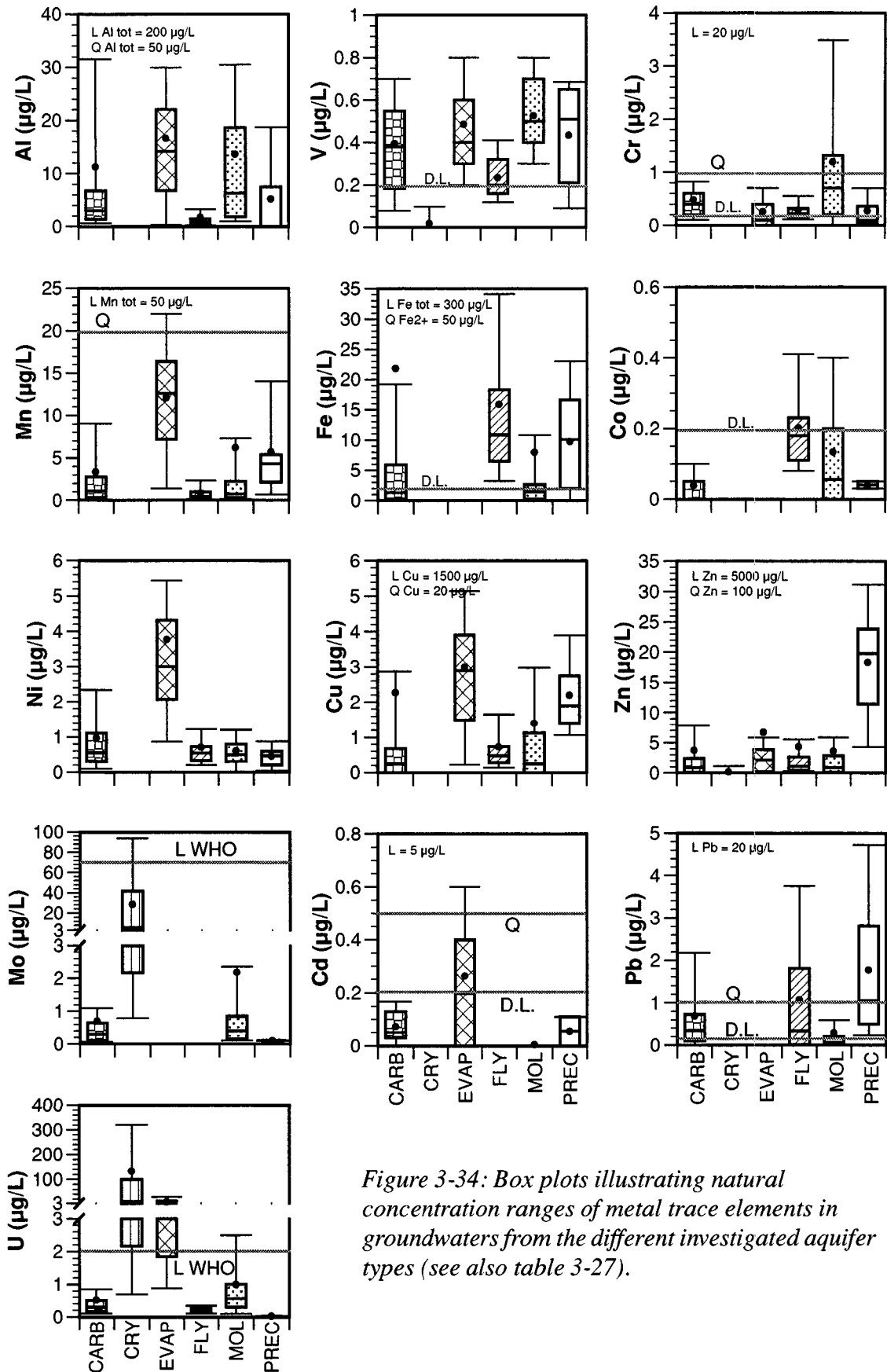


Figure 3-34: Box plots illustrating natural concentration ranges of metal trace elements in groundwaters from the different investigated aquifer types (see also table 3-27).

Natural tracers of groundwaters in the crystalline Mont-Blanc and Aiguilles-Rouges Massifs

Dubois (1993) has proposed Mo, U, W and Rb as specific marker elements of granite groundwaters, and As and Ba as specific markers of gneiss groundwaters of the Mont-Blanc and Aiguilles-Rouges Massifs.

The comparison with the concentrations found in the other groundwater types shows that **Mo**, **U**, **As** and **W** represent excellent tracers of recent groundwaters in the Mont-Blanc granite. In these granite groundwaters, the median concentration of dissolved **As** is about half that found in the gneiss groundwaters, but still higher than in the groundwaters from the other aquifer types. The **Rb** concentrations are particularly elevated in certain sub-thermal granite springs. The median **Rb** concentration is about twice as high as in the groundwaters from gneiss, carbonate, flysch and molasse rocks. However, in the evaporite groundwaters the **Rb** concentrations are an order of magnitude higher.

Besides the high **As** contents, the gneiss groundwaters contain also higher **U** and **Mo** concentrations than the other groundwater types, while **W** is usually near the detection limit. The dissolved **Ba** is more elevated than in granite groundwaters, but compared to the groundwaters from the other aquifer types they are among the lowest. **Ba** can therefore not be considered as a general marker of gneiss groundwaters.

Mo, **As** and **U** are excellent tracers of recent groundwaters in the crystalline Mont-Blanc and Aiguilles-Rouges Massifs, as their sources are hydrothermal minerals which are exposed along the major groundwater flow paths. At the observed concentrations, pH and redox conditions no solubility control exists for these elements and they are transported in the groundwater as dissolved anionic complexes. At these conditions, the only possible process to remove these elements from solution is sorption on secondary Fe-hydroxides.

Natural tracers of groundwaters from carbonate rocks

The total trace element content in groundwaters from carbonate rocks is relatively low compared to groundwaters from the other aquifer types, due to the short residence times and the low potential for specific trace elements of calcite.

Dematteis (1995) proposed iodine as a general tracer of groundwaters from carbonate rocks. In addition, he proposed additional trace elements as specific tracers of the groundwaters from certain lithologic units, including **Ba** as a tracer of groundwaters from deep sea limestones, **V** as a tracer of groundwaters from "Malm" aquifers of the western Swiss Jura mountains and from Cretaceous units of the Trieste region, and **Mo** and **U** as tracers of groundwaters from dolomite-bearing aquifers.

The comparability of **iodine** contents in the groundwaters from the different aquifer types is very limited because analytical artefacts occurred (see chapter "Quality control of the chemical data" on page 29). Only 20 reliable iodine analyses are available for groundwaters from carbonate rocks and 9 for molasse groundwaters. Nevertheless, the concentration of this element is one order of magnitude higher in groundwaters from carbonate rocks than in these molasse groundwaters. The biogenic origin of carbonate sediments and the related content of bitumen and kerogen is a plausible reason for the elevated iodine contents in the corresponding groundwaters. Iodine is present as highly soluble anion (**I⁻**) in solution.

The other trace elements **Ba**, **V**, **U** and **Mo** may be useful locally to distinguish groundwaters from different carbonate units, but they do not allow a discrimination of carbonate karst groundwaters from those of other aquifer types.

Natural tracers of groundwaters from evaporite rocks

The groundwaters from the Triassic evaporite series in the Rhone valley contain the highest amount of geogenic tracer of all groundwater types. Mandia (1993) proposed Li, Rb, Ni, Cu, Y, and Sc as geogenic tracers of groundwaters from evaporite rocks.

The comparison with the groundwaters from the other aquifer types shows that groundwaters from evaporite rocks contain distinctively higher concentrations of **Li, Rb, Ni, Cu, Y**, and in addition **Mn** and **Cd** than the other groundwater types. The enrichment of these elements is connected to the primary enrichment of relatively soluble elements in evaporite rocks. Dissolved trace elements originate mainly from the dissolution of dolomite (Mn, Ni) and apatite (Y, Cd), and from the oxidation of associated sulphide minerals (Cu, Ni, Cd). In addition, complexation with SO_4^{2-} enhances the solubility of metals such as Mn, Ni, and Cu. Elevated concentrations of highly soluble Li^+ and Rb^+ may be related to brine inclusions in evaporite minerals. The elevated values of Sc, however, are due to an analytical artefact and do not represent in-situ conditions (see chapter “Quality control of the chemical data” on page 29).

Natural tracers of molasse groundwaters

The trace element content of molasse groundwaters depends strongly on the mineralogic compositions of the corresponding molasse formations. A number of trace elements including have been proposed as specific natural tracers for particular molasse formations (Hesske, 1995). These elements may be useful locally to distinguish groundwaters from different molasse formations:

- **Chromium** is a good geogenic tracer of groundwaters from the OMM in western Switzerland. The dissolved Cr is related to the weathering of ophiolite detritus contained in the OMM sandstones.
- **Barium** occurs in high concentrations in the groundwaters from the conglomerates of the Gibloux fan (OMM) and the “Rigi-Rossherg” fan (USM) and in the groundwaters from the “Grès de la Cornalle” sandstone. Compared to the groundwaters from the other aquifer types, Ba is present at similarly high concentrations in molasse groundwaters as in flysch groundwaters.
- The groundwaters from the “Gypsum-bearing Molasse” contain elevated amounts of **Li, Mo, U, Br, and B**, similar to the groundwaters from the Triassic evaporites in the Rhone valley.
- The groundwaters from the “Glimmersand” formation contain distinctive elevated **Mo** and **U** contents and slightly elevated **Li** concentrations.

Natural tracers of groundwaters in the flysch

Groundwaters derived from the shallow flysch aquifers in the Niesen and Gurnigel nappes have a low trace element content situated between that of groundwaters from molasse and carbonate rocks. The comparison with the groundwaters from the other investigated aquifer types revealed no particular marker element in groundwaters from

flysch rocks. **Barium** is the most concentrated trace element, present in similar concentrations as in molasse groundwaters. Although Fe and Co are present at higher concentrations than in the other aquifer types, these elements cannot be used as a reliable tracers, because they are likely to be linked to colloidal matter in the unfiltered water samples.

It appears from the comparison of trace element concentrations in different groundwater types that dissolved Mo and U are correlated (see figure 3-35). This can be explained by the simultaneous occurrence of Mo and U minerals in rocks and by the similar chemical behaviour of these two elements in solution. This characteristic has long been known from U-ore prospecting, where Mo in soils and plants is used as a pathfinder to locate U mineralisations for exploitation (Wedepohl, 1978). In groundwater dissolved U and Mo both occur as soluble anion complexes. Elevated concentrations of these two elements occur primarily in the groundwaters from the crystalline rocks of the Mont-Blanc and Aiguilles-Rouges Massifs, but they are also found in groundwaters from certain molasse formations such as the “Glimmersande” and the “Gypsum-bearing Molasse”, and in groundwaters from dolomite-bearing carbonate rocks.

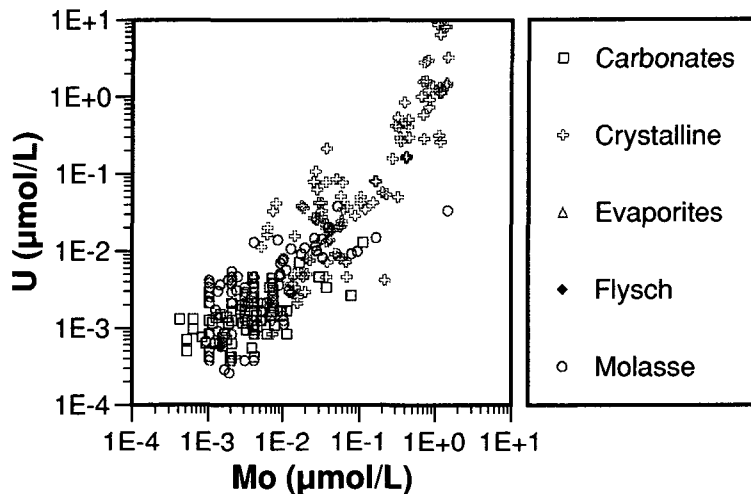


Figure 3-35: Comparison of dissolved Mo and U in the groundwaters from the different aquifer types.

Barium is a widespread trace element in the investigated recent groundwaters. The comparison of the calculated barite solubility to the Ba^{2+} and SO_4^{2-} activities in groundwaters shows, that high barium concentrations can only occur in SO_4^{2-} -poor groundwaters (figure 3-36). In SO_4^{2-} -rich groundwaters, such as those found in evaporite rocks, only small amounts of barite can be dissolved before saturation is attained.

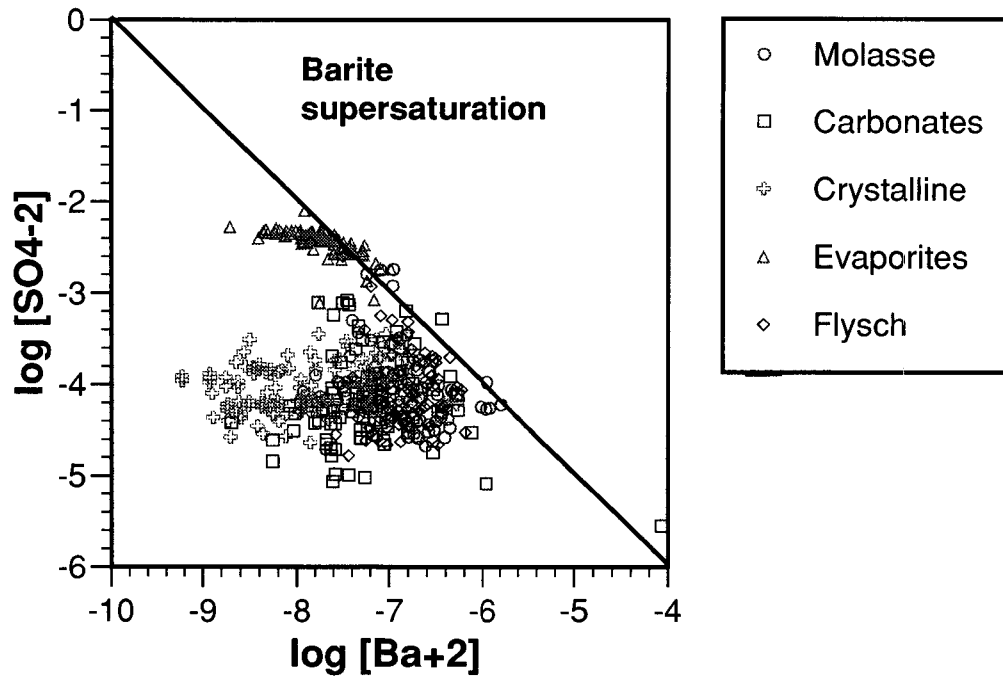


Figure 3-36: Comparison of the calculated barite solubility in SO_4^{2-} -poor groundwaters and in SO_4^{2-} -rich groundwaters such as those found in evaporite rocks. Plotted values are activities.

3. 6. Groundwater quality

In Switzerland about 80% of the drinking water is produced from groundwater. Besides groundwater from quaternary deposits, groundwater from solid-rock aquifers represents an important source of drinking water in large regions of Switzerland, such as carbonate karst groundwaters in the Jura, molasse groundwaters in the plateau region, and groundwater from granite and gneiss massifs in the Alps. Yet, groundwater is not always suited as drinking water as regards its chemical composition.

In order to assess the quality of the investigated groundwaters from different lithologic environments as drinking waters, the concentrations of chemical elements are compared to the Swiss drinking water standards. Limit concentrations (“Valeurs limite”, OSEC, 2000) and quality target values (“Valeurs de tolérance”, OSEC, 2000; “Erfahrungswerte”, SLMB, 1999) are listed in table 3-28 and compared to the investigated groundwaters (table 3-29). In addition, they are also displayed in the box plots in chapter 3. 5. on page 106.

The Swiss limits for drinking water are fixed for tap water based on toxicology, whereas quality target values are fixed based on practical aspects such as corrosion (low pH, high Cl⁻, high SO₄²⁻), depositions (high hardness, Fe, Mn, Al), taste and odour (S²⁻, NH₄⁺, Cl⁻, Na⁺, Zn, high pH), or staining of laundry and sanitary ware (Fe, Mn, Cu). Elements at concentrations above the quality target value are also used as indicators of a pollution.

The dissolved element concentrations of the investigated groundwaters represent the *natural composition* at the outlet of the aquifer, whereas the drinking-water quality standards are established for *tap water*. Tap water that has stood a certain time within metal conduits can contain elevated amounts of metals, particularly Cu, Zn, and Pb, which should not occur in natural groundwaters. The quality requirement for *groundwater* which is used as drinking water are described in the “Gewässerschutzverordnung” (GSchV/Oeaux, Anhang 2). Accordingly, the concentrations of Cl⁻ and SO₄²⁻ have to be below 40 mg/L and the NO₃⁻ concentrations have to be below 25 mg/L.

It is recalled that in the AQUITYP project the sampling sites were chosen in remote regions, where point source pollution was thought to be minimal. This does however not exclude diffuse pollution from sources including the atmosphere, and in rare cases agriculture. As the molasse occurs in the most densely populated area of Switzerland, it is difficult to find many catchments in the molasse where the influence of agriculture can be excluded completely. Furthermore, in the usually very large carbonate karst catchments, it is difficult to exclude even point source pollution, as unofficial waste deposits in dolines and shafts have been a common practice. Nevertheless, the reported groundwater composition can be regarded as close to natural for all constituents except NO₃ and Pb.

Further, the groundwater samples were generally not filtered before analysed (see chapter 2. 1. 3. on page 23). As has been shown by filtration tests (see chapter “Filtration test” on page 26), especially the Al and Fe concentrations represent total amounts including a potential colloidal fraction. These elements are therefore not included in the discussion.

Note that not all of the investigated springs are actually used for drinking water purposes. While the investigated molasse and flysch groundwaters and a large part of the carbonate karst groundwaters are used for public water supply, this is not the case of the tunnel springs in the granite and gneiss, which constitute a large part of the database, but are directed into surface water courses. The latter is also the case for most evaporite groundwaters. However, a number of evaporite springwaters are used for various purposes, such as drinking water (usually blended with other water to lower the SO₄²⁻ and Mg²⁺ content), mineral water (commercial use), thermal spas, and irrigation.

Parameters	Units	Switzerland			World	
Parameters	Units	OSEC ^a		SLMB ^b	WHO recommendations ^c	
		“Valeur limite”	“Valeur de tolérance”	“Erfahrungswert”	Guideline value	Levels likely to give rise to consumer complains
T	°C			8-15		should be acceptable
pH	pH units			6.8-8.2		
dissolved O ₂	% sat.			(30-100%)		
TDS	mg/L					1000
E.C.	µS/cm			200-800		
Na ⁺	mg/L			<20		200
K ⁺	mg/L			<5		
NH ₄ ⁺	mg/L		<0.5 (red.) <0.2 (ox.)	<0.05		1.5
Cl ⁻	mg/L			<20		250
F ⁻	mg/L	1.5		<0.5	1.5	
NO ₂ ⁻	mg/L	0.1		<0.01	3 acute 0.2 chronic	
NO ₃ ⁻	mg/L		40	<25	50	
SO ₄ ⁻²	mg/L			<50		250
S ²⁻	mg/L		not perceptible	not perceptible		0.05
P	mg/L			<0.05		
CN ⁻	mg/L	0.05			0.07	
Al	µg/L		<200	<50 (Al ³⁺)		200
Ag	µg/L		<100			
As	µg/L	50		<2	10	
Ba	µg/L				700	
B	µg/L				500	
Cd	µg/L	5		<0.5	3	
Cr	µg/L	20 (Cr ^{VI})		<1 (Cr ^{VI})	50	
Cu	µg/L		1500	<20	2000	1000
Fe	µg/L		<300 (Fe tot)	<50 (Fe ²⁺)		300
Hg	µg/L	1		<0.1	1	
Mn	µg/L		<50 (Mn tot)	<20 (Mn ²⁺)	500	100
Mo	µg/L				70	
Ni	µg/L				20	
Pb	µg/L	10		<1	10	
Sb	µg/L				5	
Se	µg/L	10		<1	10	
U	µg/L				2 (chem.)	
Zn	µg/L		5000	<100		3000

Table 3-28: Swiss drinking water standards and WHO recommendations.

- a. Ordonnance sur les substances étrangères et les composants dans les denrées alimentaires (OSEC, 22.2.2000)
- b. Lebensmittelhandbuch / Manuel des denrées alimentaires, 1999
- c. World Health Organisation: Guidelines for drinking-water quality. WHO 1993, 1998

Parameter	Aquifer type	Number of springs	> Limit	> Quality target	< Quality target
pH	Cry	52		1%	22%
	Carb	85			2%
	Mol	94			3%
	Fly	46			23%
E.C.	Cry	111			99%
	Evap	91		98%	
	Carb	86			8%
	Mol	96		5%	6%
	Fly	53			11%
Na⁺	Cry	119		1%	
	Evap	91		3%	
	Carb	87		2%	
	Mol	96		2%	
K⁺	Evap	91		8%	
	Carb	87		1%	
	Mol	96		1%	
Cl⁻	Evap	91		7%	
	Carb	87		3%	
	Mol	96		13%	
F⁻	Cry	119	23%	22%	
	Evap	91		3%	
NO₃⁻	Evap	91		1%	
	Carb	87		1%	
	Mol	96		18%	
SO₄²⁻	Evap	91		100%	
	Carb	87		9%	
	Mol	96		10%	
As	Cry	100	7%	71%	
	Evap	72		7%	
	Mol	96		1%	
Cd	Evap	73		10%	
Cr	Evap	73		1%	
	Carb	87		9%	
	Mol	96		33%	
	Fly	53		2%	
Cu	Carb	87		5%	
	Mol	96		1%	
Mn	Evap	73		11%	
	Carb	87		3%	
	Mol	96		5%	
Mo (WHO)^a	Cry	100	15%		
Ni (WHO)	Evap	78	2%		
Pb	Carb	87		18%	
	Mol	96		6%	
	Fly	53		32%	
U (WHO)	Cry	100	65%		
	Evap	78	58%		
	Carb	87	1%		
	Mol	96	14%		
Zn	Evap	78		2%	
	Mol	96		1%	

Table 3-29: Comparison of groundwaters from different aquifer types to Swiss drinking-water standards. Given are the percentages of groundwaters with concentrations of specific elements above the limit and above or below the quality target value.

a. WHO recommendations are used if no limits are given in the Swiss drinking-water standards.

3. 6. 1. Groundwaters from granite and gneiss aquifers in the Mont-Blanc region

22% of the springs in the crystalline, particularly those from granite aquifers, have **pH** values between 5.9 and 6.8, below the quality target of 6.8. Such low pH groundwaters can induce corrosion of tubing and dissolution of metals.

Further, crystalline groundwaters have a very low mineralisation and total hardness. 99% of the springs are below the quality target value for E.C. of 200 $\mu\text{S}/\text{cm}$. On the other hand, the critical value of 1.5 mg **F**⁻/L is often exceeded in these groundwaters (23% of the springs, mainly in granite). Due to the very low Ca^{2+} concentrations in granite and gneiss groundwaters, the solubility control by fluorite only sets in at a **F**⁻ concentration of about 5 mg/L, more than three times the admitted concentration (see figure 3-32 page 114).

Further, the natural **As** concentrations are substantially higher than the quality target value of 2 $\mu\text{g As}/\text{L}$ in a majority of the springs (71%), including those that are tapped for drinking water purposes. In 7% of the springs the **As** concentration exceeds even the intervention value of 50 $\mu\text{g As}/\text{L}$ (a maximum **As** concentration of 225 $\mu\text{g}/\text{L}$ has been measured). The chemical form of **As** greatly influences its toxicity. Arsenic (**As**^{III}) complexes are more toxic than arsenate (**As**^V) complexes and organic **As**-compounds. Speciation calculations suggest that the **As** in the investigated oxygenated granite and gneiss groundwaters is predominantly present as **As**^V-complexes. For **U** there is only a drinking water limit concerning its radioactivity but not for its chemical toxicity, and no limit is fixed for **Mo** in the current Swiss drinking water standards. However, the WHO recommends that drinking water should not exceed 2 $\mu\text{g U}/\text{L}$ and 70 $\mu\text{g Mo}/\text{L}$ based on the chemical toxicity of these elements. As shown earlier, the groundwaters from granite and gneiss aquifers often have conspicuous **U** and **Mo** contents, which exceed the WHO guideline value for **U** in 65% of the cases and for **Mo** in 15% of the cases.

3. 6. 2. Groundwaters from carbonate karst aquifers

The carbonate karst groundwaters normally satisfy the Swiss drinking water standards regarding the investigated chemical constituents. The pH, E.C., and major element concentrations are within or close to the recommended range. Only the SO_4^{2-} concentrations are higher than the quality target in 9% of the springs. In addition, the karst groundwaters may contain certain trace elements at concentrations above the drinking water quality targets:

18% of the investigated carbonate karst groundwaters have **Pb** concentrations exceeding the quality target value of 1 $\mu\text{g Pb}/\text{L}$. Other trace elements occurring at concentrations exceeding the quality target values include **Cr** (9%), **Cu** (5%), **Mn** (3%), and **U** (1%).

3. 6. 3. Groundwaters from evaporite rocks in the Swiss Rhone valley

The groundwaters from aquifers containing abundant gypsum and dolomite are not suited for drinking water purposes. Their SO_4^{2-} concentrations and E.C. values exceed the prescribed drinking water quality targets in all springs. A few springs also have too high concentrations of **K**⁺ (8% of the springs), **Cl**⁻ (7% of the springs), **Na**⁺ (3% of the springs), and **F**⁻ (3% of the springs).

Although the **U** values in evaporite groundwaters are not as high as in the groundwaters from the crystalline, still 58% of the springs contain **U** at values exceeding the WHO guideline value. Bosshard and others (1992) have found that high **U** concentrations also occur in several commercially available mineral waters. Further, the quality target of 20 µg **Mn** /L is exceeded in 11% of the evaporite groundwaters. In addition, 10% of the evaporite groundwaters have **Cd** concentrations exceeding the quality target of 0.5 µg/L. Other trace elements occurring at concentrations exceeding the quality target values include **As** (7%), **Ni** (2%), **Cr** (1%), and **Pb** (1%).

3. 6. 4. Groundwaters from molasse aquifers

Most of the investigated molasse groundwaters satisfy the Swiss drinking water standards, while the groundwaters from the “Gypsum-bearing Molasse” display similar quality problems as those from the Triassic evaporite series in the Alps (see above).

The **pH** of the molasse groundwaters, ranging from 6.5 to 8.1, is below quality target of 6.8 in 3% of the springs. Some molasse springwaters have **E.C.** values below (5%) or above (6%) the quality target range. Major element concentrations are generally within or close to the recommended range, except **NO₃**; which attains values above the quality target for drinking water in 18% of the springs. Further, in 13% of the springs **Cl** values and in 1% of the springs **K⁺** values are above the quality target value. In addition, the groundwaters of certain molasse units may contain trace elements at concentrations above the drinking water limits and quality targets:

The quality target of 1 µg **Cr** /L is exceeded in 33% of the investigated molasse springs, mainly in the springs in the OMM in western Switzerland. The toxicity of **Cr** strongly depends on its chemical form. Under the oxidising conditions reigning in the investigated groundwaters, **Cr** prevails in solution predominantly in its highly soluble and toxic hexavalent state (**CrO₄²⁻**). Further, the **U** concentrations of 14% molasse groundwaters, mainly those from the “Gypsum-bearing Molasse” and the “Glimmersand” molasse, exceed the WHO guideline value. The **Mn** concentrations are above the Swiss quality target value for drinking water in 5% of the springs. Other trace elements occurring in molasse groundwaters at concentrations exceeding the quality target values include **Pb** (6%), **As** (1%), and **Zn** (1%).

3. 6. 5. Groundwaters from flysch aquifers

The flysch groundwaters satisfy the Swiss drinking water standards. However, 23% of these flysch groundwaters have a **pH** ranging from 5.9 to 6.8, which is below the quality target of 6.8. 11% of the flysch groundwaters have **E.C.** values below the quality target range.

In addition, 32% of the investigated flysch groundwaters have **Pb** concentrations exceeding the quality target value.

3.6.6. Conclusions

The comparison of groundwater compositions in the different aquifer types and Swiss drinking water standards shows that the investigated groundwaters from carbonate, flysch, and molasse rocks normally satisfy the Swiss drinking water quality standards. However, it also shows that many elements of importance to drinking-water quality may occur at naturally elevated levels exceeding the prescribed limits or representing a cause of inferior drinking water quality. Particularly the groundwaters from crystalline rocks, from evaporite rocks and from certain molasse units, contain geogenic major and trace elements at concentrations exceeding the drinking water limits. In aquifers in the granite and gneiss of the Mont-Blanc and Aiguilles-Rouges massifs, problematic elements in the groundwater including F, As, U, and Mo are due to the particular mineralogy of the water conducting fractures and fissures containing fluorite, As- and Mo-bearing sulphides, and soluble U minerals. The high SO_4^{2-} concentrations in groundwaters from the Triassic evaporite series in the Rhone valley and from the "Gypsum-bearing Molasse" result from the high solubility of gypsum. These groundwaters may contain also U and Ni at levels exceeding the WHO guideline values from the weathering of U-minerals and sulphides. In addition, many geogenic elements including Cr, As, Cd, Mn, Zn and U occur at levels above the quality target values in groundwaters from different aquifer types containing minerals such as Cr-spinels, sulphides, dolomite or U-minerals.

As has been shown earlier, the hydrodynamic characteristics of the aquifer have a critical influence on the groundwater composition, in addition to the mineralogic composition. In groundwaters with a relatively long residence time, such as those in the porous molasse rocks, even relatively insoluble minerals disseminated in the rock, such as Cr-bearing pyroxene and spinels, are exposed to prolonged weathering and may release significant amounts potentially toxic trace elements. On the other hand, in fractured aquifers, or even more in karst aquifers, groundwater flow is usually very fast and takes place essentially in fractures or karst conduits, and only the soluble minerals present along these preferential flow paths are dissolved. Depending on which minerals are present along the preferential flow paths, groundwater of a good (flysch and carbonate karst groundwater) or a bad (crystalline groundwater) drinking water quality develops.

Furthermore, the hydrodynamic and infiltration characteristics of the aquifer also have an influence on the transport of problematic elements. For instance, groundwaters from karst aquifers or fractured aquifers are more sensitive to diffuse pollution than groundwaters from aquifers with interstitial porosity, because of the usually very fast transit time and the poor filtration of the water. With Pb being a typical atmospheric pollutant (e.g. Atteia, 1992), the elevated Pb concentrations in certain carbonate karst and flysch groundwaters may result from transport of atmospheric Pb down into the aquifer.

This comparison shows that the geogenic concentrations of major and trace elements derived for groundwaters from crystalline, carbonate, evaporite, molasse and flysch rocks would represent valuable additional information for the evaluation of groundwater quality. It has been shown that a certain element concentration occurring naturally in the groundwater of one aquifer type can mean a pollution in another. It is hoped that the geo-reference presented in this study will provide a contribution for a more discerning view in cantonal and federal groundwater quality management.

IV. CHEMICAL WEATHERING
OF BURDIGALIAN
SANDSTONE:
SOURCES AND BEHAVIOUR
OF CHROMIUM

4. 1. Introduction

The processes and physical-chemical conditions, which lead to the observed typical trace element concentrations in the studied recent groundwaters are not fully understood. Detailed studies considering field conditions are necessary to evaluate the influence of the mineralogic, chemical and time factors responsible for the observed concentration of a particular geogenic tracer element in the groundwater. Therefore, this part of the present study is focused on a detailed investigation of one geogenic tracer, in order to test the more general approach adopted for the synthesis of the hydrochemistry in the different aquifer types chapter “Typology of Recent Groundwaters” on page 41. A detailed hydro-geochemical study was carried out on the origin and chemical behaviour of Cr, the potentially toxic tracer of groundwaters from Burdigalian molasse sandstone in western Switzerland.

For the characterisation of Cr in the groundwater from a molasse sandstone (OMM, Burdigalian) a comprehensive field study has been conducted of two selected catchments in western Switzerland (Lutry spring catchment and Pierre-Ozaire spring catchment). A quantitative description of the processes controlling the dissolved Cr content in these groundwaters has been made based on mineralogical, geochemical, and hydrological investigations in addition to the groundwater chemical data.

Column experiments have been carried out in the laboratory with molasse sandstone from the field site, in order to support the field study findings and to derive additional constraints for the quantitative geochemical description of the system. Oxidised and reduced sandstone were collected from within the saturated zone of the aquifer. Two experiments with mountain-wet oxidised and reduced sandstone have been carried out over a time span of two months each, to obtain information about the influence of the alteration state of the substratum. The mineralogic composition of these samples has been analysed by optical microscopy and by X-ray diffraction (appendix E); the chemical composition has been analysed by X-ray fluorescence (appendix F). In order to obtain information about surface etching phenomena, mineral grains were separated from these sandstone samples and soil samples and investigated by scanning electron microscopy (SEM).

4. 1. 1. Selection of the study site

The upper marine molasse sandstone (OMM, Burdigalian) is an important aquifer in the Swiss plateau region (Keller, 1992). In western Switzerland, Hesske (1995) proposed that Cr is the natural marker element of recent groundwaters from this formation (see table 4-1). It is interesting to note that groundwaters from mafic and ultra-mafic rocks in the Alps, rocks that generally contain higher Cr concentrations than the studied molasse sandstone, have lower Cr concentrations than the molasse groundwaters (Derron, 1999). Compared to recent groundwaters from flysch, evaporite and carbonate aquifers, the Cr concentrations in these molasse groundwaters are also significantly higher.

The quality target for drinking water in Switzerland of 1 µg Cr/L (Manuel Suisse des denrées alimentaires, 1994) is exceeded in the groundwaters from the OMM sandstone in western Switzerland. It is therefore very important to recognise the sources of Cr in this sandstone and the processes controlling its concentration and its chemical form, i.e. trivalent or hexavalent, in the groundwater.

	Mol	OMM W-CH ^a	Mafic	Ultram	Fly	Evap	Carb
Cr (µg/L)	0.8 (<0.2-7.1) n = 100	4.2 (1.9-6.9) n = 15	1.4 (0.2-4.4) n = 30	1.5 (1.0-4.0) n = 14	0.2 (<0.2-1.4) n = 74	<0.2 (<0.2-1.1) n = 83	0.4 (<0.2-2.8) n = 97

Table 4-1: Chromium concentrations in groundwaters from different aquifer types (median, minimum and maximum values, and number of springs). Mol = molasse groundwaters in general and OMM W-CH = groundwaters from OMM sandstone in western Switzerland (Hesske, 1995); Mafic = groundwaters from mafic rocks and Ultram = groundwaters from ultramafic rocks (Derron, 1999); Fly = flysch groundwaters (Basabe, 1993); Evap = evaporite groundwaters (Mandia, 1993); Carb = carbonate karst groundwaters (Dematteis, 1995).

Two catchments situated entirely in the OMM sandstone in western Switzerland have been chosen for this hydro-geochemical study: The catchment of the Lutry spring is covered by forest and represents natural conditions. This catchment is used for the characterisation of the processes controlling the dissolved Cr content in the groundwater under natural conditions. The Pierre-Ozairé spring lies a few kilometres further south of the Lutry spring and drains a catchment covered by farm land (grass land). This spring is used to assess the influence of the different land use on the geochemical processes.

Previous studies provide an almost complete set of mineralogic, hydrologic, and hydrochemical data for the Lutry catchment. Such a data set is required for a quantitative description of the processes controlling the geogenic trace element composition of the groundwater. The hydrogeology of the investigated catchments and the hydrochemistry of the springwaters are well known. Both springs are part of the long-term monitoring network of the AQUITYP project, which provides a complete hydrochemical data set covering a time span of 19 years. In addition, the geochemical behaviour of trace elements has been studied in the soil of the Lutry catchment within the scope of the AQUISOL project.

4.1.2. Previous studies and data

The hydrogeology of the studied area is well known from earlier studies (GEOLEP, 1984, 1991). In addition, the hydrogeology of the Lutry spring has recently been described in detail, including isotope data and results of tracer tests (Etcheverry & Parriaux, 1999). The groundwater discharged at the Lutry spring is a recent, tritium-containing water (20 to 99 TU in waters sampled between 1985 and 1990). Its mean residence time calculated from tritium data with an exponential model is 3 to 4 years. This result is consistent with the outcome of the tracer tests made in this catchment, where the concentrations of the tracers in the springwater have still been rising one and a half years after injection.

Being part of the long-term monitoring network of the AQUITYP project, discharge, and physical-chemical parameters, as well as major and trace element concentrations in the groundwaters of both springs have been measured since 1982.

In the Lutry catchment, the geochemical behaviour of trace elements at soil level has been studied by Atteia (1992) and Dalla Piazza (1996) within the scope of the AQUISOL project. Chemical analyses have been made of rainwater, throughfall solutions collected under the forest canopy, and soil solutions. In addition, soil and bedrock material has been sampled and the mineralogy of the different soil levels has been studied in detail.

Atteia (1992) and Dalla Piazza (1996) have concentrated their investigations on the sources of dissolved trace elements (atmospheric input versus soil weathering). Atteia (1992) has calculated water fluxes and chemical element fluxes in the soil. He proposed that small amounts of Cr are leached from the sandy substratum by a slow weathering process. The study of Dalla Piazza (1996) was focused on the petrographic and geochemical evolution of the soil. This researcher has suggested that the primary ferro-magnesian sheet-silicates (biotite, chlorite, glauconite, serpentine) and heavy minerals such as spinel and epidote present in the soil are possible Cr-sources. He has also shown that the geochemistry of the fine-grained fraction in the soil evolves most strongly under the influence of weathering processes.

For the present study, analyses of rainwater, throughfall solution, soil solutions and spring water, as well as mineralogic and chemical data of soil and bedrock have been compiled from the studies of Atteia (1992), Dalla Piazza (1996), and Hesske (1995), and completed in this study where necessary.

4.2. Hydrogeologic setting

4.2.1. Localisation of the study site

The catchments of the Lutry and Pierre-Ozaire springs selected for this case study are located in western Switzerland, 8 km north-east of Lausanne. They are situated in the autochthonous Upper Marine Molasse (see figure 4-1). The catchments are located close to one another and present the same geological characteristics. Both cover a surface of approximately 2.5 ha (figure 4-2).

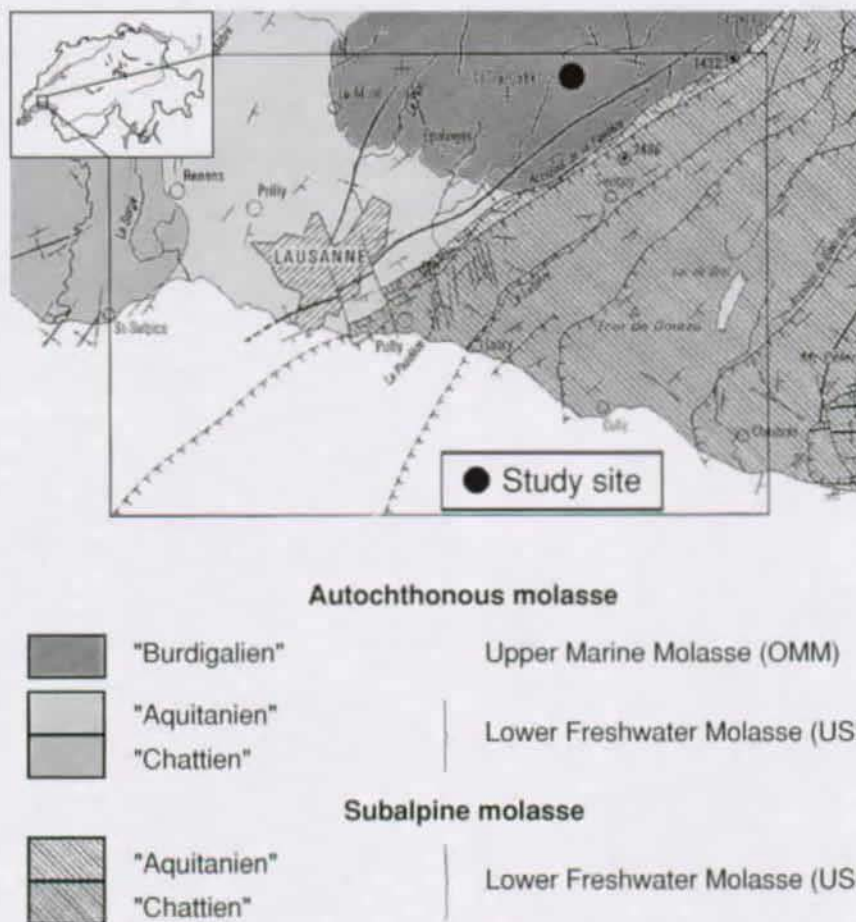


Figure 4-1: Geographic and tectonic situation (after Weidmann, 1988).

The Lutry catchment is situated in the region of the Bois du Grand Jorat at an altitude of about 900 m (see figure 4-2). It is entirely covered by a well-tended 80 years old coniferous forest (Atteia, 1992). The highest point of the topographic catchment is situated at 891 m, 13 m higher than the spring, which is situated in a small valley at an altitude of 878 m. The spring is tapped by means of a shallow, 25 m long drain in western direction, parallel to the small valley (GEOLEP, 1984). A second, smaller spring drains the immediate surroundings

of the spring. The discharge of this smaller spring is less than 1/10 of the larger one. Samples for chemical analyses have been taken only at the large spring and the small one is neglected in the following study. Discharge measurements, however, include both springs. The Pierre-Ozaire spring is located a few kilometres further south and drains a catchment occupied by grass land. The Pierre-Ozaire spring is the number 2 of a series of 15 springs tapped within a 665 m long gallery in the OMM sandstone. The spring is tapped by means of a shallow, 15 m long Y-shaped drain in south-eastern direction from the gallery (GEOLEP, 1984) and the water is led to the collector in the gallery. The highest point of the topographic catchment lies approximately 18 m higher than this drain.

The Lutry and the Pierre-Ozaire springs are used for the public drinking water supply of the city of Lausanne.

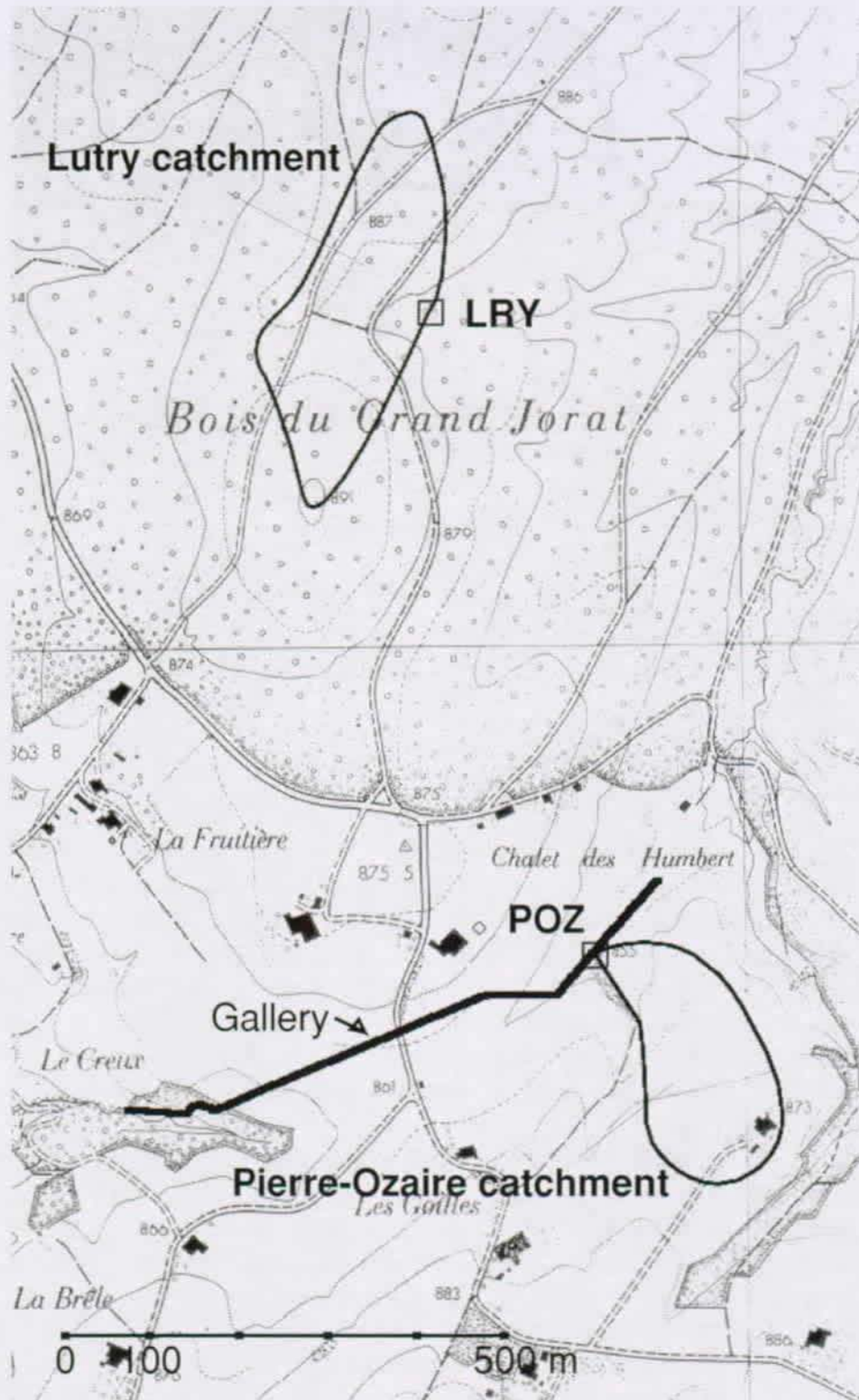


Figure 4-2: Close-up map showing the locations of the Lutry spring (LRY, coordinates 544'620 / 157'350) and the Pierre-Ozair spring (POZ, coordinates 544'860 / 156'690), and the approximate extension of the catchments.

4.2.2. Geological background

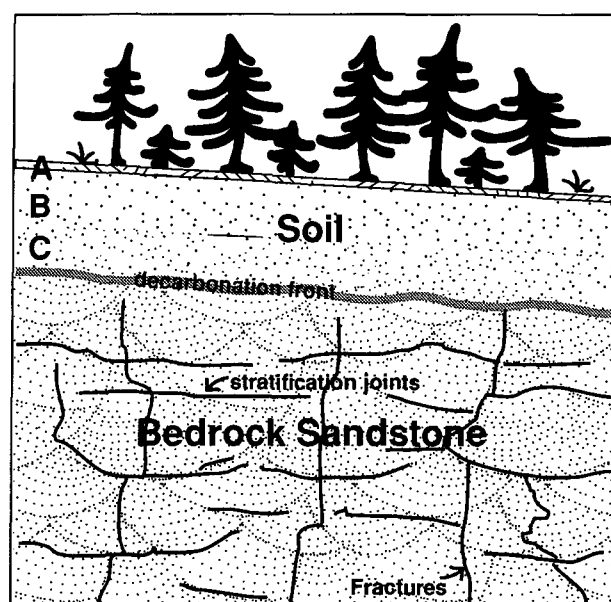


Figure 4-3: Lutry catchment: schematic profile through soil and bedrock sandstone.

Soil

The forest soil covering the Lutry catchment is a deep acid brown soil (also known as dystric cambisol, FAO soil classification). Generally, acid brown soils are characterised by weak or absent depletion in Fe and clay (Lozet & Mathieu, 1990). A description of the soil layers in the Lutry catchment is given in table 4-2. The B-horizon contains little organic matter and exhibits a reddish-brown colour from the presence of Fe-oxides and -hydroxides. This reddish-brown colour decreases at depth and becomes more and more greenish-beige until similar to the colour of the bedrock sandstone. The contacts between the different soil layers are gradual. The soil is completely decarbonated from the action of acid solutions seeping downwards.

Grain-size and mineralogic analyses showed that the soil developed by in situ alteration of the underlying OMM sandstone (Dalla Piazza, 1996). The soil development is favoured by the superficially loosened and fissured sandstone exposed after the retreat of Pleistocene glaciers, and by a locally preserved thin glacial sediment cover with an average thickness of about 1 metre (GEOLEP, 1984). The glacial sediments consist of weakly compacted silty sands with very few gravel sized components. This material is of local origin, composed of reworked molasse sandstone without significant external material. The thickness of the soil in the Lutry catchment varies as a function of the thickness of this glacial material: The soil is thinner on top of the hills (A + B horizon \approx 0.8 m in auger profile) and thicker in the small depressions, where the glacial sediment cover is more important. In a typical soil profile in the Lutry catchment the decarbonation front is situated at a depth of 2.5 m (Atteia, 1992).

Depth (cm)	Soil horizon		Description
0 - 2	litter	OL	Organic horizon, consisting of weakly decomposed organic matter from the forest
2 - 4	moder	OF	Weakly evolved forest humus in aerated environment
4 - 10	A-horizon	Aalh	Mixture of mineral and organic material, dark brown colour
10 - 45	B-horizon	Sal	Mineral soil horizon. Silty sand showing no more visible structures of the original bedrock, numerous roots
45 - 100		Salg1,2	Similar to Sal, but with rusty spots from variation in oxidation and reduction state resulting from bad drainage conditions
100 - 250	C-horizon	SC	Altered, completely decarbonated bedrock
250		SCca	Decarbonation front
> 250	bedrock		Carbonate-bearing bedrock

Table 4-2: Description of the soil layers in a typical profile in the Lutry catchment (after Dalla Piazza, 1996).

Bedrock sandstone

In the investigated area the Burdigalian OMM sandstone reaches a total thickness of approximately 200 m (Weidmann, 1988). The 660 m long Pierre-Ozaire gallery (see figure 4-2), which is situated a few meters below surface (20 m at most) in the OMM sandstone, allows an insight into the surface-near structure of the OMM sandstone in the studied area. In this surface-near zone, the bedrock is a calcareous, fine- to coarse-grained cross-bedded sandstone with mm to cm thick marly interlayers. Grain-size analyses have shown that the fine-grained fraction (<50 μm) makes up 5 to 20% in different sandstone varieties (Dalla Piazza, 1996). The sedimentary beds are flat-lying, with a very flat dip of 2 to 4° to the north. Sub-vertical fissures cut the sedimentary beds.

From a hydrogeologic point of view, the cross-bedded and fissured structure of the sandstone determines the preferential flow paths of the groundwater. Springs and seepage zones observed in the gallery are usually situated on top of the thin marl beds, which act as small-scale confining layers. This fissured sandstone is characterised by a so-called double porosity. The primary porosity, i.e. the interstitial porosity measured on unfissured sandstone samples ranges from 16 to 22% depending on grain size, clay content and degree of cementation and alteration (see appendix D). Groundwater flow in this interstitial porosity is slow, the hydraulic conductivity calculated from these measured porosity values is in the order of 10^{-6} to 10^{-8} m/s. The most permeable sandstone is coarse-grained and poorly cemented (originally or due to dissolution of the cement) and has little clay content. On the other hand, the secondary porosity formed by open stratification joints and fissures provides pathways for rapid horizontal and vertical groundwater flow.

The alteration state of the Burdigalian sandstone is distinctly displayed by its colour. In its unaltered state the sandstone has a bluish colour, while in its altered state it displays a yellowish rusty colour due to the presence of Fe-hydroxides. Bläuer (1987) has shown that the $\text{Fe}_2\text{O}_3/\text{FeO}$ ratio is higher in the yellow varieties of the OMM sandstone, which accounts for their more oxidised state. Along preferential flow paths in joints and fissures these alteration processes reach deeper into the reduced, bluish sandstone (figure 4-4) than in undisturbed, homogeneous sandstone. A thin reddish Fe-hydroxide film also covers the surfaces of marl beds, which act as confining layers. Oxidised and reduced sandstone, as

well as a clay layer that separates these zones were sampled within the saturated zone of the aquifer in the Pierre-Ozaire Gallery for mineralogical and chemical analysis (see chapter 4. 3. "Weathering of the Burdigalian sandstone" on page 142).

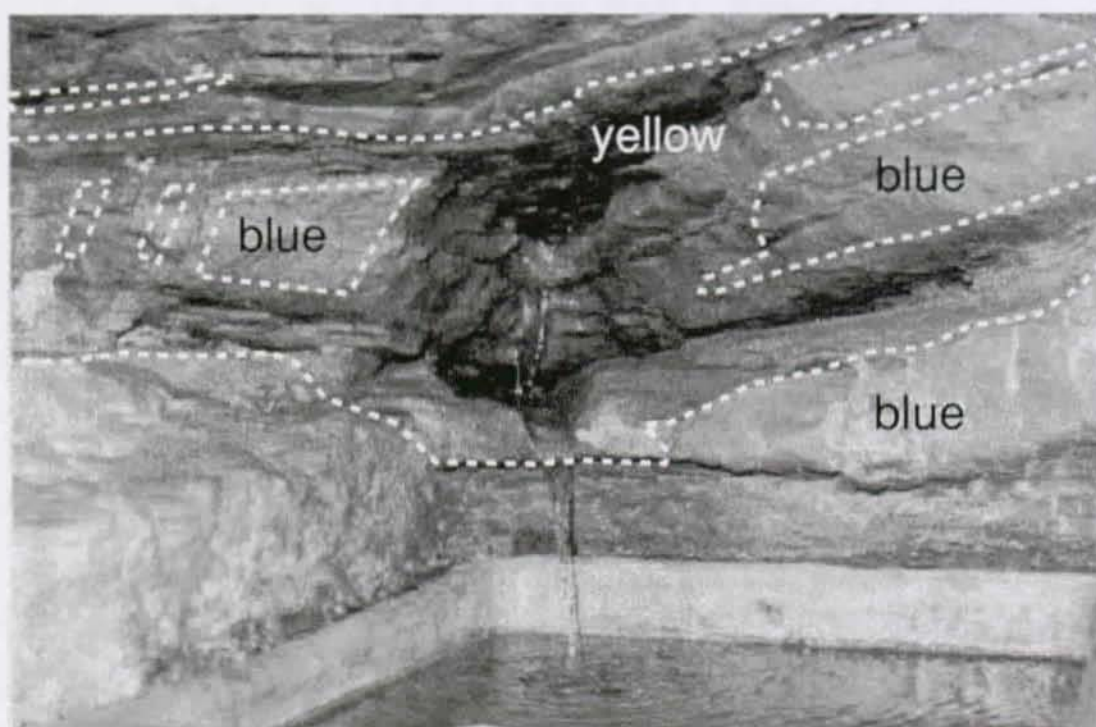


Figure 4-4: Colour variations of the OMM sandstone according to its alteration state. The springs emerge in the yellow parts of the sandstone, usually on top of impermeable marl beds. The sandstone which is not in direct contact with oxygenated groundwater remains in the reduced state displayed by its bluish colour.

Origin of the detrital material

During the Burdigalian a shallow sea flooded the molasse plateau, in which thick-bedded feldspar-rich and glauconitic marine sandstones were deposited (Trümpy, 1980a). Pebbles and sand were transported into this sea by rivers coming from the Alps and further along the axis of the basin by long-shore currents. Along the southern margin of the OMM outcrop belt, marine conditions prevailed outside of these rivers deltas, and fluvial conditions within. Paralic facies is encountered in the transitional zone. In these paralic areas abundant coal seams occur. In the investigated catchments carbonised pieces of driftwood and leaves can often be found. Some pyrite is found associated with the coal. In the outcrop these coal concretions are easily spotted, because the sandstone around the coal shows a red halo from impregnation with Fe-hydroxide formed from the oxidation of pyrite.

The mineralogic composition of clastic sediments and particularly their heavy mineral assemblage are characteristic for the lithology of the source rocks. The heavy mineral assemblage can therefore be used to identify these source rocks. In western Switzerland the heavy mineral assemblage of the OMM sandstone is dominated by epidote, apatite, pyroxenes, amphiboles, biotite, serpentine and spinels (magnetite and chromite), and minor amounts of pumpellyite, laumontite, sphene, zircon, tourmaline, garnet and rutile occur (Allen and others, 1985). This heavy mineral assemblage points to a source region

containing mafic and ultra-mafic rocks. The source region of the OMM in western Switzerland is thought to lie in the western Prealps, more specifically in the Upper Cretaceous to Eocene flysch nappes of the Prealps. Particularly the source of the pyroxenes, chromite, serpentine and part of the amphiboles can be traced back to the Gêts nappe (Simmen nappe s.l.) south of lake Geneva (see figure 4-5). In this unit, Early Jurassic to Cretaceous ophiolite rocks have been described by several authors (e.g. Jaffé, 1955; Salimi, 1965; Bertrand, 1970; Mevel, 1975; Bertrand & Delaloye, 1976). The ophiolites of the Gêts nappe include serpentinite rocks and a variety of mafic rocks comprising mafic sills, pillow lava, gabbro, and various mafic volcanic breccias. Radiometric dating of sand-sized rounded glauconite pellets in the molasse sandstone indicates that glauconite is partly reworked from lower Cretaceous source rocks (Fischer, 1983). In addition, glauconite also occurs as void fillings and replacements of various components, indicating diagenetic glauconitisation of the OMM sandstone.

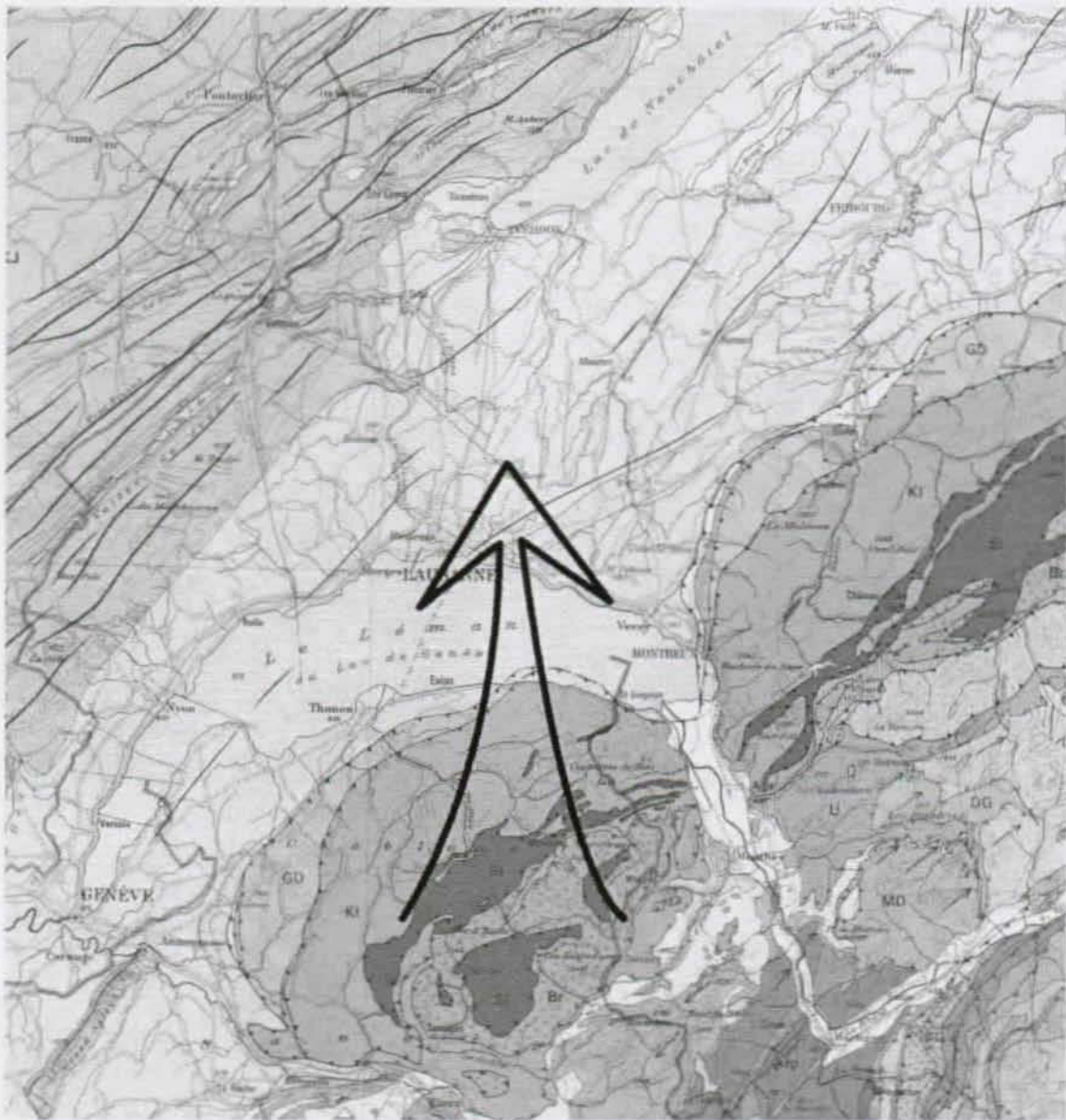


Figure 4-5: Origin of diagnostic heavy minerals such as hornblende, serpentine and pumpellyite occurring in the Burdigalian sandstone in western Switzerland (after Allen, 1985).

4. 2. 3. Hydrogeology

In the Lutry catchment the unsaturated zone includes the upper soil and the decarbonated sandstone layers. Atteia (1992) has shown by lysimeter measurements and hydrologic modelling, that the water fluxes in the soil are generally downwards directed.

The water table is normally situated near the depth of the decarbonation front. During high water periods a temporary rising of the water table has been observed. In a piezometer in the Lutry catchment the water table was situated at a depth of -2.7 m at low water periods, while during high water periods it rose to -1.2 m depth (GEOLEP, 1984). This is consistent with the rusty spots observed in the lower soil levels, resulting from variation in redox state due to a temporary high water table (see table 4-2). During high water periods, and due to the higher permeability of the surface-near decarbonated sandstone compared to the underlying carbonate-bearing bedrock, considerable amounts of groundwater seem to flow through these surface-near layers.

The discharge volume of the Lutry spring is closely connected to precipitation (see figure 4-6). The spring responds to precipitation within days. The main high water period generally occurs in winter, while secondary maxima can occur during the summer months. Snow thaw plays a minor role in the groundwater recharge of this area, because the snow cover is not very persistent at this low altitude. The Lutry spring has an average discharge of 33 L/min (period 1984 to 1994), and attains a maximum discharge of up to 100 L/min. During low water periods, normally in October-November, the discharge can drop as low as 5 L/min.

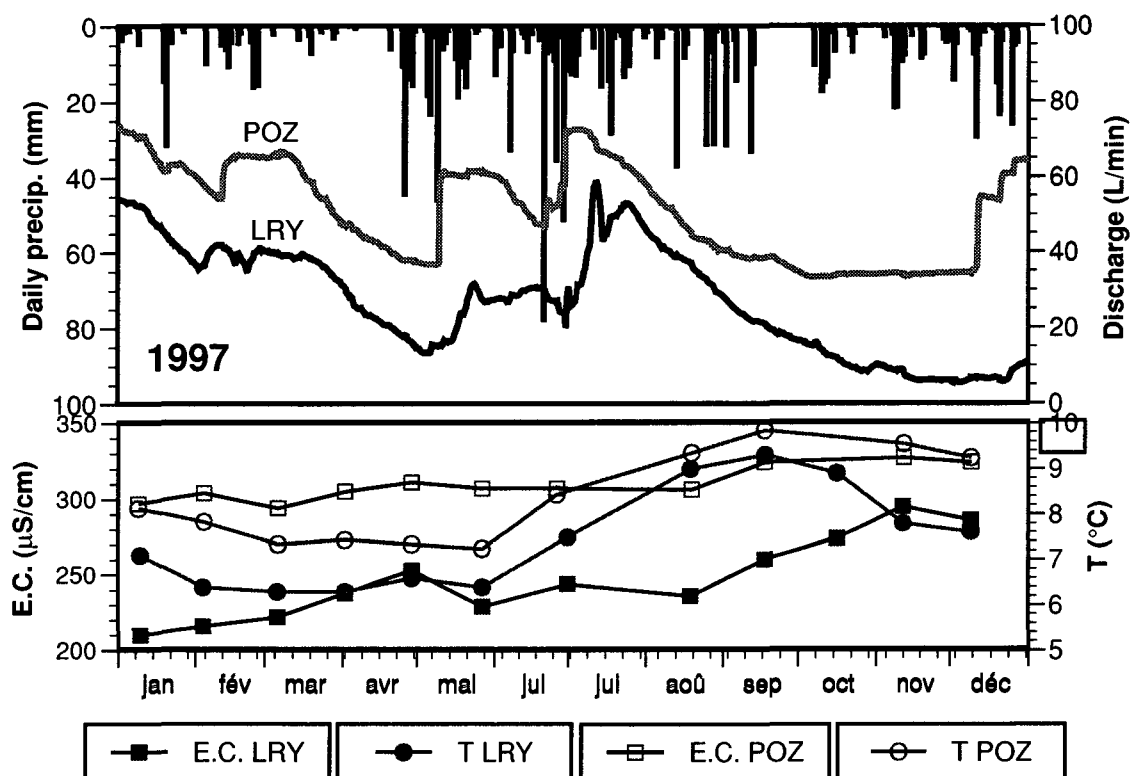


Figure 4-6: Discharge hydrographs of the Lutry (LRY) and Pierre-Ozair (POZ) springs (example 1997), compared to daily precipitation at Villars-Tiercelin (SMA meteorologic station, altitude 850 m), as well as water temperature and electric conductivity (E.C.).

Mean annual precipitation at the studied site is 1401 mm (SMA meteorologic station of Villars-Tiercelin, average of the years 1984 to 1997). In the Lutry catchment, the evapotranspiration calculated from median Cl concentrations in throughfall solutions under the forest canopy (0.98 mg Cl/L) and in groundwater (1.72 mg Cl/L) totals 43%. Following from this, approximately 800 mm of the mean annual rainfall infiltrate into the aquifer and 600 mm are lost by evapotranspiration. The surface of the Lutry catchment deduced from this calculated *effective precipitation* and the mean discharge of the Lutry spring is 2.17 ha. Considering analytical uncertainties and the rough assumptions made for this estimation, this corresponds well with the catchment surface of 2.5 ha estimated from topography.

The seasonal variation of discharge is usually accompanied by a small opposite variation in groundwater mineralisation. In the Lutry spring the electric conductivity ranges from 200 to 250 $\mu\text{S/cm}$. The lowest electric conductivity values have been measured during high water periods, while during low water periods, the electric conductivity can rise as high as 362 $\mu\text{S/cm}$. The highest value has been measured during the extreme low water period in 1989, after six and a half months of drought. Water temperature of the Lutry spring ranges from a minimum of 5 to 6°C in February-March to a maximum of 9 to 10°C usually in September.

The Pierre-Ozaire spring shows a similar behaviour as the Lutry spring. Its discharge volume is well correlated with precipitation (see figure 4-6) and responds within hours. Average discharge (60 L/min, measuring period 1984 to 1994) and peak discharge (up to 200 L/min) are roughly the double of the Lutry spring. During low water periods in autumn, the discharge can drop as low as 5 L/min as well. The higher discharge of the Pierre-Ozaire spring, in spite of its similar estimated catchment size, may be related to the lower evapotranspiration of grass compared to forest vegetation.

The springwater of the Pierre-Ozaire spring is slightly more mineralised than of the Lutry spring. The electric conductivity varies between 248 and 332 $\mu\text{S/cm}$ (average 290 $\mu\text{S/cm}$). The water temperature at the Pierre-Ozaire spring is about 1°C higher than at the Lutry spring. This is probably related to the absence of shading by forest and the resulting higher soil temperature.

The relatively constant groundwater mineralisation occurring despite the fast response of the springs to precipitation is consistent with an average residence time of the groundwater of 3 to 4 years calculated from tritium data of the Lutry spring (Etcheverry & Parriaux, 1999). Based on the results of a simple reservoir-type mathematic model (a homogeneous reservoir with a lower saturated zone and an upper unsaturated zone) Atteia (1992) has suggested that fast vertical water transfer occurs in the unsaturated zone and slow groundwater flow in the saturated zone. As an approximation, this simplified model is valid. The small variation in water mineralisation opposite to the variation of discharge indicates, that during high water periods faster water flow in the surface-near decarbonated sandstone and along preferential flow path in fissures and open stratification joints becomes more important.

The marked seasonal variation of the water temperature, and the small shift of the water temperature relative to air temperature are indicators for the shallowness of groundwater flow near the spring.

4. 3. Weathering of the Burdigalian sandstone

4. 3. 1. Mineralogy

The Burdigalian sandstone is composed of 30 to 40% quartz, 5 to 15% K-feldspar, 10 to 25% plagioclase, 5 to 30% calcite, less than 3% dolomite and 15 to 30% sheet silicates. The relative amounts of these detrital minerals vary depending on the amount of diagenetic carbonate cement. The sheet silicates consist mainly of clay minerals and glauconite, as well as small amounts of biotite and white mica (see figure 4-7). Heavy minerals including epidote, apatite, pyroxenes, amphiboles, spinels (magnetite and chromite), and minor amounts of sphene, zircon, and rutile and a serpentine-type mineral have also been observed. Clay minerals include montmorillonite, illite, and chlorite. No significant kaolinite has been identified in any sample. The clay mineral composition of the reduced sandstone is similar to that found in the marl layers, i.e. montmorillonite, illite and chlorite are present at a ratio of about 1:1:1, while in the oxidised sandstone montmorillonite is more

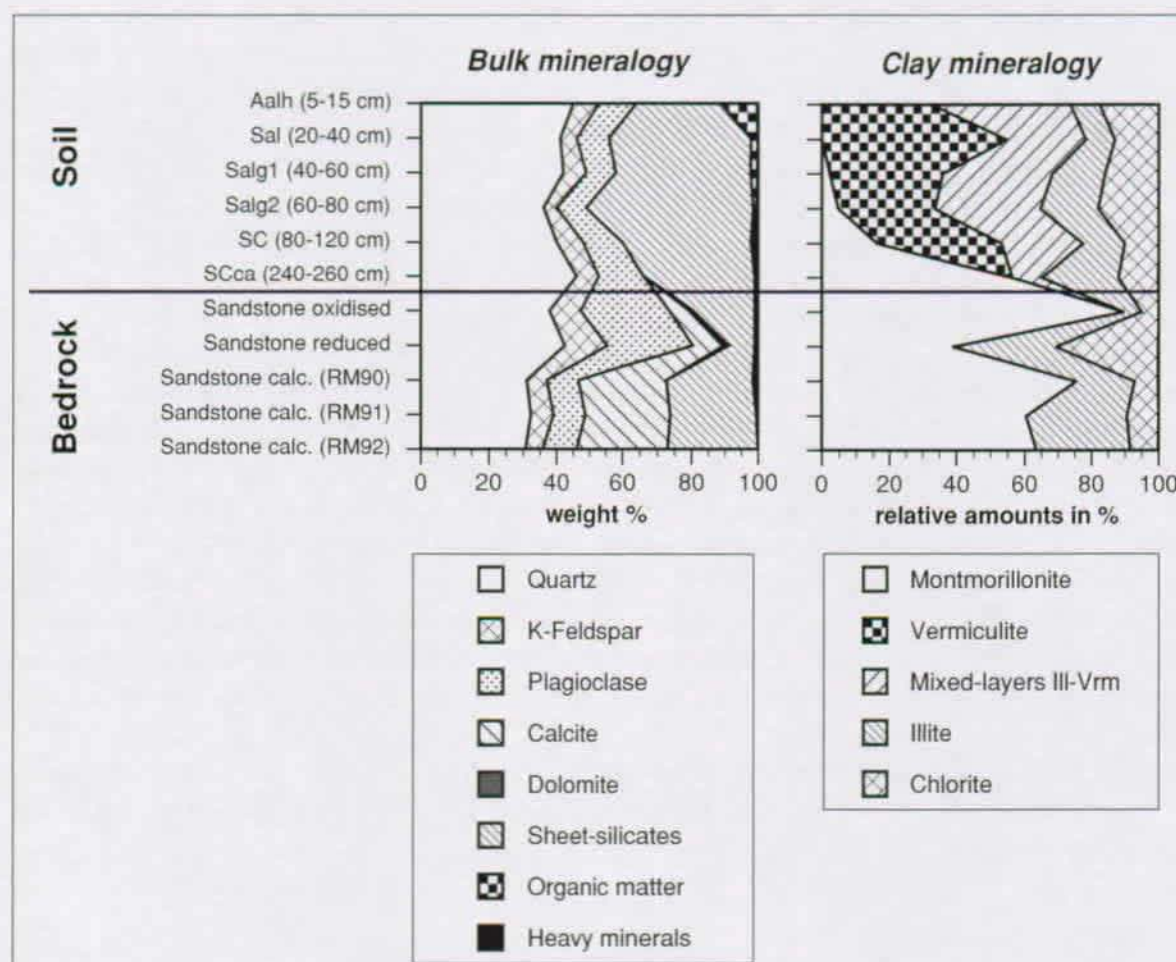


Figure 4-7: Relative amounts of main and clay minerals in a depth profile through the soil and in different varieties of the bedrock sandstone. Mineralogic data of soil (abbreviations see table 4-2) and the bedrock samples RM90 to RM92 are from Dalla Piazza, 1996.

abundant. This rock composition is comparable to that of other OMM sandstone samples in western Switzerland (Pancella, 1995). Thin section microscopy has shown that the mafic mineral grains in the sandstone are chloritised and feldspars are internally altered to clay minerals. Clay minerals are present together with carbonates in an intricate mixture forming the rock matrix. In the oxidised sandstone Fe-hydroxides coat the detrital mineral grains.

The bulk mineralogy of the soil closely reflects the parent material (i.e. the Burdigalian sandstone), except for the carbonates, which have been dissolved in the soil (see figure 4-7). Quartz, K-feldspar and plagioclase are present in similar proportions in the soil as in the bedrock sandstone underneath. In contrast to this, the clay mineralogy of the soil is significantly different from the bedrock. It is characterised by the appearance of important amounts of vermiculite and illite-vermiculite mixed-layered clay minerals in the upper soil layers, while montmorillonite is declining from the deeper soil to the top. The serpentine-type mineral vanishes in the upper soil levels (Dalla-Piazza, 1996), while chlorite and white mica persist. In addition to the mineralogic differences between the soil and the bedrock sandstone, there is a relative enrichment of the fine fraction in the soil (15 to 47% of fraction <50 µm in the soil, compared to 5 to 20% of fraction <50 µm in the sandstone), which is supposed to be the result of mainly physical fragmentation (Dalla Piazza, 1996).

The evolution of the mineralogic composition from the unaltered bedrock sandstone to the upper soil (figure 4-7) reflects the alteration processes in the watershed induced by infiltrating rain water. In the following, detrital and diagenetic minerals are termed "primary" minerals, and minerals, which formed due to the alteration of the sandstone by the infiltrating rain water are termed "secondary" minerals.

SEM back scattered electron images of different detrital mineral grains separated from the soil and the bedrock sandstone show corroded surfaces (figure 4-8 to figure 4-15). The photographs show that all major minerals are corroded, particularly the mafic minerals. Plagioclase is generally more altered than K-feldspar and biotite is more altered than white mica. This is consistent with the stability of these minerals in soil environments and the different weathering kinetics of these minerals (see table 1-2 on page 11).

The differences between the bedrock sandstone and the soil include mainly the type of sheet-silicates and their proportions (see figure 4-7). The most conspicuous changes are the disappearance of montmorillonite and the simultaneous appearance of important amounts of vermiculite and illite-vermiculite mixed-layered clay minerals in the soil. Further, in the grain size fraction >100 µm, biotite and associated chlorite decrease strongly and the serpentine-type mineral disappears towards the upper soil levels (Dalla Piazza, 1996). From these mineralogical changes Dalla Piazza (1996) has identified the following mineral alteration processes occurring in the soil:

- Montmorillonite is transformed to vermiculite. In addition, vermiculite can also be a product of the alteration of chlorite, glauconite, pyroxenes and amphiboles (Deer and others, 1992).
- Biotite is altered to illite-vermiculite mixed-layered clay minerals.
- The serpentine-type mineral dissolves in the upper soil layers.

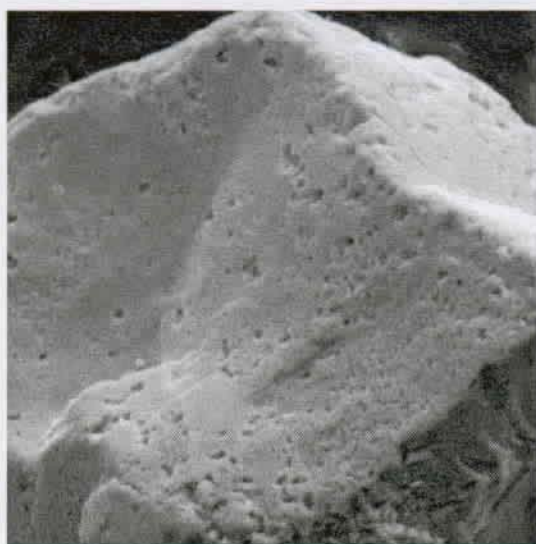


Figure 4-8: Corroded chromite grain (picture width 87 μm .)

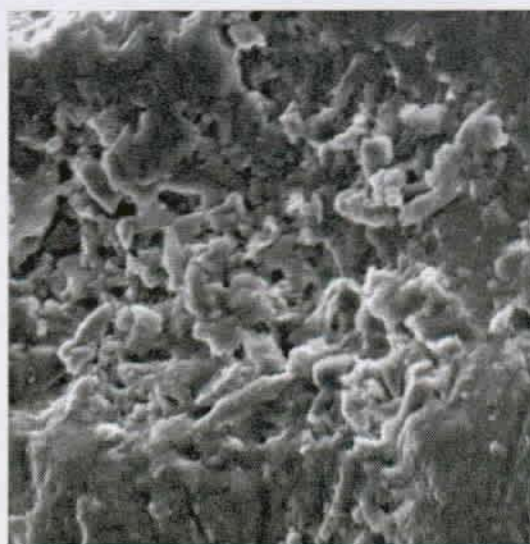


Figure 4-9: Strongly corroded Cr-bearing pyroxene grain (picture width 43 μm .)

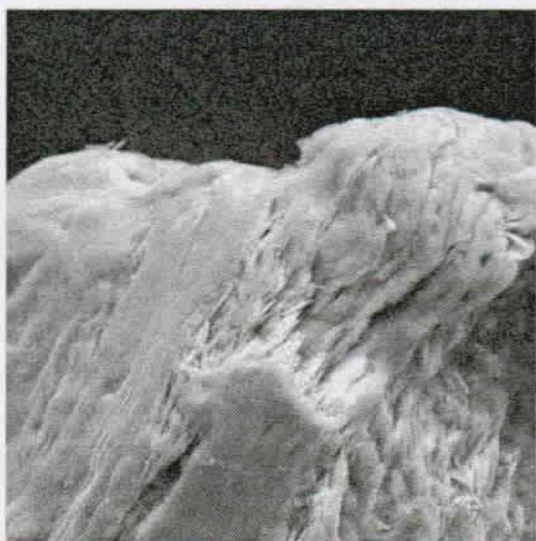


Figure 4-10: Exfoliated and chloritised biotite flake (picture width 87 μm .)

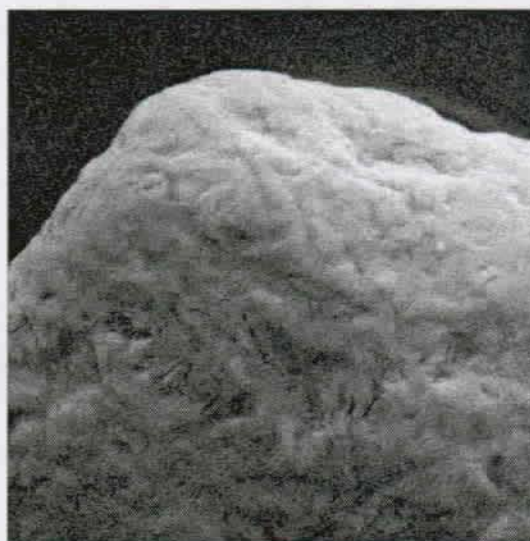


Figure 4-11: Typical aggregate of weathered glauconite (picture width 87 μm .)

The most prominent mineralogical changes induced by weathering of the sandstone can be derived from the comparison of the oxidised, yellow sandstone and the reduced, bluish sandstone. These weathering processes include:

- The oxidised sandstone contains secondary Fe-hydroxides, which lead to its characteristic yellowish colour. The Fe-hydroxides form from the *alteration of Fe-bearing minerals* such as spinels, pyroxenes, glauconite, and biotite. These Fe-bearing minerals contain mainly Fe^{II} , which is oxidised to Fe^{III} during the alteration process and precipitates as Fe-hydroxide coatings on the grain surfaces.

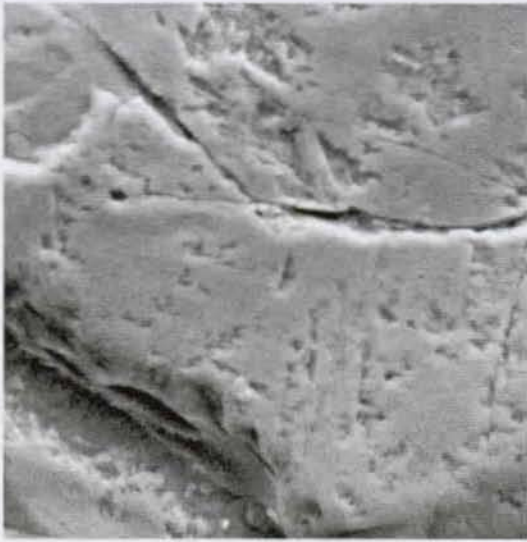


Figure 4-12: Corroded quartz grain (picture width 87 μm).

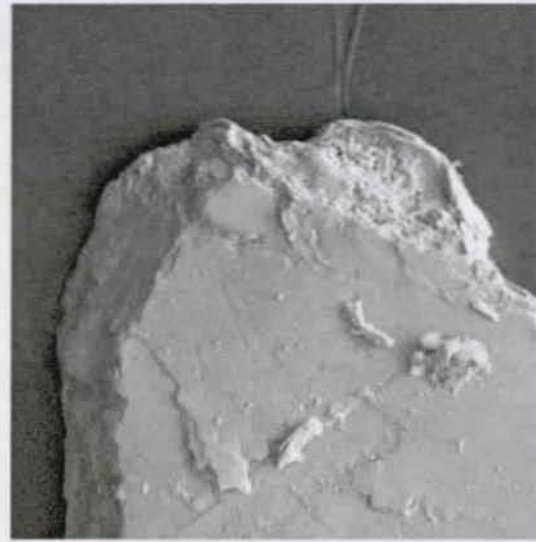


Figure 4-13: Relatively fresh muscovite grain (picture width 580 μm).

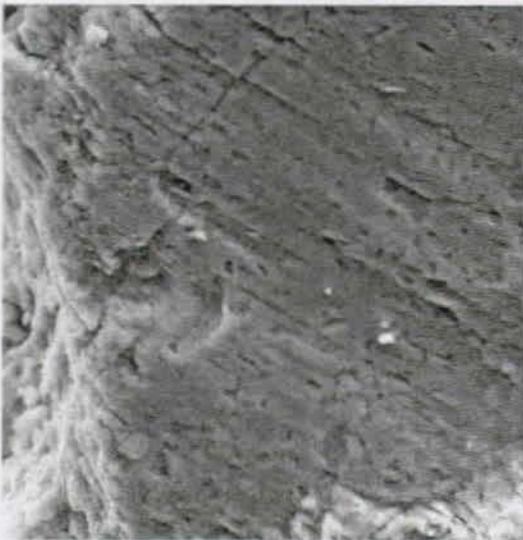


Figure 4-14: Corroded plagioclase grain (picture width 87 μm).

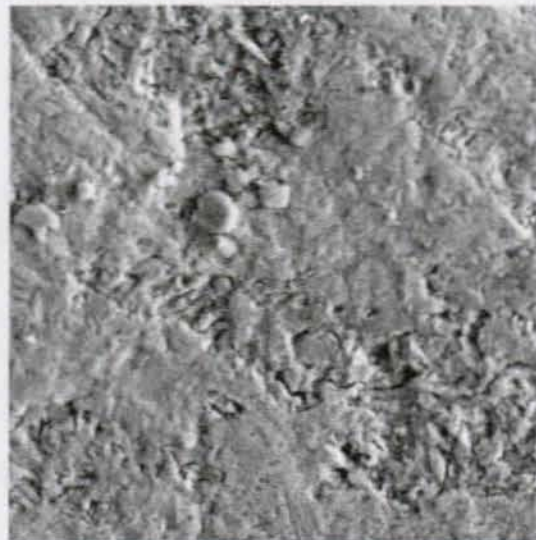


Figure 4-15: Slightly corroded K-feldspar grain (picture width 87 μm).

- The oxidised sandstone contains a smaller amount of carbonates (7%) than the reduced sandstone (11%). In western Switzerland, OMM sandstone can contain up to 30% carbonates (Pancella, 1995; Dalla Piazza, 1996). This indicates a *partial decarbonation*, particularly of the oxidised sandstone in the surface-near zones.
- The oxidised sandstone contains a higher portion of montmorillonite than the reduced sandstone (90% compared to 40% of total clay minerals, see figure 4-7). The greater portion of montmorillonite in the oxidised sandstone is due to the presence of secondary montmorillonite. Montmorillonite typically forms by the slow alteration of Al-silicate minerals such as biotite, amphiboles and feldspars, and other clay minerals such as chlorite and illite.

4.3.2. Geochemistry

The evolution of the chemical composition along a synthetic depth profile through the soil and bedrock sandstone is illustrated in figures 4-16 and 4-17 and data are listed in appendix F.

The strong decrease of Ca and loss on ignition (LOI) in the soil reflects the decarbonation of the parent material. The remaining LOI of the soil belongs mainly to the presence of abundant clay minerals. Strontium shows a similar evolution as Ca and LOI, indicating that this element is associated mainly with carbonate minerals (see figure 4-17).

The major element chemistry within the bedrock sandstone shows only small variations as a function of variations in grain-size and depth. The intercalated marl layers are enriched in Al, Fe, K and Mg compared to the sandstone. These elements are major elements in the present clay minerals chlorite, illite and montmorillonite, which explains their enrichment in marl.

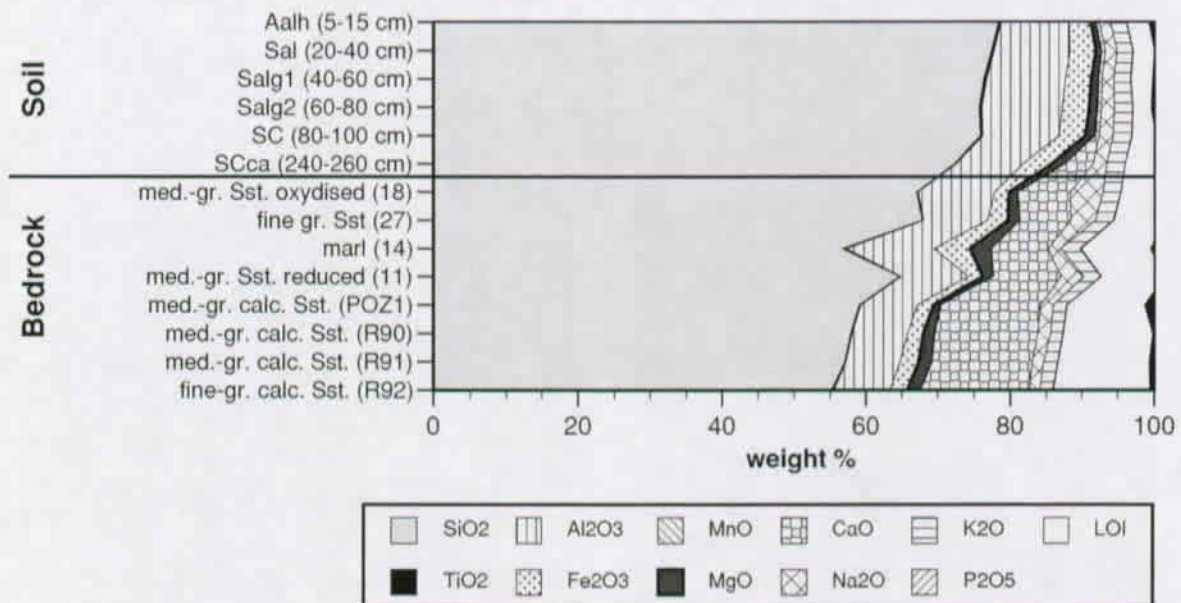


Figure 4-16: Major element composition along a compiled depth profile through the soil and bedrock sandstone. Chemical data from the soil and partly from the bedrock are from Dalla Piazza (1996) and Hesske (1995).

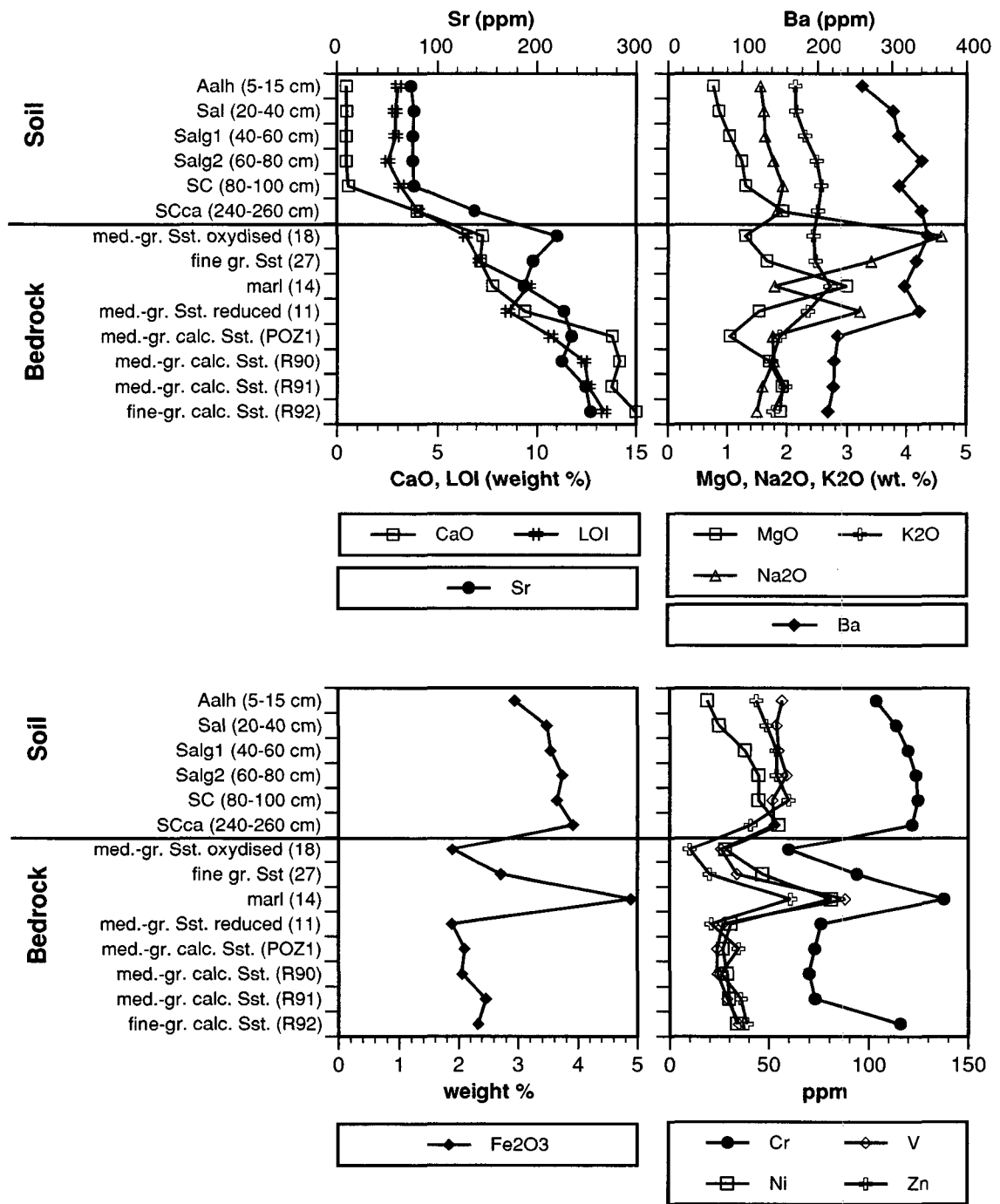


Figure 4-17: Major and trace element composition along a compiled depth profile through the soil and bedrock sandstone. Chemical data from the soil and partly from the bedrock are from Dalla Piazza (1996) and Hesse (1995).

Compared to other sandstones - the worldwide average Cr-content in sandstones is 27 ppm (Nriagu & Nieboer, 1988) - the Burdigalian sandstone occurring at the study site contains relatively high concentrations of Cr ranging from 60 to 138 ppm.

The Cr content is correlated with the total Fe content, as well as with Ni, V, and Zn throughout the profile from bedrock sandstone to soil. Chromium is enriched in marl layers, together with Fe, Ni, Zn, V, Ti, and Zr (see figure 4-17). This enrichment can be due to a primary, sedimentary enrichment of the marl and to a secondary enrichment resulting from alteration processes:

1.) Primary sedimentary enrichment:

- The enrichment can be related to the **abundance of clay minerals**. Certain trace metals can substitute for major elements in the structure of clay minerals, particularly in chlorite and montmorillonite. This is consistent with the observed elevated Cr, Ni, Zn and V concentrations in separated fine fractions (0 to 2 μm , 2 to 5 μm , 5 to 20 μm) of the soil and bedrock material (Dalla Piazza, 1996).
- The marl layers can be enriched in **heavy minerals**. Particularly the elevated Ti and Zr values point to an enrichment in heavy minerals, as these elements occur essentially in ilmenite, rutile and zircon. These heavy minerals are among the most insoluble minerals occurring in the OMM sandstone. Furthermore, it has been shown that the Cr, V, Ni, and Zn concentrations are 10 to 100 times higher in the heavy mineral fraction than in the bulk sand of the same grain-size (Dalla Piazza, 1996). This further indicates a heavy mineral enrichment of the marl layers.

2.) Secondary enrichment resulting from alteration processes:

- The metal enrichment can be due to the thin **Fe- and Mn-hydroxide film**, which often covers the top of marl layers (see chapter 4. 2. 2. "Geological background" on page 136). Dissolved metals can co-precipitate together with Fe-hydroxides.
- The metal enrichment can be due to **adsorption** of metal ions onto clay minerals and Fe-hydroxides. These materials have a much larger surface than the sand grains in the coarser layers and are therefore much more efficient in adsorbing metal ions.

The apparent enrichment of Cr, Fe, V, Ni and Zn in the soil compared to the bedrock sandstone results from the concentration of these elements in the decarbonated residue during the early stage of alteration, i.e. during carbonate dissolution. However, Dalla Piazza (1996) has shown by recalculating the total element amounts for the carbonate free portion of the bedrock sandstone, that these elements are increasingly *depleted* towards the upper soil levels. The same is also true for major elements including K, Na, Mg, Si, and Al, as well as for Ba. This indicates progressive leaching of the decarbonated silicate and (hydr-)oxide residue of the upper soil levels by the infiltrating rainwater.

4. 4. Chromium in the Burdigalian sandstone

The Burdigalian sandstone at the study site in western Switzerland contains 2 to 5 times higher Cr concentrations than the world wide average of 27 ppm (Nriagu & Nieboer, 1988). The origin of the detrital material from the ophiolite rocks occurring in the Prealpine Gêts nappe explains the relatively elevated Cr-content in this sandstone (see page 138). It appears that the geogenic tracer Cr persists from the igneous source rock (ophiolites of the Gêts nappe) to the detrital sediment equivalent (Burdigalian sandstone) through inherited heavy minerals and is finally found in elevated concentrations in the groundwater evolving in this sandstone.

In order to find out which minerals are relevant in the processes controlling the dissolved Cr-content in the groundwater, the potential to be a Cr-source or Cr-sink of the minerals constituting the OMM sandstone and soil have been compared (see table 4-3). In particular, the Cr-content, the relative abundance, the solubility, and the reactivity of primary and secondary minerals occurring in the Burdigalian sandstone and in the soil have been compared. The Cr-contents of the minerals have been derived partly from micro-probe analyses of samples from the study site (Dalla Piazza, 1996) and partly from literature. In all of the discussed minerals Cr is present in its trivalent form.

4. 4. 1. Primary Cr-minerals

The primary minerals with the highest Cr-concentrations are contained in the heavy mineral fraction. In particular there are **chromite** ($\text{Fe}^{\text{II}}\text{Cr}^{\text{III}}_2\text{O}_4$), **Cr-bearing magnetite** ($\text{Fe}^{\text{II}}(\text{Fe}^{\text{III}},\text{Cr}^{\text{III}})_2\text{O}_4$), and **Cr-bearing pyroxenes**. SEM images of these minerals show etched surfaces, which prove their chemical corrosion (figure 4-8 and figure 4-9). Although these heavy minerals are present in relatively small quantities (<1%), their alteration may release significant amounts of Cr into solution, because of their high Cr-content of 44 wt.% Cr_2O_3 in spinel and up to 0.27 wt.% Cr_2O_3 in pyroxene. The fact that chromite is still found in the upper soil levels is due to its resistance against weathering. Coating with hydroxide phases may considerably slow the chemical weathering of such Fe-rich minerals.

Glaucanite is more abundant than spinel and pyroxenes (estimated amount 5 to 10% in the sand-sized fraction), but contains only small amounts of Cr of around 0.043 wt.% Cr_2O_3 . **Biotite** and **amphibole** contain similarly small amounts of Cr as glaucanite (an average of 0.032 wt.% Cr_2O_3 has been measured in biotite) but occur only in very small amounts. Like spinel and pyroxenes, glaucanite, biotite, and amphiboles have slow dissolution kinetics. In the soil biotite and glaucanite are altered to vermiculite and in the bedrock they are probably altered to montmorillonite. The alteration of biotite and glaucanite is not likely to liberate significant amounts of Cr, because vermiculite and montmorillonite can absorb some Cr. Microprobe analyses of biotite and glaucanite from the soil indicate that the Cr content in these minerals is conserved or even increases during alteration (Dalla Piazza, 1996).

The Cr-content in **chlorite** has not been analysed, but chlorites may contain small amounts of Cr in octahedral sites. Chlorite is present in important amounts throughout the profile. Although no decrease of the amount of chlorite towards the surface can be discerned from sedimentary variation, Dalla Piazza (1996) has suggested that the chlorite in the smallest grain-size fraction (<2 μm) of the soil loses Fe and probably other substituting metals such as Ni, Mn and Cr. Chlorite usually undergoes a slow alteration to montmorillonite or to vermiculite. Because these secondary minerals can accommodate

small amounts of Cr in their structure, the alteration of chlorite is not likely to release important amounts of Cr.

The Cr-content in **serpentine** has not been analysed, but literature data indicate that minerals of the serpentine group can only contain small amounts of substituting metals due to misfits in the structure. Therefore, Fe, Cr, and other metals contained in the original olivine or pyroxene are generally accommodated in associated magnetite or Fe-hydroxides and only very small amounts of these elements enter the structure of serpentine. A maximum of 0.020 wt.% Cr₂O₃ has been reported (Deer and others, 1992). This and the relatively small amount of serpentine in the total rock lead to the conclusion that serpentine is probably not an important Cr-source.

White mica, epidote, ilmenite and rutile may contain trace amounts of Cr in their structure. However, these minerals are very resistant against weathering and therefore no relevant Cr-sources.

Dalla Piazza (1996) has shown that the **clay fraction** (<2 µm) of the uppermost soil levels have significantly lower amounts of Cr, Ni, Al, Mn, Fe, Si, Ca, Na and K than the clay fraction in deeper parts of the soil. In this small grain-size fraction of the soil probably a mixture of inherited clay minerals from the underlying sandstone and secondary clay minerals formed during soil formation are present. In the uppermost soil this fine-grained material is leached more intensively than the coarser sand grains, because the small grain-size enhances the reaction with infiltrating water. At a total amount of about 15% in the soil material, the most fine-grained fraction of the soil may have a significant influence on the mineralisation of the groundwater and possibly on the dissolved Cr content.

4. 4. 2. Secondary Cr-minerals

Fe-hydroxides such as amorphous to crystalline ferrihydrite (Fe(OH)₃), goethite (FeOOH), or limonite (FeOOH·nH₂O) are ubiquitous in the soil and in the oxidised parts of the Burdigalian sandstone. Ferrihydrite forms solid-solutions with Cr-hydroxide (Cr(OH)₃) and the concentration of dissolved Cr^{III} has been shown to be limited by the solubility of amorphous Cr_xFe_{x-1}(OH)₃ solid-solutions (Amonette & Rai, 1990). In addition, hydroxide minerals, particularly amorphous hydroxides have very large surfaces. They are therefore powerful sorbing materials. Goethite has a pH_{PZNPC} of 7.3 and ferrihydrite of 8.5 (see table 1-4 on page 14). If the pH of the solution is higher than the pH_{PZNPC} the surfaces are negatively charged and the Fe-hydroxides have a capacity for cation adsorption chapter "Sorptions" on page 12. If the pH of the solution is lower than the pH_{PZNPC}, as it is the case in the soil, anion adsorption can occur.

Clay minerals are the second potential Cr sink. Particularly *vermiculite* and *montmorillonite*, which are the most abundant clay minerals in the soil and in the oxidised sandstone, respectively, can take up some Cr in their structure (Deer and others, 1992). In addition, these minerals have a very large surface. Montmorillonite has a pH_{PZNPC} <2.5, indicating that this mineral can act as a powerful cation sorbing substratum. This is consistent with the observed enrichment of Cr in the marl layers and in the soil.

Dalla Piazza (1996) has shown by sequential leaching of soil material, that in the soil less than 10% of the total Cr is located on mineral surfaces (adsorbed on clay minerals or on Fe-hydroxides or Mn-oxides), in interlayer sites of clay minerals, or associated with organic matter. The remaining 90% of the Cr appear to be fixed in the structure of the soil minerals.

Components	Origin and description	Abundance wt. %	Cr-content wt. % Cr ₂ O ₃
Quartz	detrital	30-40	-
K-feldspar	detrital orthoclase and microcline	6-16	-
Plagioclase	detrital albite and more An-rich plagioclase in variable alteration states	10-25	-
Calcite	detrital calcite grains and carbonate lithoclasts; sparry diagenetic calcite	6-25	-
Dolomite	diagenetic cement	0-3	-
Spinels	detrital magnetite and chromite	accessory	up to 44 ^b
Pyroxenes	strongly altered detrital relics	accessory	up to 0.27 ^a
Glauconite	detrital grains (sand sized rounded dark green pellets) and diagenetic glauconite replacing other minerals or as void fillings	3-8%	0.043 ^a
Biotite, amphiboles	detrital biotite and amphibole grains showing chloritisation along cleavage planes	accessory	0.032 ^b
White mica	detrital flakes, concentrated in layers	accessory	0.024 ^a
Serpentine	detrital heavy mineral and clay mineral fraction	<1	up to 0.020 ^b
Ilmenite, rutile, epidote	detrital heavy minerals	accessory	traces ^b
Zircon, apatite, sphene	detrital heavy minerals	accessory	-
Illite	clay mineral fraction (detrital, diagenetic, and in the soil possibly authigenic)	1-5	-
Chlorite	clay mineral fraction (detrital, diagenetic, and in the soil possibly authigenic)	<1-4	traces ^b
Montmorillonite	clay mineral fraction (detrital and/or diagenetic and in the oxidised sandstone possibly authigenic)	<25	traces
Vermiculite	clay mineral fraction of the soil (authigenic)	<10	traces
Fe- and Mn-hydroxides	weathering products commonly associated with ferro-magnesian minerals (Bt, Grt, Hem, Glt, Ep, Chl), as coating on mineral grains and as thin films on top of clay layers. Cr _x Fe _{x-1} (OH) ₃ solid-solutions	accessory	several%
Coal	carbonised driftwood and leaves, with a surrounding red halo of Fe-hydroxide impregnation and some pyrite	accessory	
Pyrite	diagenetic, mainly associated with coal	accessory	-

Table 4-3: Primary (detrital and diagenetic) and secondary minerals (authigenic weathering products formed due to the alteration of the sandstone by the infiltrating rain water) constituting the OMM sandstone and soil at the study site and their properties as potential Cr-sources or Cr-sinks.

- a. Deer and others, 1992. Value for Mg-chlorite in ultramafic rocks
b. mean value of micro-probe analyses (Dalla Piazza, 1996)

4.4.3. Summary

The Cr-sources identified in the aquifer sandstone include glauconite and chlorite, and accessory spinel, pyroxene, serpentine, biotite, and amphibole. All of these minerals are unstable and tend to be dissolved, as shown by their corroded surfaces. From a mass balance point of view, the smallest amount of a chromium mineral to be dissolved to reach the Cr-content observed in the groundwater (4.5 µg Cr/L) would be chromite (15 µg/L). In contrast, much larger amounts of Cr-rich pyroxene (2'436 µg/L) or biotite (20'553 µg/L) would be required to dissolve. Slow alteration of chromite and to a lesser degree pyroxene therefore appear to be the most important Cr-releasing processes in the studied sandstone aquifer.

During the alteration of these mafic minerals, however, a large part of the Cr is retained in secondary Fe- and Mn-hydroxide coatings on the grain surfaces and clay minerals.

4. 5. Hydrochemistry

4. 5. 1. Water compositions

Chemical data are available for the springwaters of the Lutry and Pierre-Ozaire sites (table 4-5). The time series for the Lutry and Pierre-Ozaire springwaters covering 19 years are illustrated in figures 4-19 to 4-22. In addition, chemical data of rain water, throughfall solutions under the forest canopy, and soil solutions (Atteia, 1992; table 4-4) are available for the Lutry site.

Rainwater and throughfall solution

The rainwater at the Lutry site is a very dilute, acid solution with a median total mineralisation of 6.6 mg/L and a pH of 4.7 (see table 4-4). Major dissolved anions are NO_3^- , SO_4^{2-} and Cl^- . On the cation side Ca^{2+} , NH_4^+ , and Na^+ dominate, besides minor amounts of Mg^{2+} and K^+ . Atteia (1992) divided the chemical elements present in rainwater into three groups, summarising their different sources as follows:

- marine origin: Na, Cl, and Mg
- terrestrial origin (dust): Ca, Sr, Ba, K, Rb, Si, Ni, Cr, and Fe
- anthropogenic origin: S, N (NO_3^- and NH_4^+), Cl, Cu, Zn, Pb, B, V, and Mn

Compared to the atmospheric pollution recorded for several sites in Sweden and Germany, in the Lutry catchment the anthropogenic input of metals including V, Cr, Mn, Ni, Cu, Zn and Pb via rain is rather low. Atteia (1992) has further shown, that despite the low altitude and proximity to the city of Lausanne, there is no significant difference in the annual element fluxes via precipitation between the Lutry catchment and catchments located in more remote mountain areas in Switzerland. Despite of the low anthropogenic pollution level, dissolved compounds such as NH_4^+ , NO_3^- , SO_4^{2-} and Cl^- , as well as Cu, Zn, Pb, V, and Mn in the rainwater and throughfall sampled at the Lutry site have a largely anthropogenic origin (Atteia, 1992).

The throughfall solution has a higher total mineralisation than rainwater (median value 16.5 mg TDS/L) and a similarly low pH of 4.5. During its passage through the forest canopy the throughfall solution becomes enriched with most elements, particularly with K, N (NO_3^- and NH_4^+), Rb, Mn, Cu, V, and Pb, due to evaporation on the vegetation surface (interception), dissolution of dry deposition, and selective uptake or release of elements by the vegetation. An estimated interception by the forest canopy of 25% (Atteia, 1992) results in an increase of element concentrations of 33%. However, this is still less than the observed enrichment, indicating that the higher total mineralisation of the throughfall solution must be a result mainly of the dissolution of dry deposition. This is consistent with the fact that compared to deciduous trees or grass, conifer trees have a large surface leading to important dry deposition (Appelo & Postma, 1996).

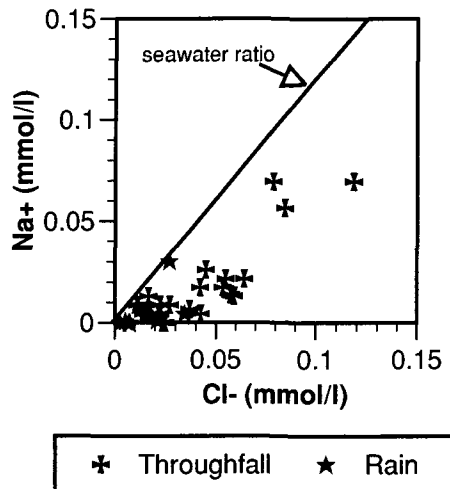


Figure 4-18: Comparison of the Na^+/Cl^- ratios in the precipitation at the Lutry site with the ratio of sea water.

A close look at the data has revealed, that the rainwater and throughfall are enriched in Cl^- relative to Na^+ (see figure 4-18). This indicates that an additional source of Cl^- besides marine aerosols must exist, contrary to the suggestion of Atteia (1992). In industrialised areas possible Cl^- sources are the burning of waste plastics or coal, which produces HCl . The calculation of the marine part of Cl^- by assuming an exclusively marine origin of Na^+ shows that 40 to 80% of the Cl^- must have a non-marine origin. This is also consistent with the values observed by the BUWAL (1999) and with the findings of Zobrist & Stumm (1979), who estimated that over 50% of the Cl^- in Swiss rainwater has a non-marine origin.

Soil solutions

The soil solutions sampled in the forest soil of the Lutry catchment at 30 cm and 80 cm depth are characterised by slightly higher total mineralisations than the throughfall solution (TDS 19.3 mg/L and 25.6 mg/L, respectively) and a higher pH of around 6.0. The major anions are dominated by SO_4^{2-} , and HCO_3^- , and to a lesser extent by NO_3^- and Cl^- , and the major cations are dominated by Ca^{2+} , and Mg^{2+} and minor amounts of Na^+ .

The soil solutions show an important increase of Mg, Ca, Sr, Na, Mn, Al, and Si compared to rainwater and throughfall solution. These major elements are accompanied by increased amounts of trace elements including V, Fe, Ni, Zn, and Ba. In contrary, K, Rb, Pb and partly NO_3^- , B, and Cu from atmospheric sources are retained in the soil and their concentrations are lower in the soil solutions than in the throughfall solution (see figure 4-24).

		Rainwater				Throughfall				Soil solution -30 cm				Soil solution -80 cm			
		Med	Min	Max	n	Med	Min	Max	n	Med	Min	Max	n	Med	Min	Max	n
pH	pH-units	4.7	3.7	6.5	9	4.5	3.5	5.5	13	6.2	4.7	7.2	12	6.0	4.1	7.1	15
TDS	mg/L	6.6	1.4	24.5	11	16.5	3.1	62.6	30	19.3	9.3	35.8	16	25.6	10.0	43.3	19
Cl ⁻	mg/L	0.3	n.d.	1.2	10	1.0	n.d.	4.2	29	1.3	n.d.	3.2	10	1.0	n.d.	3.2	16
NO ₃ ⁻	mg/L	2.2	n.d.	9.7	10	6.1	1.3	23.0	29	n.d.	n.d.	1.8	10	n.d.	n.d.	7.3	16
SO ₄ ²⁻	mg/L	2.1	n.d.	5.1	10	5.2	1.4	21.6	29	7.5	1.8	8.5	5	7.9	n.d.	11.1	15
Ca ²⁺	mg/L	0.7	0.2	3.7	11	1.4	0.4	8.1	30	2.1	1.3	5.0	16	3.0	1.6	7.1	19
Mg ²⁺	mg/L	n.d.	n.d.	0.2	11	n.d.	n.d.	1.0	30	1.6	1.2	3.6	16	1.3	0.9	1.9	19
Sr ²⁺	mg/L	0.002	0.001	0.009	11	0.005	0.001	0.012	16	0.011	0.008	0.012	10	0.014	0.011	0.028	13
Na ⁺	mg/L	n.d.	n.d.	0.7	9	0.2	n.d.	1.6	28	0.9	0.2	1.6	15	1.0	0.6	1.6	18
K ⁺	mg/L	n.d.	n.d.	0.4	11	1.1	n.d.	4.1	30	0.2	n.d.	0.5	16	0.3	n.d.	2.1	19
NH ₄ ⁺	mg/L	1.1	0.4	2.3	5	1.9	0.3	4.4	10	0.3	n.d.	0.4	3	n.d.	n.d.	0.4	6
Si total	mg/L	0.4	n.d.	0.8	11	n.d.	n.d.	0.8	30	5.8	1.0	10.8	16	4.1	0.6	8.6	19
Rb total	µg/L	n.d.	n.d.	1.0	11	6.0	1.0	24.0	30	0.8	n.d.	2.0	16	1.0	n.d.	7.0	19
Ba total	µg/L	2.0	1.0	3.0	11	4.0	1.0	38.0	29	8.0	2.0	16.0	16	26.0	12.0	59.0	19
Al total	µg/L	n.d.	n.d.	n.d.	6	n.d.	n.d.	300	20	70	n.d.	400	15	160	n.d.	8600	18
V total	µg/L	0.3	n.d.	2.0	11	1.0	n.d.	5.0	30	1.0	n.d.	3.0	16	1.0	n.d.	2.0	19
Cr total	µg/L	n.d.	n.d.	0.2	11	n.d.	n.d.	2.0	30	0.2	n.d.	1.0	16	n.d.	n.d.	0.3	19
Mn total	µg/L	9.0	4.2	30.0	11	111.0	21.0	862.0	30	100.5	37.0	316.0	16	184.0	0.3	1142.0	19
Fe total	µg/L	9	n.d.	58	6	12	n.d.	52	19	19	7	42	16	5	n.d.	308	19
Ni total	µg/L	n.d.	n.d.	2.2	11	1.0	n.d.	5.0	30	1.4	n.d.	5.0	16	2.8	1.0	5.0	19
Cu total	µg/L	1.7	0.7	5.9	11	3.3	1.4	15.9	30	3.7	1.8	23.0	10	2.8	0.8	9.0	12
Zn total	µg/L	19.4	4.7	85.9	11	33.0	8.0	138.0	30	62.5	39.0	481.0	16	84.0	44.0	585.0	19
Pb total	µg/L	1.8	0.6	8.0	11	3.8	1.8	16.0	30	0.4	n.d.	2.0	16	n.d.	n.d.	6.4	19
B total	µg/L	4	1	94	11	10	4	22	30	12	5	26	16	12	6	24	19

Table 4-4: Compositions of rain water, throughfall solution, and soil solutions at the Lutry site (Atteia, 1992; n.d. = not detected).

Groundwater

In the Lutry springwater the pH varies between 6.6 and 8.0 and the E_H between 390 and 570 mV (table 4-5). In the Pierre-Ozaire springwater the variation of pH and E_H is similar, ranging from 6.7 and 8.0 and from 360 and 540 mV, respectively.

The groundwaters discharged at the Lutry and Pierre-Ozaire springs have an intermediate total mineralisation, with median values of 227.4 mg TDS/L and 261.9 mg TDS/L, respectively (table 4-5). The Lutry springwater is of the Ca-(Mg)-HCO₃-(SO₄) water type and the Pierre-Ozaire of the Ca-(Mg)-HCO₃-(Cl)-(NO₃) water type.

The most abundant ions in the springwaters from both catchments are Ca²⁺, and HCO₃⁻ together with minor amounts of Mg²⁺, Na⁺, SO₄²⁻, and NO₃⁻ (see table 4-5). The alkaline earth elements Ca²⁺, Mg²⁺, and Sr²⁺ are fairly well correlated among each other and with alkalinity, as well as with the discharge volume of the spring. As pointed out earlier, a higher total mineralisation and thus higher concentrations of these elements occur during low water periods and vice-versa (see figures 4-19 and 4-20). The Pierre-Ozaire springwater generally shows poorer correlations between these dissolved elements than the Lutry spring, but the variation with discharge can also be observed (see figures 4-21 and 4-22).

Compared to the Lutry springwater, the Pierre-Ozaire springwater is characterised by higher NO_3^- , Cl^- , K^+ , and Na^+ concentrations and to a lesser degree higher Mg^{2+} , Sr^{2+} , and Ba^{2+} concentrations. It however shows slightly lower SO_4^{2-} concentrations. The observed differences in groundwater composition can be related to the different settings of the two catchments, i.e. forest in the Lutry catchment and cultivated grass land in the Pierre-Ozaire catchment. In the Lutry springwater the concentrations of Na^+ , K^+ , NO_3^- , and Cl^- are lower and show less variation than in the Pierre-Ozaire springwater. Chloride is typically present in lower concentrations than Na^+ and it is not correlated with Na^+ and K^+ . In the Pierre-Ozaire springwater, on the other hand, Cl^- is present at higher concentrations than Na^+ . This suggests that in the Pierre-Ozaire catchment an input of K^+ , NO_3^- , Cl^- , and Na^+ by fertilisers exists in addition to the atmospheric input and the geogenic sources of K^+ and Na^+ in the aquifer.

The variation with time of the dissolved SO_4^{2-} concentrations shows that in the last years this compound has slightly decreased in the groundwaters at both sites. In Switzerland the SO_4^{2-} concentrations in rainwater have slightly decreased in the last years as well (BUWAL, 1999). Since in the Burdigalian sandstone a small amount of homogeneously distributed pyrite is the only geogenic source of SO_4^{2-} , the decrease of the atmospheric SO_4^{2-} input seems to have an influence on the SO_4^{2-} concentrations in the springwater. The fact that SO_4^{2-} concentrations are higher in the Lutry springwater compared to the Pierre-Ozaire springwater supports this explanation, because dry deposition on the forest canopy is higher than on the grass land and consequently leads to a higher atmospheric input.

		Lutry Groundwater				Pierre-Ozaire Groundwater			
		Med	Min	Max	n	med	Min	Max	n
T	°C	7.8	5.0	9.4	40	8.4	6.2	10.1	38
E.C. at 20°	µS/cm	234	193	362	40	282	215	331	37
pH	pH-units	7.2	6.6	8.0	39	7.3	6.7	8.0	37
E _H	mV	445	387	565	28	451	356	544	27
O ₂ (aq)	mg/L	9.7	7.7	11.8	23	9.2	7.2	10.8	23
TDS	mg/L	226.4	177.5	284.7	38	259.1	188.4	316.5	38
Total Hardness	°F	13.6	10.5	16.7	37	15.1	9.5	17.6	38
Alkalinity as HCO ₃ ⁻	mg/L	145.0	107.0	183.6	38	145.8	102.5	182.8	38
F ⁻	mg/L		n.d.		24		n.d.		28
Cl ⁻	mg/L	1.5	n.d.	3.3	36	11.4	5.8	16.6	38
NO ₃ ⁻	mg/L	6.5	4.5	10.0	38	23.9	9.8	37.5	38
SO ₄ ²⁻	mg/L	13.2	8.2	17.7	38	8.1	4.3	13.7	37
Ca ²⁺	mg/L	44.6	35.2	56.3	38	52.0	35.0	62.5	38
Mg ²⁺	mg/L	4.8	4.1	7.2	38	6.4	3.2	9.1	38
Sr ²⁺	mg/L	0.112	0.064	0.161	38	0.142	0.113	0.193	38
Na ⁺	mg/L	2.1	1.8	3.2	38	3.9	1.7	5.8	38
K ⁺	mg/L	0.3	0.2	0.6	38	1.0	0.2	1.5	38
Si total	mg/L	5.4	4.4	6.4	34	4.9	3.9	5.9	35
Li total	µg/L	1	1	2	38	1	1	2	38
Rb total	µg/L	0.3	0.2	0.4	38	0.3	n.d.	0.6	38
Ba total	µg/L	5.7	3.0	9.6	38	10.9	8.2	14.6	38
Al total	µg/L	6	2	121	38	4	1	120	38
Ti total	µg/L		n.d.			0.2	n.d.	0.3	38
V total	µg/L	0.7	0.5	1.3	38	0.8	0.6	1.3	38
Cr total	µg/L	4.6	2.9	7.1	38	4.0	2.7	6.9	38
Mn total	µg/L	n.d.	n.d.	0.7	36	0.2	n.d.	0.4	38
Fe total	µg/L	4.1	1.9	24.1	37	2.8	1.5	6.8	38
Co total	µg/L		n.d.			n.d.	n.d.	0.2	38
Ni total	µg/L	1.4	0.5	2.5	38	0.4	0.2	2.1	38
Cu total	µg/L	n.d.	n.d.	1.5	37	0.2	n.d.	0.7	38
Zn total	µg/L	1.6	n.d.	3.4	36	1.5	0.3	7.5	38
Mo total	µg/L	n.d.	n.d.	1.6	38	n.d.	n.d.	0.3	38
Cd total	µg/L	n.d.	n.d.	0.3	38	n.d.	n.d.	0.5	37
Pb total	µg/L	n.d.	n.d.	0.3	38	n.d.	n.d.	1.0	38
U total	µg/L	n.d.	n.d.	0.2	38	0.2	n.d.	0.3	38
Br total	µg/L	8	6	11	38	11	6	16	38
I total	µg/L	n.d.	n.d.	6	38	1	n.d.	2	37
B total	µg/L	7	5	17	38	7	5	14	38
As total	µg/L		n.d.			0.4	n.d.	0.7	30

Table 4-5: Chemical compositions of the Lutry and Pierre-Ozaire springwaters (n.d. = not detected).

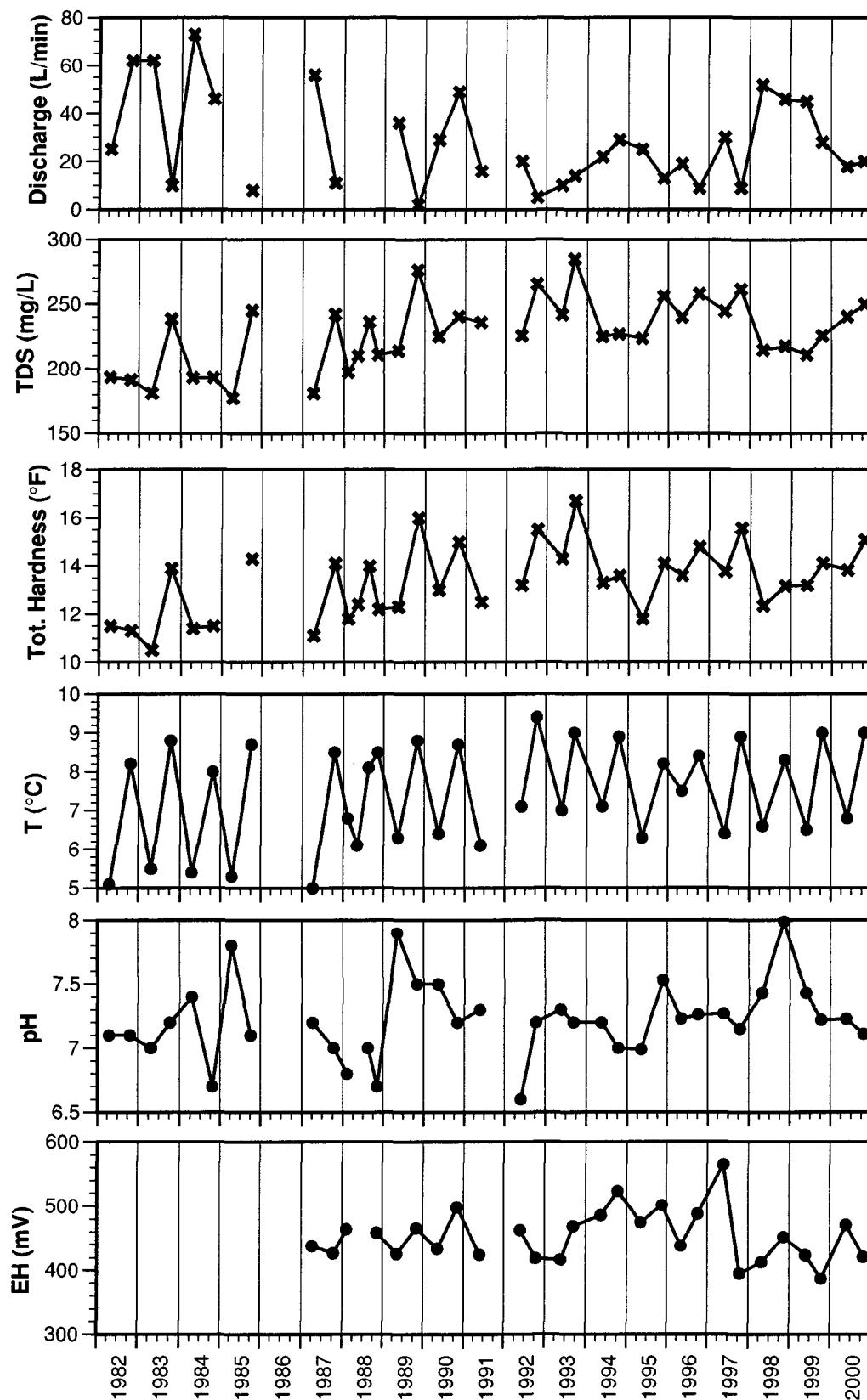


Figure 4-19: Lutry springwater: Time series of discharge, total mineralisation (TDS), total hardness, water temperature, pH and E_H .

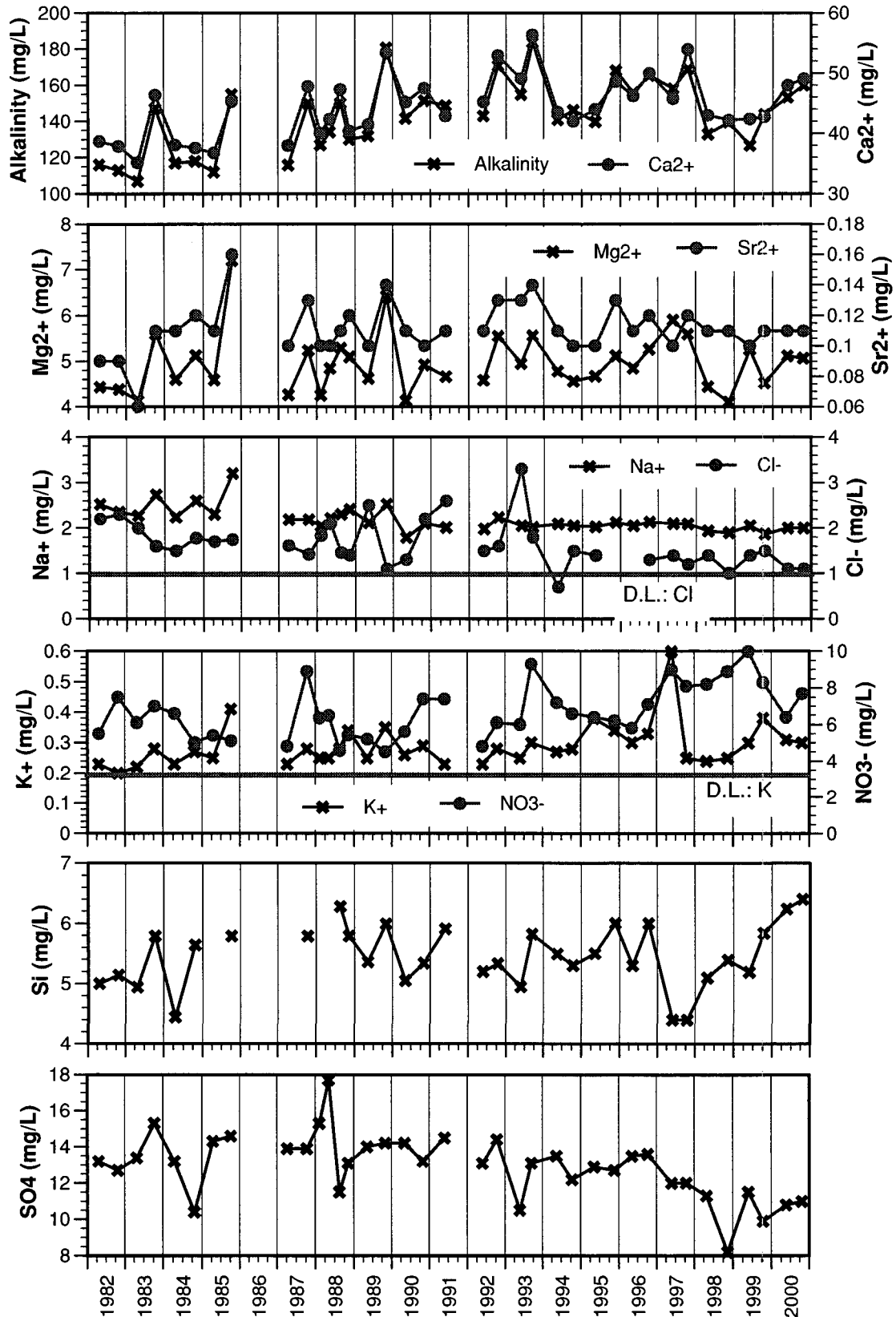


Figure 4-20: Lutry springwater: Time series of major elements.

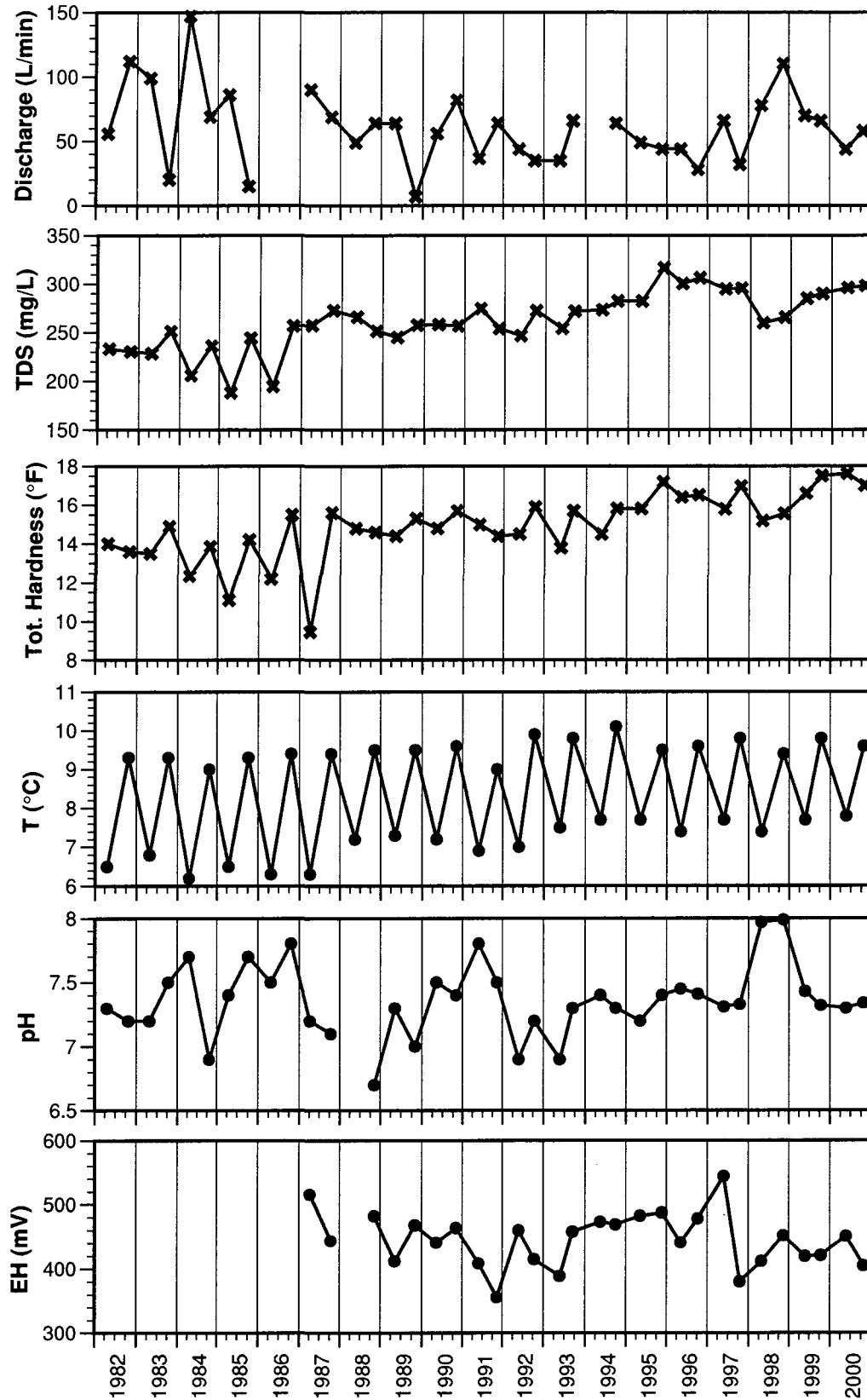


Figure 4-21: Pierre-Ozaire spring: Time series of discharge, total mineralisation (TDS), total hardness, water temperature, pH and E_H .

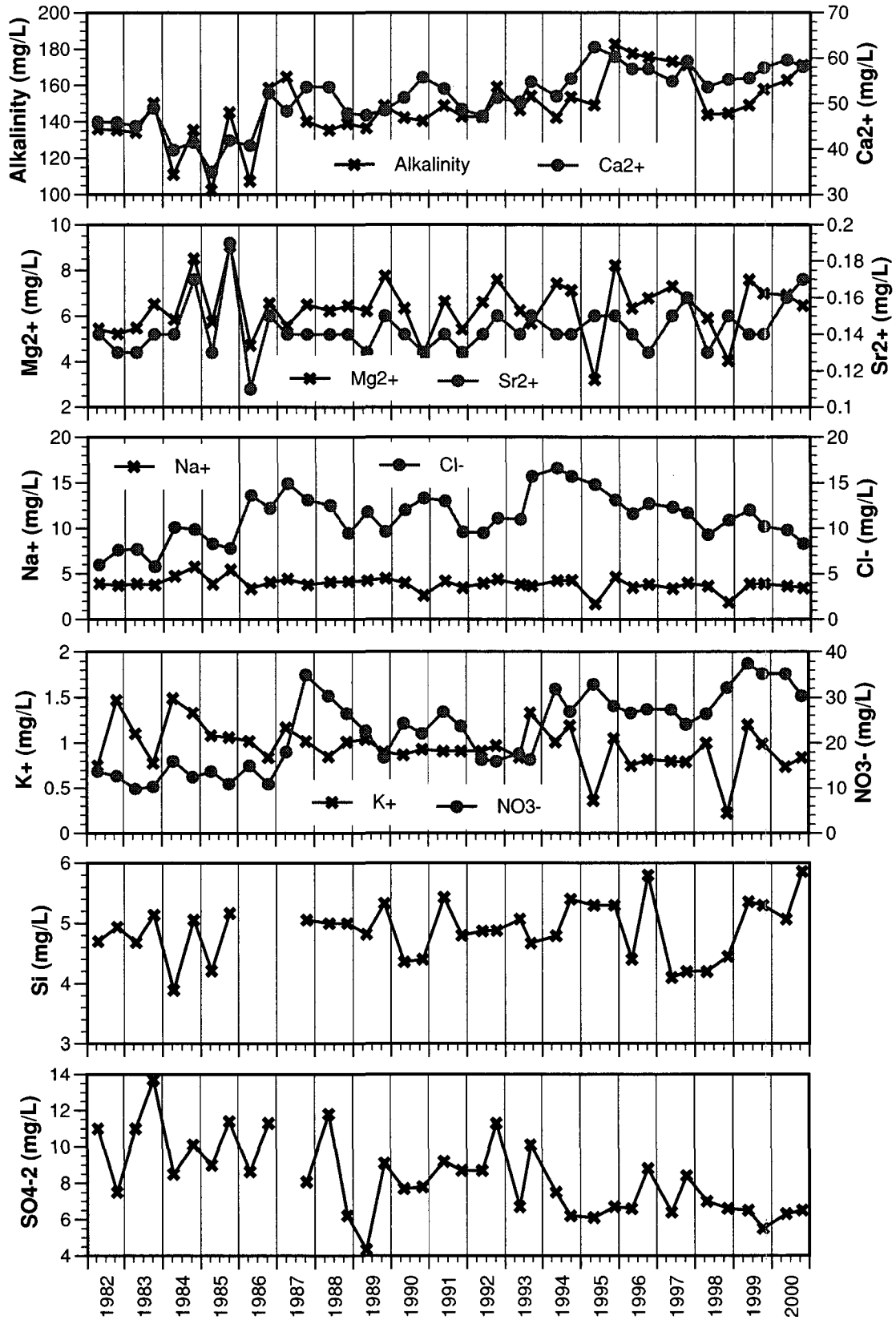


Figure 4-22: Pierre-Ozaire springwater: Time series of major elements.

4. 5. 2. Chromium as geogenic tracer

Chromium is only detected in the groundwater, while it has almost never been detected in rainwater, throughfall and soil solutions. This indicates that atmospheric input of Cr can be neglected. Certain mineral fertilisers and sewage sludge can contain elevated amounts of Cr (BUWAL, 1991). However, the Lutry springwater (forest) contains slightly higher Cr concentrations compared to the Pierre-Ozaire springwater (grassland) (see figure 4-23). Therefore, the use of fertilisers in the Pierre-Ozaire catchment does not appear to influence the Cr-content of the groundwater. As there are no other anthropogenic sources of Cr in the Lutry and Pierre-Ozaire catchments, the Cr found in the groundwater must have a geogenic origin, and is therefore a natural tracer of groundwater from the Burdigalian sandstone.

Chromium shows neither a correlation with discharge or water temperature, nor with any major or trace element. This indicates that this element is subjected to a complex chemical control. Furthermore, no correlation exists between the dissolved Cr-contents and the pH or redox potential measured in the groundwater.

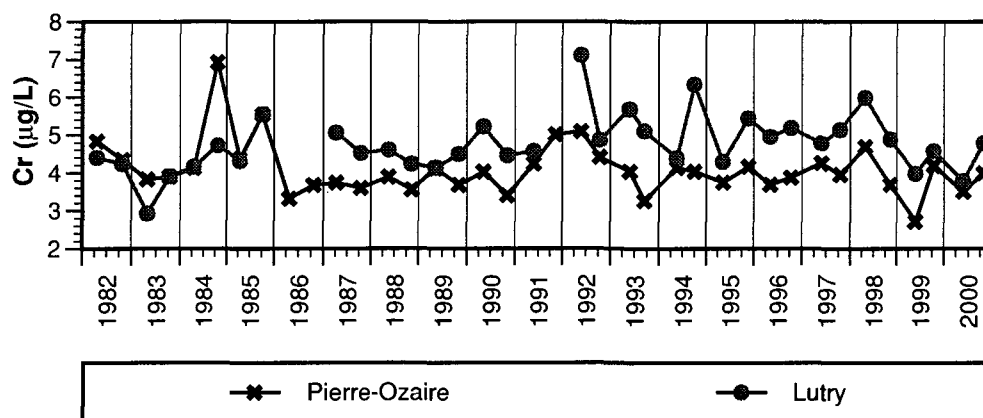


Figure 4-23: Time variation of the Cr concentration in the Lutry and Pierre-Ozaire springwaters.

4. 5. 3. Chemical evolution of the Lutry springwater

The general chemical evolution of molasse springwaters has been described in chapter 3. 4. 4. "Recent groundwaters derived from molasse" on page 91. In the present chapter the chemical evolution of the Lutry springwater is discussed in detail.

The distribution of aqueous species and mineral saturation indices have been calculated based on median values rather than mean values of rainwater, throughfall, soil solutions and springwater, in order to diminish the influence of extreme values (table 4-6 and figure 4-24).

No data are available for dissolved carbon contents in rainwater, throughfall and in soil solutions. To enable model calculations, total dissolved inorganic carbon (TDIC) contents in rainwater and throughfall solution have been calculated assuming equilibrium with the atmospheric CO_2 content ($P_{\text{CO}_2} = 10^{-3.5}$). In the soil solutions TDIC contents have been derived from charge balance calculations, resulting in a P_{CO_2} in the soil solutions of $10^{-2.48}$ and $10^{-2.38}$ at 30 and 80 cm depth, respectively. The calculated values are in agreement with literature average values of soil P_{CO_2} ranging from $10^{-1.5}$ to $10^{-2.5}$ (Brook and others, 1983; Buyanovsky & Wagner, 1983; see also page 76).

The redox potential in rainwater and throughfall solution was calculated assuming the same conditions as in groundwater (equilibrium with atmospheric oxygen; $P_{\text{O}_2} = 10^{-0.68}$). For the soil solutions, oxidising conditions are indicated by the presence of oxidised Fe mineral phases (reddish colour of the soil) and the very low dissolved Fe content in the soil solutions.

Measured Al concentrations in the soil solutions vary strongly, which is probably related to the presence of Al-colloids or sample contamination. The solubility of amorphous Al-hydroxide generally sets an upper limit to the Al^{3+} activity in solution. Therefore, calculated Al concentrations in equilibrium with $\text{Al}(\text{OH})_{3(\text{am})}$ are used for the soil solutions. These calculated concentrations lie in the same range as the measured values from the ceramic lysimeter sampling (Atteia, 1992). This method for the sampling of soil solutions proved to be more reliable than the sampling by membrane lysimeters.

		Rainwater	Throughfall solution	Soil solutions ^a		Groundwater
				-30 cm	-80 cm	
	Units	median n=11	median n=30	median n=16	median n=19	median n=38
T	°C	10.0	10.0	10.0	10.0	7.8
pH	pH-units	4.7	4.5	6.2	6.0	7.2
E_H	mV	1020 ^b	1032 ^b	933 ^b	943 ^b	445
Alk. as HCO₃⁻	µmol/L	0.3 ^c	0.2 ^c	95	80 ^d	2377
F⁻	µmol/L	n.d.	n.d.	n.d.	n.d.	2
Cl⁻	µmol/L	7	28	38	30	42
SO₄²⁻	µmol/L	22	54	78	106	137
NO₃⁻	µmol/L	36	99	14	14	104
Ca²⁺	µmol/L	18	34	52	75	1112
Mg²⁺	µmol/L	n.d.	6	64	54	199
Sr²⁺	µmol/L	0.02	0.06	0.13	0.16	1.27
Na⁺	µmol/L	1	9	39	44	91
K⁺	µmol/L	3	28	5	8	7
NH₄⁺	µmol/L	59	106	15	4	n.a.
Si total	µmol/L	15	4	205	146	191
Ba total	µmol/L	0.015	0.029	0.058	0.189	0.042
Al total	µmol/L	n.d.	n.d.	4.515 ^d	8.266 ^c	0.231
Cr total	µmol/L	n.d.	n.d.	0.003	n.d.	0.088
Mn total	µmol/L	0.164	2.021	1.838	3.349	0.003
Fe total	µmol/L	0.165	0.215	0.331	0.072	0.073
P_{CO2}		10 ^{-3.5}	10 ^{-3.5}	10 ^{-2.5}	10 ^{-2.4}	10 ^{-2.14}
P_{O2}		10 ^{-0.7}	10 ^{-0.7}	10 ^{-0.9}	10 ^{-0.9}	10 ^{-0.9}
SI Calcite		-8.69	-8.81	-4.24	-4.36	-0.65
SI Dolomite		-	-18.50	-8.50	-8.97	-2.19
SI Chalcedony		-1.10	-1.71	0.05	-0.10	0.04
SI Kaolinite		-	-	7.47	7.18	4.87
SI Gypsum		-4.88	-4.22	-3.90	-3.62	-2.51
SI Barite		-2.31	-1.64	-1.20	-0.57	-1.25
SI Strontianite		-10.70	-10.73	-5.98	-6.16	-2.70
SI Celestite		-5.73	-4.97	-4.48	-4.25	-3.41
SI Fe(OH)₃(am)		-0.69	-0.81	1.11	0.26	1.31
SI Cr(OH)₃(am)		-	-	-23.32	-	-2.29
SI Gibbsite		-	-	2.83	2.83	1.53
SI Al(OH)₃(am)		-	-	0.00	0.00	-1.33
SI Birnessite		2.86	3.54	6.76	6.74	-8.62
SI Manganite		-0.81	-0.14	3.15	3.07	-4.95

Table 4-6: Median chemical compositions and saturation states with respect to selected minerals of rainwater, throughfall, soil solutions (data from 1990-1991; Atteia, 1992) and springwater (sampling period 1981 to 2001, median values, high water and low water periods). Concentrations are in µmol/L. n.d. = not detected; n.a. = not analysed.

a. Sampled by means of a ceramic lysimeter

b. Calculated value, assuming equilibrium with O₂(g) at atmospheric P_{O2} = 10^{-0.7}

c. Calculated value, assuming equilibrium with CO₂(g) at atmospheric P_{CO2}=10^{-3.5}

d. Calculated value, assuming equilibrium with amorphous Al-hydroxide

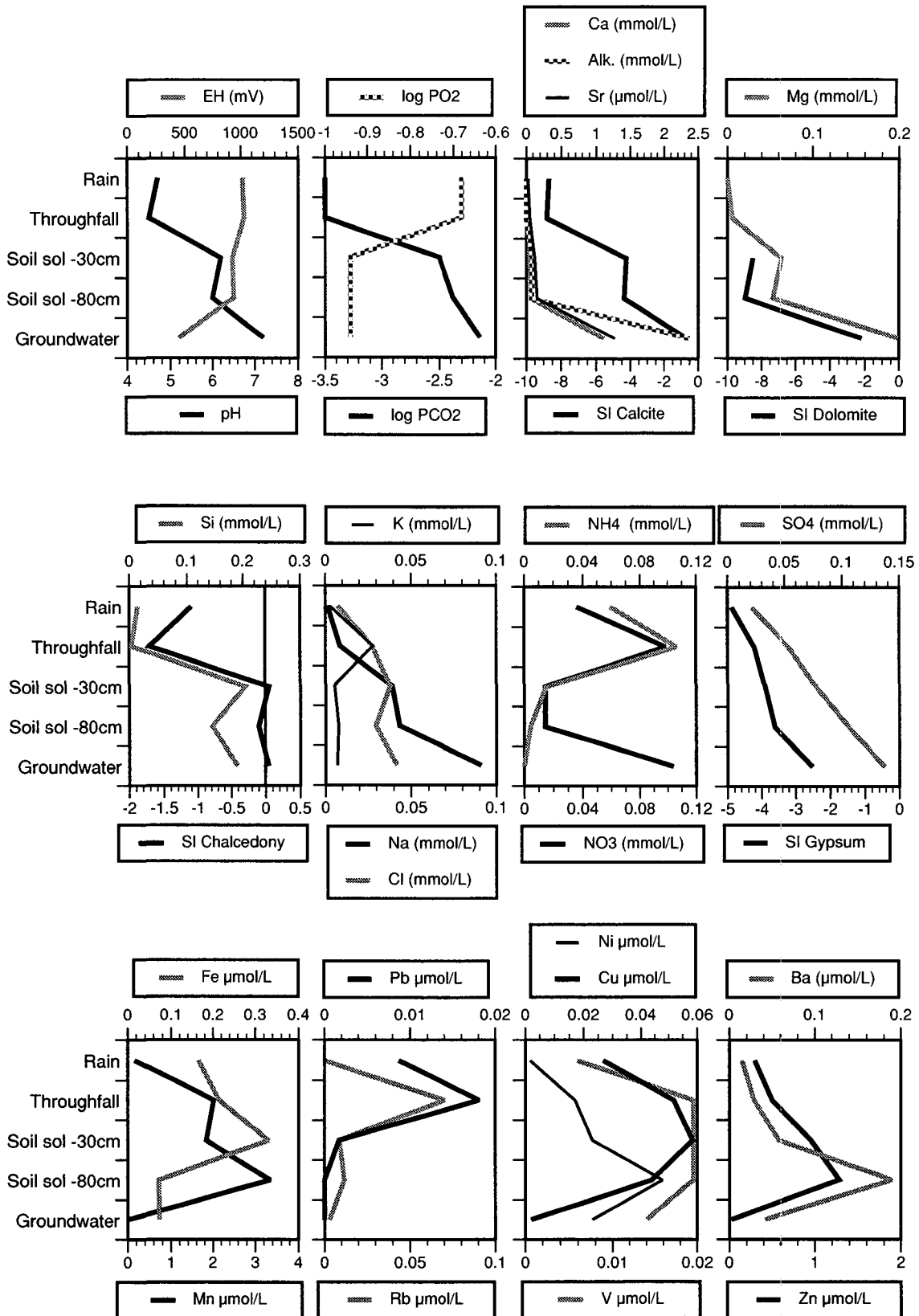
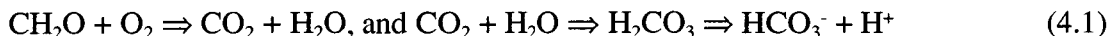


Figure 4-24: Distribution of dissolved major and trace elements and saturation state from rainwater to groundwater (data see table 4-6).

Major elements

Compared to the rainwater and throughfall solutions the soil solutions at 30 and 80 cm depth show an increase in alkalinity (see table 4-6, and figures 4-24 and 4-25). This increase is the result of the dissolution of CO₂ from the decay of organic matter and root respiration in the soil. In the soil solutions with a pH of about 6.0, the thus produced carbonic acid dissociates to bicarbonate.



The oxidation of organic matter in the soil consumes oxygen (reaction 4.1), leading to a slight drop of the redox potential. The subsequent dissolution of CO₂ and dissociation of carbonic acid produces acidity. Additional acidity is produced by the oxidation of atmospheric NH₄⁺ input (reaction 4.2; e.g. Appelo & Postma, 1996). The soil solution analyses show that NH₄⁺ disappears in the soil.



If plants consume all the nitrate in the soil solution, the proton production from the oxidation of NH₄⁺ would be balanced by the HCO₃⁻ production from the denitrification process (reaction 4.3). Yet, the presence of NO₃⁻ in the springwater is proof of incomplete denitrification.

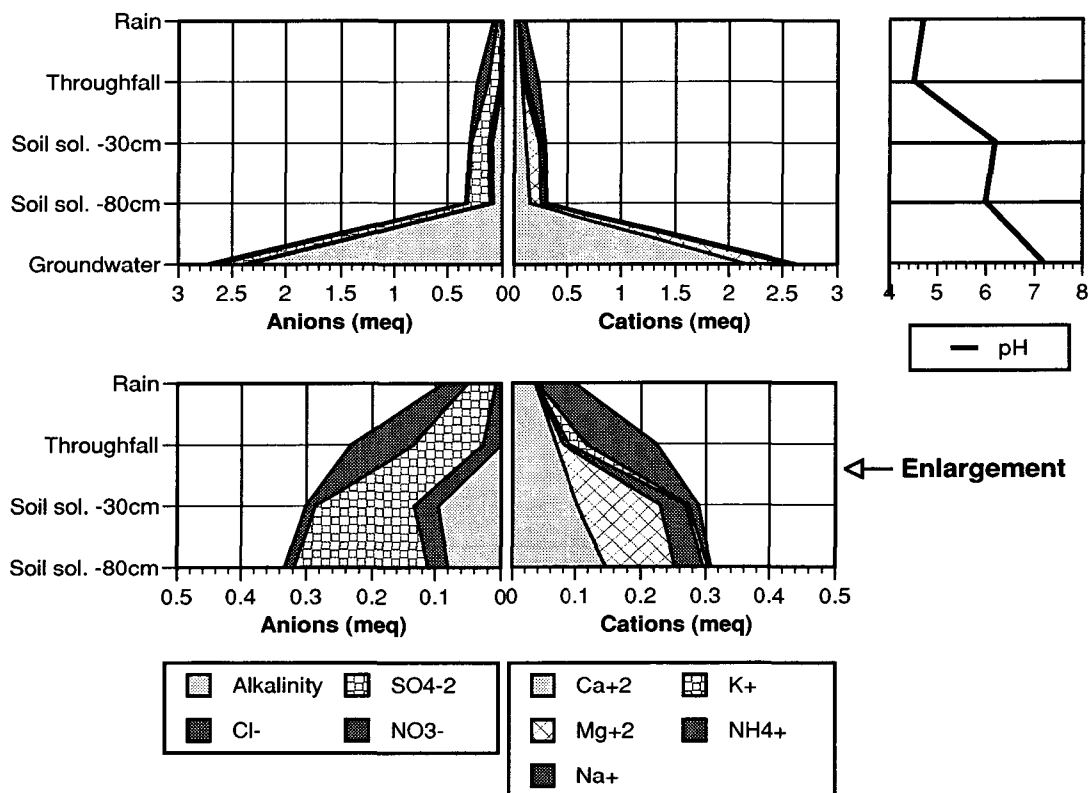
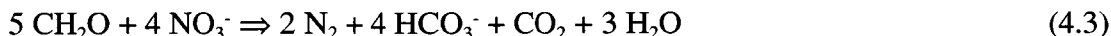


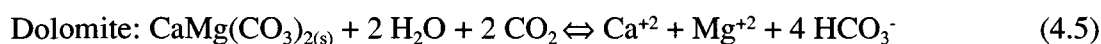
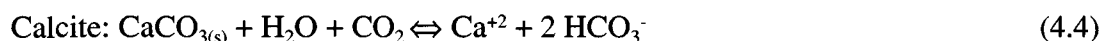
Figure 4-25: Evolution of the major element composition from rainwater to groundwater. Chemical data of rainwater, throughfall and soil solutions are from Atteia (1992).

Despite the input of acid rain and further acidification of the soil solution by the oxidation of organic matter and atmospheric NH_4^+ , soil solutions have a higher pH than the rainwater. This increase of the pH is the result of mineral alteration reactions, which buffer the acidity input and release base cations into solution.

The dissolved silica concentration already reaches a value of about 5 mg Si/L in the soil solution at 30 cm depth and remains constant down to the springwater (see table 4-6 and figure 4-24). This indicates that silicate minerals dissolve in the upper most soil levels. The soil solutions and the springwater are saturated with chalcedony and supersaturated with respect to quartz, which is in agreement with the extremely sluggish precipitation kinetics of quartz (Rimstidt & Barnes, 1980). The relatively constant Si concentration in the soil solutions and in springwater (see time series in figure 4-20) and their equilibrium with chalcedony indicate that the silica concentration in the soil solutions and in the groundwater is controlled by the solubility of chalcedony.

Together with the increase in dissolved silica a small increase of dissolved Mg^{2+} and Ca^{2+} characterises the soil solutions. As no more carbonate minerals are present in the soil, this increase must be due to the weathering of Ca- and Mg-bearing silicate minerals in the soil. The slow weathering of mafic silicate minerals such as chlorite, serpentine, pyroxenes, biotite, and glauconite releases silica, Mg^{2+} , and Ca^{2+} into solution. The observed alteration phenomena of these minerals supports this explanation (see chapter 4. 3. 1. "Mineralogy" on page 142). The very low Mg^{2+} and Ca^{2+} content of the soil solution is consistent with the slow dissolution kinetics of these silicate minerals (see table 1-2 on page 11).

As the infiltrating solution reaches the water table, which is situated approximately at the depth of the decarbonation front, the pH attains near neutral values and a massive increase in Ca^{2+} and alkalinity and to a lesser extent Mg^{2+} occurs. The strong increase of these compounds is the result of the rapid dissolution of carbonate minerals as soon as the soil solution attains the carbonate-bearing bedrock sandstone:



Saturation state calculations indicate that saturation with calcite is nearly reached in the Lutry springwater, while saturation with dolomite is not reached. This is due to the slower dissolution kinetics of dolomite compared to calcite on the other hand (see page 78).

The molar Na^+/Cl^- ratio rises from about 0.2 in rainwater to 2.2 in springwater, indicating that a geogenic source of Na^+ must exist. Possibilities include the alteration of the abundant plagioclase and Na-Ca cation exchange on clay minerals. The etched surfaces of plagioclase grains observed by SEM are consistent with the alteration of plagioclase. However, compared to cation exchange reactions, the alteration of plagioclase is extremely slow. As the molasse sediments were formed in a marine, Na-dominated environment, clay minerals were originally saturated with Na^+ . However, the sandstone has been exposed to freshwater conditions for at least 10'000 years (since soil formation began after the last retreat of pleistocene glaciers). The capacity to release Na^+ must therefore have decreased. Nevertheless, cation exchange cannot be excluded completely as a potential Na-source, since no cation exchange data of the Burdigalian sandstone are available.

As the K^+ concentration in springwater are only hardly above the detection limit (0.2 mg/L), K-bearing minerals including biotite and K-feldspar appear to be the most important geogenic sources of K^+ . For example, exfoliated, chloritised biotite flakes have been observed in thin-section and in SEM images (figure 4-10), and Dalla Piazza (1996) has

shown by microprobe analysis, that altered biotite and the altered rims of K-feldspar are depleted in K.

Alteration products from the weathering of silicate minerals in the bedrock sandstone are montmorillonite and possibly illite or illitic material. The relative amount of montmorillonite is higher in the more altered parts of the bedrock sandstone compared to the unaltered parts, indicating that montmorillonite is a likely alteration product in the bedrock sandstone. The alteration of primary silicate minerals to montmorillonite mainly leads to a release of base cations into solution, whereas Al and silica are retained in the solid phase.

The small increase of dissolved SO_4^{2-} in the springwater compared to the soil solutions is due to the oxidation of small amounts of pyrite contained in the sandstone.

Trace elements

Microprobe analyses have shown that particularly biotite, glauconite and chlorite lose Fe and associated trace metals in the upper soil levels (Dalla Piazza, 1996). This author has also shown that Ba is essentially leached from K-feldspar, and to a minor extent from biotite and white mica. In these minerals, Ba occurs as a primary substitute for K.

The mainly divalent Fe in mafic minerals including biotite, chlorite, glauconite, pyroxenes, and spinels is released and oxidised to Fe^{III} , and associated Ni, V, Cr, Zn, and Mn are released in the alteration process. The Fe^{III} subsequently precipitates as Fe-hydroxides on mineral surfaces. Together with Fe and Mn most trace elements such as Zn, Ni, Cu, Rb, and Ba become immobile in the lower soil levels or in the surface near parts of the bedrock. Retention processes including co-precipitation with Fe-hydroxides and Mn-oxides or adsorption result from the increasing pH at the decarbonation front. Fe-hydroxides and Mn-oxides represent a powerful substratum for the adsorption of trace elements. In addition, secondary vermiculite and montmorillonite also incorporate some Fe^{III} , Cr^{III} , Ba, Ni, Zn, Rb, Li. Lead, which has an essentially anthropogenic origin, is retained already in the upper soil levels due to its strong association with organic matter (Atteia, 1992).

Contrasting this, Cr (see below) and Sr^{2+} are mobilised in substantial amounts in the saturated zone of the aquifer. Dissolved Sr^{2+} shows an evolution parallel to dissolved Mg^{2+} , Ca^{2+} and alkalinity, which indicates that the origin of this element is predominantly associated with the dissolution of carbonates. Equilibrium with the minerals strontianite or celestite is not reached.

Mass balance calculations

Mass balance calculations have been performed to test the likelihood of different mineral phases to get involved in the hydrochemical evolution of the Lutry groundwater from the lowest soil level to the spring. The mass balance calculations were performed using the median compositions of the soil solution at 80 cm depth (initial water composition) and the springwater (final water composition; see table 4-7). The difference in composition between these two solutions is due to reactions of the groundwater with minerals in the aquifer. The weathering reactions observed in the mineralogic investigations (see chapter 4. 3. 1. "Mineralogy" on page 142) and discussed in the preceding section were used to calculate the mass transfer for every geologically reasonable combination of these plausible phases to fit the observed changes in solute composition. A model is realistic when the results are consistent,

- a) with thermodynamic considerations (saturation states), and
- b) with the observed mineralogy and surface shape of minerals (corroded vs. not corroded surface).

In the present case (b) is the better constraint for the likeliness of a mass transfer model, because of the uncertainties attached to, or the lack of, thermodynamic data for Al-silicates, and the extremely different reaction kinetics of the minerals present in the weathering column.

	Unit	Initial solution: Soil solution -80 cm (median composition)	Final solution: Groundwater (median composition)
pH	pH-units	6.0	7.2
C	μmol/L	80	2377
S	μmol/L	106	137
Ca	μmol/L	75	1112
Mg	μmol/L	54	199
Na	μmol/L	44	91
K	μmol/L	8	7
Si	μmol/L	146	191
Al	μmol/L	8.266	0.231
Fe	μmol/L	0.072	0.073
P _{CO2}		10 ^{-2.4}	10 ^{-2.14}
SI Calcite		-4.36	-0.65
SI Dolomite		-8.97	-2.19
SI Chalcedony		-0.10	0.04
SI Fe(OH) ₃ (am)		0.26	1.31

Table 4-7: Compositions of the initial and final solutions used in the mass balance calculations.

In the calculations all major cations and anions except Cl⁻ were included. In addition, Al, Si and Fe were included to investigate the mass transfer of Al-silicates and Fe-bearing mineral phases. Chloride was not considered, because of the strong variation of Cl⁻ in the soil solution, which is likely to be linked to its partly anthropogenic origin.

As primary minerals calcite, dolomite, albite, K-feldspar, pyrite, chlorite, biotite, serpentine (chrysotile), and enstatite have been tested. All of these minerals are unstable in the weathering profile (see chapter 4. 3. 1. "Mineralogy" on page 142) and were allowed to dissolve in the models.

Calcite and dolomite are the most rapidly dissolving minerals present in the bedrock sandstone. In the Burdigalian sandstone, dolomite makes up approximately $\frac{1}{10}$ of the amount of calcite. Calcite and dolomite are the most important sources of dissolved Ca²⁺, Mg²⁺, and HCO₃⁻. Their dissolution is enhanced by the dissolved CO₂ contained in the soil solution (reactions 4.4 and 4.5). Biotite, chlorite, pyroxene (enstatite), and serpentine (chrysotile) have been taken into consideration as additional Mg-sources in different model runs. The dissolution of these mafic silicate minerals has been observed in SEM images.

Albite is the most plausible Na source, as it is the only Na-containing mineral considered. Alternatively, Na may originate from Ca-Na cation exchange. Both possibilities were tested.

Biotite and K-feldspar are the most prominent sources for K. Biotite has a faster weathering rate than K-feldspar, but it is only present in very small amounts (less than 1% biotite compared to 10 to 15% K-feldspar). Both minerals have therefore been tested.

The low Al and Fe concentrations in the springwater and the Si concentration remaining constant between the soil solution and springwater suggest that these elements are subject to a solubility control. This needs the consideration of secondary minerals acting as Al, Fe, and Si sinks. Mineralogic investigations have shown that montmorillonite is a plausible product phase from the alteration of various silicate minerals. However, montmorillonite can have a wide variety of chemical compositions, which has an influence on solute cations such as Mg^{2+} , K^+ , Ca^{2+} , and Fe^{2+} . A montmorillonite termed "Mont-mafic" with the composition $K_{0.07}Mg_{0.4}Ca_{0.13}Fe_{0.1}Al_{1.99}Si_{3.65}O_{10}(OH)_2$ has been used in the models. In addition, the precipitation of SiO_2 and amorphous $Fe(OH)_3$ was allowed because chalcedony and Fe-hydroxide reach saturation in the soil solution and in the springwater.

The small increase of SO_4^{2-} in the springwater is attached to the oxidation of small amounts of pyrite, which occur associated with carbonised organic matter in the Burdigalian sandstone. Because pyrite is the only sulphur-bearing phase in all models, the amount of oxidising pyrite is determined only by the difference in dissolved SO_4^{2-} between initial and final water composition. It therefore remains the same in all models.

Mineral phases	Formula	Model 1	Model 2	Model 3	Model 4	Model 5	Model 6
CO ₂ gas	CO ₂	1344	1342	1342	1340	1447	1403
Calcite	CaCO ₃	890	888	888	886	1036	991
Dolomite	CaMg(CO ₃) ₂	151	153	153	155	27	71
Albite	NaAlSi ₃ O ₈	47	47	47	47	n.c.	n.c.
Ca-Na Exchange	Ca ²⁺ ⇌ 2 Na ⁺	n.c.	n.c.	n.c.	n.c.	24	24
Biotite	KMg _{1.5} Fe _{1.5} AlSi ₃ O ₁₀ (OH) ₂	1	1	n.c.	n.c.	n.c.	n.c.
K-feldspar	KAlSi ₃ O ₈	n.c.	n.c.	1	1	n.c.	n.c.
Serpentine	Mg ₃ Si ₂ O ₅ (OH) ₄	1	n.c.	1	n.c.	32	n.c.
Enstatite	Mg _{0.8} Fe _{0.2} SiO ₃	n.c.	3	n.c.	3	n.c.	64
Chlorite	Mg ₅ Al ₂ Si ₃ O ₁₀ (OH) ₈	n.c.	n.c.	n.c.	n.c.	6	6
Pyrite	FeS ₂	15.5	15.5	15.5	15.5	15.5	15.5
Mont-mafic	K _{0.07} Mg _{0.4} Ca _{0.13} Fe _{0.1} Al _{1.99} Si _{3.65} O ₁₀ (OH) ₂	-29	-29	-29	-29	-10	-10
Fe(OH) ₃	Fe(OH) ₃	-15	-15	-13	-13	-15	-27

Table 4-8: Six different models obtained by NETPATH mass balance calculations using different mineral assemblages. Amounts of mass transfer of dissolving (positive) and precipitating (negative) mineral phases are given in $\mu\text{mol/kg H}_2\text{O}$; n.c. = not considered.

With the above presented dissolved components and mineral phases, six plausible models were obtained (table 4-8). The models 1 to 4 are very similar. They differ mainly in

the type of K- and Mg-bearing silicate minerals, i.e. biotite vs. K-feldspar and enstatite vs. serpentine. The models 5 and 6 use Ca-Na cation exchange as Na-source instead of albite.

The most important reactions in all models are the dissolution of CO₂, calcite and dolomite. The importance of carbonate dissolution is consistent with the observed decarbonation of the bedrock. The required CO₂-source is the abundant CO₂ production in the soil.

In the models 1 to 4 an amount of 47 µmol (12.5 mg) albite is weathering per kg water. It is balanced with an equally high amount of montmorillonite that should precipitate. Alternatively, Na can be released by Ca-Na cation exchange (models 5 and 6). The effect of using Ca-Na cation exchange instead of albite weathering is mainly the much lower amount of precipitating montmorillonite, the slightly higher amount of calcite dissolution, and the implication of important chlorite, serpentine and pyroxene dissolution as additional Mg-sources.

The molar amounts of biotite and K-feldspar are the same, because both minerals contain 1 mole of K per formula unit. The amount of 1 µmol of these minerals that should dissolve per kg of solution corresponds to 0.6 mg biotite or 0.3 mg K-feldspar.

The use of different Mg- and K-bearing minerals has an influence on the amount of secondary minerals that must precipitate. Mainly the amount of Fe(OH)₃, which is presumed to be the Fe-sink in this aquifer material, is higher if biotite is the K-source. In models 5 and 6 the amount of Fe(OH)₃ that should precipitate is higher, because less Fe-containing montmorillonite precipitates. If in addition chromite dissolves, the amount of Fe(OH)₃ would be even higher. Silica is balanced by montmorillonite in all models, and no SiO₂ phase needs to precipitate.

The comparison of the models with plagioclase alteration (models 1 to 4) and the models with Ca-Na cation exchange (models 5 and 6) shows that the models 1 to 4 appear to be the most plausible ones, as only very small amounts of serpentine and pyroxene are present in the Burdigalian sandstone. In the models 5 and 6 using Ca-Na cation exchange as source of Na unrealistically high amount of serpentine, enstatite and chlorite must dissolve to explain the dissolved Mg²⁺ concentration occurring in the groundwater. These models are therefore less probable to represent the natural conditions in the aquifer. This indicates that Ca-Na cation exchange probably plays a minor role compared to albite alteration.

4. 6. Geochemistry of chromium

4. 6. 1. Natural and anthropogenic sources of chromium

In different rock types the chromium content can vary widely (table 4-9). Granites, carbonate rocks and sandy sediments have low Cr contents, whereas ultramafic and mafic rocks and shales typically exhibit high Cr contents. In rocks Cr occurs mostly in its trivalent form (Matztat & Shiraki, 1978). Common Cr-bearing rock forming minerals are spinels, such as chromite (FeCr_2O_4) and magnetite (Fe_3O_4), pyroxenes, and sheet-silicates. Trivalent Cr (Cr^{III}) closely resembles Fe^{III} and Al^{III} in its ionic size and chemical properties and it normally substitutes for these elements in minerals. During weathering processes Cr also behaves similar to Fe^{III} and Al^{III} : Chromium is especially concentrated in the residual weathering products such as clays and oxide or hydroxide phases. Therefore the clay fraction of clastic sediments is usually richer in Cr than are the coarser fractions. Similarly, Fe-rich concretions show an increase of Cr over the parent rocks. The Cr content of soils is largely determined by the parent material.

Dissolved Cr in water is a trace element with a typical concentration of 0.3 $\mu\text{g/L}$ in sea water and an average of 1 $\mu\text{g/L}$ in freshwater (Adriano, 1986; table 4-9). Naturally elevated Cr-concentrations of several hundred $\mu\text{g Cr/L}$ have been reported in groundwaters from ultramafic rocks in regions with dry climate (Robertson, 1975). The highest known natural Cr-concentration, about 7500 $\mu\text{g/L}$, was measured in a pH 12.5 groundwater near Maqarin, Jordan (Khoury and others, 1992).

Rock types	typical Cr concentration (ppm)	Water	typical Cr concentration ($\mu\text{g/L}$)
Continental crust ^a	100	Freshwater ^b	1
Ultramafic rocks ^a	2400	Sea water ^b	0.3
Basalts ^a	200		
Limestone ^a	9		
Granite ^c	4		
Sandstone ^a	27		
Shale ^a	83		

Table 4-9: Average Cr-concentrations in different rock types and in water.

a. Nriagu & Nieboer, 1988: 82

b. Adriano, 1986

c. Matztat & Shiraki, 1978

Chromium is used in many industrial processes, including chromium-plating industry, refractory brick production and chemical industry (mainly chromate manufacturing and pigment production), leather-tanning and wood-treatment facilities, and last but not least in mining and smelting of Cr-ore and metallurgical industry (Nriagu & Nieboer, 1988; Adriano, 1986). Common sources of Cr contamination are waste water, dust, and fumes from these industries, fly ash from power plants (fuel combustion) and waste incineration plants. Due to spill, leakage and improper waste disposal, Cr has been released into the environment at many sites and is a widespread soil and groundwater contaminant (e.g.

Baron and others, 1996; Basler Zeitung, 4.5.1994; Calder, 1988; Nikolaidis and others, 1994; Palmer & Wittbrodt, 1991; Puls and others, 1994a, 1994b; Stollenwerk & Grove, 1985). In contaminated groundwaters, dissolved hexavalent Cr has been reported to reach concentrations as high as 14'600 mg/L (United Chrome Products site in Corvallis, USA; Palmer & Wittbrodt, 1991).

4. 6. 2. Toxicology

Hexavalent Cr compounds are 10 to 100 times more toxic when ingested than are trivalent Cr compounds (Katz & Salem, 1993). Carcinogenicity appears to be associated primarily with inhalation of the less soluble hexavalent Cr-compounds including Ca-, Sr-, Ba-, Pb-, and Zn-chromates (Yassi & Nieboer, 1988). On the other hand, trivalent Cr in amounts of a few µg is an essential nutrient required for normal sugar and fat metabolism (Anderson, 1989). In Switzerland, the drinking water limit is fixed at 20 µg Cr^{VI}/L (Lebensmittelhandbuch / Manuel des denrées alimentaires, 1994), while the WHO recommend a maximum of 50 µg total Cr /L (WHO, 1993).

4. 6. 3. Aqueous geochemistry of chromium

Oxidation-reduction reactions

Cr can exist in oxidation states from 0 (metallic form) to VI. However, only trivalent Cr (Cr^{III}) and hexavalent Cr (Cr^{VI}) are important in the pH-E_H range of natural aquatic systems. The redox transformation of Cr^{III} into Cr^{VI} or vice versa can only take place in presence of another redox couple, which accepts or provides the three necessary electrons. In natural environments such redox couples include H₂O/O₂(aq), Mn^{II}/Mn^{IV}, NO₂/NO₃⁻, Fe^{II}/Fe^{III}, S²⁻/SO₄²⁻, and CH₄/CO₂.

Hexavalent Cr is a strong oxidant, which is reduced in presence of electron donors. A low pH favours such reduction reactions. Laboratory studies have shown that hexavalent Cr can be reduced to trivalent Cr in presence of organic matter (Bartlett & Kimble, 1976b), or dissolved sulphide (Schroeder & Lee, 1975). In addition, dissolved Fe²⁺ ions from the weathering of Fe^{II}-bearing minerals, such as biotite, magnetite, or chlorite can be involved in Cr^{VI} reduction as follows (Rai and others, 1988):

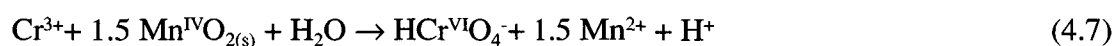


This reaction was found to be very rapid, with equilibrium being established in less than 5 min in presence of dissolved oxygen (Eary & Rai, 1988). The Cr³⁺ and Fe³⁺ subsequently precipitate as hydroxide phases. In acid solutions the Cr^{III} concentration is limited by the solubility of (Cr^{III},Fe^{III})(OH)_{3(s)} co-precipitates (Rai and others, 1988; Stollenwerk & Grove, 1985) and at neutral to alkaline conditions probably by Cr(OH)_{3(s)}. Davis-Anderson and others (1994) have suggested that heterogeneous reduction of Cr^{VI} (first surface adsorption, then reduction) on the surface of Fe^{II}-bearing minerals and the subsequent precipitation of (Fe,Cr)(OH)_{3(s)} is the primary mechanism immobilising dissolved Cr^{VI}. In the described case, the fine fraction making up only 1 wt.% of the aquifer material, dominated the amount of aqueous Cr^{VI} reduction because of its great surface area and reactivity.

The inverse reaction, the oxidation of Cr^{III} to Cr^{VI}, is considerably slower. Dissolved oxygen has been found to oxidise Cr^{III} to Cr^{VI} (Schroeder & Lee, 1975; Nakayama, 1981a; Eary & Rai, 1987), but the rate of this oxidation reaction at room temperature is very slow and allows Cr^{III} to become involved in faster sorption and precipitation reactions. Therefore, the oxidation of Cr^{III} by dissolved oxygen is unlikely in soils. Several studies on Cr^{III} oxidation in soils have shown that freshly precipitated Cr^{III} in form of CrCl_{3(s)} or Cr(OH)_{3(s)}, and some Cr^{III} forms in tannery waste and sewage sludge are oxidised by Mn-oxides contained in the soil (Bartlett & James, 1979; Amacher & Baker, 1982; James & Bartlett, 1983a). This oxidation reaction occurs in three steps:

- 1) adsorption of Cr^{III} onto MnO_{2(s)} surface sites,
- 2) oxidation of Cr^{III} to Cr^{VI} by surface Mn^{IV},
- 3) desorption of the reaction products Cr^{VI} and Mn^{II}

Aged precipitates of Cr(OH)_{3(s)} are less prone to oxidation than the freshly precipitated forms. Similar to the reduction of Cr^{VI}, the rate and amount of Cr^{III} oxidation increases with decreasing pH and increasing ratio of surface area per solution volume (Eary & Rai, 1987). The following theoretical stoichiometries have been suggested by Amacher & Baker (1982) and by Eary & Rai (1987):



The MnOOH_(s) produced in the second reaction then decays into aqueous Mn²⁺. The oxidation rate of Cr^{III}, which is related to the amount and surface area of Mn-oxides is initially rapid and slows down significantly after 20 to 60 min, so that the reaction does not appear to reach completion (Schroeder & Lee, 1975; Eary & Rai, 1987).

Under certain special conditions, reduction of aqueous Cr^{VI} may occur simultaneously with oxidation of Cr^{III}, so that the relative rates of oxidation and reduction establish an equilibrium level of Cr^{VI} in the soil (James and others, 1997).

Speciation

The chemical speciation of dissolved Cr is determined by pH and redox conditions. A pH-E_H diagram of aqueous inorganic Cr hydrolysis species based on the study of Ball and Nordstrom (1998) is shown in figure 4-26.

Under oxidising conditions Cr occurs in its hexavalent state (Cr^{VI}). At total Cr concentrations below 10 mM (about 520 mg/L), aqueous Cr is present in an anionic Cr^{VI} form, HCrO₄⁻(aq) at pH <6.5, and CrO₄²⁻(aq) at neutral and alkaline pH (Palmer and others, 1987). Thus, in most oxygenated natural groundwaters chromate (CrO₄²⁻(aq)) is the dominant Cr-species. The presence of the Cr-species HCrO₄⁻(aq) and CrO₄²⁻(aq) in concentrations above 1 mg/L in Cr contaminated waters is recognised by the yellow colour of the water.

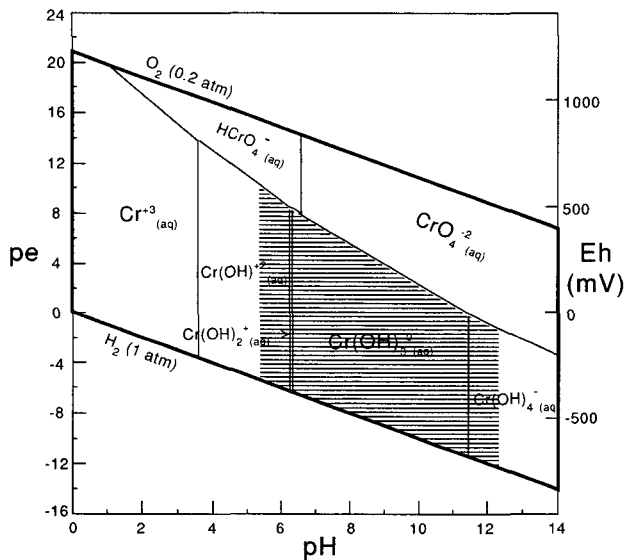


Figure 4-26: Areas of dominance of aqueous inorganic Cr hydrolysis species at equilibrium in the system $Cr + H_2O + O_2$ at standard state conditions (Ball and Nordstrom, 1998). The hatched area indicates the predominance region of $Cr(OH)_{3(cr)}$ at $[Cr_{10}] = 10^{-6} M$ (i.e. 52 µg/L).

Trivalent Cr (Cr^{III}) is the most stable form of Cr under reducing conditions. In dilute waters Cr^{III} forms complexes mainly with hydroxyl. In strongly mineralised waters Cr^{III} -complexes with a variety of ligands occur, including sulphate, ammonium, cyanide, sulphocyanide, fluoride, and chloride (to a lesser extent), well as organic ligands (Bartlett & Kimble, 1976a; Nakayama, 1981a). The most important aqueous Cr^{III} -species occurring in natural groundwaters are listed in table 4-10. The $Cr^{3+}_{(aq)}$ -species prevails only at a pH below 3.6 (figure 4-26). Polymeric species such as $Cr_2(OH)_2^{+4}_{(aq)}$, $Cr_3(OH)_4^{+5}_{(aq)}$, or $Cr_4(OH)_6^{+6}_{(aq)}$ are never significant in natural systems (Rai and others, 1987).

Cr^{VI} species^a:	$HCrO_4^-_{(aq)}$	$CrO_4^{2-}_{(aq)}$		
Cr^{III} species^b:	$Cr^{3+}_{(aq)}$	$Cr(OH)^{2+}_{(aq)}$	$Cr(OH)_3^0_{(aq)}$	$Cr(OH)_4^-_{(aq)}$

Table 4-10: Main aqueous Cr-species in natural groundwaters.

a. Palmer and others, 1987

b. Rai and others, 1987

Solubility of chromium compounds

Hexavalent Cr is considerably more soluble than trivalent Cr. There are no significant solubility constraints on the Cr^{VI} concentration in natural groundwaters. Only at relatively high Cr^{VI} concentrations such as found at contaminated sites, there will be a solubility control by Cr^{VI} -minerals. Therefore, because of their generally high solubility, minerals containing Cr^{VI} are rare in nature. Baron & Palmer (1996a, 1996b, 1998) have identified and described a red chromate analog of the sulphate mineral jarosite ($KFe_3(CrO_4)_2(OH)_6$), and $KFe(CrO_4)_2 \cdot 2H_2O_{(s)}$, a more soluble reddish-yellow precipitate in a soil strongly contaminated by acid chromium-plating solutions. In addition, Rai and others (1988) have suggested that $BaCrO_{4(s)}$ may be an important Cr^{VI} -mineral in soils at Cr-contaminated sites. This mineral forms a continuous solid-solution salt with barite ($BaSO_4$). Further, crocoite ($PbCrO_4$), iranite ($PbCrO_4 \cdot H_2O$) and $K_2CrO_{4(s)}$ salt were found in chromium plating sludge

dumped at a contaminated site, and the yellow chromate (CaCrO₄) occurred at evaporative conditions in a drainage ditch.

In contrary to the highly soluble Cr^{VI}, the low solubility of Cr^{III}-minerals significantly limits the concentration of Cr^{III} in groundwater already under moderately oxidising and under reducing conditions and pH conditions found in most natural aquifers (see figure 4-26). Amorphous Cr(OH)₃ and Cr^{III}-Fe^{III}-hydroxide solid-solutions (Cr_xFe_{x-1}(OH)_{3(am)}) are the main Cr^{III} solubility controlling phases in natural environments (Amonette & Rai, 1990; Ball & Nordstrom, 1999). The solubility of amorphous Cr-Fe-hydroxide solid-solutions increases with increasing amount of Cr^{III} (Sass & Rai, 1987). Direct precipitation of chromite (FeCr₂O₄) from aqueous solutions is not expected at the low temperatures in natural systems (Hem, 1977).

Adsorption and complexation

Anions such as HCrO₄⁻ and CrO₄²⁻ are attracted to positively charged surfaces, such as Fe-hydroxides that commonly coat aquifer materials. Laboratory experiments have shown that at low pH Fe-hydroxides are strong adsorbates of Cr^{VI} (James & Bartlett, 1983; Stollenwerk & Grove, 1985). These substances have a high pH_{PZNPC} (point of zero net proton charge) of 7.3 to 8.5 (see table 1-4 page 14). Adsorption decreases with increasing pH, because of the decrease of positive surface charge of the sorbing substratum, and no adsorption is expected to occur at a pH above 8.5. Based on batch and column experiments with Fe-hydroxide coated sandy alluvium, Stollenwerk & Grove (1985) have found that Cr^{VI} adsorption was strongly non-linear, i.e. fractional adsorption decreased with increasing Cr-concentration, following a Langmuir-type adsorption model. These authors observed that the equilibrium adsorption of Cr^{VI} was achieved within three days during batch tests.

Like other metals, Cr^{III} is rapidly and strongly adsorbed by soil Fe-hydroxides and Mn-oxides, clay minerals and sand (Schroeder & Lee, 1975; Bartlett & Kimble, 1976a). In batch experiments this process has been found to be rapid, about 90% of the added Cr is adsorbed by clay minerals and Fe-oxides after 24 h. The adsorption of Cr^{III} increases with increasing pH and organic matter content of the soil. On the other hand, adsorption decreases with the presence of other inorganic cations or dissolved organic ligands.

Summary

In nature Cr exists as Cr^{VI} and Cr^{III}, which differ greatly in their toxicity and mobility. Under oxidising conditions, Cr prevails in solution in its toxic hexavalent form (CrO₄²⁻). In natural groundwaters Cr^{VI} is moderately to highly mobile due to the lack of solubility constraints and the moderate to low adsorption of the anionic CrO₄²⁻ species by the aquifer material. In contrast, Cr^{III} is subjected to solubility control by amorphous Cr(OH)_{3(am)} and Cr^{III}-Fe^{III}-hydroxide solid-solutions (Cr_xFe_{x-1}(OH)_{3(am)}). Dissolved concentrations of Cr^{III} are generally well below water quality standards. In addition, in neutral to slightly acid groundwaters Cr^{III} is removed from the solution by adsorption on clay minerals and hydroxides. This adsorption process increases with increasing pH.

Hexavalent Cr can be reduced to trivalent Cr in presence of organic matter, dissolved Fe²⁺ from the weathering of Fe^{II}-bearing minerals, or dissolved sulphide. The inverse reaction, the oxidation of Cr^{III} to Cr^{VI}, occurs in presence of oxygen and Mn-oxides contained in the soil. The oxidation of Cr^{III} to Cr^{VI} is considerably slower than the reduction

of Cr^{VI} to Cr^{III} . The reaction rate and amount of Cr oxidation or reduction is highest at low pH and a high ratio of surface area per solution volume.

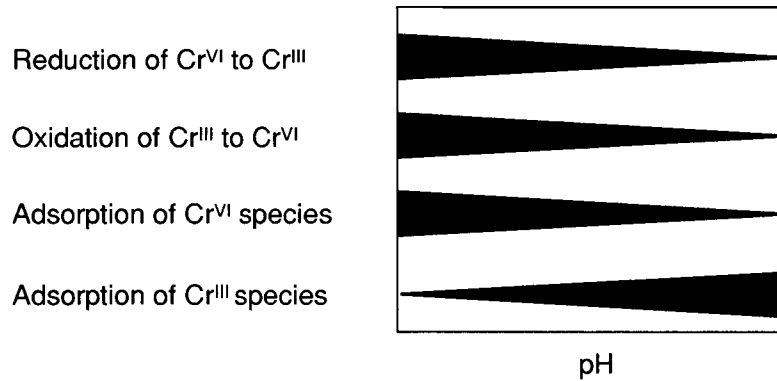


Figure 4-27: Qualitative influence of the solution pH on different processes influencing the mobility of Cr.

4. 6. 4. Chromium in groundwater from the Burdigalian sandstone

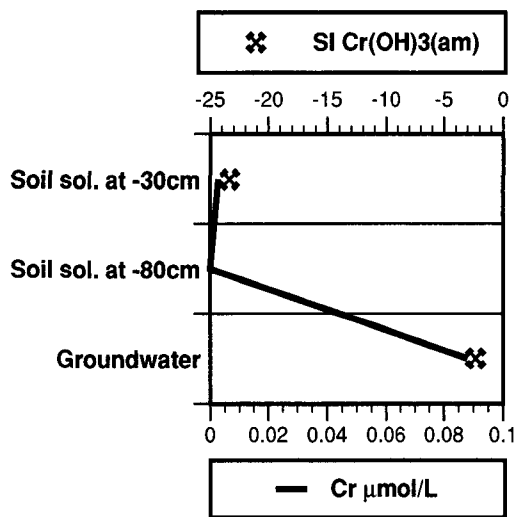


Figure 4-28: Evolution of the dissolved Cr concentration and the saturation state with amorphous Cr-hydroxide from rainwater to groundwater.

In the present chapter, the evolution of Cr and its chemical behaviour in the Lutry springwater are discussed in detail.

At the Lutry site, the Cr-concentrations in the soil solutions at 30 and 80 cm depth are very low compared to the Cr-concentration in the groundwater emerging at the spring (figure 4-28). Chromium is released by the weathering of mafic minerals such as pyroxenes, chlorite, glauconite, biotite, serpentine, and Cr-spinels (see chapter 4. 5. 3. “Chemical evolution of the Lutry springwater” on page 163). Chromite is considered to be the most important Cr-source in the Burdigalian sandstone (see chapter 4. 4. “Chromium in the Burdigalian sandstone” on page 149). The etch pits on the surfaces of chromite, pyroxenes and biotite observed in SEM images prove that these minerals indeed dissolve (see figures 4-8, 4-9, and 4-10). All primary and secondary Cr-bearing minerals occurring in the Burdigalian sandstone and in

the overlying soil contain Cr in its trivalent form.

Despite the important weathering processes releasing Cr in the soil, the Cr-concentrations of the soil solutions are very low compared to the groundwater. This suggests, that higher amounts of Cr are released in the bedrock sandstone and/or that a retention mechanism exists in the soil. Possibilities include:

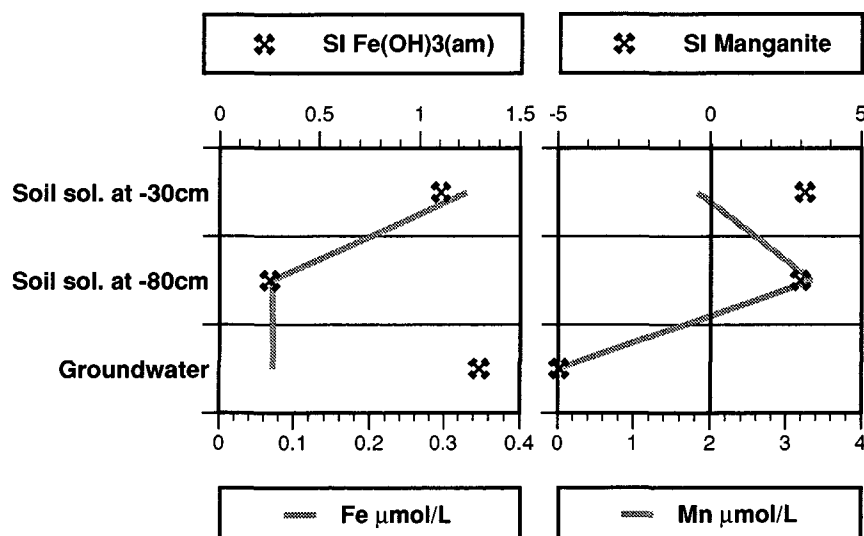


Figure 4-29: Evolution from rainwater to groundwater of the dissolved Fe and Mn concentrations and saturation states with amorphous Fe-hydroxide and manganite.

- 1.) All of the present Cr-bearing minerals have very slow weathering rates. The infiltrating water remains only a short time in the soil before it attains the bedrock (i.e. the time to cover a distance of about 2.5 m), while it remains for an average of 3 to 4 years in the bedrock sandstone before it emerges at the spring. Due to this difference in residence time the Cr concentration in the soil solution remains too small to be detected.
- 2.) In the soil vermiculite is the most important secondary mineral produced by the weathering of mafic silicates including biotite, glauconite, chlorite, and pyroxene. Vermiculite can take up significant amounts of Cr^{III} in its structure. Therefore, the Cr contained in the primary minerals tends to be retained in the weathering residue.
- 3.) The Cr-concentration in the soil solutions is limited by the co-precipitation with secondary Fe-hydroxides: The soil solutions are strongly subsaturated with respect to amorphous Cr-hydroxide, but slightly supersaturated with the less soluble Fe-hydroxide. This suggests that the dissolved Cr^{III} in the soil solutions can co-precipitate with Fe-hydroxides in the form of (Cr^{III},Fe^{III})(OH)₃ solid-solutions.
- 4.) Adsorption on clay minerals and hydroxides limits the dissolved Cr concentration in the soil solutions.

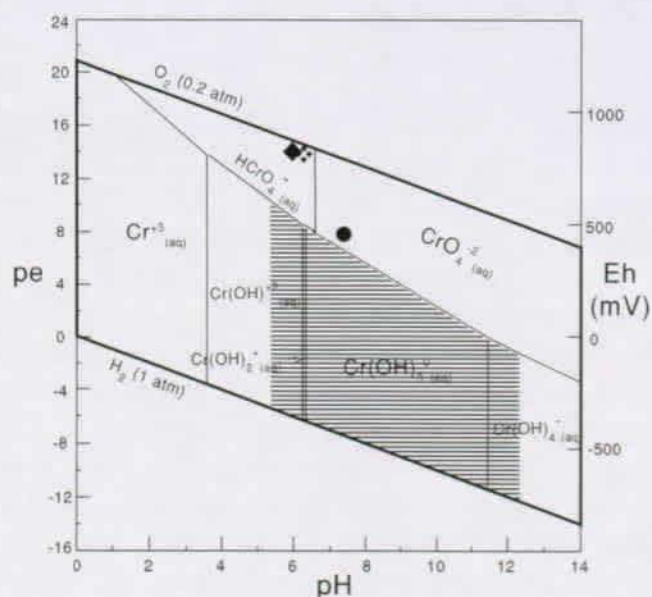
The residual enrichment of Cr in the soil and in the marly layers of the sandstone indicates that during the weathering of primary Cr-bearing minerals part of the Cr may be incorporated in secondary clay minerals such as vermiculite or montmorillonite.

The soil solutions and the groundwater are subsaturated with amorphous Cr-hydroxide, indicating that the precipitation of this secondary Cr-mineral does not limit the dissolved Cr-content in the groundwater. Nevertheless, co-precipitation with Fe-hydroxides can occur. The dissolved Fe-concentration decreases strongly from the soil solution to the groundwater (see figure 4-29) and the soil and the weathered parts of the bedrock sandstone show the typical rusty colour of Fe-hydroxides. This indicates that Fe-hydroxide phases are important

secondary minerals in addition to clay minerals. The Cr-bearing minerals always contain Fe, which partly precipitates as Fe-hydroxide, and partly becomes incorporated into clay minerals.

In addition to the incorporation into secondary clay minerals and Fe-hydroxides, Cr^{III} is also adsorbed onto clay minerals. Dzombak and Morel (1990) have shown that at a pH above 5.5 dissolved Cr³⁺ becomes completely adsorbed.

After all these Cr retention processes, practically no dissolved Cr should be contained in the groundwater. However, at the pH and redox conditions prevailing in the soil solutions and in the groundwater, the Cr^{III} liberated by mineral alteration can be oxidised to Cr^{VI} (see figure 4-30). Hexavalent Cr is much more soluble than trivalent Cr and in natural aquifers no minerals occur that limit the Cr^{VI} concentration. It has been shown that Cr^{III} oxidation to Cr^{VI} is enhanced by an acid pH and the presence of Mn-oxides (see chapter 4. 6. 3. "Aqueous geochemistry of chromium" on page 173). Such conditions are present in the soil at the Lutry site. The soil solutions are slightly acid and Mn-oxides seem to be produced readily in the lower soil levels from the precipitation of dissolved Mn. The median dissolved Mn concentrations in the soil solutions are as high as 184 µg/L, while in the groundwater the Mn concentration is near the detection limit (figure 4-29). As the groundwater penetrates the carbonate-bearing bedrock the pH rises and all the dissolved Mn precipitates. An oxidant for Cr^{III} is thus produced. Due to the oxidation of Cr^{III} to Cr^{VI} the Cr^{III} activity in solution becomes very low, which explains the subsaturation with amorphous Cr^{III}-hydroxide.



✧ Soil solution at -30 cm
 ◆ Soil solution at -80 cm
 ● Groundwater

Figure 4-30: pH and redox conditions of the average soil solutions and groundwater of the Lutry site plotted in the pH-EH diagram for Cr (after Ball and Nordstrom, 1998; see figure 4-26)

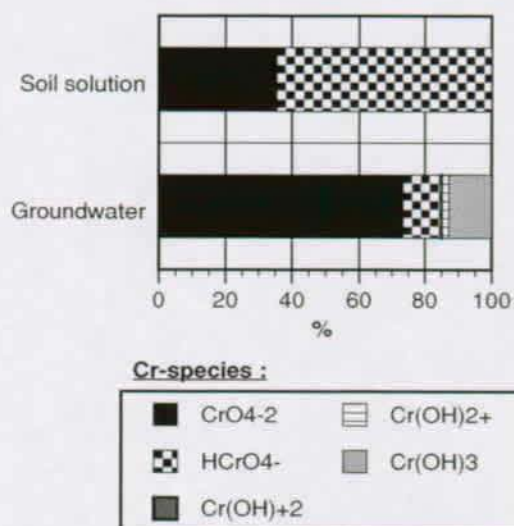


Figure 4-31: Results of speciation calculations of dissolved Cr in soil solution and groundwater.

Speciation calculations indicate, that at equilibrium conditions the dissolved Cr is indeed present in its toxic hexavalent form (figure 4-31): In the soil solutions dissolved Cr is mainly present as HCrO_4^- , while in the groundwater it is predominantly present as CrO_4^{2-} , due to the higher pH.

At a pH of 6.0 or less reigning in the soil solutions, even the anions HCrO_4^- and CrO_4^{2-} may partly get adsorbed onto Fe-hydroxide phases (Stumm & Morgan, 1996). Stollenwerk & Grove (1985) found that equilibrium adsorption of Cr^{VI} was achieved within 3 days during batch tests. This is probably sufficient to allow local equilibrium to be established in the soil. So even if Cr^{III} is oxidised to Cr^{VI} , the Cr concentration will be limited by adsorption. On the other hand, at the neutral to alkaline pH prevailing in the groundwater the adsorption of Cr^{VI} is

moderate to low. Anion adsorption characteristically decreases with increasing pH because of the decrease in positive charge of the sorbing medium. As the infiltrating solution reaches the decarbonation front, the dissolution of carbonate minerals causes the pH to rise. Therefore the adsorption of Cr^{VI} is lower in the carbonate-bearing sandstone than in the soil.

Considering all of these mechanisms the observed strong Cr-increase between the soil solution and the groundwater can be explained by the longer residence time of the water in the bedrock sandstone than in the soil, and by the absence of retention processes in the bedrock sandstone: In the soil, dissolved Cr^{VI} is partly retained by adsorption on Fe- and Mn-hydroxides due to the low pH. In contrary, in the bedrock sandstone, no adsorption of dissolved Cr^{VI} occurs due to the higher pH buffered by the dissolution of carbonate minerals.

4.7. Leaching experiments

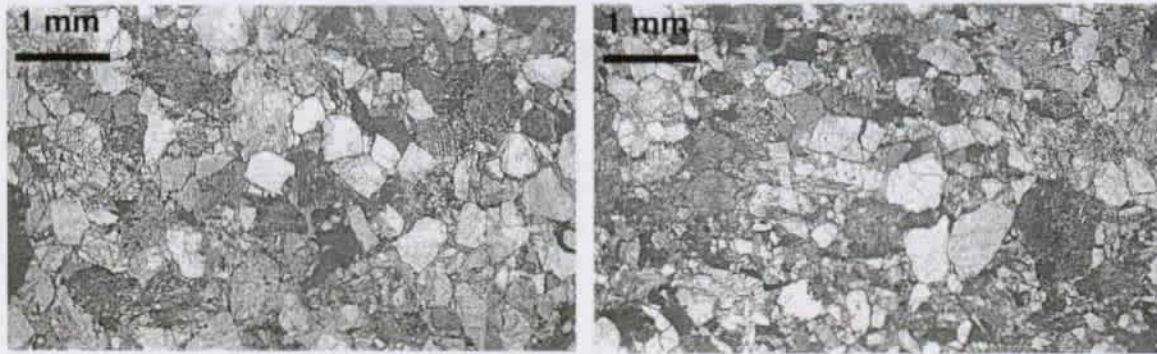
Column experiments have been carried out with Burdigalian molasse sandstone from the field site, in order to support the field study findings. These experiments were aimed to further identify and quantify the processes responsible for the Cr mineralisation and the overall geochemical evolution observed in the Lutry groundwater. The leaching experiments have been designed to determine the contribution of the bedrock sandstone to the chemical groundwater composition under natural conditions as a function of time. Under laboratory conditions the physical-chemical parameters including flow, P_{CO_2} , and pH can be better controlled than in the field, thus making the investigation of the chemical interactions between the substratum and the solution easier. These experiments can thus be used as an additional constraint on the geochemical evolution of the groundwater derived for the Lutry catchment, which allows to improve the knowledge of the relevant processes in the system.

The P_{CO_2} and pH in the experiment were adjusted in order to simulate the natural conditions as closely as possible. The setup allowed to measure physical-chemical parameters such as electric conductivity, pH, and redox potential during the experiment, and to take repeated samples for chemical analysis. The leaching experiments were conducted in a system with circular solution flow from the reservoir into the column with the sand substratum and back into the reservoir. In the reservoir the solution was constantly re-equilibrated with a P_{CO_2} of $10^{-2.0}$ (open system), representing soil conditions. The chemical evolution of the solution percolating repeatedly through the substratum has been studied. With this experimental setup the chemical weathering near the top of the bedrock sandstone is simulated.

Two experiments with mountain-wet oxidised and reduced sandstone from the field site were carried out over a time span of 2 months each, to obtain information about the influence of the alteration state of the substratum. The comparison of rock and water analytical data of both experiments allowed to identify the processes responsible for the mobilisation (desorption/mineral dissolution) and retardation (adsorption/mineral co-precipitation) of Cr.

4.7.1. Substratum

In the leaching experiments Burdigalian sandstone in its reduced and oxidised state was used as substratum. The two sandstone varieties were collected within the saturated zone of the aquifer in the Pierre-Ozaire gallery chapter "Bedrock sandstone" on page 137.



1.) Oxidised (yellow), Fe-hydroxide coated sandstone 2.) Reduced (bluish) sandstone.

Both sandstone samples have a similar grain-size distribution. The median grain-size is 0.4 mm, and the fine fraction (<63 µm) determined by dry sieving, makes up about 5.5 wt.% in the reduced sandstone and 4.5 wt.% in the oxidised sandstone (figure 4-32).

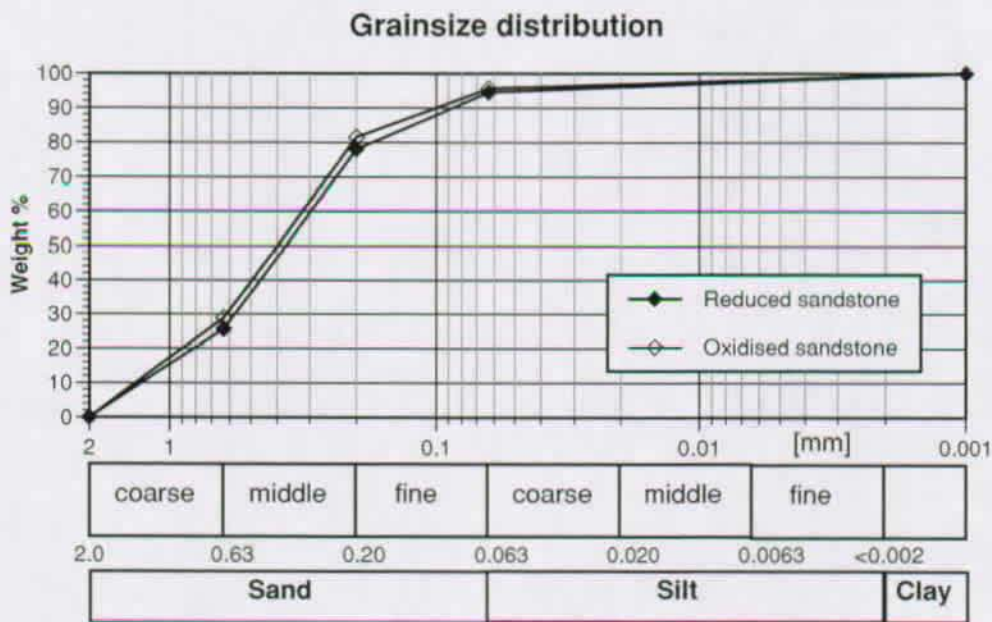


Figure 4-32: Grain-size distribution of the reduced and oxidised sandstone used in the leaching experiments determined by dry sieving.

The mineralogic composition of the samples is summarised in table 4-11 and the chemical composition is given in appendix F. The primary mineralogy (detrital and diagenetic minerals) is similar in both samples (see chapter 4. 3. 1. “Mineralogy” on page 142). However, X-ray diffraction analyses showed that the oxidised sandstone is slightly more decarbonated and contains a higher sheet-silicate content and a different clay mineralogy compared to the reduced sandstone. Particularly the proportion of montmorillonite is higher in the oxidised sandstone (see table 4-11). The higher sheet-silicate content of the oxidised sandstone can be explained by the stronger argillitisation of feldspars, mica, and mafic minerals observed in thin-section. These

secondary clay minerals contained within the larger detrital grains contribute to the total sheet-silicate content, but do not appear in the grain-size analysis. The higher content of montmorillonite in the oxidised sandstone is thus due to the stronger alteration of primary silicate minerals.

In contrast to the reduced sandstone the detrital grains of the oxidised sandstone are coated with Fe-hydroxides giving the rock its characteristic yellow colour. Both the oxidised and the reduced sandstone have a total Fe content of 0.66 wt.%. Assuming that in the oxidised sandstone all Fe would be present as Fe-hydroxide, this would yield a maximum Fe-hydroxide content of 1.3 wt.% of the bulk rock. This number, however, is certainly too high, because remnants of detrital Fe-bearing phases and Fe-bearing newly formed secondary phases such as montmorillonite are still present in the oxidised sandstone. Therefore, the Fe-hydroxide content is very small (<1 wt.%).

Bulk mineralogy			Clay mineralogy		
Minerals (weight%)	Oxidised sandstone	Reduced sandstone	Minerals (relative amounts,%)	Oxidised sandstone	Reduced sandstone
Quartz	38	42	Montmorillonite	90	40
K-Feldspar	9	13	Illite	5	30
Plagioclase	26	25	Chlorite	5	30
Calcite	6	9			
Dolomite	(0.9)	(0.2)			
Sheet silicates ^a	19	8			
Heavy minerals ^b	<1	<1			

Table 4-11: Bulk mineralogy (weight%) and clay mineralogy (relative amounts in percent) of the sandstones used in the leaching experiments determined by X-ray diffraction analysis. The values in brackets are qualitative.

- a. Sheet silicates include clay minerals (montmorillonite, illite, and chlorite), glauconite, biotite, white mica, and traces of serpentine
- b. Heavy minerals include epidote, pyroxenes, amphiboles, spinels (magnetite and chromite), apatite, and minor amounts of sphene, zircon, and rutile

4.7.2. Experimental method

The following procedure was developed for sample preparation and the packing of the columns with the sand substratum.

A sufficient quantity (5 to 8 kg) of mountain-wet oxidised and reduced sandstone was disaggregated with a plastic hammer and sieved through a 2 mm screen to remove coarse particles and rock debris. The sand was then homogenised to obtain representative samples. From the moment of sampling all rock material prepared for the column experiments was stored in plastic bags in a humid chamber, to prevent clay minerals, particularly the montmorillonite, from drying and shrinking. A subsequent swelling of the clay minerals within the column is thus minimised, which is important to prevent clogging of the column. In addition, filling the column with mountain-wet material prevents stratification of the

substratum within the column, because the fine-grained fraction sticks to the larger grains, thus allowing a homogeneous packing.

A borosilicate glass column of 50 cm length and 2.5 cm diameter was used. The adjustable end pieces were equipped with teflon filters (70 μm pore size). To pack the column, one of the end pieces was twisted half into the column to have enough space for later adjustments. Then, 300 g of wet sand was filled into the column in small portions and slightly compacted with a stick. The top of the column was plugged with the second end piece, and the top plug was lowered onto the sand. No further column conditioning was made, as the experiments need to start with the first passage of the solution through the column. This means, that the hydraulic column parameters can only be determined in a separate run.

The leaching experiments were conducted in a closed system with circular solution flow (see set-up scheme in figure 4-33), where the solution is pumped upwards through a glass column filled with approximately 300 g of sand substratum and back into the reservoir bottle. In this way the solution gets more and more concentrated in ions leached from the substratum. The leaching experiments were performed at laboratory temperature (20 to 22°C, air-conditioning) and under a constant CO_2 partial pressure of approximately 1%.

The solutions were pumped through the column with a HPLC pump (Dionex DQP-1) at a flow rate of about 4.5 ml/min. The use of a HPLC pump has the advantage that the flow rate is maintained constant, because this type of pump compensates for an eventual pressure increase in case of slight clogging.

The length of the connecting tubes (Teflon) and the volume of the flow through cells (adapted in size) were kept as small as possible in order to minimise dead volume and resulting delay. The total dead volume was approximately 40 ml.

One litre of high purity water (Millipore®) has been used as an elution solvent. The solvent volume of 1 litre was chosen in order to be as small as possible to obtain sufficient concentrations of dissolved ions (especially trace elements) for analysis and large enough to allow sampling without disturbing the system too much. During the experiment, the solution contained in a 2 L PE reservoir bottle was homogenised with a magnetic stirrer. In order to simulate a P_{CO_2} in the reservoir atmosphere similar to that occurring in the soil, the solution was kept under a gas atmosphere containing 10% CO_2 and 90% N_2 at an over-pressure of approximately 0.1 bar. In this way, a constant P_{CO_2} of $10^{-2.0}$ bar, i.e. 1% CO_2 , is maintained in the reservoir.

Three subsequent flow-through cells (glass) at the column outlet were equipped with measuring electrodes for periodical measurements of electric conductivity, pH, temperature and redox potential of the solution. The electric conductivity was measured with a WTW LF 340 apparatus, the pH with a WTW 197-S apparatus with a Ag/AgCl pH electrode, and the redox potential with a WTW pH 340 apparatus with a Ag/AgCl reference electrode. After the measurements the flow-through cells were emptied and by-passed.

Before the experiment is started, the system with connected measuring electrodes was rinsed with Millipore water during one hour. Then, before connecting the sand-filled column, the Millipore water used as solvent was out-gassed by ultrasonic treatment during 10 minutes, and the reservoir bottle was connected to the gas pressure bottle to allow the solution to equilibrate with the gas phase.

The column output solution was sampled through a three-way valve in 15 ml PE tubes. During sampling, the flow rate was measured for control. The samples for chemical analysis were filtered immediately with a syringe equipped with a 0.45 μm Teflon filter and subsequently stocked in the refrigerator until analysis. The sampling tubes and filter device were previously rinsed with Millipore water.

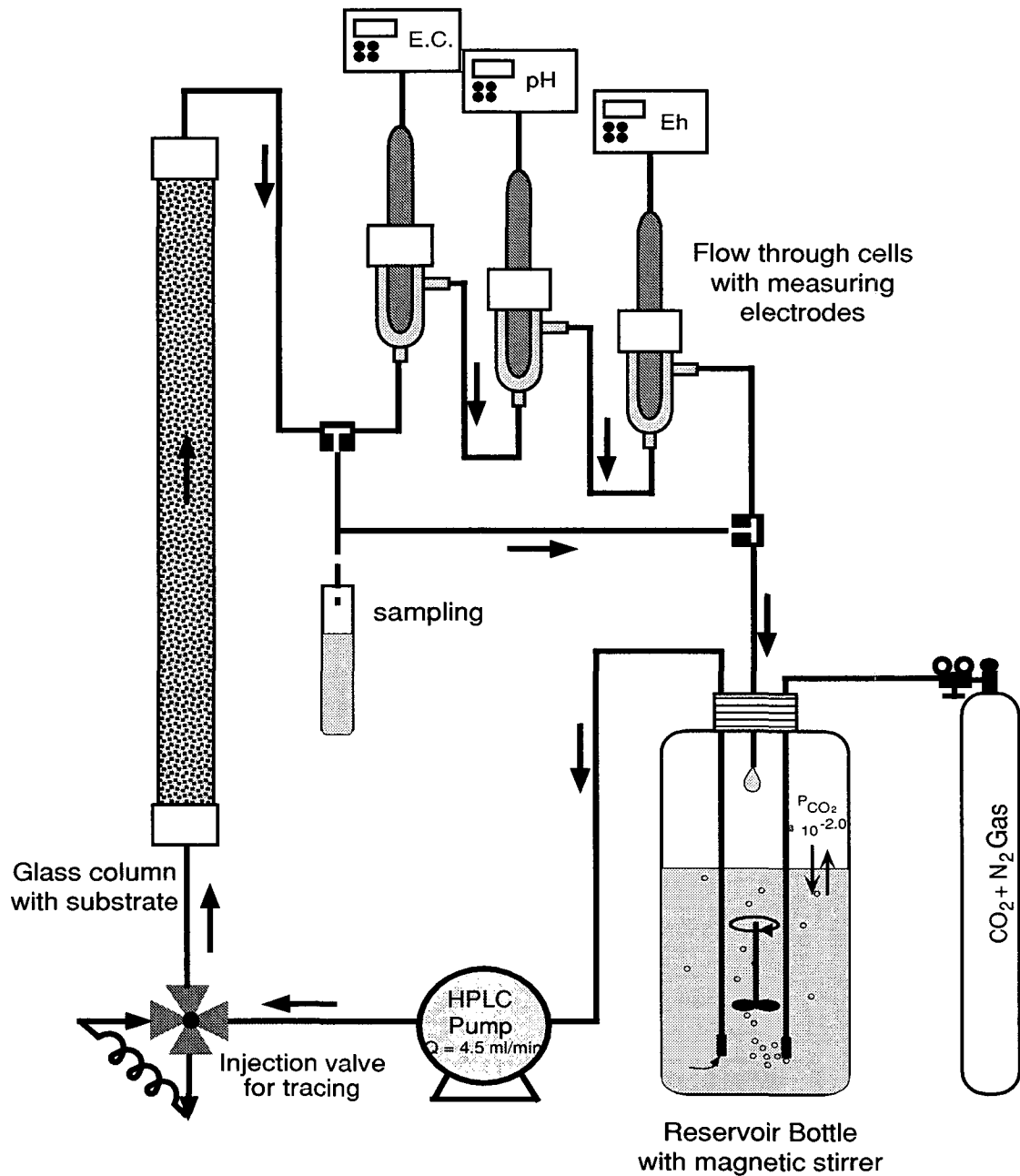


Figure 4-33: Experimental setup.

Alkalinity was determined immediately after sampling by titration with HCl 0.1 mol to a pH of 4.3. Alkalinity was not analysed in every sample, because this analyse needs at least 20 ml of solution to obtain an accurate result. For the other samples the alkalinity was calculated using charge balance considerations. Major cations and anions (Mg^{2+} , Ca^{2+} , Na^+ , K^+ , F^- , Cl^- , NO_3^- , SO_4^{2-}) were analysed by ion chromatography. The samples for trace elements were acidified with HNO_3 supra-pure 65% to a pH 2 and stored in the refrigerator ($4^\circ C$) until analysed by HR-ICP-MS (see chapter 2. 1. 4. "Laboratory analytical methods" on page 28).

Column characteristics

Column characteristics such as the porosity of the substratum and the average residence time of the solution in the column are used to determine the volume of solution circulating through the substratum during the leaching experiments. The standard deviation of the break through curve and the dispersivity and Peclet number (Pe) give additional information about the flow conditions. The dimension-less Peclet-number depends on the length and diameter of the column, the grain-size distribution of the substratum and the dispersivity. The higher the dispersivity in the column, the smaller is Pe.

In a chromatographic column the transport of a substance through a water-saturated porous substratum can be described by the convection-dispersion equation (4.9) of Villermaux (1981). This formula applies for conservative tracers that do not undergo any interaction with the substratum and therefore migrate with the same velocity as the solution.

(4.9)

$$\frac{\partial c_{\text{tot}}}{\partial t} = D \frac{\partial^2 c}{\partial x^2} - v \frac{\partial c}{\partial x}$$

where c_{tot} = total concentration of the dissolved substance [g/L]
 c = concentration of the substance in solution [g/L]
 t = time [s]
 x = distance in travelling direction [m]
 v = pore flow velocity [m/s]
 D = dispersion coefficient [m²/s]

The column characteristics were determined in four tracer test runs with the same sand substratum as used for the leaching experiments. A pulse of NaCl solution was injected as conservative tracer. The tracer peak was monitored by continuously recording the electric conductivity at a time interval of 30 seconds. On-line data acquisition was carried out using a NB-MIO-16L ADC board (National Instruments) and a home-made LabView program. The results of the four tracer tests are shown in table 4-12.

The porosity of the substratum in the column is about 0.5, with a total pore volume of approximately 100 ml. The pore volume and porosity calculated from the flow rate are larger than the pore volume and porosity calculated from the substratum density. This is due to the fact that the pore volume determined from the flow rate also includes the dead volume in the measuring cell. In the four tests similar porosity values were obtained indicating a good reproducibility of the column packing and allows to extrapolate the column characteristics determined in these tests to the leaching experiments. A Peclet-number of about 60 was obtained for the present setup.

In the experiment the porosity of the substratum in the column is 2.3 to 3.3 times higher than the matrix porosity of undisturbed sandstone in the field (matrix porosity = 0.15 to 0.21). This indicates that in the experiment a larger amount of solution gets in contact with the substratum than in undisturbed sandstone in the field. The ratio of substratum surface per solution volume is thus smaller than in the undisturbed sandstone in the field. In the field, however, groundwater flow takes place not only through the matrix porosity, but also through the secondary porosity, i.e. through fissures and joints, thus decreasing the rock surface per solution volume. The hydraulic conditions in the experiments are therefore presumed to be fairly well comparable to the field conditions.

Column Parameters	Formula	Unit	Test 1	Test 2	Test 3	Test 4	Average
Tracer solution (NaCl) total concentration	C_{tot}	g/L	10	20	20	20	
Measuring interval	dt	s	30	30	30	30	30
Column length	L	cm	40.5	40.5	38.8	38.5	39.6
Column section	A	cm ²	4.91	4.91	4.91	4.91	4.91
Flow	Q	ml/min	4.43	4.43	4.39	4.45	4.43
substratum mass	m_s	g	272	272	258	270	268
substratum density	ρ_s	g/cm ³	2.76	2.76	2.76	2.76	2.76
mean residence time	$t_m = \sum t_i C_i / \sum C_i$ ^a	s	1747	1475	1590	1402	1553
mean residence time	t_m	min	29	25	27	23	26
Variance	$\sigma^2 = \sum t_i^2 C_i / \sum C_i - t_m^2$	s ²	84815	62768	104424	80225	83058
Standard deviation of the breakthrough-curve	σ	s	291	251	323	283	287
Peclet number Pe	$Pe = 2 (t_m / \sigma)^2$ or Lv/D	-	72	69	48	49	60
Pore flow velocity	$v = L / t_m$	cm/min	1.4	1.7	1.5	1.7	1.5
Total column volume	$V_{\text{tot}} = A L$	ml	199	199	191	189	194
Pore volume determined by flow	$V_{\text{PQ}} = Q t_m$	ml	129	109	116	104	115
Pore volume determined by density	$V_{\text{Pd}} = V_{\text{tot}} - (m_s / \rho_s)$	ml	100	100	97	91	97
Porosity determined by flow	$\Phi_Q = V_{\text{PQ}} / V_{\text{tot}}$	-	0.65	0.55	0.61	0.55	0.59
Porosity determined by density	$\Phi_d = V_{\text{Pd}} / V_{\text{tot}}$	-	0.50	0.50	0.51	0.48	0.50
Dispersion coefficient	$D = L v / Pe$	-	0.78	0.96	1.17	1.30	1.05
Dispersivity	$\lambda = D / v \cdot 10$	mm	5.63	5.84	8.02	7.86	6.84

Table 4-12: Column characteristics: results of four tracer experiments.

a. $C_i =$ concentration as a function of time

Experimental artefacts

During the different leaching experiments carried out over a time span of two years, the experimental setup has been improved strongly. Nevertheless, different experimental artefacts could not be eliminated completely.

In the first tests the physical-chemical parameters such as pH, redox potential, electric conductivity and temperature were measured in-line and recorded continuously with a LabView program. In this setup a contamination with KCl from the pH-electrode occurred, because the measuring electrodes remained in contact with the solution during the whole experiment. A blank test carried out using the same setup and measuring electrodes but without the sand substratum confirmed the origin of the high K^+ and Cl^- concentrations found in solution (figure 4-34).

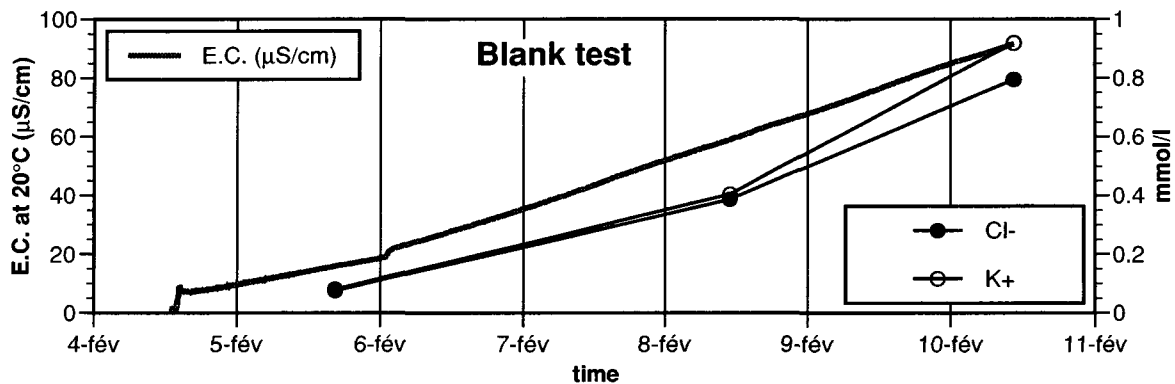


Figure 4-34: Results of a blank-test using the same experimental setup and measuring electrodes as in the leaching experiments but without substratum indicating K and Cl input from the pH-electrode.

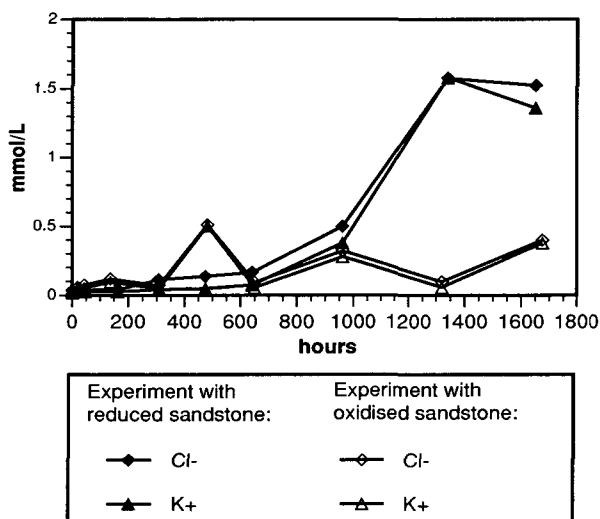


Figure 4-35: Contamination with KCl from the pH electrode occurring in the leaching experiments with reduced and oxidised sandstone.

After this, the setup was changed and the physical-chemical parameters were measured periodically during sampling. In this way the contamination by the pH-electrode was reduced considerably, but not excluded completely. The relatively elevated K^+ and Cl^- concentrations and their good correlation in the first leaching experiment carried out with the reduced sandstone indicate, that a small contamination still occurred (figure 4-35). Therefore, in the experiment with the oxidised sandstone carried out afterwards, the pH was measured even less often, which allowed to further reduce this contamination (figure 4-35). Due to this contamination problem, the K^+ and Cl^- values are not used in the interpretation of the leaching experiments.

The concentrations in milliequivalents of K^+ and Cl^- make up between 2% of the solution mineralisation in the first samples (least polluted) and 30% in the last samples (most polluted). In the first samples the effect of the KCl contamination on other rock-water reactions by increasing the ionic strength of the solution can therefore be neglected. In addition, both K^+ and Cl^- are nearly conservative tracers, and do not react with other dissolved elements.

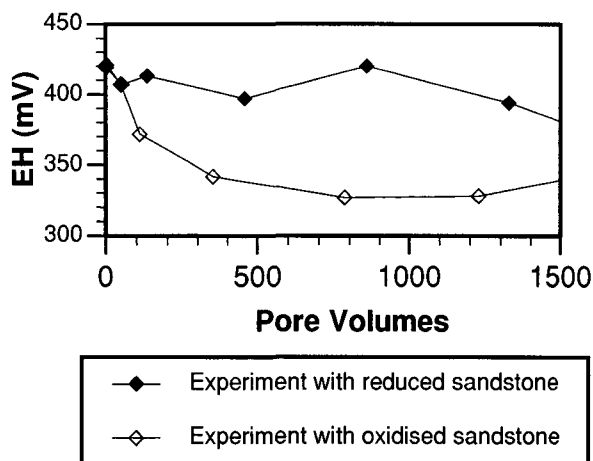


Figure 4-36: Decrease of the redox potential resulting from the presence of oxygen consuming micro-organisms.

the species distribution and saturation state of the solutions with this lowered redox potential, conditions are simulated that are not observed in nature. Therefore, only the first E_H measurement is used for these calculations.

Another problem has occurred due to leakages in the HPLC pump and resulting loss of solution. The leaching experiments with the oxidised and reduced sandstone substratum were carried out with 1 litre of solution over a time span of 2 months each. During this time span, 10 samples were taken in each experiment: 5 samples of 35 ml for a complete analysis of major and trace elements and 5 samples of 15 ml for major and trace element analysis without alkalinity. Thus a volume of 250 ml of solution has been removed by sampling. However, after the two months time significantly less than 750 ml solution were left due to losses of solution in the pump (see figure 4-38).

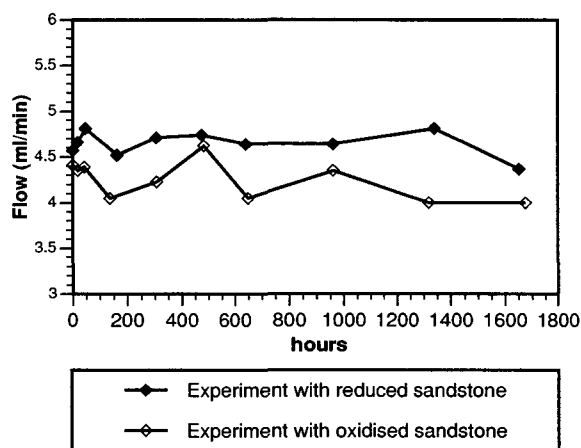


Figure 4-37: Evolution of the flow rate with time, showing that a fairly constant flow rate has been attained by using a HPLC pump.

the true increase of dissolved ions by reactions with the sand substratum, but to the concentration effect resulting from the leakage.

The use of mountain-wet sand substratum without further treatment and the storage in a humid chamber of over a year has caused an artefact in the evolution of the redox potential, which is probably related to the presence of micro-organisms (see figure 4-36). Particularly during the long-term experiment with the oxidised sandstone, it is believed that the presence of micro-organisms lead to a slight decrease of the redox potential due to the consumption of dissolved oxygen. In the end of this experiment local growth of algae has been observed in the sand substratum. The E_H measurements in this experiment are therefore unreliable except for the first one. When calculating

This problem is probably related to an over-pressure resulting from slight clogging of the filters at the outflow of the column. By using a HPLC pump the flow rate is maintained constant, because this type of pump compensates for eventual pressure increases (see figure 4-37). However, due to the high amount of clay minerals in the substratum the pressure became too high and solution escaped drop-wise through the security valve of the pump. The consequence of this leakage is that the increase in the solution mineralisation occurs step-wise after each loss (see figure 4-38). Therefore, the increase of the solution mineralisation during the last two thirds of the experiment does not correspond to

After the long-term experiment with the reduced sandstone the pump has been repaired and in the experiment with the oxidised sandstone the leakage problem could almost be prevented. An attempt has been made to reconstruct the solution volume from the observed solution losses at the pump and the resulting step-wise increase of the electric conductivity. The result is shown in figure 4-38.

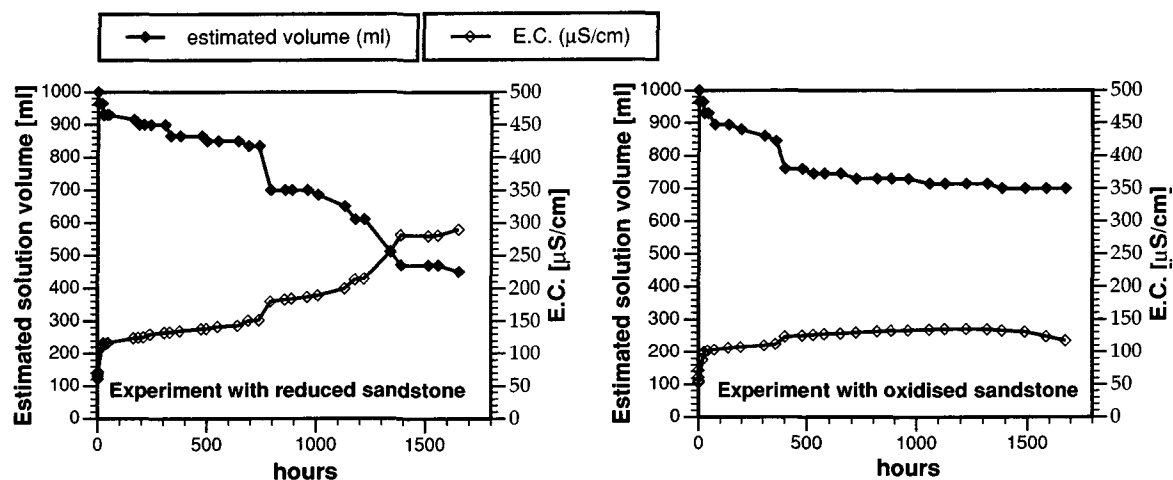


Figure 4-38: Estimated volume of solution and electric conductivity measured during the experiments. The evolution of these two parameters suggests that the step-wise increase of the electric conductivity is due to the losses of solution which occurred in the pump.

Due to these experimental artefacts, only the first 500 hours of the experiments corresponding to the percolation of approximately 1400 pore volumes of solution through the substratum are used for further interpretation. During this time span the volume decrease due to sampling and the resulting concentration effect are relatively small. In order to calculate saturation states of the solutions, which correspond to the true conditions in the experiments, the measured element concentrations have not been corrected for this small concentration effect.

4.7.3. Results

The chemical compositions of the solutions sampled during the experiments with reduced and oxidised sandstone are listed in table 4-13 and table 4-14.

Leaching experiment with reduced Burdigalian sandstone											
Parameter	Unit	1	2	3	4	5	6	7	8	9	10
Date		30.3.99	31.3.99	1.4.99	6.4.99	12.4.99	19.4.99	26.4.99	10.5.99	26.5.99	7.6.99
Time		15:15	9:15	14:40	10:45	9:45	10:30	8:45	16:15	11:00	11:00
Flow rate	ml/min	4.57	4.66	4.81	4.52	4.71	4.74	4.64	4.64	4.81	4.37
E.C.	µS/cm	70	109	117	124	133	138	143	187	256	290
E _H	mV	419	407	413	397	420	394	359	337	417	373
pH	pH-units	8.9	8.4	8.2	8.2	8.2	8.1	8.1	7.9	7.6	7.5
Alkalinity as HCO ₃ ⁻	mg/l	47.3	70.9	n.a.	n.a.	83.9	n.a.	n.a.	n.a.	n.a.	177.0
HCO ₃ ⁻ calc ^a	mg/l	41.2	67.7	76.7	65.0	91.7	107.2	106.3	131.3	198.8	230.4
Cl ⁻	mg/l	1.3	1.2	1.4	1.4	4.0	4.8	5.9	17.7	55.8	54.0
F ⁻	mg/l	0.3	0.3	0.4	0.4	0.3	0.5	0.5	0.4	0.3	0.4
SO ₄ ²⁻	mg/l	9.5	4.6	4.7	4.5	2.4	4.0	3.8	4.8	5.6	7.8
Ca ²⁺	mg/l	12.1	18.2	20.7	17.6	24.1	29.2	28.9	36.3	52.3	64.5
Mg ²⁺	mg/l	3.8	4.2	4.6	4.0	5.1	5.9	5.9	7	9.3	11.1
Sr ²⁺	mg/l	0.906	0.146	0.150	0.160	0.165	0.168	0.171	0.224	0.298	0.340
Na ⁺	mg/l	1.9	0.7	0.7	0.6	1.6	1.6	1.6	1.6	2.0	2.0
K ⁺	mg/l	0.9	1.1	1.0	1.0	1.6	1.9	2.9	14.8	61.7	53.2
Si total	(mg/l)										5.5
Li total	µg/l	3.6	2.4	2.2	2.3	2.9	3.3	3.0	3.1	4.0	5.1
Rb total	µg/l	1.4	1.4	1.7	1.8	2.4	2.4	2.5	4.3	6.1	7.3
Ba total	µg/l	8.8	9.2	13.6	13.9	15.5	10.9	14.9	25.7	42.4	48.5
Al total	µg/l	15.9	15.1	13.9	12.3	12.6	12.3	11.3	10.5	7.6	7.7
Cr total	µg/l	0.6	0.2	0.2	0.2	0.2	0.4	0.4	0.7	0.4	0.5
Mn total	µg/l	0.6	0.3	0.3	0.9	<0.2	<0.2	<0.2	<0.2	0.4	0.4
Fe total	µg/l	2.5	0.8	0.8	1.5	1.1	<1	<1	1.2	1.4	<1
Co total	µg/l	<0.2	<0.2	<0.2	<0.2	<0.2	<0.2	<0.2	<0.2	<0.2	<0.2
Ni total	µg/l	0.7	0.3	0.4	0.4	0.4	0.4	0.5	0.5	0.7	0.7
Cu total	µg/l	2.8	0.2	0.2	<0.2	<0.2	0.2	<0.2	<0.2	<0.2	<0.2
Zn total	µg/l	3.1	2.6	1.7	1.9	1.3	1.6	1.8	1.8	1.9	1.6
Mo total	µg/l	0.8	0.5	0.7	0.6	0.8	0.7	0.8	0.7	0.8	0.7
Cd total	µg/l	<0.2	<0.2	<0.2	<0.2	<0.2	<0.2	<0.2	<0.2	<0.2	0.22
Pb total	µg/l	0.4	<0.2	<0.2	0.2	0.3	0.2	0.4	1.6	6.4	4.2
U total	µg/l	0.2	<0.2	<0.2	0.2	0.3	<0.2	0.2	0.3	0.6	0.4
As total	µg/l	5.1	1.7	1.8	1.9	1.6	1.6	1.5	1.3	1.0	0.8

Table 4-13: Chemical composition of the solution sampled during the leaching experiment with the reduced sandstone (n.d. = not detected; n.a = not analysed).

a. charge balance

Leaching experiment with oxidised Burdigalian sandstone											
Parameter	Unit	1	2	3	4	5	6	7	8	9	10
Date		15.6.99	16.6.99	17.6.99	21.6.99	28.6.99	5.7.99	12.7.99	26.7.99	10.8.99	24.8.99
Time		16:15	10:30	10:15	8:50	11:00	17:15	17:35	17:00	15:35	11:00
Flow rate	ml/min	4.41	4.35	4.39	4.05	4.23	4.62	4.05	4.35	4.00	4.00
E.C.	µS/cm	61	88	102	106	110	125	129	134	135	118
E _H	mV	421	407	372	342	327	328	346	339	334	324
pH	pH-units	8.7	8.4	8.2	8.2	8.1	8.0	7.9	7.9	7.9	7.8
Alkalinity as HCO ₃ ⁻	mg/l	35.1	56.4	65.6	n.a.	71.7	n.a.	n.a.	n.a.	n.a.	74.7
HCO ₃ ⁻ calc ^a	mg/l	34.9	53.8	62.2	63.5	77.5	87.9	88.5	78.1	90.3	82.4
Cl ⁻	mg/l	0.5	2.0	2.6	4.1	2.5	18.2	3.3	11.3	3.4	14.1
F ⁻	mg/l	0.5	0.3	0.3	0.4	0.4	0.2	0.4	0.3	0.4	0.4
SO ₄ ²⁻	mg/l	n.d.	n.d.	n.d.	n.d.	n.d.	n.d.	n.d.	n.d.	n.d.	n.d.
Ca ²⁺	mg/l	8.5	15.0	17.4	17.8	21.7	23.9	25.0	22.1	25.6	22.6
Mg ²⁺	mg/l	1.2	1.7	2.0	2.0	2.4	2.7	2.8	2.5	2.9	2.5
Sr ²⁺	µg/l	0.091	0.091	0.146	0.150	0.150	0.160	0.165	0.168	0.171	0.224
Na ⁺	mg/l	2.7	1.2	1.2	1.2	1.4	1.8	1.3	1.2	1.3	1.6
K ⁺	mg/l	0.7	1.9	2.0	3.7	1.8	19.7	2.1	10.9	2.2	14.9
Si total	(mg/l)										2.8
Li total	µg/l	1.0	1.1	1.6	1.7	1.4	1.9	2.3	2.1	2.2	1.6
Rb total	µg/l	1.4	1.4	1.4	1.7	1.7	1.8	2.4	2.4	2.5	4.3
Ba total	µg/l	8.8	8.8	9.2	13.6	13.6	13.9	15.5	10.9	14.9	25.7
Al total	µg/l	20.7	11.6	10.0	8.4	8.3	9.2	9.5	7.8	8.8	8.6
Cr total	µg/l	0.7	0.7	0.6	0.6	0.9	1.2	1.4	1.3	1.8	1.6
Mn total	µg/l	<0.2	<0.2	<0.2	<0.2	<0.2	<0.2	<0.2	<0.2	<0.2	<0.2
Fe total	µg/l	10.0	1.1	<1	<1	<1	1.5	1.1	<1	<1	1.2
Co total	µg/l	<0.2	<0.2	<0.2	<0.2	<0.2	<0.2	<0.2	<0.2	<0.2	<0.2
Ni total	µg/l	0.7	0.7	0.3	0.4	0.4	0.4	0.4	0.4	0.5	0.5
Cu total	µg/l	2.8	2.8	<0.2	<0.2	<0.2	<0.2	<0.2	0.2	<0.2	<0.2
Zn total	µg/l	3.1	3.1	2.6	1.7	1.7	1.9	1.3	1.6	1.8	1.8
Mo total	µg/l	0.8	0.8	0.5	0.7	0.7	0.6	0.8	0.7	0.8	0.7
Cd total	µg/l	<0.2	<0.2	<0.2	<0.2	<0.2	<0.2	<0.2	<0.2	<0.2	<0.2
Pb total	µg/l	0.4	0.4	<0.2	<0.2	<0.2	0.2	0.3	0.2	0.4	1.6
U total	µg/l	0.2	0.2	<0.2	<0.2	<0.2	0.2	0.3	<0.2	0.2	0.3
As total	µg/l	5.1	5.1	1.7	1.8	1.8	1.9	1.6	1.6	1.5	1.3

Table 4-14: Chemical composition of the solution sampled during the leaching experiment with the oxidised sandstone (n.d. = not detected; n.a = not analysed).

a. charge balance

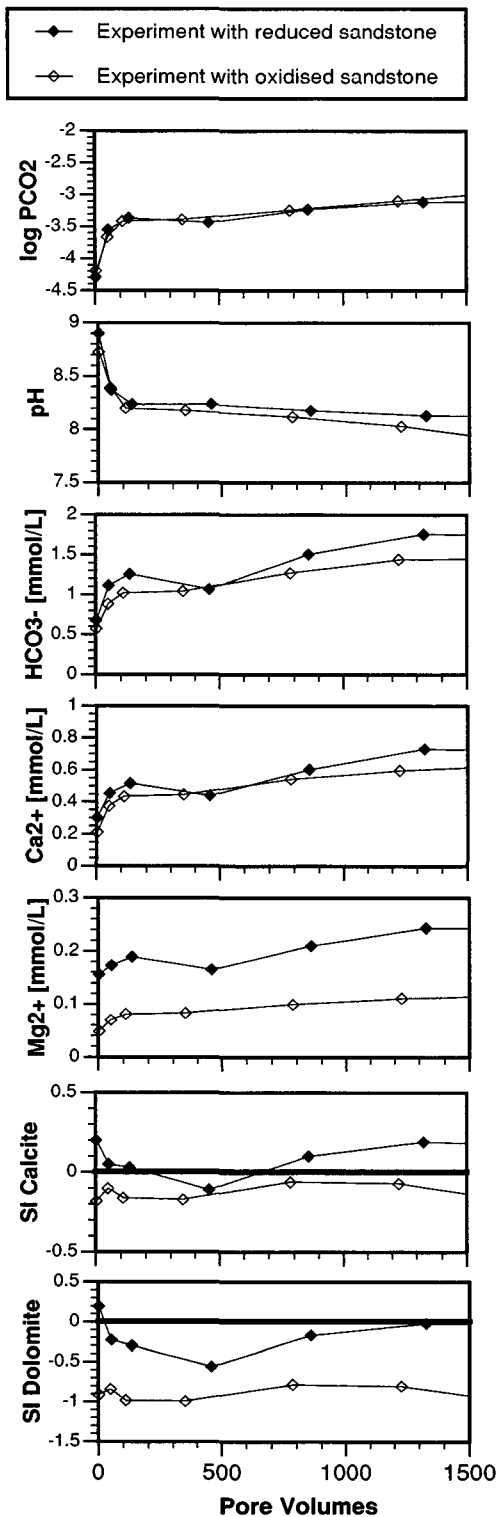


Figure 4-39: Evolution of the P_{CO_2} and pH, and of the alkalinity, Ca^{2+} , and Mg^{2+} concentrations in the solutions from the leaching experiments, as well as their saturation states with respect to calcite and dolomite.

With the setup used in the experiments a system is simulated that is replenished with CO_2 in the reservoir, thus corresponding to the conditions in the soil (open system, $P_{\text{CO}_2} = 10^{-2}$). At these conditions the initial solution, i.e. Millipore water saturated with CO_2 , has a pH of 5.0. In the column itself the dissolved CO_2 for one pore volume is used up by mineral reactions before it gets replenished again. Thus, for one pore volume of percolating water, this corresponds to the *closed system* conditions of the saturated zone of the aquifer. The P_{CO_2} of the solution emerging from the column is therefore lower than in the reservoir and the pH is considerably higher due to buffering reactions (see figure 4-39). With this experimental setup the chemical evolution of the solution percolating downwards from the soil into the aquifer is simulated.

The solution chemistry is dominated by alkalinity, Ca^{2+} , and minor amounts of Mg^{2+} in the long-term leaching experiments with reduced and oxidised sand substratum. There is a good positive correlation between these ions. The Ca^{2+} and Mg^{2+} contents are elevated already in the first samples, which were taken after less than two hours. This indicates that these dissolved elements originate from a fast mineral reaction such as the dissolution of calcite and dolomite (see reactions 4.4 and 4.5 on page 167). The weathering of silicate minerals is very much slower than the dissolution of carbonates. This potential source of Ca and Mg can thus be excluded, at least in the first samples. The molar alkalinity/ Ca^{2+} ratios in the solutions vary between 2.2 and 2.5, indicating that the dissolution of calcite dominates over the dissolution of dolomite, similar to the Lutry springwater. The solutions from the experiment with the reduced sandstone contain about twice the amount of Mg^{2+} compared to the solutions from the experiment with the oxidised sandstone. This is consistent with the slightly higher dolomite content in the reduced substratum. Saturation state calculations indicate that the solutions from both experiments are about in equilibrium with calcite. The solutions evolving in the reduced substratum also reach saturation with dolomite, while this is not the case in the solutions from the oxidised sandstone substratum due to their lower Mg^{2+} activities.

The rapid dissolution of carbonate minerals acts as the principal pH-buffer. The result is a sharp pH increase from 5.0 in the solution entering the column for the first time to a value near 9.0 in the solution leaving the column. The subsequent slow decrease of the pH is due to the ongoing re-equilibration of the solution with the P_{CO_2} of the reservoir and the carbonate minerals in the substratum.

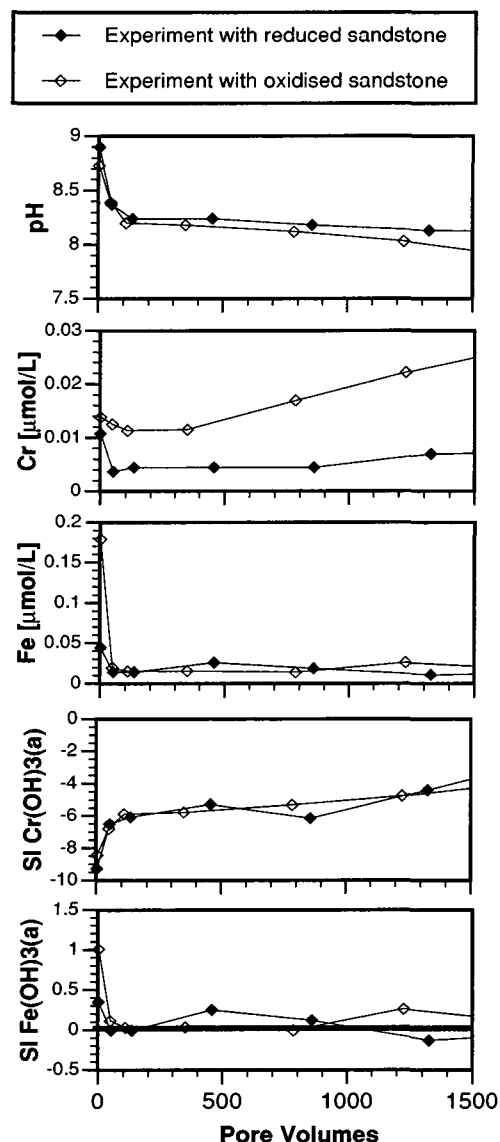


Figure 4-40: Evolution of pH and Cr and Fe concentrations in the solutions from the leaching experiments, as well as their saturation states with respect to amorphous Cr- and Fe-hydroxide.

Cr-bearing mineral phase dissolves very fast. Alternatively, in the oxidised sandstone Cr might be desorbed from weak sorption sites on the surfaces of Fe-hydroxides as a result of the high pH.

The peak in the first samples of both experiments can be explained by the washing out of moisture contained in the substratum. During a test run with oxidised sandstone an even higher Cr concentration of 4.1 µg/L was measured in the first pore volume of solution that

Trace element analyses have shown that Cr is immediately released into solution in both experiments and concentrations in the same order of magnitude as found in the groundwater (median 4.6 µg Cr/L in Lutry springwater) are reached at the end of the experiments (see figure 4-40 and tables 4-13 and 4-14).

In the experiment with the reduced sandstone the dissolved Cr concentration evolved from 0.6 µg/L in the first sample, to 0.2 µg/L in the second sample, and only slowly increased to 0.4 µg/L in the 6th sample after 20 days (or after the percolation of about 1300 pore volumes of solution). Contrasting this, in the experiment with the oxidised, Fe-hydroxide coated sandstone the dissolved Cr concentrations evolved from 0.7 µg/L in the first sample to 0.6 µg/L in the third sample and then slowly increased to 1.2 µg/L in the 6th sample. After the percolation of about 1300 pore volumes of solution the dissolved Cr concentration in the experiment with the oxidised sandstone attained three times the concentration obtained with the reduced sandstone.

Speciation calculations indicate that Cr is present as Cr^{VI} , mostly in form of the CrO_4^{2-} -complex and to a minor extent in form of the $HCrO_4^-$ -complex. Similar to the findings of the field study, a solubility control by the precipitation of Cr-hydroxides was not reached. This indicates that, once released, Cr remains in solution, and that no retention occurs by the precipitation of secondary Cr-hydroxide.

The relatively high Cr content occurring already in the first samples points to a very rapid Cr-releasing process. Several Cr-releasing processes are possible. A first possibility is the washing out of Cr-containing moisture from the substratum. The second possibility is that a

percolated through the substratum. This concentration is practically identical with the concentration observed in the Lutry springwater and thus confirms this hypothesis. In addition, the presence of elevated concentrations of other elements such as Na, Cu, Ni, Zn, Pb, Mo, and As in the first samples of both experiments further supports this hypothesis.

In the oxidised sandstone the rapid dissolution of Cr-bearing Fe-hydroxides may be an additional source of Cr. The elevated Fe contents that are present in the first sample are consistent with this. As the CO₂ saturated solution with a pH of 5 enters the column such hydroxides become unstable and tend to dissolve. Then, as the pH shortly afterwards rises to a value near 9, resulting from the dissolution of carbonate minerals, the dissolved metals remain in solution. The supersaturation of the first sample with amorphous Fe-hydroxide and the saturation of the subsequent samples is consistent with this hypothesis.

With ongoing leaching, the Cr concentration increases faster in the solutions from the oxidised sandstone than in the solutions from the reduced sandstone. This indicates that in the oxidised sandstone, the Cr-releasing reactions are faster than in the reduced sandstone. This differential increase of dissolved Cr in the two experiments can be explained by the following two processes: (1) the dissolution of primary Cr-bearing minerals and (2) the ongoing desorption of Cr^{VI} adsorbed on the surfaces of Fe-hydroxides in the oxidised sandstone. In the oxidised sandstone, the primary Cr-bearing minerals such as spinels and pyroxenes are more strongly corroded and therefore have a larger surface than in the reduced sandstone. As the dissolution rate of a mineral depends on its surface, the primary Cr-bearing minerals may dissolve slightly faster in the oxidised sandstone than in the reduced sandstone. In addition, Cr^{VI} may be desorbed from the surfaces of Fe-hydroxides in the oxidised sandstone, due to the high solution pH resulting from the buffering by the dissolution of carbonates. As Fe-hydroxide coatings are absent in the reduced sandstone, this desorption of Cr probably accounts for the difference in the dissolved Cr content of the two experiments.

4.7.4. Conclusions

The leaching experiments carried out with Burdigalian sandstone from the field site were aimed to support the field study findings and to further investigate the processes responsible for the Cr mineralisation observed in the Lutry groundwater. With the adopted setup between a true column experiment and a batch experiment, not all the processes occurring in nature can be modelled. However, despite of the experimental artefacts that occurred due to the particular setup, the rapid leaching of Cr from the Burdigalian sandstone has been confirmed. It has been shown that the potential Cr-releasing processes are fast enough to explain the Cr contents found in the springwater. Several Cr-releasing processes including the washing out of moisture from the field, the dissolution of Fe-hydroxides and primary Cr-bearing by the aggressive CO₂ saturated solutions, and the desorption of Cr from the surfaces of Fe-hydroxides have been discussed. The leaching experiments have shown, that in the oxidised, Fe-hydroxide-coated sandstone Cr is faster released into solution than in the less altered reduced sandstone. This indicates that the Cr contained in the reduced sandstone is in a more stable state, i.e. mainly incorporated the structure of detrital minerals, while in the oxidised sandstone the Cr is partly in a unstable state, i.e. adsorbed on the surface of secondary Fe-hydroxides, from where it is more easily leached. The experiments clearly show that in the Burdigalian sandstone the release of Cr into the groundwater depends on the weathering state of the sandstone.

V. SUMMARY AND CONCLUSIONS

The present study allowed to attain the following objectives:

- 1.) **Creation of a groundwater database**
Setup of a consistent groundwater database over a time span of 20 years
- 2.) **Definition of an aquifer typology**
Identification of the chemical characteristics and differences of recent groundwaters from five aquifer types in the alpine belt: natural major and trace element concentration ranges (Geo-reference)
Identification of potential sources of the geogenic tracers and of the rock-water interaction processes controlling groundwater chemistry under natural conditions by using geochemical modelling strategies
- 3.) **Identification of the leaching processes of Cr from a molasse sandstone**
Identification of the origin and the processes controlling the concentration of the geogenic tracer **chromium** in groundwaters from the Burdigalian Molasse sandstone in western Switzerland.

5. 1. Creation of a groundwater database

A rigorous quality control of the entire database was made in order to enable a comparison of the chemical groundwater data gathered and analysed over a time span of 20 years. An overview of the sampling techniques, the sample treatment and the analytical methods applied in the AQUITYP project since 1981 is given.

Different tests were carried out to evaluate the quality and comparability of the data, including charge balance calculations, comparison of different analytical techniques (particularly those used for trace element analysis) and tests to estimate the influence of the filtration procedure.

These tests showed that in general the data quality was satisfactory. From a total of 1824 groundwater analyses 1674 analyses passed the quality check. From these, 1475 are analyses of *recent* groundwaters and were selected for further investigation. Groundwater analyses with a charge balance with $> \pm 5\%$ error and certain trace elements such as Sc and I, which present analytical difficulties that were not recognised at the time of their analysis were not used. The filtration tests showed that mainly the Fe and Al concentrations may be overestimated due to the presence of particulate or colloidal matter in the normally non-filtered samples.

In order to make this large number of quality controlled data accessible also for future investigations, a groundwater data storage system was developed (*AQUITYP-DataBase*).

5. 2. Definition of an aquifer typology

A synthesis of the geology and hydrogeology of five aquifer types, including crystalline, carbonate, evaporite, molasse, and flysch rocks, and the hydrochemistry of natural recent groundwaters (springwaters) from these aquifer types was made. This synthesis is based on quality controlled groundwater data acquired during previous studies in the AQUITYP project (Basabe, 1993; Dematteis, 1995; Dubois, 1993; Hesske, 1995; Mandia, 1993).

The composition of recent groundwaters is determined by the following principal factors:

- **Mineralogy of the aquifer rock:** Abundance, chemical composition and reactivity of rock forming minerals
- **Hydrogeology:** Composition and type of infiltration, type of groundwater circulation (rock-water contact), and residence time
- **Chemical reactions between groundwater and aquifer rock:** Dissolution and precipitation of minerals, oxidation and reduction of aqueous species, and sorption

A summary of the essential structural and mineralogic aspects, as well as of the typical hydrogeologic features of each aquifer type is given, based on hydrogeologic investigations made during the previous studies and on mineralogical and geochemical data from the literature. This information was used to derive potential sources of the major and trace element compositions of the corresponding groundwaters and to model their hydrochemical evolution.

The hydrochemical characteristics of the groundwaters in the different aquifer types were summarised and compared, and concentration ranges of major and trace elements for groundwaters in each aquifer type were deduced. The geogenic tracers proposed by the previous researchers were evaluated and the potential sources of these tracers identified.

The emphasis was laid on the hydro-geochemical evolution leading to the characteristic major and trace element composition in each of the five aquifer types. The dominant geochemical processes were investigated using geochemical modelling strategies: Using an equilibrium approach, the distribution of aqueous species, ion activities, and saturation indices of the investigated groundwaters were calculated as a function of measured solution compositions, pH, E_H , and temperature. These calculations proved very useful to investigate the chemical form of dissolved elements at equilibrium. Possible limitations of the element concentrations by the solubility of secondary minerals, such as calcite, gypsum, barite, celestite, strontianite, fluorite, and chalcedony, as well as metalliferous oxide- and hydroxide phases of Fe, Ni, Mn, Cu and Cr were explored. Mass balance calculations allowed to test the likelihood of geologically reasonable mineral phases to get involved in the hydrochemical evolution of selected groundwaters from infiltrating rainwater to the spring.

5. 2. 1. Hydrochemical characteristics of recent groundwaters from the different aquifer types

Physical-chemical parameters

The investigated groundwaters are generally cold and oxygenated and have a mildly acid to mildly alkaline pH, as it is typical for recent groundwaters. The lowest pH values occur in the least mineralised springwaters, particularly in flysch and crystalline aquifers.

Major and trace elements

The fact, that the investigated groundwaters have short residence times in the order of a few hours (karst aquifers) to a few years (porous molasse aquifers) establishes a boundary condition for potential chemical reactions. The dominating rock-water interaction processes in all aquifer types are limited to relatively fast reactions such as the dissolution of carbonate (Ca^{2+} , Mg^{2+} , HCO_3^-) and sulphate minerals (Ca^{2+} , Ba^{2+} , SO_4^{2-}), the oxidation of sulphides (SO_4^{2-} , metals) and to a minor extent cation-exchange processes (Na^+ , K^+). Primary Al-silicate minerals are very insoluble and have sluggish reaction kinetics. They are therefore not likely to contribute large amounts of dissolved ions.

The comparison of the groundwaters from the different aquifer types showed that each rock type contributes in a characteristic way to the major and trace element composition of the corresponding groundwaters (see also table 5-1 on page 206):

- Groundwaters from the **crystalline** rocks of the Mont-Blanc and Aiguilles-Rouges Massifs are very dilute groundwaters (TDS 22 to 158 mg/L). Their major element composition is dominated by Ca^{2+} , Na^+ , Mg^{2+} , alkalinity, SO_4^{2-} , and F^- (Ca-Na- HCO_3 - SO_4 waters). Elevated amounts of Mo, U, W, and As occur. The mineralogy along fracture planes acting as groundwater flow paths (hydrothermal minerals) is more important in the groundwater mineralisation than the composition of the bulk rock (Al-silicates). Processes significant for the mineralisation of recent crystalline groundwaters include the dissolution of carbonates (Ca^{2+} , Mg^{2+} , HCO_3^-), fluorite (F^- , Ca^{2+}), as well as U- and W-minerals (U, W), ion exchange processes on clay minerals (Na^+), and oxidation of sulphides (SO_4^{2-} , As, Mo). In these Ca^{2+} -poor groundwaters the F^- concentrations attain values as high as 4.0 mg/L before fluorite saturation is reached. At oxidising conditions and at the given pH values U, As, Mo and W are present in solution in a soluble anion form, including U^{VI} -carbonate complexes, $\text{As}^{\text{V}-}$, $\text{Mo}^{\text{V, VI}-}$, and W^{VI} -oxy-anions, respectively. At the given concentrations, there is no solubility control for these elements. Only sorption on secondary Fe-hydroxides can limit the concentrations.
- **Carbonate karst** groundwaters obtain their low to intermediate mineralisation (TDS 161 to 547 mg/L) from the dissolution of calcite (Ca- HCO_3 waters), as well as in certain regions dolomite (Ca-Mg- HCO_3 waters) and gypsum (Ca-Mg- HCO_3 - SO_4 waters). Due to their very short residence times, and because calcite can only contain very restricted amounts of certain trace elements, the carbonate karst groundwaters normally contain very low trace element contents. However, **iodine** is generally elevated in carbonate groundwaters, probably due to fossil organic matter contained in

carbonate rocks. In addition, specific geogenic trace elements allow to distinguish groundwaters from certain carbonate units: Elevated **Ba** values occur in karst waters from deep sea limestones containing accessory barite. Barite solubility places an upper limit on the dissolved Ba concentrations at SO_4^{2-} contents surpassing 0.1 mmol. **U** and **Mo** can reach high concentrations in groundwaters from dolomite-bearing aquifers. Elevated Sr^{2+} and **Li** concentrations are associated with the dissolution of evaporite layers. Finally, elevated **V** values occur in groundwaters from the “Malm” of the western Swiss Jura and from bituminous Cretaceous limestones near Trieste (clay minerals, Fe-hydroxides and organic matter). V appears to be present as soluble anion-complexes, which explains its high mobility in oxygenated groundwaters.

- The groundwaters from Triassic **evaporites** in the Swiss Rhone basin are by far the most mineralised groundwaters (TDS 760 to 2788 mg/L), usually of the Ca-Mg-SO₄-HCO₃ type. Major element composition is characterised by elevated amounts of Ca^{2+} , Mg^{2+} , Sr^{2+} , SO_4^{2-} , and alkalinity (Ca-Mg-SO₄-HCO₃ waters). The hydrochemical evolution of these groundwaters is governed by incipient dedolomitisation, involving dissolution of gypsum, celestite and dolomite and simultaneous precipitation of calcite. The Na^+ and K^+ concentrations are probably controlled by ion-exchange reactions on clay minerals. Elevated amounts of the trace elements Mn, Ni, Cu, Li, Rb, Y, and Cd are characteristic. As gypsum is fairly close in composition to pure CaSO₄, these trace elements are probably contained in associated carbonate minerals (dolomite: Mn, Ni), phosphates (apatite: Y, Cd), sulphides (Cu, Ni, Cd), and clay minerals and/or in brine inclusions (Li and Rb).
- Recent groundwaters circulating in the porous and fissured **molasse** sandstones and conglomerates acquire their intermediate total mineralisation (TDS 48 to 714 mg/L) primarily by dissolution of calcite and minor dolomite (Ca-Mg-HCO₃ waters). Molasse groundwaters tend to have longer residence times than the groundwaters from carbonate and flysch rocks resulting in higher Mg^{2+} , alkalinity, and silica concentrations. The particular mineralogy of certain Molasse formations is reflected in specific trace element compositions of corresponding groundwaters: ophiolite detritus in OMM sandstones in western Switzerland (Cr), barite fracture mineralisations in subalpine and folded Molasse units (Ba), granitic detritus containing sulphides (Mo), U-minerals (U) and abundant mica (Li) in the “Glimmersand” (OSM, Ca-Mg-HCO₃-SO₄ waters), and evaporite minerals (Li, Sr), sulphides (Mo), and U-minerals (U) in the “Gypsum-bearing Molasse” (USM, highly mineralised Ca-Mg-SO₄-HCO₃ waters, TDS 984 to 1346 mg/L).
- Recent groundwaters derived from **flysch** aquifers in the Niesen and Gurnigel nappes are poorly evolved Ca-(Mg)-HCO₃ waters. Their low to intermediate total mineralisation (TDS 160 to 459 mg/L) is primarily acquired by the dissolution of calcite and small amounts of dolomite. The low trace element content is dominated by Ba originating from the dissolution of barite fracture mineralisations. The poor chemical evolution of recent flysch groundwaters results from (1) their short residence time in the fractured flysch rocks, and (2) the absence of readily dissolving minerals except carbonates and barite.

5. 2. 2. Groundwater quality

The concentrations of chemical elements in the groundwaters from the different aquifer types were compared to Swiss and WHO drinking water standards in order to assess the quality of the investigated groundwaters. This comparison showed that the natural major and trace element composition of groundwaters does not necessarily comply with drinking water standards. Particularly the concentrations of F, As, U, and Mo in groundwater from the crystalline, SO₄, Mg, U, and Ni concentrations of evaporite groundwaters, and U concentrations of certain molasse groundwaters may exceed the limits for drinking water. Further, it was found that several geogenic trace elements including As, Cd, Cr, Cu, Mn, and Zn can be present at concentrations exceeding the quality target values of the Swiss drinking water standards.

5. 3. Identification of the leaching processes of Cr from a molasse sandstone

The groundwaters of the Burdigalian molasse sandstone (OMM) in western Switzerland are characterised by elevated concentrations of the potentially toxic tracer element Cr. The Cr concentrations in these groundwaters exceed the quality target value of the Swiss drinking water standards. In these molasse groundwaters the Cr concentrations are also higher than in groundwaters from mafic and ultramafic rocks, which typically contain much higher Cr-concentrations than sandstones.

5. 3. 1. Field study

In order to characterise the sources and geochemical behaviour of Cr, a comprehensive field study was carried out on a selected catchment (Lutry spring catchment near Lausanne). The investigation of the processes controlling the dissolved Cr content in these groundwaters was based on groundwater chemical data from 1982 to 2000, as well as on hydrological, mineralogical, and geochemical data.

Compared to the worldwide mean concentrations of Cr in sandstones, the Burdigalian molasse sandstone in western Switzerland presents elevated values. The origin of this high Cr-content can be explained by the presence of ophiolite detritus originating from the Nappe de Gêts (Simmen-nappe, Prealps).

Relic Cr-bearing spinel and pyroxene in this sandstone were identified to be the primary sources of Cr. An electron microscope study showed that in the Burdigalian sandstone and overlying soil these minerals are strongly corroded. The slow weathering of these minerals is thought to be the major Cr releasing process.

Under the oxidising conditions reigning in the investigated groundwaters, Cr prevails in solution in its highly soluble and toxic hexavalent state (CrO₄²⁻). Geochemical model calculations showed that in this case retention by the precipitation of secondary Cr-hydroxide phases does not occur. In addition, at the near-neutral pH of these groundwaters there is only very weak adsorption of CrO₄²⁻ by Fe-hydroxides.

5.3.2. Leaching experiments

Leaching experiments were carried out in the laboratory with Burdigalian molasse sandstone from the field site, in order to support the field study findings and to quantify the processes responsible for the Cr mineralisation observed in the Lutry groundwater. Two experiments with disaggregated mountain-wet oxidised and reduced sandstone were conducted over a time span of 2 months each, in order to obtain information about the influence of the oxidation state of the substratum on the mobilisation of Cr.

The experiments clearly showed that the Cr-releasing processes are fast enough to explain the Cr contents found in the groundwater, and that the release of Cr into the groundwater depends on the weathering state of the sandstone: In the oxidised, Fe-hydroxide-coated sandstone, Cr was faster released into solution than in the less altered reduced sandstone. This indicates that the Cr contained in the reduced sandstone is in a more stable state, i.e. mainly incorporated in the detrital minerals, while in the oxidised sandstone, the Cr is partly in a unstable state, i.e. adsorbed on the surface of secondary Fe-hydroxides, from where it is more easily leached.

5.4. Applicability of the groundwater typology

The database of geogenic major and trace element compositions of groundwaters in different lithologic environments, the so-called geo-reference, is without doubt of great value in dealing with groundwater contamination. It is particularly useful to differentiate between anthropogenic contamination and natural background concentrations of dissolved trace elements in a particular aquifer type.

Furthermore, this detailed groundwater typology contributes to a better understanding of groundwater flow paths. In engineering geology this will for example allow a better evaluation of the impact of underground work on groundwater resources.

Groundwaters from crystalline and evaporite rocks are clearly distinguished by their particular major element composition and their low, respectively high total mineralisation. The hydrochemistry of recent groundwaters from Molasse, Flysch and carbonate karst units, however, is dominated by the dissolution of calcite and minor dolomite, yielding in all three cases Ca-(Mg)-HCO₃ type groundwaters of similar total mineralisation. To distinguish such groundwaters from different lithologic environments, but with a similar major element composition trace elements proved to be particularly useful.

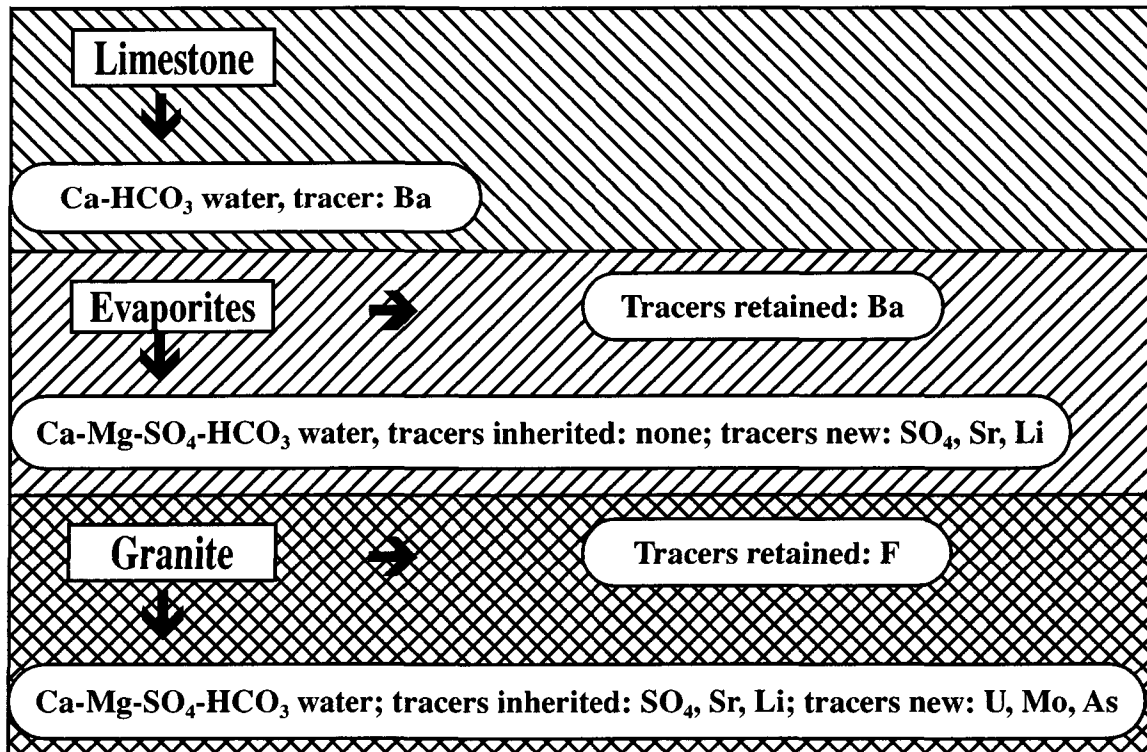
So, chemical groundwater compositions can indeed be used to determine the origin of groundwater encountered in underground work or in boreholes, as far as specific and readily soluble minerals are present in the different aquifers. Therefore, such investigations should in every case be based on sound knowledge of geological structures and mineralogical compositions of the different aquifer rock types.

The investigated springwaters are from aquifers composed of, as far as possible, a single lithologic unit within a simple tectonic context, thus minimising the influence of other lithologic units. However, aquifer systems are often more complex and involve several rock types, especially in the Alps with their complicated tectonic structure. In addition, a number of the discussed natural tracers are subjected to solubility control by precipitating secondary

minerals and may thus be removed from the solution (see table 5-1). Therefore, the groundwater composition in aquifers composed of different rock types does not represent a simple addition of the chemical marking from the different rock types. It is thus not simple to interpret the chemical compositions of groundwaters from mixed aquifers.

The following example of the evolution of groundwater in a “mixed” aquifer composed of a succession of carbonate, evaporite and crystalline silicate rocks is given to illustrate the possibilities and limits of this method (see sketch below):

A groundwater infiltrates into a barite containing limestone and is mineralised with the tracer element Ba (Ca-HCO₃ water type, intermediate total mineralisation). At the base of the limestone the groundwater reaches an evaporite layer. Due to the rapid dissolution of gypsum and dolomite the groundwater now attains a high total mineralisation with elevated Ca²⁺, Mg²⁺, SO₄²⁻, Sr²⁺, and Li values (Ca-Mg-SO₄-HCO₃ water type). The geogenic tracer Ba from the overlying carbonate rock, however, is removed from the groundwater, due to the precipitation of barite in the now SO₄²⁻-rich groundwater. So, the geochemical marking from the carbonate rock is erased by the passage of the groundwater through the evaporite rocks. If this groundwater then infiltrates further down into a fissured granite, the water type will then remain the same (Ca-Mg-SO₄-HCO₃) and also the markers Sr²⁺ and Li from the evaporite rocks will remain in solution due to their high solubility. In addition, the groundwater will acquire elevated U, As, and Mo concentrations from the interaction with hydrothermal U-minerals and sulphides in the granite. The commonly present fluorite, on the other hand, will not dissolve, because of the high Ca²⁺ concentration from the previous dissolution of gypsum. While the elevated U, As and Mo values indicate the presence hydrothermal minerals in crystalline rocks, the typical tracer F⁻ of granite groundwaters will not be present in solution.



So, although rock-water interaction processes are complex, a detailed chemical groundwater analysis can give valuable information about its flow path. This example also shows, that according to their chemical characteristics the different tracer elements show a more or less conservative behaviour in solution. To summarise the typical geochemical behaviour of these different tracer elements, an attempt has been made to classify them according to their capacity to remain in solution. The sources and solubility limiting processes of the different tracer elements are listed in table 5-1. The most conservative tracers are the highly soluble alkaline elements (Li, Rb) and iodine, elements which are only retained by weak adsorption. Then, there is a group of relatively conservative, but redox-sensitive tracers in anionic form including As, Cr, Mo, U, V, and W, which are only limited by weak adsorption in oxygenated groundwater. Finally, there are non-conservative tracers including elements that are limited by the solubility of precipitating secondary minerals and/or by adsorption.

Tracer	Potential sources	Solubility limiting processes in recent groundwaters
1.) Highly conservative tracers: not redox-sensitive, not limited by the solubility of precipitating secondary minerals and poorly adsorbed		
Li	evaporite rocks (brine inclusions, clay minerals) and mica	
Rb	evaporite rocks, clay minerals	weak adsorption by clay minerals and org. matter
I	organic matter in carbonate rocks	weak adsorption by org. matter
2.) Relatively conservative tracers: redox-sensitive tracers in anionic form, which are limited by weak adsorption		
As	As-bearing sulphides	As ^V -complexes: adsorption on Fe-hydroxides
Cr	Cr-bearing mafic minerals (spinel, pyroxenes, etc.)	Cr ^{VI} -complexes: adsorption on Fe-hydroxides at acid pH reduction and precipitation of Fe, Cr ^{III} (OH) ₃ , adsorption of Cr ^{III} at alkaline pH
Mo	molybdenite	Mo ^{V,VI} -complexes: adsorption on hydroxides and org. matter
U	U-minerals (pitchblende)	U ^{VI} -carbonate complexes: adsorption on hydroxides and org. matter
V	Fe-minerals, fossil organic matter, clay minerals	V ^V -complexes: adsorption on and co-precipitation with Fe-hydroxides
W	scheelite, wolframite	W ^{VI} -complexes: adsorption on Fe-hydroxides
SO ₄	gypsum, sulphides	weak adsorption, precipitation of gypsum in Ca-rich groundwaters only at SO ₄ concentrations above 1'400 mg/L
3.) Non-conservative tracers: Elements that are limited by the solubility of precipitating secondary minerals and/or by adsorption		
F	fluorite	precipitation of fluorite in Ca-rich groundwaters
Sr	celestite, strontianite	precipitation of celestite in SO ₄ ²⁻ -rich groundwaters, precipitation of strontianite in CO ₃ ²⁻ -rich groundwaters
Y	phosphates (apatite)	adsorption on Fe-hydroxides
Ba	barite	precipitation of barite in SO ₄ -rich groundwaters, adsorption
Mn	Mn-hydroxides, -oxides, and -carbonates (dolomite)	precipitation as Mn-hydroxides and co-precipitation with carbonates, adsorption
Ni	evaporite rocks with dolomite	adsorption on Fe-hydroxides, precipitation as Ni-hydroxides and carbonates
Cu	Cu-sulphides	adsorption on Fe-hydroxides, co-precipitation with oxides, precipitation of malachite
Cd	sulphides, apatite	adsorption, co-precipitation with hydroxides and carbonates

Table 5-1: Potential sources and solubility limiting processes for geogenic tracer elements at the given conditions reigning in the investigated recent groundwaters, i.e. at temperatures below 20°C, oxidising conditions, near-neutral pH, and typical element concentrations.

5. 5. Further research

This work gives an overview of possible sources of the geogenic tracers in groundwaters based on mineralogic and geochemical data from the literature. The lack of mineralogic and geochemical field data does however not allow a conclusive determination of the origins of all the geogenic tracers in the different lithologic environments. Therefore further geochemical field studies, such as the study made on the Lutry site, on the processes governing the concentrations of the different tracer elements are needed to confirm the proposed origins of these tracers. Furthermore, isotope studies would also help to confirm the origins of major element mineralisation.

The predominant species of the different dissolved tracer elements were calculated based on physical-chemical solution conditions and analysed concentrations and using an equilibrium approach. It is well recognized, however, that especially the transformation of redox-sensitive elements is subject to sluggish reaction kinetics and influences of microbiological processes. The calculated species distribution may therefore not correspond to the real species distribution in solution. In order to get a more realistic judgment, chemical analyses of the different species are needed. This is particularly important for elements which have a species-dependant toxicity, such as Cr or As.

REFERENCES

References

- ABERER, F. (1957): Die Molassezone im westlichen Oberösterreich und in Salzburg. *Mitt. Geol. Ges. Wien*, Vol. 50, 23-94
- ACKERMANN, A. (1986): Le Flysch de la nappe du Niesen. *Eclogae Geol. Helv.*, Vol. 79/3, 641-684
- ADAMS, C., & SWINNERTON, A. C. (1937): The solubility of calcium carbonate. *Transactions, American Geophysical Union*, Vol. 11/2, 504-508
- ADRIANO, D. C. (1986): *Trace elements in the terrestrial environment*. Springer, New York
- ALLEN, P. A., MANGE-RAJETZKY, M., MATTER, A., & HOMEWOOD, P. (1985): Dynamic palaeogeography of the open Burdigalian seaway, Swiss Molasse basin. *Eclogae Geol. Helv.*, Vol. 78/2, 351-381
- AMACHER, M. C., & BAKER, D. E. (1982): Redox reactions involving chromium, plutonium and manganese in soils (US Dept. of Energy Final Report DOE/DP/04515-1). Institute for research on Land and Water Resources, Pennsylvania State University, University Park, PA
- AMONETTE, J. E., & RAI, D. (1990): Identification of non crystalline (Fe,Cr)(OH)₃ by infrared spectroscopy. *Clays and Clay Minerals*, Vol. 38/2, 129-136
- ANDERSON, R. A. (1989): Essentiality of chromium in humans. *The Science of the Total Environment*, Vol. 86, 75-81
- ANDERSON, G. M. (1996): *Thermodynamics of natural systems*. John Wiley & Sons
- ANGELILLO, V. T. (1987): Les marnes et grès gris à gypse ("Molasse grise") du bassin Genevois. *Diplôme, Inst. Géol. Univ. Genève*
- APPELO, C. A. J., BEEKMAN, H. E., & OOSTERBAAN, W. A. (1984): Hydrochemistry of springs from dolomite reef in the Southern Alps of Northern Italy. *IAHS Publication*, Vol. 150, 125-138
- APPELO, C. A. J., & POSTMA, D. (1996): *Geochemistry, Groundwater and Pollution*. Balkema, Rotterdam, Brookfield
- ARRÀ, A., CREMA, G. C., DEMATTEIS, A., PAMBIANCHI, G., & PUCCIARELLI, R. (1994): Idrogeologia della dorsale Mt. Catria-Mt. Acuto. In *Rencontre Internationale des Jeunes Chercheurs en Géologie de l'Ingénieur*, 1 (pp. 5-10). Lausanne
- ATKINSON, T. C. (1975): Diffuse flow and conduit flow in limestone terrain in the Mendip Hills, Somerset, England. In *IAH Congress*,. Huntville, Alabama
- ATKINSON, T. C. (1977): Carbon dioxide in the atmosphere of the unsaturated zone: an important control of groundwater hardness in limestones. *J. Hydrol.*, Vol. 35, 111-123
- ATKINSON, T. C. (1983): Growth mechanisms of speleothems in Castleguard cave, Columbia Icefields, Alberta, Canada. *Arct. Alpine Res.*, Vol. 15, 523-536
- ATTEIA, O., VEDY, J.-C., PARRIAUX, A., & DAMBRINE, E. (1990): Soil influence on the physical-chemical evolution of recharge water of aquifers: AQUISOL-Project. In A. Parriaux (Ed.), *Proceedings of the 22nd Congress of IAH: Water Resources in Mountainous Regions*, 1 (pp. 254-262). Lausanne
- ATTEIA, O. (1992): Rôle du sol dans le transfert des éléments traces en solution - Application à l'étude de quelques écosystèmes d'altitude. Thèse de doctorat, N° 1031, Ecole Polytechnique Fédérale de Lausanne, Dép. Génie Rural
- ATTEIA, O. (1994): Transport of major and trace elements in soils and aquifers of different ecosystems of Switzerland. *Eclogae Geol. Helv.*, Vol. 87/2, 409-428
- AUBERT, D., BADOUX, H., & LAVANCHY, Y. (1979): La carte structurale et les sources du Jura Vaudois. *Bull. Soc. Vaudoise Sci. Nat.* N°356, Vol. 74/4, 333-343
- AYRTON, S., BARFÉTY, J. C., BELLÈRE, J., GUBLER, Y., & JEMELIN, L. (1987): Carte géologique et notice explicative de la feuille Chamonix BRGM, Orléans
- BACK, W., & HANSHAW, B. B. (1970): Comparison of chemical hydrogeology of the carbonate peninsula of Florida and Yucatan. *Journal of Hydrology*, Vol. 10, 330-368

- BACK, W., HANSHAW, B. B., PLUMMER, L. N., RAHN, P. H., RIGHTMIRE, C. T., & RUBIN, M. (1984): Process and rate of dedolomitisation: mass transfer and C14 dating in a regional carbonate aquifer. *Geol. Soc. Am. Bull.*, Vol. 95, 1415-1429
- BADOUX, H. (1963): Les unités ultrahelvétiques de la Zone desCols. *Eclogae Geol. Helv.*, Vol. 56/1, 1-13
- BADOUX, H. (1965): Atlas Géologique de la Suisse et notice explicative, Feuille 1264 Montreux Comm. Géol. Suisse
- BADOUX, H., BURRI, M., GABUS, J. H., KRUMMENACHER, D., LOUP, G., & SUBLET, P. (1971): Atlas géologique de la Suisse, Carte géologique au 1:25'000 et notice explicative de la feuille 1305 Dt. de Morcles. Comm. Géol. Suisse
- BADOUX, H., & GABUS, J.-H. (1991): Atlas Géologique de la Suisse, Carte géologique au 1:25'000 et notice explicative, feuille 1285 Les Diablerets Comm. Géol. Suisse
- BAES, C. F. J., & MESSMER, R. E. (1977): *The hydrolysis of cations*. John Wiley & Sons, New York
- BAGGIO, P. (1958): Il granito del Monte Bianco, e le sue mineralizzazioni uranifere. In *Studi e ricerche della Divisione Geomineraria, Comitato Nazionale per le Ricerche Nucleari (527-652)*. Roma
- BAKALOWICZ, M. (1974): Géochimie des eaux d'aquifères karstiques. 1. Relation entre minéralisation et conductivité. *Ann. Spéléol.*, Vol. 29/2, 167-173
- BAKALOWICZ, M. (1979): Contribution de la géochimie des eaux à la connaissance de l'aquifère karstique et de la karstification. Thèse de doctorat, Univ. P. et M. Curie, Paris
- BALDERER, W. (1979b): Die Obere Süswassermolasse als hydrogeologisches Gesamtsystem. *Bull. Centre d'Hydrogéologie de l'Université de Neuchâtel*, Vol. 3, 27-39
- BALDERER, W. (1990): Hydrogeologische Charakterisierung der Grundwasservorkommen innerhalb der Molasse der Nordostschweiz aufgrund von hydrochemischen und Isotopenuntersuchungen. *Steir. Beitr. z. Hydrogeologie*, Vol. 41, 35-104
- BALDERER, W. (1990a): Paleoclimatic trends deduced in groundwaters within Swiss molasse basin as evidence for the flow systems definition. In *Mémoires du XXII. Congrès de l'IAH*, 1 (pp. 731-740). Lausanne (Suisse)
- BALDERER, W. (1990b): Past and future evolution of flow systems as response to changing climatic conditions and anthropogenic influences. In *Mémoires du XXII. congrès de l'IAH*, 1 (pp. 741-750). Lausanne (Suisse)
- BALL, J. W., & NORDSTROM, D. K. (1998): Critical evaluation and selection of standard state thermodynamic properties for chromium metal and its aqueous ions, hydrolysis species, oxides and hydroxides. *J. Chem. Eng. Data*, Vol. 43, 895-918
- BARON, D., PALMER, C. D., & STANLEY, J. T. (1996): Identification of two iron-chromate precipitates in a Cr(VI)-contaminated soil. *Environ. Sci. Technol.*, Vol. 30, 964-968
- BARON, D., & PALMER, C. D. (1996): Solubility of $KFe_3(CrO_4)_2(OH)_6$ at 4-35°C. *Geochimica et Cosmochimica Acta*, Vol. 60/20, 3815-3824
- BARON, D., & PALMER, C. D. (1998): Solubility of $KFe(CrO_4)_2 \cdot 2H_2O$ at 4-75°C. *Applied Geochemistry*, Vol. 13/8, 961-973
- BARTLETT, R. J., & KIMBLE, J. M. (1976b): Behaviour of Cr in soils: II. Hexavalent forms. *Journal of Environ. Qual.*, Vol. 5, 383-386
- BARTLETT, R. J., & JAMES, B. (1979): Behaviour of Cr in soils: III. Oxidation. *Journal of Environ. Qual.*, Vol. 8, 31-34
- BASABE, P., & PARRIAUX, A. (1990): Hydrochemical characterization of the flysch groundwater in the Niesen tectonic nappe (Swiss Prealps). In A. Parriaux (Ed.), *Proceedings of the 22nd Congress of IAH: Water Resources in Mountainous Regions*, 1 (pp. 514-524). Lausanne, EPFL
- BASABE, P. P. (1993): Typologie des eaux souterraines du flysch de la nappe tectonique du Niesen (Préalpes Suisses). Thèse de doctorat, EPF Lausanne, Dép. Génie Civil

References

- BAU, M., MÖLLER, P., & DULSKI, P. (1997): Yttrium and lanthanides in eastern Mediterranean seawater and their fractionation during redox-cycling. *Marine Chemistry*, Vol. 56, 123-131
- BAU, M. (1999): Scavenging of dissolved yttrium and rare earths by precipitation of iron hydroxide: experimental evidence for Ce oxidation, Y-Ho fractionation, and lanthanide tetrad effect. *Geochimica et Cosmochimica Acta*, Vol. 63/1, 67-77
- BAUD, A. (1972): Observations et hypothèses sur la géologie de la partie radicale des Préalpes Médiannes. *Eclogae Geol. Helv.*, Vol. 65/1, 43-55
- BAUD, A. (1987): Stratigraphie et sédimentologie des calcaires de Saint-Triphon (Trias, Préalpes, Suisse et France). Laboratoires de géologie, minéralogie, géophysique et du musée géologique de l'Université de Lausanne, Lausanne
- BAUMANN, A. R. (1987): Geologie und Hydrogeologie des Embracher Tales und des unteren Tösstales (Kanton Zürich). Thèse de doctorat, no 8357, ETH Zürich
- BASLER ZEITUNG (1994, 4.5.1994): Neuallschwiler Altlast - eine teure Geschichte. p. 3
- BEARTH, P. (1953): Atlas géologique de la Suisse, Carte géologique au 1:25'000 et notice explicative de la feuille 1348 Zermatt Comm. Géol. Suisse
- BEHRENS, H., BENISCHKE, R., BRICELJ, M., HARUM, T., KÄSS, W., KOSI, G., LEDITSKY, H. P., LEIBUNDGUT, C., MALOSZEWSKI, P., MAURIN, V., RAJNER, V., RANK, D., REICHERT, B., STADLER, H., STICHLER, W., TRIMBORN, P., ZOJER, H., & ZUPAN, M. (1992): Investigation with natural and artificial tracers in the karst aquifer of the Lurbach system (Peggau-Tanneben-Semriach, Austria). *Steir. Beitr. z. Hydrogeologie*, Vol. 43, 9-158
- BELLUCCI, F., GIULIVO, I., PELELLA, L., & SANTO, A. (1991): Carsismo ed idrogeologia del settore centrale dei Monti Alburni (Campania). *Geologia Tecnica*, Vol. 3, 5-12
- BENSIMON, M., LOOSER, M. O., PARRIAUX, A., & REED, N. (1994): Characterisation of groundwater and polluted water by ultra trace element analysis, using High Resolution Plasma Source Mass Spectrometry (HR-ICP-MS). *Eclogae Geol. Helv.*, Vol. 87/2, 325-334
- BERGER, J.-P. (1985): La transgression de la molasse marine supérieure (OMM) en Suisse occidentale. *Münchner geowissenschaftliche Abhandlungen, Reihe A*, Vol. 5, 207
- BERGER, J.-P. (1992): Correlative chart of the European Oligocene and Miocene: Application to the Swiss Molasse Basin. *Eclogae Geol. Helv.*, Vol. 85/3, 571-610
- BERNER, R. A. (1975): The role of magnesium in the crystal growth of calcite and aragonite from sea water. *Geochimica et Cosmochimica Acta*, Vol. 39, 489-504
- BERNOULLI, D. (1964): Zur Geologie des Monte Generoso
- BERTRAND, J. (1970): Etude pétrographique des ophiolites et des granites du Flysch des Gets (Haute-Savoie, France). *Archives des Sciences de la Soc. de Phys. et d'Hist. nat. de Genève*, Vol. 23/2, 279-548
- BERTRAND, J., & Delaloye, M. (1976): Datation par la méthode K-Ar de diverses ophiolithes du flysch des Gets (Haute Savoie, France). *Eclogae Geol. Helv.*, Vol. 69, 335-341
- BESSON, O. (1990): Etude des aquifères fissurés associés au synclinal Permo-Carbonifère de Salvan-Dorénaz. In *Mémoires of the 22nd Congress of IAH*, (pp. 1113-1117). Lausanne
- BESSON, O. (1993): Méthodologie des essais de traçage en milieu fissuré alpin: Exemple du synclinal Permo-Carbonifère de Salvan-Dorénaz CRSFA (Centre de recherches scientifiques fondamentales et appliquées de Sion)
- BITTERLI, T. (1988): Das Karstsystem Sieben Hengste-Hohgant-Schrattenfluh. *Stalactite*, /1-2, 10-22
- BITTERLI, T., FUNCKEN, L., & JEANNIN, P.-Y. (1991): Le Bärenschaft: un vieux rêve de 950 mètres de profondeur. *Stalactite*, /2, 71-92

- BITTERLI, T. (1998): Ungewöhnliche speläologische Phänomene in der Schweiz; Höhlen in Nicht-Kalkgesteinen und Nicht-Karsthöhlen. *Stalactite*, Vol. 98/2, 101-114
- BLATT, H., MIDDLETON, G., & MURRAY, R. (1980): *Origin of sedimentary rocks*. Prentice-Hall Inc., Englewood Cliffs
- BLÄUER, C. (1987): *Verwitterung der Berner Sandsteine*. Dissertation, Mineralogisch-Petrographisches Institut, Universität Bern
- BLUM, J. D., GAZIS, C. A., JACOBSON, A. D., & CHAMBERLAIN, C. P. (1998): Carbonate versus silicate weathering in the Raikhot watershed within the high Himalayan crystalline series. *Geology*, Vol. 26/5, 411-414
- BONI, C., BONO, P., & CAPELLI, G. (1986): Schema idrogeologico dell'Italia centrale. *Mem. Soc. Geol. It.*, Vol. 35, 991-1012
- BORNHAUSER, M. (1929): *Geologische Untersuchung der Niesenkette*. *Mitt. natf. Ges. Bern*, 33-114
- BOSELLINI, A. (1989): *La storia geologica delle Dolomiti*. Edizioni Dolomiti, Lema di Maniago (PN)
- BOSSHARD, E., ZIMMERLI, B., & SCHLATTER, C. (1992): Uranium in the diet: risk assessment of its nephro- and radiotoxicity. *Chemosphere*, Vol. 24/3, 309-321
- BÖGLI, A. (1978): *Karsthydrographie und physische Speläologie*. Springer Verlag, Berlin
- BROOK, G. A., FOLKHOFF, M. E., & BOX, E. O. (1983): A world model of soil carbon dioxide. *Earth surface processes*, Vol. 8, 79-88
- BROOKINS, D. G. (1988): *Eh-pH diagrams for geochemistry*. Springer, Berlin, Heidelberg, New York
- Bundesamt für Umweltschutz (1982): *Wegleitung zur Auscheidung von Gewässerschutzbereichen, Grundwasserschutzzonen und Grundwasserschutzarealen*. Bern
- BURRI, M., & JEMELIN, L. (1983): *Atlas géologique de la Suisse 1:25'000, Feuille 1325 Sembrancher, Notice explicative Commission Géologique Suisse*
- BUSSY, F. (1990): *Pétrogenèse des enclaves microgrenues associées aux granitoïdes calco-alkalins: Exemple des massifs varisques du Mont Blanc (Alpes occidentales) et miocène du Monte Cappane (Ile d'Elbe, Italie)*. Thèse de doctorat N° 486, Université de Lausanne
- BUWAL (Bundesamt für Umwelt, Wald und Landschaft) (1991): *Schwermetalle und Fluor in Mineraldüngern*. Bern
- BUWAL (Bundesamt für Umwelt, Wald und Landschaft)(1998): *Nationale Grundwasserqualitätsbeobachtung (NAQUA)*. Bern
- BUWAL (Bundesamt für Umwelt, Wald und Landschaft) (1999): *NABEL Luftbelastung 1999*. Bern
- BUYANOVSKY, G. A., & WAGNER, G. H. (1983): Annual cycles of carbon dioxide level in soil air. *Soil Sci. Soc. Am. J.*, Vol. 47, 1139-1145
- BÜCHI, U. P. (1950): *Zur Geologie und Paläogeographie der südlichen mittelländischen Molasse zwischen Toggenburg und Rheintal*. Dissertation, Universität Zürich
- BÜCHI, U. P., & WELTI, G. (1951): *Zur Geologie der südlichen mittelländischen Molasse der Ostschweiz zwischen Goldingertobel und Toggenburg*. *Eclogae Geol. Helv.*, Vol. 44/1, 183-206
- BÜCHI, U. P. (1958): *Zur Geologie der Molasse zwischen Reuss und Seetal (Baldegger- / Hallwilersee / Aabach)*. *Eclogae Geol. Helv.*, Vol. 51/2, 279-298
- BÜCHI, U. P., & SCHLANKE, E. (1977): *Zur Paläogeographie der schweizerischen Molasse*. *Erdöl-Erdgas-Z.*, Vol. 93/Sonderausgabe, 57
- BÜRGISSER, H. M. (1980): *Zur mittel-miozänen Sedimentation im nordalpinen Molassebecken*. Thèse de doctorat, ETH Zürich

References

- CALAMITA, F., CELLO, G., INVERNIZZI, C., & PALTRINIERI, W. (1990): *Stile strutturale e cronologia della deformazione lungo la traversa M. S. Vicino-Polverigi (Appennino Marchigiano esterno)*. Studi geologici camerti, /volume speciale, 69-86
- CALDER, L. M. (1988): Chromium contamination of groundwater. In J. O. Nriagu & E. Nieboer (Eds.), *Chromium in the Natural and Human Environments* (215-229, Chapter 8). Wiley
- CANET, J. (1960): *Etude bibliographique sur les gîtes et gisements des départements de Haute-Savoie et Isère* BRGM
- CANTONE TICINO (1990): Monte Generoso. Studio multidisciplinare: geologia tettonica e geofisica, carsismo, idrologia, idrogeologia, chimismo isotopi e multiracciamiento (Quad. di geol. e geof. appl. 3, Dip. Econ. Pubbl., Ist. Geol. Cant., Bellinzona Cantone Ticino)
- CARON, C., HOMEWOOD, P., & WILDI, W. (1989): The original swiss flysch: a reappraisal of the type deposits in the Swiss Prealps. *Earth Science Reviews*, Vol. 26, 1-45
- CASTIGLIONI, B. (1931): *Il gruppo della Civetta (Alpi Dolomitiche)*. Padova
- CAVALLI, I., & BIANCHI-DEMICHELI, F. (1982): Il carsismo del Selcifero Lombardo del Mte. Generoso. *Stalactite*, /2, 93-102
- CELICO, P. (1983): *Idrogeologia dei massicci carbonatici, delle piane quaternarie e delle aree vulcaniche dell'Italia centro-meridionale (Marche e Lazio meridionali, Abruzzo, Molise e Campania)*. Quaderni della Cassa per il Mezzogiorno, Vol. 4/2, 225
- CENTAMORE, E., & VALLETTA, M. (1976): *Carta Geologica d'Italia alla scala 1:50'000, carta idrogeologica F° 291 Pergola e note illustrative Servizio Geologico d'Italia, Roma*
- CERLING, T. E., & QUADE, J. (1993): Stable carbon and oxygen isotopes in soil carbonates. In P. K. Swart, K. C. Lohmann, J. A. McKenzie, & S. M. Savin (Eds.), *Climate change in continental isotopic records*. (217-231)
- CHAUVE, P., DUBREUCQ, F., FRANCHON, J.-C., GAUTHIER, A., METTETAL, J.-P., & PEGUENET, J. (1987): *Inventaire des circulations souterraines reconnues par traçage en Franche-Comté Géologie Mem. n° 2*. Ministère de l'Environnement, Ann. Sci. Uni. Besançon
- CHOU, L., & WOLLAST, R. (1984): Study of the weathering of albite at room temperature and pressure with a fluidized bed reactor. *Geochimica et Cosmochimica Acta*, Vol. 48, 2205-2217
- CHURCH, T. M. (1979): Marine barite. In G. Burns (Eds.), *Marine minerals* (175-209)
- Clarix Corporation (1997): *FileMaker Pro User's Guide*
- CLAYTON, J. L. (1986): An estimate of plagioclase weathering rate in the Idaho batholith based upon geochemical transport rates. In S. M. Coleman & D. P. Dethier (Eds.), *Rates of chemical weathering of rocks and minerals* (453-466)
- CLOW, D. W., MAST, M. A., & CAMPBELL, D. H. (1993): Controls on surface water chemistry in the upper Merced River Basin, Yosemite National Park, California. *Hydrological Processes*, Vol. 10, 727-746
- COLACICCHI, R. (1967): *Geologia della Marsica orientale*. *Geologica Romana*, Vol. 4, 189-316
- COLLET, L. W., Oulianoff, N., & Reinhard, M. (1952): *Atlas géologique de la Suisse 1:25'000, Feuille 1324 Finhaut (Barberine)*, Notice explicative Service hydrologique et géologique national, Commission Géologique Suisse
- COLLET, G. (1986): *Aux sources de la Noches. Etude d'une source de l'Ultrasuisse. Mémoire de licence, Faculté des lettres, Université de Lausanne*
- CORBIN, P., & OULIANOFF, N. (1959): *Note explicative de la carte géologique du massif du Mont Blanc*
- COLOMBI SCHMUTZ DORTHE AG (1985): *Wasserversorgungsgenossenschaft der Gemeinde Weissenberg, Bern-Liebefeld: Hydrogeologischer Bericht und Dimensionierung der Schutzzonen*

- DALLA PIAZZA, R. (1994): Transfert des éléments traces en solution au cours de l'altération: Exemple du Cr dans un sol brun acide (Lutry, Suisse). In S. S. d. P. (SSP/BGS) (Ed.), Aktuelle Bodenforschung in der Schweiz, Symposium der BGS anlässlich der Jahresversammlung der SANW., 7.10.1994, document 6. Aarau
- DALLA PIAZZA, R. (1996): Géochimie des altérations dans trois écosystèmes sol tempérés - Application à l'acquisition des caractéristiques chimiques des solutés. Thèse de doctorat, N° 1483, EPF Lausanne, Dép. Génie Rural
- DAUCHY, X. (1994): Usage de l'ICP-MS haute résolution dans l'étude de sites contaminés par des décharges (Rapport de stage de formation EPFL-GEOLEP
- DAVIS, J. A., & KENT, D. B. (1990): Surface complexation modelling in aqueous geochemistry. In M. F. Hochella & A. F. White (Eds.), Mineral-Water Interface Geochemistry (177-260). Washington
- DEER, W. A., HOWIE, R. A., & ZUSSMAN, J. (1992): An introduction to the rock-forming minerals (2nd ed.). Longman Scientific & Technical
- DEMATTEIS, A., & HESSKE, S. (1993): Elementi in traccia come traccianti geogenici, due esempi: acquiferi in rocce carbonatiche e in sedimenti molassici. Risultati preliminari. In 3ème Rencontre Internationale des jeunes chercheurs en géologie appliquée., Potenza, 28. - 30.10.1993
- DEMATTEIS, A., & SALVATI, R. (1995): Contributo alla caratterizzazione idrogeologica ed idrogeochimica dell'acquifero della Montagna Grande (Abruzzo, Italia). In IMYRAG, 2eme edition., Peveragno
- DEMATTEIS, A. (1995): Typologie géochimique des eaux des aquifères carbonatés des chaînes alpines d'Europe centrale et méridionale. Thèse de doctorat, N° 1419, EPF Lausanne, Dép. Génie Civil
- DERRON, M.-H. (1999): Interaction eau-roche de basse température: géochimie des métaux dans l'altération météorique des roches mafiques alpines. Thèse de doctorat, Université de Lausanne
- DRAKE, J. J., & WIGLEY, T. M. (1975): The effect of climate on the geochemistry of carbonate terrains. Water Resour. Res., Vol. 11/6, 958-962
- DREVER, J. I. (1988): The geochemistry of natural waters. Prentice Hall Inc., Englewood Cliffs, N.J.
- DREVER, J. I., & ZOBRIST, J. (1992): Chemical weathering of silicate rocks as a function of elevation in the southern Swiss Alps. Geochimica et Cosmochimica Acta, Vol. 56, 3209-3216
- DREYBRODT, W. (1998): Limestone dissolution rates in karst environments. Bulletin d'Hydrogéologie, Centre d'Hydrogéologie, Université de Neuchâtel, Vol. 16, 167-183
- DRONKERT, H. (1987): Diagenesis of Triassic evaporites in northern Switzerland. Eclogae Geol. Helv., Vol. 80/2, 397-413
- DRONKERT, H., BLÄSI, H.-R., & MATTER, A. (1990): Fazies und Entstehung der Trias-Evaporite in den NAGRA-Tiefbohrungen, Nordschweiz (Geologische Berichte 12). Landeshydrologie und -geologie
- DUBOIS, J.-D. (1983): Etude hydrogéologique et géothermique de la région de Saillon (rapport non publié Comm. féd. énergie géothermie, Dépt. de Minéralogie Univ. Genève
- DUBOIS, J.-D., & PARRIAUX, A. (1990): Hydrogeological characteristics of the Mont Blanc and Aiguilles Rouges Massifs (France, Italy and Switzerland): First results. In A. Parriaux (Ed.), Proceedings of the 22nd Congress of IAH: Water Resources in Mountainous Regions, 1 (pp. 254-262). Lausanne
- DUBOIS, J.-D. (1993): Typologie des aquifères du cristallin: Exemple des massifs des Aiguilles Rouges et du Mont Blanc (France, Italie et Suisse). Thèse de doctorat, N° 950, EPFL, Dép. Génie Civil
- DUBOIS, J.-D., MAZOR, E., JAFFE, F., & BIANCHETTI, G. (1993): Hydrochimie et géothermie de la région de Saillon. Bulletin du CHYN, Neuchâtel, 71-85
- DUCLUZEAUX, B. (1990): Le Gouffre du Grand Cor. Stalactite, Vol. 40/1, 3-8
- DUCLUZEAUX, B., & PERRIN, J. (1995): Le Réseau du Grand Cor. In Actes du 10ème Congrès Nat. Spéléologique, (pp. 165-169). Breitenbach

References

- DUMONT, D. (1988): Campagne géochimique dans la Combe d'Orny et étude à grande échelle d'un secteur molybdénifère. Diplôme, Lausanne
- DZOMBAK, D. A., & MOREL, F. M. M. (1990): Surface complexation modelling - Hydrous Ferric oxide. Wiley-Interscience, New-York
- EARY, L. E., & RAI, D. (1987): Kinetics of chromium(III) oxidation to chromium(VI) by reaction with manganese oxides. Environ. Sci. Technol., Vol. 21/12, 1187-1193
- EARY, L. E., & RAI, D. (1988): Chromate removal from aqueous wastes by reduction with ferrous iron. Environ. Sci. Technol., Vol. 22/8, 972-977
- EISENLOHR, L. (1995): Variabilité des réponses naturelles des aquifères karstiques. De l'identification de la réponse globale vers la connaissance de la structure de l'aquifère. Thèse de doctorat, Université de Neuchâtel
- ESCHER, A., MASSON, H., & STECK, A. (1987): Coupes géologiques des Alpes occidentales suisses (Rapports géologiques Nr.2). Service hydrologique et géologique national, Berne
- ESCHER, A. (1988): Structure de la nappe du Grand St-Bernard entre le Val de Bagnes et les Mischabel (Rapports géologiques 7). Service Hydrogéologique et Géologique National, Bern
- ETCHEVERRY, D., & PARRIAUX, A. (1999): Etude hydrogéologique et isotopique de la source de Savigny GEOLEP-EPFL
- FALCONNIER, A. (1931): Etude géologique de la région du Col du Marchairuz. Thèse de doctorat n° 897, Faculté de Sciences de l'Université de Genève
- FASEL, J.-M. (1986): Sédimentologie de la Molasse d'eau douce subalpine entre le Léman et la Gruyère. Thèse de doctorat, Université de Fribourg
- FISCHER, H. (1983): K-Ar und Rb-Sr Altersbestimmungen an Glaukoniten der Helvetischen Kreide, des Tertiärs und des Oberen Jura sowie Geologie des Nord-Pilatus. Diplomarbeit, unpubl., Univ. Zürich
- FLÜCK, J. (1984): Etude hydrogéologique et géothermique des sources de Combioula, Val d'Hérens, Valais. Diplôme, non publié, Université de Genève
- FORD, D., & WILLIAMS, P. (1989): Karst geomorphology and hydrology. Unwin Hyman, London
- FORD, D. C. (1998): Perspectives in karst hydrogeology and cavern genesis. Bulletin d'Hydrogéologie, Vol. 16, 9-29
- FRAPPORTI, G., VRIEND, S. P., & VAN GAANS, P. F. M. (1996): Trace elements in the shallow groundwater of the Netherlands. A geochemical and statistical interpretation of the National Monitoring Network data. Aquatic Geochemistry, Vol. 2, 51-80
- FREEZE, R. A., & CHERRY, J. A. (1979): Groundwater. Prentice-Hall Inc., Englewood Cliffs New Jersey
- FROGNER, P., & SCHWEDA, P. (1998): Hornblende dissolution kinetics at 25°C. Chemical Geology, Vol. 151, 169-179
- FÜCHTBAUER, H. (1954): Transport und Sedimentation der westlichen Alpenvorlandmolasse. Heidelb. Beitr. Mineral. Petrogr., Vol. 4/26
- FÜCHTBAUER, H. (1955): Die Sedimentation der westlichen Alpenvorlandmolasse. Zeitschrift der deutschen geol. Ges. Jg. 1953, Vol. 105/3
- FÜCHTBAUER, H. (1964): Sedimentpetrographische Untersuchungen in der älteren Molasse nördlich der Alpen. Eclogae Geol. Helv., Vol. 57, 157-298
- GAGNEBIN (1916): Les Sources du Massif de Morcles. Bull. Soc. Vaudoise Sc. Nat., Vol. 51/189, 81-107
- GAINES, G. L., & THOMAS, H. C. (1953): Adsorption studies on clay minerals. II. A formulation of the thermodynamics of exchange adsorption. J. Chem. Phys., Vol. 21, 714-718
- GAPON, E. N. (1933): Theory of exchange adsorption. V. J. Gen. Chem. (USSR), Vol. 3, 667-669

- GARRELS, R. M., & CHRIST, C. L. (1965): *Solutions, Minerals and Equilibria*. Harper & Row, New York
- GARRELS, R. M., & MACKENZIE, F. T. (1967): Origin of the chemical composition of some springs and lakes. In W. Stumm (Eds.), *Equilibrium Concepts in natural water systems* (222-242)
- GARRELS, R. M., MACKENZIE, F. T., & HUNT, C. (1975): *Chemical cycles and the global environment*. W. Kaufmann Inc., Los Altos, CA
- GASSER, U. (1966): Sedimentologische Untersuchungen in der äusseren Zone der subalpinen Molasse des Entlebuch (Kt. Luzern). *Eclogae Geol. Helv.*, Vol. 59/2, 723-772
- GASSER, U. (1968): Die innere Zone der subalpinen Molasse des Entlebuch (Kt. Luzern), *Geologie und Sedimentologie*. *Eclogae Geol. Helv.*, Vol. 61, 229-313
- GAUTELIER, M., OELKERS, E. H., & SCHOTT, J. (1999): An experimental study of dolomite dissolution rates as a function of pH from -0.5 to 5 and temperature from 25 to 80°C. *Chemical Geology*, Vol. 157, 13-26
- GEOLEP (1984): Etude des zones de protection du groupe des sources de Pierre-Ozaire – Rapport pour la Ville de Lausanne, service des eaux Etude N° 8201). GEOLEP - EPFL
- GEOLEP (1991): Potentialités de recapture dans la région de la Pierre-Ozaire – Rapport pour la Ville de Lausanne, service des eaux Etude N° 8201.1). GEOLEP - EPFL
- Geologisches Landesamt Baden-Württemberg (1990): Hydrogeologisches Abschlussgutachten zur Ausweisung eines Wasserschutzgebietes für die Quelfassungen Mösser, Soss und Taubental (Rapport non publié Geologisches Landesamt Baden-Württemberg, Freiburg i. Br.
- Geologisches Landesamt Baden-Württemberg (1992): Hydrogeologisches Abschlussgutachten zur Abgrenzung von Wasserschutzgebieten für die Quelfassungen “Nonnenebene”, “Hattental”, “Himberg” und “Priel” der Gemeinde Sipplingen (Rapport non publié Geologisches Landesamt Baden-Württemberg, Freiburg i. Br.
- GEOTEST (1982): Hydrogeologischer Bericht und Schutzzonengutachten für die Quelfassungen Augant und Zünigwald der Gemeinde Wimmis Geotest, Bern-Zollikofen
- GILLIÉRON, F. (1986): Zur Geologie der Uranmineralisation in den Schweizer Alpen Geotech. Serie 77). *Beiträge zur Geologie der Schweiz*
- GOVERNA, M. E., LOMBARDI, S., MASCIOTTO, L., RIBA, M., & ZUPPI, G. M. (1989): Karst and geothermal water circulation in the central Apennines (Italy). In IAEA Advisory Group meeting, 329.2/9 (pp. 173-202). Wien, 17-21 nov. 1986
- GRASSO, D. A., & JEANNIN, P.-Y. (1998): Statistical approach to the impact of climatic variations on karst spring chemical response. *Bulletin d'Hydrogéologie*, CHYN, Univ. Neuchâtel, Vol. 16, 59-74
- GRIMM, W. D. (1965): Schwermineralgesellschaften in Sandschüttungen, erläutert am Beispiel der süddeutschen Molasse. *Abh. Bayer. Akad. Wiss.*, Vol. 121
- GWINNER, M. P. (1978): *Geologie der Alpen* (2nd ed.). Schweizerbart'sche Verlagsbuchhandlung, Stuttgart
- HABICHT, J. K. A. (1945): Geologische Untersuchungen im südlichen St.Gallisch-Appenzellischen Molassegebiet. *Beitr. geol. Karte Schweiz*, Vol. 83, 118
- HABICHT, J. K. A. (1987): *Lexique stratigraphique international - Volume I Europe, Fascicule 7 Schweiz, Schweizerisches Mittelland (Molasse) (Fascicule 7b)*. Birkhäuser AG, Reinach/Basel
- HANDA, B. K. (1988): Occurrence and distribution of chromium in natural waters of India. In J. O. Nriagu & E. Nieboer (Eds.), *Chromium in the Natural and Human Environments* (Chapter 7). Wiley
- HANSEN, B. K., & POSTMA, D. (1995): Acidification, buffering, and salt effects in the unsaturated zone of a sandy aquifer, Klosterhede, Denmark. *Water resources research*, Vol. 31/11, 2795-2809
- HARMON, R. S., WHITE, W. B., DRAKE, J. J., & HESS, J. W. (1975): Regional hydrochemistry of North American carbonate terrains. *Water Resour. Res.*, Vol. 11, 963-967

References

- HARRIS, N., BICKLE, M., CHAPMAN, H., FAIRCHILD, I., & BUNBURY, J. (1998): The significance of Himalayan rivers for silicate weathering rates: evidence from the Bhote Kosi tributary. *Chem Geol*, Vol. 144/3-4, 205-220
- HEM, J. D. (1977): Reactions of metal ions at surfaces of hydrous iron oxide. *Geochimica et Cosmochimica Acta*, Vol. 41, 527-538
- HEM, J. D. (1985): Study and interpretation of chemical characteristics of natural waters, 3rd ed. (Water Supply Paper 2254). U.S. Geol. Survey
- HESSKE, S. (1994): Typisierung von Molassequellwässern zwischen Chambéry (F) und Linz (A): Konzept, Vorgehen und erste allgemeine Datenauswertung. In *Rencontre Internationale des jeunes chercheurs en géologie appliquée*, (pp. 115-119). Lausanne, 21.4.1994
- HESSKE, S. (1995): Typologie des eaux souterraines de la Molasse entre Chambéry et Linz (France, Suisse, Allemagne, Autriche). Thèse de doctorat, EPF Lausanne, Dép. Génie Civil
- HESSKE, S., PARRIAUX, A., & BENSIMON, B. (1997): Geochemistry of springwaters in Molasse aquifers: Typical mineral trace elements. *Eclogae Geol. Helv.*, Vol. 90/1, 151-171
- HOCELLA, M. F., & WHITE, A. F. (Eds.) (1990): *Mineral-Water Interface Geochemistry*. Washington
- HOFMANN, F. (1957): Untersuchungen in der subalpinen und mittelländischen Molasse der Ostschweiz. *Eclogae Geol. Helv.*, Vol. 50, 289-322
- HOFMANN, F. (1959): Materialherkunft, Transport und Sedimentation im schweizerischen Molassebecken. *Bericht der St.Gallischen naturforschenden Gesellschaft*, Vol. 76 (1956-58)
- HOFMANN, F. (1960): Beitrag zur Kenntnis der Glimmersandsedimentation in der oberen Süßwassermolasse der Nord- und Nordostschweiz. *Eclogae Geol. Helv.*, Vol. 53/1
- HOLSER, W. T. (1979a): Mineralogy of evaporites. In R. G. Burns (Eds.), *Marine minerals*, Miner. Soc. of America, short course notes (211-294)
- HOLSER, W. T. (1979b): Trace elements and isotopes in evaporites. In R. G. Burns (Eds.), *Marine minerals*, Miner. Soc. of America, short course notes (295-346)
- HOMEWOOD, P. W., & ALLEN, P. A. (1981): Wave-, tide-, and current-controlled sandbodies of Miocene Molasse, western Switzerland. *Bull. amer. Assoc. Petrol. Geol.*, Vol. 65/12, 2534
- HOMEWOOD, P. W., ALLEN, P. A., & MATTER, A. (1982): Die Obere Meeresmolasse der Westschweiz (Region Freiburg). *Exkursion V*, 13. April 1982. *Jber. Mitt. oberrhein. geol. Ver.*, Vol. 64, 13-16
- HOMEWOOD, P., & LATELTIN, O. (1988): Classic swiss clastics (flysch and molasse). The alpine connection. *Geodinamica acta*, Vol. 2/1, 1-11
- HOMEWOOD, P. W., KELLER, B., SCHOEPFER, P., & YANG, C. S. (1989a): Faciès, processus de sédimentation et reconstitution des conditions paléomarines dans la Molasse marine supérieure suisse. *Bull. Soc. géol. France*, Vol. 8/5, 1015-1027
- HOMEWOOD, P. W., RIGASSI, & WEIDMANN, M. (1989b): Le bassin molassique Suisse. In B. Pursen (Eds.), *Dynamique et méthodes d'étude des bassins sédimentaires* (299-314). Technip, Paris
- HÖLTING, B. (1992): *Hydrogeologie - Einführung in die Allgemeine und Angewandte Hydrogeologie* (4th ed.). Enke, Stuttgart
- HYMAN, M. E., JOHNSON, C. E., BAILEY, S. W., APRIL, R. H., & HORNBECK, J. W. (1998): Chemical weathering and cation loss in a base-poor watershed. *Geol. Soc. Amer. Bull.*, Vol. 110/1, 85-95
- Institut Français du Pétrole (1967): Etude géologique de l'Epire (Grèce Nord-Occidentale) Etude réalisé par l'Institut de Géologie et Recherches du Sous-sol, Athènes, et l'Institut français du Pétrole - Mission Grèce. Royaume de Grèce, Ministère de l'Industrie

- JAFFÉ, F. C. (1955): Les ophiolites et les roches connexes de la région du Col des Gets. *Schweizerische Mineralogische und Petrographische Mitteilungen*, Vol. 35/1, 1-150
- JAHNKE, C. (1999): Ein neues Klassifikationssystem für Grundwasser und seine Anwendung in känozoischen Porengrundwasserleitern. *Grundwasser*, Vol. 2, 62-72
- JAMES, B. R., & BARTLETT, R. J. (1983a): Behaviour of Cr in soils: VI. Interactions between oxidation-reduction and organic complexation. *Journal of Environ. Qual.*, Vol. 12/2, 173-177
- JAMES, B. R., & BARTLETT, R. J. (1983b): Behaviour of Cr in soils: VII. Adsorption and reduction of hexavalent forms. *Journal of Environ. Qual.*, Vol. 12, 177-181
- JAMES, B. R., PETURA, J. C., VITALE, R. J., & MUSSOLINE, G. R. (1997): Oxidation-reduction of chromium: relevance to the regulation and remediation of chromate-contaminated soils. *Journal of Soil Contamination*, Vol. 6/6, 569-580
- JAMIER, D. (1975): Etude de la fissuration, de l'hydrogéologie et de la géochimie des eaux profondes des massifs de l'Arpille et du Mont Blanc. Thèse de doctorat, Université de Neuchâtel
- JÄCKLI, H. (1970): Kriterien zur Klassifikation von Grundwasservorkommen. *Eclogae Geol. Helv.*, Vol. 63/2, 389-434
- JEANBOURQUIN, P., & BURRI, M. (1989): La zone de Sion-Courmayeur dans la région du Simplon (Rapports géologiques Nr.11). SHGN, Bern
- JEANNIN, P.-Y. (1991): Températures dans la zone vadose du karst. In *Actes du 9e Congrès Nat. Spéléologique*, (pp. 71-76)
- JORDI, H. A. (1955): Geologie der Umgebung von Yverdon (Jurafuss und mittelländische Molasse). Kümmerly & Frey AG, Bern
- KATZ, S. A., & SALEM, H. (1993): The toxicology of chromium with respect to its chemical speciation: a review. *Journal of applied toxicology*, Vol. 13/3, 217-224
- KELLER, B. (1987): Lithostratigraphische Gliederung der Oberen Meeresmolasse. In *Jahresversammlung der Schweizerischen Geologischen Gesellschaft*, Luzern
- KELLER, B. (1989): Fazies und Stratigraphie der Oberen Meeresmolasse zwischen Napf und Bodensee. Dissertation, Bern
- KELLER, B. (1992): Hydrogeologie des schweizerischen Molasse-Beckens: Aktueller Wissensstand und weiterführende Betrachtungen. *Eclogae Geol. Helv.*, Vol. 85/3, 611-651
- KENNEDY, V. C., ZELLWEGER, G. W., & JONES, B. F. (1974): Filter pore-size effects on the analysis of Al, Fe, Mn, and Ti in water. *Water Resources Research*, Vol. 10/4, 785-790
- KHOURY, H. N., SALAMEH, E., CLARK, I. D., FRITZ, P., BAJJALI, W., MILODOWSKY, A. E., CAVE, M. R., & ALEXANDER, W. R. (1992): A natural analogue of high pH cement pore waters from the Maqarin area of northern Jordan. I: Introduction to the site. *Journal of Geochem. Expl.*, Vol. 46, 117-132
- KIRALY, L. (1975): Rapport sur l'état actuel des connaissances dans le domaine des caractères physiques des roches karstiques. In *IAH (Ed.), International Union of Geol. Sciences: Hydrogeology of karstic terrains*, (pp. 53-67). Paris
- KIRALY, L., & MULLER, I. (1979): Hétérogénéité de la perméabilité et de l'alimentation dans le karst: effet sur la variation du chimisme des sources karstiques. *Bull. Centre Hydrogéol.*, Neuchâtel, Vol. 3, 273-285
- KISSLING, D. (1974): L'Oligocène de l'extrémité occidentale du bassin molassique suisse. Stratigraphie et aperçu sédimentologique. Thèse de doctorat, Université de Genève
- KLIMCHOUK, A. B., Ford, D. C., Palmer, A. D., & Dreybroth, W. (2000): Speleogenesis - Evolution of Karst Aquifers
- KLIMCHOUK (2000): Speleogenesis in sulphate rocks. In A. B. Klimchouk, D. C. Ford, A. N. Palmer, & W. Dreybroth (Eds.), *Speleogenesis - Evolution of Karst Aquifers* (431-442)

References

- KRAUSKOPF, K. B., & BIRD, D. K. (1995): Introduction to geochemistry (3. ed.). McGraw-Hill, Inc.
- KUNZ, F. (1986): Notes de terrain sur quelques sources de la nappe tectonique du Niesen et essais de traçage (field notes GEOLEP-EPFL, Lausanne)
- LABHART, T., & RYBACH, L. (1972): Der Vallorcine Granit und seine radiometrischen Anomalien. Schweiz. Min. Petr. Mitt., Vol. 52, 357-388
- LABHART, T., & Rybach, L. (1974): Granite und Uranvererzungen in den Schweizer Alpen. Geologische Rundschau, Vol. 63/1, 357-388
- LASAGA, A. C., SOLER, J. M., GANOR, J., BURCH, T. E., & NAGY, K. L. (1994): Chemical weathering rate laws and global geochemical cycles. *Geochimica et Cosmochimica Acta*, Vol. 58/10, 2361-2386
- LASTENNET, R. (1994): Rôle De la zone non-saturée dans les fonctionnement des aquifères karstiques. Thèse de doctorat, Université d'Avignon et des pays de Vaucluse
- LAURSEN, S. (1991): On gaseous diffusion of CO₂ in the unsaturated zone. *Journal of Hydrology*, Vol. 122, 61-69
- LEBDIOUI, S., MICHELOT, J.-L. & FONTES, J. CH. (1990): Origine de la minéralisation sulphatée et carbonaté des eaux du tunnel sous le Mont-Blanc. In A. Parriaux (Ed.), *Proceedings of the 22nd Congress of IAH: Water Resources in Mountainous Regions*, 1 (pp. 496-503). Lausanne, EPFL
- LEMCKE, K., ENGELHARDT, W., & FÜCHTBAUER, H. (1953): Geologische und sedimentpetrographische Untersuchungen im Westteil der ungefalteten Molasse des süddeutschen Alpenvorlandes. *Beih. Geol. Jb. Hannover*, Vol. 11
- LEMCKE, K. (1972): Die Lagerung der jüngsten Molasse im nördlichen Alpenvorland. *Bull. schweiz. Ver. Petroleum.-Geol. u. Ing.*, Vol. 39/95
- LEONARDI, P. (1968a): Le Dolomiti. *Geologia dei monti tra Isarco e Piave*. In C.N.R. (Eds.), (1019). Manfrini, Rovereto
- LEONARDI, P. (1968b): Tettonica e tetto-genesi delle Dolomiti. In P. L. e. Coll. (Eds.), *Le Dolomiti (407-508)*. *Ist. Geol. Univ. Ferrara*
- LIU, X., & BYRNE, R. H. (1997): Rare earth and yttrium phosphate solubilities in aqueous solution. *Geochimica et Cosmochimica Acta*, Vol. 61/8, 1625-1633
- LOMBARD, A., BAUD, A., & STEINHAUSER, N. (1975): Atlas géologique de la Suisse, 1:25'000: carte et notice explicative feuille 1265 Les Mosses Comm. Géol. Suisse
- LOMBARDI, P. (1968): Tettonica e tetto-genesi delle Dolomiti
- LOZET, J., & MATHIEU, C. (1990): Dictionnaire de Science du Sol (2nd ed.). *Technique et Documentation - Lavoisier*, Paris
- LUGEON, M., & JEREMINE (1911): Les bassins fermés des Alpes Suisses. *Bull. Soc. Vaudoise Sc. Nat.*, Vol. 174, 461-650
- LUGEON, M., ARGAND, E., OULIANOFF, N., REINHARD, M., & POLDINI, E. (1937): Atlas géologique 1:25'000, feuille Saxon-Morcles N° 1305 et notice explicative Comm. géol. Suisse
- LUGEON, M. (1940): Atlas géologique de la Suisse: Carte géologique au 1:25'000 et notice explicative de la feuille n° 19 Les Diablerets Comm. Géol. Suisse
- MALARODA, R. (1970): Note illustrative della Carta geologica del Massiccio dell'Argentera alla scala 1:50'000. *Mem. Soc. Geol. It.*, Vol. 9, 557-663
- MANCEAU, A., SCHLEGEL, M. L., MUSSO, M., SOLE, V. A., GAUTHIER, C., PETIT, P. E., & TROLARD, F. (2000): Crystal chemistry of trace elements in natural and synthetic goethite. *Geochimica et Cosmochimica Acta*, Vol. 64/21, 3643-3661

- MANDIA, Y., & PARRIAUX, A. (1990): Hydrochemical study of evaporitic aquifers in the Rhone Basin Trias (Western Swiss Alps). First results. In A. Parriaux (Ed.), Proceedings of the 22nd Congress of IAH: Water Resources in Mountainous Regions, 1 (pp. 304-314). Lausanne, EPFL
- MANDIA, Y. (1993): Typologie des aquifères évaporitiques du Trias dans le Bassin lémanique du Rhône (Alpes occidentales). Thèse de doctorat, EPF Lausanne, Dép. Génie Civil
- MANGIN, A. (1975): Contribution à l'étude hydrodynamique des aquifères karstiques. Thèse de doctorat ès science, Univ. de Dijon (publié dans Ann. Spéléol. C.N.R.S. T. 29/3, pp. 283-332, T. 29/4, pp. 495-601, T. 30/1, pp. 21-124). In Paris
- Schweizerisches Lebensmittel Handbuch (1999). Bern
- MARÉCHAL, J. C. (1998): Les circulations d'eau dans les massifs cristallins alpins et leurs relations avec les ouvrages souterrains. Thèse de doctorat, N° 1769, EPF Lausanne, Dép. Génie Civil
- MARRO, C. (1986): Les granitoïdes du Mont-Blanc en Suisse. Thèse de doctorat, N° 909, Université de Fribourg
- MARTHALER, M. (1984): Géologie des unités penniques entre le Val d'Anniviers et le Val de Tourtemagne Valais, Suisse. *Eclogae Geol. Helv.*, Vol. 77/2, 395-448
- MASSON, H., HERB, R., & STECK, A. (1980): Excursion N°I. In R. Trümpy Schweizerische Geologische Kommission (Eds.), *Geology of Switzerland, a Guide Book. Part B: Geological Excursions* Wepf & Co Publishers, Basel, New York
- MASSON, D. (1992): L'unité karstique de Naye, inventaire des cavités. *Bulletin des cals terreux*, Vol. 152 et suivants
- MATTER, A., HOMEWOOD, P., CARON, C., RIGASSI, D., VAN STUIJVENBERG, J., WEIDMANN, M., & WINKLER, W. (1980): Flysch and Molasse of western and central Switzerland. Excursion No. 126 of the 26th International Geological Congress. In *Geology of Switzerland - a guide book (261-293)*. Wepf & Co, Basel
- MATTHESS, G. (1994): Die Beschaffenheit des Grundwassers. *Lehrbuch der Hydrogeologie*. Borntraeger
- MATZTAT, E., & SHIRAKI, K. (1978): *Chromium*. Springer Verlag, Berlin, Heidelberg, New York
- MAURER, H., FUNK, H. P., & NABHOLZ, W. (1978): Sedimentpetrographische Untersuchungen an Molasse-Abfolgen der Bohrung Linden 1 und ihrer Umgebung (Kt. Bern). *Eclogae Geol. Helv.*, Vol. 71/3, 497-515
- MAURER, H. (1983): Sedimentpetrographische Analysen an Molasseabfolgen der Westschweiz. *Jb. Geol. B.-A.*, Wien, Vol. 126/1, 23-69
- MAY, H. M., ACKER, J. G., SMYTH, J. R., BRICKER, O. P., & DYAR, M. D. (1995): Aqueous dissolution of low-iron chlorite in dilute acid solutions at 25°C. In 32nd Annual Meeting of the Clay Mineral Society, (pp. 88). Baltimore, MD
- MAYER, L. M. (1999): Spatial and temporal variation of groundwater chemistry in Pettyjohns Cave, Northwest Georgia, USA. *Journal of Cave and Karst Studies*, Vol. 61/3, 131-138
- MÄDER, U., & WABER, N. (1997): Geochemical modelling of natural and contaminated groundwaters. Short course Geologisches und Mineralogisch-Petrographisches Institut, Universität Bern
- MCCARTHY, J. F., & ZACHARA, J. M. (1989): Subsurface transport of contaminants. *Environ. Sci. Technol.*, Vol. 23, 496-502
- MEVEL, C. (1975): Les "Pillow-Lavas" spillitiques des massifs ophiolithiques du Chenaillet et des Gets (Alpes françaises). Thèse de 3ème cycle, Paris
- MÉNAGER, M.-T., MENET, C., & PETIT, J.-C. (1989): U, Th, REE mobilisation during water-rock interactions in a U-mineralised granite. In D. L. Miles (Ed.), Proceedings of the 6th international Symposium on Water-Rock Interaction, (pp. 475-478). Malvern, 3-8 Aug. 1989, Balkema

References

- MIDDLESWORTH, P. E., & WOOD, S. A. (1998): The aqueous geochemistry of rare earth elements and yttrium. Part 7. REE, Th and U contents in thermal springs associated with the Idaho batholith. *Applied Geochemistry*, Vol. 13/7, 861-884
- MILANOVIC, P. T. (1981): *Karst hydrogeology*. Littleton, CO
- MONNIER, F. (1979): *Corrélation minéralogiques et diagenèse dans le bassin molassique suisse*. Thèse de doctorat, Université de Neuchâtel
- MONNIER, F. (1982): Thermal diagenesis in the Swiss molasse basin: implications for oil generation. *Canadian J. Earth Sci.*, Vol. 19/2, 328-342
- MOORE, W. S., & Ramamoorthy, J. (1984): *Heavy metals in natural waters: applied monitoring and impact assessment*. Springer-Verlag, New York
- MOORE, D. M., & Reynolds, R. C. (1997): *X-Ray diffraction and the identification and analysis of clay minerals* (2nd ed.). Oxford University Press, Oxford
- MORNOD, L. (1949): *Géologie de la région de Bulle (Basse-Gruyère): Molasse et bord alpin*. Kümmerly & Frey, Bern
- MORSE, J. W., & MACKENZIE, F. T. (1990): *Geochemistry of Sedimentary Carbonates*. Elsevier, Amsterdam
- MOSAR, J. (1988): *Structures, déformation et métamorphisme dans les Préalpes romandes (Suisse)*. Thèse de doctorat, Faculté des Sciences, Université de Neuchâtel
- MOSAR, J., & BOREL, G. (1992): Paleostress from the Préalpes Médiannes (Switzerland). *Annales Tectonicae*, Vol. 6/2, 115-133
- MURPHY, S. F., BRANTLEY, S. L., BLUM, A. E., WHITE, A. F., & DONG, H. (1998): Chemical weathering in a tropical watershed, Luquillo Mountains, Puerto Rico: II. Rate and mechanism of biotite weathering. *Geochimica et Cosmochimica Acta*, Vol. 62/2, 227-243
- NAGRA (1993): *Résultats des recherches effectués sur le site potentiel du Bois de la Glaive (Commune d'Ollon, VD)*
- NIGGLI, P., DE QUERVAIN, F., & WINTERHALTER, R. U. (1930): *Chemismus schweizerischer Gesteine*. Bern
- NORBERT, J. (1988): *Etude hydrogéologique. Délimitation des zones de protection. Bassin sourcier de la Torneresse (4 sources), bassin sourcier de l'Eau Froide (5 sources)* Service des eaux de la ville de Lausanne
- NORDSTROM, D. K., PLUMMER, L. N., LANGMUIR, D., BUSENBERG, B., MAY, H. M., JONES, B. F., & PARKHURST, D. L. (1990): Revised chemical equilibrium data for major water-mineral reactions and their limitations. In D. C. Melchior & R. L. Basset (Eds.), *Chemical Modelling of Aqueous Systems II* (398-413). American Chemical Society Symposium Series
- NRIAGU, J. O., & NIEBOER, E. (1988): *Chromium in the natural and human environments*. Wiley
- NRIAGU, J. O. (1991): *Trace metals in the environment*. Elsevier, Amsterdam
- OSEC Ordonnance sur les substances étrangères et les composants dans les denrées alimentaires (22.2.2000)
- PACYNA, J. M., & NRIAGU, J. O. (1988): Atmospheric emissions of chromium from natural and anthropogenic sources. In J. O. Nriagu & E. Nieboer (Eds.), *Chromium in the Natural and Human Environments* (105-123, Chapter 4). Wiley
- PALMER, D. A., WESOLOWSKI, D., & MESMER, R. E. (1987): A potentiometric investigation of the hydrolysis of chromate (VI) ion in NaCl media to 175°C. *Journal of Solution Chemistry*, Vol. 16/6, 443-463
- PALMER, C. D., & WITTBRODT, P. R. (1991): Processes affecting the remediation of chromium-contaminated sites. *Environmental Health Perspectives*, Vol. 92, 25-40
- PANCELLA, R. (Ed.). (1995): *In Actes du congrès LCP, Conservation et restauration des biens culturels*, (pp. 773). Montreux

- PARKHURST, D. L., THORSTENSON, D. C., & PLUMMER, N. L. (1980): PHREEQE - A computer program for geochemical calculations U.S. Geological Survey
- PARKHURST, D. L. (1995): User's guide to PHREEQC - a computer program for speciation, reaction-path, advective-transport, and inverse geochemical calculations (Water-Resources Investigations Report 95-4227). U.S. Geological Survey
- PARKHURST, D. L., & APPELO, C. A. J. (1999): User's guide to PHREEQC (version 2) - a computer program for speciation, batch reaction, one-dimensional transport, and inverse geochemical calculations (Water-Resources Investigations Report 99-4259). U.S. Geological Survey
- PARKS, G. A. (1967): Surface chemistry of oxides in aqueous systems. In W. Stumm (Eds.), *Equilibrium concepts in aqueous systems* (121-160). Washington
- PARRIAUX, A. (1981): Contribution à l'étude des ressources en eau du bassin de la Broye. Thèse de doctorat, N° 393, EPFL Lausanne
- PARRIAUX, A., DUBOIS, J.-D., MANDIA, Y., BASABE, P., & BENSIMON, M. (1990a): The AQUITYP Project: Towards an aquifer typology in the alpine orogen. In A. Parriaux (Ed.), *Proceedings of the 22nd Congress of IAH: Water Resources in Mountainous Regions*, 1 (pp. 254-262). Lausanne, EPFL
- PARRIAUX, A., MAYORAZ, R., & MANDIA, Y. (1990c): Impact assessment of deep underground works on a mineral water resource in an alpine evaporitic context. In A. Parriaux (Ed.), *Proceedings of the 22nd Congress of IAH: Water Resources in Mountainous Regions*, 2 (pp. 1249-1258). Lausanne, EPFL
- PAUL, A. (1993): Solhebungen beim Tunnelbau im Gipskeuper, Mechanismen - Auswirkungen - Bemessungsphilosophien (Vortrag Nr. 8). In *Lehrgang Felsmechanik und Ingenieurgeologie*, Technische Akademie Esslingen, Niederlassung Sarnen, Sargans, 13./14.5.1993
- PAVONI, N. (1957): Geologie der Zürcher Molasse zwischen Albiskamm und Pfannenstiel. *Vjschr. natf. Ges. Zürich*, Vol. 102, 117
- PEARSON, F. J., LOLCAMA, J. L., & SCHOLTIS, A. (1986): Chemistry of Waters in the Böttstein, Weiach, Riniken, Schafisheim, Kaisten and Leuggern Boreholes: A Hydrochemical Consistent data set. Baden
- PEARSON, F. J., BALDERER, W., LOOSLI, H. H., LEHMANN, B. E., MATTER, A., PETERS, T., SCHMASSMANN, H., & GAUTSCHI, A. (1991): Applied isotope hydrogeology. A case study in northern Switzerland. Elsevier, Amsterdam
- PERRIN, J. (1996): Etude géologique et hydrogéologique de la région Dent de Morcles - Grand Château. Diplôme ès sciences de la Terre, Université de Lausanne, Institut de Géologie
- PETCH, M. (1970): Contribution à l'étude hydrogéologique de la plaine de l'Orbe
- PFEIFER, H.-R., HANSEN, J., HUNZIKER, J., REY, D., SCHAFER, M., & SERNEELS, V. (1995): Arsenic in Swiss soils and waters and their relation to rock composition and mining activities. In 3rd International Conference on the Biogeochemistry of Trace Elements, Paris
- PFEIFER, H.-R., DERRON, M.-H., REY, D., SCHLEGEL, C., ATTEIA, O., DALLA PIAZZA, R., DUBOIS, J.-P., & MANDIA, Y. (2000): Natural trace element input to the soil-sediment-water-plant system: examples of background and contaminated situations in Switzerland, Eastern France and Northern Italy. In B. Markert & K. Friese (Eds.), *Trace elements - Their distribution and effects in the environment* Elsevier
- PHILPOTTS, A. R. (1990): Principles of igneous and metamorphic petrology. Prentice Hall, Englewood Cliffs
- PIPER, A. M., GARRET, A. A., & others (1953): Native and contaminated groundwaters in the Long Beach-Santa Ana area, California (Water Supply Paper 1136, 320p.). U.S. Geol. Survey
- PLUMMER, L. N. (1975): Mixing of sea water with calcium carbonate groundwater. *Geol. Soc. Am. Mem.*, Vol. 42, 219-236
- PLUMMER, L. N., WIGLEY, T. M. L., & PARKHURST, D. L. (1978): The kinetics of calcite dissolution in CO₂-water systems at 5° to 60°C and 0.0 to 1.0 atm CO₂. *American Journal of Science*, Vol. 278, 179-216

References

- PLUMMER, L. N., & BACK, W. (1980): The mass balance approach: Application to interpreting the chemical evolution of hydrologic systems. *Amer. J. Sci.*, Vol. 280, 130-142
- PLUMMER, L. N., BUSBY, J. F., LEE, R. W., & HANSHAW, B. B. (1990): *Geochemical Modelling of the Madison Aquifer in Parts of Montana, Wyoming, and South Dakota*. Water Resources Research, Vol. 26/9, 1981-2014
- PLUMMER, L. N. (1992): Geochemical modelling of water-rock interaction: Past, present, future. In Kharaka & Maest (Eds.), *Water-Rock Interaction* (23-33). Balkema, Rotterdam
- PLUMMER, L. N., PRESTEMON, E. C., & PARKHURST, D. L. (1994): An interactive code (NETPATH) for modelling NET geochemical reactions along a flow PATH, version 2.0 (Water-Resources Investigations Report 94-4169). U.S. Geological Survey
- PULS, R. W., & BARCELONA, M. J. (1989): Filtration of ground water samples for metals analysis. *Hazardous Waste & Hazardous Materials*, Vol. 6/4, 385-393
- PULS, R. W., CLARK, D. A., PAUL, C. J., & VARDY, J. (1994a): Transport and transformation of hexavalent chromium through soils and into ground water. *Journal of Soil Contamination*, Vol. 3, 203-224
- PULS, R. W., CLARK, D. A., CARLSON, C., & VARDY, J. (1994b): Characterisation of chromium-contaminated soils using field-portable X-ray fluorescence. *GWMR*, 111-115
- RAI, D., SASS, B. M., & MOORE, D. A. (1987): Chromium(III) hydrolysis constants and solubility of chromium(III) hydroxide. *Inorg. Chem.*, Vol. 26, 345-349
- RAI, D., ZACHARA, J. M., EARY, L. E., AINSWORTH, C. C., AMONETTE, E., COWAN, E. E., SZELMECZKA, R. W., RESCH, C. T., SCHMID, R. L., SMITH, S. C., & GIRVIN, D. C. (1988): Chromium reactions in geologic materials Report EA-5741). Electric Power Research Institute, Palo Alto, CA
- RAVAGNANI, D. (1974): *I giacimenti uraniferi italiani e i loro minerali*. Milano
- RENZ, H. H. (1937): Zur Geologie der östlichen St.Gallisch-Appenzellischen Molasse. *Jb. St.Gall. natw. Ges.*, Vol. 69
- RICHARD, F. C., & BOURG, A. C. (1991): Aqueous chemistry of chromium: A review. *Water research*, Vol. 25/7, 807-816
- RICKARD, D., & SJÖBERG, E. L. (1983): Mixed kinetic control of calcite dissolution rates. *Am. J. Sci.*, Vol. 283, 815-830
- RIGAULT, G., & FERRARIS, G. (1962): Ricerche sulla fluorite rosea del Monte Bianco. *Atti. Accad. Sc. Torino*, Vol. 96, 12
- RIMSTIDT, J. D., & BARNES, H. L. (1980): The kinetics of silica-water reactions. *Geochimica et Cosmochimica Acta*, Vol. 44, 1683-1699
- RIZZOLI, G. (1997): XRD Röntgendiffraktometrie. Teil 1: Präparation und Auswertung (Labor-Arbeitsanleitung Mineralogisch-Petrographisches Institut Universität Bern
- ROBERTSON, F. N. (1975): Hexavalent Cr in the groundwater in Paradise Valley, Maricopa County, Arizona. *Ground Water*, Vol. 13, 516-527
- RODIER, J. (1996): *L'analyse de l'eau - eaux naturelles, eaux résiduares, eau de mer (8ème ed.)*. Dunod, Paris
- ROLLINSON, H. (1993): *Using geochemical data: evaluation, presentation, interpretation*. Longman, Singapore
- ROSE, N. M. (1991): Dissolution rates of prehnite, epidote and albite. *Geochimica et Cosmochimica Acta*, Vol. 55, 3273-3286
- ROSSI, D. (1967): Dolomitizzazione delle formazioni Anisiche e Ladino-Carniche delle Dolomiti. *Mem. Museo Tridentino Scienze Naturali*, Trento, Vol. 16/3
- RYBACH, L., VON RAUMER, J., & ADAMS, J. A. S. (1966): A gamma spectrometric study of Mont Blanc granite samples. *Beiträge zur Geologie der Schweiz, kleinere Mitteilungen*, Vol. 37

- SALIMI, F. (1965): Etude pétrographique des roches ophiolitiques des Préalpes romandes. Schweizerische Mineralogische und Petrographische Mitteilungen, Vol. 45/1, 189-280
- SALOMONS, W., & FÖRSTNER, U. (1984): Metals in the Hydrocycle. Springer-Verlag, Berlin Heidelberg
- SALOMONS, W., & MOOK, W. G. (1986): Isotope Geochemistry of Carbonates in the Weathering Zone. In B. P. Fritz & J. C. Fontes (Eds.), Handbook of Environmental Isotope Geochemistry (239-269). Elsevier, Amsterdam
- SASS, B. M., & RAI, D. (1987): Solubility of amorphous chromium(III)-iron(III) hydroxide solid solutions. Inorg. Chem., Vol. 26/14, 2228-2232
- SCHEFFER, F., & SCHACHTSCHABEL, P. (1979): Lehrbuch der Bodenkunde (10 ed.). Ferdinand Enke Verlag, Stuttgart
- SCHLANKE, S. (1974): Geologie der Subalpinen Molasse zwischen Biberburg SZ, Hütten ZH und Aegerisee ZG, Schweiz. Eclogae Geol. Helv., Vol. 67/2, 243-332
- SCHLUNEGGER, F., MATTER, A., & MANGE, M. A. (1993): Alluvial fan sedimentation and structure of the southern Molasse Basin margin, Lake Thun area, Switzerland. Eclogae Geol. Helv., Vol. 86/3, 717-750
- SCHMASSMANN, H., BALDERER, W., KANZ, W., & PEKDECKER, A. (1984): Beschaffenheit der Tiefengrundwässer in der zentralen Nordschweiz und angrenzenden Gebieten. (Technischer Bericht NTB 84-21). NAGRA
- SCHMASSMANN, H. (1990): Hydrochemische Synthese Nordschweiz: Tertiär- und Malm-Aquifere (Technischer Bericht 88-07). NAGRA, Baden
- SCHMASSMANN, H., KULLIN, M., & SCHNEEMANN, K. (1992): Hydrochemische Synthese der Nordschweiz: Buntsandstein-, Perm-, und Kristallin-Aquifere (Technical Report NTB 91-30). NAGRA, Baden
- SCHMID, G. (1970): Geologie der Gegend von Guggisberg und der angrenzenden subalpinen Molasse. Kümmerly & Frey AG, Bern
- SCHMIDT, C. (1921): Bericht über die Salzbohrung bei Sitten und über den Stellen von Combioula in Wallis Archives Géologiques Suisses, Berne
- SCHOELLER, H. (1960): Salinity of groundwater, evapotranspiration and recharge of aquifers. IASH Publikation, Vol. 52, 488-494
- SCHOELLER, H. J. (1980): Influence du climat, de la température sur la teneur en HCO₃⁻ et H₂CO₃ des eaux souterraines. Journal of Hydrology, Vol. 46, 365-376
- SCHOEPFER, P. (1989): Sédimentologie et stratigraphie de la Molasse marine supérieure entre le Gibloux et l'Aare. Thèse de doctorat, Université de Fribourg
- SCHOTT, J., BRANTLEY, S., CRERAR, D., GUY, C., BORCSIK, M., & WILLAIME, C. (1989): Dissolution kinetics of strained calcite. Geochimica et Cosmochimica Acta, Vol. 53, 373-382
- SCHROEDER, D. C., & Lee, G. F. (1975): Potential transformations of chromium in natural waters. Water Air Soil Pollution, Vol. 4, 355-365
- SCHWEDT, G. (1995): Analytische Chemie. Georg Thieme Verlag, Stuttgart
- Schweizerische Meteorologische Anstalt SMA (1974-1986): Annalen der Schweizerischen Meteorologischen Anstalt. Zürich.
- Schweizerische Gewässerschutzverordnung (GSchV)(1998)
- SCHWERD, K., & Unger, H. (1981): Molassebecken. In M. Bayerisches Geologisches Landesamt (Eds.), Erläuterungen zur geologischen Karte von Bayern 1:500'000 (88-95).
- Servizio Geologico d'Italia (1967): Carta Geologica d'Italia alla scala 1:100'000, foglio 152 "Sora" e note illustrative
- Servizio Geologico d'Italia (1972): Carta geologica d'Italia alla scala 1:50'000, foglio 290 "Cagli" e note illustrative.

References

- SIEGEL, F. R. (1967): Properties and uses of the carbonates. In G. V. Chilingar, H. J. Bissel, & R. W. Fairbridge (Eds.), *Developments in Sedimentology* (342-393)
- SIGG, L., & STUMM, W. (1981): The interaction of anions and weak acids with the hydrous goethite (α -FeOOH) surface. *Colloids Surf.*, Vol. 2, 101-117
- SPECK, J. (1953): Geröllstudien in der subalpinen Molasse am Zugersee und Versuch einer paläogeographischen Auswertung. Thèse de doctorat, Universität Zürich
- STOLLENWERK, K. G., & GROVE, D. B. (1985): Adsorption and desorption of hexavalent chromium in an alluvial aquifer near Telluride, Colorado. *J. Environ. Quality*, Vol. 14/1, 150-155
- STUMM, W., & MORGAN, J. J. (1996): *Aquatic Chemistry* (3rd edition ed.). Wiley-Interscience, New York
- SVERDRUP, H. U. (1990): *The kinetic of base cation release due to chemical weathering*. Lund University Press
- Swedish nuclear fuel and waste management (1985): Stripa project: Hydrogeological and hydrogeochemical investigations in boreholes. Final report on the phase I: Geochemical investigations of the Stripa groundwaters (Technical report 85-86)
- THIERRIN, J. (1990): Contribution à l'étude des eaux souterraines de la région de Fribourg (Suisse occidentale). Thèse de doctorat, CHYN, Université de Neuchâtel
- TOPKAYA, M. (1950): Recherches sur les silicates authigènes dans les roches sédimentaires. *Bull. Lab. Géol. Min. Géophys. Mus. géol. Lausanne*, Vol. 97, 1-132
- TRÜMPY, R. (1980a): *Geology of Switzerland, a Guide Book. Part A: An Outline of the Geology of Switzerland*. Wepf & Co Publishers, Basel, New York
- TRÜMPY, R. (1980b): *Geology of Switzerland, a Guide Book. Part B: Geological Excursions*. Wepf & Co Publishers, Basel, New York
- UNGER, H. J. (1989): Die Lithozonen der Oberen Süßwassermolasse Südostbayerns und ihre vermutlichen zeitlichen Äquivalente gegen Westen und Osten. *Geologicae Bavarica*, Vol. 94, 195-237
- VANSELOW, A. P. (1932): Equilibria of the base-exchange reactions of bentonites, permutites, soil colloids and zeolites. *Soil Sci.*, Vol. 33, 95-113
- VELBEL, M. A. (1993): Constancy of silicate-mineral weathering-rate ratios between natural and experimental weathering: implications for hydrologic control of differences in absolute rates. *Chemical Geology*, Vol. 105, 89-99
- VERNET, J. D. (1964): Pétrographie sédimentaire dans la molasse de la région de Bulle à Vevey. *Bull. assoc. suisse géol. ing. pétrole*, Vol. 31/80, 25
- VON MOOS, A. (1935): Sedimentpetrographische Untersuchungen an Molassesandsteinen. *Schweiz. Min. Petr. Mitt.*, Vol. 15/2, 169-265
- VON RAUMER, J. (1984): The external massifs, relics of Variscan basement in the Alps. *Geol. Rundschau*, Vol. 73/1
- VON RAUMER, J. (1987): Les massifs du Mont-Blanc et des Aiguilles Rouges: Témoins de la formation de croûte varisque dans les Alpes occidentales. *Géologie alpine*, Vol. 63
- VON RAUMER, J., GALETTI, G., PFEIFER, H. R., & OBERHÄNSLI, R. (1990): Amphibolites from Lake Emosson / Aiguilles Rouges, Switzerland: Tholeiitic basalts of a Paleozoic continental rift zone. *Schweiz. Min. Petr. Mitt.*, Vol. 70, 419-435
- WEDEPOHL, K. H. (1978): *Handbook of Geochemistry*. Springer Verlag, Berlin, Heidelberg, New York
- WEIDMANN, M. (1988): Atlas géologique de la Suisse 1:25'000, Feuille 1243 Lausanne, Notice explicative Service hydrologique et géologique national

- WEIDMANN, M. (1993): Atlas géologique de la Suisse et notice explicative, feuille 1244 Châtel-St-Denis Service hydrologique et géologique national
- WEYL, P. K. (1958): Solution kinetics of calcite. *J. Geol.*, Vol. 66, 163-176
- WHITE, A. F., BLUM, A. E., SCHULZ, M. S., VIVIT, D. V., STONESTORM, D. A., LARSON, M., MURPHY, S. F., & EBERL, D. (1998): Chemical weathering in a tropical watershed, Luquillo Mountains, Puerto Rico: I. Long-term versus short-term weathering fluxes. *Geochimica et Cosmochimica Acta*, Vol. 62/2, 209-226
- WHITE, A. F., BULLEN, T. D., VIVIT, D. V., SCHULZ, M. S., & CLOW, D. W. (1999): The role of disseminated calcite in the chemical weathering of granitoid rocks. *Geochimica et Cosmochimica Acta*, Vol. 63/13/14, 1939-1953
- WHO (1993): Guidelines for drinking-water quality. Recommendations (2nd ed.). Geneva.
- WHO (1998): Guidelines for drinking-water quality. Recommendations (2nd ed.). Geneva.
- WIGLEY, T. M. L. (1973): The incongruent dissolution of dolomite. *Geochimica et Cosmochimica Acta*, Vol. 37, 1397-1402
- WILLIAMS, M. W., BROWN, A. D., & MELACK, J. M. (1993): Geochemical and hydrologic controls on the composition of surface water in a high-elevation basin, Sierra Nevada, California. *Limnology and oceanography*, Vol. 38, 775-797
- WOODTLI, R., JAFFÉ, F., & VON RAUMER, J. (1987): Prospection minière en Valais: Le projet Uromine. Kümmerli & Frey SA, Bern
- YASSI, A., & NIEBOER, E. (1988): Carcinogenicity of chromium compounds. In J. O. Nriagu & E. Nieboer (Eds.), *Chromium in the Natural and Human Environments* (443-495, Chapter 17). Wiley
- ZIEGLER, P. A. (1992): Swiss molasse basin: Geodynamics, resources, hazards: an introduction. *Eclogae Geol. Helv.*, Vol. 85/3, 511-517
- ZOBRIST, J., & STUMM, W. (1979, N°146, 27 Juni 1979): Wie sauber ist das Schweizer Regenwasser? *Neue Zürcher Zeitung*, p. Beilage Forschung und Technik

APPENDIX A

MEDIAN CHEMICAL COMPOSITION OF PRECIPITATION WATER

Median chemical composition of precipitation water at five sites in Switzerland and adjacent France, as well as throughfall solutions under the forest canopy at two sites (sampling period 1990-1991, data from Atteia, 1992). JU: Jura mountains; LRY: plateau region near Lausanne; BOR: Préalpes (Vaud); SAR: Alps near Martigny (Valais), ARG: Alps near Argentières (France). - = not detected.

Site		LRY		JU		ARG	BOR	SAR
		Rain 885 m n=11	Throughfall 885 m n=30	Rain/Snow 1350 m n=27	Throughfall 1350 m n=25	Rain/Snow 2000 m n=13	Rain/Snow 2100 m n=8	Rain/Snow 2100 m n=14
pH		4.9	4.5	5.6	5.0	5.25	6.3	6.8
Cl⁻	mg/L	0.3	1.0	0.4	0.8	0.3	0.7	0.4
SO₄²⁻	mg/L	2.1	5.2	1.2	2.4	0.9	0.7	1.0
NO₃⁻	mg/L	2.3	6.1	1.3	3.8	1.0	1.6	1.3
Mg²⁺	mg/L	-	0.1	-	0.1	-	-	-
Ca²⁺	mg/L	0.7	1.4	0.4	1.2	0.3	0.8	1.2
Sr²⁺	mg/L	0.002	0.005	0.001	0.003	0.002	0.002	0.003
Na⁺	mg/L	0.03	0.2	0.1	0.4	0.1	0.1	0.2
K⁺	mg/L	0.1	1.1	0.1	1.1	0.1	0.5	0.2
NH₄⁺	mg/L	1.1	1.9	0.2	0.2	-	0.3	0.1
Si total	mg/L	0.4	0.1	0.4	0.1	0.2	0.3	0.3
Rb total	µg/L	-	6.0	-	7.0	-	0.7	-
Ba total	µg/L	2.0	4.0	1.0	7.0	1.9	16.7	6.2
V total	µg/L	0.3	1.0	-	1.0	-	0.3	-
Cr total	µg/L	-	-	0.2	-	-	-	-
Mn total	µg/L	9.0	111.0	3.1	23.0	4.0	1.0	2.8
Fe total	µg/L	9.2	12.0	2.0	5.0	7.0	-	2.0
Ni total	µg/L	0.1	1.0	-	0.4	-	-	-
Cu total	µg/L	1.7	3.3	3.4	1.3	1.4	0.9	2.5
Zn total	µg/L	19.4	33.0	22.6	22.0	19.0	6.8	19.0
Pb total	µg/L	1.8	3.8	4.0	2.0	1.0	-	-
B total	µg/L	3.6	10.0	5.0	6.8	2.0	1.4	2.1

APPENDIX B

GROUNDWATER COMPOSITION IN DIFFERENT AQUIFER TYPES

- Recent groundwaters in gneiss and granite aquifers of the Mont-Blanc and Aiguilles-Rouges Massifs
- Recent groundwaters from carbonate aquifers in southern Europe (Switzerland, France, Austria, Italy, Slovenia, and Greece)
- Recent groundwaters from evaporite aquifers in the Swiss Alps (Cantons Valais and Vaud); Pennine, Ultrahelvetic, Préalpes Médiannes and Helvetic units.
- Recent groundwaters from molasse aquifers in Switzerland and adjacent regions in France, Germany and Austria
Special cases: recent groundwaters from “Gypsum-bearing molasse” and “Glimmersand” molasse aquifers
- Recent groundwaters from flysch aquifers in the Niesen and Gurnigel nappes in western Switzerland

Composition of recent groundwaters from gneiss aquifers in the Mont-Blanc and Aiguilles Rouges Massifs. - = not analysed.

Parameter	Unit	min	25th percentile	median	75th percentile	max	n
Altitude	m	570	1523	1953	2000	2080	64
Discharge	L/min	0.1	5	12	60	3467	62
T	°C	1.4	3.9	4.7	6.3	8.6	63
pH	pH-units	6.6	7.4	7.6	7.8	8.5	17
Eh	mV	284	322	439	479	511	6
O2 diss.	mg/L	-	-	13	-	-	1
E.C. at 20°C	µS/cm	21	52	83	120	190	63
Total Hardness	°F	0.98	2.9	4.1	6.1	8.8	64
TDS	mg/L	22.25	50.8	75.2	108.6	157.7	64
Alkalinity	mg/L	9.15	25.6	39.1	53.3	77.5	64
F ⁻	mg/L	<0.2	<0.2	<0.2	0.4	1.4	64
Cl ⁻	mg/L	<1	<1	<1	<1	<1	64
NO ₃ ⁻	mg/L	<1	<1	<1	<1	2.5	64
SO ₄ ²⁻	mg/L	4.60	7.3	12.1	23.7	46.0	64
Mg ²⁺	mg/L	<0.2	0.5	0.7	1.3	6.1	64
Ca ²⁺	mg/L	3.45	10.6	14.2	22.2	33.1	64
Si ²⁺	mg/L	<0.01	0.01	0.04	0.14	0.85	63
Na ⁺	mg/L	0.60	1.0	1.5	2.1	5.4	64
K ⁺	mg/L	<0.2	0.3	0.7	1.2	3.3	64
Si total	mg/L	1.24	2.1	2.5	3.2	4.6	63
Li total	µg/L	<5	<5	<5	7	43	64
Rb total	µg/L	<0.2	0.4	0.7	1.2	7.6	58
Ba total	µg/L	0.20	1.0	2.9	10.2	40.1	57
Al total	µg/L	-	-	21.8	-	-	1
V total	µg/L	-	-	0.2	-	-	1
Cr total	µg/L	-	-	0.6	-	-	1
Mn total	µg/L	-	-	0.4	-	-	1
Fe total	µg/L	-	-	11.4	-	-	1
Co total	µg/L	-	-	<0.2	-	-	1
Ni total	µg/L	-	-	0.6	-	-	1
Cu total	µg/L	-	-	0.5	-	-	1
Zn total	µg/L	-	-	2.4	-	-	1
Y total	µg/L	-	-	-	-	-	0
Mo total	µg/L	<0.2	1.6	3.1	5.4	21.6	58
Cd total	µg/L	-	-	0.2	-	-	1
W total	µg/L	<0.2	<0.2	0.2	0.3	32.4	40
Pb total	µg/L	-	-	<0.2	-	-	1
U total	µg/L	<0.2	1.1	5.1	10.0	50.5	58
Br total	µg/L	-	-	4	-	-	1
I total	µg/L	-	-	1	-	-	1
B total	µg/L	<25	<25	<25	25	47	45
As total	µg/L	<0.5	6.1	13.8	32.0	225.2	58
Tritium	TU	17.0	40.5	47.0	54.5	79.0	43
Deuterium	‰	-	-	-99.6	-	-	1
Oxygen-18	‰	-20.0	-13.9	-13.4	-13.0	-13.0	6
Carbon-13	‰	-	-	-	-	-	0

Composition of recent groundwaters from granite aquifers in the Mont-Blanc and Aiguilles Rouges Massifs. - = not analysed.

Parameter	Unit	min	25th percentile	median	75th percentile	max	n
Altitude	m	1100	1300	1491	1548	2014	50
Discharge	L/min	5	55	112	242	2450	54
T	°C	0.2	6.8	8.9	11.5	18.3	46
pH	pH-units	5.9	6.3	6.5	7.0	8.0	35
Eh	mV	254	374	402	408	428	6
O2 diss.	mg/L	-	-	-	-	-	0
E.C. at 20°C	µS/cm	22	66	79	94	159	55
Total Hardness	°F	2.0	2.8	3.1	3.8	6.8	47
TDS	mg/L	28.7	56.5	69.1	79.4	145.8	54
Alkalinity	mg/L	15.0	26.1	29.9	32.5	54.1	55
F ⁻	mg/L	<0.2	0.4	1.1	2.8	4.0	55
Cl ⁻	mg/L	<1	<1	<1	<1	17.1	55
NO ₃ ⁻	mg/L	<1	<1	<1	<1	5.0	55
SO ₄ ²⁻	mg/L	3.0	7.5	12.5	18.4	38.7	55
Mg ²⁺	mg/L	<0.2	0.2	0.3	0.4	1.4	55
Ca ²⁺	mg/L	7.0	10.6	11.8	14.1	25.6	55
Sr ²⁺	mg/L	<0.01	0.02	0.04	0.05	0.45	55
Na ⁺	mg/L	0.5	2.2	3.4	5.2	23.7	55
K ⁺	mg/L	<0.2	0.7	1.3	2.0	3.2	55
Si total	mg/L	1.6	2.5	3.2	3.8	9.8	46
Li total	µg/L	<5	<5	<5	11	210	55
Rb total	µg/L	<0.2	0.5	1.4	3.7	7.2	42
Ba total	µg/L	<0.2	0.3	0.6	0.9	10.4	41
Al total	µg/L	-	-	-	-	-	0
V total	µg/L	-	-	-	-	-	0
Cr total	µg/L	-	-	-	-	-	0
Mn total	µg/L	-	-	-	-	-	0
Fe total	µg/L	-	-	-	-	-	0
Co total	µg/L	-	-	-	-	-	0
Ni total	µg/L	-	-	-	-	-	0
Cu total	µg/L	-	-	-	-	-	0
Zn total	µg/L	-	-	-	-	-	0
Y total	µg/L	-	-	-	-	-	0
Mo total	µg/L	0.2	32.1	66.9	106.2	140.4	42
Cd total	µg/L	-	-	-	-	-	0
W total	µg/L	<0.2	1.2	3.1	5.8	14.0	38
Pb total	µg/L	-	-	-	-	-	0
U total	µg/L	<0.2	64.2	135.2	335.2	2092.7	42
Br total	µg/L	-	-	-	-	-	0
I total	µg/L	-	-	-	-	-	0
B total	µg/L	<25	<25	26	32	56	38
As total	µg/L	<0.5	3.6	5.8	9.9	76.4	42
Tritium	TU	8.0	27.0	45.0	65.0	90.0	37
Deuterium	‰	-	-	-	-	-	0
Oxygen-18	‰	-14.0	-14.0	-14.0	-13.0	-13.0	5
Carbon-13	‰	-	-	-	-	-	0

Composition of recent groundwaters from carbonate aquifers in southern Europe. - = not analysed.

Parameter	Unit	min	25th percentile	median	75th percentile	max	n
Altitude	m	1	368	510	735	1550	83
Discharge	L/min	2	143	900	1875	60000	44
T	°C	3.3	7.3	9.8	11.0	14.1	86
pH	pH-units	6.5	7.1	7.2	7.5	7.9	85
Eh	mV	207	423	440	471	519	72
O ₂ diss.	mg/L	6	10	12	13	16	66
E.C. at 20°C	µS/cm	147	268	347	445	609	79
Total Hardness	°F	9.5	15.0	20.0	27.3	47.8	86
TDS	mg/L	160.5	254.8	345.4	424.5	547.2	87
Alkalinity	mg/L	78.0	169.3	213.5	274.5	372.1	87
F ⁻	mg/L	<0.2	<0.2	<0.2	<0.2	0.4	87
Cl ⁻	mg/L	<1	1.1	2.7	7.4	52.9	87
NO ₃ ⁻	mg/L	<1	2.0	3.0	6.0	30.1	87
SO ₄ ²⁻	mg/L	<1	4.7	8.6	14.1	148.9	87
Mg ²⁺	mg/L	<0.2	2.6	4.1	6.4	19.8	87
Ca ²⁺	mg/L	28.7	54.5	72.3	90.7	126.6	87
Sr ²⁺	mg/L	0.01	0.08	0.15	0.30	1.75	87
Na ⁺	mg/L	<0.2	0.8	1.6	4.0	45.2	87
K ⁺	mg/L	<0.2	0.5	0.8	1.6	6.5	87
Si total	mg/L	<0.5	1.5	3.0	3.8	8.2	87
Li total	µg/L	<1	<1	<1	2	6	87
Rb total	µg/L	<0.2	0.3	0.6	0.9	7.5	87
Ba total	µg/L	<0.2	5.1	11.1	18.0	220.0	87
Al total	µg/L	<0.2	1.5	3.0	6.7	137.0	87
V total	µg/L	<0.2	<0.2	0.4	0.5	1.4	87
Cr total	µg/L	<0.2	0.2	0.4	0.6	2.8	87
Mn total	µg/L	<0.2	0.4	1.1	2.8	36.9	87
Fe total	µg/L	<2	<2	<2	5.8	1352.9	87
Co total	µg/L	<0.2	<0.2	<0.2	<0.2	0.5	87
Ni total	µg/L	<0.2	0.3	0.5	0.9	4.0	78
Cu total	µg/L	<0.2	<0.2	0.3	0.7	50.8	87
Zn total	µg/L	<0.2	<0.2	0.9	2.4	86.6	87
Y total	µg/L	-	-	-	-	-	0
Mo total	µg/L	<0.2	<0.2	0.3	0.6	10.7	87
Cd total	µg/L	<0.2	<0.2	<0.2	<0.2	0.2	18
W total	µg/L	-	-	-	-	-	0
Pb total	µg/L	<0.2	<0.2	0.4	0.7	6.0	87
U total	µg/L	<0.2	<0.2	0.3	0.5	3.1	87
Br total	µg/L	<1	1	3	6	96	87
I total	µg/L	<1	2	18	21	38	19
B total	µg/L	<1	4	8	13	49	87
As total	µg/L	<0.5	<0.5	<0.5	<0.5	1.4	87
Tritium	TU	-	-	-	-	-	0
Deuterium	δ‰	-	-	-	-	-	0
Oxygen-18	δ‰	-	-	-	-	-	0
Carbon-13	δ‰	-14.8	-13.0	-11.3	-9.3	-7.0	34

Composition of recent groundwaters from evaporite aquifers in the Swiss Alps (cantons Valais and Vaud). - = not analysed.

Parameter	Unit	min	25th percentile	median	75th percentile	max	n
Altitude	m	375	605	1020	1380	2220	91
Discharge	L/min	2	25	71	184	2111	35
T	°C	4.2	6.6	8.7	9.7	13.8	91
pH	pH-units	7.0	7.0	7.0	7.3	7.6	20
Eh	mV	-	-	406	-	-	1
O2 diss.	mg/L	-	-	7	-	-	1
E.C. at 20°C	µS/cm	750	1403	1693	1915	2347	91
Total Hardness	°F	49.5	102.9	130.3	154.8	196.3	91
TDS	mg/L	760.3	1433.9	1782.2	2136.6	2787.5	91
Alkalinity	mg/L	85.0	207.2	237.9	286.2	593.7	91
F ⁻	mg/L	<0.2	<0.2	<0.2	<0.2	0.9	83
Cl ⁻	mg/L	<1	1.4	2.9	8.1	78.1	91
NO ₃ ⁻	mg/L	<1	<1	<1	1.1	41.7	91
SO ₄ ²⁻	mg/L	165.0	847.3	1043.3	1271.6	1620.0	91
Mg ²⁺	mg/L	16.6	41.2	57.7	73.1	227.7	91
Ca ²⁺	mg/L	114.3	348.5	426.0	508.2	573.6	91
Sr ²⁺	mg/L	1.00	5.93	8.22	10.08	17.60	91
Na ⁺	mg/L	1.0	2.5	4.8	7.3	30.6	91
K ⁺	mg/L	0.4	1.0	1.6	2.5	17.7	91
Si total	mg/L	1.6	2.3	3.0	3.9	9.4	85
Li total	µg/L	<5	19	28	33	114	91
Rb total	µg/L	1.5	12.6	17.4	21.4	53.3	78
Ba total	µg/L	1.3	6.1	9.6	14.5	38.3	78
Al total	µg/L	<0.2	7.0	14.1	21.1	93.8	73
V total	µg/L	<0.2	0.3	0.4	0.6	1.1	70
Cr total	µg/L	<0.2	<0.2	<0.2	0.4	1.1	73
Mn total	µg/L	<0.2	7.3	12.7	16.4	31.2	73
Fe total	µg/L	-	-	4.5	-	-	1
Co total	µg/L	-	-	<0.2	-	-	1
Ni total	µg/L	<0.2	2.1	3.1	4.3	35.7	78
Cu total	µg/L	<0.2	1.5	2.9	3.9	14.4	78
Zn total	µg/L	<0.2	<0.2	2.1	3.7	156.2	78
Y total	µg/L	<0.2	0.4	0.6	0.7	2.4	72
Mo total	µg/L	-	-	2.8	-	-	1
Cd total	µg/L	<0.2	<0.2	0.2	0.4	0.9	73
W total	µg/L	-	-	-	-	-	0
Pb total	µg/L	-	-	1.3	-	-	1
U total	µg/L	<0.2	1.8	5.2	12.8	67.0	78
Br total	µg/L	<1	2	8	12	58	73
I total	µg/L	-	-	2	-	-	1
B total	µg/L	<25	<25	<25	42	95	80
As total	µg/L	<0.5	<0.5	<0.5	0.6	4.3	72
Tritium	TU	-	-	-	-	-	0
Deuterium	‰	-	-	-	-	-	0
Oxygen-18	‰	-	-	-	-	-	0
Carbon-13	‰	-	-	-	-	-	0

Composition of recent groundwaters from evaporite aquifers in the Ultrahelvetic unit. - = not analysed.

Parameter	Unit	min	25% Percentile	median	75% Percentile	max	n
Altitude	m	395	800	1170	1390	1810	33
Discharge	L/min	2.5	26.0	100.0	600.0	2110.7	9
T	°C	4.2	6.0	7.7	10.0	12.0	33
pH	pH-units	7.0	7.0	7.0	7.1	7.2	6
Eh	mV	-	-	406	-	-	1
O2 diss.	mg/L	-	-	6.8	-	-	1
E.C. at 20°C	µS/cm	956	1389	1730	1895	2120	33
Total Hardness	°F	64.4	99.5	135.8	152.0	171.5	33
TDS	mg/L	980.0	1417.3	1849.2	2085.7	2370.7	33
Alkalinity	mg/L	183.0	216.7	244.0	270.9	366.0	33
F ⁻	mg/L	<0.2	<0.2	<0.2	<0.2	0.5	33
Cl ⁻	mg/L	<1	<1	3.7	13.4	77.9	33
NO ₃ ⁻	mg/L	<1	<1	<1	1.3	41.7	33
SO ₄ ²⁻	mg/L	388.1	758.7	1056.3	1239.1	1440.0	33
Mg ²⁺	mg/L	16.6	31.3	41.7	61.0	83.2	33
Ca ²⁺	mg/L	204.8	356.7	471.0	520.0	573.3	33
Sr ²⁺	mg/L	3.82	6.67	8.48	9.66	12.20	33
Na ⁺	mg/L	1.7	2.7	4.6	7.4	29.9	33
K ⁺	mg/L	0.4	0.8	1.2	1.6	5.2	33
Si total	mg/L	1.6	2.0	2.4	3.6	4.3	33
Li total	µg/L	10	19	29	32	42	33
Rb total	µg/L	1.5	13.4	17.3	18.1	26.5	30
Ba total	µg/L	4.4	7.5	11.3	15.1	38.3	30
Al total	µg/L	<0.2	5.0	14.0	17.6	46.2	30
V total	µg/L	<0.2	0.3	0.4	0.4	0.9	28
Cr total	µg/L	<0.2	<0.2	0.2	0.6	0.9	30
Mn total	µg/L	<0.2	10.7	14.0	17.0	22.7	30
Fe total	µg/L	-	-	4.6	-	-	1
Co total	µg/L	-	-	0.03	-	-	1
Ni total	µg/L	0.6	2.4	3.5	4.4	5.5	30
Cu total	µg/L	<0.2	1.4	3.0	3.5	5.2	30
Zn total	µg/L	<0.2	0.5	2.6	4.4	153.4	30
Y total	µg/L	<0.2	0.4	0.6	0.7	1.0	29
Mo total	µg/L	-	-	2.8	-	-	1
Cd total	µg/L	<0.2	<0.2	0.2	0.4	0.7	30
W total	µg/L	-	-	-	-	-	0
Pb total	µg/L	-	-	1.3	-	-	1
U total	µg/L	<0.2	1.1	1.9	2.3	5.4	30
Br total	µg/L	<1	2	8	16	38	30
I total	µg/L	-	-	2	-	-	1
B total	µg/L	<25	<25	32	49	95	33
As total	µg/L	<0.5	<0.5	<0.5	0.6	2.7	29
Tritium	TU	-	-	-	-	-	0
Deuterium	‰	-	-	-	-	-	0
Oxygen-18	‰	-	-	-	-	-	0
Carbon-13	‰	-	-	-	-	-	0

**Composition of recent groundwaters from evaporite aquifers in the Préalpes Médiannes. -
= not analysed.**

Parameter	Unit	min	25% Percentile	median	75% Percentile	max	n
Altitude	m	375	380	385	385	1140	13
Discharge	L/min	41.0	96.5	138.2	155.8	373.0	5
T	°C	5.3	8.8	9.3	9.7	9.9	13
pH	pH-units	7.0	7.0	7.0	7.0	7.0	3
Eh	mV	-	-	-	-	-	0
O2 diss.	mg/L	-	-	-	-	-	0
E.C. at 20°C	µS/cm	1110	1352	1480	1510	1837	13
Total Hardness	°F	80.5	101.7	114.4	115.7	147.6	13
TDS	mg/L	1127.3	1411.1	1574.3	1607.9	2045.6	13
Alkalinity	mg/L	192.6	202.5	207.9	250.0	262.5	13
F ⁻	mg/L	<0.2	<0.2	<0.2	0.2	0.2	11
Cl ⁻	mg/L	<1	1.2	1.5	2.4	3.0	13
NO ₃ ⁻	mg/L	<1	<1	<1	<1	1.3	13
SO ₄ ²⁻	mg/L	613.0	814.7	899.5	922.5	1262.1	13
Mg ²⁺	mg/L	18.8	44.6	56.8	59.5	65.1	13
Ca ²⁺	mg/L	267.7	346.0	357.0	375.0	512.8	13
Sr ²⁺	mg/L	2.65	7.06	10.46	16.43	17.60	13
Na ⁺	mg/L	1.0	4.2	4.9	4.9	5.6	13
K ⁺	mg/L	0.8	1.0	1.4	1.6	1.8	13
Si total	mg/L	1.6	2.7	3.2	3.4	3.8	8
Li total	µg/L	16	20	34	47	51	13
Rb total	µg/L	8.2	12.3	14.2	24.7	53.3	7
Ba total	µg/L	6.3	14.4	18.8	22.9	27.0	7
Al total	µg/L	<0.2	7.0	14.1	25.0	93.8	7
V total	µg/L	0.2	0.4	0.4	0.6	0.6	7
Cr total	µg/L	<0.2	<0.2	<0.2	0.4	0.9	7
Mn total	µg/L	1.4	5.4	7.9	19.6	28.7	7
Fe total	µg/L	-	-	-	-	-	0
Co total	µg/L	-	-	-	-	-	0
Ni total	µg/L	2.1	2.6	4.7	5.8	35.7	7
Cu total	µg/L	1.5	2.5	3.5	3.9	14.4	7
Zn total	µg/L	<0.2	0.4	2.1	5.5	22.5	7
Y total	µg/L	0.4	0.5	0.6	1.1	2.4	7
Mo total	µg/L	-	-	-	-	-	0
Cd total	µg/L	<0.2	0.3	0.3	0.5	0.8	7
W total	µg/L	-	-	-	-	-	0
Pb total	µg/L	-	-	-	-	-	0
U total	µg/L	0.6	1.0	1.6	2.0	2.5	7
Br total	µg/L	<1	5	6	12	28	7
I total	µg/L	-	-	-	-	-	0
B total	µg/L	39	44	63	90	91	8
As total	µg/L	<0.5	<0.5	<0.5	0.7	1.0	7
Tritium	TU	-	-	-	-	-	0
Deuterium	‰	-	-	-	-	-	0
Oxygen-18	‰	-	-	-	-	-	0
Carbon-13	‰	-	-	-	-	-	0

Composition of recent groundwaters from evaporite aquifers in the Pennine. - = not analysed.

Parameter	Unit	min	25% Percentile	median	75% Percentile	max	n
Altitude	m	480	625	1160	1395	2220	39
Discharge	L/min	2.0	19.0	40.6	140.3	1500.0	19
T	°C	4.2	7.0	8.7	9.6	13.8	39
pH	pH-units	7.0	7.3	7.4	7.4	7.6	8
Eh	mV	-	-	-	-	-	0
O2 diss.	mg/L	-	-	-	-	-	0
E.C. at 20°C	µS/cm	750	1346	1717	1966	2347	39
Total Hardness	°F	49.5	98.9	131.0	164.2	196.3	39
TDS	mg/L	760.3	1372.4	1786.4	2227.8	2787.5	39
Alkalinity	mg/L	85.0	162.9	221.9	295.9	593.7	39
F ⁻	mg/L	<0.2	<0.2	<0.2	<0.2	0.9	33
Cl ⁻	mg/L	0.3	1.8	4.3	9.0	78.1	39
NO ₃ ⁻	mg/L	<1	<1	<1	1.3	17.9	39
SO ₄ ²⁻	mg/L	165.0	819.8	1080.0	1312.5	1596.7	39
Mg ²⁺	mg/L	20.2	52.1	70.7	98.6	227.7	39
Ca ²⁺	mg/L	114.3	295.5	409.3	476.5	553.7	39
Sr ²⁺	mg/L	1.00	5.31	6.88	8.33	11.73	39
Na ⁺	mg/L	1.0	2.5	5.1	8.9	30.6	39
K ⁺	mg/L	0.7	1.8	2.2	3.5	17.7	39
Si total	mg/L	2.0	2.8	3.6	4.5	9.4	38
Li total	µg/L	<5	18	21	31	114	39
Rb total	µg/L	2.3	11.8	16.3	22.5	39.3	35
Ba total	µg/L	2.2	5.5	7.9	11.2	30.9	35
Al total	µg/L	<0.2	10.0	14.2	27.4	68.2	30
V total	µg/L	<0.2	0.3	0.5	0.8	1.1	29
Cr total	µg/L	<0.2	<0.2	<0.2	0.4	1.1	30
Mn total	µg/L	<0.2	6.0	11.0	14.0	31.2	30
Fe total	µg/L	-	-	-	-	-	0
Co total	µg/L	-	-	-	-	-	0
Ni total	µg/L	<0.2	1.1	2.5	3.6	28.5	35
Cu total	µg/L	<0.2	0.9	2.9	4.6	7.4	35
Zn total	µg/L	<0.2	<0.2	1.8	2.8	156.2	35
Y total	µg/L	<0.2	0.3	0.5	0.7	1.0	30
Mo total	µg/L	-	-	-	-	-	0
Cd total	µg/L	<0.2	<0.2	<0.2	0.4	0.9	30
W total	µg/L	-	-	-	-	-	0
Pb total	µg/L	-	-	-	-	-	0
U total	µg/L	0.2	9.2	13.3	27.1	67.0	35
Br total	µg/L	<1	3	8	1	58	30
I total	µg/L	-	-	-	-	-	0
B total	µg/L	<25	<25	<25	<25	89	33
As total	µg/L	<0.5	<0.5	<0.5	0.7	4.3	30
Tritium	TU	-	-	-	-	-	0
Deuterium	δ‰	-	-	-	-	-	0
Oxygen-18	δ‰	-	-	-	-	-	0
Carbon-13	δ‰	-	-	-	-	-	0

Composition of recent groundwaters from evaporite aquifers in the Helvetic. - = not analysed.

Parameter	Unit	min	25% Percentile	median	75% Percentile	max	n
Altitude	m	720	795	855	877.5	880	6
Discharge	L/min	2.8	177.1	351.4	525.7	700.0	2
T	°C	7.1	7.7	9.0	10.7	11.3	6
pH	pH-units	7.0	7.0	7.0	7.0	7.0	3
Eh	mV	-	-	-	-	-	0
O2 diss.	mg/L	-	-	-	-	-	0
E.C. at 20°C	µS/cm	1870	1973	2040	2117	2190	6
Total Hardness	°F	152.2	161.5	170.7	185.0	190.0	6
TDS	mg/L	2058.6	2207.9	2363.1	2451.2	2565.4	6
Alkalinity	mg/L	173.1	250.1	265.9	298.5	403.2	6
F ⁻	mg/L	<0.2	<0.2	<0.2	<0.2	0.4	6
Cl ⁻	mg/L	<1	1.3	2.3	2.8	3.5	6
NO ₃ ⁻	mg/L	<1	<1	<1	<1	<1	6
SO ₄ ²⁻	mg/L	1236.7	1326.9	1361.6	1490.0	1620.0	6
Mg ²⁺	mg/L	53.9	67.1	103.5	130.5	134.0	6
Ca ²⁺	mg/L	461.4	506.3	532.5	556.5	573.6	6
Sr ²⁺	mg/L	10.10	10.34	10.60	10.92	12.00	6
Na ⁺	mg/L	1.6	1.7	2.2	3.4	5.8	6
K ⁺	mg/L	0.6	1.0	1.6	2.3	3.2	6
Si total	mg/L	2.5	2.7	3.0	3.3	4.0	6
Li total	µg/L	21	28	30	39	51	6
Rb total	µg/L	21.9	22.4	23.8	26.0	30.5	6
Ba total	µg/L	1.3	2.8	3.0	3.4	6.6	6
Al total	µg/L	4.7	5.7	13.3	22.6	25.2	6
V total	µg/L	0.2	0.2	0.3	0.4	0.6	6
Cr total	µg/L	<0.2	<0.2	<0.2	<0.2	0.3	6
Mn total	µg/L	6.8	7.9	12.2	15.9	24.8	6
Fe total	µg/L	-	-	-	-	-	0
Co total	µg/L	-	-	-	-	-	0
Ni total	µg/L	2.5	2.8	4.1	5.2	6.2	6
Cu total	µg/L	1.5	2.0	3.0	4.0	8.1	6
Zn total	µg/L	<0.2	<0.2	1.1	2.9	5.0	6
Y total	µg/L	0.4	0.6	0.7	0.7	1.2	6
Mo total	µg/L	-	-	-	-	-	0
Cd total	µg/L	<0.2	<0.2	0.2	0.2	0.7	6
W total	µg/L	-	-	-	-	-	0
Pb total	µg/L	-	-	-	-	-	0
U total	µg/L	6.2	6.9	8.9	10.2	11.0	6
Br total	µg/L	<1	2	3	4	10	6
I total	µg/L	-	-	-	-	-	0
B total	µg/L	<25	<25	<25	<25	<25	6
As total	µg/L	<0.5	<0.5	<0.5	0.6	0.7	6
Tritium	TU	-	-	-	-	-	0
Deuterium	‰	-	-	-	-	-	0
Oxygen-18	‰	-	-	-	-	-	0
Carbon-13	‰	-	-	-	-	-	0

Composition of recent groundwaters from molasse aquifers.- = not analysed.

Parameter	Unit	min	25th percentile	median	75th percentile	max	n
Altitude	m	340	581	650	910	1430	96
Discharge	L/min	1	9	22	50	1260	95
T	°C	6.5	8.2	8.7	9.4	12.9	96
pH	pH-units	6.5	7.0	7.2	7.4	8.1	94
Eh	mV	288	374	391	421	484	94
O2 diss.	mg/L	5	9	11	12	15	32
E.C. at 20°C	µS/cm	22	338	420	512	806	96
Total Hardness	°F	1.2	19.9	25.0	30.5	43.3	96
TDS	mg/L	48.4	329.9	418.3	509.2	714.4	96
Alkalinity	mg/L	7.3	224.6	281.5	338.4	432.9	96
F ⁻	mg/L	<0.2	<0.2	<0.2	<0.2	0.2	96
Cl ⁻	mg/L	<1	1.5	3.0	4.8	32.0	96
NO ₃ ⁻	mg/L	<1	6.2	8.1	15.4	157.9	96
SO ₄ ²⁻	mg/L	<1	7.5	12.1	17.5	60.6	96
Mg ²⁺	mg/L	0.7	7.4	13.5	21.1	36.1	96
Ca ²⁺	mg/L	6.5	61.1	82.2	92.9	117.4	96
Sr ²⁺	mg/L	0.010	0.138	0.215	0.287	0.996	96
Na ⁺	mg/L	0.3	1.5	2.4	3.8	36.4	96
K ⁺	mg/L	0.2	0.5	0.8	1.3	4.2	96
Si total	mg/L	2.0	4.1	5.9	7.3	19.0	96
Li total	µg/L	<1		2	3	29	96
Rb total	µg/L	<0.2	0.3	0.5	0.9	3.0	96
Ba total	µg/L	2.4	14.2	26.8	47.0	333.7	96
Al total	µg/L	<0.2	2.2	8.2	19.7	80.5	96
V total	µg/L	<0.2	0.4	0.5	0.7	1.1	96
Cr total	µg/L	<0.2	0.3	0.8	1.7	6.9	96
Mn total	µg/L	<0.2	0.4	0.8	2.1	374.1	96
Fe total	µg/L	<2	<2	<2	2.7	155.0	96
Co total	µg/L	<0.2	<0.2	<0.2	0.2	0.8	96
Ni total	µg/L	<0.2	0.3	0.5	0.7	3.2	96
Cu total	µg/L	<0.2	<0.2	<0.2	0.8	15.2	96
Zn total	µg/L	<0.2	<0.2	0.9	2.8	155.0	96
Y total	µg/L	-	-	-	-	-	0
Mo total	µg/L	<0.2	<0.2	0.3	0.5	1.9	96
Cd total	µg/L	<0.2	<0.2	<0.2	<0.2	0.3	96
W total	µg/L	-	-	-	-	-	0
Pb total	µg/L	<0.2	<0.2	<0.2	0.2	8.7	96
U total	µg/L	<0.2	0.2	0.5	0.9	3.3	96
Br total	µg/L	<1	4	9	15	126	96
I total	µg/L	<1	1	2	4	8	4
B total	µg/L	<1	2	3	5	99	96
As total	µg/L	<0.5	<0.5	<0.5	<0.5	1.2	96
Tritium	TU	20.0	27.5	30.0	44.2	86.8	4
Deuterium	δ‰	-80.1	-78.6	-77.1	-74.4	-71.6	3
Oxygen-18	δ‰	-11.3	-11.1	-11.0	-10.6	-10.2	3
Carbon-13	δ‰	-	-	-	-	-	0

Special case: Composition of recent groundwaters from “Gypsum-bearing molasse” aquifers.- = not analysed.

Parameter	Unit	min	25th percentile	median	75th percentile	max	n
Altitude	m	435	461	473	477	484	4
Discharge	L/min	0	1	4	20	60	4
T	°C	9.8	10.5	11.4	13.2	16.3	4
pH	pH-units	7.4	7.5	7.5	7.6	7.8	4
Eh	mV	333	390	417	427	434	4
O2 diss.	mg/L	-	-	-	-	-	0
E.C. at 20°C	µS/cm	1008	1108	1141	1187	1326	4
Total Hardness	°F	55.2	67.0	73.3	78.3	86.0	4
TDS	mg/L	984.4	1079.7	1146.9	1223.3	1346.0	4
Alkalinity	mg/L	375.8	386.3	403.9	429.3	463.5	4
F ⁻	mg/L	0.2	0.2	0.2	0.2	0.2	4
Cl ⁻	mg/L	28.0	32.5	34.5	38.8	50.0	4
NO ₃ ⁻	mg/L	28.0	31.0	33.5	36.3	40.0	4
SO ₄ ²⁻	mg/L	255.0	336.8	386.5	418.0	445.0	4
Mg ²⁺	mg/L	35.4	38.1	39.5	40.7	43.2	4
Ca ²⁺	mg/L	168.5	215.5	234.3	250.4	289.2	4
Sr ²⁺	mg/L	4.030	4.516	4.693	4.730	4.797	4
Na ⁺	mg/L	7.6	8.8	9.6	14.9	29.5	4
K ⁺	mg/L	2.0	3.1	3.9	5.3	8.1	4
Si total	mg/L	3.7	3.8	4.9	6.3	7.4	4
Li total	µg/L	17	19	20	23	29	4
Rb total	µg/L	0.9	1.0	1.1	1.3	1.8	4
Ba total	µg/L	20.7	28.0	32.9	37.3	43.0	4
Al total	µg/L	<0.2	2.1	3.6	4.9	6.3	4
V total	µg/L	0.4	0.5	0.6	0.6	0.7	4
Cr total	µg/L	0.6	0.7	0.7	0.8	0.8	4
Mn total	µg/L	<0.2	0.4	0.5	0.6	0.6	4
Fe total	µg/L	<2	<2	<2	3.9	11.4	4
Co total	µg/L	0.4	0.4	0.4	0.5	0.6	4
Ni total	µg/L	0.7	0.9	1.3	1.6	1.7	4
Cu total	µg/L	2.3	2.7	2.9	14.7	49.5	4
Zn total	µg/L	5.6	8.0	9.1	9.7	11.0	4
Y total	µg/L	-	-	-	-	-	0
Mo total	µg/L	1.3	1.9	2.6	2.6	2.7	3
Cd total	µg/L	<0.2	<0.2	<0.2	<0.2	<0.2	4
W total	µg/L	-	-	-	-	-	0
Pb total	µg/L	0.4	0.4	0.5	1.0	2.1	4
U total	µg/L	2.4	2.5	3.0	3.5	3.6	4
Br total	µg/L	28	30	37	44	45	4
I total	µg/L	2	2	3	6	15	4
B total	µg/L	12	18	26	36	52	4
As total	µg/L	<0.5	<0.5	<0.5	<0.5	0.5	4
Tritium	TU	-	-	-	-	-	0
Deuterium	‰	-	-	-	-	-	0
Oxygen-18	‰	-	-	-	-	-	0
Carbon-13	‰	-	-	-	-	-	0

Special case: Composition of recent groundwaters from "Glimmersand" molasse aquifers.- = not analysed.

Parameter	Unit	min	25th percentile	median	75th percentile	max	n
Altitude	m	440	508	564	602	618	8
Discharge	L/min	2	11	23	28	127	8
T	°C	9.1	9.4	9.8	10.0	11.9	8
pH	pH-units	7.5	7.6	7.7	7.9	8.1	8
Eh	mV	337	371	401	408	440	8
O2 diss.	mg/L	-	-	9	-	-	1
E.C. at 20°C	µS/cm	561	619	642	679	698	8
Total Hardness	°F	16.7	37.1	37.9	38.6	39.4	8
TDS	mg/L	556.9	612.6	638.0	647.5	674.4	8
Alkalinity	mg/L	357.7	372.6	394.3	408.7	430.1	8
F ⁻	mg/L	<0.2	<0.2	<0.2	<0.2	<0.2	8
Cl ⁻	mg/L	2.0	4.0	8.3	13.3	27.7	8
NO ₃ ⁻	mg/L	<1	<1	3.5	9.1	32.3	8
SO ₄ ²⁻	mg/L	32.9	42.6	56.3	66.9	92.6	8
Mg ²⁺	mg/L	25.3	25.9	26.1	27.1	30.8	8
Ca ²⁺	mg/L	94.7	110.6	117.3	122.7	123.7	8
Sr ²⁺	mg/L	0.160	0.220	0.265	0.293	0.681	8
Na ⁺	mg/L	2.4	2.4	2.6	5.0	8.5	8
K ⁺	mg/L	0.6	0.7	0.8	0.8	0.9	8
Si total	mg/L	2.8	6.7	7.0	7.2	8.6	8
Li total	µg/L	5	6	8	9	13	8
Rb total	µg/L	0.6	0.7	0.8	1.2	1.9	8
Ba total	µg/L	10.1	21.2	31.1	40.4	65.3	8
Al total	µg/L	1.1	1.2	1.4	1.4	212.0	8
V total	µg/L	0.2	0.3	0.3	0.3	1.0	8
Cr total	µg/L	0.2	0.2	0.2	0.2	1.1	8
Mn total	µg/L	<0.2	<0.2	5.5	20.8	45.7	8
Fe total	µg/L	<2	<2	<2	5.7	161.8	8
Co total	µg/L	<0.2	<0.2	<0.2	<0.2	0.2	8
Ni total	µg/L	0.3	0.7	1.0	1.3	3.9	8
Cu total	µg/L	<0.2	<0.2	0.3	1.1	2.8	8
Zn total	µg/L	<0.2	0.3	0.4	1.5	4.9	8
Y total	µg/L	-	-	-	-	-	0
Mo total	µg/L	2.6	3.2	3.8	6.3	9.2	7
Cd total	µg/L	<0.2	<0.2	<0.2	<0.2	<0.2	8
W total	µg/L	-	-	-	-	-	0
Pb total	µg/L	<0.2	<0.2	<0.2	<0.2	0.5	8
U total	µg/L	2.0	2.3	3.1	5.6	9.0	8
Br total	µg/L	2	13	22	28	37	8
I total	µg/L	-	-	4	-	-	1
B total	µg/L	2	2	3	4	7	8
As total	µg/L	<0.5	<0.5	<0.5	<0.5	2.5	8
Tritium	TU	20.0	22.5	25.0	38.5	52.0	3
Deuterium	‰	-	-	-	-	-	0
Oxygen-18	‰	-10.4	-10.4	-10.4	-10.4	-10.4	2
Carbon-13	‰	-	-	-	-	-	0

Composition of recent groundwaters from flysch aquifers in the Niesen and Gurnigel nappes. - = not analysed.

Parameter	Unit	min	25th percentile	median	75th percentile	max	n
Altitude	m	915	1345	1502	1700	1950	53
Discharge	L/min	1	12	111	398	2967	50
T	°C	1.2	4.5	5.7	6.7	9.2	50
pH	pH-units	5.9	6.7	7.0	7.2	7.7	46
Eh	mV	449	450	454	455	477	5
O2 diss.	mg/L	-	-	12	-	-	1
E.C. at 20°C	µS/cm	159	233	270	331	474	53
Total Hardness	°F	9.7	14.2	16.3	20.0	27.9	53
TDS	mg/L	159.7	230.8	267.1	314.6	458.8	53
Alkalinity	mg/L	113.7	164.9	186.9	223.5	314.2	53
F ⁻	mg/L	<0.2	<0.2	<0.2	<0.2	<0.2	53
Cl ⁻	mg/L	<1	<1	<1	<1	3.5	51
NO ₃ ⁻	mg/L	<1	<1	2.4	5.0	8.1	53
SO ₄ ²⁻	mg/L	2.5	5.2	8.2	11.9	36.2	53
Mg ²⁺	mg/L	1.3	2.7	3.2	5.3	23.5	53
Ca ²⁺	mg/L	24.0	49.2	56.2	69.6	97.3	53
Sr ²⁺	mg/L	0.111	0.286	0.368	0.547	3.114	53
Na ⁺	mg/L	0.3	0.5	0.8	1.6	10.2	51
K ⁺	mg/L	<0.2	0.3	0.4	0.7	3.0	53
Si total	mg/L	<0.5	1.1	1.5	2.0	4.6	53
Li total	µg/L	<1	2	3	6	29	53
Rb total	µg/L	0.3	0.4	0.6	1.0	5.8	53
Ba total	µg/L	5.1	17.8	26.5	51.0	128.0	53
Al total	µg/L	<0.2	0.4	0.9	1.5	23.2	53
V total	µg/L	<0.2	<0.2	0.2	0.3	0.5	53
Cr total	µg/L	<0.2	<0.2	0.2	0.3	1.1	53
Mn total	µg/L	<0.2	0.2	0.5	1.0	4.9	53
Fe total	µg/L	<2	6.4	10.7	16.9	57.9	44
Co total	µg/L	<0.2	<0.2	<0.2	0.2	0.6	53
Ni total	µg/L	<0.2	0.3	0.5	0.7	4.0	49
Cu total	µg/L	<0.2	0.3	0.5	0.8	3.7	48
Zn total	µg/L	<0.2	0.5	1.1	2.7	75.0	46
Y total	µg/L	-	-	-	-	-	0
Mo total	µg/L	-	-	<0.2	-	-	1
Cd total	µg/L	-	-	0.4	-	-	1
W total	µg/L	-	-	-	-	-	0
Pb total	µg/L	<0.2	<0.2	0.3	1.6	6.3	53
U total	µg/L	<0.2	<0.2	0.2	0.3	0.9	53
Br total	µg/L	<1	2	3	4	8	53
I total	µg/L	-	-	<1	-	-	1
B total	µg/L	2	5	7	11	73	53
As total	µg/L	-	-	-	-	-	0
Tritium	TU	-	-	-	-	-	0
Deuterium	‰	-	-	-	-	-	0
Oxygen-18	‰	-	-	-	-	-	0
Carbon-13	‰	-	-	-	-	-	0

APPENDIX C

CHEMICAL GROUNDWATER CLASSIFICATION

The water types after Jäckli (1970) refer to a classification based on the proportions of major cations and anions. The water types are named using a multiple-ion designation in decreasing dominance order. The dominant ions are determined from the percentage of milliequivalents for each major cation (Ca^{2+} , Mg^{2+} , Na^+ , K^+) and anion (HCO_3^- , SO_4^{2-} , Cl^- , F^- , NO_3^-) in solution. For example, in a Ca- HCO_3 -(SO_4) water Ca (underlined) accounts for more than 50% of the total cations, HCO_3 makes up between 20 and 50% of the total anions and SO_4 (in brackets) between 10 and 20%.

The water types occurring in each aquifer type (crystalline, carbonate, evaporite, molasse, and flysch rocks) have been determined after Jäckli (1970) and their distribution is given in percents. The number of sites is given if there are less than 3 springs per water type.

Distribution of water types according to JÄCKLI (1970) between the different aquifer types. CRY = crystalline aquifers, CARB = carbonate karst aquifers, EVAP = evaporite karst aquifers, MOL = molasse aquifers, FLY = flysch aquifers

Water Type	Cry	Carb	Evap	Fly	Mol
<u>Ca</u> -(Mg)-(Na)- HCO_3 - SO_4	3.1%	1 site			
<u>Ca</u> -(Mg)- HCO_3		18.4%		35.1%	15.7%
<u>Ca</u> -(Mg)- HCO_3 -(Cl)-(NO ₃)					1 site
<u>Ca</u> -(Mg)- HCO_3 -(NO ₃)					1 site
<u>Ca</u> -(Mg)- HCO_3 -(NO ₃)-(Cl)					1 site
<u>Ca</u> -(Mg)- HCO_3 -(SO ₄)	2 sites			1 site	1 site
<u>Ca</u> -(Mg)- HCO_3 -SO ₄	4.7%	5.7%		1 site	
<u>Ca</u> -(Mg)-SO ₄			2 sites		
<u>Ca</u> -(Mg)-SO ₄ -(HCO ₃)			36.7%		
<u>Ca</u> -(Mg)-SO ₄ -HCO ₃			10.0%		1 site
<u>Ca</u> -(Mg)-SO ₄ -HCO ₃ -(Cl)			2 sites		
<u>Ca</u> -(Mg)-SO ₄ -HCO ₃		2 sites			1 site
<u>Ca</u> -(Na)-(K)- HCO_3 -SO ₄	1 site				
<u>Ca</u> -(Na)-(Mg)- HCO_3 -SO ₄	2.4%				
<u>Ca</u> -(Na)-(Mg)- HCO_3 -SO ₄ -(F)	1 site				
<u>Ca</u> -(Na)-(Mg)-SO ₄ -HCO ₃	1 site				
<u>Ca</u> -(Na)-(Mg)-SO ₄ -HCO ₃ -(NO ₃)					1 site
<u>Ca</u> -(Na)- HCO_3 -(F)-(SO ₄)	1 site				
<u>Ca</u> -(Na)- HCO_3 -(SO ₄)	1 site	1 site			
<u>Ca</u> -(Na)- HCO_3 -(SO ₄)-(F)	1 site				
<u>Ca</u> -(Na)- HCO_3 -SO ₄	16.5%				
<u>Ca</u> -(Na)- HCO_3 -SO ₄	2.4%				
<u>Ca</u> -(Na)- HCO_3 -SO ₄ -(Cl)	1 site				
<u>Ca</u> -(Na)- HCO_3 -SO ₄ -(F)	3.1%				
<u>Ca</u> -(Na)- HCO_3 -SO ₄ -(F)	1 site				
<u>Ca</u> -(Na)-SO ₄ -HCO ₃	2.4%				
<u>Ca</u> -(Na)-SO ₄ -HCO ₃	1 site				
<u>Ca</u> - HCO_3	1 site	51.7%		50.9%	11.1%
<u>Ca</u> - HCO_3 -(Cl)		2 sites			

Distribution of water types according to JÄCKLI (1970) between the different aquifer types. CRY = crystalline aquifers, CARB = carbonate karst aquifers, EVAP = evaporite karst aquifers, MOL = molasse aquifers, FLY = flysch aquifers

Water Type	Cry	Carb	Evap	Fly	Mol
<u>Ca</u> -HCO ₃ -(SO ₄)	8.7%	1 site			
<u>Ca</u> -HCO ₃ -SO ₄	23.6%				
<u>Ca</u> -Mg-(Na)-HCO ₃				1 site	
<u>Ca</u> -Mg-HCO ₃	3.9%	10.3%		2 sites	49.1%
<u>Ca</u> -Mg-HCO ₃ -(Cl)					1 site
<u>Ca</u> -Mg-HCO ₃ -(NO ₃)-(Cl)					2 sites
<u>Ca</u> -Mg-HCO ₃ -(NO ₃)-(SO ₄)-(Cl)					1 site
<u>Ca</u> -Mg-HCO ₃ -(SO ₄)	1 site			1 site	9.3%
<u>Ca</u> -Mg-HCO ₃ -(SO ₄)				1 site	
<u>Ca</u> -Mg-HCO ₃ -NO ₃ -(SO ₄)					1 site
<u>Ca</u> -Mg-HCO ₃ -SO ₄	1 site	1 site	1 site		1 site
<u>Ca</u> -Mg-HCO ₃ -SO ₄		1 site			
<u>Ca</u> -Mg-HCO ₃ -SO ₄			1 site		
<u>Ca</u> -Mg-HCO ₃ -SO ₄ -(Cl)					1 site
<u>Ca</u> -Mg-Na-HCO ₃					1 site
<u>Ca</u> -Mg-SO ₄			4.4%		
<u>Ca</u> -Mg-SO ₄ -(HCO ₃)			30.0%		
<u>Ca</u> -Mg-SO ₄ -HCO ₃			4.4%		1 site
<u>Ca</u> -Mg-SO ₄ -HCO ₃			1 site		
<u>Ca</u> -Na-(Mg)-HCO ₃ -(Cl)		1 site			
<u>Ca</u> -Na-HCO ₃ -(F)-(NO ₃)-(SO ₄)	1 site				
<u>Ca</u> -Na-HCO ₃ -Cl-(SO ₄)		1 site			
<u>Ca</u> -Na-HCO ₃ -F-(SO ₄)	3.1%				
<u>Ca</u> -Na-HCO ₃ -SO ₄	1 site				
<u>Ca</u> -Na-HCO ₃ -SO ₄	1 site				
<u>Ca</u> -Na-HCO ₃ -SO ₄ -(Cl)	1 site				
<u>Ca</u> -Na-HCO ₃ -SO ₄ -(F)	3.1%				
<u>Ca</u> -Na-HCO ₃ -SO ₄ -(F)	4.7%				
<u>Ca</u> -Na-SO ₄ -HCO ₃	1 site				
<u>Ca</u> -SO ₄ -(HCO ₃)			3.3%		
<u>Ca</u> -SO ₄ -HCO ₃	2 sites	1 site	3.3%		
Mg-Ca-HCO ₃				1 site	
<u>Na</u> -Ca-HCO ₃ -SO ₄ -Cl	1 site				
<u>Na</u> -Ca-SO ₄ -HCO ₃ -Cl	1 site				

APPENDIX D

LUTRY SITE: POROSITY AND SPECIFIC PERMEABILITY OF BEDROCK SANDSTONE SAMPLES

The grain density and bulk rock density as well as specific permeability were measured on four sandstone samples (small rock cylinders). Porosity and hydraulic conductivity were calculated from the density and permeability measurements. The two numbers represent the results of double analyses.

samples		grain density	density determined by He-porosimetry	bulk rock density determined by Hg-pycnometry	porosity determined by He-porosimetry	Total porosity	Specific permeability determined by N-percolation		Hydraulic conductivity
		ρ_{gr}	ρ_{He}	ρ_{tot}	θ_{He}	θ	k		K^a
Nr		g/cm ³	g/cm ³	g/cm ³	%	%	darcy	cm ²	m/s
					$\frac{\rho_{He} - \rho_{tot}}{\rho_{He}} \cdot 100$	$\frac{\rho_{gr} - \rho_{tot}}{\rho_{tot}} \cdot 100$		$k \text{ (darcy)} \cdot 9.87 \cdot 10^{-9b}$	$k \text{ (darcy)} \cdot 9.66 \cdot 10^{-6}$
11	reduced medium-grained Sandst.	2.78	2.75	2.32	15.7	16.7	0.105	$1.04 \cdot 10^{-9}$	$1.01 \cdot 10^{-6}$
		2.77	2.74	2.32	15.5	16.4	0.109	$1.08 \cdot 10^{-9}$	$1.05 \cdot 10^{-6}$
18	oxidised medium-grained Sandst.	2.75	2.76	2.17	21.5	21.4			
		2.76	2.76	2.17	21.5	21.6			
24	near surf. medium-grained Sandst..	2.78	2.74	2.29	16.6	17.7	0.051	$5.03 \cdot 10^{-10}$	$4.93 \cdot 10^{-7}$
		2.79	2.74	2.29	16.5	18.1	0.054	$5.33 \cdot 10^{-10}$	$5.22 \cdot 10^{-7}$
25	near surf. fine-gr. Sandst	2.79	2.76	2.33	15.7	16.4	0.004	$3.95 \cdot 10^{-11}$	$3.86 \cdot 10^{-8}$
		2.81	2.76	2.33	15.5	16.9	0.005	$4.94 \cdot 10^{-11}$	$4.83 \cdot 10^{-8}$

a. $K=k\rho g/\mu$,

where K = hydraulic conductivity, k = specific permeability, ρ = fluid density, μ = dynamic viscosity (centipoise cP; $N\cdot s/m^2 \cdot 10^{-3}$), g = earth acceleration

b. Conversions: [Freeze, 1979 #398], p. 29

APPENDIX E

LUTRY SITE: MINERALOGICAL COMPOSITION OF BEDROCK AND SOIL

Bulk mineralogical composition and clay mineral associations of oxidised and reduced Burdigalian sandstone and marl were analysed by X-ray diffraction. Sample preparation and analyses were performed at the Institute of Mineralogy and Petrography of the University of Bern according to the methods described in the XRD laboratory manual (Rizzoli, 1997). A Phillips PW 1800 diffractometer with a copper tube ($\text{CuK}\alpha$) was used. The diffraction patterns were measured over a range of $2-60^\circ 2\theta$ for random powder mounts (bulk mineralogy) and over a range of $2-35^\circ 2\theta$ for oriented samples (clay mineralogy). The diffraction patterns were treated by the PC-APD program (Phillips).

XRD analyses of oxidised and reduced Burdigalian sandstone and marl are presented together with compiled mineralogical data of the different soil horizons and calcareous Burdigalian sandstone.

Horizon	Soil ^a						Bedrock			
	Aalh	Sal	Salg1	Salg2	SC	SCca	Bedrock ox.. ^c	Bedrock red. ^b	Bedrock calc. ^c	Marl ^d
Depth (cm)	5-15	20-40	40-60	60-80	80-120	240-260				
Bulk mineralogy (wt.%)										
Quartz	45	41	42	36	40	46	38	42	31	-
K-Feldspar	8	5	7	4	8	7	9	13	6	-
Plagioclase	11	10	9	9	12	13	26	25	10	-
Calcite	0	0	0	0	0	0	6	9	25-27	-
Dolomite	0	0	0	0	0	0	1	2	-	-
Sheet-silicates	25	42	41	50	40	34	19	8	27	-
Organic matter	11	2	2	1	1	0	0	0	0	-
Heavy minerals >100 μm	0.4	0.2	0.3	0.5	1.2	1	-	-	1	-
Clay mineralogy (relative amounts in%)										
Vermiculite	33	55	34	29	37	0	0	0	0	0
Mixed-layers Ill-Vrm	40	24	32	31	24	8	0	0	1	0
Smectite	0	0	2	5	16	57	90	40	67	35
Illite	9	9	16	17	13	23	5	30	24	35
Chlorite	18	13	16	18	11	12	5	30	8	33

Mineralogy of soil and bedrock (- = not analysed)

a. Dalla Piazza, 1996

b. this work, material used for leaching experiment

c. mean of 3 samples (RM90, RM91, RM92; Dalla Piazza, 1996)

d. this work

APPENDIX F

LUTRY SITE: CHEMICAL COMPOSITION OF BEDROCK AND SOIL

Three samples of Burdigalian sandstone and one marl sample were analysed chemically by X-ray fluorescence. After measuring the loss on ignition, major elements were measured on glass pellets and trace elements were measured on pressed powder pellets. Measurements were carried out at the University of Fribourg. The results are presented together with compiled mineralogical data of other sandstone samples and of the different soil horizons.

Chemical composition of soil and bedrock samples at Lutry site. n.a. = not analysed; n.d. = not detected.

Sample	Soil ^a						Bedrock								
	Aalh	Sal	Salg1	Salg2	SC	SCca	18 ^b	27 ^b	14 ^b	11 ^b	POZ1 ^c	R90 ^a	R91 ^a	R92 ^a	
	5-15 cm	20-40 cm	40-60 cm	60-80 cm	80-100 cm	240-260 cm	med.-gr. oxidised Sst.	fine gr. Sst	marl	med.-gr. reduced Sst.	med.-gr. calc. Sst.	med.-gr. calc. Sst.	med.-gr. calc. Sst.	fine-gr. calc. Sst.	
Major elements (weight %)															
SiO ₂	78.32	77.35	76.34	75.71	75.89	72.33	67.07	67.84	56.69	64.65	59.07	57.88	57.05	55.21	
TiO ₂	0.39	0.42	0.41	0.40	0.36	0.24	0.22	0.23	0.60	0.23	0.23	0.18	0.20	0.35	
Al ₂ O ₃	9.57	10.64	10.97	11.15	10.57	9.19	10.55	8.81	12.23	9.35	7.87	7.75	7.53	7.76	
Fe ₂ O ₃	2.95	3.48	3.54	3.74	3.65	3.92	1.90	2.72	4.90	1.89	2.11	2.06	2.47	2.34	
MnO	0.04	0.09	0.08	0.07	0.08	0.09	0.06	0.07	0.05	0.06	0.13	0.07	0.08	0.08	
MgO	0.76	0.86	1.04	1.25	1.32	1.94	1.31	1.67	2.99	1.54	1.05	1.71	1.93	1.90	
CaO	0.46	0.48	0.46	0.46	0.57	3.95	7.31	7.19	7.81	9.39	13.80	14.18	13.78	14.99	
Na ₂ O	1.56	1.62	1.64	1.78	1.94	1.85	4.59	3.41	1.80	3.22	1.77	1.79	1.60	1.51	
K ₂ O	2.14	2.15	2.30	2.49	2.57	2.52	2.44	2.47	2.72	2.35	1.89	1.75	1.98	1.78	
P ₂ O ₅	0.09	0.08	0.09	0.07	0.09	n.d.	0.08	0.11	0.16	0.10	0.08	0.07	0.10	0.13	
LOI	3.02	2.87	2.90	2.51	3.15	4.00	6.43	7.13	9.58	8.57	10.70	12.38	12.61	13.40	
SUM	99.30	100.04	99.77	99.63	100.19	100.03	101.96	101.65	99.53	101.36	98.70	99.82	99.33	99.45	
Trace elements (ppm)															
Ba	260	302	310	341	311	341	349	334	318	338	228	223	222	215	
Cr	104	114	120	124	125	122	60	94	138	76	73	70	73	116	
Cu	n.d.	n.d.	n.d.	n.d.	12	1	<5	<5	<5	<5	9	n.d.	n.d.	n.d.	
Nb	n.a.	n.a.	n.a.	n.a.	n.a.	n.a.	5	<5	10	6	5	n.a.	n.a.	n.a.	
Ni	19	25	38	45	45	55	28	47	81	31	27	29	30	34	
Pb	20	15	9	9	8	1	23	16	36	22	6	0	2	1	
Rb	82	88	98	98	94	91	72	68	110	70	67	61	69	65	
Sr	73	76	75	75	76	138	220	196	187	227	235	225	249	254	
V	57	54	55	59	52	53	26	34	88	27	24	24	29	35	
Y	10	13	13	20	26	23	16	27	34	19	21	10	15	22	
Zn	44	49	54	54	60	41	10	20	61	21	35	26	36	39	
Zr	151	168	160	155	121	91	80	84	173	113	82	53	54	199	

a. Dalla Piazza, 1996

b. This work: Relative errors for oxides in weight percent can be given as follows: 100 wt.% \pm 1.5 %, 50 wt.% \pm 2 %, 10 wt.% \pm 3 %, 5 wt.% \pm 4 %, 1 wt.% \pm 5 %, 0.5 wt.% \pm 7 %. Relative errors for trace element concentrations in ppm are 1000 ppm \pm 12 %, 500 ppm \pm 15 %, 100 ppm \pm 25 %, 50 ppm \pm 30 %, 10 ppm \pm 50 %.

c. Hesske, 1995

Curriculum Vitae

KILCHMANN Sybille

born on March 13th 1971

Swiss

Education

1986-1990 Collège Ste Croix, Fribourg,
Matura Type B (languages)

1991-1996 Geological and Mineralogical Institutes, University of Berne
Graduate studies in earth sciences (mineralogy)
Dipl. phil. nat.

1997-2001 Swiss Federal Institute of Technology - Lausanne
PhD studies in hydro-geochemistry